

Jefferson Luiz Brum Marques
Cesar Ramos Rodrigues
Daniela Ota Hisayasu Suzuki
José Marino Neto
Renato García Ojeda *Editors*

IX Latin American Congress on Biomedical Engineering and XXVIII Brazilian Congress on Biomedical Engineering

Proceedings of CLAIB and CBEB 2022,
October 24–28, 2022, Florianópolis,
Brazil—Volume 4: Clinical
Engineering and Health
Technologies



Series Editor

Ratko Magjarević, *Faculty of Electrical Engineering and Computing, ZESOI, University of Zagreb, Zagreb, Croatia*

Associate Editors

Piotr Ładyżyński, *Warsaw, Poland*

Fatimah Ibrahim, *Department of Biomedical Engineering, Faculty of Engineering, Universiti Malaya, Kuala Lumpur, Malaysia*

Igor Lackovic, *Faculty of Electrical Engineering and Computing, University of Zagreb, Zagreb, Croatia*

Emilio Sacristan Rock, *Mexico DF, Mexico*

The IFMBE Proceedings Book Series is an official publication of *the International Federation for Medical and Biological Engineering* (IFMBE). The series gathers the proceedings of various international conferences, which are either organized or endorsed by the Federation. Books published in this series report on cutting-edge findings and provide an informative survey on the most challenging topics and advances in the fields of medicine, biology, clinical engineering, and biophysics.

The series aims at disseminating high quality scientific information, encouraging both basic and applied research, and promoting world-wide collaboration between researchers and practitioners in the field of Medical and Biological Engineering.

Topics include, but are not limited to:

- Diagnostic Imaging, Image Processing, Biomedical Signal Processing
- Modeling and Simulation, Biomechanics
- Biomaterials, Cellular and Tissue Engineering
- Information and Communication in Medicine, Telemedicine and e-Health
- Instrumentation and Clinical Engineering
- Surgery, Minimal Invasive Interventions, Endoscopy and Image Guided Therapy
- Audiology, Ophthalmology, Emergency and Dental Medicine Applications
- Radiology, Radiation Oncology and Biological Effects of Radiation
- Drug Delivery and Pharmaceutical Engineering
- Neuroengineering, and Artificial Intelligence in Healthcare

IFMBE proceedings are indexed by SCOPUS, EI Compendex, Japanese Science and Technology Agency (JST), SCImago. They are also submitted for consideration by WoS.

Proposals can be submitted by contacting the Springer responsible editor shown on the series webpage (see “Contacts”), or by getting in touch with the series editor Ratko Magjarevic.

Jefferson Luiz Brum Marques ·
Cesar Ramos Rodrigues ·
Daniela Ota Hisayasu Suzuki ·
José Marino Neto ·
Renato García Ojeda
Editors

IX Latin American Congress on Biomedical Engineering and XXVIII Brazilian Congress on Biomedical Engineering

Proceedings of CLAIB and CBEB 2022
October 24–28, 2022
Florianópolis, Brazil—Volume 4: Clinical
Engineering and Health Technologies

 Springer

Editors

Jefferson Luiz Brum Marques
Institute of Biomedical Engineering
Department of Electrical and Electronic
Engineering
Federal University of Santa Catarina
Florianópolis, Brazil

Cesar Ramos Rodrigues
Institute of Biomedical Engineering
Department of Electrical and Electronic
Engineering
Federal University of Santa Catarina
Florianópolis, Brazil

Daniela Ota Hisayasu Suzuki
Institute of Biomedical Engineering
Department of Electrical and Electronic
Engineering
Federal University of Santa Catarina
Florianópolis, Brazil

José Marino Neto
Institute of Biomedical Engineering
Federal University of Santa Catarina
Florianópolis, Brazil

Renato García Ojeda
Institute of Biomedical Engineering
Department of Electrical and Electronic
Engineering
Federal University of Santa Catarina
Florianópolis, Brazil

ISSN 1680-0737

ISSN 1433-9277 (electronic)

IFMBE Proceedings

ISBN 978-3-031-49409-3

ISBN 978-3-031-49410-9 (eBook)

<https://doi.org/10.1007/978-3-031-49410-9>

© The Editor(s) (if applicable) and The Author(s), under exclusive license to Springer Nature
Switzerland AG 2024

This work is subject to copyright. All rights are solely and exclusively licensed by the Publisher, whether the whole or part of the material is concerned, specifically the rights of translation, reprinting, reuse of illustrations, recitation, broadcasting, reproduction on microfilms or in any other physical way, and transmission or information storage and retrieval, electronic adaptation, computer software, or by similar or dissimilar methodology now known or hereafter developed.

The use of general descriptive names, registered names, trademarks, service marks, etc. in this publication does not imply, even in the absence of a specific statement, that such names are exempt from the relevant protective laws and regulations and therefore free for general use.

The publisher, the authors, and the editors are safe to assume that the advice and information in this book are believed to be true and accurate at the date of publication. Neither the publisher nor the authors or the editors give a warranty, expressed or implied, with respect to the material contained herein or for any errors or omissions that may have been made. The publisher remains neutral with regard to jurisdictional claims in published maps and institutional affiliations.

This Springer imprint is published by the registered company Springer Nature Switzerland AG
The registered company address is: Gewerbestrasse 11, 6330 Cham, Switzerland

Paper in this product is recyclable.

Preface

The IX Latin American Congress on Biomedical Engineering and XXVIII Brazilian Congress on Biomedical Engineering (CLAIB&CBEB 2022) took place simultaneously on October 24–28, 2022, in Florianópolis-SC, Brazil, and were organised by the Institute of Biomedical Engineering of The Federal University of Santa Catarina (IEB-UFSC), the Regional Council of Biomedical Engineering for Latin America (CORAL) and the Brazilian Biomedical Engineering Society (SBEB). These events were held remotely for the most part, with a small set of conferences taking place in person on the premises of IEB-UFSC (Florianópolis, Brazil). They included 11 hands-on technical workshops for students, 26 keynote speakers and symposia, and 40 oral and poster presentation sessions attended by about a thousand participants, including undergraduate and graduate students, academic researchers, and public and private sector agents.

We are proud to present in this book a selection of papers presented at this event by researchers from all over the world, reporting recent and innovative findings and technological outcomes in the many areas of interest of biomedical engineering. These papers represent nearly 50% of those original contributions presented at the CLAIB&CBEB 2022. Their academic quality has been warranted by careful peer review coordinated by an expert scientific committee of leading Latin American senior researchers in biomedical engineering. The content is organised into four volumes and eleven chapters, covering the most relevant areas of scientific and technological developments within the broad spectrum of biomedical engineering interests. We are sure that the contributions presented in this book give a deep overview of the leading edge in your expertise and other areas.

On behalf of Scientific and Organising Committees, we thank authors, academic reviewers and sponsoring societies such as CORAL, SBEB, UFSC, FAPESC and IEB-UFSC for their contributions. Moreover, we encourage readers to enjoy this amazing piece of scientific literature as a breadth of knowledge in the biomedical engineering field.

Florianópolis, Brazil

Jefferson Luiz Brum Marques
Cesar Ramos Rodrigues
Daniela Ota Hisayasu Suzuki
José Marino Neto
Renato García Ojeda

Organisation

CLAIB&CBEB 2022 was organised by the Regional Council of Biomedical Engineering for Latin America (CORAL) and the Brazilian Biomedical Engineering Society (SBEB) in cooperation with the International Federation for Medical and Biological Engineering (IFMBE).

Committees

The Organizing Committee of the IX Latin American Congress of Biomedical Engineering (CLAIB 2022) and the XXVIII Brazilian Congress of Biomedical Engineering (CBEB 2022) was composed of the following members:

Organising Committee

President: Renato Garcia Ojeda

Vice-President: Jefferson Luiz Brum Marques

Scientific Committee

Jefferson Luiz Brum Marques

Programme Committee

José Marino-Neto

Special Events Committee

Cesar Ramos Rodrigues

Finance and Disclosure Committee

Daniela Ota Hisaysu Suzuki

Follow-Up Committee

Helio Schechtman—President of the Brazilian Society of Biomedical Engineering (SBEB)

Elliot Vernet—President Regional Council of Biomedical Engineering for Latin America (CORAL)

Shankar Krishnan—President International Federation of Medical and Biological Engineering (IFMBE)

Part Editors

Biomedical Robotics, Assistive Technologies and Health Informatics	<i>Teodiano Freire Bastos Filho (UFES-Brazil)</i> <i>Luis Eduardo Rodriguez Cheu (CSEJG-Colombia)</i> <i>Renato Garcia Ojeda (UFSC-Brazil)</i>
Biomedical Image and Signal Processing	<i>Márcio Holsbach Costa (UFSC-Brazil)</i> <i>Virginia Laura Ballarin (UNMDP-Argentina)</i> <i>Jurandir Nadal (UFRJ-Brazil)</i>
Biomedical Optics and Systems and Technologies for Therapy and Diagnosis	<i>Renato Amaro Zângaro (UAM-Brazil)</i> <i>Regiane Albertini de Carvalho (UNIFESP-Brazil)</i>
Biomedical Devices and Instrumentation	<i>Percy Nohama (PUC-PR-Brazil)</i> <i>Guilherme; Nunes Nogueira (PUC-PR-Brazil)</i>
Bioengineering, Modelling and Simulation, Bioinformatics and Computational Biology	<i>Antonio Carlos Guimarães de Almeida (UFSJ-Brazil)</i> <i>Antônio Márcio Rodrigues (UFSJ-Brazil)</i> <i>Luis Enrique Bergues Cabrales (UO-Cuba)</i>
Biomaterials, Tissue Engineering and Artificial Organs	<i>Idágene Aparecida Cestari (USP-Brazil)</i> <i>Sônia Maria Malmonge (UFABC-Brazil)</i>
Biosensors, Bioinstrumentation and Micro-nanotechnologies	<i>Alcimar Barbosa Soares (UFU-Brazil)</i>
Biomechanics, Neural Engineering and Rehabilitation	<i>Adriano de Oliveira Andrade (UFU-Brazil)</i>
Clinical Engineering and Health Technology Assessment	<i>Fabiola Margarita Martínez-Licona (UAM-Mexico)</i> <i>Roberto Macoto Ichinose (UFRJ-Brazil)</i>
Health Technology Innovation and Development	<i>Antonio Adilton Oliveira Carneiro (USP-Brazil)</i>
Metrology and Quality of Healthcare Technologies	<i>Carlos Rubén Dell'Aquila (UNSJ-Argentina)</i> <i>Rodrigo Pereira Barretto da Costa Félix (InMetro-Brazil)</i>

Special Topics*Adson Ferreira da Rocha (UnB-Brazil)**Renato Garcia Ojeda (UFSC-Brazil)***Support Committee**

Alexandre Holzbach Junior
Bruna Fanchin
Clara Teresa de Souza Ramos
Daniella de Lourdes Luna Santana de Andrade
Daniel Ribeiro de Moraes
Esteferson Quadros
Felipe Rettore Andreis
Flavio Maurício Garcia Pezzolla
Guilberth Alves de Matos
Henrique Rezer Mosquér
Israel Santana
Jéssica Rodrigues da Silva
Jonas Martins Maciel
Jone Follmann
Juliano Martins
Lucas Bertinetti Lopes
Maicon Francisco
Marcelo Dérick Oliveira das Chagas
Maria Angelica Martins
Mariana Ribeiro Brandão
Mateus Andre Favretto
Matheus Gama Costa
Paulo Miguel Rodrigues da Rocha
Pedro Paulo Santos Gomes da Silva
Rafael Glatz
Rafael Schantone Silva
Raul Guedert
Sandra Cossul
Susana Bartnikowsky
Victor Hugo de Freitas Morales
Vinícius Rodrigues Zanon

Scientific Reviewers

Adilmar Coelho Dantas	Universidade Federal de Uberlândia, BR
Adriana Gabriela Scandurra	Universidad Nacional de Mar del Plata, AR
Adriana Kauati	State University of Western Paraná, BR
Adriane Parraga	Universidade Estadual do Rio Grande do Sul, BR
Adriano Pereira	Universidade Federal de Uberlândia, BR
Adriano Péricles Rodrigues	Universidade Federal de Goiás, BR
Agustina Bouchet	Universidad de Oviedo, ES
Agustina Garces Correa	Universidad Nacional de San Juan, AR
Alberto López Delis	Universidad de Oriente, CU
Aldira Domínguez	Universidade de Brasília, BR
Alejandro Espinel Hernández	Universidad do Oriente, CU
Alexander Alexeis Suárez-León	Universidad de Oriente, CU
Alexandre Balbinot	Universidade Federal do Rio Grande do Sul, BR
Alexandre Luís Cardoso Bissoli	Instituto Nacional da Propriedade Industrial, BR
Alexandre Romariz	Universidade de Brasília, BR
Alfredo de Oliveira Assis	Universidade Federal de Goiás, BR
Alvaro David Orjuela Cañon	Universidad del Rosario, AR
Ana B Pimentel-Aguilar	Instituto Nacional de Enfermedades Respiratorias, MX
Ana Karoline Almeida da Silva	Universidade de Brasília, BR
André Adami	Universidade de Caxias do Sul, BR
André Dantas	Instituto Santos Dumont, BR
Andre Lazzaretti	Universidade Tecnológica Federal do Paraná, BR
André Luís Fonseca Furtado	Instituto Federal do Sudeste de Minas Gerais, BR
Andrés Alberto Ramírez Duque	Universidad El Bosque, CO
Andrés Felipe Ruíz Olaya	Universidad Antonio Nariño, CO
Angela Abreu Rosa de Sá	Universidade Federal de Uberlândia, BR
Angela Salinet	Universidade de São Paulo, BR
Antonio Mauricio Miranda de Sá	Universidade Federal de Rio de Janeiro, BR
Aparecido Carvalho	Centro Universitário Salesiano São Paulo, BR
Argenis Adrian Soutelo Jimenez	Universidad de Oriente, CO
Ariana Moura Cabral	Universidade Federal de Uberlândia, BR
Ariel Braidot	Universidad Nacional de Entre Rios, AR
Arnaldo Fim Neto	Universidade Federal do ABC, BR
Arquímedes Montoya Pedrón	Hospital General Docente Juan Bruno Zayas Alfonso, CU
Arthur Carvalho Pires	Universidade Federal de São João Del-Rei, BR
Aura Ximena González Cely	Universidad Pedagógica y Tecnológica, CO
Ayayacatl Morales	Universidad Autónoma Metropolitana Iztapalapa, MX

Beatriz Fernandes	Pontificia Universidad Catolica de Parana, BR
Beatriz Janeth Galeano Upegui	Universidad Pontificia Bolivariana, CO
Belkys Amador	Universidad Austral de Chile, CL
Bruno Bispo	Universidade Federal de Santa Catarina, BR
Caio C. E. De Abreu	Universidade do Estado de Mato Grosso, BR
Carla Scorza	Universidade Federal de São Paulo, BR
Carlos Alirio Lozano Ortiz	Universidade Federal de Rio de Janeiro, BR
Carlos Araujo	Instituto Federal do Paraná, BR
Carlos Castillo	Fundación Universitaria del Área Andina, CO
Carlos Danilo Miranda Regis	Instituto Federal da Paraíba, BR
Carlos Galvão Pinheiro Júnior	Universidade Federal de Goiás, BR
Carlos Maciel	Universidade de São Paulo, BR
Carlos Magno Medeiros Queiroz	Instituto Federal do Triângulo Mineiro, BR
Carlos Valadao	Instituto Federal do Espírito Santo, BR
Carolina Tabernig	Universidad Nacional de Entre Ríos, AR
Cesar Ferreira Amorim	Universidade Federal de Uberlândia, BR
Cesar Rodrigues	Universidade Federal de Santa Catarina, BR
César Teixeira	University of Coimbra, PT
Cicero Hildenberg Lima De Oliveira	Universidade Tecnológica Federal do Paraná, BR
Claudia Lescano	Universidad Nacional de San Juan, AR
Claudia Mirian de Godoy Marques	Universidade do Estado de Santa Catarina, BR
Cleber Zanchettin	Universidad Nacional de San Juan, AR
Cleison Daniel Silva	Universidade Federal do Pará, BR
Cristian Blanco	Universidad Antonio Nariño, CO
Cristian David Guerrero Mendez	Universidad Antonio Nariño, CO
Cristiano Jacques Miosso	Universidade de Brasília, BR
Cristina Shimoda Uechi	MCTIC, BR
Dafne Mendes Soares	Universidade Federal de São João del-Rei, BR
Damien Depannemaecker	Universidade Federal de São Paulo, BR
Daniel Cavalieri	Instituto Federal do Espírito Santo, BR
Daniela del Carmen Gonzalez	Universidad Nacional de San Juan, AR
Daniela O H Suzuki	Universidade Federal de Santa Catarina, BR
Daniella De Lourdes L S Andrade	Universidade Federal de Santa Catarina, BR
Danilo Melges	Universidade Federal de Minas Gerais, BR
Danilo Silva	Universidade Federal de Santa Catarina, BR
David Sérgio Adães de Gouvêa	Universidade Federal de Juiz de Fora, BR
Débora de Fátima Camillo Ribeiro	Pontificia Universidade Católica do Paraná, BR
Delmo Benedito Silva	Universidade Federal de São João Del-Rei, BR
Denis Delisle Rodriguez	Instituto Santos Dumont, BR
Diana Gutierrez	Universidad Manuela Beltran, CO
Diego Beltramone	Universidad Nacional de Córdoba, AR

Diego Sebastián Comas	National University of Singapore, SG
Éberte Freitas	Universidade Federal do Espírito Santo, BR
Edgard Morya	Instituto Santos Dumont, BR
Edras Pacola	Universidade Positivo, BR
Eduardo Antonio Fragoso Dias	Universidade Federal do Espírito Santo, BR
Eduardo M. Scheeren	Pontifícia Universidade Católica do Paraná, BR
Eduardo Naves	Universidade Federal de Uberlândia, BR
Elgison Da Luz Dos Santos	Centro Universitário Internacional Uninter, BR
Eliete Maria De Oliveira Caldeira	Universidade Federal do Espírito Santo, BR
Elisa Perez	Universidad Nacional de San Juan, AR
Elisangela Manffra	Pontifícia Universidade Católica do Paraná, BR
Elisângela Oliveira Carneiro	Universidade Estadual de Feira de Santana, BR
Emanuel Tello	Universidad Nacional de San Juan, AR
Enrique J. Marañón	Universidad de Oriente, CU
Enrique Mario Avila Perona	Universidad Nacional de San Juan, AR
Eric Laciár Leber	Universidad Nacional de San Juan, AR
Ernesto Suaste	CINVESTAV Sección Bioelectrónica, MX
Esmirna Cascaret Fonseca	Centro Provincial de Medicina Deportiva, CU
Esteban Lanzarotti	Universidad de Buenos Aires, AR
Eugenio Orosco	universidade Nacional de San Juan, AR
Euler Garcia	Universidade de Brasília, BR
Evandro Salles	Universidade Federal do Espírito Santo, BR
Fabiana Bertoni	Universidade Estadual de Feira de Santana, BR
Fabiana da Silveira Bianchi Perez	Faculdades Alfredo Nasser, BR
Fabio Viegas Caixeta	Universidade de Brasília, BR
Fabricio Lima Brasil	Instituto Santos Dumont, BR
Fabricio Neves Mendonca	Instituto federal de Minas Gerais, BR
Fabrício Noveletto	Universidade do Estado de Santa Catarina, BR
Fátima L. S. Nunes	Universidade de São Paulo, BR
Felipe Rettore Andreis	HST Aalborg University, DK
Fellipe Allevalo Martins da Silva	Universidade Federal do Rio de Janeiro, BR
Fernando Henrique Magalhães	Universidade de São Paulo, BR
Fernando Jorge Muñoz Zapata	Universidad Nacional de San Juan, AR
Fernando Valdés-Pérez	Universidade do Oriente, CU
Flavio Buiochi	Universidade de Sao Paulo, BR
Floriano Salvaterra	Universidade Federal de Rio de Janeiro, BR
Francisco Assis de Oliveira Nascimento	Universidade de Brasília, BR
Franco Simini	Universidad de la Republica de Uruguay, UY
Frieda Saicla Barros	universidade Tecnológica Federal do Paraná, BR
Gabriel Bruno M. Fernandes	Universidade Federal de Santa Catarina, BR
Gabriel Domingo Vilallonga	Universidade Nacional de Catamarca, AR

Gabriel Eduardo Cañadas Fragapane	Universidad Nacional de San Juan, AR
Gabriel Motta Ribeiro	Universidade Federal de Rio de Janeiro, BR
Gilcélío Silveira	Universidade Federal de São João del-Rei, BR
Glauco Cardozo	Instituto Federal de Santa Catarina, BR
Glécia Luz	Universidade de Brasília, BR
Gonzalo Quiroga	Universidad Nacional de San Juan, AR
Guilherme Augusto Gomes De Villa	Universidade Federal de Goiás, BR
Guillermo Abras	Universidad Nacional de Mar del Plata, AR
Gustavo Meschino	Universidad Nacional de Mar del Plata, AR
Gustavo Vivas	Empresa Brasileira de Serviços Hospitalares, BR
Harlei Leite	Universidade Federal do Espírito Santo, BR
Henrique Takachi Moriya	Universidade de Sao Paulo, BR
Hugo Líbero	Instituto Federal de Goiás, BR
Humberto Gamba	Universidade Tecnológica Federal do Paraná, BR
Humberto Romano	INTECNUS Foundation, AR
Isabela Alves Marques	Universidade Federal de Uberlândia, BR
Isabela Miziara	Universidade Federal do Pará, BR
Ismar Cestari	Instituto do Coração Universidade de São Paulo, BR
Jair Trapé Goulart	Universidade de Brasília, BR
Javier Camacho	Universidade EIA, CO
Jerusa Marchi	Universidade Federal de Santa Catarina, BR
Jessica Lara	Universidade Federal de São João Del-Rei, BR
João Henrique Kleinschmidt	Universidade Federal do ABC, BR
João Lameu	Universidade Federal do ABC, BR
Joao Marques	University of Saint Joseph, US
João Otávio Bandeira Diniz	Instituto Federal do Maranhão, BR
João Panceri	Instituto Federal do Espírito Santo, BR
Joaquim Cezar Felipe	Universidade de São Paulo, BR
Joaquim Mendes	Universidade do Porto, PT
Joaquin Azpiroz Leehan	UAM Iztapalapa, MX
Jorge Takenaga	Universidad de Monterrey, MX
Jose Carlos Cunha	Pontificia Universidade Católica do Paraná, BR
José Di Paolo	Universidad Nacional de Entre Ríos, AR
José Felício Da Silva	Universidade de Brasília, BR
José Foggiatto	Universidade Tecnológica Federal do Paraná, BR
José María Flores	Universidad Nacional de Entre Rios, AR
José Wilson Bassani	Universidade de Campinas, BR
Juan Carlos Iturrieta Gimeno	Universidad Nacional de San Juan, AR
Juan Carlos Perfetto	Universidad de Buenos Aires, AR

Juan Enrique Palomares Ruiz	Instituto Tecnológico Superior de Cajeme, MX
Juan Graffigna	Universidad Nacional de San Juan, AR
Juan I. Montijano	University of Zaragoza, ES
Juan Ignacio Pastore	Universidad Nacional de Mar del Plata, AR
Juan Pablo Tello Portillo	Universidad del Norte, CO
Juan Pastore	Universidad Nacional de Mar del Plata, AR
Juan Vorobioff	Comisión Nacional de Energía Atómica CNEA, AR
Juliana Santa Ardisson	Universidade Federal do Espírito Santo, BR
Juliano Costa Machado	Instituto Federal Sul-Rio-Grandense, BR
Julio Alberto Rojas Vargas	Universidade do Oriente, CU
Julio Cesar Nievola	Pontifícia Universidade Católica do Paraná, BR
Karla Aparecida Ferreira	Universidade Federal de São João Del-Rei, BR
Katia Prus	Universidade Tecnológica Federal do Paraná, BR
Kelison Tadeu Ribeiro	Instituto Federal do Espírito Santo, BR
Lacordaire Kemel Pimenta Cury	Instituto Federal de Educação, Ciência e Tecnologia Goiano, BR
Leandro Bueno	Instituto Federal do Espírito Santo, BR
Lena Perez Font	Universidad de Oriente, CU
Leonardo Abdala Elias	Universidade Estadual de Campinas, BR
Leonardo Abrantes	Universidade Federal de Rio de Janeiro, BR
Leonardo Batista	Universidade Federal da Paraíba, BR
Leonardo Ramirez	Universidad Militar Nueva Granada, CO
Leticia Silva	Universidade Federal do Espírito Santo, BR
Lorena Orosco	Universidad Nacional de San Juan, AR
Lourenço Madruga Barbosa	Universidade Tecnológica Federal do Paraná, BR
Lucas Côgo Lampier	Universidade Federal do Espírito Santo, BR
Lucenildo Cerqueira	Universidade Federal de Rio de Janeiro, BR
Luciana Menezes Xavier de Souza	Universidade Federal de Santa Catarina, BR
Luciana Roberta Peixoto	Universidade de Brasília, BR
Luciane Aparecida Pascucci de Souza	Universidade Federal do Triângulo Mineiro, BR
Luciano Menegaldo	Universidade Federal de Rio de Janeiro, BR
Luis Carlos Hernandez Barraza	National University of Singapore, SG
Luis Eduardo Maggi	Universidade Federal do Acre, BR
Luis Jiménez-Angeles	Universidade Nacional Autónoma do México, MX
Luis Miguel Zamudio	Universidade do Oriente, CU
Luis Pulenta	Universidad Nacional de San Juan, AR
Luis Roberto Barriere	Universidad Don Bosco, SV
Luis Sifuentes	Universidad Cuauhtémoc Aguascalientes, MX
Luis Vilcahuaman	Pontificia Universidad Católica del Peru, PE

Maikel Noriega Alemán	Universidad del Oriente, CU
Maira Ranciaro	Pontificia Universidad Católica del Paraná, BR
Malki-çedheq Benjamim C. Silva	Universidad Federal de Pernambuco, BR
Marcella Carneiro	Universidad de Brasília, BR
Marcelo Lencina	National Technological University, AR
Marcio Nogueira de Souza	Universidad Federal de Rio de Janeiro, BR
Marcio Rodrigues	Instituto Federal del Sudeste de Minas Gerais, BR
Marco Antonio Garcia	Universidad Federal de Juiz de Fora, BR
Marcos Hara	Instituto Federal del Paraná, BR
Marcus Vieira Fraga	Universidad de Goiás, BR
Maria Claudia F. Castro	Centro Universitario da FEI, BR
Mariana de Mello Gusso	Pontificia Universidad Católica del Paraná, BR
Mariela Azul Gonzalez	Universidad Nacional de Mar del Plata, AR
Mário Fabrício Fleury Rosa	Universidad de Brasília, BR
Marly Guimaraes Fernandes Costa	Universidad Federal del Amazonas, BR
Martha Ortiz	Universidad Autonoma de Mmexico - Iztapalapa, MX
Martha Ribeiro	Universidad de São Paulo, BR
Martha Zequera	Pontificia Universidad Javeriana, CO
Martín Guzzo	Universidad Nacional de San Juan, AR
Maryangel Jhoseline Medina	Comisión Nacional de Energía Atómica, AR
Mateus Andre Favretto	Universidad del Estado de Santa Catarina, BR
Mauren Abreu de Souza	Pontificia Universidad Católica del Paraná, BR
Mauricio Cagy	Universidad Federal del Rio de Janeiro, BR
Mauricio Kugler	Nagoya Institute of Technology, JP
Mauricio Tavares	Contronic Tecnologia para Diagnósticos, BR
Mayra Aarao	Universidad Federal de São João del-Rei, BR
Mohamed Ahmed	Universidad Federal de São João Del-Rei, BR
Monica Teresita Miralles	Universidad de Buenos Aires, AR
Munir Gariba	Universidad de São Paulo, BR
Murilo Contó	Boston Scientific, BR
Nahuel M Olaiz	Universidad de Buenos Aires, AR
Nicolas Jacobo Valencia Jimenez	Universidad Santiago de Cali, CO
Nilton Correia Da Silva	Universidad de Brasília, BR
Olavo Luppi Silva	Universidad Federal del ABC, BR
Pablo Caicedo	Universidad Autónoma de Colombia, CO
Pablo Daniel Cruces	Universidad de Buenos Aires, AR
Pablo Diez	Universidad Nacional de San Juan, AR
Pablo Turjanski	Universidad de Buenos Aires, AR
Patrick Marques Ciarelli	Universidad Federal del Espíritu Santo, BR
Paula Brandao Furlan	Universidad Federal de Rio de Janeiro, BR
Paula Hembecker	Pontificia Universidad Católica del Paraná, BR

Paulo Ambrosio	Universidade Estadual de Santa Cruz, BR
Paulo Broniera Junior	Federação das Indústrias Estado de São Paulo, BR
Paulo Eduardo Narcizo de Souza	Universidade de Brasília, BR
Paulo Gubert	Universidade Católica de Pelotas, BR
Paulo Jose Abatti	Universidade Tecnológica Federal do Paraná, BR
Paulo Roberto Sanches	Hospital de Clínicas de Porto Alegre, BR
Paulo Rogerio Scalassara	Universidade Tecnológica Federal do Paraná, BR
Pedro Bertemes Filho	Universidade do Estado de Santa Catarina, BR
Pedro Gewehr	Universidade Tecnológica Federal do Paraná, BR
Pedro Moisés de Sousa	Universidade Federal de Uberlândia, BR
Pedro Xavier de Oliveira	Universidade Estadual de Campinas, BR
Rafael Sanchotene Silva	Universidade Federal de Santa Catarina, BR
Raimes Moraes	Universidade Federal de Santa Catarina, BR
Raul Guedert	Universidade Federal de Santa Catarina, BR
Renata Coelho Borges	Universidade Tecnológica Federal do Paraná, BR
Renato de Araujo	Universidade Federal de Pernambuco, BR
Renato Naville Watanabe	Universidade Federal do ABC, BR
Ricardo Borsoi	University of Lorraine, FR
Ricardo Ruggeri	Autoridad Regulatoria Nuclear, AR
Ricardo Suyama	Universidade Federal do ABC, BR
Roberto Sagaró Zamora	Universidad de Oriente, CU
Rocio Belén Buenamaizón	Universidad Nacional de San Juan, AR
Rodolfo Dias Correia	Hospital das Clínicas de Ribeirão Preto, BR
Rodrigo Gomide	Instituto Federal Goiano, BR
Rodrigo Pinto Lemos	Universidade Federal de Goiás, BR
Rodrigo Santos	Universidade Federal de Juiz de Fora, BR
Rodrigo Varejão Andreão	Instituto Federal do Espírito Santo, BR
Roger Gomes Tavares de Mello	Universidade Federal do Rio de Janeiro, BR
Ronni Amorim	Universidade de Brasília, BR
Rosa Itzel Flores	Universidad Autonoma de Mexico - Iztapalapa, MX
Rosangela Jakubiak	Universidade Tecnológica Federal do Paraná, BR
Rossana Rivas Tarazona	Pontificia Universidad Catolica del Peru, PE
Rubén Acevedo	Universidad Nacional de Entre Ríos, AR
Sandra Cossul	Universidade Federal de Santa Catarina, BR
Sandra Rocha Nava	Universidad La Salle, CO
Sara Rosa de Sousa Andrade	Faculdades Estácio de Sá, BR
Sérgio Francisco Pichorim	Universidade Tecnológica Federal do Paraná, BR
Sergio Furuie	Universidade de São Paulo, BR
Sergio Ioshii	Pontificia Universidade Católica do Paraná, BR
Sheila da Luz Schreider	Universidade Federal do Espírito Santo, BR
Shirley Quintero	Escuela de Ingenieros, CO

Silas Moreira de Lima	Universidade Federal de São João Del-Rei, BR
Silvia Rodrigo	Universidad Nacional de San Juan, AR
Suélia Rodrigues Fleury	Universidade de Brasília, BR
Suelia Rosa	Universidade de Brasília, BR
Sylvia Faria	Universidade de Brasília, BR
Sylvia Pires	Universidade Federal de São João Del-Rei, BR
Tatiane Ramalho	Universidade Federal de São Paulo, BR
Tenysson W. Lemos	Universidade de São Paulo, BR
Teodiano Bastos Filho	Universidade Federal do Espírito Santo, BR
Thaína Aparecida Azevedo Tosta	Universidade Federal de São Paulo, BR
Thais Winkert	Universidade Federal de Rio de Janeiro, BR
Thomaz Botelho	Instituto Federal do Espírito Santo, BR
Vanessa Pereira Gomes	Instituto de Pesquisas Tecnológicas, BR
Vesna Zeljkovic	Lincoln University, UK
Victor Diego Cupertino Costa	Universidade Federal de São João Del-Rei, BR
Victor Hugo C de Albuquerque	Universidade Federal do Ceará, BR
Victor Luciano Carmona Viglianco	Universidad Nacional de San Juan, AR
Wally Auf der Strasse	Colégio Militar de Curitiba, BR
Wellington Pinheiro Dos Santos	Universidade Federal de Pernambuco, BR
Wemerson Parreira	Universidade do Vale do Itajaí, BR
Willian Bispo	Universidade Estadual de Londrina, BR
Yann Morère	Université de Lorraine, FR
Yolanda Torres Perez	Universidad Pedagógica y Tecnológica, CO

Sponsoring Institutions



CORAL: Consejo Regional de Ingeniería
Biomédica para América Latina
www.coralbiomedica.org

SBEB: Sociedade Brasileira de Engenharia
Biomédica
www.sbeb.org.br

IFMBE: International Federation of Medical and
Biological Engineering
www.ifmbe.org



UFSC: Universidade Federal de Santa Catarina
www.ufsc.br



IEB-UFSC: Instituto de Engenharia Biomédica da UFSC
www.ieb.ufsc.br



FAPESC: Fundação de Amparo à Pesquisa e Inovação do Estado de Santa Catarina
www.fapesc.sc.gov.br

Contents

Clinical Engineering and Health Technology Assessment

Importance of the Department of Biomedical Engineering in the Conversion of a High Specialty Hospital to a COVID-Hospital	3
<i>A. B. Pimentel-Aguilar, R. Rodríguez-Vera, and M. R. Ortiz-Posadas</i>	
Ventilatory Support Associated with Extubation Success in Preterm Infants Can Reduce the Hospitalization Days	14
<i>Hellen Hillary Oliva, Adriane Muller Nakato, Paula Karina Hembercker, Débora de Fátima Camillo Ribeiro, Maria Eduarda Rossari Porto, and Percy Nohama</i>	
Analysis of the Causes of Failures in a Dental Unit in Primary Health Care	23
<i>Mariana Ribeiro Brandão, Jonas Maciel, Juliano Martins, and Renato Garcia Ojeda</i>	
Principal Components and Neural Networks Based Linear Regression to Determine Biomedical Equipment Maintenance Cost in the Peruvian Social Security Health System	31
<i>E. Toledo, C. de la Cruz, and C. Mamani</i>	
Study of Technical Productivity as a Tool for the Development of the IPS Universitaria Infrastructure Master Plan	43
<i>Lucía Uribe-Herrera, Mabel Zapata-Álvarez, Óscar Saldarriaga-Saldarriaga, Juan Barreneche-Ospina, Javier García-Ramos, Daniela Cardona-Alzate, and Juan Manuel-Galeano</i>	
EPID-Based Patient-Specific Quality Assurance in VMAT Radiation Therapy Using Split Arcs	55
<i>William Correia Trinca and Ana Maria Marques da Silva</i>	
Clinical Decision Support System to Managing Beds in ICU	67
<i>Edgar D. Báez, Sofia J. Vallejos, and Maria I. Pisarello</i>	
Development of Best Practices Virtual Resources to Assist in the Safe Use of Health Technologies in an Interdisciplinary Ecosystem	78
<i>Mariana Ribeiro Brandão and Renato Garcia Ojeda</i>	

Use of a HAPI FHIR Server and Development of a Multi-user Web Interface for Visualization and Analysis of Data from Patients with Diabetes Mellitus	88
<i>Maicon Francisco and Jefferson Luiz Brum Marques</i>	
Analysis of Failure Causes in the Mammography Machines	98
<i>Indira Hernandez-Contreras and Fabiola M. Martinez-Licona</i>	
An Overview of the Postgraduate Courses in Clinical Engineering Offered in Brazil	107
<i>N. C. B. L. Koch, A. P. Romani, T. R. Oliveira, and H. Tanaka</i>	
Features of Computerized Systems for the Management of Medical-Hospital Equipment in Clinical Engineering Departments in Brazil	118
<i>Perseu Filho Rosa and Frieda Saicla Barros</i>	
Investigation of Probable Causes of Patient Damage in the Multifactorial Environment of Adverse Events: Analysis of Adverse Event Notifications for Pulmonary Ventilator	128
<i>Alexandre Holzbach Júnior, Mariana Ribeiro Brandão, and Renato Garcia Ojeda</i>	
Analysis of Maintenance Events in Medical Equipment in the Largest Trauma Hospital in Natal/RN	139
<i>Lyssandra Paz, Lucas Moura, Tiago Barreto, Marcelo Lima, and Alice Suassuna</i>	
Indexes for Health Technology Assessment Two Case Studies: Computer Tomography Scan and Linear Accelerator	150
<i>L. Guzmán-Canizales, J. A. Lozano-Suárez, and M. R. Ortiz-Posadas</i>	
A Proposed Model for Calculate the Number of Mammography Machines for the South-West Area of Mexico	163
<i>Fabiola M. Martinez-Licona and Cipactli M. Martinez-Vazquez</i>	
Productivity Index Applied to Clinical Engineering	174
<i>D. N. Araújo and J. W. M. Bassani</i>	
Reliability Analysis Techniques Applied to Highly Complex Medical Equipment Maintenance	184
<i>M. C. C. Rezende, R. P. Santos, F. C. Coelli, and R. M. V. R. Almeida</i>	

Health Technology, Innovation and Development

- Multi-platform Mobile Application for Elderly Care Management 195
*R. S. Navarro, R. K. Chagas, A. Baptista, L. A. M. Pereira,
 and S. C. Nunez*
- Comparative Study of Therapeutic Ultrasound and Copaiba Oil
 Phonophoresis Therapies for Shoulder Tendinitis 203
*J. P. S. Martins, A. B. Fernandes, R. A. Lazo-Osório, L. P. Alves,
 A. B. Villaverde, and C. J. de Lima*
- Home Dental Whitening: Preliminary Clinical Study of the Technique
 and Patients' Perception 212
A. Baptista, L. H. V. Dantas, R. S. Navarro, A. Pinto, and S. C. Nunez
- Experimental Determination of Vascular Pulsatility During
 Continuous-Flow LVAD Assistance 219
Marcelo Mazzetto, Daniel S. Torres, Simão Bacht, and Idágene A. Cestari
- Augmented Reality for Gait Rehabilitation: A Scoping Review 228
Laís Souza Amorim and Alana Elza Fontes Da Gama
- IoT System for Elbow Angle Assessment Applied to Orthosis Device 241
Beatriz Cunha, Jean Schmith, and Rodrigo Marques de Figueiredo
- Analysis of the Exposure of PLA Surfaces to Ozone Gas, Ozonated Water,
 and Ultraviolet Radiation, Preliminary Evaluation 253
*M. C. O. Carvalho, F. T. C. S. Balbina, L. L. Azevedo, G. V. Schmitz,
 A. B. Fernandes, and C. J. Lima*
- Therapeutic Approaches in the Sequence of Pierre Robin: A Systematic
 Review of the Literature 263
*J. E. P. Nunes, R. S. Navarro, M. S. A. Mota, B. P. Santos, G. P. Nunes,
 and N. A. Parizotto*
- Cardiopulmonary Exercise Testing Data Processing and Storage Tools 273
*G. B. Penteado, V. R. Uemoto, F. C. Araujo, R. D. D. Buchler,
 C. A. C. Hossri, R. S. Meneghelo, R. V. Freitas, R. A. Hortegal,
 and H. T. Moriya*
- Application for Mobile Devices to Measure Daily Protein Intake
 in the Elderly: PROT + First Results 281
*F. C. D. Silva, A. P. S. Martins, F. C. D. F.C.D.Silva, L. E. Simonato,
 and D. S. F. Magalhães*

Qualitative Analysis of Different Formulations of Losartan Potassium Using Raman Spectroscopy	285
<i>T. R. O. Heinzlmann, C. J. Lima, H. C. Carvalho, A. B. Fernanades, and L. Silveira</i>	
Application Development for Canine Hearing Monitoring	294
<i>R. S. Navarro, D. C. L. Martins, A. Baptista, L. A. M. Pereira, and S. C. Nunez</i>	
Design of Technical Support for Stand-Up	302
<i>Y. J. Fonseca, R. A. Espinosa, and M. E. Lambertinez</i>	
Use of Ozonized Oil in Chronic Wounds of Lower Limbs: Preliminary Results	309
<i>T. K. Serra, L. Dos Santos, L. Assis, J. C. Tarocco, P. C. O. Z. Pimente, and C. Tim</i>	
COVIData: A Web Platform for Tracking, Classification and Monitoring Cases Suspects of COVID-19	317
<i>Beatriz L. Gandolfi, Clarissa S. R. Merino, Vitor I. da Silva, Diego S. Costa, Gabriel de M. Fiali, André S. Carvalheiro, Luiz R. C. da Silva, Camila C. Rocha, Giovanna B. Lins, Saul C. Leite, and Fernanda N. Almeida</i>	
Mechanical Ventilator and Oxygen Concentrator System: Tinki's Proof of Concept	328
<i>Pierol Quispe, Daniela Gómez-Alzate, and Sandra Pérez-Buitrago</i>	
Optimized Performance Pulse Oximeter Based on the MAX30102 Commercial Sensor	338
<i>Ricardo Cebada-Fuentes, José Valladares-Pérez, José Antonio García-García, and Celia Sánchez-Pérez</i>	
Antimicrobial Photodynamic Therapy with Methylene Blue and Urea in <i>Escherichia Coli</i> and <i>Staphylococcus Aureus</i>	349
<i>P. I. B. P. Silva, M. A. K. Saleh, A. Baptista, D. Honorato, S. Campos, S. C. Nunez, and R. S. Navarro</i>	
360 Immersion System: A Work at Height Safety Training Experience with Physiological Monitoring	357
<i>Guilherme Agnolin, Maira Mieko Botome, Bruno Pires Bastos, Lazaro Ismael Hardy Llins, Bruno Garcia da Rocha, and Marcela Purificação</i>	

Metrology and Quality of Healthcare Technologies

Mass Estimation in Body Photography for Obesity Assessment Using Deep Learning and Linear Regression 369
Alexandre G. Silva, Lucas N. Ziza, Rangel Arthur, and Franklin C. Flores

Development of a Neonatal Lung Simulator with Variable Compliance 380
S. G. Mello, A. E. Lino-Alvarado, G. D. Valério, C. A. Estevam, M. S. Dias, K. N. Barros, A. F. G. Ferreira Junior, and H. T. Moriya

Typical Values in Digital Mammography Within the Framework of Diagnostic Reference Levels 386
J. V. Real and A. L. M. C. Malthez

Metrological Conformity Assessment of Pulmonary Ventilators During the Covid-19 Pandemic in Brazil 395
Benedito Vital Ribeiro Junior, Henrique Alves de Amorim, Matheus Cardoso Moraes, and Thiago Martini Pereira

Influence of Phototype, Sweating and Moisturizing Lotions on Human Skin Emissivity: A Possible Cause of Screening Errors of Feverish People in Sanitary Barriers 403
Andriele Ninke, João Thomaz Lemos, Pablo Rodrigues Muniz, Reginaldo Barbosa Nunes, Hércules Lázaro Morais Campos, and Josemar Simão

Assessing the Quality of Behavioral Data Obtained by Human Observers Using Cohen’s Kappa and Accessory Metrics: Development of the Algorithms and an Open-Source Library 413
João Antônio Marcolan, Jefferson Luiz Brum Marques, and José Marino-Neto

Assessment of Lung Ventilators’ Pressure Alarms System in a Controlled Scenario 424
S. G. Mello, A. E. Lino-Alvarado, R. L. Vitorasso, D. A. O. Rosa, M. H. G. Lopes, A. F. G. Ferreira Junior, and H. T. Moriya

Maternal Near Miss in the State of Rio Grande Do Norte (Brazil) Between 2003 to 2019: A Preliminary Analysis of Identification and Monitoring 431
T. S. Rêgo, S. P. Silva, D. V. Vieira, R. A. O. Freitas-Júnior, and A. C. Rodrigues





Radiation Dose Optimization for Contrast-Free Adult Skull CT Protocol 439
F. N. Torres, J. V. Real, and A. M. Malthez

Author Index 449

Clinical Engineering and Health Technology Assessment



Importance of the Department of Biomedical Engineering in the Conversion of a High Specialty Hospital to a COVID-Hospital

A. B. Pimentel-Aguilar¹ , R. Rodríguez-Vera¹ , and M. R. Ortiz-Posadas²  

¹ Biomedical Engineering Department, National Institute of Respiratory Diseases, Mexico City, Mexico

² Electrical Engineering Department, Universidad Autónoma Metropolitana Iztapalapa, Mexico City, Mexico

posa@xanum.uam.mx

Abstract. The National Institute of Respiratory Diseases (INER, its Acronym in Spanish) is a Mexican tertiary-care-hospital specialized in respiratory diseases. On February 27, 2020, the first case of COVID-19 in Mexico was confirmed at the INER. As of this date, the Institute began its conversion process to a COVID hospital. The challenge was to achieve the maximum capacity of 250 beds for the care of critical patients and turn the Institute into a 100% COVID hospital, becoming the largest Intensive Care Unit in the country. The participation of the Department of Biomedical Engineering (DBE) in this process was crucial; since it re-engineered a set of processes related to the planning, installation, training, use and management, maintenance and performance of medical technology. The DBE defined the technological and logistical changes to increase the capacity for intensive care in each of the clinical areas. It evaluated aspects related to infrastructure, supply of medicinal gases and medical equipment; particularly ventilators, which were the most demanded equipment for the care of COVID patients. This paper presents the process of converting the INER to a COVID-Hospital accompanied by the functions performed by the Biomedical Engineering Department in said process.

Keywords: Biomedical Engineering Department · COVID-Hospital · National Institute of Respiratory Diseases

1 Introduction

The National Institute of Respiratory Diseases (INER, its Acronym in Spanish) is a tertiary-care-hospital specialized in respiratory diseases. Its primary objectives are scientific research, the formation and training of qualified human resources as well as the provision of highly specialized medical care services in respiratory system diseases throughout the Mexican territory. The INER is the main institution in Mexico that treats respiratory diseases such as tuberculosis, Chronic Obstructive Pulmonary Disease (COPD), lung cancer, asthma, interstitial diseases and other diseases of the upper airway through specialists in Otorhinolaryngology [1].

On January 7, 2020, Chinese health authorities reported that a new coronavirus (SARS-CoV2) had been identified as a possible origin of the COVID-19 disease. On February 27, 2020, the first case of COVID-19 in Mexico was confirmed and it was treated at the INER [2]. As of this date, the Mexican Government mandated the Institute begin its hospital reconversion process, following the guidelines for the implementation of temporary COVID-19 care centers and mobile hospitals, whose objective is to establish the technical foundations necessary for the care of patients with COVID. To contribute in a comprehensive and timely response to the provision of health services for the population infected by SARS-COV-2 with criteria based on the quality and safety of patient care, with respect to the rights human beings and with a focus on the preservation of life, the well-being of people and mental health [3, 4].

It is through this undertaking that the Department of Biomedical Engineering (DBE) participated in the reengineering of processes related to planning, installation, training, use and management, maintenance and optimal functionality of medical technology. This paper presents the activities subscribed for converting the INER to a COVID-Hospital and the functions performed by the DBE in this process.

2 Background (Before COVID-19)

On April 24, 2020, the Government of Mexico City decreed the INER to become a COVID-Hospital. The challenges were to achieve the conversion of beds with all the infrastructure and equipment for the care of COVID patients, reach the maximum capacity of 250 beds for the care of patients in critical condition due to SARS-CoV2, refer patients with other pneumological and otorhinolaryngology diseases (non-covid patients) to other hospitals and, convert the Institute into a 100% COVID-Hospital. It would become the largest Intensive Care Unit in the country.

2.1 Department of Biomedical Engineering

In order to increase the physical and technical capacity of intensive care, the Biomedical Engineering Department (DBE) defined the medical technology, healthcare facilities and logistical changes in each of the clinical areas of the Institute. The DBE considered the following aspects: infrastructure, supply of medicinal gases, and medical equipment, in particular those related to ventilatory support; monitoring, and diagnostic imaging, since these were the highest demanded equipment in relation to the care of COVID patients [5]. The DBE is a member of the Infection Prevention and Control Committee as well as the Biosafety Committee, which is why it was also involved in cleaning and disinfection protocols, both for medical technology and for the physical spaces of the Institute's clinical areas.

2.2 Infrastructure

The Institute has a horizontal architecture distributed in six independent buildings corresponding to different clinical services, which facilitated the conversion and adaptation of the hospital's infrastructure. The fourteen clinical areas and the total distribution of the 250 beds is shown in Table 1.

Table 1. Clinical areas and distribution of the 250 beds.

Clinical Area	Beds
Clinical Service 1. Interstitial diseases (CS1)	28
Clinical Service 2. Tuberculosis (CS2)	28
Clinical Service 3. Oncology (CS3)	30
Clinical Service 4. Pneumology (CS4)	27
Clinical Service 5. COPD (CS5)	29
Clinical Service 6. Pharmacological Research (CS6)	10
Surgery Unit (UQX)	4
Recovery of Surgery (REC)	20
Intensive Care Unit (ICU)	15
Otolaryngology (ORL)	12
Pneumopediatrics (UNP)	29
Emergency Room (ER)	18
Total	250

2.3 Medicinal Gases

The Institute had 250 hospital beds with medical gas intakes distributed in clinical areas as shown in Table 2. Note that, despite having the capacity to supply medical gases, a ventilator was not available in all cases. For example, in Clinical Service 1. Interstitial Diseases, there are 28 beds with intakes, but only eight have an associated ventilator; while critical areas (Intensive Care Unit (ICU), Surgery Unit (UQX) and Emergency Room (ER)) have a ventilator for each oxygen intake.

2.4 Mechanical Ventilators

At the end of 2019 the Institute had 66 ventilators and 113 vital sign monitors available. Of the total, six ventilators (9%) were over 15 years old; 46 ventilators (70%) were between 15 and 10 years of age; nine ventilators (14%) had an antiquity between 10 and 5 years; and five ventilators (7%) less than five years (Table 3). The largest number of ventilators acquired coincides with the declaration of the H1N1/09 virus pandemic in Mexico in 2009. Regarding the vital signs monitors, there were 113 devices of which 22 (20%) presented functional problems due to deterioration as a result of their intensive use.

3 Reconversion Covid Hospital (Results)

3.1 Department of Biomedical Engineering

The reconversion to a COVID-Hospital required a vast quantity of human, material and financial resources. The Institute hired more medical and paramedical personnel. To meet the permanent high demand for medical services, work shifts were increased in the

Table 2. Medicinal intakes and oxygen consumption per ventilator in the clinical areas of INER, prior to conversion.

Clinical service	Gas intake	Intake+V	%Beds+V	O ₂ consumption (L/min)	
				For V	Total for intake+V
CS1	28	8	29	60	480
CS2	28	8	29	60	480
CS3	30	10	33	60	600
CS4	27	15	56	60	900
CS5	29	10	34	60	600
CS6	10	10	100	60	600
UQX	4	6	100	60	360
REC	20	10	50	60	600
ICU	15	15	100	60	900
ORL	12	4	33	60	240
UNP	29	13	45	60	780
ER	18	18	100	60	1080
Total	250	127	50.8		7,620

clinical areas, respiratory therapy, radiology and biomedical engineering. The hospital staff increased 60% and in the specific case of the Department of Biomedical Engineering (DBE), the staff increased by 300%. Since prior to the conversion there were only six biomedical engineers and, 18 additional ones were hired to cover all hospital operating shifts (Table 4). This growth derived from the great demand of technical support required for the optimal functionality of medical technology, since all the hospital beds were converted to intensive care beds. The DBE collaborated with the medical area in order to identify the medical equipment needed for the care of COVID patients in critical condition. The technological capacity increased globally by 119%. Equipment such as: infusion pumps, beds, stretchers, electrocardiographs, X-ray equipment, immunology analyzers, blood gas analyzers, bariatric lifts, hemodialysis machines, vital signs monitors, deep freezers, refrigerators, ultrasounds, video laryngoscopes and ventilators were acquired.

Each of the hospital beds was equipped with monitoring, ventilation, electrocardiography and drug infusion devices. The increase in the amount of medical equipment for the care of critical patients due to SARS-CoV2 is shown in Table 5. In some types of medical equipment, such as ventilators, monitors and beds, it was possible to have a surplus that provided a technological reserve for the hospital.

Due to the increase in the technological capacity, the personnel and the medical services of the Institute, the DBE also increased and modified the technical service routines. In order to promptly detect operating problems in both, the critical equipment and in the medical gas supply. Continuous tours were implemented during all work shifts.

Table 3. Number of mechanical ventilators and monitors available at INER in 2019

Purchase year	Number of ventilators	Number of monitors	Antiquity
1998	1		22
1999		1	21
2001	1		19
2002	1		18
2003	1	2	17
2005	2	3	15
2006	3	2	14
2007	6	9	13
2008	1	4	12
2009	35	14	11
2010	1	8	10
2011	3	6	9
2012	1	4	8
2013	5	21	7
2014		31	6
2015	2		5
2016	3	2	4
2018		6	2
Total	66	113	

Table 4. Distribution of Biomedical Engineering staff in shifts

Shift	M	E	N _A	N _B	D _W	N _W	Total
Pre-Conversion	6	0	0	0	0	0	6
Post-Conversion	7	5	3	3	4	2	24

M. Morning
E. Evening

N_A Night A
N_B Nigh B

D_W Day weekend
N_W Night Weekend

Preventive maintenance was advanced before the Hospital conversion, and a calendar of preventive services based on the surplus of medical equipment was programmed on a rotating basis, so as not to deter from bed care.

On the other hand, the DBE participated in the development of protocols for the disinfection of medical devices and clinical areas in conjunction with the Hospital Epidemiological Surveillance Unit (UVEH). It also developed the methodology for the internal and external cleaning of medical equipment, and medium and high level disinfection. It trained workers, internal technical staff and suppliers in the use of personal

protective equipment (PPE). A biological safety strategy was carried out in the maintenance of medical equipment and its accessories, as well as the safe disposal of its consumables.

Table 5. Growth of medical equipment to attention of COVID19 critical patients.

Medical equipment	Before	After	Growth
Video-laryngoscopes	0	14	
Mechanical ventilators	66	240	264%
Ultrasound	6	19	217%
Hemodialysis machines	2	6	200%
Vital Signs Monitor	113	324	187%
Portable X-rays	4	11	175%
Gasometer	4	11	175%
Infusion pumps	650	1400	115%
Electrocardiograph	17	30	76%
Hospital beds	230	314	37%
Defibrillators	50	51	2%
Total	1142	2499	119%

Regarding the processes of acquisition, delivery and installation of new medical equipment, execution times had to be shortened due to the urgency of requiring immediate equipment for intensive care beds. In this sense, the installation and operation tests of the medical equipment, as well as training of the user personnel had to be carried out in parallel and in compliance with the biosafety protocols in the corresponding clinical areas.

3.2 Medicinal Gases

In order to have a homogeneous distribution of constant gas supply (without saturation in critical points of the network) the pneumatic load of the medical gas supply network (oxygen and medical air) was distributed in the critical areas: ICU, UQX and ER in addition to inpatient clinical services in the first stage of conversion.

Initially, a physical separation of the hospitalization areas was made to distribute and separate the supply lines in each clinical service. The supply lines were changed, the electrical capacity of each building was adapted, and the spaces were distributed to ensure the safe accommodation of medical equipment and furniture.

Using an oxygen and nitrogen mixing system in proportions of 21% and 79% respectively, synthetic air (free of moisture and particles) was supplied to the clinical areas. Simultaneous pneumatic support was guaranteed for 100 mechanical ventilators with a safety margin of at least 10%. In an extreme case, the maximum gas capacity would

allow feeding at least 10 additional ventilators; considering a consumption average of 3,600 L per hour. The synthetic air production capacity is limited to a production of up to 480,000 l/h. The oxygen is limited by the storage capacity of up to 6,500 gallons of liquid oxygen. This allows for the use of 100 ventilators for 48 continuous hours without recharging gas. However, a five-hour backup was also envisaged in the event of a main supply system failure.

In the second stage of conversion—named “Magna Hospital Reconversion” by the Mexican government, the medical gas supply network was divided into three blocks, each with its own gas supply plant. This division guaranteed the pneumatic oxygen and air support for 200 ventilators to its maximum capacity. Out of the three plants supplying medicinal gases, one already existed prior to the first stage of conversion; subsequently, two more with mobile oxygen units and medical grade compressors were implemented. Table 6 shows the distribution of the oxygen and medical air supply network into these three blocks of hospital services that ensured an adequate supply of medicinal gases for each clinical service.

Table 6. Segmentation of the medical oxygen and air supply network into three blocks of hospital services.

Block	Clinical service	Beds	Beds + V 1 st stage	Beds + V Magna R	Total Beds + V per block
Block 1	SC1	28	6	20	82
	SC2	28	6	20	
	SC3	30	8	22	
	SC4	27	13	20	
Block 2	SC5	29	8	20	77
	SC6	10	8	10	
	UQX	4	4	4	
	REC	20	10	16	
	UCI	15	15	15	
	ORL	12	4	12	
Block 3	UNP	29	13	21	41
	URG	18	15	20	
Total		250	110	200	200

3.3 Mechanical Ventilators

Owing to the fact that the most demanded medical equipment in critical areas was the mechanical ventilator, another very important area for the reconversion of the Institute

was Respiratory Therapy. The availability of this equipment and the control of the consumption of its accessories were essential to guarantee the safety of the patients who required ventilatory support.

Throughout 2020, the Institute bought eleven mechanical ventilators, borrowed 25 and received 138 more ventilators in donation. This raised the ventilatory support capacity by 264% with 240 available ventilators. The existing and newly acquired ventilators are of four types: basic pneumatic (BN), non-invasive (NI), volumetric (VL) and volumetric transfer (VT); distributed in 13 different brands (Table 7). Note that most of the devices (200) are volumetric ventilators, followed by transfer ventilators with 24, twelve basic pneumatic ventilators, and four non-invasive ventilators. In relation to brands, four dominate: the M7 brand totaling 96 devices; the M1 brand with 35; the M12 with 26 and the M4 and M13 brands with 20 ventilators each. The rest of the ventilators (43) are distributed among the nine remaining brands.

The variety of ventilators and brands forced the DBE to oversee the control of accessories and consumables. The design of training and the qualification of technical staff in maintenance procedures, along with the modification and/or updating of preventive maintenance routines adhering to the corresponding calendar. Likewise, respiratory therapy technicians were trained in the use and management of the new ventilators, as well as to keep a record of adverse events derived from the use of a wide variety of equipment.

Table 7. Ventilators available after COVID19 Hospital conversion

Brand	NB	NI	VL	VT	Total
M1	12		23		35
M2		4			4
M3			1		1
M4			20		20
M5			5		5
M6			12	5	17
M7			80	16	96
M8			2	1	3
M9			4		4
M10			6	1	7
M11			2		2
M12			25	1	26
M13			20		20
Total	12	4	200	24	240

3.4 Disinfection Procedures

Other relevant tasks for the reconversion of the Institute included control of infections associated with health care, and scouting of appropriate technologies to carry out the disinfection processes of physical spaces. The DBE worked in conjunction with the Institutional Biosafety Committee to learn about the disinfection protocols for the safe handling of medical equipment, so as to help reduce the risk of cross-infection between patients. Some of the protocols that the DBE participates in are described below:

- Cleaning surfaces by mechanically removing organic matter in equipment and accessories.
- Medium level disinfection by high pressure biphasic mixture spraying of areas including furniture and biomedical equipment.
- Application of a high-level disinfectant using a bactericidal and bacteriostatic film.
- High level disinfection using hydrogen peroxide vapor methods or Ultraviolet-C (UV-C) light irradiation. Evaluation of the effectiveness of the high-level disinfection process (HLD) using surface and environmental (air) cultures.

It is important to mention that the application of the HLD techniques were carried out only in the event that the patient was occupied the bed presented some drug or multidrug resistant bacteria, or in the case of empty clinical services. The selection of the HLD protocol by hydrogen peroxide, or by UV-C irradiation was determined for the emergency services or for the “Field Hospital” (described below) due to its characteristics of being an open space.

4 Covid Hospital Magna Reconversion (Results)

The work of the Department of Biomedical Engineering consisted of planning, implementing and evaluating the hospital reconversion of the Institute in relation to medical technology, medicinal gases and the critical infrastructure. The objective was to increase the physical and technical capacity of the ICU, expanding the intensive care beds to a maximum care capacity of 250 patients in critical condition.

This stage was consolidated with the installation of a Field Hospital, donated by the Mexican Red Cross, with a capacity of 50 additional beds, of which 30 were enabled for the intensive care of COVID patients. Said hospital was installed in the parking lot next to the Emergency Room and was made up of five tents for medical care, with beds designed to provide intensive care. Furthermore, it required the design and installation of an air conditioning system with filters of High Efficiency Protection Air (HEPA) to ensure a safe environment. Additionally, ambient temperatures were controlled and monitored to ensure the correct functionality of equipment and comfortability of the units. A continuous air and oxygen distribution network was implemented to enable the continuous supply of airflow; assure safe ranges of ventilation and aspiration of patients, as well as the installation, training, operational tests and commissioning of medical equipment.

The supply of medicinal gases was guaranteed and distributed in a total of 250 beds throughout the Institute. This considered 230 beds available for use with a mechanical ventilator and 20 additional beds with low oxygen requirement as nasal tips (Table 8).

Note that in the first stage of the reconversion (R_{1st}) the supply was expanded from 15 to 110 intensive care beds (44%), and in the “Magna Reconversion” (MR) 200 beds (80%) were completed. These were distributed in the three blocks defined: 82, 77 and 41 respectively. Additionally, the “Magna Reconversion” was completed with more than 30 beds of the Field Hospital.

In this way, the largest Intensive Care Unit in Mexico was created, reaching a capacity of 250 beds equipped with the infrastructure requirements, medical equipment and paramedical personnel for the care of critical COVID patients.

Table 8. Total facilities provide by the COVID Hospital Magna Reconversion at the National Institute of Respiratory Diseases from Mexico.

Clinical area	Beds (B)	B+V (R_{1st})	B+V (MR)	%(B+V) By block
Block 1	113	33	82	36%
Block 2	90	49	77	33%
Block 3	47	28	41	18%
INER	250	110	200	87%
Red Cross (Field Hospital)	30	0	30	13%
Total capacity	280	110	230	100%

5 Conclusion

The National Institute of Respiratory Diseases (INER) has treated 5,746 critically ill patients with SARS-CoV2 and other coronaviruses. As of February 27, 2020, when the first case was presented in Mexico, the INER treated a monthly average of 60% of patients with ventilatory support. The installed infrastructure has sustained solid care of critically ill patients during the 15 months of pandemic—even in the maximum occupancy in which 200 hospitalized patients were treated, out of which 185 required mechanical ventilatory support. Likewise, the Field Hospital for emergency room care, was reconfigured into a unit for the care of critically ill patients and infectious diseases, thus complementing the Institute’s health care capacity.

The planning and execution of the growth of the Institute’s infrastructure carried out by the BDE for the “Magna Reconversion”, mandated by the Government of Mexico, has correctly covered the care of critically ill patients, placing the INER as the health institution with the highest intensive care capacity in the history of the country.

For all the above, the Department of Biomedical Engineering has become a fundamental piece in regard to the decision-making of all processes that concern medical technology in the National Institute of Respiratory Diseases.







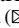
Acknowledgment. The authors of this paper greatly thank each of the members of the Department of Biomedical Engineering (DBE) who participated in this huge labor, for their effort, strength and dedication to carry out their activities inside and outside the COVID areas. We also extend our thanks to the INER authorities who fully trusted in the capacity of our DBE to contribute towards the “Magna Reconversion” of the Institute.

References

1. National Institute of Respiratory Diseases: Specific Organization Manual for the National Institute of Respiratory Diseases Ismael Cosío Villegas. Ministry of Health, Mexico (2016). http://iner.salud.gob.mx/descargas/normatecainterna/MOdirgeneral/MO_INER_2016-2.pdf
2. Suárez, V., Suárez Quezada, M., Oros Ruiz, S., Ronquillo De Jesús, E.: Epidemiology of COVID-19 in Mexico: from the 27th of February to the 30th of April 2020. *Rev. Clin. Esp.* **220**(8), 463–471 (2020). (in Spanish)
3. Mexican Health Ministry: Hospital reconversion guidelines (2020). <https://coronavirus.gob.mx/wp-content/uploads/2020/04/Documentos-Lineamientos-Reconversion-Hospitalaria.pdf>. (in Spanish). Accessed 15 Apr 2021
4. Mexican Health Ministry: Guidelines for the implementation of COVID-19 temporary care centers and Mobile Hospitals (2020). https://coronavirus.gob.mx/wp-content/uploads/2020/04/Lineamientos_Centros_Atencion_Temporal.pdf. (in Spanish). Accessed 15 Apr 2021
5. World Health Organization: Priority medical devices list for the COVID-19 response and associated technical specifications (2020). <https://www.who.int/publications/i/item/WHO-2019-nCoV-MedDev-TS-O2T.V2>. (in Spanish). Accessed 15 Apr 2021



Ventilatory Support Associated with Extubation Success in Preterm Infants Can Reduce the Hospitalization Days

Hellen Hillary Oliva¹ , Adriane Muller Nakato¹ , Paula Karina Hembecker¹ ,
Débora de Fátima Camillo Ribeiro^{1,2} , Maria Eduarda Rossari Porto¹ ,
and Percy Nohama¹  

¹ Graduate Program on Health Technology, Pontifícia Universidade Católica do Paraná, Rua Imaculada Conceição, 1155, Curitiba, Paraná, Brazil
percy.nohama@pucpr.br

² Neonatal Services, Waldemar Monastier Hospital, Campo Largo, Paraná, Brazil

Abstract. In this research, we aimed to investigate the clinical, ventilatory and physiological characteristics associated with extubation and verify the days in ventilator support in premature infants. This retrospective study analyzes 102 medical records of preterm infants who needed invasive mechanical ventilation from the Neonatal Intensive Care Units between January 2018 and December 2020. Data were divided into extubation success (i.e., 72 h without the need for re-intubation) and failure groups. Clinical data, ventilatory parameters, and arterial blood gas data were analyzed and compared between groups. Differences were considered statistically significant if p-value <0.05. The number of days in ventilatory support was high in the failure group but without statistical significance. The noninvasive ventilation support was high (81.4%) and higher in extubation success group. The majority of the preterm infants had extubation success (80.6%). The frequency mandatory were significantly higher and the oxygen saturation smaller in the failure group ($p \leq 0.05$). The preterm infants that failed in the extubation process presented more respiratory instability, using higher pressure levels and mandatory frequency and higher days in hospitalization.

Keywords: Premature Infants · Mechanical Ventilation · Airway Extubation

1 Introduction

Invasive ventilatory support in preterm infants remains one of the highest evidence methods, especially in treating extreme preterms respiratory failure (<28 weeks) [1–3]. About 85% of the babies born at <30 weeks of gestational age are mechanically ventilated at some time during their stay in the NICU, and the Respiratory Distress Syndrome (RDS) is the leading cause of preterm infants mortality [1, 4]. Indications for mechanical ventilation in premature infants include cases of respiratory failure (characterized by a $\text{PaO}_2 < 50$ mmHg and a $\text{PaCO}_2 > 65$ mmHg), persistent pulmonary hypertension in

the newborn (PPHN), meconium aspiration syndrome (MAS), pneumonia and respiratory distress (ARDS), asphyxia, traumatic brain injury (TBI), spinal muscular atrophy, congenital diaphragmatic hernia, congenital heart disease or after thoracic surgery. The parameters to be adjusted in invasive mechanical ventilation will depend on the type of pathology and the respiratory and gasometric disorders found [5]. Although the type and duration of mechanical ventilatory support used in the first 48 h of life by preterm infants is critical [6]. The invasive mechanical ventilation (IMV) is crucial, prolonged use in very premature lungs can cause injuries due to exposure to high pressures, volumes, and oxygen. It contributes to the development of pneumonia, pneumothorax, and bronchopulmonary dysplasia (BPD) and, in addition, can provoke complications in the children's neuropsychomotor development process [7, 8].

It is essential to remove the IMV as soon as possible because it reduces early ventilator trauma and minimizes short and long-term complications [9].

Currently, the IMV weaning and extubation process is mainly based on clinical judgment and on factors that indicate the premature infants' capacity to maintain independent breathing, with hemodynamic stability, improved oxygenation, and the ventilation lung [9, 10]. Time of the weaning, criteria for extubation, and support after removal of IMV are different in several Neonatal Intensive Care Units (NICU) due to the lack of standardized guidelines [9, 11]. So, it becomes necessary to find predictive parameters that reduce the chances of extubation failure and, consequently, the reintubation.

Extubation failure is associated with greater respiratory instability in premature infants. Furthermore, the stress on the airways caused by the passage of the tube during the prolonged use of IMV and increased hospitalization time are characteristics associated with preterm infants who need reintubation [12]. Early extubation failure and reintubation requirement within 48 h may increase in 83% the risk of morbidity and mortality in preterm infants compared to those who did not need reintubation [13, 14]. Some of the main factors predisposing to extubation failure are low birth weight and low gestational age. Approximately 50% of preterm infants less than 28 weeks of gestation will fail in their first extubation attempt [15].

In addition, failure may occur due to airway obstructions such as spasms, edema, and secretions accumulation; the non-resolution of the primary pathology or other hospitalization caused pathology; inability of the respiratory muscles to perform contraction or prolonged time in IMV [12, 16–18].

Aiming to attend the requirement in finding the predictive parameters that allow the extubation success and, consequently, the reduction of the complications in a short and long time, this study describes clinical, ventilatory, and physiological characteristics of preterm infants associated with the extubation failure. It is important to highlight that the study about ventilatory support is relevant for biomedical engineering context, as it enables the innovation of ventilatory equipment, as well as the correct adjustments of ventilatory parameters.

2 Materials and Methods

We conducted a retrospective cohort study with preterm infants born at Waldemar Monastier Regional Children's Hospital, Paraná, Brazil, from January 2018 to December 2020. All data were obtained from medical records. The study was approved by the Ethics

Committee on Research with Human Beings of Universidade Federal do Paraná (ID 18296113.0.0000.0096).

All newborn infants admitted to the Neonatal Intensive Care Unit (NICU) with gestational age up to 36 weeks and 6 days, of both sexes, and who required invasive mechanical ventilation were included. The exclusion criteria consisted of neonates who died or were transferred to another hospital before an extubation attempt, or those who had missing or incomplete data regarding the extubation process. A total of one hundred and two neonates met eligibility criteria and were enrolled in our study.

A spreadsheet was developed to collect neonatal demographics (gestational age, gender, birth weight, Apgar scores at 1 and 5 min, type of delivery, presence of patent ductus arteriosus, retinopathy of prematurity and bronchopulmonary dysplasia, surfactant doses, length in IMV, mode of IMV, caffeine doses, successful or failed extubation, the reason for failure and whether noninvasive ventilation was used after extubation), maternal characteristics (age, mechanical ventilator settings (peak inspiratory pressure (PIP), support pressure (SP), mean airway pressure (MAP), exhaled tidal volume, positive end-expiratory pressure (PEEP), the fraction of inspired oxygen (FiO_2), mandatory frequency (Fmand), inspiratory time and arterial blood gas analysis (fraction of inspired oxygen (FiO_2)/partial pressure of arterial oxygen (PaO_2), oxygen saturation (SpO_2), the potential of hydrogen (pH), partial pressure of arterial carbon dioxide (PaCO_2), bicarbonate (HCO_3), base excess (BE)). Data entry was performed by one research assistant.

The parameters used to assess the possibility of extubation in the NICU corresponded to the newborn being hemodynamically stable, with PaCO_2 below 65 mmHg, SpO_2 above 85%, the FiO_2 below 30%, heart rate higher than 100 bpm, PIP lower than 20 mmHg and PEEP inferior to 7. Mechanical ventilators present in the NICU were from the Imbramed brand, namely the Inter V, Inter VII, and Inter Neo.

The primary outcome assessed was successful extubation, defined as no need for invasive ventilatory support for 72 h or more [9]. Immediately after extubation, the need to use noninvasive ventilatory support (NIV) was assessed according to the necessity of the baby, without a protocol. Preterm infants who remained on IMV for a long time or already had a history of extubation failure were chosen to use conventional CPAP. When had occurred a complication, the medical team opted for the bilevel or NPPV. After 2019, bubble-CPAP use in the NICU was started, being used more frequently than conventional CPAP.

Data were summarized using descriptive statistics. The assumption of normality was tested using the Kolmogorov-Smirnov test. We used chi-square tests or Fisher exact test to compare dichotomous outcome, and the appropriate parametric test (Student's t-test) or nonparametric test (Mann-Whitney U test) to compare continuous outcomes.

We used multivariate logistic regression model to estimate odds ratios and 95% confidence limits for the independent variables associated with failure extubation as the dependent variable. Variables found to have a statistically significant differences ($p < 0.05$) in the univariate analysis were entered into a backward logistic regression model with extubation failure. The level of significance was set at $p < 0.05$. Statistical analysis was performed using the Statistical Package for the Social Sciences, version 22.0 (SPSS Inc., Chicago, IL, USA).

3 Results

We analysed 102 medical records from infants who were intubated during their hospital stay and met our inclusion criteria. One hundred and two preterm infants were included in the final analysis, fifty-one (50.0%) were female. Their median GA was 30 weeks (IQR 29-33), and median birthweight was 1505 g (IQR 1055-2075). Extubation succeeded in 91 (89.2%) infants and failed in 11 (10.8%) (Table 1).

Infants in the failure extubation group were older and heavier at birth in comparison with the ones who succeed, but there were no significant differences between the two groups. The preterm infants who had successful extubation differed significantly in having more doses of surfactant compared with infants who failed ($p = 0.05$). We did not find any statistically significant differences in ventilatory settings and respiratory parameters at the time of extubation between the two groups, but it is important to mention that the success group remained for fewer days on MV compared to the failure group.

Univariate analysis revealed that extubation failure was associated with PIP (OR 1.30; IC95% 0.99–1.71; $p = 0.05$) and Fmand (OR 1.13; IC95% 1.00–1.27; $p = 0.04$). After adjustment for variables that were significant in our univariate analysis, no variable remained as a significant factor ($p < 0.05$) for extubation failure. Thus, an elevated PIP and Fmand can be related to extubation failure (Table 2).

4 Discussion

Predicting the ideal time for extubation in these preterm infants requires high diagnostic skills and clinical judgments because even with technological advances and new adjuvant therapies, such as the use of caffeine, administration of surfactant, and application of prenatal corticosteroids, there is still a lack of guidelines that can optimize and ensure an optimal weaning and extubation process [9, 19]. The newborn having a spontaneous respiratory rate that is adequate for the weight and age, there is no apnea or signs of respiratory effort, the vital signs are stable, as well as blood gas parameters, there is no need for sedation and $SpO_2 > 90\%$ are some criteria to be considered by the medical team at the time of extubation [5].

In our study, the most preterm infants had extubation successful (89.2%). Similar studies verified the relevance of the association between low birth weight and low gestational age to extubation failure, which the impairment of respiratory function can explain due to nutritional deficiency [17, 20–23]. Thus, it is demonstrated that preterm infants with greater weight and higher gestational age denote a higher incidence of successful extubation. However, according to the results found in our study, both birth weight and gestational age in the failure group were higher. While these data were not statistically significant, they can be explained by the sample's small number of preterm infants with low weight and gestational age, as shown by the respective medians of 1505 g and 30 weeks of gestational age.

The significant factors for extubation failure were the PIP ($p = 0.05$) and the Fmand ($p = 0.04$). In addition, an increase was found regarding the maximum inspiratory pressure and the mandatory frequency in the failure group. Another study also demonstrated significance in the PIP value, demonstrating that the failure group required a high inspiratory pressure compared to the successful group [19]. Although there was no statistical

Table 1. Demographic characteristics, ventilatory support parameters and blood gas measurements of preterm infants who had successful or failed extubation (n = 102).

Variables	Extubation		p-value
	Failure	Success	
Infants characteristics			
Female sex	46 (50.5)	5 (45.5)	0.75 ^a
GA (weeks)	30.0 (28.0; 33.0)	33.0 (30.0; 34.0)	0.07 ^c
Birth weight (grams)	1480 (1035; 1960)	1925 (1335; 2375)	0.08 ^c
5-min APGAR	7.0 (5.0; 8.0)	7.0 (6.0; 8.0)	0.52 ^c
Surfactant doses	1.0 (0.0; 1.0)	0.0 (0.0; 1.0)	0.05^c
Corticosteroids doses	1.0 (0.0; 1.0)	1.0 (0.0; 1.0)	0.60 ^c
Ventilatory settings			
MV duration (days)	5.0 (2.0; 9.0)	6.0 (5.0; 7.0)	0.22 ^c
PS (cm/H ₂ O)	13.0 (12.0; 14.0)	13.5 (13.0; 14.0)	0.15 ^c
MAP (cm/H ₂ O)	9.0 (8.0; 9.0)	9.0 (8.0; 9.0)	0.72 ^c
Tidal vol	10.0 (73; 16.0)	13.0 (9.0; 15.0)	0.54 ^c
PIP (cm/H ₂ O)	16.0 (15.0; 17.0)	17.0 (16.0; 17.0)	0.07 ^c
PEEP (cmH ₂ O)	6.0 (5.0; 6.0)	6.0 (5.0; 6.0)	0.74 ^c
FiO ₂	0.25 (0.21; 0.30)	0.21 (0.21; 0.30)	0.49 ^c
NIV after extubation	83 (91.2)	9 (81.8)	0.29 ^b
Blood Gases			
pH	7.43 ± 0.08	7.44 ± 0.05	0.25 ^d
PCO ₂ , mmHg	29.7 (24.4; 33.5)	32.1 (30.0; 37.3)	0.19 ^c
HCO ₃ mmol/L	22.4 (17.9; 23.9)	23.5 (22.4; 25.2)	0.12 ^c
PaO ₂ , mmHg	101.0 ± 36.6	88.5 ± 43.8	0.34 ^d
BE, mEq/L	-2.8 ± 3.7	-0.05 ± 4.09	0.99 ^d
SpO ₂ , %	97.3 (93.2; 98.5)	95.4 (88.9; 98.5)	0.37 ^c

^a Pearson's chi-squared test; ^b Fisher Exact test; ^c Mann-Whitney U test; ^d Student's t test. GA, gestational age; MV, mechanical ventilation; PS, pressure support; MAP, mean airway pressure; TV, tidal volume; PIP, peak inflation pressure; PEEP, Positive end-expiratory pressure; FiO₂ inspired oxygen concentration; NIV, noninvasive ventilation; PCO₂, partial pressure of carbon dioxide in arterial or capillary blood; PCO₂, Partial pressure of arterial oxygen; BE, base excess; SpO₂, arterial blood oxygen saturation

significance in the previous analyses, other studies have shown a tendency for the mandatory frequency to be higher in the failure group [23–26]. This can be explained by the fact that the babies who fail in the extubation usually require higher ventilation settings, present respiratory effort, and tend to retain carbon dioxide [18].

Table 2. Significant variables after univariate logistic regression analysis for failure extubation.

Variables	Extubation failure OR (IC 95%)	p-value	Summary model
PIP (cm/H ₂ O)	1.30 (0.99–1.71)	0.05	X ² (1) = 4.15 R ² Nagelkerke = 0.08
Fmand	1.13 (1.00–1.27)	0.04	X ² (1) = 3.8 R ² Nagelkerke = 0.07

PIP, peak inspiratory pressure; Fmand, mandatory frequency.

The benefits of applying the surfactant with less than two hours of life has been reported in the literature and demonstrates a significantly reduced the rates of bronchopulmonary dysplasia development and mortality, in addition to contributing to better adaptation to the mechanical ventilator [27, 28]. The present analysis showed that the successful group received more surfactant doses than the failure group, thus presenting a positive significance relative to this group ($p = 0.05$). This finding, however, is not consistent with other studies since the administration of surfactant doses is related to the pulmonary immaturity of preterm infants, being directly associated with gestational age [10, 21]. It is possible that the success group received higher doses of surfactant because it had a lower gestational age (median of 30 weeks).

Regarding the time of preterm infants on VM, it was shown that in the success group had earlier extubation (median of 5 days) to the detriment of the failure group (median of 6 days). According to another study that compared the time spent on the VM of preterm infants, it also showed that the failing group remained with support for a longer time [29]. It could be partly due to higher initial illness severity or from lung injury occurring from delayed extubation [10].

After the extubation procedure, most preterm infants use NIV (92%); thus, it may be correlated to the high rate of successful extubation. Another study that obtained a similar success rate (87.18%) found that most preterm infants in the success group used noninvasive CPAP ventilation support after extubation, and only two preterm infants failed [30]. The use of NIV is associated with a lower incidence of reintubation because it maintains functional residual capacity, preventing post-extubation atelectasis and apneas and avoiding the need for reintubation [30, 31].

This study has limitations. This was a retrospective analysis of several extubation parameters conducted in a single-center study. Multicenter prospective studies with clearly delineated extubation protocols would be helpful in addressing these limitations. Despite this, the results of this study indicate that weaning protocols may be valuable in standardizing the process of weaning. Furthermore, the weaning protocol applied in the hospital considering the minimal criteria required for assessment of readiness for weaning associated with the use of post-extubation NIV seems to be a promising alternative to reduce adverse effects related to conventional ventilation.

5 Conclusions

The surfactant doses and the adjustable ventilatory parameters of IMV, such as the PIP and the mandatory frequency value, can be important parameters to be considered at the time of extubation of premature infants. In addition, was observed the majority use of noninvasive ventilatory support after extubation, helping to prevent atelectasis and apneas, thus reducing the extubation failure incidence. Identifying factors that can influence extubation failure or success is essential to assist the multidisciplinary team in the process of early extubation in preterm infants. There is the possibility of reducing the permanence of the preterm infants in IMV and the number of hospitalization days, enabling their insertion in their family environment and thus reducing the losses arising from the long period of hospitalization. We emphasize the importance of ventilatory support with well-adjusted parameters for the improvement of the ventilation in neonates, as well as for the evolution improvement of the pulmonary condition.

Acknowledgment. This work has been supported by the following Brazilian research agencies: Conselho Nacional de Desenvolvimento Científico e Tecnológico (CNPq), Araucária Foundation, and Coordenação de Aperfeiçoamento de Pessoal de Nível Superior (CAPES). In addition, the authors would like to acknowledge support from Waldemar Monastier Children's Hospital directors board.

Conflict of Interest. The authors declare that they have no conflict of interest.

References

1. Beltempo, M., Isayama, T., Vento, M., Lui, K., Kusuda, S., Lehtonen, L., et al.: Respiratory management of extremely preterm infants: an international survey. *Neonatology* **114**, 28–36 (2018)
2. Da Fonseca, E.B., Damião, R., Moreira, D.A.: Preterm birth prevention. *Best Pract. Res. Clin. Obstet. Gynaecol.* **69**, 40–49 (2020). Bailliere Tindall Ltd.
3. Vliegenthart, R.J.S., Van Kaam, A.H., Aarnoudse-Moens, C.S.H., Van Wassenaer, A.G., Onland, W.: Duration of mechanical ventilation and neurodevelopment in preterm infants. *Arch. Dis. Child.: Fetal Neonatal Ed.* **104**, 631–635 (2019)
4. Choi, Y.B., Lee, J., Park, J., Jun, Y.H.: Impact of prolonged mechanical ventilation in very low birth weight infants: results from a national cohort study. *J. Pediatr.* **194**, 34–39 (2018)
5. Wilkins, R.L., Stoller, J.K., Kacmarek, R.M.: *Egan's Fundamentals of Respiratory Care*. Elsevier, Rio de Janeiro (2009)
6. Nascimento, C.P., Maia, L.P., Alves, P.T., de Paula, A.T., Cunha Junior, J.P., Abdallah, V.O.S., et al.: Invasive mechanical ventilation and biomarkers as predictors of bronchopulmonary dysplasia in preterm infants. *Jornal de Pediatria* **97**, 280–286 (2021)
7. Dumpa, V., Bhandari, V.: Surfactant, steroids and non-invasive ventilation in the prevention of BPD. In: *Seminars in Perinatology*, vol. 42, pp. 444–52 (2018)
8. Wielenga, J.M., Van den Hoogen, A., Van Zanten, H.A., Helder, O., Bol, B., Blackwood, B.: Protocolized versus non-protocolized weaning for reducing the duration of invasive mechanical ventilation in newborn infants. In: *Cochrane Database of Systematic Reviews*, pp. 1–18 (2016)

9. Kaczmarek, J., Kamlin, C.O.F., Morley, C.J., Davis, P.G., Sant'Anna G.M.: Variability of respiratory parameters and extubation readiness in ventilated neonates. *Arch. Dis. Child.: Fetal Neonatal Ed.* **98**, 70–73 (2013)
10. Chawla, S., Natarajan, G., Shankaran, S., Carper, B., Brion, L.P., Keszler, M., et al.: Markers of successful extubation in extremely preterm infants, and morbidity after failed extubation. *J. Pediatr.Pediatr.* **189**, 113–119 (2017)
11. Cordeiro, A.M.G., Fernandes, J.C., Troster, E.J.: Possible risk factors associated with moderate or severe airway injuries in children who underwent endotracheal intubation. *Pediatr. Crit. Care Med.* **5**, 364–8 (2004)
12. Shehadeh, A.M.H.: Non-invasive respiratory support for preterm infants following extubation from mechanical ventilation. A narrative review and guideline suggestion. *Pediatr. Neonatol.* **61**, 142–7 (2020)
13. Shalish, W., Kanbar, L., Kovacs, L., Chawla, S., Keszler, M., Rao, S., et al.: The impact of time interval between extubation and reintubation on death or bronchopulmonary dysplasia in extremely preterm infants. *J. Pediatr.Pediatr.* **205**, 70–76 (2019)
14. Sweet, D.G., Carnielli, V., Greisen, G., Hallman, M., Ozek, E., Te Pas, A., et al.: European consensus guidelines on the management of respiratory distress syndrome—2019 update. *Neonatology* **115**, 432–450 (2019)
15. Cavallone, L.F., Vannucci, A.: Extubation of the difficult airway and extubation failure. *Anesth. Analg.. Analg.* **116**, 368–383 (2013)
16. Hiremath, G.M., Mukhopadhyay, K., Narang, A.: Clinical risk factors associated with extubation failure in ventilated neonates. *Indian Pediatr.Pediatr.* **46**, 887–890 (2009)
17. Dassios, T., Kaltsogianni, O., Greenough, A.: Relaxation rate of the respiratory muscles and prediction of extubation outcome in prematurely born infants. *Neonatology* **112**, 251–257 (2017)
18. Mueller, M., Wagner, C.L., Annibale, D.J., Knapp, R.G., Hulsey, T.C., Almeida, J.S.: Parameter selection for and implementation of a web-based decision-support tool to predict extubation outcome in premature infants. *BMC Med. Inform. Decis. Mak.Decis. Mak.* **6**, 1–13 (2006)
19. Dimitriou, G., et al.: Prediction of extubation failure in preterm infants. *Arch. Dis. Child.: Fetal Neonatal* **86**, 32–35 (2002)
20. Tana, M., Lio, A., Tirone, C., Aurilia, C., Tiberi, E., Serrao, F., et al.: Extubation from highfrequency oscillatory ventilation in extremely low birth weight infants: a prospective observational study. *BMJ Paediatr. Open* **2**, 1–7 (2018)
21. Hermeto, F., Martins, B.M.R., Ramos, J.R.M., Bhering, C.A., Sant'Anna, G.M.: Incidence and main risk factors associated with extubation failure in newborns with birth weight < 1,250 grams. *Jornal de Pediatria* **85**, 397–402 (2009)
22. Martin, C.R., Brown, Y.F., Ehrenkranz, R.A., O'Shea, T.M., Allred, E.N., Belfort, M.B., et al.: Nutritional practices and growth velocity in the first month of life in extremely premature infants. *Pediatrics* **124**, 649–657 (2009)
23. Nakato, A.M., Ribeiro, D.F., Simão, A.C., da Silva, R.P.G.V.C., Nohama, P.: Impact of spontaneous breathing trials in cardiorespiratory stability of preterm infants. *Respir. Care* **66**, 286–91 (2021)
24. Robles-Rubio, C.A., Kaczmarek, J., Chawla, S., Kovacs, L., Brown, K.A., Kearney, R.E., et al.: Automated analysis of respiratory behavior in extremely preterm infants and extubation readiness. *Pediatr. Pulmonol.. Pulmonol.* **50**, 479–486 (2015)
25. Kaczmarek, J., Chawla, S., Marchica, C., Dwaihy, M., Grundy, L., Sant'Anna, G.M.: Heart rate variability and extubation readiness in extremely preterm infants. *Neonatology* **104**, 42–48 (2013)

26. Davidson, J., Miyoshi, M.H., Miyashiro, A., dos Santos, N., Brunow De Carvalho, W.: Medida da frequência respiratória e do volume corrente para prever a falha na extubação de recém-nascidos de muito baixo peso em ventilação mecânica. *Revista Paulista de Pediatria* **26**, 36–42 (2008)
27. Finer, N.N., et al.: Early CPAP versus surfactant in extremely preterm infants. *N. Engl. J. Med.* **362**(21), 1970–79 (2010)
28. Walsh, M.C., Morris, B.H., Wrage, L.A., Vohr, B.R., Poole, W.K., Tyson, J.E., et al.: Extremely low birthweight neonates with protracted ventilation: mortality and 18-month neurodevelopmental outcomes. *J. Pediatr.Pediatr.* **146**, 798–804 (2005)
29. Mukerji, A., Razak, A., Aggarwal, A., Jacobi, E., Musa, M., Alwahab, Z., et al.: Early versus delayed extubation in extremely preterm neonates: a retrospective cohort study. *J. Perinatol.Perinatol.* **40**, 118–123 (2020)
30. Chawla, S., Natarajan, G., Gelmini, M., Kazzi, S.N.J.: Role of spontaneous breathing trial in predicting successful extubation in premature infants. *Pediatr. Pulmonol.* **48**, 443–448 (2013)
31. Al-Hadidi, A., Lapkus, M., Karabon, P., Akay, B., Khandhar, P.: Respiratory modalities in preventing reintubation in a pediatric intensive care unit. *Glob. Pediatr. Health* **8**, 1–6 (2021)



Analysis of the Causes of Failures in a Dental Unit in Primary Health Care

Mariana Ribeiro Brandão^(✉) , Jonas Maciel , Juliano Martins ,
and Renato Garcia Ojeda 

Department of Electrical Engineering (DEEL), Biomedical Engineering Institute (IEB-UFSC),
Federal University of Santa Catarina (UFSC), Florianópolis, Brazil
marianaribeirobrandao@gmail.com

Abstract. Failure cause analysis is an essential tool for Clinical Engineering. One of the essential equipment in dental care in Primary Health Care is the Dental Unit. Due to its importance, the study of the causes of failures to elucidate the main risks associated with this equipment in users is necessary to assist in its safe use based on evidence. The identification of failures occurred through a survey of open service orders in the Health Centers of Florianópolis, Brazil. Data were stratified, categorized with respect to fault location. A total of 77 failure modes were categorized and the failure mode with the highest occurrence was hose leak, followed by unregulated pressure valve and clogged venturi and debris filter. It was observed that approximately 70% occurred in the following parts of the technology: dental element (including hand instruments) and water unit. For the failure mode with the highest occurrence rate, hose leak, the quality tool, Ishikawa Diagram, was applied to determine the main causes of failures and presented some risk mitigation strategies. This study consolidated the importance of analyzing failures retrospectively to establish risk mitigation strategies prospectively, in order to improve quality and safety for the end user of the technology.

Keywords: Dental Unit · Primary Health Care · Clinical Engineering

1 Introduction

Primary Health Care (PHC) is the first stage of the integrated health care network, being responsible for health promotion and protection, disease prevention, diagnosis, treatment and rehabilitation [1]. One of the main PHC programs in Brazil is the National Oral Health Policy, which aims to expand access to dental treatment for the Brazilian population [2]. Oral health is a component of general health and its integration with primary care is essential in the accessibility to health care of the population [3].

PHC is characterized by the provision of low-complexity services, but this factor is not a limiting factor for the presence and technological dependence in these establishments. Thus, it is necessary to manage their technologies in order to ensure the maintenance of quality and safety for the patient. Therefore, the execution of Clinical Engineering activities that aim to seek quality in technological processes through Health Technology Management (HTM) becomes fundamental.

The Biomedical Engineering Institute (IEB-UFSC) bases the performance of HTM on three pillars, called technology, infrastructure and human resources, in which the interaction between them results in an improvement in safety, reliability and effectiveness in the use of technologies in health establishments [4]. One of the steps included in the HTM process to be developed and implemented by Clinical Engineering throughout its life cycle is the analysis of failures involving medical equipment, taking into account not only a technological failure, but involving a broader analysis encompassing the device installation environment and the human factors that are operating. Operational failures in the health area can harm both patients and operators, reducing productivity and quality of care [5].

The Dental Unit, also called Equipment or Dental System, consists of the main technology in the dentistry service due to its various functionalities, being a product to support the patient's dental treatment [6]. The study of errors and damages in dental environments should be treated as fundamental priorities in the area [7]. Research carried out on patient safety for dentistry in PHC has determined that one of the recurring incidents is equipment failures [8]. A study found that equipment failures were responsible for the second largest cause of incidents in dental establishments, with the most common problems involving the dental set or individual units connected to it [9]. In another survey, it showed that failures in medical devices appeared as the majority of incidents in dental units [10].

Due to the importance in PHC and the recurrence of equipment problems in dental care establishments, it is necessary to study failures involving this technology in order to prevent the occurrence and ensure greater safety. In order to standardize the classification of incidents, studies suggest a categorization of failures as shown in Table 1 [11, 15].

The use of quality tools to analyze risks and failures in medical equipment is important to evidence the data in a clearer and more standardized way, such as the Ishikawa Diagram. This consists of a recommended quality tool to analyze problems in different domains of probable causes [12]. Thus, this failure analysis study aims to contribute to Clinical Engineering in the generation of evidence of the main problems involving malfunctions of dental sets in order to prioritize the implementation of improvements in order to increase patient safety.

2 Materials and Methods

The analysis of the failures that occurred in the Dental Unit in the PHC came from information collected from the service order system of the health centers in the city of Florianópolis, in Brazil, between January 2015 and June 2018, through 5 steps explained below. The first stage consists of studying the equipment; followed by data collection in the management system used at the IEB-UFSC and data export to an Excel spreadsheet; stratification and classification of fault data; application of the Ishikawa diagram to analyze the cause of reported problems; and finally, analysis of the results. The study consisted of mixed steps of quantitative and qualitative analysis.

The first step was the study of the Medical Equipment to be analyzed. At this time, technical training was carried out on the operation of the Dental Unit, where their practical experiences on the device were shared. The manufacturer's instruction manuals

were also read. After having greater knowledge about the technology, data collection was carried out in the Clinical Engineering information system through the extraction of Service Orders. A total of 1185 service orders were exported to an Excel spreadsheet where data was stratified and classified into failure modes according to the type of problem identified and its location in the equipment.

The determination of failure modes was made from a compilation and organization of the operators' failure reports, the activity performed by the technicians after the opening of the call and the final finding of the problem, analyzed retrospectively during the study period. Thus, failure modes were characterized, finding the main cause of the problem, number of failures observed in the period and consequently the frequency compared to all other failure modes. The failures were also classified according to Wang, explained in Table 1. The operators' failure reports were carefully analyzed by the Clinical Engineering team.

For the failure modes with higher occurrences, a more in-depth study was carried out to verify the main causes of these problems in order to seek strategies and implement actions to correct these problems. The Ishikawa Diagram quality tool was chosen to help identify the causes generated and elucidate the main causes of the problem with greater recurrence of calls in dental establishments. The construction of the Ishikawa Diagram is based on a few steps, namely: problem definition, identification of groups of causes, identification of causes and classification of causes [12]. At the IEB-UFSC, the groups selected for analysis are technology, human resources, infrastructure, measurement, materials and methods. With this, some actions were proposed to be implemented in the establishment in order to reduce the occurrence of failures and improve patient safety.

Table 1. Fault classification [11, 15].

Code	Failure cause description
NPF	No problem found
UPF	Unpreventable failure caused by normal wear and tear
ACC	Accessory failure (including supplies)
BATT	Battery failure
NET	Failure related to network
USE	Failure induced by use (i.e. abuse, accident, environment conditions)
PPF	Predictable and preventable failure
EF	Evident failure (i.e. evident to user but not reported)
SIF	Induced by service (i.e. caused by a technical intervention not properly completed or premature failures of a part just replaced)
PF	Potential failure (i.e. in process of occurring)
HF	Hidden failure (i.e. not detectable by the user unless special test or measurement equipment)

3 Results

3.1 Dental Unit Study

The Dental Unit is a medical equipment that depends on the supply of air, water and electricity to conduct procedures in dental offices [13]. According to ABNT NBR IEC 80601-2-60:2015, which covers basic safety and performance requirements of the Dental Set, this technology consists of a combination of dental hand instruments, dental units, the patient's dental chair and a dental light operator [14]. In addition to this regulation, ABNT NBR ISO 6875:2014 and ABNT NBR IEC 60601-1:2010 are also applicable.

This is the main technology in the dental service due to its various uses, including: patient accommodation during the procedure, connection of hand instruments, instrument support, provision of lighting, among others. Its main components used are: the Patient Chair (consisting of a base, backrests, geared motor and pedal), Dental Element (can also be called a carter, composed of the support of instruments and hand instruments for carrying out procedures, such as the triple syringe, high and low rotation pen), Dental Operation Light (responsible for lighting the procedure field), Auxiliary Unit (also called Water Unit, consisting of cuspidors, suction, debris filter, auxiliary syringe, Distilled water reservoir and air filter) and saddle chair or dentistry chair. The study of the equipment consisted of a fundamental initial step in the development of the work, since the better understanding of the functionality and mode of use of the device facilitated the stratification, classification and analysis of data.

3.2 Data Stratification and Classification

When stratifying the data from the 1185 service orders with reports of problems involving the Dental Unit and relating them to the location of the equipment failure, it was found that 364 were related to the dental element; 276 in the hand instruments; 179 in the Auxiliary Unit; 165 on the dental operatory light; 93 in the patient chair; 65 in pedal; 9 in the saddle chair and 34 were related to problems in the infrastructure of the environment, as shown in Fig. 1.

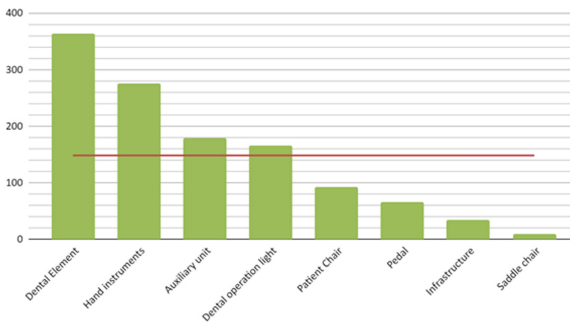


Fig. 1. Number of failures according to the location in the equipment. Dental Element = 364; Hand Instruments = 276; Auxiliary unit = 179; Dental Operation Light = 165; Patient Chair = 93; Pedal = 65; Infrastructure = 34; Saddle Chair = 9.

With these results, it can be seen that approximately 70% of failures in Dental Units involve the Dental Element, hand instruments and the Auxiliary Unit. When analyzing the reports of problems associated with the technology, it resulted in the identification of 77 failure modes involving the technology, with the 9 failure modes with the highest occurrence factors elucidated in Table 2.

When analyzing the data according to the standard failure classification presented in Table 1, it appears that, of the 1185 failure reports, 614 (equivalent to 51.8%) came from usage problems - USE - (these were deregulation of parts, wear, accidents, breakage), 404 (34.%) were obvious failures that could have been detected earlier - EF - (such as leaks, clogging of filters), 151 unpredictable failures - UPF - (such as burning of lamp, fuse) and 16 faults arising from the service performed - SIF, as shown in Fig. 2. It can be seen that more than 80% of fault reports are caused by use and obvious faults.

Table 2. The main failure modes in the dental unit.

Failure Modes	N° Failure	%
Leak in hoses	135	12.44
Unregulated high speed valve	84	7.09
Blockage in venturi and debris filter	104	9.59
Burnt out lamp and unregulated focus	40	3.38
Venturi/ejector wear	37	3.12
Water and/or air leak in the Borden	38	3.21
Electrical wiring fatigue in operation light	35	2.95
Faulty pilot valve	52	4.39
Regulator broken or unregulated air filter	17	1.43

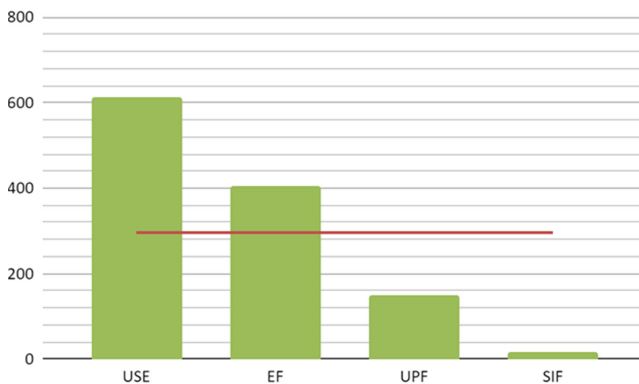


Fig. 2. Faults classification. USE (Use-Induced Failures) = 614; EF (Evident Faults) = 404; UPF (Unpredictable Failure) = 151; SIF (Service Induced Failure) = 16.

Another indicator analyzed was the average time to repair faults, which corresponds to the period between the opening of a work order until its closure. Among the 1185 work orders, this average period was 37 days, indicating a high rate of unavailability of Dental Unit. Administrative and financial bottlenecks are among the main problems highlighted for this high rate.

3.3 Analysis of the Causes: Ishikawa Diagram

Through the analysis of failure modes, it was found that the leakage in hoses was the one with the highest expressive occurrence, therefore, from the quality tool Ishikawa Diagram, the causes for the elucidated problem were established, as shown in Fig. 3. From the analysis of the causes of the failure mode, it was possible to establish actions to improve Clinical Engineering to contribute to the most appropriate use of technology, such as specific training to assist in safer use, infrastructure adaptations and performance of operational procedures for the standardization of usage protocols.

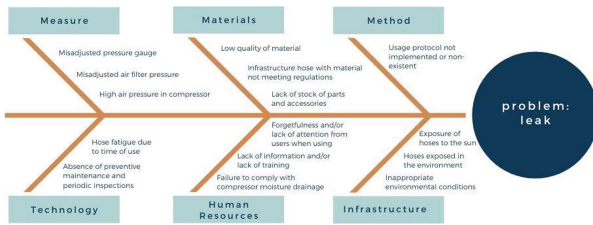


Fig. 3. Ishikawa Diagram.

4 Discussion

The analysis of failures in dental units demonstrated the importance for Clinical Engineering in technological processes in dental environments by investigating the causes and proposing more assertive solutions that improve the use of technology with less risk to the user. When analyzing the reports of failures through the classification, it was observed the high incidence resulting from problems of use and failures that could have been detected earlier. These problems suggest the need to implement a program of continuous training to operators for proper use and early identification of problems that may trigger. This categorization was also presented and discussed by Iandanza [15] and applied to various medical devices. The methodology proposed and applied in the Dental Unit consists of a useful tool for Clinical Engineering and which includes several factors for identifying the causes of failures, through a systemic view of the entire context of use as discussed by Signori [4].

The Ishikawa Diagram was a useful tool to identify the causes of the failure report, when considering several factors that contribute to the incidents, according to the Health Technology Management model developed at the IEB-UFSC [4]. With this instrument, the causes related to problems could be observed: in the infrastructure in which the

equipment is located, such as exposure to the sun; human resources such as lack of attention and lack of training in use; technology itself as the natural fatigue of its parts and pieces; as the deregulation and lack of quality control in the products; materials such as lack of stock in the units and method such as lack of technology use protocols.

Problems involving this device lead to delays and/or cancellation of service, leading to pent-up demand, in addition to impacting the quality of health care and financial implications for the institution. As shown, the high average repair time causes a high rate of technological unavailability, which implies a reduction in patient care, and therefore, loss of financial resources. Thus, some suggestions for actions by Clinical Engineering for improvement consist of periodic training for the entire team involved; carry out incorporations of inputs and accessories with better quality, carry out more preventive inspections; analyze the infrastructure involved in the equipment and prevent environmental conditions from interfering with the use of the equipment. The main limitations for this work were the lack of standardization in the reporting of failures by both operators and service providers, making it difficult to categorize and analyze data. In some cases, a lack of technical detail of the reported and resolved problem was also observed. Something that can be solved is to show those involved the importance of detailing so that the data can be as clear and objective as possible and in this way be able to show evidence as close to reality as possible. It is also suggested to improve the information system to reduce the fields for filling in failure reports and thus facilitate the study. Another limitation of the work is related to the lack of standardization of technology nomenclature. The lack of standardization makes the search for evidence difficult.

5 Conclusion

The analysis of the cause of failures is an essential tool for Clinical Engineering in order to elucidate and assist in the elaboration and implementation of strategies that aim to reduce the occurrence of problems. The occurrence of failures involving Dental Unit directly impacts the quality of care in dental environments, as it is an essential technology for patient care. A total of 77 failure modes were categorized and the failure mode with the highest occurrence was hose leakage, followed by unregulated pressure valves and clogged venturi and debris filters. The failures identified in this research, which usually occur due to the time of use of accessories and technology, in addition to human factors such as lack of knowledge and lack of carrying out protocols, can generate negative impacts on care, such as pause in treatment, damage to the patient in addition to financial losses. This work contributed significantly to the identification of the main problems faced in the use of Dental Units, identifying the causes so that preventive actions can be established in PHC aiming at greater quality in care.

Through this work, it was identified the need to establish Clinical Engineering programs not only in hospitals, but also in PHC, thus helping health professionals in the proper, safe and reliable use of health technologies, such as in dental environments. Analyzing failures retrospectively was essential to understand and generate evidence for the entire community and improve improvements in the use of technologies in the context of PHC. The main actions that must be taken for future planning and process improvements are training for operators, improvement in the incorporation of better

quality material, and planning for possible replacements of the technology park. However, the implementation of the proposed improvement actions in order to reduce the risks of errors involving the Dental Unit, aims to increase patient safety and reduce costs for the establishment.

References

1. Ministry of health in Brazil: Primary Health Care. Disponibile (2019). <http://aps.saude.gov.br/smp/smpoquee>
2. Ministry of health in Brazil: National oral health policy. Disponibile (2019). <http://www.saude.gov.br/acoee-e-programas/politica-nacional-de-saude-bucal>
3. Prasad M, et al.: Integration of oral health into primary health care: a systematic review. *J. Family Med. Prim. Care* (2019)
4. Signori, M., Garcia, R.: Clinical engineering incorporating human factors engineering into risk management. In: World Congress on Medical Physics and Biomedical Engineering, September 7–12, 2009, Munich, Germany. Diagnostic and Therapeutic Instrumentation, Clinical Engineering, vol. 25, pp. 449–452 (2009)
5. Tucker, A.L.: The impact of operational failures on hospital nurses and their patients. *J. Oper. Manag.* (2004)
6. Brazilian National Standards Organization: ABNT NBR ISO 6875:2014. Dentistry—Dental chair for patient (2014)
7. Black, I., Bowie, P.: Patient safety in dentistry: development of a candidate ‘never event’ list for primary care. *Br. Dent. J.*, 782–788 (2017). <https://doi.org/10.1038/sj.bdj.2017.456>
8. Bailey, E., Tickle, M., Campbell, S.: Patient safety in primary care dentistry: where are we now? *Br. Dent. J.* **217**, 339–344 (2014). <https://doi.org/10.1038/sj.bdj.2014.857>
9. Thusu, S., Panesar, S., Bedi, R.: Patient safety in dentistry—state of play as revealed by a national database of errors. *Br. Dent. J.* (2012)
10. Chappy, S.: Perioperative patient safety: a multisite qualitative analysis. *AORN J.* **83**, 871–888 (2006)
11. Wang, B., et al.: Evidence-based maintenance: part I—measuring maintenance effectiveness with failure codes <https://doi.org/10.1097/JCE.0b013e3181e6231e>
12. National Health Surveillance Agency: Risk Management and Investigation of Adverse Events Related to Health Care (2017)
13. Food & Drug Administration: Dental Unit Waterlines Disponibile (2018). <https://www.fda.gov/medical-devices/dental-devices/dental-unit-waterlines>
14. Brazilian National Standards Organization: ABNT NBR IEC 80601-2-60:2015. Medical electrical equipment Part 2–60: Particular requirements for the basic safety and essential performance of dental equipment (2015)
15. Iadanza, E., Gonnelli, V., Satta, F., et al.: Evidence-based medical equipment management: a convenient implementation. *Med. Biol. Eng. Comput. Comput.* **57**, 2215–2230 (2019). <https://doi.org/10.1007/s11517-019-02021-x>



Principal Components and Neural Networks Based Linear Regression to Determine Biomedical Equipment Maintenance Cost in the Peruvian Social Security Health System

E. Toledo¹ , C. de la Cruz² , and C. Mamani³ 

¹ Facultad de Ingeniería y Arquitectura, Universidad de Lima, Lima, Perú
etoledo@ulima.edu.pe

² Facultad de Ingeniería Eléctrica y Electrónica, Universidad Nacional de Ingeniería, Lima, Perú

³ Facultad de Ingeniería de Producción y Servicios, Universidad Nacional de San Agustín de Arequipa, Arequipa, Perú

Abstract. In this study, multivariate linear regression models and principal component analysis, and artificial neural networks (ANN) were designed to predict the monthly cost of biomedical equipment maintenance services in the Peruvian Social Health Insurance (EsSalud). The data employed in the development of these models were obtained from maintenance contracts and their execution, from 2019 to present. The results demonstrate that the multivariable linear regression model acquires adequate metrics; still, such a model has four correlated variables. Hence, the use of the principal component regression model enhanced the outcomes by using two components, thus acquiring greater interpretability. Finally, the ANN model obtained the best performance predictor.

Keywords: Linear regression · Principal components regression · Artificial neural network · Machine learning · Equipment maintenance cost

1 Introduction

EsSalud is a public entity attached to the Peruvian Ministry of Labor and Employment Promotion, which delivers health, social, and economic benefits to employees of public and private companies. EsSalud possesses 61,349 pieces of hospital equipment, out of which 47,661 are biomedical and 13,688 are electromechanical, distributed among 30 Decentralized Organizations (ODC). The maintenance of such equipment is performed through the contracting of specialized companies that offer personnel and physical means to the hospitals of EsSalud [1].

There are several reasons, which in most cases occur simultaneously, as to why insufficient money is invested in maintenance: limited availability of resources, low capacity to implement, corruption, favoritism, and lack of contractual incentives for adequate maintenance [2]. Thus, the determination of the monthly cost of maintenance

will enable the implementation of anti-corruption policies in EsSalud, in addition to establishing parameters for a sufficient estimate of the maintenance budget.

This article proposes the development of models according to multiple linear regression, principal component regression (PCR), and multilayer neural networks to predict the monthly cost of hospital equipment maintenance in EsSalud.

2 Data Analysis

2.1 Machine Learning for Maintenance Management

Machine learning techniques have been used in numerous research to offer important information for decision-making in equipment maintenance management. The applications include: the prediction of equipment failures [3, 4], prediction of neonatal incubator performance [5], spare parts for planned maintenance [6], and prediction of the useful life of the equipment and its components [7, 8], among other applications; all of them are oriented to enable efficient asset management and optimize maintenance costs.

Machine learning procedures are majorly split into two groups: supervised and unsupervised learning. In a supervised learning problem, the objective is to learn general rules (model) that map inputs to outputs, so that it will be possible to estimate the output for new unseen data, where we have observed input values but not their associated output [9].

There are two major groups of supervised learning: (i) classification where the output values are categorical, and (ii) regression where the output values are numeric [9].

2.2 Multiple Linear Regression

Multiple linear regression is a very flexible system for evaluating the association of a collection of independent variables (or predictors) to a single dependent variable (or criterion) [10]. In a simple form, a simple linear regression model can be calculated as:

$$Y_i = a + bX_i + e_i, \quad (1)$$

where each element of the independent variable Y_i is linearly associated with predictor X_i via the regression coefficients b (slope) and intercept a ; e_i is the residual term elucidating the deviation of the actual value from the predicted value Y_i .

An important step when performing a regression analysis is to select the predictor variables that offer the most information and identify the values of the dependent variable. Following [11], it is first necessary to generate the correlation matrix of all variables with each other. Then the best predictors are those that have the highest correlation with the dependent variable, and have a low correlation with each other, since highly correlated variables have redundant information and influence the accuracy of the determination of the dependent variable.

2.3 Principal Component Regression (PCR)

In multiple regression, one of the main challenges with the usual least squares estimators is the issue of multicollinearity, which happens when there are near-constant linear functions of two or more of the predictor, or regressor, variables [12].

The best way to overcome this challenge is by principal components (PCs) regression, where the PCs of the predictor variables are employed rather than the predictor variables themselves. As the PCs are uncorrelated, there are no multicollinearities between them, and the regression calculations are also simplified. The combination of PC analysis (for lowering dimensionality) and multivariate linear regression produces the first-order multivariate model known as PCR [13].

2.4 Multilayer Neural Network

Neural networks encompass a collection of neurons and edges, inspired from circuit analysis. Various weights can be applied to each edge connecting the neurons. At each neuron, an activation function is applied to a weighted input signal to produce an output signal. A sigmoidal function is frequently utilized, comprising a first-order low-pass filter of a unit step function.

Neurons are then subdivided into an input layer, hidden layer(s), and output layer. The number of hidden layers defines whether the system is a shallow learning system (with one or a few hidden layers) or deep learning (with many hidden layers) [9].

A single-layer perceptron (SLP) is a simple linear binary classifier. It takes inputs and associated weights and combines them to generate output that is used for classification. It has no hidden layers [14]. The training model is given by the equation given below:

$$\hat{y} = f(x, w^T) = \sigma\left(\sum_i^n x_i w_i\right), \quad (2)$$

$$\sigma = \frac{1}{1 + e^{-x}}, \quad (3)$$

$$\hat{y} = \begin{cases} 1 & \text{if } y \geq p^* \\ 0 & \text{elsewhere} \end{cases} \quad (4)$$

where:

- $[x_1, x_2, x_3, \dots, x_n]^T$ is the vector of vector of inputs
- $[w_1, w_2, w_3, \dots, w_n]$ is the vector of weights
- Σ is the activation function
- \hat{y} is the model result
- p^* is the threshold.

The major limitation of the SLP models is that perceptron models are only precise when working with data that is linearly separable, this led to the development of subsequent neural network models [15].

A multilayer perceptron (MLP) is a simple example of feedback artificial neural networks (ANNs). An MLP comprises at least one hidden layer of nodes other than the input

layer and the output layer. Each node of a layer other than the input layer is called a neuron that employs a nonlinear activation function including the sigmoid or rectified linear unit (ReLU) function. An MLP utilizes a supervised learning technique called backpropagation for training while minimizing the loss function like cross-entropy. It employs an optimizer for tuning parameters (weight and bias). Its multiple layers and nonlinear activation differentiate an MLP from a linear perceptron. A multilayer perceptron is a basic form of a deep neural network [14].

2.5 Data Collection

In the current study, information associated with equipment maintenance contracts and information on the implementation of their maintenance was acquired from the institutional computer platforms (SAP and SISMAC) and public domain applications (Electronic System of State Contracting - SEACE), from 2019 to present.

Once the information from the different systems was obtained, the classification by ODC and standardization was performed, considering that each record corresponds to a time interval of one month.

2.6 Determination of the Independent Variables

It is necessary to determine which independent maintenance variable influences the dependent variable since the independent variable is the monthly contracting cost of a given preventive and corrective maintenance service. The main significant parameters that are associated with the performance and cost of equipment maintenance are established in the contract and are categorized into qualitative and quantitative variables, as follows:

Qualitative variables. These are variables that enable establishing differentiated maintenance costs based on a given classification. In [20], the prices of biomedical equipment maintenance services have been determined based on qualitative variables. For the current examination, the following qualitative variables were considered:

- Type of equipment: biomedical, electromechanical, hemodialysis, diagnostic imaging.
- Zone or region: Lima, Central, North, South, and East.
- Year: 2019, 2020, 2021.

Quantitative variables. These are numerical variables that enter the model for the computation of correlation with the dependent variable. For the current investigation, the following quantitative variables were carried out:

- Number of equipment included in the maintenance contract
- Number of technicians
- Number of supervisors
- Number of man-hours worked in a month
- Number of preventive and corrective work orders executed in a month
- Working capital: Is the monthly amount available to contracted companies for the purchase of spare parts.

2.7 Data Cleaning

Considering that the data were acquired from various systems that are not integrated with each other, they were consolidated and the records were manually integrated. For this reason, the date of award of the bid for the contracted maintenance services was considered and from that date, the information recorded in the maintenance management system for each month was collected.

This information was integrated in Excel, and then, employing filters, records consisting of incomplete information and non-congruent data were eliminated.

Next, groups of data were constructed with the qualitative variables to assess the type of classification to be employed. Analysis of variance and boxplots were conducted, and it was observed that categorizing the data by type of equipment caused greater homogeneity of the data. It was also observed that of all the types of equipment, the contracts for biomedical equipment demonstrate a better composition of the data.

Subsequently, it was identified that the data that best denotes the maintenance cost are: work orders implemented, man-hours executed, and the number of equipment and personnel. To identify the last variable, a weighted average function was employed according to the average monthly remuneration of specialist technicians, non-specialist technicians, and resident engineers.

3 Results

Linear regression, principal component, and multilayer perceptron analysis were conducted utilizing the sklearn, numpy, keras and pandas libraries in the google colab environment. The metrics used to examine the performance of our model were the squared error (R^2), mean squared error (MSE), and their level of significance was tested using the analysis of variance (ANOVA) test.

3.1 Multivariable Linear Regression

For this instance, the standardized predictor variables depicted above were utilized, which were renamed as V1, V2, V3, and V4 respectively. Similarly, the dependent variable was renamed Y. After performing the linear regression model, the outcomes depicted in Table 1 were acquired.

Table 1. Multivariate linear regression results

R^2	MSE	ANOVA
0.8491	0.1245	0.850

Finally, the equation of the linear regression model, considering the coefficients and the intercept, is as follows:

$$Y = 0.083 \times V1 + 0.2186 \times V2 + 0.6639 \times V3 + 0.0029 \times V4 - 0.0087 \quad (5)$$

3.2 Linear Regression Using Principal Components

Before the analysis, standardization of features were performed by removing the mean and scaling to unit variance, which results are shown in Table 2.

Table 2. Data standardization

No	WORK ORDERS	MAN-HOURS	EQUIPMENT	PERSONNEL
0	2.001117	1.924265	1.558619	1.366508
1	1.968141	2.005268	1.558619	1.366508
2	2.028597	1.905847	1.558619	1.366508
3	1.786771	1.757009	1.558619	1.213231
...

Consequently, the correlation matrix was developed (Table 3), and it was detected that the correlation between the explanatory variables was considerable in most cases. This shows the presence of multicollinearity and the need to conduct Principal Component Analysis (PCA) to attain purely independent variables in the form of PCs that can act as explanatory variables [16].

Table 3. Correlation matrix

	WORK ORDERS	MAN-HOURS	EQUIPMENT	PERSONNEL
WORK ORDERS	1	0.874741	0.865729	0.814418
MAN-HOURS	0.874741	1	0.796736	0.882751
EQUIPMENT	0.865729	0.796736	1	0.795278
PERSONNEL	0.814418	0.882751	0.795278	1

Likewise, employing Bartlett's test, the following statistical variables were found, which show that it is suitable to carry out the PCA: $\text{Chi}^2 = 1657.40373$, Degrees of freedom = 6; p-value = 0. Thus, the null hypothesis, which considers that explanatory variables are independent, can be rejected and purely independent variables that can function as new explanatory variables can be attained [16].

The Kaiser criterion and the sedimentation diagram were employed to determine the suitable number of PCs. For the Kaiser criterion, only one eigenvalue = 3.524 (greater than unity) was obtained, which signifies that only with the first component PC1, it is possible to represent the model with the greatest explanatory variability.

In the sedimentation plot, illustrated in Fig. 1, the variability elucidated by each component can be observed: 87.88% for PC1, 6.14% for PC2, 3.85% for PC3, and 2.13% for PC4.

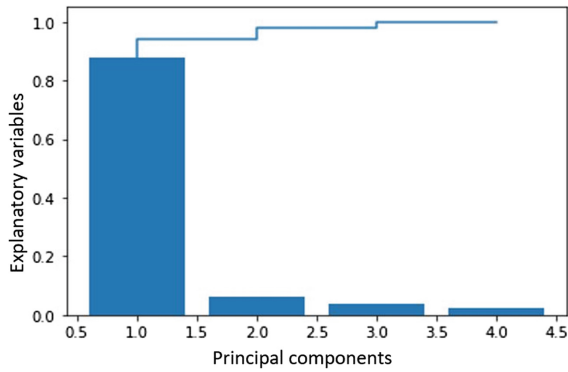


Fig. 1. Sedimentation rate graph

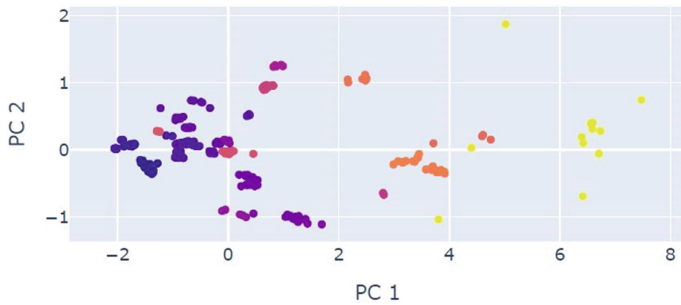


Fig. 2. Principal component-oriented data

Using the sedimentation plot illustrated in Fig. 1, it was identified that by employing two components PC1 and PC2, 94.02% of the variability of the data can be described.

Figure 2 illustrates the outcomes of the application of the PCA, considering only two components.

With the two PCs obtained, multiple linear regression was carried out, utilizing 80% of the samples for training and 20% of the samples for testing. After running the regression, the outcomes displayed in Table 4 were attained.

Table 4. Principal Component Regression Results

R^2	MSE	ANOVA
0.8215	0.1709	0.8225

Finally, the equation of the linear regression according to the PCs, considering the coefficients and the intercept, is as follows:

$$Y = 0.4873 \times PC1 + 0.4356 \times PC2 + 0.0062 \quad (6)$$

3.3 Linear Regression Using Multilayer Perceptron

Before the neural network analysis, the data were standardized to acquire a mean of zero and a unit variance, as illustrated in Table 5.

Table 5. Data standardization

	WORK ORDERS	MAN-HOURS	EQUIPMENT	PERSONNEL
AVERAGE	-0.0214435	-0.02606172	-0.03434693	-0.03175927
VARIANCE	0.98342658	0.98060481	0.94661916	0.93470986

The Keras library was used for the neural network design, employing the Sequential class, considering an input layer for the four independent variables, two hidden layers (of 128 nodes and 16 nodes respectively), and an output layer, see Table 6, having a total of 2721 parameters to train. Additionally, a ReLU function was employed as an activation function, an Adaptive Moment Estimation (ADAM) as optimizer algorithm with an initial learning rate of 0.001 and MSE as a loss function.

Table 6. Neuronal Network Configuration

Layer (type)	Output shape	Parameters #
Hidden layer_1 (Dense)	(None, 128)	640
Hidden layer_2 (Dense)	(None, 16)	2064
Output_layer (Dense)	(None, 1)	17

Similarly, it was established that 80% of the data would be employed for training and 20% for testing. Additionally, 30% of the training data was used for validation. Finally, the number of iterations was set to 1000 to lower the MSE.

Considering the information demonstrated in Fig. 3, it is observed that in approximately 350 iterations in both training and validation data, there is a stable MSE that does not continue to decline.

Table 7 shows the results of the trained Neural Network.

Consequently, the results obtained from the model were assessed, employing it as a predictor. For this, the test data were taken and provided in the model, obtaining the graph illustrated in Fig. 4.

As a result of the validation process, Table 8 displays the monthly maintenance cost obtained with the three models employing randomly selected training data.

Finally, in Table 9 the predicted monthly maintenance cost was determined, utilizing a sample of updated data, which were not employed in the test and training process.

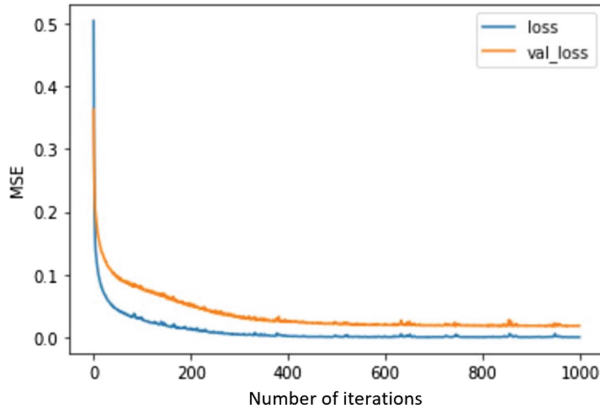


Fig. 3. MSE vs Number of Iterations

Table 7. Neural Network Results

R^2	MSE
0.985	0.01787296

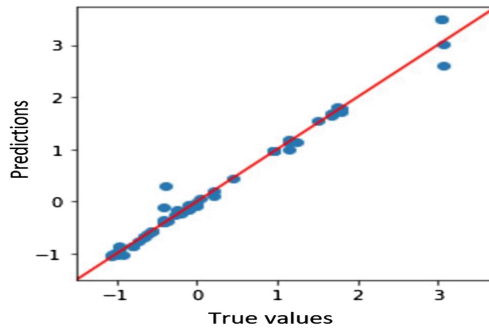


Fig. 4. Accuracy of the neural network model

4 Discussion

Two models following the machine learning techniques were developed to identify the cost of monthly contracting of preventive and corrective maintenance services for biomedical equipment, acquiring an R^2 of 0.8215 and 0.985 for the PCR and neural network model, respectively. Some authors have developed models to set up the parameters that have the greatest impact on the cost of maintenance of biomedical equipment; for instance, in [17] a model following mean time to failure, failure rate, and risk functions for preventive and corrective maintenance were determined, based on historical information on the maintenance of anesthesia machines. Similarly, the maintenance costs of electromedical equipment are correlated with the number of beds and the number of

Table 8. Estimated monthly maintenance cost

ODC	MLR	PCR	ANN	REAL COST
Piura	104,408	117,570	105,921	130,190
Cusco	51,234	58,719	62,627	53,258
Puno	47,025	55,638	46,149	46,398
Huancavelica	30,381	41,607	35,003	39,600
Almenara	51,904	87,252	92,658	95,708

Table 9. Predicted monthly maintenance cost

ODC	MLR	PCR	ANN	REAL COST
Juliaca	58,239	56,297	51,538	44,542
Pasco	54,295	54,083	53,557	41,073
Cusco	75,616	66,808	63,461	62,940
La Libertad	193,996	171,438	192,787	182,000
INCOR	58,842	55,015	55,171	57,183

operating rooms, the number of nursing staff, the acquisition value of the equipment, the number of admissions, surgical interventions, and the total length of hospital stay, based on [18].

A small number of biomedical equipment (between 7% and 13% of the total) necessitate 80% of the annual cost of maintenance, based on [19]. Then it is possible to acquire considerable economic savings by concentrating the policy of cost optimization exclusively on this small fraction of technologies. In the current work, regression models were developed for estimating biomedical equipment cost of maintenance services, without considering other types of equipment, for instance: electromechanical equipment, and hemodialysis equipment, among others.

As maintenance costs may rely on several equipment-dependent characteristics, e.g., the operating environment, service fees should also be distinguished based on these characteristics. In [20] predictive models for different machine profiles were developed to identify differentiated maintenance service fee schedules.

5 Conclusions

In this work, the monthly cost of maintenance of biomedical equipment of EsSalud was estimated through the design and training of multiple linear regression models, regression based on PCs, and ANNs. The latter indicates the most accurate results, with a coefficient of multiple determination of 0.985 and a mean square error of 0.0179.

In future research, we hope to collect more data and further exploit the performance of deep learning.

Acknowledgments. The authors would like to thank EsSalud for providing relevant information related to the maintenance of hospital equipment.

Conflict of Interest. The authors declare that they have no conflict of interest.







References

1. Seguro Social de Salud del Perú at <http://www.essalud.gob.pe/transparencia/>. Accessed 07 May 2022
2. Pastor, C.: El mantenimiento como herramienta para conseguir infraestructura de alta calidad y durabilidad (2020)
3. Nikfar, M., Bitencourt, J., Mykoniatis, K.: A two-phase machine learning approach for predictive maintenance of low voltage industrial motors. *Procedia Comput. Sci.* **200**, 111–120 (2022)
4. Abdurakipov, S.S., Butakov, E.B.: Comparative analysis of algorithms of machine learning for predicting pre-failure and failure states of aircraft engines. *Optoelectron. Instrum. Data Process* **56**, 586–597 (2020)
5. Kovačević, Ž., et al.: Prediction of medical device performance using machine learning techniques: infant incubator case study. *Health Technol.* **10**(1), 151–155 (2020)
6. Taigel, F., Tueno, A.K., Pibernik, R.: Privacy-preserving condition-based forecasting using machine learning. *J. Bus. Econ.* **88**, 563–592 (2018)
7. Vietze, D., Hein, M., Stahl, K.: Method for a cloud based remaining-service-life-prediction for vehicle-gearboxes based on big-data-analysis and machine learning. *Forsch. Ingenieurwes.. Ingenieurwes.* **84**(4), 305–314 (2020)
8. Huang, H.-Z., et al.: Support vector machine based estimation of remaining useful life: current research status and future trends. *J. Mech. Sci. Technol.* **29**, 151–163 (2015)
9. Badillo, S., et al.: An introduction to machine learning. *Clin. Pharmacol. Ther.* **107**(4), 871–885 (2020)
10. Aiken, L.S., West, S.G., Pitts, S.C.: Multiple linear regression. *Handb. Psychol.*, 481–507 (2003)
11. Vallejo, P.M.: Correlación y regresión, simple y múltiple. Universidad Pontificia Comillas, Madrid (2012)
12. Jolliffe, I.T.: *Principal Component Analysis for Special Types of Data*. Springer, New York (2002)
13. Olivieri, A.C.: *Introduction to Multivariate Calibration: A Practical Approach*. Springer (2018)
14. Manaswi, N.K., Manaswi, N.K., John, S.: *Deep Learning with Applications Using Python*. Apress, Berkeley, CA, USA (2018)
15. Beysolow II, T., Beysolow II, T.: Single and Multilayer Perceptron Models. *Introduction to Deep Learning Using R: A Step-by-Step Guide to Learning and Implementing Deep Learning Models Using R*, pp. 89–100 (2017)
16. Manoj, J., Suresh, K.K.: Forecast model for price of gold: multiple linear regression with principal component analysis. *Thail. Stat.* **17**(1), 125–131 (2019)
17. Khalaf, A., et al.: Maintenance strategies and failure-cost model for medical equipment. *Qual. Reliab. Eng. Int.* **31**(6), 935–947 (2015)
18. Aunión-Villa, J., Gómez-Chaparro, M., Sanz-Calcedo, J.G.: Assessment of the maintenance costs of electro-medical equipment in Spanish hospitals. *Expert. Rev. Med. Devices* **17**(8), 855–865 (2020)

19. Puntoni, V., Masselli, G.M.P., Silvestri, S.: An adaptation of Pareto's parametric distribution as a support tool for the analysis of maintenance costs of biomedical equipment. In: 2021 IEEE International Workshop on Metrology for Industry 4.0 & IoT (MetroInd4. 0&IoT). IEEE (2021)
20. Deprez, L., Antonio, K., Boute, R.: Pricing service maintenance contracts using predictive analytics. *Eur. J. Oper. Res. Oper. Res.* **290**(2), 530–545 (2021)



Study of Technical Productivity as a Tool for the Development of the IPS Universitaria Infrastructure Master Plan

Lucía Uribe-Herrera¹ , Mabel Zapata-Álvarez¹ ,
Óscar Saldarriaga-Saldarriaga¹, Juan Barreneche-Ospina¹ ,
Javier García-Ramos¹ , Daniela Cardona-Alzate¹ ,
and Juan Manuel-Galeano² 

¹ Bioinstrumentation and Clinical Engineering Research Group - GIBIC, Bioengineering Department, Engineering Faculty, Universidad de Antioquia UdeA, Calle 70 No. 52-21, Medellín, Colombia
lucia.uribeh@udea.edu.co

² Institución Prestadora de Servicios de Salud IPS Universitaria, Universidad de Antioquia - UdeA, Medellín, Colombia

Abstract. The design of an infrastructure roadmap was elaborated for the IPS Universitaria of the city of Medellín, which has an approximate execution time of 10 years and is made up of a total of 71 infrastructure improvement projects with which it seeks to achieve national accreditation in health services. An important challenge was the existence of an old physical plant in structure and in the composition of its technical networks. The plan was designed with special emphasis on improving hospital productivity, through the implementation of different strategies that would allow an adequate separation and independence of hospital flows, technical capacity improvement, for vertical and horizontal transport between floors and blocks, guaranteeing a proper relation between each clinical service and their interdependent services, reducing the physical critical connections between services passing from 33 to 0% in them, from 30.01 to 22.8% in moderately critical connections and from 34.4 to 77.2% in no critic type relations.

Keywords: Productivity · Interdependence · Hospital infrastructure · Technical capacity

1 Introduction

Though the world trend for healthcare is the homecare migration, the critical care and high complexity procedures will have a place in hospital environments, because of that, in countries like Colombia it is still necessary the strengthen hospital facilities. According to Linda Luxon, hospital infrastructure plays a big role in healthcare improvement, it provides quality in the patient experience and the right design can improve the efficient workflow of clinical staff. It is

important to highlight that hospital infrastructure covers the access, processes, networks and technical equipment [3].

Regarding to efficiency, the suitable facility planning can reduce the mixing between clean and solid circulation as well as the mixing between patient and public circulation, with which it is achieved a better patient experience and increase de patient safety. Then, it is possible to maintain different routes for materials, medical devices, supplies, food and waste materials and avoid de cross flow with patients, clinical staff, support service and the general public [1]. To achieve a facility design according to the features presented above, it is necessary to meet national and international standards and good practices adopted from benchmarking processes.

The national regulation (minimum requirements) for authorizing the hospitals to provide health services are established in the 3100 resolution of 2019 [6], one of the standards are focused on infrastructure requirements, nevertheless are not so demanding. On the other hand, resolution 5095 of 2018 [5], where it is adopted the health accreditation manual for hospitals is a demanding standard, focused on patient safety with high requirements for infrastructure design. Colombian healthcare institutions have been working to meet the regulation and quality standards: 3100 and 5095 resolutions respectively. However, this is an arduous task due to factors such as the building's age, original architectural designs, the challenge of renewing networks without suspending services, and contingency planning implementation, among others.

The IPS Universitaria (Institución Prestadora de Servicios de Salud Universitaria for its acronym in Spanish) is a hospital facility founded in 1950, it is a high complexity hospital which receive many patients of the city, the infrastructure has more than 40,000 m². The services briefcase includes emergency, surgery (14 operating rooms), hospitalization (630 beds), diagnostic imaging, hemodynamics, dialysis, blood bank, clinical laboratory, and external consultation, among others. In the strategic planning for the next 10 years (2022–2032) one of the strategy hospital managerial team objectives, is to become in a university hospital, which implies the meeting of the 5095 and 3409 [4] national resolutions. Some challenges regarding achieving this objective are related to facility design it is that hospital is constituted of three large buildings which were built in different years and additionally are connected through two pedestrian bridges located on two high-traffic public avenues. It is common to find in each building different structures, corridors, and columns that avoid fluid circulation and condition any reform. Another big challenge is the facades of the buildings are of heritage interest in the city.

According to the strategic objective stated, the IPS Universitaria needs to establish a roadmap to renew the buildings and minimize the redundant circulation of patients, staff, clinical, and technical support. Additionally, it is important to relocate some clinical departments in order to reduce the patient waiting time for procedures, improve the clinical staff comfort and patient safety, and finally to get the great objective of being a university hospital meeting the regulatory and quality standards. An analysis of the facility efficiency related to the sufficiency

of the technical conditions and interdependence standard of the 3100 resolution was carried out with the objective of raising the roadmap required for the hospital projections. The next sections will expose the implemented methodology and the main results and conclusions of this study.

2 Methodology

The methodology (Fig. 1) that was carried out included three phases, the first one involves a review of regulatory issues, secondly the diagnosis and recognition of the current state of the framework, the hospital workflows, and focal group perspectives, and thirdly the analysis of critical findings and arising of the roadmap.

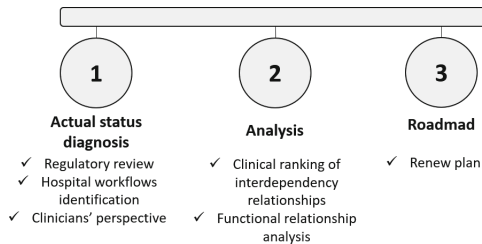


Fig. 1. Methodological scheme

2.1 Actual Status Diagnosis

Regulatory Review The starting point of this study is the identification of the actual status of the facility including technical network, systems, and environments according to Colombian regulatory requirements. Each hospital aspect is associated to a technical standard, it is summarized on Table 1.

Identification of Hospital Workflows In interest of prevent disease transmission and warranty a higher patient safety; clean, dirty, public, technical, and clinical staff workflows were contemplated and included in the characterization of hospital flows [2].

Endeavoring to improve the times of attention and obtain high quality patient care, all the flows (each aisle in every floor) were analyzed together on the same plane. In this way, it was possible to observe the redundant circulation, those that contain workflows that should not come together because it would create a major risk for patients, were regarded critical. On this wise, the workflow critical raking (CR) in every aisle was established according to Eq. 1:

$$CR = a + b + c \tag{1}$$

where:

Table 1. Regulatory framework for the inspection of networks and systems

Network wires	Applicable standard
Electrical	RETIE, NTC 2050/1998
Air-conditioning	AMCA, ANSI, AIHA, AHRI, ASHRAE, ASME, SMACNA
Hydrosanitary	NTC 1500/2017, resolution 0631/2015
Firefighting	NSR 10 chapter J
Voice and data	TIA 1179, ANSI/TIA/EIA 568A
Vertical transport	NTC 4349, NTC 5926-1, NTC 6047, Decree 0471/2018
Waste management	Decree 4741/2005, Decree 0440/2009, Decree 351/2014
Infrastructure	Infrastructure standard, resolution 3100 of 2019

- $a = 1$ if there is a multiplicity of paths of interdependence
- $b = 1$ if there is a crossing of dirty and clean flows
- $c = 1$ if it is a corridor with public flow.

If they do not meet the condition, the value for a , b , c is zero.

Focal Groups to Explore Clinicians’ Perspectives Knowing the perspective of people who shape the workflows offers the possibility to identify what is arduous to see being out of the process, therefore was necessary look for a method that promote the participants to share their real views.

Focus groups have been a commonly used technique in health research because it boosts a safe zone for people to talk plainly about what they real think about a specific topic with “synergy and spontaneity” [7]. Taking this into consideration, the focal groups were conformed by managerial, administrative, clinical, technical and support profiles.

The discussion topic was aimed to classify the importance level and current state of each one of hospital’s aspects (Table 1) according to the collaborators perception.

In the order to quantify the importance level and the current state of the infrastructure, the information was scored from one to three in the following way; Importance level have three choices: Very important - 3, Important - 2 and Little important - 1, as Actual state with: good - 3, middle - 2 and Bad - 1.

2.2 Analysis

Critical Ranking of Interdependent Relationships Once the critical infrastructure aisle were identified and accepted as the areas where the patient waiting increased rapidly, was necessary to determine priorities that would feed the action plan, it means that the changes and improvement proposed would be reflected on the infrastructure roadmap.

The first step was to correlate the clinical services, their interdependencies, and the hospital infrastructure with a relationship matrix. After that, the assessment of interdependent interactions was ranked from one to three depending on the grade of criticality, as follows; High critical: 3, Medium critical: 2 and Low critical: 1.

Functional Relationships Analysis Based on the interdependence standard from 3100 resolution of 2019 [3] and the diagnosis results, is essential to design some functional interdependence relationships to improve productivity and fulfilling regulatory requirements. Outset is imperative to know if the relationship between two services exists and if it is commonly used in clinical flow or whether the relationship must be included because is a mandatory requirement. Those terms are introduced in Eq. 2:

$$SR = m + n \quad (2)$$

where:

- $m = 1$ if in the Resolution 3100 the relationship between services was considered as “it has it”
- $n = 1$ if it exists, if from the institutional experience both services had a relationship of interdependence with high demand.

If they do not meet the condition, the value for m and n is zero.

According to the definition of the equation 2, there are three possible results about the relationship of clinical services which are:

- High Relationship: Score 2, implies contiguity between the pair of services
- Medium relationship: Score 1, non-contiguous but fluid relationship
- Low Relationship: Score 0, only logistic relationship.

2.3 Roadmap Proposal

Renew Plan Considering the first and second stages of methodology, a renew plan were raised. From the actual status diagnosis were identified the different technical and clinical aspects that needs an immediate response regarding to the more critical ranked workflow aisles. Also, where identified the regulation meeting gaps that it is mandatory to correct in order to improve the standard meetings and to assure the patient safety. Likewise, from the focal groups were identified the main aspects to build on relate to clinicians’ perspectives. With the ranking of functional relationship analysis, were possible to identify the necessary movements between clinical services. Once identified the critical issues to solve, an intervention plan was proposed, with the aim of reduce the redundant circulation, improve the clinical staff comfort and minimize the critical relationship between interdependency hospital clinical services.

3 Results and Analysis

This section is present according to the methodology that was executed and presented previously, thus, every phase has its own results.

3.1 Actual Status Diagnosis

Regulatory Review According to Table 1, each aspect was analyzed in the light of the standards summarized. Some relevant recommendations were raised focused on the meeting of the criteria analyzed.

- Enhance the capacity of the electrical substation and the water reservoir.
- Fire protection network implementation.
- Improve the waste system management in order to reduce the cross-contamination.
- Improve the data communication both with wireless and wired infrastructure.
- Specifically, vertical transport recommendation, will be exposed in the section of hospital workflows because have a high impact on hospital circulation.

Identification of Hospital Workflows The hospital buildings are located over public spaces without enclosures and are joined by a pedestrian bridge which all the hospital workflows converge, as can be seen in Fig. 2.

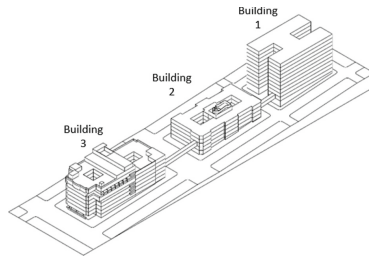


Fig. 2. IPS University architectural scheme

The IPS Universitaria communicates vertically by means of 14 elevators and 2 freight elevators distributed in each building as follows:

- Building 1: 5 elevators, 1 freight elevator
- Building 2: 2 elevators
- Building 3: 7 elevators, 1 freight elevator.

Related to the lifts of the buildings there were identified some features to improve such as the total elevator ride does not cover all floors in the building, which generate the necessity of change between them to go from the highest to the lowest floors. Also, the elevators are used for clean and soiled circulation indiscriminately. Regarding some technical spares and parts, were identified that are old and exceed the useful life by three times.

Focal Groups to Explore Clinicians' Perspectives During the meetings was possible to connect with 83 individuals of the IPS Universitaria collaborators, people from sterilization process, pharmaceutical service, the clinicians and some other that participate in support and logistic services like food chain supply, cleaning, laundry, surveillance, etc. filled out the form and answered the open questions during the meetings creating a space of discussion where each one of them could share their point views, agreements, and disagreements.

Their perspective about the current state of the infrastructure and the level of importance were averaged and clustered by facility aspects, each finding is illustrated on Fig. 3.



Fig. 3. Illustration of the study of routes carried out at each level of each block of the IPS Universitaria.

This result indicates that in the daily hospital operation all facilities aspect represents a high level of importance, but the current state of the infrastructure is poorly and must be attended at least on the infrastructure roadmap. In this manner, is indispensable for the institution to focus on the improvement of the following items:

- Updating and renewal of technical networks
- Vertical transport
- Horizontal connection between blocks
- Flow separation
- Proximity of interdependent services.

Taking advantage of focus group methodology's particularities, the meetings also allow to know what the clinicians' perspectives are about interdependence services. The responses exhibit that sterilization process and, pharmaceutical service and surgery are the most critical interdependence in people's perspectives.

Target clinical service	Amount of intersecting interdependent clinical services
Chemotherapy	1
Ionizing radiation (medical imaging)	1
Vascular diagnosis	1
Hemodynamic interventions	1
Laboratory testing	1
Dialysis	1
Medium complexity hospitalization unit	1
High complexity hospitalization unit	1
Intermediate care unit	1
Intensive care unit	1
High complexity surgery	1
Medium complexity emergency department	1
High complexity emergency department	1
Pharmaceutical service	
TOTAL	13

Fig. 4. Color code for diagram flow

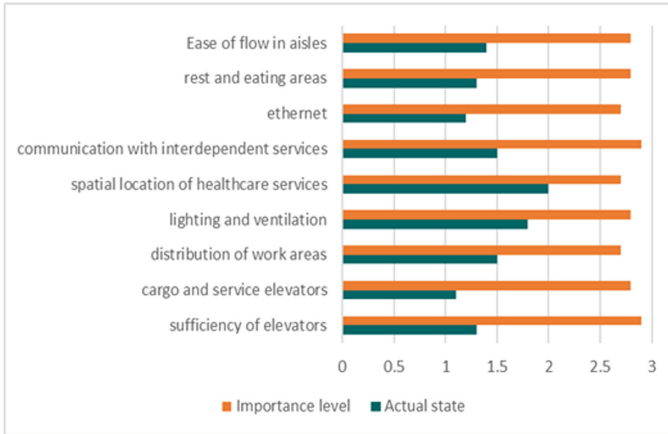


Fig. 5. Results of perception of the state of the infrastructure associated with the productivity of the IPS Universitaria

3.2 Analysis

Critical Ranking of Interdependent Relationships The correlation matrix was carried out through the relationship matrix that correlate the interdepends services with the available services of the hospital and each one of them were scored by little, medium and very critical. That information was related with facilities aspects and three very critical spots were found; those are vertical transport, the connection bridges, and the aisles. Considering the multiple inter-dependence workflows, soiled flows, and public circulation.

Comprehending the hospital facilities aspects and the critical ranking of the interdependent relationships every aisle was analyzed, an example of this is presented on Fig. 4 is an aisle located on the first flow of the third building which has many different workflows. The color code for this example is summarized in Fig. 5.

In addition, equivalent examinations were executed for 9 critical aisles of the hospital, after that was pertinent to the study define a criticality level of all aisles. The outcomes demonstrated that one aisle has low criticality, 3 of them have medium criticality, and the rest 5 have high criticality.

Functional Relationships Analysis According to methodology proposed for identified the critical interdependence relationship, the matrix of functional relationship was raised, and a summarized version is presented in Fig. 6. The original matrix contemplates 29 clinical services. Of the 93 interdependence relationships of the IPS Universitaria, 33 were ranked in very high criticism, 28 in medium, and 32 in low. The most critical relationship is related to the most complex clinical services which are the medical imaging diagnostic and emergency services.

On the other hand, the less critical interdependency services are hospitalization with supply services (food and laundry supply), this is due to the services being in the same building. Also, these services present less critical communication problems regarding vertical transport.

Pursuant to the colors in the matrix, the optimal distance between two interdependent clinical services was identified and it is a great input to propose the movement of different areas.

3.3 Roadmap Proposal

Renew Plan Understanding that is further complicated to establish an action plan to improve the productivity of the hospital by enhancing facilities aspects not only because the extent of the inversion but also for the dynamic of a hospital institution, was necessary to prioritize the interventions during the next 10 years.

From the previous analysis, in the roadmap proposed were summarized 71 activities focused on meeting resolution 5095 of 2018. It is important to highlight some of them:

1. Updating and improvement of all networks (electrical, hydro sanitary, fire protection, data, waste system) and technical equipment and moving them to the terraces and basements with an exclusively technical approach.
2. Construction of a technical tunnel, which will allow the networks' management and the separation of clean and soiled circulation.
3. Movement of the medical imaging diagnostic services to reduce the distance between them and emergency, surgery, and intensive care unit
4. Allocate similar clinical services in each building, in summary: in the building 3 will be place the high complexity services relate to surgery, emergency and intensive care unit, in 2 will be place the medical imaging diagnostics services and, in building 1 will place the hospitalization services.

Functional relationship	Emergencies	Hemodynamics	Surgery	IUC	ECU	Hospitalization	Clinical laboratory	diagnostic imaging	Esterilization center	Pharmacy	Feeding	Laundry
Emergencies	High	High	Medium	Medium	Medium	Medium	Medium	High	Medium	Medium	Medium	Medium
Hemodynamics	High	High	Medium	High	High	High	High	High	High	High	High	High
Surgery	Medium	Medium	High	High	High	High	High	High	High	High	High	High
ICU	Medium	Medium	Medium	High	High	High	High	High	High	High	High	High
ECU	Medium	Medium	Medium	Medium	High	High	High	High	High	High	High	High
Hospitalization	Medium	Medium	High	High	High	High	High	High	High	High	High	High
Clinical laboratory	Medium	Medium	Medium	Medium	Medium	High	High	High	High	High	High	High
Diagnostic imaging	Medium	Medium	Medium	Medium	Medium	Medium	High	High	High	High	High	High
Esterilization center	Medium	Medium	Medium	Medium	Medium	Medium	Medium	High	High	High	High	High
Pharmacy	Medium	Medium	Medium	Medium	Medium	Medium	Medium	Medium	High	High	High	High
Feeding	Medium	Medium	Medium	Medium	Medium	Medium	Medium	Medium	Medium	High	High	High
Laundry	Medium	Medium	Medium	Medium	Medium	Medium	Medium	Medium	Medium	Medium	High	High

	High relationship: Contiguity, immediacy
	Medium relationship: Non-contiguous but fluid connection
	Low relationship: logistic ratio only

Fig. 6. Matrix of functional relationships for the design of the roadmap

5. Increase in the horizontal connection with the other two bridges between buildings. In this way will be possible to reduce the redundant circulation and workflow convergence.
6. To increase the elevators and expand their ride to all floors in the buildings.
7. Generate leisure and rest areas for the clinical staff.

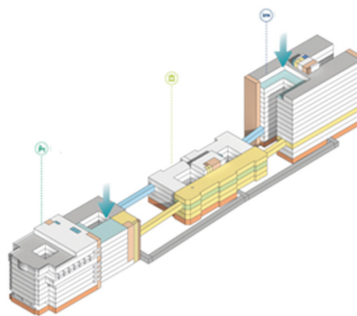


Fig. 7. Planimetric projection of the IPS Universitaria after the implementation of the roadmap.

In Fig. 7 is presented the overview of IPS universitaria facility in a projection of the roadmap implementation. It is possible to observe the clean and soiled

circulation mainly with blue and yellow bridges, also the tunnel for technical circulation and technical networks and equipment movement. As well as the grouping of buildings according to similar clinical services.

In a simulation of the roadmap implementation, the critical ranking of interdependent relationships was ranked again. In Table 2, the comparison between this relationship after and before the roadmap is presented. It is possible to observe that every high relationship will disappear and the medium will be reduced to one. Almost all relationships will have low critical level.

Table 2. Comparison between levels of criticality between relationships of interdependence today and after the implementation of the roadmap

Criticality level	Current relationships	Relationships after roadmap implementation
High	33	0
Medium	28	21
Low	32	71

4 Conclusions

Owing to the implementation of the model described in this study, the characterization of features that were generating higher delays in the healthcare and its support processes offered by the IPS Universitaria was achieved.

The identification of times that decrease institutional productivity associated to infrastructure aspects because represents off times allow to obtain a very close diagnosis to the reality which are responsible for the existence of dead times that generate a decrease in institutional productivity related to physical, technical and infrastructure environment factors.

The items identified were validated with a group of 83 collaborators from the IPS Universitaria with different occupational profiles, guaranteeing coverage in the analysis of critical points on all institutional fronts.

By identifying the critical or failure points, it was possible to classify the most critical technical and care needs, with the aim that they are taken into account for the institution's road map proposal.

The elaboration of an exclusive functional relationship design for the IPS Universitaria was achieved, built based on Colombian regulatory requirements and institutional experience, which served as the basis for the design of the roadmap proposal with the objective of improving the interdependence of services.

After the global proposal of the roadmap and through the same model for calculating the criticality of interdependence relationships, a reduction in the criticality of physical connections between services was achieved by going from 33 to 0% of critical relationships, from 30.01 to 22.8% of moderately critical relationships and from 34.4 to 77.2% of relationships without any type of criticality.

The proposed roadmap raises the possibility of a free space that can be used for the opening of a new service or for a possible increase in the installed capacity of an existing service and there is a significant increase in the common and rest areas for the operational staff of the institution, which indirectly also influence the improvement of institutional productivity.

Conflict of Interest. The authors declare that they have no conflict of interest.



Acknowledgments. The authors would like to thank Bioinstrumentation and Clinical Engineering Research Group (GIBIC) and IPS Universitaria.

References

1. KMD Architects: Design Efficiency in Healthcare (2022)
2. Gregory, L., Weston, L.E., Harrod, M., Meddings, J., Krein, S.L.: Understanding nurses' workflow: batching care and potential opportunities for transmission of infectious organisms, a pilot study. *Am. J. Infect. Control* **47**(10), 1213–1218 (2019)
3. Luxon, L.: Infrastructure—The key to healthcare improvement. *Future Hosp. J.* **2**(1), 4–7 (2015)
4. Ministerio de Salud y de la Protección Social de Colombia. Resolución 3409 (2012)
5. Ministerio de Salud y de la Protección Social de Colombia. Resolución 5095 (2018)
6. Ministerio de Salud y de la Protección Social de Colombia. Resolución 3100 (2019)
7. Tausch, A.P., Menold, N.: Methodological aspects of focus groups in health research: results of qualitative interviews with focus group moderators. *Glob. Qual. Nursing Res.* **3** (2016)



EPID-Based Patient-Specific Quality Assurance in VMAT Radiation Therapy Using Split Arcs

William Correia Trinca¹(✉)  and Ana Maria Marques da Silva² 

¹ Radiotherapy Department, Mãe de Deus Hospital, Porto Alegre, Brazil
william.trinca@gmail.com

² Medical Image Computing Laboratory, Pontifical Catholic University of Rio Grande do Sul, PUCRS, Porto Alegre, Brazil

Abstract. Electronic Portal Imaging Device (EPID) with Portal Dosimetry software (Varian Medical Systems) is a widely used and efficient strategy for performing quality control tests for radiation therapy treatments using Volumetric Modulated Arc Therapy (VMAT). However, a significant limitation is that we have a 3D dose representation projected in a 2D plane along the arcs, which brings many uncertainties to the analysis and is not recommended in many modern studies. This work aims to propose a quality control strategy for treatments with VMAT technique, using division of treatment arcs for quality control measures, in two, four and eight segments, as well as to analyze the best division of arcs in two clinical cases: prostate and head and neck cancers. We analyzed the results using the Portal Dosimetry regarding the required number of arc divisions and how it affects the measurements specificity and sensitivity based on gamma index analysis in Portal Dosimetry software, by inserting controlled errors into the Multileaf Collimator (MLC) positions. We conclude that the division into at least four segments and the careful analysis against the historical baseline results of the service can help to identify cases where some corrective action is necessary or to carry out even more segmented analysis, such as the division into eight parts. We also emphasize that this strategy becomes especially useful due to its practicality in clinical routine, as it is a practical and widely available tool.

Keywords: Radiotherapy · Quality Assurance · VMAT · EPID · Portal Dosimetry

1 Introduction

In modern radiation therapy, one of the main techniques is the volumetrically modulated arc technique (VMAT), which allows high conformation and shorter treatment times through continuous gantry movement, dose rate variation, and dynamic changes in the position of the multi-leaf collimator (MLC). VMAT is typically delivered by performing one or two full rotations around the patient. Several studies confirm the accuracy of dose delivery in VMAT, the stability of these systems, and their clinical results [1, 2]. However, the requirements for careful quality control, particularly the recommendations

for carrying out patient-specific tests, as described in the main international guideline, the Task Group Report 218 of the American Association of Physicists in Medicine (AAPM) [3], can be quite challenging and time-consuming in clinical practice.

In this context, a tool that has gained a lot of space in the clinic is the Electronic Portal Imaging Device (EPID). EPIDs are amorphous silicon panels capable of generating images for positioning verification, with spatial resolution and characteristics capable of making them reliable and practical detectors for dosimetry [4, 5]. EPIDs also showed good results even when compared to detector arrays or volumetric detectors [6, 7]. However, there are at least two important criticisms of its use: the first is detecting a three-dimensional (3D) treatment delivering the dose predicted for a volume, being verified in a two-dimensional (2D) projection. Another critical point is a geometric issue that incidences referring to different treatment regions are absorbed in the same region of the panel when we radiate a complete arc of 360 degrees. These limitations often allow doubts or even create a limitation regarding the EPID use as a means of verification for modulated arc treatments. TG 218 report clearly recommends the tests should not be performed with what it defines as “perpendicular composite - PC” [3], a category where the EPID measurement for arc treatments is inserted. The report, however, allows field-to-field acquisition, which is defined as “perpendicular field-to-field (PFF)”. Normally true for treatments performed with static fields, the EPID use in quality tests is not clearly defined for VMAT treatments.

This study aims to analyze the results of patient-specific quality assurance (PSQA) tests, performing the acquisitions in divisions of the treatment arcs. The strategy divides the main treatment arcs into several segments and analyzes them separately, with controlled error insertions, in the Varian Portal Dosimetry software. In other words, we hypothesize that a PC acquisition could be transformed into something equivalent to a PFF and analyze the strategy sensitivity.

2 Materials and Methods

2.1 Patient Selection

We randomly selected data from twenty patients treated in our institution using the VMAT technique, duly anonymized, for this retrospective study. There were 10 cases of tumors in head and neck (H&N) and 10 prostate cancer treatment cases.

The project was approved by the institutions’ ethics committee (CAAE 55015222.2.0000.5336, report 5.223.470).

2.2 Planning and Error Insertion

All cases were planned on the Eclipse V13.6 software (Varian Medical System, Palo Alto, CA, USA), which has already been validated and irradiated in a Varian Trilogy™ linear accelerator, equipped with a high-definition multi-leaf collimator (HDMLC). Prostate cases were planned with two complete arcs (181° – 179° and 179° – 181°), with collimators rotated at 30° and 330° , while the H&N cases were planned with two complete arcs (181° – 179° and 179° – 181°) with the collimator angles adjusted for each case. We always

used 6 MV energy beams in both group cases, with a nominal maximum dose rate of 600 MU/min.

According to Mu et al. [8], MLC position errors around 1 mm can generate clinical impact, especially on systematic gap errors. Oliver et al. [9] reported that open/closed type MLC errors tended to have a more significant effect on the clinical dose than random or other systematic MLC shift errors that do not open/close gaps. The International Atomic Energy Agency [10] also estimates the acceptable uncertainty of the MLC dynamic position at <1 mm. Therefore, we created three scenarios of systematic errors around 1 mm magnitude, simulated by moving the MLC leaves on a specific segment of each arc. These errors were arbitrarily inserted into a 45° segment of each arc ($1/8$ of arc). This choice was made so that we could control the sensitivity to errors in the expected position. These movements were made by moving the banks in opposite directions resulting in an opening of MLC apertures to avoid collision between leaves, facilitating the error reproduction. Thus, the error was inserted in all pairs of leaves on that segment, always opening half of the desired error in each bank (Fig. 1). The first error inserted was one with the least expected impact, 0.5 mm; the second one was a 1 mm gap, and then a proposition with the highest expected impact, defined as 3 mm. Likewise, we chose different segments for the two clinical sites to avoid a bias in the gantry position, which could be relevant according to Rahman et al. [11] (Fig. 2).

To allow the insertion of these controlled errors, the plan files of the MLC collimators position in DICOM, were exported from the Eclipse system and modified in a Jupyter™ environment, with a specific Python in-house code developed for the purpose. Later, they were be reinserted into the system to carry out the measurements.

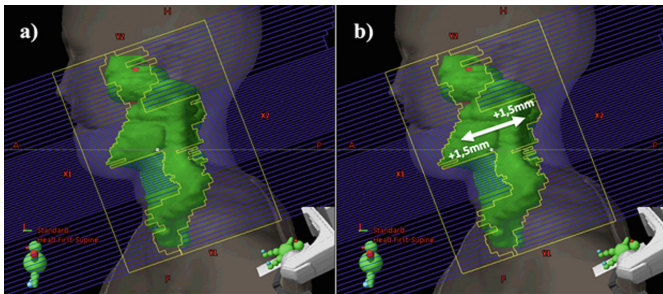


Fig. 1. Beam's eye view for two plans: (a) original Plan and (b) plan with a 3 mm opened MLC.

We evaluated four different types of plans: the original plans without errors and the plans with errors of 0.5 mm, 1 mm, and 3 mm.

2.3 Measurements

We propose an arc splitting strategy to detect mismatch positions, analyzing the sensitivity to these errors using a Varian EPID (model 1000), placed at 100 cm of the source. The original plans had their expected fluence map on the EPID calculated with the Varian PDIP V13.6 algorithm for irradiation with full arcs, dividing each arc into two half arcs,

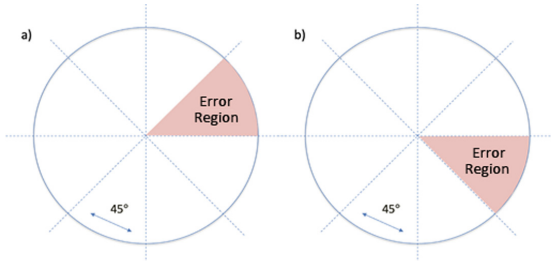


Fig. 2. Position of the segments containing errors for the two clinical cases: (a) Prostate and (b) Head and Neck.

in four semi-arcs or in eight semi-arcs. So, the measurements based on this strategy lead us to analyze the expected fluency in these four arc division scenarios for each of the four types of plans, performing a total of 120 measurements of arcs or semi-arcs on each patient (Fig. 3).

Another important dosimetric aspect is that the measurements of each case were always carried out after absolute dosimetry and always acquired on the same day.

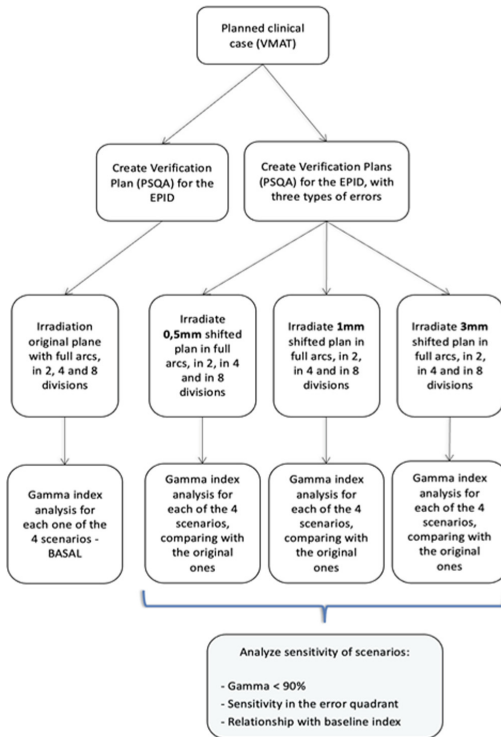


Fig. 3. Flowchart of measurements.

2.4 Planning Analyses

We performed all the analyses using the gamma index evaluation [12] in the Varian Portal Dosimetry V13.6 software (PD). Fluence maps were globally normalized in an absolute way, seeking a distance-to-agreement of 3%/2 mm, and using a 10% threshold. Cases with more than 90% of points within the fields with a gamma index <1 were considered approved. All images were aligned using the auto-alignment tool, seeking to mitigate the problem of arm position during acquisitions.

An essential tool of the PD system is evaluating the fluence measurements of the plans with errors concerning the expected fluences in the original plan (Fig. 4). In addition, it is important to point out that this is a widespread system easily accessible to many radiotherapy departments around the world.

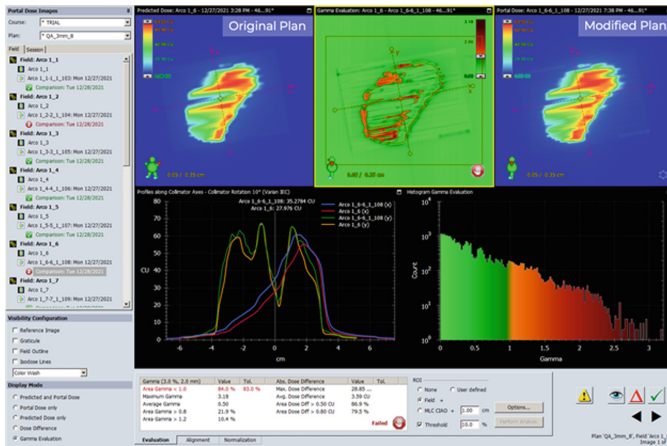


Fig. 4. Gamma Index analyses of a modified plan, compared to the originally expected fluence.

Our goal was to compare the results of the gamma index with the baseline for each scenario, seeking to verify the system’s ability to locate the segment where the errors were inserted. For this, we analyzed the ability to highlight these errors through two variables: segment gamma index below 90%, and a degradation greater than 5% of the basal plan index, in addition to the statistical significance of these variations.

3 Results

3.1 Dosimetric Impact

Given our arbitrary choice of location and segment sizes, we performed an analysis of the dosimetric impact that these errors could have on planning. The dose-volume histograms (DVH) of the plans were calculated to evaluate changes in coverage of the planning target volumes (PTV) and variations in main organs at risk (OAR) for both clinical cases (Table 1). For HN plans we used the spinal cord as surrogate and for prostate plans the

rectum, as both are the most critical structures for each case. The Spinal Cord, as a serial organ, we analyzed maximum dose. For the Rectum, as a parallel organ, we focused on the mean dose.

Table 1. Variation of Dosimetric Parameters of Modified Plans

		PTV _{H&N} D _{95%}			Spinal Cord % D _{max}		
Case	Site	0,5 mm	1 mm	3 mm	0,5 mm	1 mm	3 mm
1	H&N	0.1%	0.3%	0.9%	-0,1%	0,3%	1,9%
2	H&N	0.0%	0.2%	0.8%	-0,1%	0,3%	2,3%
3	H&N	0.2%	0.4%	1.1%	-0,3%	0,0%	1,4%
4	H&N	0.1%	0.3%	1.0%	-0,2%	0,2%	1,9%
5	H&N	0.1%	0.3%	1.0%	-0,2%	0,1%	1,7%
6	H&N	0.1%	0.3%	1.0%	-0,2%	0,1%	1,8%
7	H&N	0.1%	0.2%	0.5%	0,4%	0,7%	2,2%
8	H&N	0.1%	0.2%	0.8%	0,1%	0,4%	2,0%
9	H&N	0.1%	0.2%	0.6%	0,2%	0,6%	2,1%
10	H&N	0.1%	0.2%	0.7%	0,2%	0,5%	2,0%
Mean		0.1%	0.3%	0.8%	0,2%	0,3%	1,9%
		PTV _{Prostate} D _{95%}			Rectum % D _{mean}		
		0.5 mm	1 mm	3 mm	0.5 mm	1 mm	3 mm
11	Prostate	0.2%	0.5%	1.2%	0.5%	1.0%	2.8%
12	Prostate	0.2%	0.4%	1.1%	0.5%	1.0%	3.1%
13	Prostate	0.2%	0.3%	0.9%	0.4%	0.8%	2.2%
14	Prostate	0.2%	0.4%	1.1%	0.3%	0.7%	2.1%
15	Prostate	0.3%	0.5%	1.5%	0.4%	0.8%	2.3%
16	Prostate	0.2%	0.4%	1.1%	0.4%	0.7%	2.0%
17	Prostate	0.1%	0.2%	0.6%	0.3%	0.6%	1.7%
18	Prostate	0.2%	0.3%	0.9%	0.3%	0.6%	1.6%
19	Prostate	0.2%	0.3%	0.9%	0.3%	0.6%	1.8%
20	Prostate	0.2%	0.3%	0.9%	0.3%	0.7%	2.0%
Mean		0.2%	0.4%	1.0%	0.4%	0.7%	2.2%

It is important to consider that errors from 1 mm are considered a level of action by the IAEA and that they can generate clinical impact. We can also note that the uncertainty of dose delivery in radiotherapy is on the order of 2.1% [10]. So, we conclude that the sub-millimetric errors of 0.5 mm had practically no dosimetric significance, with the variations ranging from 0,1 to 0,4%. The 1 mm case produced a low impact, varying

from 0,3% to 0,7%. However, a higher error of 3 mm, even only in one segment, has generated a result that could lead to clinical impact, with a variation of $D_{95\%}$ of $0.8\% \pm 0.2\%$ for the H&N cases and $1.0\% \pm 0.2\%$ for the prostate cases, while for the OARs we found a variation of $1.9\% \pm 0.3\%$ on the spinal cord D_{\max} and $2.2\% \pm 0.5\%$ for the D_{mean} of the rectum.

3.2 Prostate Plans

Ten prostate cases were irradiated for the four scenarios and analyzed concerning the expected original fluences. The variations of the gamma indexes and their significance are shown in the table below (Table 2):

Table 2. Variation of gamma index values for prostate cases in relation to baseline values. In red, the segments where the errors are inserted; in Bold the results out of tolerance and with p value $<0,05$

Setup	Arcs	Error 0,5mm		Error 1mm		Error 3mm	
		Var (%)	<i>P</i>	Var (%)	<i>P</i>	Var (%)	<i>P</i>
Full Arcs	1	0,1	0,108	0,1	0,165	-1,0	0,001
	2	-0,2	0,148	0,1	0,048	-0,6	<0,001
Split 2	1.1	-0,2	0,510	0,2	0,033	0,2	0,067
	1.2	-0,2	0,003	-0,3	0,001	-3,0	<0,001
	2.1	-0,4	0,178	0,1	0,616	-2,5	<0,001
	2.2	0,0	0,745	0,3	0,014	0,1	0,136
Split 4	1.1	-0,2	0,305	0,2	0,277	0,0	0,709
	1.2	-0,1	0,223	0,0	0,430	0,0	0,918
	1.3	-0,5	<0,001	-0,9	<0,001	-7,2	<0,001
	1.4	-0,2	0,185	0,2	0,153	-0,1	0,283
	2.1	-0,4	0,274	0,3	0,036	0,1	0,594
	2.2	-0,4	0,018	-0,3	0,021	-5,9	<0,001
	2.3	0,0	0,438	0,2	0,054	0,1	0,167
	2.4	-0,2	0,027	0,1	0,462	0,0	0,775
Split 8	1.1	-0,2	0,306	0,5	0,126	0,5	0,016
	1.2	0,0	0,631	0,4	0,007	0,4	0,027
	1.3	-0,1	0,771	0,2	0,018	0,1	0,295
	1.4	-0,1	0,154	0,0	0,622	-0,1	0,181
	1.5	0,0	0,783	0,2	0,274	0,2	0,198
	1.6	-0,7	0,007	-1,7	<0,001	-13,5	<0,001
	1.7	-0,2	0,060	0,0	0,927	-0,3	0,026
	1.8	-0,6	0,106	0,3	0,192	0,3	0,084
	2.1	-0,2	0,333	0,2	0,694	0,3	0,647
	2.2	0,0	0,975	0,1	0,458	0,2	0,113
	2.3	-0,7	0,002	-1,7	<0,001	-14,5	<0,001
	2.4	-0,2	0,035	0,1	0,513	-0,1	0,708
	2.5	0,0	0,772	0,6	0,080	0,4	0,166
	2.6	0,2	0,380	0,3	0,067	0,0	0,711
2.7	-0,1	0,131	0,3	0,051	0,2	0,132	
2.8	-0,3	0,244	0,2	0,265	0,4	0,011	

We observed the errors in the 0.5 mm plans were practically not detected in any of the arc divisions, while the 1 mm errors, even with smaller values systematically detected ($p < 0.05$) also do not clearly sign the presence of mismatches when we analyze the absolute values and its clinical significance. However, in the 3 mm error scenario, where we know that there is a real important dosimetric variation, an important reduction in the approval of points for division into 4 quadrants was noted, with reductions of $6.6 \pm 1.7\%$ and $5.6 \pm 1.8\%$ (both $p < 0.001$), but gamma indexes (Table 3) of $91.2\% \pm 1.6\%$ and $93.0\% \pm 2.2\%$, respectively, touching the borderline of the 90% approval. In the division into 8 octants, we could see an evident abrupt drop, with variations of $13.7\% \pm 3.5\%$ and $15\% \pm 2\%$ (both $p < 0.001$) and gamma indexes pass rates of $85.1\% \pm 4.0\%$ and $83.6\% \pm 2.5\%$.

Table 3. Gamma index absolute values of Prostate cases for divisions in four and eight segments. In red, values below 90%.

Prostate	Arcs	Orig	Mod 0,5mm	Mod 1mm	Mod 3mm
Split 4	1.3	98,2	97,7	97,3	91,0
	2.2	98,4	98,0	98,1	92,5
Split 8	1.6	98,7	98,1	97,1	85,2
	2.3	98,2	97,5	96,5	83,7

3.3 Head and Neck Plans

Ten head and neck cases were irradiated for the four scenarios and analyzed in relation to the expected original fluences. The variations of the gamma indexes and their significance are shown in the table below (Table 4):

As we noticed on the Prostate plans, the errors in the 0.5 mm plans were practically not detected in any of the arc divisions, while the 1 mm errors, even with smaller values again systematically detected ($p < 0.05$), also do not clearly sign the presence of mismatches on the absolute values. For the 3 mm errors cases, we found an important reduction in the approval of points for division into 4 quadrants, with reductions of $6.5 \pm 1.7\%$ and $4.9 \pm 1.8\%$ ($p < 0.001$) and gamma indexes of $91.0\% \pm 1.6\%$ and $87.9\% \pm 2.2\%$, respectively. In the division into 8 octants, we could see again an evident abrupt drop, with variations of $17.8\% \pm 3.5\%$ and $15\% \pm 2\%$ ($p < 0.001$) and Gamma Indexes pass rates of $78.1\% \pm 4.0\%$ and $82.6\% \pm 2.5\%$ (Table 5).

Table 4. Variation of gamma indexes for head and neck cases in relation to the baseline. In red, the segments where the errors are inserted; in bold results out of tolerance and with $p < 0.05$

Setup	Arcs	Error 0,5mm		Error 1mm		Error 3mm	
		Var (%)	<i>P</i>	Var (%)	<i>P</i>	Var (%)	<i>P</i>
Full Arcs	1	0,2	0,514	0,0	0,804	-0,3	0,059
	2	0,2	0,377	0,1	0,587	-0,3	0,098
Split 2	1.1	0,1	0,563	-0,2	0,174	0,0	0,846
	1.2	-0,2	0,007	-0,4	0,015	-1,9	0,010
	2.1	-0,2	0,051	0,0	0,754	-1,5	0,017
	2.2	0,0	0,789	0,0	0,741	0,0	0,801
Split 4	1.1	-0,2	0,111	0,0	1,000	0,1	0,376
	1.2	0,0	0,714	-0,1	0,264	0,1	0,633
	1.3	-0,2	0,096	0,0	0,702	0,0	0,922
	1.4	-0,5	<0,001	-0,9	<0,001	-6,0	<0,001
	2.1	-0,9	0,022	-0,9	<0,001	-5,3	<0,001
	2.2	0,0	0,704	0,0	0,427	-0,1	0,454
	2.3	-0,1	0,302	-0,1	0,279	-0,1	0,487
	2.4	0,1	0,359	0,4	0,022	0,1	0,578
Split 8	1.1	-0,1	0,238	0,1	0,589	0,0	1,000
	1.2	0,1	0,586	0,1	0,502	0,0	0,898
	1.3	0,1	0,384	0,0	0,904	0,1	0,457
	1.4	-0,1	0,244	-0,1	0,387	-0,1	0,757
	1.5	0,1	0,405	0,0	0,931	0,1	0,410
	1.6	0,0	0,832	-0,2	0,223	-0,1	0,337
	1.7	-1,5	<0,001	-3,9	<0,001	-16,2	<0,001
	1.8	-0,1	0,391	-0,1	0,621	0,0	0,956
	2.1	0,0	0,938	0,2	0,113	0,1	0,832
	2.2	-1,1	0,001	-2,8	<0,001	-13,7	<0,001
	2.3	-0,3	0,128	-0,1	0,506	-0,3	0,026
	2.4	0,1	0,490	0,0	0,733	0,0	0,954
	2.5	0,2	0,197	1,0	0,392	0,1	0,825
	2.6	-0,1	0,215	0,0	0,809	-0,1	0,120
2.7	-0,1	0,454	-0,1	0,513	-0,1	0,382	
2.8	0,0	0,780	0,0	0,670	0,2	0,341	

Table 5. Gamma index absolute values of head and neck cases for divisions in four and eight segments. In red, values below 90%.

Head and Neck	Arcs	Orig	Mod 0,5 mm	Mod 1 mm	Mod 3 mm
Split 4	1.4	96.6	96.1	95.7	90.6
	2.1	94.9	94.0	94.0	89.6
Split 8	1.7	93.8	92.2	89.9	77.6
	2.2	94.1	93.0	91.3	80.4

3.4 Error-Free Arcs

A secondary result obtained is also the analysis of the variation of the readings along the sub-arcs where there is no insertion of errors. We analyzed the differences between the three measurements done for each sub-arc, focusing only on the segments where we had no insertion of mismatch positions. For the prostate cases, we found an average error of $0.0 \pm 0.2\%$, and for the H&N plans, $-0.1 \pm 0.4\%$, with only four segments (in a total of 132) showing significant values ($p < 0.05$), but all with absolute differences below 1%.

4 Discussion

Our results indicate that the measurements carried out with arc divisions in the EPID have an outstanding sensitivity for detecting errors of small magnitude, even if they are below the threshold of clinical relevance, according to the analysis of the impact on PTV coverage and doses in organs at risk.

Yan et al. [13] evaluated the sensitivity of patient-specific IMRT quality assurance procedures to minor MLC leaf positioning errors. Random errors of up to 2 mm and systematic errors of ± 1 mm and ± 2 mm in MLC leaf positions were introduced into clinical IMRT plans. They found that the detectors (film and array) could only detect 2 mm or above errors. Tatsumi et al. [14] studied systematic leaf position errors generated by directly changing a leaf offset in a linac controller measured on the array. Using three TPS, they concluded that 1 mm was defined as an upper limit that maintains pass rates of 2% under a dose difference of 2%.

In our study, the 0.5 mm errors were undetected in any configuration, and we attribute it to both the small dosimetric impact and the small segment size. Perhaps systematic errors along the entire arc might be more relevant, although the literature shows that submillimeter errors have little effect in any situation [8, 9, 13, 14].

Errors of the magnitude of 1 mm, placed in an octant of the arc, were detected in a systematic and statistically significant way from the division into four sub arcs for the two clinical cases, although the results themselves were not consistently below the criteria of acceptance of gamma index analysis. This phenomenon demonstrates that the EPID with PD is capable of detecting small variations, of the order of 1 mm, even with subclinical relevance, in a context of setup errors inserted in the MLC along a single octant. However, for these small errors and segment magnitudes, at least a division into 4 quadrants was necessary to demonstrate this difference.

When we analyzed the 3 mm errors in an octant, where we estimate a clinical impact of up to 2%, the system was able to consistently detect the errors since from the division into 4 quadrants, already approaching the threshold of gamma index approval. In the division into 8 parts, the error is detected clearly and unequivocally, with pass rates systematically below 90% for the defined criteria.

These results corroborate the theory suggested by TG 218 that PC-type acquisitions could mask and dilute errors along the arcs, not even showing any of the setup errors inserted. Although the magnitude of the errors chosen was not large, we demonstrated that the strategy of division into sub-arcs proved to be effective for detecting small errors, from divisions of at least 4 quadrants, in the two studied clinical cases.

Among the limitations of this work, we can point out the arbitrary choice of magnitude errors and their extension along the arc, limiting our conclusions on other scenarios. Likewise, the selection of two clinical cases and 20 patients is limited. However, it is important to highlight that the analysis of the clinical impact of the errors inserted shows that the system was able to systematically detect errors of the magnitude where they could start to impact the treatment effectively. Another issue, as explained by Bailey et al. [15], is that PD compares calibrated response plans to a TPS portal dose prediction algorithm based on the actual fluence calculation. Consequently, PD does not directly audit the TPS dose calculation algorithm beyond the actual fluency. Therefore, other forms of QA (e.g., secondary MU calculations) are necessary to supplement this limitation.

As a suggestion for further work, other types of errors could be addressed, as well as different extensions along the arcs, or even different segmentations for analysis, contributing to even more effective conclusions about what is the best strategy to leave the analysis of sub-arcs the most sensitive and closest to a PFF analysis. This study also did not consider other sources of possible errors in VMAT, such as gantry variations, collimators, and dose rate, which could also be performed with EPID [16].

5 Conclusions

We conclude that the strategy of dividing the EPID-based patient-specific quality assurance with portal dosimetry into sub-arcs is effective for detecting errors in the setup, especially for divisions of at least four quadrants. Errors with possible clinical relevance were identified, even when they were not detected in the setup of full arc., We believe that the division into at least four sub-arcs and the careful analysis concerning the service's baseline results could help identify cases where some corrective action is necessary or carry out even more investigations, as in the division into eight segments. We also emphasize that the strategy becomes especially useful due to its practicality in clinical routine, as it is practical and widely available.

Acknowledgment. We thank the Mãe de Deus Hospital for allowing the use of the systems and PUCRS for academic support.

Conflict of Interest. The authors declare that they have no conflict of interest.

References

1. Otto, K.: Volumetric modulated arc therapy: IMRT in a single gantry arc. *Med. Phys.* **35**(1), 310–317 (2008). <https://doi.org/10.1118/1.2818738>
2. Teoh, M., et al.: Volumetric modulated arc therapy: a review of current literature and clinical use in practice. *Br. J. Radiol. Radiol.* **84**(1007), 967–996 (2011). <https://doi.org/10.1259/bjr/22373346>
3. Miften, M., et al.: Tolerance limits and methodologies for IMRT measurement-based verification QA: recommendations of AAPM task group No. 218. *Med. Phys.* **45**(4), e53–e83 (2018). <https://doi.org/10.1002/mp.12810>

4. van Elmpt, W., et al.: A literature review of electronic portal imaging for radiotherapy dosimetry. *Radiother. Oncol.: J. Eur. Soc. Ther. Radiol. Oncol.* **88**(3), 289–309 (2008). <https://doi.org/10.1016/j.radonc.2008.07.008>
5. Bakhtiari, M., et al.: Using an EPID for patient-specific VMAT quality assurance. *Med. Phys.* **38**(3), 1366–1373 (2011). <https://doi.org/10.1118/1.3552925>
6. Kausar, A., Mani, K., Azhari, H., Zakaria, G.: Patient-specific quality control for intensity-modulated radiation therapy and volumetric-modulated arc therapy using electronic portal imaging device and two-dimensional ion chamber array. *J. Radiother. Pract.* **18**(1), 26–31 (2019). <https://doi.org/10.1017/S1460396918000328>
7. El Kafhali, M., Khalis, M., Tahmasbi, M., Sebihi, R., Velasquez Sierra, L.: Clinical experiment on quality control comparison of complex treatment plans of the VMAT technique using a diode-based cylindrical phantom (ArcCHECK) and an amorphous silicon-based planar detector (A-Si1000). *Phys. Med.* **12**, 100044 (2021). <https://doi.org/10.1016/j.phmed.2021.100044>
8. Mu, G., et al.: Impact of MLC leaf position errors on simple and complex IMRT plans for head and neck cancer. *Phys. Med. Biol.* **53**(1), 77–88 (2008). <https://doi.org/10.1088/0031-9155/53/1/005>
9. Oliver, M., et al.: Clinical significance of multi-leaf collimator positional errors for volumetric modulated arc therapy. *Radiother. Oncol.: J. Eur. Soc. Ther. Radiol. Oncol.* **97**(3), 554–560 (2010). <https://doi.org/10.1016/j.radonc.2010.06.013>
10. International Atomic Energy Agency: Accuracy Requirements and Uncertainties in Radiotherapy, Human Health Series (2016)
11. Rahman, M.M., et al.: Segmental analysis trial of volumetric modulated arc therapy for quality assurance of linear accelerator. *Prog. Med. Phys.* **30**(4), 128–138 (2019)
12. Low, D.A., et al.: A technique for the quantitative evaluation of dose distributions. *Med. Phys.* **25**(5), 656–661 (1998). <https://doi.org/10.1118/1.598248>
13. Yan, G., et al.: On the sensitivity of patient-specific IMRT QA to MLC positioning errors. *J. Appl. Clin. Med. Phys.* **10**(1), 120–128 (2009). <https://doi.org/10.1120/jacmp.v10i1.2915>
14. Tatsumi, D., et al.: Direct impact analysis of multi-leaf collimator leaf position errors on dose distributions in volumetric modulated arc therapy: a pass rate calculation between measured planar doses with and without the position errors. *Phys. Med. Biol.* **56**(20), N237–N246 (2011). <https://doi.org/10.1088/0031-9155/56/20/N03>
15. Bailey, D.W., et al.: EPID dosimetry for pretreatment quality assurance with two commercial systems. *J. Appl. Clin. Med. Phys.* **13**(4), 3736 (2012). <https://doi.org/10.1120/jacmp.v13i4.3736>
16. Liang, B., et al.: Comparisons of volumetric modulated arc therapy (VMAT) quality assurance (QA) systems: sensitivity analysis to machine errors. *Radiat. Oncol. (London, England)* **11**(1), 146 (2016). <https://doi.org/10.1186/s13014-016-0725-4>



Clinical Decision Support System to Managing Beds in ICU

Edgar D. Báez , Sofia J. Vallejos , and Maria I. Pisarello  

Faculty of Exact and Natural Sciences and Surveying, Northeast National University, Av.
Libertad 5400, Corrientes, Argentina
mainespisarello@exa.unne.edu.ar

Abstract. This work proposes an AI-based machine learning model using the supervised learning algorithm and a decision tree that allows analyzing and predicting the degree of affectation in patients for their corresponding hospitalization in a Coronary Intensive Care Unit (CICU). The methodology used follows the scientific method that allowed us to investigate and examine all kinds of studies, results and research. The dataset used was obtained from the repository, coming from a hospital specialized in cardiovascular diseases. The total performance of the model reaches 79.27% of accuracy. With these f-score it is possible to determine the state of gravity of a patient and the action to take according to their state.

Keywords: Hospital record · Medical informatics · Artificial intelligence · Prediction

1 Introduction

In comparison to other sections of hospitals, the intensive care unit (ICU) is one of the most complex and specialized ones. In consequence, having a patient treated in these therapies is extremely costly. Moreover, it has one of the highest mortality rates and admits a relatively large number of patients.

Modern hospitals tend to optimize their services and reduce costs. In this intelligence, ICU becomes a critical section where evaluation, comparison and improvement of their performance results significant in order to achieve these goals. This motivation carries out to measure outcomes indices, including hospital mortality and length of stay [1].

However, most of the medical information systems that are collected in a hospital, in general, traditionally focus on collecting data for management and not on increasing the quality of care, efficiency and patient safety, which should be the purpose of these health information systems. It is common not to take advantage of the prediction of the future behavior of some health problems present in the Electronic Health Records (EHR), based on the understanding of the past. For this reason, the implementation of electronic systems designed to help clinical decision-making was promoted. These systems are intended to improve the accuracy, timeliness, quality and overall effectiveness of a particular decision or set of related decisions [2].

The huge amount of clinical data, recorded in the EHR, allows the use of algorithms that could predict diseases, get statistical information and help in the management of beds in critical sections such as ICU. Machine Learning (ML) and Deep Learning models depend on data for training, and the amount of data needed to reach adequate performance must be large enough. In the clinical context, data comes from various sources, and sometimes sits in databases without much use. In the case of Electronic Medical Records, detailed information about patients is stored indefinitely and could be handled to train predictive models that enable precision healthcare. One of the main impediments for widespread adoption of advanced ML and DL in healthcare is lack of interpretability [3, 4].

Additionally, predictions are tools that allow us to increase the certainty in the diagnosis. Many critically ill patients remain in inadequate wards due to lack of space in special cardiology care units. This last situation is particularly frequent when the patient, who has passed the most critical period of his illness, remains in the coronary unit (CU), either due to lack of beds in the conventional hospitalization ward or because his risk, although not justified admission to the UC exceeds the care capacity of a conventional ward [5].

In this sense, clinical decision support systems (CDSs) are active knowledge systems that use one or more sets of patient data to generate medical recommendations that integrate with EHR. Their ultimate goal is to support health professionals in decision-making and to help improve the interaction between scientific evidence and patient information. The lack of information given the lack of efficient computer systems makes it difficult to make informed and timely decisions [6].

The objective of this manuscript is to link the innovation context of the technoscientific activity process with the construction of knowledge, using machine learning algorithms (ML) to model and simulate the implicit inferences of experts in decision making. AI algorithms discover knowledge or patterns by proposing alternatives to understand the problem posed, renewing the abstracted reality. A System is proposed that allows the visualization of relevant information to support decision-making, with the aim of maximizing clinical and social benefits, and minimizing the costs associated with the management of basic hospital beds, intermediate and critical therapies.

2 Methods

Statement of the research question.

The purpose of the research is to identify the machine learning (ML) algorithm that allows classifying and predicting the degree of complexity of the state of the heart of a patient [7]. For systematic mapping, the following research question is defined:

Q: What is the impact of using a ML algorithm to obtain a model that identifies severity for patient care?

This will make it possible to obtain a record of current studies for the analysis and prediction of the degree of complexity of cardiovascular diseases.

2.1 The CRISP-DM Model

In this project, the CRISP-DM model was selected for its flexibility since it is necessary to perform an exploration of large amounts of data without a specific modeling objective. To collect the necessary data in the investigation, interviews were conducted with specialists in this area. Data contained in the data table was submit to a rigorous analysis based fundamentally on the representation of reality, consistency, unnecessary fields, empty fields and data of a hybrid or not very genuine nature. The medical team assesses blood tests, laboratory tests and vital signs.

2.2 Data Preparation and Analysis

Data were taken from patients who had been admitted to the Hospital specialized in Cardiology, which is the object of our study. A time window of 1 year -2019 was taken. Patients considered were women, men and children with different cardiac pathologies. The hospital is a highly complex health center specializing in cardiovascular diseases. It has digital medical records that make up relational data tables from which we extracted the data. To collect the necessary data in the investigation, interviews were conducted with specialists in this area. Each of the variables that were taken into account was described to optimize their understanding. The data contained in the warehouse was subjected to a rigorous analysis based fundamentally on the representation of reality, consistency, unnecessary fields, empty fields and data of a hybrid or not very genuine nature. Access and retrieval are manual processes. These steps required a combination of IT and healthcare professional expertise. Within this framework, data recovery was performed with a small multidisciplinary team of professionals. The analysis of the data begins with the description of the results of each variable separately. For some variables there are reference intervals that are established in healthy people using statistical methods. The data considered were: age; sex; number of times the patient has been admitted to each section of the hospital: emergency, floor, ICU; etc.; latest laboratory values such as potassium, red blood cells, hemoglobin, blood glucose, hematocrit, serum creatinine, cardiac ultrasound data, electrical activity, death or not of the patient.

The set of actions and technologies for data preparation and analysis consists of the following steps:

1. Access to data: from multiple sources
2. Data retrieval: In the exploration, a combination of structured and semi-structured data in different types of repositories emerges. Data of the electronic medical record type that record events of the current disease or medical history. Other data are laboratory tests, vital signs, pharmacotherapy that the patient is receiving or has received.

For some variables there are reference intervals that are established in healthy people using statistical methods. Being out of this range can indicate the presence or absence of disease or risk of suffering from it. For this reason this extra information was added to the set of data provided, in addition to being out of range it is important to know how far out it is. The variables out of range were proposed by the team of IT professionals.

3. Data cleansing: All information in the file is anonymous and cannot be traced back to any specific patient. Although not all security concerns are eliminated, this ensures that individual patient data will not be misused if the data is stolen or hacked. Information dissociation procedures were applied, so that the owners of the data are NOT unidentifiable, the dissociation technique that was used does not allow any person to be identified, in accordance with the provisions of article 28 of Law 25326 (Protection Law of personal data).

Among the most frequent situations can be named: missing values, values out of range, null values and blank spaces that hide values. There were also some outliers that could bias the results of the analysis. Errors in the data that affect quality had to be corrected.

4. Data formatting: Once the data set was cleaned, it needed to be formatted to continue with data preparation and analysis. This step includes troubleshooting how to fit multiple date formats in the data. Also some data variables are not necessary for the analysis and therefore had to be removed from the data set.

5. Merge the data: When the data has been cleaned and formatted, the next step for data preparation and analysis is to transform it by merging, splitting, or joining the input sets. Once the data has been loaded into the data warehouse staging area, there is a second chance for validation.

In the construction of Dataset1, some data taken into account were the following:

The initial dataset with which the work began contained 696 records and 31 columns.

Blank spaces in text-type fields and periods in numeric-type fields correspond to missing or missing values.

Each record has a unique record or index identifier (InCabNPrin). Figure 1 shows the initial dataset.

InCabNPrin	FacieNro	Edad	FacieSexo	InternacionesEnEMER	InternacionesEnPISO	InternacionesEnRCVA	InternacionesEnRCVP	\	
0	64261	385508	60	F	0	1	0	0	
1	62107	474566	61	M	0	1	0	0	
2	60406	381482	48	M	0	2	0	0	
InternacionesEnUTI	UltPotasio	...	ECO_FEY	ECO_IndiceDeMasa	ECO_Tisular	ECO_VolumenAuriIzq	FueraRangoFEY50-75	\	
0	0	4.3	...	33	NaN	16.0	NaN	1	
1	0	4.0	...	55	NaN	8.0	NaN	0	
2	0	4.7	...	46	71.0	5.0	20.0	1	
FueraRangoIxMasc<95F<115M	FueraRangoECO_Tisular<15	FueraRangoECO_VolumenAuriIzq<34	ECGAnormal	Obito					
0	0	1	0	0					
1	0	0	0	0					
2	0	0	0	0					

Fig. 1. Initial Dataset.

With a data set processed and explored, it is necessary to create a matrix of independent variables and a vector of dependent variables. The variable selection method used was Forward Stepwise Regression. In this method, variables are sequentially entered into the model. The first variable that is introduced is the one with the highest correlation (+ or -) with the dependent variable. In this case Deaths in the first instance. After performing the pertinent analysis, we observed that the results were highly influenced

by the imbalance in the data set. Almost 99% of the “alive” class, compared to 1% of the “death” class. In both the training and test groups, the data set is unbalanced; therefore, the accuracy rate obtained is falsely high. For example, in unbalanced data, when the ratio of positive and negative samples is 9:1, when its precision is 90%, the model prediction tends to classify the samples in the majority class. It leads to an ineffective prediction. The information contained in the minority class is very limited, so it is difficult to determine the distribution of its data, that is, it is difficult to find the rules within it.

For this reason, we chose to take another target variable that allows an analysis closer to reality.

2.3 Proposed Strategy

By using the death variable as a target, an important part of the information has been left out, since those who died outside the medical institution considered are not included. It seeks to generalize and establish business rules on how to grant a bed in the CICU to those patients classified as high risk with a high score, and refer those patients with less care to another type of hospitalization. This makes it possible to significantly reduce the workload of medical specialists, and/or increase the volume of data processed with the same number of staff.

Unlike the previous dataset, only the patient’s last hospitalization is taken if he or she had more than one. The sample period covers a period of one year.

Our main objective is to predict if a patient should go to the CICU. The results of how many patients in reference to the number of hospitalizations in the CICU are illustrated in Fig. 2. It is observed that the maximum number of hospitalizations in the CICU is 6, most of the values are 0 (zero) hospitalizations accounting for 548 cases. In this situation, it is convenient to convert the numerical value to nominal, in a discretization process.

Decision tree model

We build a model using decision trees. We create the parameters “x” and “y” and use the fit() method to perform the training and then the predict() instruction to make a prediction. To set up the model we specify the mean squared error to implement data separation.

We evaluate the predictive capacity of the tree by calculating the accuracy in the test data set. Next, we evaluate the proportion of correctly predicted instances (TP and TN) over the total sum of elements evaluated. We perform the corresponding calculation:

$$\text{Accuracy} = \frac{270 + 1}{270 + 1 + 73 + 1} = \frac{271}{345} =$$

$$\text{Accuracy} = 0.78550724.$$

$$\text{Accuracy for the test} = 0.78550724$$

To find the balance between the depth and complexity of the tree with respect to the predictive capacity of the model on test data, the decision tree is usually grown to its greatest extent and then the pruning process is executed to identify the optimal sub-tree, in this case the depth is increased to six.

Fitting the model using formulas

We apply the Exploratory Regression tool to evaluate all the possible combinations of possible input explanatory variables, looking for models of Ordinary Least Squares (Ordinary Least Squares OLS). Results are shown and explained in the following section.

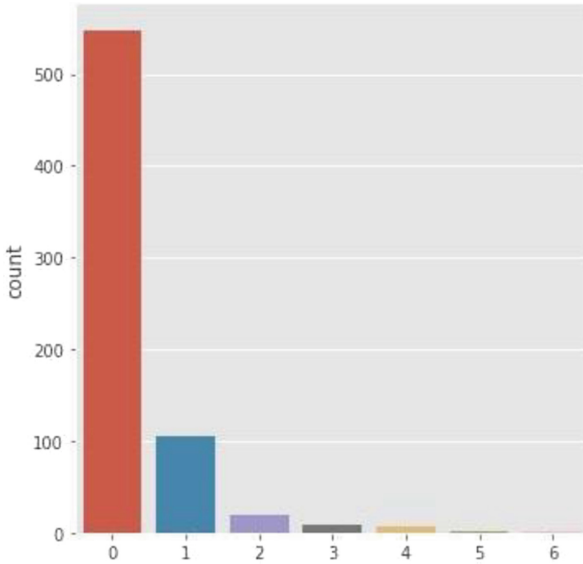


Fig. 2. Initial Dataset

3 Results

When creating a model, it is important to study the distribution of the response variable, which is our main interest, and the independent variables, those that determine the value of the dependent variable.

The independent variables are analyzed graphically using histograms, as shown in the figures. We show the data graphically to get an idea of their dispersion. Figure 3 shows the histograms of the variables Serum Creatinine and of the Ultrasound of the ejection fraction. In the model, these are the variables that contribute the most. Our results were validated by the team of advisors.

The peak of the density graph shows where the values are concentrated in the interval value 1.22 mg/l. The minimum value 0.4 mg/l and the maximum 7.3 mg/l. Figure 4 shows the histogram of the Potassium variable and Fig. 5 shows statistical data corresponding to the same variable. The average value 4.1215 mmol/L coincides with the highest peak of the histogram.

We categorized admissions to the CICU into two groups: those who had never been to the CICU 0 and another group, those who had been to the CICU 1 or more times.

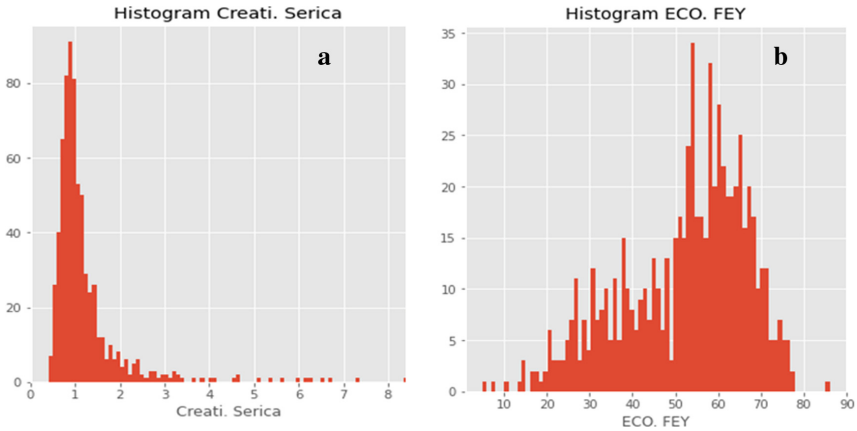


Fig. 3. a) Histogram of creatinine serica; b) Histogram of ECO.FEY

The total in each category yields 548 patients who were never hospitalized (0) and 142 patients who were hospitalized once or more.

Figure 6 illustrates the correlations between variables when CICU admissions have been categorized.

With this information about the distribution, we can analyze the data, make statistical inferences, and identify which distribution the data best fit. The distance that separates the cluster represented by the red points (0 hospitalizations) from the others that are more mixed is appreciable.

As mentioned in Section II, we compute the correlation coefficient, R , to look at the influence of each of the independent variables separately with the dependent variable. We also calculate the coefficient of determination, also known as R^2 (R squared), to determine how well the regression line fits to the data. We take the dependent variable InterEnUCICEncoded using the Least Squares method, multiple R-squared and adjusted R-squared values are measures of model performance.

Possible values range from 0.0 to 1.0. For this model, the R-squared value is 0.012 and the adjusted R-squared is 0.010. The adjusted R-squared value is always slightly lower than the multiple R-squared value, because it reflects the complexity of the model (the number of variables), as it relates to the data and is therefore a more accurate measure of performance of the model. An adjusted R-squared value of 0.012 will indicate that the model explains approximately 1 percent of the variation in the dependent variable. In other words, the model counts approximately 1% of cases of CICU admissions.

Logistic Regression (RL) aims to estimate the parameters of the equation ($\beta_0, \beta_1, \beta_2, \dots, \beta_k$), for this case the values are those shown in Fig. 7.

$$Z = 0.241634 - 0.005071 \times \text{UltPotasio} + 0.046359 \\ \times \text{CreatiSerica} - 0.001403 \times \text{ECO_FEY}$$

Once the classifier model has been trained on the data, it is possible to make predictions on the test set data.

The model has been trained and can now be used to predict new instances in the test dataset.

It is expected that the predictive model developed from these data will serve as a guide for the center specialist to make a decision about admission to the CICU. As an example, a patient with: Potassium = 4.9 mmol/L, Creati.Snerica = 0.4 mg/dL and Ultrasound FEY = 37.0% SHOULD NOT go to CICU.

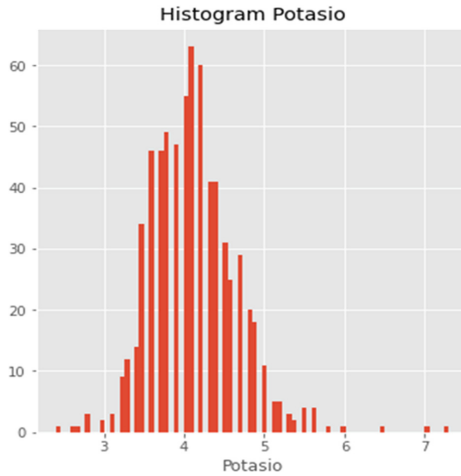


Fig. 4. Histogram of Potassium

```
Potasio Promedio: 4.12159420289855
Desvio Std Potasio: 0.5405854032395461
Intervalo para asignar Potasio aleatoria: 3 a 4
```

Fig. 5. Statistical data of Potassium

Figure 8 illustrates the application of these values to the model and the returned result [0] indicating that it should not go to CICU.

Next, we try to make a decision about admission to the CICU, a patient with: Potassium = 3.0 mmol/L, Creati.Serica = 8.5 mg/dL and Ultrasound FEY = 31.0% SHOULD go to the ICCU. Figure 9 illustrates the application of the case.

The returned result [1] indicating that YES you should go to UCIC. For this model, its confusion matrix is the one illustrated in Fig. 10.

We evaluate the predictive capacity of the model by calculating the F1-score, which takes into account the precision and recall in the test data set. The values are illustrated in Fig. 11.

To validate our results, we presented and discussed them with the center’s team of specialists. All results were positively validated.

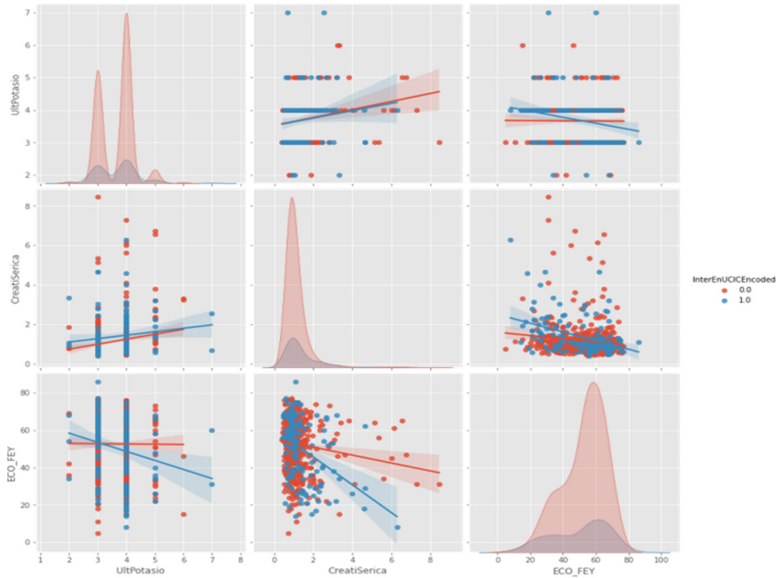


Fig. 6. Correlations between variables when admissions to the CICU have been categorized.

β estimados:

```
Intercept      0.241634
UltPotasio     -0.005071
CreatiSerica   0.046359
ECO_FEY        -0.001403
dtype: float64
```

Fig. 7. Parameters of the equation.

```
: # Relaciona Input con Output
# define input
new_input = [[4.9 , 0.94, 37.0]]
# get prediction for new input
new_output = model.predict(new_input)
print("Prueba:",new_input, new_output)
```

```
Prueba: [[4.9, 0.94, 37.0]] [0.]
```

```
: model.score(X,y)
```

```
: 0.7927536231884058
```

Fig. 8. Model test for return result [0].

```
# predigo
# define input
new_input = [[3.0 , 8.5, 31.0 ]]
# get prediction for new input
new_output = model.predict(new_input)
print("Pruebo:",new_input, new_output)

Pruebo: [[3.0, 8.5, 31.0]] [1.] ←
```

Fig. 9. Test of the model where YES you should go to CICU

```
print(confusion_matrix(Y_validation, predictions))

[[270  1]
 [ 73  1]]
```

Fig. 10. Confusion matrix

```
# Reporte de clasificación
print(classification_report(Y_validation, predictions))
```

	precision	recall	f1-score	support
0.0	0.79	1.00	0.88	271
1.0	0.50	0.01	0.03	74
accuracy			0.79	345
macro avg	0.64	0.50	0.45	345
weighted avg	0.73	0.79	0.70	345

Fig. 11. Predictive ability of the mode

4 Conclusions

One of the most important conclusions that emerged from this work is the importance of the use of AI in the medical field, through the application of ML algorithms that allow improved data classification and interpretation techniques, disease prediction, time saving and available resources. After the analysis, we can deduce that the rules of behavior identified collaborate with the decision making of the doctors of the CICU. In effect, it allows determining the state of severity of a patient and what action to take according to their state, substantially reducing the time that a doctor must invest to identify it.

The main objective of this study was to develop a ML model that allows predicting, analyzing, and forecasting the degree of severity in patients with coronary heart disease by using decision trees to prevent CICU congestion.

It is concluded that, referring to the study and the experimental analyzes that have been carried out in other prediction models, the decision tree model assured us almost an 80% of effectiveness in the prediction.

The greatest achievement of this work is the development of a tool that, based on the hospital's own data, obtains an applicable and functional model that takes into account the particularities of the population under study.

A future project would be to design of a computer prototype capable to provide support to specialists in an average of a few seconds, with a high success rate and with a clear display that minimizes ambiguities.

Acknowledgment. This development was carried out as a transfer project under the call phase zero of the Sadosky Foundation dependent on the Ministry of Science, Technology and Innovation of Argentina.

Authors would like to acknowledge the Secretary General of Science and Technology of the Northeast National University, for their support through PI18-F008.

Conflict of Interest The authors declare that they have no conflict of interest.

References

1. Maharlou, H., Kalhori, S.R.N., Shahbazi, S., Ravangard, R.: Predicting length of stay in intensive care units after cardiac surgery: comparison of artificial neural networks and adaptive neuro-fuzzy system. *Healthc. Inform. Res.* **24**(2), 109–117 (2018)
2. Nanayakkara, S., Fogarty, S., Tremeer, M., Ross, K., Richards, B., Bergmeir, C., Kaye, D.M., et al.: Characterising risk of in-hospital mortality following cardiac arrest using machine learning: a retrospective international registry study. *PLoS Med.* **15**(11), e1002709 (2018)
3. Caicedo-Torres, W., Gutierrez, J.: ISeeU: visually interpretable deep learning for mortality prediction inside the ICU. *J. Biomed. Inform.* **98**, 103269 (2019)
4. Che, Z., Purushotham, S., Khemani, R., Liu, Y.: Interpretable deep models for ICU outcome prediction. In: *AMIA Annual Symposium Proceedings*, vol. 2016, p. 371. American Medical Informatics Association (2016)
5. Kim, J., Park, Y.R., Lee, J.H., Lee, J.H., Kim, Y.H., Huh, J.W.: Development of a real-time risk prediction model for in-hospital cardiac arrest in critically ill patients using deep learning: retrospective study. *JMIR Med. Inform.* **8**(3), e16349 (2020)
6. Sutton, R.T., Pincock, D., Baumgart, D.C., Sadowski, D.C., Fedorak, R.N., Kroeker, K.I.: An overview of clinical decision support systems: benefits, risks, and strategies for success. *NPJ Digit. Med.* **3**(1), 1–10 (2020)
7. Assaf, D., Gutman, Y.A., Neuman, Y., Segal, G., Amit, S., Gefen-Halevi, S., Tirosh, A., et al.: Utilization of machine-learning models to accurately predict the risk for critical COVID-19. *Intern. Emerg. Med.* **15**(8), 1435–1443 (2020)



Development of Best Practices Virtual Resources to Assist in the Safe Use of Health Technologies in an Interdisciplinary Ecosystem

Mariana Ribeiro Brandão^(✉)  and Renato Garcia Ojeda 

Department of Electrical Engineering (DEEL), Biomedical Engineering Institute (IEB-UFSC), Federal University of Santa Catarina (UFSC), Florianópolis, Brazil
marianaribeirobrandao@gmail.com

Abstract. During the pandemic, Clinical Engineering faced the need to develop virtual activities. This study presents the platform development of virtual resources, contributing to the Best Practices of safe and reliable use of health technologies, as a way of guiding the safe operation. The guiding resources were developed using the Design Thinking approach, employing the principles of user-centered development, and using the PDCA quality tool. Best Practices resources from different technologies were developed, validated and made available, as from the Interdisciplinary Internship Program at IEB-UFSC. The guiding resources of Best Practices developed were implemented through the development of folders with safe guidelines and a platform for providing webinars in a virtual way, allowing access and participation to several professionals from different locations nationally and internationally, encouraging the dissemination of qualified knowledge about the use of health technologies. This platform allowed, during this special pandemic situation, to disseminate important concepts of Best Practices by Clinical Engineering, aiming to contribute to the reduction of adverse events and the development of materials contributed to the formation of an innovative, interdisciplinary and collaborative ecosystem involving health technologies. These activities significantly contribute to the activities of Clinical Engineering, aiming to guide and train users in the safe and reliable use of health technologies.

Keyword: Best Practices · Clinical Engineering · Interdisciplinarity

1 Introduction

The safe and reliable use of health technologies requires the interaction between human resources, infrastructure and technology in the consolidation of an environment aimed at reducing risks in a multidisciplinary ecosystem in health systems, based on the methodology developed at IEB-UFSC, elucidated in Fig. 1. Aiming to contribute to the safety, reliability and effectiveness of technological processes in health environments [1], the interaction between the three pillars becomes essential to contribute to Clinical Engineering (CE) in Health Technology Management (HTM). In order for technologies to be used safely and with less risk to the patient, the correct use is essential to avoid errors

that can compromise the quality of care and cause damage. For this, it is essential to constantly manage the quality of the technological process in the development of guidance materials and the application of Best Practices. Best Practices are a valuable tool for health systems as they help standardize processes and provide professional training to perform certain activities correctly.

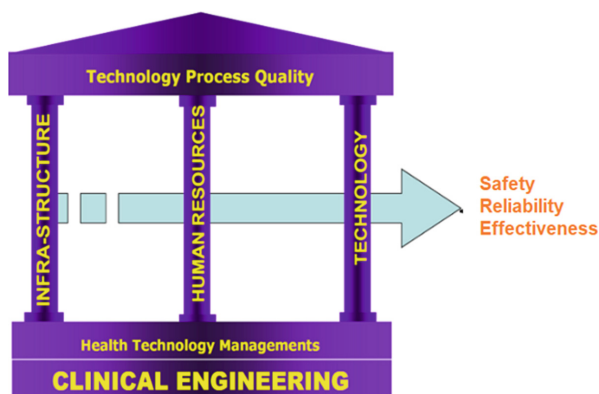


Fig. 1. Technological process in health IEB-UFSC model [1].

Best Practices consist of evidence-based health methods, interventions, procedures or techniques to obtain better health care and assist in decision making [2]. According to Perleth, it is “*the ‘best way’ to identify, collect, evaluate, disseminate, and implement information about as well as to monitor the outcomes of health care interventions for patients/population groups and defined indications or conditions.* [4]”. However, one of the great challenges of Best Practices applied in health involves adapting to the needs of each population, requiring research to be incorporated in different types of environments [2].

The term Best Practices is recurrently used in health care areas, and as technologies are increasingly present, it is necessary to implement guidance resources with evidence-based guidelines for the purpose of safer and more appropriate uses. In order to have Best Practices, it is necessary to collect information regarding available evidence on safety, efficacy, social and ethical values, in addition to the quality of health interventions [4].

As a result of the increase in the development and availability of increasingly digital content, to attend the needs of guiding and disseminating information for the proper use of technology, the Biomedical Engineering Institute (IEB-UFSC) developed a virtual platform, implemented by interdisciplinary teams, with a series of virtual resources on Best Practices in the safe and reliable use of health technologies, as a way to reduce adverse events, guiding the safe use of health technology.

Guidance materials are means used to disseminate information with the objective of training, instructing and educating equipment operators [11]. To minimize the problems involving the technologies, different virtual resources of orientation were developed based on the analysis of usability techniques and considering principles of Human Factors Engineering [12].

The elaboration and implementation of guidance resources, aims to contribute to Clinical Engineering in guaranteeing an adequate use of technologies, preventing them from being operated erroneously, compromising users of the equipment and possibly leading to damage to the patient. Best Practices aim to contain guidelines for solving a user's problem [3], and through the adoption of user-centered design principles, it collaborates to minimize possible unwanted health events [13]), by developing products centered on from the user's perspective, integrated to their context and tasks [9, 10].

One of the approaches to user-centered development widely used in different sectors, including healthcare, is Design Thinking, a methodology focused on problem solving centered on user needs, working with interdisciplinary teams in a continuous and interactive process with all stakeholders [5, 6, 14].

The IEB-UFSC incorporates into its activities the approach of the PDCA cycle (Plan-Do-Check-Act), so that activities are managed properly, and that improvement actions are identified and implemented periodically [12, 15].

This work aims to present a methodology proposal and to develop guidance resources containing Best Practices in the safe and reliable use of technologies, incorporating in its activities the process approach of the PDCA cycle. These guiding resources were carried out at the IEB-UFSC in an interdisciplinary ecosystem, with the purpose of contributing to Clinical Engineering in the safer HTM and with less risk of adverse events for users.

2 Materials and Methods

The guiding resources were developed using the principles of user-centered development, using the Design Thinking approach and using the PDCA quality tool. Initially, a multidisciplinary team was formed through the integration of undergraduate and graduate students in an interdisciplinary internship program composed of several courses, such as engineering, medicine and dentistry. Through these teams, with the support of the technical and administrative team of the IEB-UFSC, resources of Best Practices of different technologies were developed, validated and made available to society. Manuals and folders were developed, as well as a virtual platform for making webinars available. Webinar consists of a virtual event with live streaming.

For the development of manuals and folders, the steps were based on the PDCA, which consist of: planning and structuring, which includes activities to define the format and theme, responsible persons; execution, which encompasses studies, training and preparation of materials and availability; followed by critical analysis and development of an action plan in search of continuous improvements, consisting of a feedback system of information.

The proposed and applied methodology is an adaptation of the design thinking approach, and encompasses three main stages, they are: immersion, systematization and implementation, where in each of these phases there must be a continuous interaction with the users of the technology. During the immersion, a deeper understanding of the problems that users have is performed, and a data collection is carried out to explore the problem. In the systematization, a structuring and classification of the data generated in the previous phase is realized. In the implementation, prototypes must be developed to carry out evaluations and adjustments, as shown in Fig. 2.

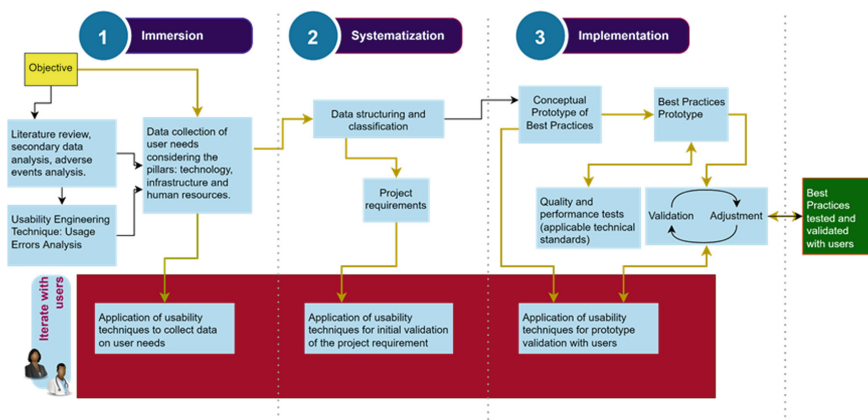


Fig. 2. Methodology proposal for the development of virtual resources of Best Practices for the safe use of health technologies.

3 Results

The guiding resources of Best Practices developed at the IEB-UFSC were manuals and folders containing guidelines with safe guidelines for the proper use of health technologies and a platform for making webinars available in a virtual way, allowing several professionals from different locations, encouraging the dissemination of qualified knowledge in the use of health technologies. For the development of these resources, an interdisciplinary team was structured and trained, through the implementation of an Interdisciplinary Internship Program.

This program included training in areas of Clinical Engineering, such as metrology in health, Dimensioning and Incorporation of Health Technologies, Health Technologies Assessment, Human Factors Engineering, in addition to specific training in Medical Equipment. During the training sessions, the technical and clinical impacts on the use of technologies were addressed and discussed, bringing perspectives from both the clinical and technical areas.

Guidance resources were developed according to the methodology presented, using the design thinking approach and the PDCA cycle, according to the methodology presented in Fig. 2. Initially, an immersion was carried out based on the collection of information and evidence; both in articles through systematic searches in databases; and in the investigation of adverse event notifications in the ANVISA (National Health Surveillance Agency, Brazil) and MAUDE-FDA (Food & Drug Administration) databases; technical standards, ordinances and resolutions; operating manuals for medical equipment; documents and reports issued by government agencies and experiences of the IEB-UFSC team.

In the systematization stage, the information collected during the immersion phase was structured and analyzed, and ended with the implementation of good practice materials. In this final stage, prototypes were developed by the IEB-UFSC interdisciplinary

team and continuous improvements were applied. An example of a best practice developed is illustrated in Fig. 3, which consists of a manual for the safe operation of infrared thermometers,

The materials developed encompassed themes related to Best Practices in the use of Clinical Infrared Thermometer, Dental Chair, Pulse Oximeter, Steam Sterilization, Infusion Pump, Lung Ventilator; in addition to other topics in the HTM, such as innovations and digital health, metrology, safety and quality in technologies, Design Thinking, Medical Equipment regularization and certification, Health Technology Assessment, Human Factors Engineering, among others, in order to provide professionals and guide them in the proper use of technologies.



Fig. 3. Best Practices Manual in the Use of Infrared Thermometer developed at IEB-UFSC, in Portuguese.

The Best Practices contributed to the provision of information in a more illustrative way, prepared through the collaboration and continuous involvement of the interdisciplinary team, following regulations, usage protocols and manuals of equipment.

Another orientation virtual resource format also developed using the PDCA methodology for execution were Webinars. A total of 25 Webinars have been developed on a recurring basis since August 2020, reaching a wide audience, both from the technical area as well as health professionals, government agencies, industries, among others. The webinars have a prior registration and are available later on the platform. A total

of 2387 people signed up for the 25 webinars, and a total of 13,000 users accessed the platform as of July 2022. The platform contains the webinars as well as short videos of safe operation of health technologies.

Among those enrolled in the Webinars, 38.7% were students (undergraduate engineering students represent 40.58% of the total number of students; 25.97% refer to undergraduates in health courses, 29.44 post graduate students from various professional areas and others were not specified); 20.5% represent professionals graduate in some Engineering; 19.7% refer to health professionals and 13% to technicians, and 8% to other areas, as shown in Fig. 4.

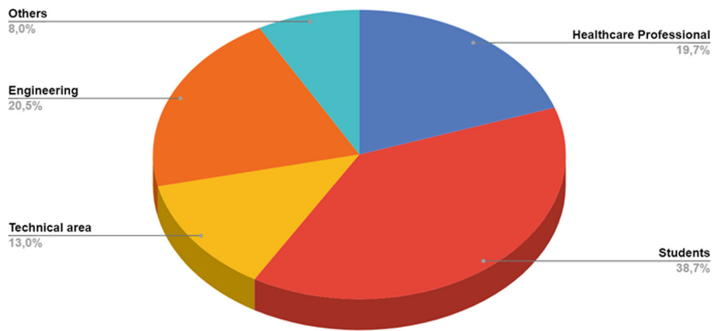


Fig. 4. Profile of IEB-UFSC webinar participants.

Regarding the course, the most expressive audience is Electrical Engineering, with a representation of 21.9%, followed by Biomedical Engineering with 14.7%, nursing with 10.9%, dentistry with 8.3%, in addition to medicine, design, other engineering and other areas, as shown in Fig. 5.

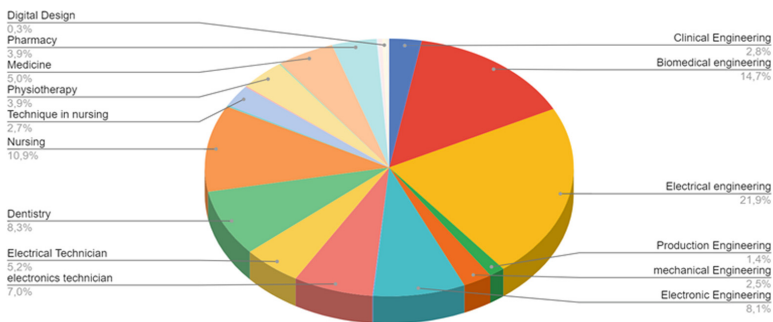


Fig. 5. Areas of IEB-UFSC webinar participants.

In addition, the webinars had national and international coverage, with the participation of professionals and students from all regions of Brazil and from different continents, with significant Latin American participation, contributing to a global impact on the safer use of technologies, as shown in Fig. 6.

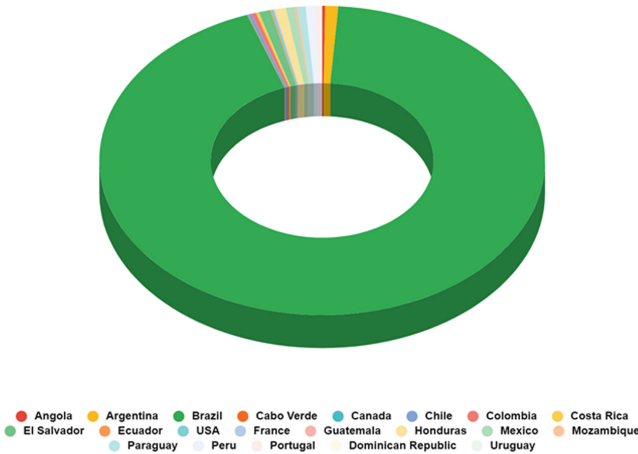


Fig. 6. Profile of IEB-UFSC webinar participants.

The themes of the Webinars were different, such as: safety and reliability of Medical Equipment; Best Practices in the processing of medical devices; Neonatology Equipment; Health Technology Assessment; Medical Equipment Usability; Technological Innovations; Medical Devices Regularization and Certification; Best Practices in the use of High Frequency Electrosurgical Units, Dental Accessories, Lung Ventilator, Multiparameter Monitor, Infusion Pump, Infrared Thermometer, among many other topics.

The choice of webinar topics and best practice materials was based on: areas of Clinical Engineering aligned with the IEB-UFSC Health Technology Management methodology; availability of medical equipment in the Health Metrology laboratories and simulated Human Factors Engineering laboratories in Primary Health Care and Intensive Care Units; resulting from the analysis of adverse events in medical devices conducted at the IEB-UFSC and other topics proposed by researchers and interdisciplinary team.

4 Discussion

The active involvement of people with a multidisciplinary profile in the technological development process was considered when designing the virtual resources involving the technologies, in convergence with discussions brought by Branaghan et al. [5]. In addition, the continuous evaluation of projects enabled rapid and dynamic improvements that better meet the needs of users.

In order to train human resources in the HTM, and aiming to stimulate the creation of an innovative ecosystem between different areas of activity, the implementation of the interdisciplinary internship program contributed to the development of an environment for stimulating ideas to improve the existing solutions in health. The interaction between different areas is essential to show the importance of integration for the improvement in the use of health technologies, as also discussed by Kim [16].

The content made available digitally contributed to the impact and wider dissemination of information, making it possible to reach audiences in different locations in Brazil as well as internationally. The development of guidance resources in a virtual way contributed to the dissemination of information that was previously restricted to presence environments, making it possible to assist in the democratization of access to safe and reliable data.

The contribution of the development of virtual guidance resources of Best Practices in the HTM goes through helping in the proper orientation in the use of technologies, preventing the occurrence of errors that can cause damages to the users. As discussed by Flewwling et al. [8], the development of training should encompass the difficulties faced by users to mitigate the occurrence of usage errors. Therefore, a continuing education program must consider the problems faced by users on a day-to-day basis with technology, both in incorporation and throughout the entire lifecycle. The methodology presented in this work for the development of guidance resources can be applied to analyze the problems faced with technologies and, thus, establish actions that can improve their use in health environments. For technologies that are already incorporated in the establishments, analyzing the difficulties that operators face and developing materials with guidelines aimed at solving the problems, consist of strategies to be introduced by Clinical Engineering, in convergence with the recommendations of Brandão and Garcia [7].

Aspects of safety and reliability, with the application of a platform of safe and reliable information, it is possible to disseminate knowledge and impact the quality of the population's health, including in critical public health situations. As future work, it is suggested to develop other virtual resources to guide the use of technologies, such as materials for training using virtual and augmented reality. Furthermore, to reach even more health professionals who work in health facilities for safer operation of technologies. Another future step is to incorporate the results generated in the work in a didactic virtual platform for safe and reliable guidance of technologies, to be made available to users, aiming to integrate and centralize all information. In addition, to integrate the information generated at work in a technological platform to contribute to the interoperability of data in medical devices.

5 Conclusion

The platform with the availability of virtual resources made it possible to disseminate important concepts of Best Practices by Clinical Engineering, aiming to contribute to the dissemination of information on health technology management and proper operation of medical equipment. With this, it contributed to the formation of an innovative, interdisciplinary and collaborative ecosystem involving health technologies. Manuals, folders and webinars were developed at the IEB-UFSC involving different themes and made available to the population, with national and international coverage. The virtual resources fostered aspects of security and reliability, with the application of a secure and reliable information platform, allowing the dissemination of knowledge and impacting the population quality of life. These activities are important and significantly contribute to the responsibilities of Clinical Engineering, aiming to guide and train users in the safe and reliable use of health technologies.

The IEB-UFSC interdisciplinary internship program aimed to integrate the areas of health and exact sciences to encourage teamwork and develop activities focused on solving users' problems regarding the safe and quality use of health technologies. The use of the PDCA methodology for the development of guidance resources allowed the establishment of a feedback system, which was possible from the application of feedback forms sent to subscribers after the webinars, making it possible to periodically analyze opinions and establish improvements and topic suggestions. Through the forms, new themes were implemented in the webinars and adjustments were made, such as having a more practical part with the technologies during the transmissions.

The interdisciplinary and collaborative involvement of different actors in Clinical Engineering is fundamental for health safety. The development of guidance resources significantly contribute to the activities of Clinical Engineering, aiming to guide and train users in the safe and reliable use of health technologies, aiming to preventively minimize the risks that occur in health care.



References

1. Garcia, S.J.A., et al.: Health care technology management applied to public primary care health. In: Pan American Health Care Exchanges, pp. 250–253 (2011)
2. Ten, H.W., Minnie, K., Van der Walt C (2020) Improving healthcare: a guide to roll-out best practices. *Afr. Health Sci.*, 1487–1495. <https://doi.org/10.4314/ahs.v20i3.55>
3. Nelson, A.M.: Best practice in nursing: a concept analysis. *Int. J. Nurs. Stud.* (2014). <https://doi.org/10.1016/j.ijnurstu.2014.05.003>
4. Perleth, M., Jakubowski, E., Busse, R.: What is 'best practice' in health care? State of the art and perspectives in improving the effectiveness and efficiency of the European health care systems (2001). [https://doi.org/10.1016/s0168-8510\(00\)00138-x](https://doi.org/10.1016/s0168-8510(00)00138-x)
5. Branaghan, R.J., et al.: Human Factors in Medical Device Design. *Critical Care Nursing Clinics of North America*, pp. 225–236 (2018). <https://doi.org/10.1016/j.cnc.2018.02.005>
6. Brandão, M.R., et al.: Systematic review of design thinking applied to medical devices. *Int. J. Knowl. Eng. Manag.*, 165–180 (2021). <https://doi.org/10.47916/ijkem-vol9n25-2020-84852>
7. Brandão, M.R., Garcia, R.: Descriptive analysis of user-centered usability techniques to health technology management. In: 43° Congreso Nacional de Ingeniería Biomédica, México (2020)
8. Flewwelling, C.J., et al.: The use of fault reporting of medical equipment to identify latent design flaws. *J. Biomed. Inform.*, 80–85 (2014). <https://doi.org/10.1016/j.jbi.2014.04.009>
9. Ritter, F., et al.: Foundations for Designing User-Centered Systems. Springer, London (2014)
10. Norman, D.: *The Design of Everyday Things* (2002)
11. International Electrotechnical Commission: IEC/TR 61258:2008 Guidelines for the Development and Use of Medical Electrical Equipment Educational Materials, 2nd ed. Geneva (2008)
12. Brandao, M.R.: Proposal for a Methodology for the Application of Usability Techniques in Clinical Engineering to Contribute to the Development and Use of Technological Solutions for Health. Federal University of Santa Catarina, Florianópolis, Brazil (2021)
13. Brazilian National Standards Organization: ABNT NBR ISO 9241-210:2011: Ergonomics of Human-System Interaction Part 210: Human-Centered Design for Interactive Systems (2011)

14. Altman, M., et al.: Design Thinking in Health Care (2018)<https://doi.org/10.5888/pcd15.180128>
15. Avelar, P.S., et al.: Medical-hospital technology management as a clinical engineering strategy in home care in Brazil. In: IV Latin American Congress on Biomedical Engineering, pp. 1203–1206 (2007). https://doi.org/10.1007/978-3-540-74471-9_279
16. Kim, H.N.: A conceptual framework for interdisciplinary education in engineering and nursing health informatics. Nurse Educ. Today (2019). <https://doi.org/10.1016/j.nedt.2018.12.010>. PMID: 30639937



Use of a HAPI FHIR Server and Development of a Multi-user Web Interface for Visualization and Analysis of Data from Patients with Diabetes Mellitus

Maicon Francisco^(✉)  and Jefferson Luiz Brum Marques 

Institute of Biomedical Engineering, Federal University of Santa Catarina, Florianópolis, Brazil
maicon.francisco@posgrad.ufsc.br

Abstract. Estimates show that from 2019 to 2045, the number of people with Diabetes Mellitus could increase from 463 million to 700 million. Brazil follows this trend, and studies have shown that the country is the third country with the highest expenditure on diabetes. Studies with secure and interoperable databases are necessary to manage the disease. The Institute of Biomedical Engineering of the Federal University of Santa Catarina is developing the Screening for Diabetes Complications project, which seeks to collect, process, store and analyse data from patients with Diabetes Mellitus. This article presents the implementation of a HAPI FHIR server, which meets the HL7 FHIR communication standard, and an ElasticSearch server to complement and facilitate requests to the FHIR server. It also presents the development of a web interface, using an MVC architecture, for multiple users to visualize and analyze the collected data, meeting the General Data Protection Law requirements in Brazil.

Keywords: Diabetes Mellitus · HAPI FHIR · ElasticSeach · Web Interface · MVC design pattern

1 Introduction

Diabetes Mellitus (DM) has become a significant health challenge, reaching alarming numbers of people with the diagnosis. It is estimated that in 2019, the number of people with DM around the world was 463 million and the projection for 2045 is that this number may reach 700 million people [1].

The number of people with DM in Brazil follows the same worldwide trend. Accordingly to epidemiological data from the Brazilian Society of Diabetes [2], between 2006 and 2018, the prevalence of men and women with DM older than 18 increased by 54% and 28%, respectively. In 2019, the number of Brazilians aged 20–79 with DM was 16.8 million. Also, Brazil is the third country with the highest health expenditure related to DM [1].

The studies and monitoring of the disease make it possible to carry out control and apply precise measures for the treatment and better quality of life. For a person with DM,

control of blood glucose and cardiometabolic risk factors, medication management, and early monitoring of complications with an organised health system reduce the acute and chronic complications of the disease and prolong the lives of these individuals [3].

Other countries report having diabetes monitoring records but do not provide sufficient information about their outcomes. In low-income countries, few vital reports are recorded, and the reliability of data collection on diabetes is dubious and incomplete. Most data on diabetes derived from monitoring systems in most countries are sparse and inadequate, and most countries do not have a system to evaluate national actions or programs [4].

In Brazil, the National Health Data Network (RNDS) was established in 2020 as the national platform for interoperability in the healthcare system; this interconnectivity environment is to be fully implemented by 2028. In addition to being a structuring project of the Connect SUS, the RNDS is a Federal Government program to carry out the digital healthcare transformation in Brazil, aiming to promote the exchange of information between the Health Care Network, allowing for the transition and continuity of care in public and private sectors [5].

The implementation of an interoperable healthcare system requires a standard protocol, and the RNDS has defined the HL7 (Health Level Seven) FHIR (Fast Healthcare Interoperability Resources) to exchange information [5].

Considering the increasing number of people with DM and the current restructuring of the health data system in Brazil, the Institute of Biomedical Engineering of the Federal University of Santa Catarina (IEB-UFSC) is developing a project to record and monitor data from patients with DM, using a system called SDC-X (Screening for Diabetes Complications).

The article presents the structuring of the SDC-X project, the use of an HL7 FHIR server complemented by the ElasticSearch server, and the development of a multi-user web platform to present the data to be monitored, seeking to comply with the current Law of Data Protection (LGPD) in Brazil.

2 Materials and Methods

2.1 SDC-X Project

The SDC-X project is a system to assess patients with DM from different locations through data collection, storage and analysis. The “X” of the acronym represents the various data acquisition modules and may represent data related to the cardiovascular, visual, and other physiological systems.

The SDC-X comprises four modules (Fig. 1): the Acquisition Module, Concentrator Module, Storage Module, and Analysis and Interface Module.

The Acquisition Module consists of a set of equipment for collecting vital signs. This data is then processed, analysed and sent to the server by the Storage Module. The Storage Module contains the HL7 FHIR server that must receive the data and make it available to the Analysis and Interface Module through an API (Application Programming Interface). The Analysis and Interface Module then presents the data in different formats for different users.

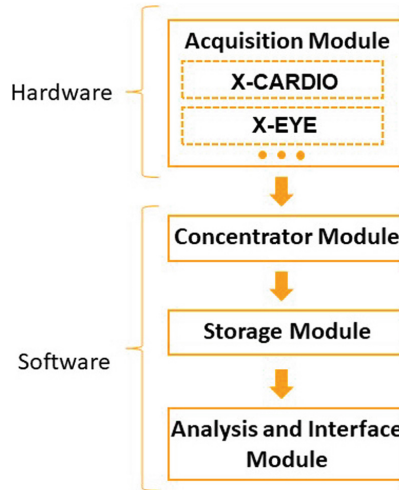


Fig. 1. SDC-X project comprises four blocks, where the Acquisition Module is essentially hardware, and the other 3 are software.

Every module was developed for different researchers at the IEB-UFSC. The Acquisition Module has, until now, three hardware developed: X-Cardio, X-Eye and X-Esc. How these modules were developed and how they work can be viewed in [6–8]. These developments involve non-invasive measurements, but other relevant information is more significant to monitoring the DM and involves invasive measures, like Hb1A1c, HDL [9, 10], blood glucose and cholesterol [10].

The Concentrator Module is software installed in a computer, where the data are collected, processed, analysed and send to the Storage Module [6].

2.2 HL7 FHIR and ElasticSearch Servers

HL7 is a non-profit organisation credited with creating standards for sharing, integrating, exchanging and requesting electronic health information. The HL7 FHIR, built in 2011, is a standard that proposes to facilitate the exchange of information by combining web standards and focusing on implementation. It is structured in a data model that can be accessed via a URL via REST (Representational State Transfer), called “Resources” [11–13].

Access to the server must be performed through RESTful requests, and the responses are delivered in XML (eXtensible Markup Language) or JSON (Javascript Object Notation) formats through an API (Application Programming Interface) [11, 12].

The data store must be mapped to specific resources described in the HL7 FHIR documentation [11].

An ElasticSearch server is implemented to assist the FHIR server in more complex tasks. ElasticSearch is a free and open distributed data search and analysis engine for all data types, including textual [14].

2.3 SDC-X Interface

The web interface represents the Analysis and Interface Module of the project. This interface intuitively presents patient information and collected data through the Acquisition Module for different user profiles (e.g., patient, clinician, health manager) [15].

The interface is developed using the MVC (Model-Views-Controller) design pattern and PHP as the programming language. This design pattern structures the project in 3 layers, which helps to reduce coupling and promotes increased cohesion in the project's classes, facilitating code maintenance and reuse [15].

Within the project structure, the three layers are separated by tasks. The Model layer communicates with servers and databases; the interface, i.e., what the user sees, is created by the Views layer, and the Controller is the layer that executes the user's actions. The communication between the layers is represented in Fig. 2, and the arrows represent information exchanges between layers [15].

All users go through the interface module, as shown in Fig. 3. The user accesses the platform through a login and password system using his previously registered profile. The servers return with the data to be presented through the interface.

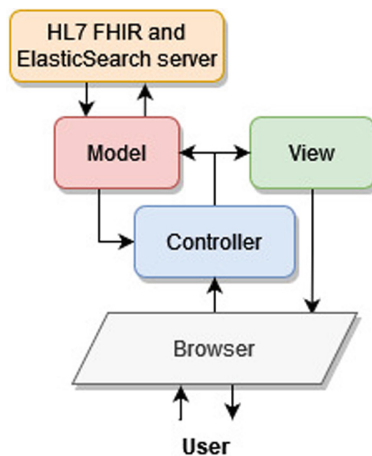


Fig. 2. Diagram of the MVC model. The user interacts with the system through a browser, interpreting the View layer. The Controller executes user requests through the browser and sends commands to the Model and View layers [15].

The interface allows five user profiles: Administrator, Patients, Researcher, Practitioner and Manager. The data accessed in each profile follow a permissions rule verified by the Controller and Model blocks. The description of each user profile is presented below.

Administrator: It controls who can access the project interface.

Patient: This user only views their data.

Researcher: This user accesses the raw data, preserving patient identification. This profile allows to export and process of data as desired.

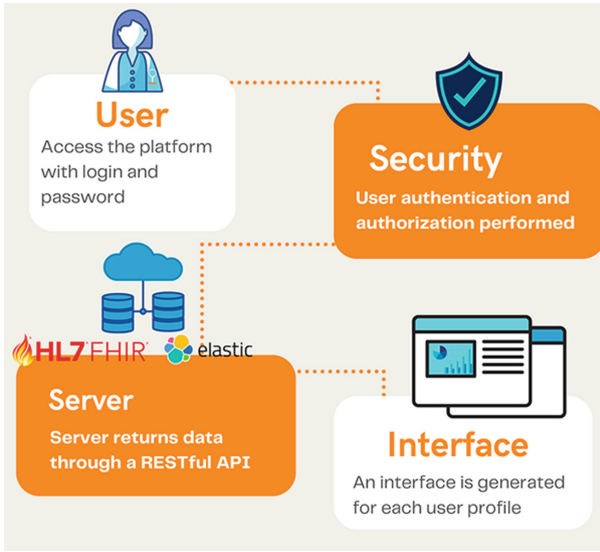


Fig. 3. SDC-X Project Analysis and Interface Module System Flowchart.

Practitioner: This profile is implemented for health practitioners who can consult direct information from patients.

Manager: This user has access to a series of analyses of the set of data collected. This profile is intended to assist in obtaining information from the health system, thus allowing the establishment of goals and solutions in an informed and accurate manner.

3 Results

All tests were performed locally, where the interface application was executed through the XAMPP server (version 3.3.0), an open-source server developed by Apache Friends. Furthermore, for the HL7 FHIR and Elasticsearch servers, Docker software (version 4.3.0) was used, an operating system-level virtualisation system that delivers software in packages called containers.

3.1 FHIR Server and Data Usage

Dummy data were used by a Synthetic Patient Population Simulator called Synthea. This simulator generates realistic data, but not from patients in different formats, including the FHIR [16]. One thousand simulated patients were developed for the tests, and 824 had diabetes, which was included in the database.

The open-source server HAPI (HL7 Application Programming Interface) was used, a complete implementation of HL7 FHIR in JAVA. This server is supported by the UHN (University Health Network), and its team of programmers is recognised for producing open-source software related to projects integrated with HL7 [17].

The HAPI FHIR server uses the HL7 FHIR R4 version and allows all access to FHIR Resources through RESTful API and the freedom to create Resources to suit the data formats of SDC-X projects.

3.2 SDC-X Interface

The interface implements login and password verification, and a MySQL database was created to store information from the users of the interface and thus verify if the login data are compatible and determine their registered profile.

Each profile has different access to the interface, meeting security and data protection criteria.

The profile registered as an Administrator has two screens, one to accept or block users from the interface and another to apply a data visualisation blocking rule through the Practitioner profile. This rule aims to comply with paragraph 5 of article 7 of Law No. 13,709 of August 14th 2018, which says that the data controller must have consent from the data owner in case of sharing information [18].

The Patient profile aims to comply with articles 6, 9 and 18 of Law No. 13,709, which determines free access to subjects' data [18]. This last aspect is covered through pages within the patient profile interface, which allows consulting all the information and contact for questions.

The Researcher profile user can see the data, but patients are anonymised, e.g., the name is replaced by the id of the database. In this profile, it is possible to download data, in JSON format, every 20 patients, as the interface loads 20 patients per page. The Researcher's profile can also see patients' information and download their data individually for analysis. It is also possible to filter patients on the patients' page, which performs a series of rules for the server to return the desired data.

The Practitioner profile contains a screen where you can search for a specific patient through their identification document (e.g., CPF); then, the server returns the patient's data, and the Practitioner has access to all the patient's information necessary to carry out a consultation and evaluate the patient. On the patient's profile screen, the Practitioner sees the exams performed previously (e.g. blood glucose, cholesterol, weight) in a graphic format. The Practitioner can also see all exams, results, and medications prescribed. Figure 4 details the patient profile page for a Practitioner.

The Manager profile contains global but not individualised patient information. So, to acquire this information, a bunch of requests to the server are needed, overloading the server, and slowing the web page. Therefore, the ElasticSearch server is implemented to minimise this issue.

ElasticSearch (version 7.9.2) was implemented in a container using Docker software, working in parallel with the FHIR server, helping with more complex requests. So, the Concentrator Module must send the data to the FHIR server and the ElasticSearch server, and both are the Storage Module. As the data in ElasticSearch is not intended for independent visualisation, it does not need to be identifiable; the Storage Module must anonymise the data when sending it to ElasticSearch.

Therefore, the SDC-X flowchart can be more understandable in Fig. 5. The data are collected by the hardware composing the Acquisition Module, manipulated by a practitioner. These data are processed by a computer with software that comprises the

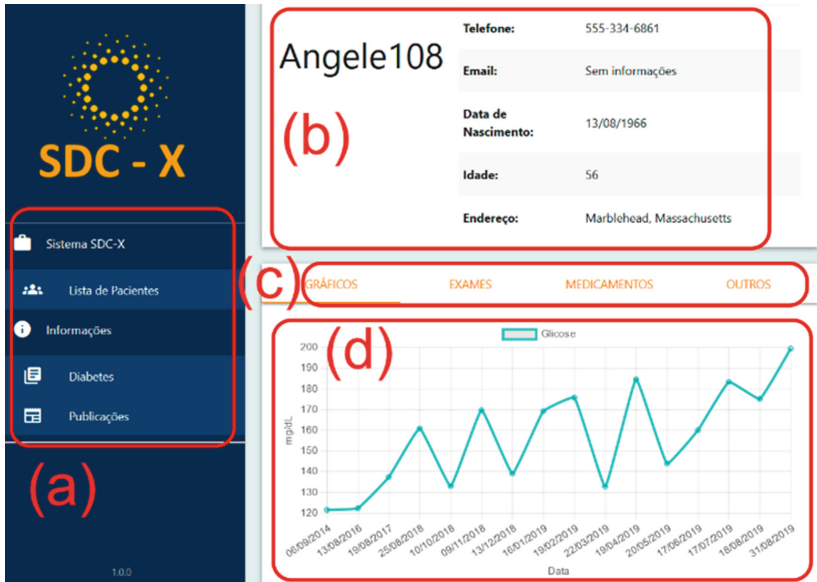


Fig. 4. Interface for the Practitioner profile viewing a patient's data. (a) Menu of interface screens. (b) Patient identification data. (c) Patient data navigation menu. (d) Graphs of patient exam data.

Concentrator Module. These data are analysed and sent to a RESTful API to the servers, composed of the FHIR server and ElasticSearch, forming the Storage Module. The Analysis and Interface Module can access these data by the RESTful API and show the application in any browser. This application web can be accessed by everyone with internet and an account in the SDC-X project.

The Manager profile allows one to view the data together; it is not allowed to see the data individually and can create policy guidelines for managing diabetes. Figure 6 displays the Manager profile statistics page.

4 Discussion

The HAPI FHIR tool was excellent for implementing the HL7 FHIR server. In addition, the ElasticSearch software proved to be a complementary tool, improving the processing time of the information.

The interface implementation presented an intuitive development when using the MVC method, allowing agile changes, and its modularity allows adding new functions as the SDC-X project develops.

The interface presented all the functions proposed in each profile, and only the Manager profile was implemented to use ElasticSearch requests.

It was observed that the rapid availability of data from diabetes patients, for the Practitioner profile, we have a quick analysis of the patient's history graphically and individually of the exams, which allows an agile and more accurate consultation.

The Researcher profile has permission to download data for other research, and the Manager profile allows for creating more decisive actions regarding diabetes.

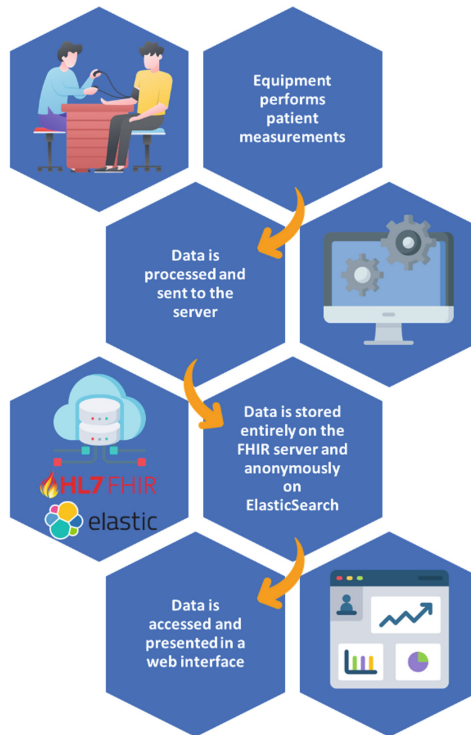


Fig. 5. The data is collected by the equipment of the Acquisition Module and sent to the Concentrator Module that analyses and processes the data. The FHIR protocol sends the data to the FHIR server, anonymises the patients and sends it to the Elasticsearch server. The users can visualise the data using the Analysis and Interface Module.

The Administrator, Patient and the other profiles aim to comply with the LGPD in force in the country, and this project must be in constant development and revision to always be in conformance with the law.

This project was entirely implemented on the same machine, and new tests must be carried out through cloud implementation. Thus, more severe security measures must be implemented, meeting data protection protocols, anonymisation, secrecy, and carrying out safety reports as described in section X of article 6 of the LGPD.

The project so far focuses on diabetes mellitus. Still, there is a possibility of adding new developments, such as the insertion of laboratory markers and new equipment for monitoring other pathologies, including systemic arterial hypertension, autoimmune diseases and chronic diseases in general. In addition, with the help of EMG and EEG equipment, we can use the system developed to provide the follow-up of pathologies such as epilepsy, stroke and cardiovascular problems in general.



Fig. 6. Statistical data is presented for the Manager profile based on the collected data. The information on this page are processed through ElasticSearch, which provides a more elaborate and faster query to the data than the FHIR server.

5 Conclusion

This work describes the implementation of a HAPI FHIR server in parallel with the ElasticSearch software and developing a web interface to complement the SDC-X project that aims to collect, store, treat, analyse and make available data from patients with diabetes. In this interface, rules were developed for five user profiles, seeking to meet the GDPR in force in the country.

Future research should conduct more tests to implement the cloud system and apply new security protocols. The interface has been created in an intuitive and modular format following the MVC design and thus can include new interpretations of data from future SDC-X projects.

Acknowledgment. This project was developed with the financial support of the Coordination for the Improvement of Higher Education Persons (CAPES) and the IEB-UFSC.

Conflict of Interest. The authors declare that they have no conflict of interest.

References

1. Federation, I.D.: IDF Diabetes Atlas. 9th ed. Brussels, Belgium (2019). [https://doi.org/10.1016/S0140-6736\(55\)92135-8](https://doi.org/10.1016/S0140-6736(55)92135-8)
2. SBD Homepage, <https://diabetes.org.br/dados-epidemiologicos>. Accessed 19 Aug 2021
3. WHO Homepage, <https://www.who.int/publications/m/item/improving-health-outcomes-of-people-with-diabetes-mellitus>. Accessed 25 Jun 2022
4. WHO: WHO Discussion paper (version dated August 9th 2021). Paper Knowledge. Toward a Media History of Documents, no. August, pp. 1–9 (2021)

5. BRASIL: Ministério da Saúde. Secretaria-Executiva. Departamento de Informática do SUS. Estratégia de Saúde Digital para o Brasil 2020–2028 [recurso eletrônico]/Ministério da Saúde, Secretaria-Executiva, Departamento de Informática do SUS.—Brasília: Ministério da Saúde (2020). ISBN 978-85-334-2841-6
6. Terra, T.G.: Software de Gerenciamento, Análise e Detecção Precoce da Disfunção Autonômica em Indivíduos com Diabetes Mellitus. 2020. Universidade Federal de Santa Catarina (2020)
7. Ücker, M.: Desenvolvimento de sistema point-of-care de pupilometria dinâmica aplicado no screening da Neuropatia Autonômica Diabética. 2020. Universidade Federal de Santa Catarina (2020)
8. Nakamura, K.K.: Sistema para avaliação da função sudomotora aplicado na detecção precoce do Diabetes Mellitus tipo 2. 2022. Universidade Federal de Santa Catarina (2022)
9. Borries, T.M., Dunbar, A., Bhukhen, A., Rismany, J., Kilham, J., Feinn, R., Meehan, T.P.: The impact of telemedicine on patient self-management processes and clinical outcomes for patients with Types I or II Diabetes Mellitus in the United States: a scoping review. *Diabetes Metab. Ic Syndr.: Clin. Res. Rev.* **13**(2), 1353–1357 (2019). Elsevier BV. <https://doi.org/10.1016/j.dsx.2019.02.014>
10. Rasmussen, O.W., Lauszus, F.F., Loekke, M.: Telemedicine compared with standard care in type 2 diabetes mellitus: a randomised trial in an outpatient clinic. *J. Telemed. Telecare* **22**(6), 363–368 (2016). SAGE Publications. <https://doi.org/10.1177/1357633x15608984>
11. Benson, T., Grieve, G.: Principles of Health Interoperability: FHIR, HL7 and SNOMED CT. Springer International Publishing, Cham (2021). <https://doi.org/10.1007/978-3-030-56883-2>
12. HL7 FHIR Homepage, <https://www.hl7.org/fhir/bundle-definitions.html>. Accessed 20 Jun 2021
13. Vieira, I.O., Francisco, M., Ojeda, R.G., Marques, J.L.B., Marino Neto, J.: Proposta de um Servidor de Interoperabilidade de Dados em Pesquisa Clínica com Padrão HL7 FHIR. XIII Seb, 10 dez. 2021. AYA Editora. <https://doi.org/10.47573/xiiiSeb.33>
14. Elasticsearch Homepage, <https://www.elastic.co/pt/what-is/elasticsearch>. Accessed 03 Mar 2023
15. Francisco, M., Vieira, I.O., Ojeda, R.G., Marques, J.L.B., Marino Neto, J.: Aplicação Web em Saúde 4.0: Uma Plataforma Multiusuário Baseada em um Servidor HAPI FHIR. XIII Seb, 10 dez. 2021. AYA Editora. <https://doi.org/10.47573/xiiiSeb.33>
16. Synthea Homepage, <https://github.com/synthetichealth/synthea>. Accessed 10 Jan 2022
17. Hussain, M.A., Langer, S.G., Kohli, M.: Learning HL7 FHIR Using the HAPI FHIR Server and Its Use in Medical Imaging with the SIIM Dataset. *J. Digit. Imaging* **31**(3), 334–340 (2018). <https://doi.org/10.1007/s10278-018-0090-y>
18. BRASIL Homepage, http://www.planalto.gov.br/ccivil_03/_ato2015-2018/2018/lei/113709.htm. Accessed 10 Mar 2022



Analysis of Failure Causes in the Mammography Machines

Indira Hernandez-Contreras² and Fabiola M. Martinez-Licona^{1,2}

¹ Electrical Engineering Department, Universidad Autonoma Metropolitana Iztapalapa, Mexico City, Mexico

fmm1@xanum.uam.mx

² Universidad Autonoma Metropolitana Biomedical Engineering Academic Program, Iztapalapa, Mexico City, Mexico

Abstract. Patient safety arises from the need to prevent and protect patients from avoidable mistakes. Two fundamental concepts that shape patient safety are error and adverse events, the consequences may range from potentially dangerous complications, slow recoveries, high medical costs, or unnecessary deaths. Breast cancer has become a global health problem with one of the most expensive burdens among non-communicative diseases. Since screening mammography is the most used method for tumor identification, patient safety applied to this technology is focused on delivering safe and effective service that results in an accurate and reliable diagnosis. This paper presents the analysis of the causes that can induce a potential failure in the mammography machine, and the actions to correct them. We used a risk analysis approach to identify the failures that may occur while using a mammography machine in screening programs. We extracted the information about the failures from specialized consultation and discussion forums and technical and operation manuals. We adapted the concepts of severity, occurrence, and detection involved in calculating the risk priority number according to the Failure Mode and Effects Analysis method, assigning them one of three levels (low, medium, and high). The adapted risk priority level was calculated from the averaged product of levels from the mentioned components. The results were mapped into an Ishikawa diagram, and an action procedure proposal was shown. The causes found are defined mainly concerning the handling of the equipment components, although causes related to the acquisition technique, patient handling, and availability of support information.

Keywords: Mammography machine · Failure causes · FMEA

1 First Section

Patient safety arises from the need to prevent and protect patients from avoidable errors. The World Health Organization (WHO) presents patient safety as a healthcare discipline that emerged as a result of the evolving complexity in health care systems and the rise of patient harm in healthcare facilities. It aims to prevent and reduce risks, errors, and harm in patients during the provision of healthcare [1]. Two basic concepts that

shape patient safety are error and adverse events. A health care error is a “mistake, inadvertent occurrence or unintended event in health care delivery that may or may not result in patient injury” [2]. An adverse event is an “injury that was caused by medical management, rather than the underlying disease, and that prolonged the hospitalization, produced a disability at the time of discharge, or both” [3]. The consequences that can appear range from potentially dangerous complications, slow recoveries, high medical costs, or unnecessary deaths. In this context, the WHO has declared patient safety a global health priority [4]. This concept of security extends to the functions not only of treatment in hospital facilities but also in diagnosis and rehabilitation both within the hospital and outpatient services, and the device manufacture which initiatives such as the unique device identifier [5]. With the arrival of the internet of things in medicine, patient safety must arrive at home.

Breast cancer has become a global health problem, with 11.7% of new cancer cases in 2020 [6]. The diagnosis, treatment, and follow-up of the disease are part of a strategy in which the early detection may make a difference between timely care and death. Screening mammography is the most used method for tumor identification in women that do not present signs or symptoms; the tumors, which cannot be perceived or felt, and the microcalcifications that might lead to the presence of breast cancer, are the targets of the mammography study. Mammography applied under the screening program in an organized population-based approach has the potential to reduce the risk of death from breast cancer by about 40% in women from 50 to 69 years old [7]. Despite its potential, several barriers prevent the consolidation of screening programs. Among them stand out lack of a healthcare provider recommendation, health insurance coverage for a mammogram, lack of access to screening services, time-consuming of receiving test results, social support, cultural norms issues, knowledge and beliefs about cancer, and expectations about screening [8].

Patient safety in screening mammography is focused on delivering safe and effective service that results in an accurate and reliable diagnosis. The mammography machine is the medical device responsible for obtaining X-ray images that show the state of the breast concerning potential tumors or microcalcifications. Some of the health care errors or adverse events related to screening involve the functionality of the device, the image acquisition technique, and the output interpretation. A false-negative mammogram does not present any abnormality although the cancer is present, and a false-positive mammogram presents abnormalities even though there is no presence of cancer. According to the American Cancer Society, screening mammograms miss about 1 in 8 breast cancers. About half of the women in an annual screening program over a 10-years period will have a false-positive finding at some point [9]. Digital mammography is a technology where the presence of artifacts related to patients (motion, antiperspirant, thin breast), hardware (field inhomogeneity, detector, collimator misalignment, grid misplacement, vibrations) and software processing (loss of edges, high-density, vertical bars) can give rise to erroneous diagnoses [10].

The factors that determine the result of a mammography study must be monitored to determine potential failures that affect the patient health. The evaluation and monitoring actions in mammography are part of the quality program. One of the tools frequently used to identify and analyze failures is the cause-effect diagram. This paper presents the

analysis of the causes that can induce a potential failure in the mammography machine, as well as the actions to correct them, as part of the medical equipment management program based on the monitoring and evaluation of its functionality.

2 Methods

We used a risk analysis approach to identify the technological and technical related failures that may occur during the use of a mammography machine in screening programs, assuming that facilities and the power grid are appropriately working. We also adapted some elements from the Failure Mode and Effects Analysis (FMEA) method. This method is based on a systematic process that identifies the potential product or process failures before they occur so they can be eliminated or at least minimized [11]. Tools such as cause-effect diagrams can be applied to identify the causes of failures. In this case, we used the Ishikawa diagram. This diagram facilitates the analysis of problems and solutions in aspects such as the quality of processes, products, and services. The Ishikawa diagram is based on a logical order to structure the information clearly and takes the form of a fishbone, where the multiple relationships of cause and effect of the variables that intervene in the processes are presented [12].

The information about the causes of failure associated with the mammogram operation and functioning was extracted from specialized consultation and discussion forums and technical and operation manuals. Among the consulted forums are medwrench.com in USA and cancerresearchuk.org in the UK. We classified the causes of failure into the following categories:

- Human resources involved in the operation of the mammography machine
- Environment under the machine operates
- Materials needed and used in the operation of the machine
- Methods required for the machine operation
- Machine components and tools required to perform the study
- Measurements and actions that conform to the study procedure

After the failure causes identification and classification, we adapted the concepts that are involved in the calculation of the risk priority number according to the FMEA method [13]; these are:

Severity: the consequence of the failure when it happens

Occurrence: the probability of the failure occurring

Detection: the probability of the failure being detected before it happens.

Based on the information reported on the forums, we assigned one of three levels (low, medium, high) to each of the concepts for every failure cause. For severity, we use the consequence level related to the patient, both during the procedure and in the result interpretation. For occurrence, we took the number of direct and indirect mentions of the failure cause. For detection, we consulted the technical and operation manuals of three mammography machine models to identify the probability of early detection according to the inspection procedures. The adapted risk priority level (RPL) was extracted from

Table 1. Level ranges and numeric RPL value.

Level	% Range	Value for RPL calculation
Low	[0–25)	12.5
Medium	[25–75)	50
High	[75–100]	87.5

the averaged product of levels from the three mentioned components using the numerical values shown in Table 1.

This information was presented in an Ishikawa diagram form in which we prioritized the failure causes and their corrective actions. Finally, an action procedure to deal with the risk levels of the failures is proposed.

3 Results

Four discussion forums were consulted for the failure causes research. Two of them had to be eliminated since they presented nonhomogeneous, inconsistent, and incomplete information. We found 17 common causes of mammography machine failure; Table 2 shows the failure causes, a brief description, the severity, occurrence, and detection level assigned as well as their RPL and the corrective actions identified. Figure 1 shows the resulting Ishikawa diagram.

The color of the failure causes shows the severity level (red-high, yellow-medium, green-low), and the position in the diagram is related to the assigned RPL level: the closest to the fishbone, the highest level it has. Figure 2 shows the action process to implement the activities aimed at containing the cause.

The cause “*compression plates functionality*” will be considered to exemplify the assignment of levels as follows:

Severity. The consequences concerning the patient are essential since a wrong action in the use of paddles can cause both discomfort in the patient and an image of questionable quality that impacts the diagnosis. Then a **high** level is assigned.

Occurrence. This cause occurred 28 times directly and indirectly. The total number of mentions registered in the forums was 95, so this cause represented 29% of the total and was assigned the **medium** level.

Detection. In the manuals consulted, the corresponding action to address this cause must be carried out immediately, which is why it was assigned a **high** value.

RPL. With the assigned levels, the calculation of the PLR is carried out by taking the numerical values of table 1 as follows:

$$RPL = (87.5 + 50 + 87.5)/3 = 75 \quad (1)$$

which corresponds to a **high level**. Due to its high severity level, it was located closest to the fishbone within the Ishikawa diagram in the machine category.

Table 2. Mammography machine failure causes, RPL calculation and corrective actions.

Failure cause	Brief description	Severity	Occurrence	Detection	RPL	Corrective Actions
Arm Functionality	Slow rotation or no rotation	Medium	Medium	High	Medium	Reboot the system
Breast location during exposition	Poor breast position causing patient discomfort	High	Low	Low	Medium	Perform periodic training on positioning the breast and communication of instructions to the patient
Bucky functionality	Engine failure. When attempting a shot, the system rotates up without being able to do so	Medium	Low	Low	Low	Inspect Bucky board. Verify that the grid moves freely along the entire path in both directions
Collimator functionality	Rear collimator failure, slip during movement, stop working after a certain number of patients, can not make an exposure	High	Medium	High	High	Perform regular cleaning and maintenance
Compression plates functionality	Plates fail quality-control tests, and compression is not detected	High	Medium	High	High	Check possible short circuits and change plates
Electric current and filaments	Filament current failure during an exposure using a small focal spot	High	Low	Medium	Medium	Check and calibrate the filament waveforms, and check the filament voltage. Check fuses
Emergency electrical system	In conditions of electrical risk, the system does not respond. Power failure causes the system to crash	Low	Low	Low	Low	When an electrical storm occurs, restore the breakers where the machine is located
Filter functionality	The filters are dirty and cause an error	Low	Low	Low	Low	Periodically inspect and clean filters
Generator battery operation	Generator battery error	Low	Low	Low	Low	Replace batteries

(continued)

Table 2. (continued)

Failure cause	Brief description	Severity	Occurrence	Detection	RPL	Corrective Actions
Lack of manuals	There are no manuals, or they are incomplete	Medium	Low	Low	Low	Request manuals or guides
Machine calibration	The equipment is not calibrated or is not calibrated after changing the batteries	Medium	Medium	Medium	Medium	Plan regular equipment maintenance and calibration
Noise artifacts in images	The images present granulations and elements that do not belong to the breast tissue, the images present artifacts that alter the interpretation	Medium	Medium	High	Medium	Periodically inspect and maintain coils
Power on functionality	The equipment turns on and off. The keyboard does not work. The equipment does not turn on. Failed to log in. The system does not boot. Error messages are not reset	High	High	High	High	Regularly check the connectors
Secure system for start procedure	The system does not turn on	Low	Medium	High	Medium	Contact the supplier and check the software
Shooting system/ exposure	Poor image quality. Signal loss during a trigger	High	Medium	Medium	Medium	Restart system. Check connectors
X-Ray tube calibration	Voltage error. The tube is not calibrated. X-rays are disabled and no exposure is allowed. Tube failure	High	Medium	High	High	Plan regular equipment maintenance and calibration
X-Ray tube noise	Noise generated from the tube head. Tube voltage fault	High	Medium	Medium	Medium	Plan regular equipment maintenance and calibration

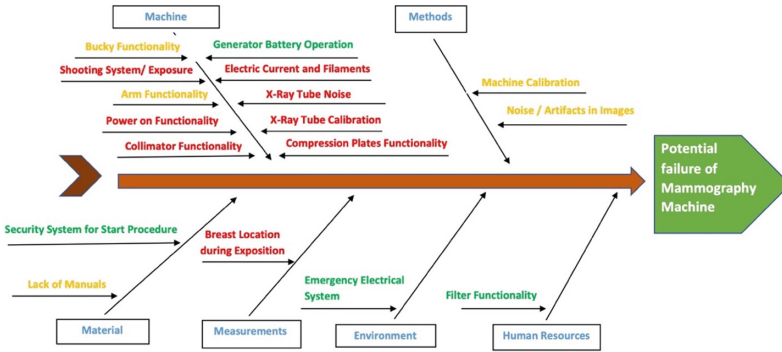


Fig. 1. Ishikawa diagram for potential failures of a mammography machine.

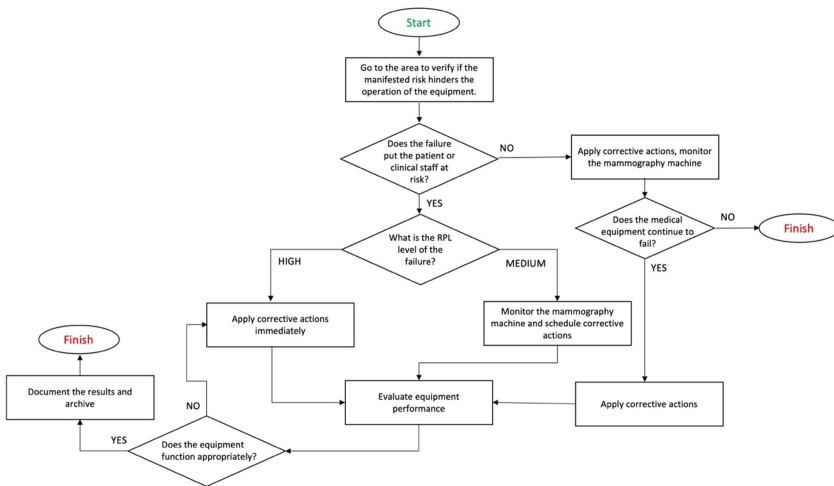


Fig. 2. Proposed action procedure.

4 Discussion

Identifying the causes of mammography failure allows an action to be taken promptly to have control over the consequences that it may have. The causes detected in the forums are mainly associated with the operation of the equipment. We assume that these causes present more problems to users due to lack of experience in its operation and maintenance or lack of technical support documentation. In the technical manuals consulted, we found that the troubleshooting sections address aspects related to radiological protection, image quality, software and hardware errors, X-ray tube, arm, and compression. Some of them are reported in Table 1.

We found that the number of forums dedicated to imaging equipment is relatively high, but they are very few when identifying those related to mammography. All the forums consulted are in English, which favors communication between users from all over the world, especially in cases where there is a lack of access to technical information.

Regarding patient safety, both in the forums and in the manuals, aspects of the equipment components predominate. In some cases, their operation to obtain an image of the breast is also present. The causes of this type of failure are training in the technique. Considering the consequences of a diagnostic failure due to poor image acquisition, training should be considered a high priority for action and continuous development. The use of support tools for image analysis, such as artificial intelligence, improves diagnostic capacity even in low-quality images [14]. However, access is limited to digital equipment that can integrate the algorithms while still depending on acquisition and interpretation skills. The list of reported failures can be taken as a starting point for developing management systems for the functionality and conservation of the mammograph; it represents the causes most reported by the technical community, which can be specified in greater detail and provide more specific solutions. Since the mammogram is a crucial element for the screening, it is essential to include the technical operation and conservation of the device in the programs for breast cancer early detection. FMEA-based approaches have been used to address the challenges of cancer radiotherapy [15, 16], demonstrating the potential utility of this methodology for studying the risks associated with cancer diagnosis and treatment.

5 Conclusions

The causes of mammography failure were analyzed, taking FMEA principles and components and Ishikawa diagrams to form an information base that prioritizes those aspects that present a high risk for patient safety. The reported causes are defined mainly concerning the handling of the equipment components, although causes related to the acquisition technique, patient handling, and availability of support information were also detected. It is planned to incorporate information from a larger number of manuals, the opinion of experts in the hospital setting, and develop technical support material for screening programs for early detection of breast cancer. The use of FMEA for risk analysis and the proposed approach presents characteristics such as the classification of the information obtained and the use of Ishikawa diagrams, which allow adaptation for application in other medical equipment.

Conflict of Interest. “The authors declare that they have no conflict of interest.”

References

1. WHO Patient Safety, <https://www.who.int/news-room/fact-sheets/detail/patient-safety>
2. Liang, B.A.: Promoting patient safety through reducing medical error: a paradigm of cooperation between patient, physician, and attorney. *SIU Law J.* **24**, 54–568 (2000)
3. Brennan, T.A., Leape, L.L., Laird, N.M., et al.: Incidence of adverse events and negligence in hospitalized patients. Results of the Harvard Medical Practice Study I. *N. Engl. J. Med.* **324**(6), 370–376 (1991). <https://doi.org/10.1056/NEJM199102073240604>
4. WHO Global action on patient safety WHA72.6, https://apps.who.int/gb/ebwha/pdf_files/WHA72/A72_R6-en.pdf?ua=1

5. Wilson, N.A., Tcheng, J.E., Graham, J., Drozda Jr., J.P.: Advancing Patient Safety Surrounding Medical Devices: Barriers, Strategies, and Next Steps in Health System Implementation of Unique Device Identifiers. *Medical devices* (Auckland, N.Z.), (15), pp. 177–186 (2022). <https://doi.org/10.2147/MDER.S364539>
6. International Agency for Research on Cancer (IARC), <https://bit.ly/3sBFVsB>, <https://gco.iarc.fr/today/data/factsheets/populations/484-mexico-fact-sheets.pdf>
7. Lauby-Secretan, B., et al.: Breast-cancer screening—viewpoint of the IARC Working Group. *N. Engl. J. Med.* **372**(24), 2353–2358 (2015). <https://doi.org/10.1056/NEJMsr1504363>
8. Sarma, E.A.: Barriers to screening mammography. *Health Psychol. Rev.* **9**(1), 42–62 (2015). <https://doi.org/10.1080/17437199.2013.766831>
9. American Cancer Society, <https://www.cancer.org/cancer/breast-cancer/screening-tests-and-early-detection/mammograms/limitations-of-mammograms.html>
10. Ayyala, R.S., Chorlton, M., Behrman, R.H., et al.: Digital mammographic artifacts on full-field systems: what are they and how do I fix them? *Radiographics* **28**, 1999–2008 (2008). <https://doi.org/10.1148/rg.287085053>
11. Mikulak, R.J., McDermott, R., Beauregard M.: *The Basics of FMEA*, 2nd ed. CRC Press, New York, NY (2009)
12. Luca L.: A new model of Ishikawa diagram for quality assessment. In: *IOP Conference Series: Materials Science and Engineering*, Kozani, Grecia, pp. 1–6 (2016). <https://doi.org/10.1088/1757-899X/161/1/012099>
13. Ben-Daya, M.: Failure mode and effect analysis. In: *Handbook of Maintenance Management and Engineering*, pp. 75–90. Springer, London. (2009). https://doi.org/10.1007/978-1-84882-472-0_4
14. Yoon, J.H., Kim, E.K.: Deep learning-based artificial intelligence for mammography. *Korean J. Radiol. Radiol.* **22**(8), 1225–1239 (2021). <https://doi.org/10.3348/kjr.2020.1210>
15. Xu, Z., Lee, S., Albani, D., et al.: Evaluating radiotherapy treatment delay using Failure Mode and Effects Analysis (FMEA). *Radiother. Oncol.* **137**, 102–109 (2019). <https://doi.org/10.1016/j.radonc.2019.04.016>
16. Rash, D., Hoffman, D., Manger, R., Dragojević, I.: Risk analysis of electronic intraoperative radiation therapy for breast cancer. *Brachytherapy* **18**(3), 271–276 (2019). <https://doi.org/10.1016/j.radonc.2019.04.016>



An Overview of the Postgraduate Courses in Clinical Engineering Offered in Brazil

N. C. B. L. Koch^(✉) , A. P. Romani , T. R. Oliveira , and H. Tanaka 

Biomedical Engineering/CECS, Federal University of ABC (UFABC), São Bernardo Do Campo, SP, Brazil
koch.natalia@ufabc.edu.br

Abstract. “Clinical Engineering” (EC) is an engineering specialty in which the primary role is to take care of the life cycle of medical equipment. Professional assignments cover activities ranging from planning the incorporation of new devices to managing the maintenance and disposal of systems in an appropriate destination. Engineers working in that field are commonly named Clinical Engineers. The first professionals with dedicated training in the field started in Brazil around four decades ago. However, despite the decades, Brazil’s educational system still lacks standardization. Our goal in this paper was to investigate how these professionals act in the field and, more importantly, how they were trained. To accomplish that, we selected all ‘Higher Education Institutions’ (IES) in Brazil that currently offers recognized Clinical Engineering specialization. The number of thirteen IES met the established criteria. The institution’s information was collected through an exploratory search on the official e-MEC portal and from their respective own electronic addresses. The data were statistically structured and further analyzed. The results could overview each EC specialization program’s structure, highlighting abilities and skills developed. Our analysis supports government officials’ standardization process and future candidate’s decisions.

Keywords: Clinical Engineering · Clinical Engineer · Postgraduate Courses

1 Introduction

Even within “Health Care Facilities” (EAS), the work of EC is still little known. Clinical Engineering seeks to combine engineering and management knowledge by applying them to health technologies [1].

One of the best-known definitions of EC in Brazil is the definition made by the “Brazilian Association of Clinical Engineering” (ABEClin) which defines the Clinical Engineer as the professional who applies engineering techniques in the management of health equipment in order to ensure the traceability, usability, quality, efficacy, effectiveness, safety and performance of this equipment in order to promote patient safety [2].

According to the American College of Clinical Engineering (ACCE), Clinical Engineer is a supportive professional who promotes patient care by applying engineering and

management skills to health technology. This engineering professional focuses on planning, evaluation, management, analysis, education, support, and regulatory compliance of healthcare technology [3].

The history of EC in Brazil begins in the early seventies. When in 1973, the 'Ministry of Health' pointed out the need for evaluation and quality of diagnostic products. This evaluation was made before authorizing its commercialization, according to Law nº 5,991 of 12/17/1973 [4–6].

In the 1980s, most of the medical equipment purchased in Brazil suffered malfunctions due to a lack of maintenance and/or spare parts. This scenario resulted from numerous variables, such as a lack of well-trained professionals, technical manuals, and other relevant documentation for maintenance and technology [1, 7].

In the following years, the activities of EC were restricted to carrying out corrective actions, delaying the consolidation of a broader and qualified process of hospital medical technology management (GTMH) [6, 8], and with the performance of corrective maintenance almost exclusively by manufacturers, it was clear the size of the waste of resources with the massive percentage of equipment failure, directly impacting the quality of health care services. This obstacle in maintaining hospital medical technology clearly showed the need to create EC departments throughout the country formally. Concomitantly, the federal government promoted the creation of training schools in EC [5].

In the early 1990s, precisely in the years 1993 and 1995 were created the first *Lato sensu* postgraduate courses in EC in Brazil. These courses were implemented at the universities UNICAMP (Campinas-SP), USP (São Paulo-SP), UFPB (João Pessoa-PB) and UFRS (Porto Alegre-RS). These courses were intended for Electrical Engineers who wanted to work in the area, within the hospital environment, to mitigate the losses accumulated by the lack of management of the technology park [5, 9].

Although the professionals have been working for at least forty years in Brazil, the profession of Clinical Engineer is not yet regulated, so there is no definition of which professional can perform this activity and its attributions [9, 10].

With the profession not regulated, professionals who work as clinical engineers face difficulties, such as proving their performance in the area and being absorbed by the labor market. The profession of Clinical Engineer does not compose the list of professions of the 'Brazilian Classification of Occupations' (CBO), a fact that makes it impossible for the professional to have his work card signed as a Clinical Engineer. However, even with the non-regulation of the profession, the area of EC has continued to expand. Over the years, more graduate courses have emerged in EC. It is possible to notice that the curricular matrix of these courses varies significantly according to the perception and experience of the coordinator who elaborates the course.

In the present study, exploratory research was carried out in the e-MEC portal of all the IES accredited by the MEC and currently offer the postgraduate course in EC in the national territory and information available in their respective electronic addresses [11–24].

Only thirteen IES met these two criteria and were selected for this study. These selected IES had their information collected through the e-MEC portal and in their electronic addresses. Data were collected on the total course load, course duration,

internship requirement and course completion work, and two IES quality measurement indices. The first was the ‘General Index of Courses’ (IGC) for the year 2019 (the last calculated index). Moreover finally, the level of teacher qualification was considered as an indirect measurement of the quality of the IES [25].

2 Method

The inclusion criteria assumed for this study were: (1) Official recognition of the program by MEC and (2) to be an active program in the current year of 2022.

Table 1. IES that offer the postgraduate course in EC, acronym of IES and year of start of offer

IES	Acronym	Beginning
Faculdade Unyleya	–	2019
Faculdade I. de C. S. Albert Einstein	FICSAE	2006
Faculdade Unimed	–	2020
Faculdade Estácio de Sá	UNESA	2017
Instituto Navigare	–	2021
Instituto Nacional de Telecomunicações	INATEL	2019
Instituto E-Class	–	2020
RTG Especialização	–	2020
Universidade de Fortaleza	UNIFOR	2010
Faculdade de Agudos	FAAG	2019
Faculdade Jardins	FACJARDINS	2020
Centro Universitário Internacional	UNINTER	2022
Senai Cimatec	SENAICIMATEC	2022

The data collection was conducted based on data available in the e-MEC portal and the official web pages of the respective programs, to verify the current offer and whether the information that was in the e-mail address of the IES corroborated the information contained in the platform of the MEC.

The e-MEC portal information collected were: IES region, teaching modality, year of the start of course offer, total workload, hours/classes per course, requirement of internship and ‘Graduation thesis’ (TCC), IGC and qualification of course coordinators [11–24]. Table 1 lists the IES selected for this study.

3 Results

Out of the thirteen IES selected in this study, 60% (8 in 13 program) are located in the Southeast region of the country (Minas Gerais, São Paulo and Rio de Janeiro), as it can be seen in Fig. 1, and others are spread across different states (Maranhão, Bahia, Sergipe, Ceará, Goiás and Paraná).

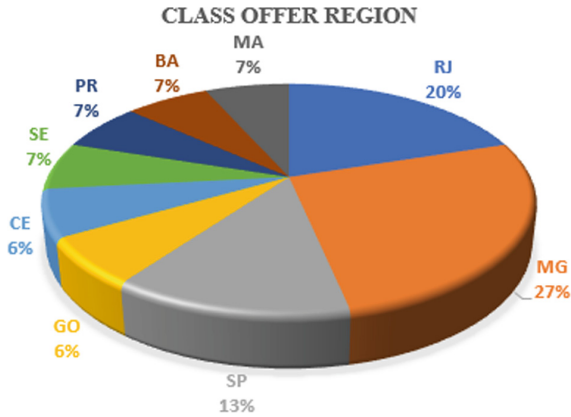


Fig. 1. Region of offer of postgraduate course in EC in The Brazilian territory

In Fig. 2, the distribution of programs workload is presented. The proportion of 38% of the IES analyzed offer the 360 h/class workload.

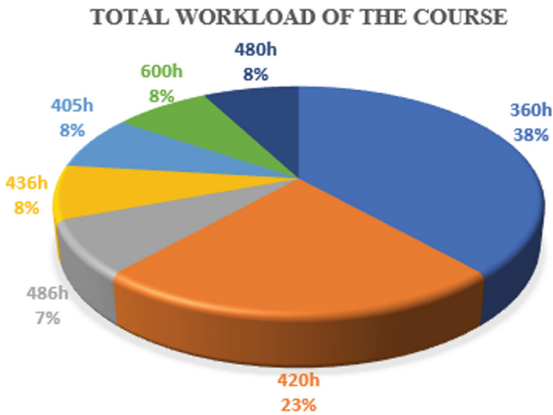


Fig. 2. Total workload of the postgraduate course in EC in hours/class

The arithmetic average total workload of the courses offered is 420.5 h/class, and the highest total workload of the postgraduate course in EC, is 600 h/class, offered by FACJARDINS. The same IES offers this course in the shortest time, in just 6 months [22].

Regarding the duration of the course, FACJARDINS offers its course in less time, of only 6 months. INATEL, UNIFOR and SENAI CIMATEC offer their courses in 24 months. The arithmetic mean duration of the course was 15.5 months. Figure 3 presents this distribution:

On the requirement of the mandatory internship, FICSAE determines 46 h of internship for fulfillment and UNIFOR determines 20 h of internship.

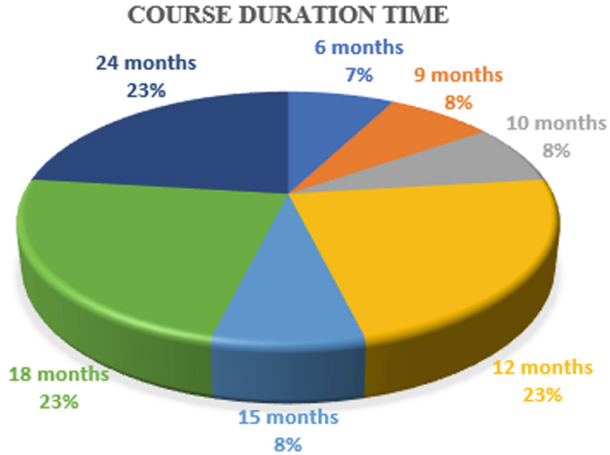


Fig. 3. Duration of the postgraduate course in EC in months.

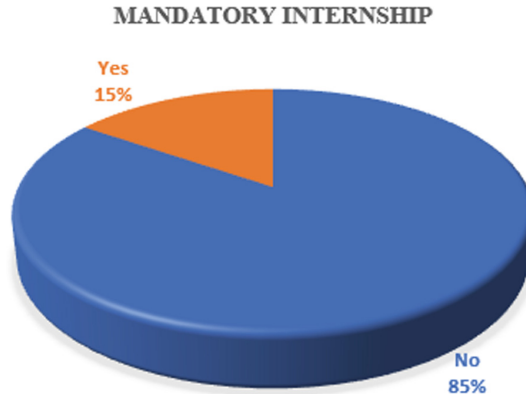


Fig. 4. Requirement of mandatory internship in the postgraduate course in EC.

These internship hours enter the total workload of the postgraduate course in EC. As shown in Fig. 4, the two IES mentioned above represent 15% of the total IES under study, and the rest of the IES (85%) does not have an internship requirement.

The CNE/CES 01 resolution of 04/06/2018 also made the TCC optional in all Lato sensu postgraduate courses. Even so, as seen in Fig. 5, the majority (62%) of the IES still require TCC as a mandatory activity for completing the Postgraduate course in EC [26].

The IGC attests the quality of all undergraduate and postgraduate courses of an IES. The calculation of the IGC is carried out by an average between the grades of the last 'Preliminary Course Concepts' (CPC) of the evaluated courses [27].

The calculated IGC is a continuous variable in the interval between 0 and 5, where indicators with levels above 3 are considered satisfactory, indicating quality.

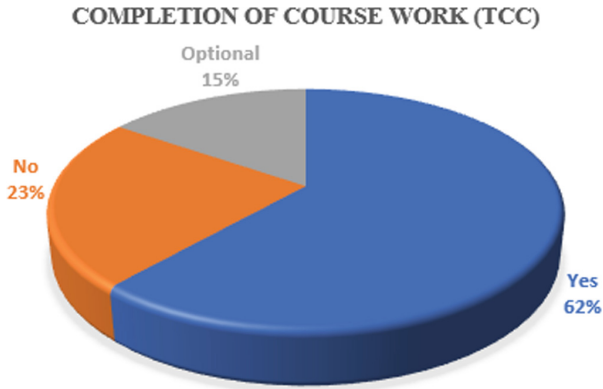


Fig. 5. Requirement of (TCC) in the Postgraduate Course in EC

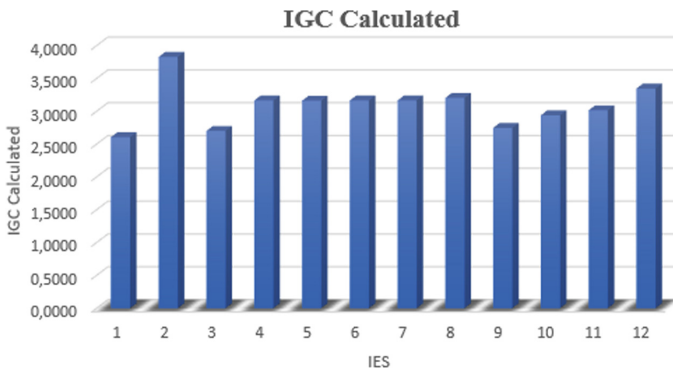


Fig. 6. IGC calculated from twelve IES selected for the study.

In the case of IES with grades between 1 and 2, they will be subject to a visit from INEP evaluators for *on-site* verification of the teaching conditions offered [27, 28].

The IGC of 12 selected IES were collected, except for Unimed College, because the calculated IGC value was not available for consultation in the e-MEC portal [11].

As shown in Fig. 6, the highest value of the calculated IGC was FICSAE, with 3.8290, and the lowest value was 2.6060, referring to Faculdade Unyleya.

The arithmetic mean of the IGC was 3.0872.

The level of teacher’s qualification is part of the goals of the ‘National Education Plan’ (PNE), which aims to increase the number of teaching staff to 75% with masters and Ph.D., being at least 35% with Ph.D. [29].

The ‘Census of Higher Education’ is conducted annually by INEP. This census is the research instrument to evaluate the institutions offering higher education courses. The level of qualification of teachers is part of the calculation of quality indicators, such as CPC and IGC. [30].

As shown in Fig. 7, 42% of the teaching coordinators have the specialization, 42% have the master’s degree, the remainder (16%) Ph.D. and postdoctoral.

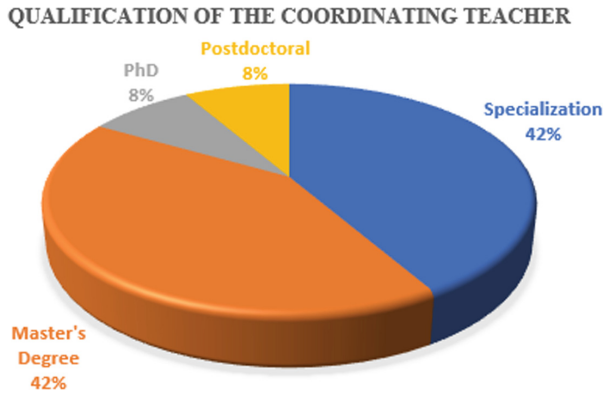


Fig. 7. Level of qualification of the teacher coordinator of postgraduate courses in EC

4 Discussion

The objective of this manuscript was to present an overview of the status of the EC postgraduate courses available in Brazil. Although the EC professionals have been acting in the country for at least four decades, the professional training programs still lack specific national legislation and professional recognition, which express no consensus regarding the professional duties of a clinical engineer and the absence of professional certification. The currently available programs vary along different parameters as the discipline's content, the number of subjects in the course, and the total workload.

Identifying national minimum requirements for Clinical Engineers who practice as health professionals have been a point of discussion globally since the 80's [31, 32].

Guaranteeing competency in their discipline by completing appropriate educational qualifications should be a common element for every global program. Therefore, standardizing the mandatory contents of the Postgraduate course in EC is necessary for Brazil.

The question regarding clinical engineering regulation and minimum curriculum has already been present in Brazilian society for at last 20 years [33]. However, more investments are needed.

As an example of EC professional definition and contradictions, the Vunesp Foundation published the EBSEH/HC-UFU (02/2019) Clinical Engineer Hire Program that required the following knowledge in its objective test: Electronics; operation of direct and indirect patient care equipment; hospital safety; management and acquisition of medical-hospital equipment, parts, and accessories; contract management; legislation and bidding [34]. This content does not superpose to the significant content covered in postgraduate courses in EC [35–37].

One of the challenges observed in this research was the collection of data through the web pages of the respective IES [12–24]. There was no course program on most web pages, or pre-registration was required to access more information about the course. Despite the challenges, our research demonstrated an asymmetrical geographic distribution of the courses offered. The southeast region is responsible for 60% of the current specializations offered. Although the demographic census conducted in 2010 by the

Brazilian Institute of Geography and Statistics (IBGE), considered a total of 80.364,410 inhabitants in the region, representing 42.1% of the Brazilian population.

The resolution CNE/CES 01 (04/06/2018) established that all *Lato sensu* postgraduate courses must meet a minimum workload of 360 h/class per course [26]. The total workload of the postgraduate course in EC ranged from 360 h/class up to 600 h/class. JACJARDINS offers its course in 600 h/class, with a completion time of only 6 months [22]. The average arithmetic duration of the postgraduate course in EC is 15.5 months. The majority of IES, around 85%, do not charge mandatory internships, but the majority (62%) still ask the TCC as a criterion for obtaining the ‘Certificate of Completion of Course’.

The highest IGC value calculated was FICSAE, which is 3.8290 and the lowest value was that of Faculdade Unyleya with 2.6060. The indicator that indirectly attests to the quality of the IES is the degree of teacher qualification.

Miranda [25] carried out a mapping of variables that affect the academic performance of students in the business area. As a result, it was concluded that four variables of academic training significantly influence academic performances: exclusive dedication, *Stricto sensu* degree, relevant publications, and strategies or teaching and learning methods.

These results show that the education level of the teaching staff, the number of teachers per course, and the volume of courses offered by the IES have a significant impact on the performance of the students and the performance measurement index by the ‘National Student Performance Exam’ (ENADE) [25].

Thus, the level of training of the teaching staff is an indirect indicator of quality used by INEP, and this is part of the goals of the ‘National Education Plan’ (PNE) [30].

Figure 7 shows that teachers need to increase their qualifications. In the thirteen IES selected, there are only two coordinators with Ph.D. On the other hand, it is important to emphasize that there is little literature considering the essential knowledge for the Clinical Engineer’s performance in Brazil. In this context, EC course instructors should have job experience in the EC. The content of some disciplines of the Postgraduate Course in EC would benefit from collected experiences in the EC job.

5 Conclusions

In this study, we presented data collection results of 13 officially recognized EC specialization courses in Brazil. All program information was publicly available and obtained on the MEC website. Despite the MEC recognition, our findings pointed out a poor standardization of the program’s curriculums. The overall content covered by each postgraduate course varies among the requirements and workloads, and activities such as mandatory internships and graduation projects do not follow a common standard. All programs require tuition payment and are asymmetrically distributed among the country territory, with the offered courses centered in the country’s Southeast region. In conclusion, our project demonstrates the current need to construct a standard national minimum curriculum.

Acknowledgments. This study was financed by a Brazilian government agency known as the ‘Coordenação de Aperfeiçoamento de Pessoal de Nível Superior’ (CAPES).

Conflict Interest

The authors declare that they have no conflict of interest.

References

1. Almeida, E.S.F., Cária, J.D.P.: Perfil da Engenharia Clínica em Hospitais de Grande Porte de Belo Horizonte. Seminários INATEL, Belo Horizonte/MG (2016)
2. Associação Brasileira de Engenharia Clínica – ABEClin. <http://www.abeclin.org.br/pagina.php?p=quem-somos>. Last accessed 16 May 2022
3. American College of Clinical Engineering – ACCE. <https://accenet.org/about/Pages/ClinicalEngineer.aspx>. Last accessed 16 May 2022
4. Lei nº 5.991 de 17 de dezembro de 1973 - Dispõe sobre o Controle Sanitário do Comércio de Drogas, Medicamentos, Insumos Farmacêuticos e Correlatos, e dá outras Providências. http://www.planalto.gov.br/ccivil_03/leis/15991.htm. Last accessed 16 May 2022
5. Ramirez, E.F.F., Calil, S.J.: ENGENHARIA CLÍNICA: PARTE I - ORIGENS (1942–1996), Semina: Ci. Exatas/Tecnologia, vol. 21, pp. 27–33. Londrina/PR (2000)
6. Porto, D., Marques, D.P.: Engenharia clínica: nova “ponte” para a bioética? Revista Bioética 24(3), 515–527 (2016)
7. Silva, A.O., Monteiro, J., Moreira e Mariana, P.D.J.: A IMPORTÂNCIA DO ENGENHEIRO CLINICO NO AMBIENTE HOSPITALAR. Congresso Técnico-Científico da Engenharia e da Agronomia – Contecc. Palmas/TO (2021)
8. Beskow, W.B.: Sistema de informação para o gerenciamento de tecnologia médico-hospitalar: metodologia de desenvolvimento e implementação de protótipo. Universidade Federal de Santa Catarina, Florianópolis/SC (2001)
9. Souza, A.F., More, R.F.: O PERFIL DO PROFISSIONAL ATUANTE EM ENGENHARIA CLÍNICA NO BRASIL. XXIV Congresso Brasileiro de Engenharia Biomédica – CBEB 2014, pp. 1086–1090. São Paulo/SP (2014)
10. Salu, S.: Regulamentação da Profissão do Engenheiro Clínico, ABEE/GO. <https://abee-go.org.br/2020/10/07/regulamentacao-da-profissao-do-engenheiro-clinico/>. Last accessed 17 May 2022
11. Cadastro Nacional de Cursos e Instituições de Educação Superior - e-MEC. <https://emec.mec.gov.br/emec/nova>. Last accessed 17 May 2022
12. Faculdade Unyleya: Curso de Pós-Graduação em Eng. Clínica EAD. [https://unyleya.edu.br/pos-graduacao-ead/curso/engenharia-clinica/?ap=google&src=search.dsa_rlsa.g&utm_source=google_y&utm_medium=cpc&utm_campaign=dsa_rlsa\(FY\)&utm_content=curso&keyword=&ap=google&gclid=EA1aIQobChMIvp3hlNXm9wIVFRXUAR37nALZEEAYASAAEgKIDvD_BwE](https://unyleya.edu.br/pos-graduacao-ead/curso/engenharia-clinica/?ap=google&src=search.dsa_rlsa.g&utm_source=google_y&utm_medium=cpc&utm_campaign=dsa_rlsa(FY)&utm_content=curso&keyword=&ap=google&gclid=EA1aIQobChMIvp3hlNXm9wIVFRXUAR37nALZEEAYASAAEgKIDvD_BwE). Last accessed 18 May 2022
13. Faculdade Israelita de Ciências da Saúde Albert Einstein, Curso de Pós-Graduação em Eng. Biomédica e Clínica. https://ensino.einstein.br/engenharia_clinica_p0055/p?gclid=EA1aIQobChMIvp3hlNXm9wIVFRXUAR37nALZEEAYAYAAEgLmtvD_BwE. Last accessed 18 May 2022
14. Faculdade Unimed: Curso em MBA em Eng. Clínica. <https://www.faculdadeunimed.edu.br/cursos/pos-graduacao/mba-em-engenharia-clinica>. Last accessed 18 May 2022
15. Faculdade Estácio de Sá: Curso de Pós-Graduação em Eng. Biomédica com Ênfase em Eng. Clínica. <https://estacio.br/cursos/pos-graduacao/engenharia-biomedica-com-enfase-em-engenharia-clinica>. Last accessed 18 May 2022

16. Instituto Navigare: Curso de Pós-Graduação em Eng. Clínica – Online. <https://www.instituto.navigare.com.br/engenharia-clinica-online>. Last accessed 18 May 2022
17. Instituto E-Class: Curso de Pós-Graduação em Eng. clínica e Hospitalar. <https://eclass.minhacontaverde.com.br/engenharia-clinica>. Last accessed 18 May 2022
18. Instituto Nacional de Telecomunicações: Curso de Especialização em Eng. Clínica e Eng. Biomédica – Online. <https://inatel.br/pos/online/engenharia-clinica-e-engenharia-biomedica>. Last accessed 18 May 2022
19. RTG Especialização: Curso de Pós-Graduação em Eng. Clínica. <https://rtgespecializacao.com.br/pos-graduacao/engenharia-clinica/>. Last accessed 18 May 2022
20. Universidade de Fortaleza: Curso de Pós-Graduação em Eng. Clínica. <https://unifor.br/web/pos-graduacao/especializacao-em-engenharia-clinica/>. Last accessed 18 May 2022
21. Faculdade de Agudos: Curso de Especialização em Eng. Clínica. <https://faag.com.br/esp-em-engenharia-clinica/>. Last accessed 18 May 2022
22. Faculdade Jardins: Curso de Pós-Graduação em Eng. Clínica e Pesquisa. https://www.faculdadejardins.com.br/ead/pos-graduacao/engenharia/eng_clinica_pesquisa/. Last accessed 18 May 2022
23. Centro Universitário Internacional: Curso de Pós-Graduação em Eng. Clínica -EAD. <https://www.uninter.com/pos-graduacao-ead/engenharia-clinica/>. Last accessed 18 May 2022
24. Senai Cimatec: Curso de Pós-Graduação em Eng. Clínica. https://www.senaicimatec.com.br/cursos_pos/especializacao-em-engenharia-clinica/#/apresentacao. Last accessed 18 May 2022
25. Miranda, G.J.: Relações entre as qualificações do professor e o desempenho discente nos cursos de graduação em Contabilidade no Brasil (2011). <https://www.teses.usp.br/teses/disponiveis/12/12136/tde-16032012-190355/publico/GilbertoJoseMirandaVC.pdf>. Last accessed 19 May 2022
26. MEC: Resolução nº1 de 6 de abril de 2018. https://blog-static.infra.grancursosonline.com.br/wp-content/uploads/2021/05/24143909/CNE_CES_01.pdf. Last accessed 19 May 2022
27. Guerra, M.F., Brito, A.C., Soares, J.L.: Avaliação de desempenho das instituições de Ensino Superior Brasileiras: Uma Reflexão a Luz da Controladoria. *Revista Espacios* **38**(15), 11–23 (2017)
28. INEP: NOTA TÉCN. Nº 39/2017/CGCQES/DAES (2017). https://download.inep.gov.br/educacao_superior/enade/notas_tecnicas/2016/nota_tecnica_n39_2017_cgcqes_daes_calculo_igc.pdf. Last accessed 19 May 2022
29. INEP - Censo da Educação Superior. Docentes da educação superior estão mais qualificados. <https://www.gov.br/inep/pt-br/assuntos/noticias/censo-da-educacao-superior/docentes-da-educacao-superior-estao-mais-qualificados>. Last accessed 19 May 2022
30. MEC/SASE: Planejando a Próxima Década: Conhecendo as 20 Metas do Plano Nacional de Educação (PNE) (2014). https://pne.mec.gov.br/images/pdf/pne_conhecendo_20_metas.pdf. Last accessed 19 May 2022
31. Pallikarakis, N.: Biomedical/clinical engineering education and certification: fifty years. *Health Technol.* **12**(3), 671–678 (2022)
32. Yadin, D., Calil, S., Pallikarakis, N., Poluta, M., Bergamasco, S., Clark, D., Judd, T., Wear, J., Fukuta, K., Mullally, S., Morse, W.: Is clinical engineering an occupation or profession? *Glob. Clin. Eng. J.* **4**(2) (2021)
33. Del Solar, J.G., Soares, F.A., Mendes, C.J.: Brazilian clinical engineering regulations: health equipment management and conditions for professional exercise. *Res. Biomed. Eng.* **33**(4), 301–312 (2017)
34. Fundação Vunesp, Edital: HC-UFU CONCURSO PÚBLICO 02/2019 – EBSERH/HC-UFU. <https://documento.vunesp.com.br/documento/stream/MTQyOTA0MA%3d%3d>. Last accessed 19 May 2022

35. Cebraspe - CESPE/UnB: Edital n° 4 abertura Concurso EBSEHR Administrativo. http://www.cespe.unb.br/concursos/EBSEHR_18_ADMINISTRATIVA/arquivos/ED_4_EBSEHR_ADMINISTRATIVA__ABERTURA.PDF. Last accessed 30 May 2022
36. Instituto AOCF: Edital de abertura do Concurso Público da área administrativa com lotação no HUIB – UFCG. https://www.institutoaocf.org.br/concursos/arquivos/hujb_edital04_anexoIII.pdf? Last accessed 30 May 2022
37. Instituto Americano de Desenvolvimento - IADES, Edital do Concurso Público 4/2014 - EBSEHR/HUPES/UFBA. <https://www.iades.com.br/inscricao/upload/104/20140220205538735.pdf>. Last accessed 19 May 2022



Features of Computerized Systems for the Management of Medical-Hospital Equipment in Clinical Engineering Departments in Brazil

Perseu Filho Rosa^(✉)  and Frieda Saicla Barros 

Graduate Program in Biomedical Engineering, Federal Technological University of Paraná,
Curitiba, Brazil

perseurosa@alunos.utfpr.edu.br

Abstract. The rapid evolution and complexity of medical-hospital equipment (EMH), as well as the appearance of adverse events that had not occurred until then, resulted, in the United States, in the emergence of the area of activity called Clinical Engineering (CE). In Brazil, although the profession does not have its proper recognition and regulation, the need for a qualified and designated professional to manage health technologies, within a Health Care Facility (EAS), has been increasingly evident. To manage these technologies, in addition to being mandatory, is the responsibility of each Hospital, requiring dedication and control. The use of computerized systems (SI), aiming at successful management of health technologies, including the preparation of inventories and control of technical intervention events (e.g., maintenance), has been consolidated. Despite having available in the market diversified software intended for the realization of maintenance management, notoriously, the foundation, structuring and functionality of these, are convergent. The present work aimed to list, through bibliographic references, parameters and essential functions, which should make up an SI for the management of EMH, applied in the Departments of CE in Hospital Units. Thus, through the study carried out, it was observed that a software for this purpose can be divided into four main modules: Module of registrations, EMH inventory, service orders (maintenance) and, reports/indicators. Finally, given the functionalities identified in the analyzed SI, it is suggested to conduct new studies related to the incorporation of specific tools and functionalities, aimed at CE in Brazil.

Keywords: Clinical engineering · Maintenance software · Medical-hospital equipment · Hospital maintenance · Health maintenance

1 Introduction

With the significant advance of technologies applied in health care establishments (EAS), in addition to the constant demand, by society, for excellence, quality and safety in the services provided by these establishments, to carry out the management of health technologies, specifically under the medical-hospital equipment (EMH), has become a major challenge for clinical engineering (CE) and hospital managers.

The quality of service provision in a hospital is directly related to the efficient management of the respective medical and hospital equipment [1].

The term clinical engineer, created in the 1970s by Thomas Hargest and César Caceres, according to Gordon [2], in order to identify the professional responsible for managing technologies in healthcare environments, despite not being a modality recognized by the Federal Council of Engineering and Agronomy (CONFEA) in Brazil, according to Souza and More [3], has undeniable importance in the face of activities developed in the hospital environment.

Although there is no recognition by the competent class body (CONFEA), as presented by the National Health Surveillance Agency (ANVISA), through the Technovigilance Manual, health services in Brazil have had these professionals for at least 30 years, however in a reduced way and concentrated only in reference services or linked to universities [4].

Furthermore, as recommended by the health authority (ANVISA), through Resolution of the Collegiate Board (RDC) No. 509, of May 27, 2021 [5], which repeals RDC No. 02 of 2010, it is the responsibility of the health establishments manage health technologies used in the provision of health services, in order to guarantee their traceability, effectiveness, quality and safety, as well as carry out the elaboration and implementation of a Management Plan for the respective technologies, including medical-hospital equipment.

For the World Health Organization [18], there is a need to establish priorities in the selection and management of health technologies, resulting from the implementation and inappropriate use of these technologies.

According to Brito [6], in specialized literature, different methods of planning and management of technologies can be found, and the use of computerized systems is the most applied resource.

Thus, aiming for success in the management of health technologies, contemplating the control of preventive, corrective and calibration maintenance events, carried out in medical-hospital equipment [7], the use of specific applications and programs, generically called software, become essential for the organization and administration of a hospital, according to Malagón-Londoño [8].

Simply called CMMS, a computerized maintenance management system is a technological tool to support the maintenance strategy, which through a set of functions promotes data processing to produce indicators to be used in support of maintenance management activities [16].

In view of the above, through articles and studies already carried out, the present work aims to list the parameters and essential functions that must compose a computerized system (SI) for the management of medical and hospital equipment, applied in the departments of Clinical Engineering in Hospital Units.

2 Methodology

The present work was elaborated through research carried out on articles and literary works related to hospital management, specifically to the clinical engineering and hospital maintenance sector.

To delimit the bibliographic references to be consulted, the following keywords were defined to be used as search filters along with renowned websites of scientific articles: clinical engineering, maintenance management, medical equipment, maintenance software, cmms and management hospital.

Through the filters, fourteen (14) scientific/academic/technical works were initially selected, among them twelve (12) articles, one (01) dissertation and one (01) technical publication of the WHO, obtained from the websites Scientific Electronic Library (SciELO), CAPES Journal Portal, UNIFACEF Journal Portal, UFRN Journal Portal, Health and Technology Journal (joint publications by Springer and IUPESM—International Union for Physical and Engineering Sciences in Medicine, in cooperation with WHO—World Health Organization), PubMed, Institute of Electrical and Electronics Engineers—IEEE, ScienceDirect, World Health Organization—WHO, Google Scholar and institutional repository of UTFPR.

Literary works, totaling three (03), related to hospital management and maintenance management, were also preliminarily selected due to their respective titles: “Hospital Management—For an Effective Administration”, “Maintenance Management in Health Services” and “Management information systems in healthcare organizations”.

After the initial selection of works and books, in order to limit the bibliographic bases to be used, the introduction of these documents was read, aimed at identifying contents associated with the use of information systems for maintenance management by the sectors of clinical engineering in health care establishments.

That said, it was defined for the development of this study to use the articles written by Barbosa [9], Oliveira [10], Silva [11], Fernandes [12] Chein [15], Medenou [17], Patrícia’s dissertation [13], the technical document prepared by the WHO [18] and the literary work of Malagón-Londoño [8].

In addition to the selection of one (01) literary work and the eight (08) works obtained via websites, the use of Collegiate Board Resolution n° 509, of May 27, 2021 [5], issued by the National Health Surveillance (ANVISA), which discusses the management of health technologies in health establishments, and the Brazilian Standard NBR 15943 [14], issued by the Brazilian Association of Technical Standards (ABNT), addressing the guidelines for a management program for infrastructure equipment for health services and equipment for health, in order to complement this study.

Therefore, the purpose of this work is to list, through the bibliographic references, the functions and the main parameters recommended to compose an information system (software) destined to the effective management of medical and hospital equipment by a clinical engineering sector, having as based on their incidence, their respective foundations and compliance with specific norms and resolutions available in Brazil.

Next, Fig. 1 illustrates the methodology applied to carry out this work.

3 Results

Through the bibliographic references used for this study, a standardized structuring of the main functions and parameters necessary in the information systems used for the management of medical and hospital equipment by the clinical engineering sector in Hospitals was obtained.

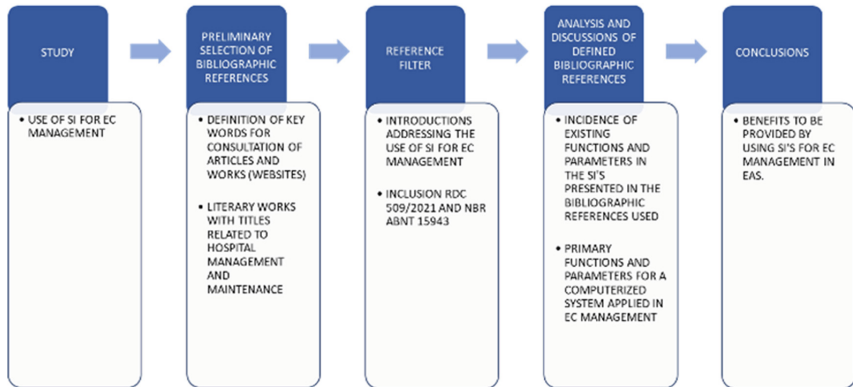


Fig. 1. Flowchart illustrating the methodology of this work. (The Author 2022).

Silva [11] presents that, in order to perform a better management control of medical-hospital equipment, an information system should basically enable the insertion of: registration/code generation/research for each medical-hospital equipment; registration and research of customers/companies/suppliers; issuance/evaluation/closure and research of service orders; registration of users/sectors with definition of usage profiles, to restrict the access of each user.

In the same way, Barbosa [9] shows that the Hospital Maintenance System 4.0, used by the clinical engineering sector in a large hospital located in Rio Grande do Sul, makes it possible to carry out an effective administrative control through the following applicability: registration of products, cost centers, employees, equipment, suppliers, payment methods, users and permissions, dollar exchange rates; issuance of maintenance service orders with priority level definitions; issuance of various reports for management controls.

Therefore, as mentioned by Malagón-Londoño [8], Oliveira [10] and Fernandes [12], the Computerized Maintenance Management System (CMMS) applied in clinical engineering provides benefits to the respective sector. The CMMS software must present as functionalities: fields and tables for entering data in general, related to the types of medical and hospital equipment, equipment models, manufacturers/sellers, warehouses/spare parts, personnel/users, maintenance (contemplating service orders) and the health establishment; equipment inventory module defined as the CMMS core, referring to the registration of information related to each medical-hospital equipment; spare parts management module; modules for preventive, predictive and corrective maintenance, with the possibility of defining calendars and schedules for efficient inspections; contract management module and diversified reporting.

Piccinini [13], in her dissertation published in the Postgraduate Program in Biomedical Engineering at Universidade Tecnológica Federal do Paraná, with the objective of developing, analyzing and implementing an information system for EMH maintenance management, called SIGMEH (Sistema of Medical-Hospital Equipment Management), presents as utilities of the respective SI: registration of users with definition of access

limits (profiles); registration of employees, positions, environments and suppliers; registration of medical-hospital equipment, values of technical maintenance hours, technical standards, EMH manuals, attachment of photos; management of preventive and corrective maintenance service orders; prioritization of equipment for maintenance and warehouse control.

For Chien [15], as exposed in his work on the development of a medical equipment management system structure for the clinical engineering department, applied in a University Hospital in Taiwan, the architecture of a CMMS for the management of EMH can be classified into four groups: the first intended for basic registration information, such as equipment inventory, cost center codes, staff data, etc.; the second comprising EMH acquisition, acceptance and disposal practices, involving the recording of dates and times, enabling monitoring and evaluations; the third, defined by the author as the busiest group in an CE sector, is dedicated to the maintenance of EMH, contemplating a system of service orders, with tracking of the progress and content of the repairs, allowing the future issuance of indicators of performance and failure trends; the latter includes warranty, maintenance and contract management systems, allowing the engineer to track information such as expired warranty, preventive maintenance or other contracted service.

With the objective of significantly improving the management and control of health technologies, especially in low-income countries, the work carried out by Medenou [17] demonstrates the application of CMMS in three hospitals located in Benin, West Africa. The implementation of a computerized system for the management of these technologies in low-income countries was motivated by the WHO. The CMMS developed, in its first version, had 35 database fields, with different purposes, enabling the registration and control of the inventory of the equipment park, the management and planning of preventive and corrective maintenance, the management of suppliers, the supplying spare parts, generating and controlling service orders and issuing reports.

In a technical document prepared by the World Health Organization [18], it is mentioned that computerized maintenance management systems always include medical equipment inventories and usually include information related to service history, maintenance procedures, performance indicators and information of costs. According to the WHO, the following are basic modules for composing a CMMS: equipment inventory module; spare parts management module; maintenance module, which includes several tools for the management of preventive and corrective interventions, service orders, schedules, parts, among others; and contract management module. In addition to the division into modules, a management system must also enable the issuance of various reports through the selection of fields, tables and existing modules.

Thus, it can be defined as the result obtained through the analyzed works, that the structuring of a computerized system intended for the management of medical-hospital equipment in clinical engineering, at least, must have the following functionalities and parameters, as illustrated in the Figs. 2 and 3.

STRUCTURING - INFORMATION SYSTEM FOR THE MANAGEMENT OF EMH IN CLINICAL ENGINEERING	
<p>1 REGISTRATION MODULE</p> <ul style="list-style-type: none"> 1.1 Cost centers; 1.2 Contracts; 1.3 EAS; 1.4 Suppliers / Companies; 1.5 Employees; 1.6 Users and permissions; 1.7 Standards and resolutions. 	<p>2 EMH INVENTORY MODULE</p> <ul style="list-style-type: none"> 2.1 EMH name; 2.2 EMH manufacturer; 2.3 EMH model; 2.4 EMH serial number; 2.5 EMH Heritage; 2.6 EMH Location/ Sector; 2.7 EMH priority level; 2.8 EMH Periodicity MP; 2.9 Date of acquisition of EMH; 2.10 EMH acquisition value; 2.11 Date of installation of the EMH; 2.12 EMH Warranty; 2.13 EMH maintenance contract; 2.14 EMH accessories; 2.15 EMH ANVISA Registration.

Fig. 2. Modules 1 and 2 of structuring an SI for EMH management (The Author 2022).

STRUCTURING - INFORMATION SYSTEM FOR THE MANAGEMENT OF EMH IN CLINICAL ENGINEERING	
<p>3 WORK ORDERS MODULE (MAINTENANCE)</p> <ul style="list-style-type: none"> 3.1 EMH data; 3.2 Applicant data; 3.3 Requested service (e.g. MP, MC); 3.4 Request date; 3.5 Defect Reported by the applicant; 3.6 Data of the person responsible for receiving the EMH; 3.7 EMH Exit Date; 3.8 Priority level; 3.9 Resp. execution of the service (e.g. internal or external); 3.10 Resp data. the execution of the service; 3.11 Failure displayed (actual defect); 3.12 Detailed description of the service performed; 3.13 EMH return date; 3.14 Status (e.g. in progress, completed); 3.15 Cost (\$) of services and parts performed; 3.16 Cost center; 3.17 Additional information (e.g. warranty). <p><i>Obs.: There is information that will automatically be filled in through the previous modules already registered.</i></p>	<p>4 REPORT AND INDICATOR MODULE</p> <ul style="list-style-type: none"> 4.1 Reporting based on the selection of information from previous modules 4.2 Issuing indicators based on the selection of information from previous modules

Fig. 3. Modules 3 and 4 of structuring an SI for EMH management (The Author, 2022).

4 Discussion

Based on the content of the nine (09) references used to carry out this work, as well as through Figs. 2 and 3, presented above, a software for the management of clinical engineering can be divided into four (04) main modules, being these: Module 01—Registration module; Module 02—EMH Inventory Module, Module 03—Service Order Module (Maintenance); Module 04—Reports and indicators module, similar to the one exposed by both Chien [15] and WHO [18].

The first module is intended for entering registration information, which are: hospital cost centers; registration of maintenance and acquisition contracts; information on the health care establishment, such as the name, the complexity of the services provided, the contacts and the respective CNES code (National Registry of Health Establishments); supplier and company information—containing fundamental data such as address, contact, company name, among others; employee data—containing name, job description

and salary, for example; data related to users of the computerized system, including creation, alteration, and definition of access permissions to be granted; the registration of current norms and resolutions, aiming at the elaboration of a technical collection of consultation to the users of the system.

Then, the second module, related to the inventory of medical-hospital equipment, has a fundamental role in the life of each EMH within the EAS, as explained by Silva [11]. In this step, data such as the name of the equipment, the manufacturer, the model, the serial number, the assets (internal information of each EAS), the location or sector in which it is located, the priority level of the equipment for the EAS, the periodicity of preventive maintenance, the purchase date and value, the installation date, the warranty provided by the supplier, the existence or not of a maintenance contract, the accessories and the registration with ANVISA, must be registered in order to obtain a “digital inventory”, such as providing effective traceability of existing technologies in the establishment, as recommended by Article 15. of Resolution RDC No. 509, of May 27, 2021 [5]. At this stage, it is appropriate to use a standard nomenclature for medical equipment, such as the Universal System of Nomenclature of Medical Devices and the Global System of Nomenclature of Medical Devices, according to WHO [18].

Through the third module, it is possible to carry out the management of technical interventions that occurred in medical-hospital equipment, meeting the requirements of ABNT NBR 15943 [14], which establishes instructions for a management program for infrastructure equipment for health services and of health equipment. Fernandes [12] defines service orders, the title of this third module, as requests for maintenance services for technologies registered in inventory. The registration and issuance of maintenance service orders are registered in this location. For each service order, information related to EMH registration data, service requester data, type of service requested (e.g. preventive or corrective maintenance), request date, EMH defect reported by the requester, data of the person responsible for receiving or withdrawal from the EMH, date of departure of the EMH from the sector of origin, service status (e.g.: in progress, completed), values with the performance of services and parts (if used), cost center and additional information (e.g.: item under warranty, maintenance unfeasible), must be completed. The use and insertion of data in this module is dynamic, conditioning the quality and effectiveness of the management to be carried out by the clinical engineering team, since through the information filled in the service orders, for example, it is possible to analyze of commonly occurring failures to prioritize interventions in EMH, according to Medenou [17].

The fourth module, aiming to provide a better managerial and technical control, in addition to being used to obtain several relevant information that can be used as complements for administrative decisions, as explained by Barbosa [9], the fourth and last module is intended for the elaboration of reports and indicators. In this module, information is obtained through the random selection of data already registered in the computerized system, having its usefulness focused on managerial and administrative actions as initially mentioned. As an example, reports showing the amount of equipment with “under maintenance” status, or the total cost spent on providing corrective maintenance services in each month, can be issued. The evaluation of the general performance

of the use of a CMMS for medical-hospital equipment, according to WHO [18], is made possible using this module.

The Table 1 aims to present in an optimized way the four modules mentioned in this discussion, in comparison to the necessary functionalities that an information system (SI) must have, identified in the nine (09) analyzed works.

In addition to the exposition of the modules proposed for the composition of a CMMS—CE, the last column of the Table 1 indicates that in none of the analyzed works, the existence of a functionality destined exclusively for the issuance of an EMH management plan, in a computerized system, is mentioned, which is necessary according to ABNT NBR 15943 [14] and RDC No. 509/2021 [5].

Table 1. Minimum modules necessary for a CMMS—CE, according to this Author, compared to the minimum functionalities mentioned in the analyzed works (The Author, 2022).

REFERENCES	APPROACH TO SIMILAR FUNCTIONALITIES IDENTIFIED IN THE REFERENCES				
	DIVISION OF MODULES PROPOSED FOR CMMS - CE				EMH MANAGEMENT PLAN ABNT NBR 15943 [14] AND RDC Nº 509/2021 [5]
	01 - REGISTRATION MODULE	02 - EMH INVENTORY MODULE	03 - WORK ORDERS MODULE (MAINTENANCE)	04 - REPORT AND INDICATOR MODULE	
Barbosa [9]	✓	✓	✓	✓	✗
Oliveira [10]	✓	✓	✓	✓	✗
Silva [11]	✓	✓	✓	✗	✗
Fernandes [12]	✓	✓	✓	✓	✗
Chein [15]	✓	✓	✓	✓	✗
Medenou [17]	✓	✓	✓	✓	✗
Patricia [13]	✓	✓	✓	✓	✗
WHO [18]	✓	✓	✓	✓	✗
Malagón- Londoño [8]	✓	✓	✓	✓	✗

5 Conclusion

Including from the initial registration of data, such as the insertion of users, suppliers, contracts, in addition to the creation of a digital inventory of medical-hospital equipment existing in a health care establishment, as well as the management of maintenance services performed in EMH's through service orders, up to the issuance of management reports and indicators, are unanimous and essential functions parameterized in the computerized systems used in the clinical engineering sectors.

In addition to corroborating with the essentiality and effectiveness in the management carried out using computerized systems, by the clinical engineering sectors in Hospitals,

the present work demonstrates that despite having available in the market diversified software destined for the accomplishment of maintenance management, their foundation, structuring, and functionality are convergent.

However, in the national conjuncture (Brazil), there is a possible gap in automated tools destined exclusively for clinical engineering attributions through current health norms and resolutions. For example, through the study carried out, the existence of functions strictly intended for the issuance of a Health Equipment Management Plan, as recommended by RDC No. 509, of May 27, 2021 [5], or, for the issuance of a health equipment management program, in compliance with the Brazilian standard ABNT NBR 15943 [14].

In conclusion, despite the already consolidated use of computerized systems intended to assist sectors responsible for managing equipment and maintenance, there are specific tools and functionalities, aimed at clinical engineering, subject to further studies and incorporations.

References

1. Amorim, A. S., Pinto, V. L., Shimizu, H. E.: O desafio da gestão de equipamentos médico-hospitalares no Sistema Único de Saúde. *Saúde Debate*. Rio de Janeiro **39**(105), 350–362 (2015)
2. Ramírez, E.F.F., Calil, S.J.: Engenharia clínica: Parte I – Origens (1942–1996). *Semina: Ciências Exatas e Tecnológicas*. **21**(4), 27–33 (2000). Available at: <http://www.uel.br/revistas/uel/index.php/semexatas/article/view/3009>. Access 29 May 2022
3. Souza, A.F., More, R.F.: O perfil do profissional atuante em engenharia clínica no Brasil. In: XXIV CONGRESSO BRASILEIRO DE ENGENHARIA BIOMÉDICA. 13 e 17 de outubro, 2014, Uberlândia. *A Engenharia Biomédica como Propulsora de Desenvolvimento e Inovação Tecnológica em Saúde*. Uberlândia: CBEB (2014). Available at: <http://www.canal6.com.br/cbeb/2014/index.html>. Access in: 29 May 2022
4. BRASIL: Agência Nacional de Vigilância Sanitária. Manual de tecnovigilância: uma abordagem sob ótica da vigilância sanitária [recurso eletrônico] / Agência Nacional de Vigilância Sanitária, Gerência Geral de Monitoramento de Produtos Sujeitos à Vigilância Sanitária, Gerência de Tecnovigilância. – Brasília: Agência Nacional de Vigilância Sanitária (2021)
5. ANVISA: Agência Nacional de Vigilância Sanitária. Resolução de Diretoria Colegiada – RDC N° 509, de 27 de maio de 2021. Brasília: Diário Oficial da União (2021). Available at: <https://www.in.gov.br/en/web/dou/-/resolucao-rdc-n-509-de-27-de-maio-de-2021-323002855>. Access in: 29 May 2022
6. BRITO: Lúcio Flávio de Magalhães. *Segurança aplicada às instalações hospitalares*. 6 ed. São Paulo: Editora Senac São Paulo (2014)
7. Dalcol, P., Gomes, L.: O papel da engenharia clínica nos programas de gerência de equipamentos médicos: estudo em duas unidades hospitalares. In: II CONGRESSO LATINOAMERICANO DE ENGENHARIA BIOMÉDICA, 23 a 25 de maio de 2001, Habana 2001. *Engenharia Clínica*. La Habana (2001). Available at: <https://pt.scribd.com/document/423662105/00131-pdf>. Access in: 29 May 2022
8. Malagón-Londoño, G.: *Gestão hospitalar para uma administração eficaz*/Gustavo Malagón-Londoño, Gabriel PontónLaverde, Jairo ReynalesLondoño; tradução Catia Franco de Santana, Iara Gonzales Gil. 4 ed. Rio de Janeiro: Guanabara Koogan (2019)
9. Barbosa, A.T., Spalding, L.E.S.: Análise do sistema de informação do setor de engenharia clínica de um hospital do sul do país. In: *Anais do X Congresso Brasileiro de Informática em*

- Saúde, pp. 14–18 (2006). Available at: https://www.researchgate.net/profile/Luiz-Spalding/publication/237266679_Analise_do_Sistema_de_Informacao_do_Sector_de_Engenharia_Clinica_de_um_Hospital_do_Sul_do_pais/links/545a11a20cf2bccc49130033/Analise-do-Sistema-de-Informacao-do-Sector-de-Engenharia-Clinica-de-um-Hospital-do-Sul-do-pais.pdf. Access in: 29 May 2022
10. Oliveira, B., Borges, L.: ESTUDO DA IMPLEMENTAÇÃO DO CMMS EM UM DEPARTAMENTO DE ENGENHARIA CLÍNICA. In.: Revista Eletrônica de Sistemas de Informação e Gestão Tecnológica **9**(3) (2018). Available at: <https://periodicos.unifacel.com.br/index.php/resiget/article/viewFile/1628/1146>. Access in: 29 May 2022
 11. Silva, L.M., Ferreira, A.C.M.: Sistema de Cadastro e Manutenção de Equipamento Médico Hospitalar: proposta para o desenvolvimento com uma ferramenta para auxiliar a gestão da manutenção da engenharia clínica nos hospitais. 2014. In: Fatec Bauru. Available at: <http://fatecbauru.edu.br/mtg/source/Sistema%20de%20cadastro%20de%20equipamento%20m%C3%A9dico-hospitalar%20.pdf>. Access in: 29 May 2022
 12. Fernandes, A.C.S. et al.: SISTEMA DE GERENCIAMENTO WEB PARA ENGENHARIA CLÍNICA: PROPOSTA DE ARQUITETURA E IMPLEMENTAÇÃO. In.: Revista Brasileira de Inovação Tecnológica em Saúde-ISSN: 2236–1103 (2017). Available at: <https://periodicos.ufm.br/reb/article/download/11623/8975>. Access in: 29 May 2022
 13. Piccinini, P.S. et al.: Sistema de informação para gerenciamento de equipamentos médicos-hospitalares. Dissertação de Mestrado. Universidade Tecnológica Federal do Paraná (2016). Available at: https://repositorio.utfpr.edu.br/jspui/bitstream/1/1870/1/CT_PPGE_M_Piccinini%2C%20Patricia%20Strapasson_2016.pdf. Access in: 29 May 2022
 14. ASSOCIAÇÃO BRASILEIRA DE NORMAS TÉCNICAS. NBR 15943: diretrizes para um programa de gerenciamento de equipamentos de infraestrutura de serviços de saúde e de equipamentos para a saúde. Rio de Janeiro, 21p (2011)
 15. Chien, C.-H., Huang, Y.-Y., Chong, F.-C.: A framework of medical equipment management system for in-house clinical engineering department. In: 2010 Annual International Conference of the IEEE Engineering in Medicine and Biology, pp. 6054–6057. IEEE (2010). Available at: <https://pubmed.ncbi.nlm.nih.gov/21097122/>. Access in: 26 Ago 2022
 16. Lopes, I. et al.: Requirements specification of a computerized maintenance management system—a case study. *Procedia Cirp* **52**, 268–273 (2016). Available at: <https://www.sciencedirect.com/science/article/pii/S2212827116307971>. Access in: 27 Aug 2022
 17. Medenou, D. et al.: Medical devices in sub-Saharan Africa: optimal assistance via a computerized maintenance management system (CMMS) in Benin. *Health and Technol.* **9**(3), 219–232 (2019). Available at: <https://link.springer.com/journal/12553/volumes-and-issues/9-3>. Access in: 24 Aug 2022
 18. World Health Organization et al.: Computerized maintenance management system (2011). Available at: <https://www.who.int/publications/i/item/9789241501415>. Access in: 29 Aug 2022



Investigation of Probable Causes of Patient Damage in the Multifactorial Environment of Adverse Events: Analysis of Adverse Event Notifications for Pulmonary Ventilator

Alexandre Holzbach Júnior¹ , Mariana Ribeiro Brandão² ,
and Renato Garcia Ojeda² 

¹ Institute of Biomedical Engineering (IEB-UFSC), Federal University of Santa Catarina/Center for Health Sciences, Florianópolis, Brazil
alexandrehj@yaho.com.br

² Institute of Biomedical Engineering (IEB-UFSC), Federal University of Santa Catarina/Technological Center, Florianópolis, Brazil

Abstract. Pulmonary ventilator is a medical equipment of big impact in patients with lung conditions or during anesthesia, making it important to evaluate the adverse events related to it and to place them in their context of occurrence. To this end, an analysis of adverse events was performed from 2011 to July 2021 based on the Food and Drug Administration (FDA) and National Health Surveillance Agency (ANVISA) platforms, along with a review of the literature on causes and contexts in which adverse events occur. In the FDA database, more than 100,000 notifications were found, with equipment defects related to display, operability, and mechanical problems predominating. The events of damage to the patient were mainly death, cardiorespiratory arrest and oxygen desaturation. On the ANVISA platform, 131 notifications were found, including complications related to the airflow of the device. Damage to the patient was, mainly, death, cardiorespiratory arrest, and respiratory failure. Applying the classification of adverse events of the Emergency Care Research Institute (ECRI) the reports of the American base, it was verified that the events were entirely caused by ventilator defects. Events related to problems intrinsic to pulmonary ventilators preponderated, a fact that is not consistent with the researched literature, which demonstrate the importance of the systemic approach to the complex environment in which adverse events occur. This study reinforces the need to generate evidence of problems related to the use of technologies for the investigation of causes, and to apply Clinical Engineering in management of health technologies in a safer way.

Keywords: Technovigilance · Pulmonary Ventilator · Adverse Event · Clinical Engineering

1 Introduction

According to the World Health Organization, medical equipment can be understood as any instrument, device, machine, software or reagent that has been manufactured for the purpose of serving in medical care, whether diagnosis, screening, treatment or its continued evaluation [1]. It is estimated that there are more than 2 million different types of medical equipment on the market, being deeply rooted in the practice of the health professional [1].

The mechanical ventilator has a great impact on patient survival and is used to maintain respiratory flow in situations of pulmonary or neuromuscular deficiency, such as severe acute respiratory syndrome (SARS), and general anesthesia [2, 3]. During the COVID-19 pandemic started in 2019, the ventilator was at the center of global debates, as well as the best techniques and modes of ventilation for patients in severe condition [4, 5].

However, it is also essential to analyze adverse events related to the use of mechanical ventilator. An adverse event is defined as a complication to the health of the user or patient that occurs during the routine use of a medical equipment, which is in conditions and parameters prescribed by the manufacturer [6]. Adverse events should be reported to health surveillance agencies, which have their respective databases, fundamental to provide information on classification and causes of these events, as well as the type of damage caused to the patient and the defects of related equipment [6, 7]. This system of surveillance of adverse events related to medical equipment is called technovigilance [6]. In fact, not only national surveillance institutions but also international private institutions such as the Emergency Care Reporting Institute (ECRI) are very active in the evaluation and classification of these events related to the use of medical devices, spreading useful reports for good health practices and also for decision-making in public policies [8].

In this sense, we highlight the relevance of understanding more deeply the cause of these incidents and their relationship with the environment represented by operator, apparatus, patient, institution and external environment, in order to assist Clinical Engineering in the management of health technologies with more safety and reliability, and consequently, reduce the damage caused to patients [9–11, 25].

Thus, this study sought to perform an analysis of adverse events related to the use of mechanical ventilator in the databases of the National Health Surveillance Agency (ANVISA) [12] and its American equivalent, the Food and Drug Administration (FDA) [13]. At the same time, the objective was a literature review on the causes and forms of classification of adverse events and how they can be situated in their context of occurrence.

2 Method

Given the current relevance of the mechanical ventilator in the face of the COVID-19 pandemic, this work selected this equipment for a review in two technovigilance databases. The analysis was carried out from 2011 to July 2021. For the analysis of the FDA database, the Manufacturer and User Facility Device Experience (MAUDE)

platform [13] was used, and for the search for mechanical fan data, the code chosen was the “CBK”, “Ventilator, Continuous, Facility Use”.

To search for Brazilian data, the Technology Notification platform was used, linked to the Ministry of Health [12].

For the analysis of the information, information was extracted from the reported problems and effects on the patient.

In addition, articles were searched in several databases such as PubMed, Embase and SciELO, in addition to gray literature, on the topics related to the subject. To carry out the search in these databases, the associated descriptors were: *pulmonary ventilator, ventilator, mechanic, mechanical respirator, medical device X adverse effect, adverse event X causes, consequences X ICU, intensive care unit, medical context, context of occurrence, place of occurrence*.

3 Results

3.1 Adverse Events Reported to the FDA

In the period from 2011 to the date of data collection, 101,791 reports were found to the FDA, totaling 102,193 adverse events. The year 2016 had the highest number of events, 16,055, while only 1877 events were recorded in 2011, the year with the lowest number of cases. On the platform, it is possible to find two main sets of information, the defects presented by the equipment and the damage that such defects cause to patients. The main mechanical fan failures reported in the period are: misguided message displayed on the fan display, equipment operating differently than expected, inoperable equipment, display not showing the parameters and images it should provide and mechanical problems. Regarding the damage inflicted on patients, although the most frequent items reported were lack of patient involvement, absence or ignorance of consequences or impact to the patient and absence of specific signs, symptoms or conditions, outcomes such as death, low oxygen saturation, difficulty breathing and cardiac arrest are also among the main ones. Figure 1 shows the FDA adverse event reports distributed over the years covered by this study.

3.2 Adverse Events Reported to Anvisa

In relation to the data of the Anvisa platform, 131 notifications were found, with the mechanical fan being the 6th device with more notifications in the delimited period. The highest number of notifications (26 reports) was recorded in 2020, the year in which the pandemic by COVID-19 was triggered, and the lowest number was recorded in 2011, with only 2 notifications. There was also an atypical fall in 2019, with only 4 notifications. The average in the period was approximately 12 notifications per year, with visible growth over time. Unfortunately, of the 131 reported, at least 100 are distributed between “Uninformed”, “Other” and “Ignored”, and there are also records regarding improper flow, lack of flow and loss of energy. Death was the most frequent patient’s damage, with 41 occurrences, followed by cardiorespiratory arrest and respiratory failure. “Unreported” data is also among the top notifications. Figure 2 shows the Anvisa adverse event reports distributed over the years covered by this study.

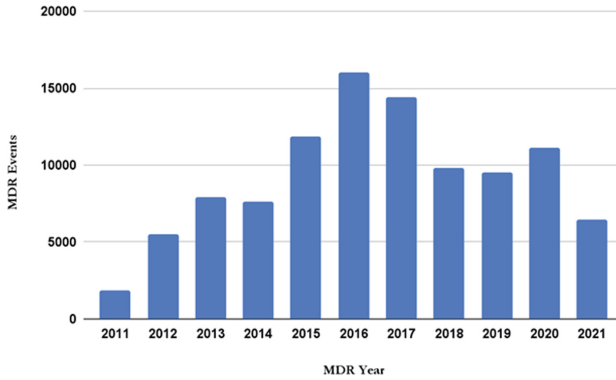


Fig. 1. Distribution of adverse events from the FDA platform in years of reporting

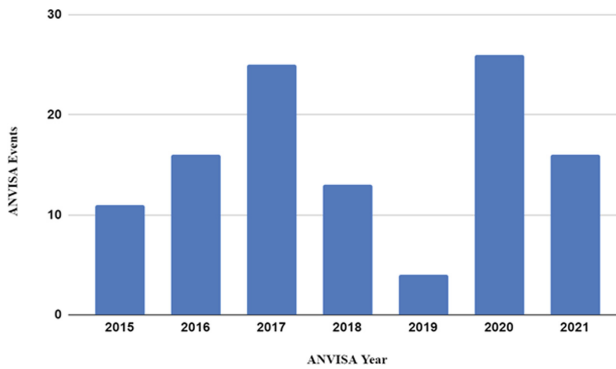


Fig. 2. Distribution of adverse events from the Anvisa platform in years of reporting.

3.3 Application of the ECRI Classification

Aiming to better understand the causes of adverse events and in view of the multifactorial context in which they occur, agencies such as Emergency Care Reporting Institute (ECRI) and researchers such as Sheperd [11, 14], elaborated classifications that could group these events into errors related to the equipment, the user/operator, external/environmental conditions, the installation/support and also to the patient and any attempts to sabotage. The similarity between the two models is in the categories “device” and “user/operator”, related to defects presented by the medical equipment itself and by human failures and lapses, respectively. In this study, the ECRI classification was applied to the data found on the FDA platform. Of the 100 types of reports of the American platform, 98 were framed as equipment failures and the remaining two as absence or informational insufficiency. It is possible to see the main flaws in the “equipment” category of ECRI in Table 1.

Table 1. FDA data applied in ECRI classification

Cause of adverse event	Number of notifications
<i>Due to equipment</i>	
Incorrect messaging devices	17,494
Device operates differently than expected	11,641
Device inoperative	8023
No display/image	7072
Mechanical problem	6038
Battery problem	4756
Failed to charge	4044
Circuit failure	3390
Failed to turn on	3087
failed to charge	4044
Circuit failure	3390
Failed to connect	3087
Failed to charge	4044
Circuit failure	3390
Failed to connect	3087
Failed to calibrate	2930
Incorrect or inappropriate test results	2628
Output problem	2415
Failed to recalibrate	2386
Device operational problem	2347
Appropriate term/code not available	2066
Device alarm system	1838
Irregular or intermittent display	1553
Loss of potency	1549
Device failure for self test	1475
Device stops intermittently	1452
Equipment cycle failure	1370
Problem of protective measures	1317
Power problem	1224
Break	1135
Failed to deliver	1025

(continued)

Table 1. (continued)

Cause of adverse event	Number of notifications
Display issue or visual feedback	1000
<i>Other causes</i>	
Adverse event with no identified device or usage issue	1817
Insufficient information	1115

4 Discussion

This work reviewed the ANVISA (Brazil) and FDA (USA) databases in search of the history of adverse events related to mechanical ventilator in the last 10 years. On both platforms, the relationship of equipment dysfunctions and damage to the patient was found. Regarding the defects of the equipment in question, the data found have a certain degree of variation, since the American agency mainly blames problems related to the visualization panel, operability (altered and absent) and mechanical problems without specification. On the other hand, ANVISA mainly reports problems with the flow of the device. However, such comparison may be inaccurate, since the Brazilian platform has a large part of its reports without the fan defect being broken down. Regarding the damage to the patient, there was convergence in the data of the platforms, with manifestations such as death, cardiac or cardiorespiratory arrest and respiratory problems occupying the first positions. In both databases, there was an increase in notifications over time, with notorious superiority in the contingent of American data.

According to studies that evaluated the main causes of adverse events, it is possible to draw a complex and multifactorial context in which these events may occur [11, 28]. Equipment failures are just one cause among the many potential actors and contributors of patient damage, such as the support provided by the health institution, maintenance and training, external factors such as radiation and infrastructure, the patient himself with his variable informational level and, certainly, professional health users, such as doctors and nurses, who effectively operate the equipment. It is even possible that problems related to usability and development of the medical device are part of the cause of adverse events and inaccuracies found in the notifications [29].

This interrelationship is illustrated in Fig. 3 [11, 14], and converges with the Methodology of Health Technology Management developed by the Institute of Biomedical Engineering (IEB-UFSC). In this model, infrastructure, technology and human resources must be analyzed and equated in their interaction, when considering the context in which the technology is inserted, to ensure safety, reliability and quality, as elucidated in Fig. 4 [26].

In this sense, Reason [9] outlines two systems in which human error could be situated, namely, the approach of the individual and that of the system. He argues that, while the mistaken approach of the individual focuses on guilt isolates errors from their situational contexts, the systemic approach emphasizes the development of the work environment and seeks to understand what defense mechanisms of a medical equipment failed for the adverse event to occur. This approach could be seen in the Swiss cheese model [9, 11],

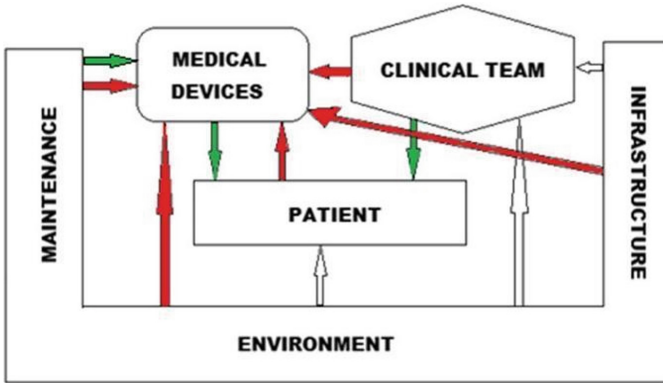


Fig. 3. Factors that can influence medical devices [11]

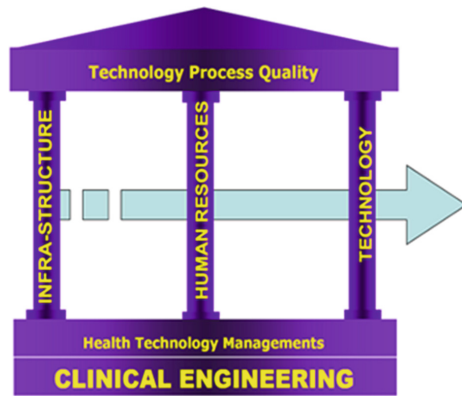


Fig. 4. Model of technological process in health IEB-UFSC [26]

with its various layers holding gaps, which represent the active failures of professionals and the latent conditions to which the whole system is subject. The adverse event occurs, thus, when all these gaps align. Within this integrated perspective, Evans et al. [15] demonstrated that, although mechanical ventilator alarms are effective and important in reporting critical situations and adverse events, they can easily be ignored, confused or not perceived in an intensive care unit (ICU), due to the fatigue of the multidisciplinary team, the multiplicity of rooms, noise pollution or acoustic issues of the site. To this end, they proposed an audiovisual alarm system that would have repercussions throughout the ICU and that would only be shut down after patient care.

Additionally, Kamio and Masamune [16] compared the use of mechanical ventilators in ICU and in a non-specialized medical environment, concluding that human factors were among the most frequent causes of adverse events in both sites, although errors based on medical knowledge were more prevalent in the non-specialized environment, given the lower preparation of professionals. These findings reinforce the need to evaluate

the entire context of probable causes, since the reports of this study referred to intrinsic errors, but may also be related to non-explicit causes of human failures.

Other studies also obtained similar results [7, 14], even showing that the human factor was predominant in other American databases such as Pennsylvania patient safety authority and university healthy system consortium, while the FDA presented a very low percentage for this factor. According to the same study [7], the types of reports and the way they are classified in a database are closely related to the purposes and characteristics of this database. Even so, it is questioned whether all events and their correct reasons have been openly reported to the American platform.

In the case of the Brazilian situation, we question why the platform has a significantly lower number of notifications when compared to the FDA. In March 2020, just before the outbreak of the pandemic in Brazil, there were about 61,000 [17] mechanical ventilators in the country, a figure that, when compared to the approximately 200,000 in the U.S. [18] up to the same period, does not justify such a lower number of reports. In Brazil, the system responsible for collecting and storing reports of adverse events is the National System of Notifications for Health Surveillance (NOTIVISA), linked to the Ministry of Health [19]. This system was inaugurated only in 2007, which contributed to the growth in the number of notifications in recent years [19]. However, this is a recent change, which seems to favor a possible posture of underreporting. In addition, studies have demonstrated low awareness, spontaneity and proactivity on the part of health professionals in reporting adverse events [20].

Beyond the Brazilian reality, however, underreporting is a significant problem for health agencies. Polisená and collaborators demonstrated [21], in an extensive systematic review, that fear of punishment, uncertainty about what should be reported, ignorance about how notifications will be used and issues related to time for notification are among the main barriers to the recognition and reporting of adverse events. More than that, there could be a lack of knowledge about the existence of an official and national reporting system for reporting events [27]. In addition, other studies have noticed [22], using simulations with patients, a relevant lack of consensus among health professionals regarding the application of protocols for reporting adverse events, demonstrating the variability with which these reports may occur. In this sense, it is important not only to develop structures for the safe processing of medical device notifications, but also to disseminate them among health professionals and make it possible for this notification to be done in an easy and intuitive way, creating a notification culture, with sense of justice and proportion on the eventual fault of the health professional [11], in addition to systemic strategies of organization, education and selection of equipment. Such pillars are fundamental not only for the increase of notifications, when there are adverse events, but also for the reduction of harm to the patient [11, 23].

Another advantage of the correct recording of adverse event reports is that an analysis of this information can be an important data generator for the Health Technology Management (GTM) carried out by the Clinical Engineering of the hospitals. Techno Surveillance programs with clinical engineering participation should carry out an up-to-date investigation of these events throughout the entire lifecycle of the ventilator and other devices, from the development stages to incorporation, use in healthcare environments [30].

Regarding data research, as well as in other studies [24], the difficulty in searching and collecting data from this research remains. Reports of adverse events constitute valuable information for researchers, health professionals and managers, in addition to patients themselves, which makes it imperative that they are properly systematized and classified and easily accessed. In this sense, one of the greatest difficulties in the use of the FDA platform is the existence of different codes for the same medical equipment, such as, in this case, the mechanical ventilator. In this study, the code “CKB” was used, but it is possible that other mechanical ventilator marks are recorded under other codes, which may constitute a limitation for this study, both by duplication of data and by lack of data under other records. On the ANVISA platform, it was noticed that, despite the 131 constant notifications, only 123 have details regarding the equipment defect and the damage to the patient described in the summary table. Moreover, there is no possibility of downloading the data from the online platform, which hinders the collection and analysis of these reports. Thus, it is possible to observe a lack of transparency and accessibility in these databases. In addition, there was inconsistency regarding the findings with regard to the models of the equipment, since the FDA platform has this data, but Anvisa’s does not. Thus, studies will be carried out to investigate a prevalence of adverse events and other mechanical devices.

Other limitations of this study are notifications recorded in more than one classification of equipment failure, which may inflate the numbers found, and the absence of information such as the site of use of the device and characteristics of the patient and the notifier, which prevents further analysis of the profile and context of the notifications.

5 Conclusion

This work reinforced the need to generate evidence of problems related to the use of technologies for the investigation of causes, and thus, to apply Clinical Engineering in the management of health technologies in a more safe and reliable way. The technovigilance platforms of Brazil (ANVISA) and the USA (FDA) present significant divergences, mainly regarding the volume of data and the degree of detail of the reports, and the FDA has superiority in these two criteria.

Despite the fact that both contribute to the knowledge and evaluation of adverse events that occurred in these countries. Cardiorespiratory arrest, respiratory failure and even death are among the main outcomes, which makes it imperative actions and studies aimed at increasing notifications and reducing harm to the patient. Given the importance of the systemic approach of the complex environment in which adverse events occur, it is necessary to stimulate scopes focused not on individual guilt but on the various factors potentially responsible for these events. Also, there is a possible culture of underreporting in Brazil, in view of the small number of ANVISA reports.

Thus, technovigilance is a fundamental program to promote the adoption of actions that lead to the protection and promotion of the health of the population. Technovigilance aims at the sanitary safety of health products in the post-marketing period (Equipment, Materials, Medical-Hospital Articles, Implants and Products for Diagnosis of “in-vitro” use), being extremely relevant in the context of health technology. It must always be known by health professionals, so that it is possible to have the correct registration and reduce the amount of technical failures and, consequently, the damage to the patient.

Acknowledgment. The authors appreciate the institutional support provided by the Federal University of Santa Catarina for the production of this research.

Conflict of Interest

The authors declare that they have no conflict of interest.




References

1. World Health Organization: Medical devices. WHO. www.who.int/health-topics/medical-devices#tab=tab_1. Last accessed July 2021
2. Hans, G.A., Sottiaux, T.M., Lamy, M.L., Joris, J.L.: Ventilatory management during routine general anaesthesia. *Eur. J. Anaesthesiol.* **26**(1), 1–8 (2009)
3. Calderon Romero, J.: Confiabilidade metrológica de ventiladores pulmonares. *Faculdades Catolicas* (2015)
4. Chang, R., Elhousseiny, K.M., Yeh, Y.C., Sun, W.Z.: COVID-19 ICU and mechanical ventilation patient characteristics and outcomes: a systematic review and meta-analysis. *PLoS One* **16**(2), e0246318 (2021)
5. Grasselli, G., Cattaneo, E., Florio, G., Ippolito, M., Zanella, A., Cortegiani, A., Huang, J., Pesenti, A., Einav, S.: Mechanical ventilation parameters in critically ill COVID-19 patients: a scoping review. *Crit Care* **25**(1), 115 (2021)
6. Centro de Vigilância Sanitária: Tecnovigilância. http://www.cvs.saude.sp.gov.br/apresentacao.asp?te_codigo=23. Last accessed July 2021
7. Pham, J.C., Williams, T.L., Sparnon, E.M., Cillie, T.K., Scharen, H.F., Marella, W.M.: Ventilator-related adverse events: a taxonomy and findings from 3 incident reporting systems. *Respir. Care* **61**(5), 621 (2016)
8. Report S.: ECRI Top 10 health technology hazards for 2020. *J Radiol Nurs* **39**(1), 6–9 (2020)
9. Reason, J.: Human error: models and management. *BMJ* **320**(7237), 768–770 (2000)
10. Amoore, J.N.: A structured approach for investigating the causes of medical device adverse events. *J. Med. Eng.* **2014**, 1–13 (2014)
11. Avendaño, G.: Critical importance of multilateral studies related with adverse events in medical devices. *Heal. Technol.* **6**(3), 213–227 (2016). <https://doi.org/10.1007/s12553-016-0151-5>
12. Agência Nacional de Vigilância Sanitária. Tecnovigilância—Português (Brasil). <https://www.gov.br/anvisa/pt-br/acesoainformacao/dadosabertos/informacoes-analíticas/tecnovigilância>. Last accessed July 2021
13. MAUDE - Manufacturer and User Facility Device Experience. <https://www.accessdata.fda.gov/scripts/cdrh/cfdocs/cfmaude/search.cfm>. Last accessed July 2021
14. De Souza, B.J.C., Mehrpour, S., Ferreira, M.M., Coelho, Y.L., Vivas, G.D.C., Rodriguez, D.D., et al.: Compilation about adverse events recorded in FDA/USA and ANVISA/Brazil databases through models available in the literature concerning analysis and prioritization of actions for medical devices. *Glob. Clin. Eng. J.* **4**(2), 5–14 (2021)
15. Evans, R.S., Johnson, K.V., Flint, V.B., Kinder, T., Lyon, C.R., Hawley, W.L., et al.: Enhanced notification of critical ventilator events. *J. Am. Med. Inform. Assoc.* **12**(6), 589 (2005)
16. Kamio, T., Masamune, K.: Mechanical ventilation-related safety incidents in general care wards and ICU settings. *Respir. Care* **63**(10), 1246–1252 (2018)
17. Veja: Coronavírus: Brasil tem 61.000 respiradores funcionando. É suficiente? | VEJA. <https://veja.abril.com.br/saude/coronavirus-brasil-tem-61-000-respiradores-funcionando-e-suficiente/>. Last accessed July 2021

18. WebMed: U.S. may not have enough ventilators for COVID-19. <https://www.webmd.com/lung/news/20200318/us-may-not-have-enough-ventilators-for-covid19>. Last accessed July 2021
19. de Oliveira, J.R., Xavier, R.M.F., de Santos Júnior, A.F.: Eventos adversos notificados ao Sistema Nacional de Notificações para a Vigilância Sanitária (NOTIVISA): Brasil, estudo descritivo no período 2006 a 2011. *Epidemiol e Serviços Saúde* **22**(4), 671–678 (2013)
20. Romeu, G.A., Távora, M.R.F., da Costa, A.K.M., de Souza, M.O.B., Gondim, A.P.S.: Notificações de reações adversas em um hospital sentinela de Fortaleza - Ceará. *An do Encontro do Programa Pós-Graduação em Ciências Farm* **I**, 1–5 (2017)
21. Polisen, J., Gagliardi, A., Urbach, D., Clifford, T., Fiander, M.: Factors that influence the recognition, reporting and resolution of incidents related to medical devices and other healthcare technologies: a systematic review. *Syst. Rev.* **4**(1), 29 (2015)
22. Yoon, C., Nam, K.C., Lee, Y.K., Kang, Y., Choi, S.J., Shin, H.M., et al.: Differences in perspectives of medical device adverse events: observational results in training program using virtual cases. *J Korean Med. Sci.* **34**(39) (2019)
23. Amoores, J., Ingram, P.: Quality improvement report: learning from adverse incidents involving medical devices. *Br. Med. J.* **325**(7358), 272–275 (2002)
24. Heinemann, L., Fleming, G.A., Petrie, J.R., Holl, R.W., Bergenstal, R.M., Peters, A.L.: Insulin pump risks and benefits: a clinical appraisal of pump safety standards, adverse event reporting, and research needs: a joint statement of the European association for the study of diabetes and the American diabetes association diabetes technology working group: a joint statement of the European association for the study of diabetes and the American diabetes association diabetes technology working group. *Diabetes Care* **38**, 716–722 (2015)
25. Brandao, M.R., Ojeda, R.G., Costa, M.G., Silvestri, C.T., Chagas, M.D., Campos, G.G.: Clinical engineering in the analysis of adverse events in medical equipment in Brazil. In: *International Clinical Engineering and Health Technology Management Congress*. Virtual Edition: [s.n.] (2021)
26. Garcia, S.J.: Health care technology management applied to pub-lic primary care health. *Pan Am. Health Care Exchanges* 250–253 (2011)
27. Alsohime, F., Temsah, M.H., Hasan, G., Al-Eyadhy, A., Gulman, S., Issa, H., Alsohime, O.: Reporting adverse events related to medical devices: a single center experience from a tertiary academic hospital. *PLoS One* **14**(10), e0224233 (2019)
28. Carlos de Souza, J., Mehrpour, S., Modolo Ferreira, M., Luduvico Coelho, Y., De Castro Vivas, G., Delisle Rodriguez, D., De Assis Santos, F., Freire Bastos-Filho, T.: Compilation about adverse events recorded in FDA/USA and ANVISA/Brazil databases through models available in the literature concerning analysis and prioritization of actions for medical devices. *GlobalCE* **4**(2), 5–14 (2021)
29. Flewwelling, C.J., Easty, A.C., Vicente, K.J., Cafazzo, J.A.: The use of fault reporting of medical equipment to identify latent design flaws. *J. Biomed. Inform.* **51**, 80–85 (2014)
30. David, Y.: Editor's Corner [Internet]. 4th ICEHTMC Proceedings. International Medical Sciences Group, LLC (2021)



Analysis of Maintenance Events in Medical Equipment in the Largest Trauma Hospital in Natal/RN

Lyssandra Paz¹ , Lucas Moura¹ , Tiago Barreto^{1,2} , Marcelo Lima³ ,
and Alice Suassuna^{1,4}  

¹ Federal Institute of Education, Science and Technology of Rio Grande do Norte,
Natal, RN, Brazil

² Department of Electrical and Computer Engineering, Federal University of Rio
Grande do Norte, Natal, RN, Brazil

³ Secretary of State for Public Health, Natal, RN, Brazil

⁴ Department of Electrical Engineering, Federal University of Uberlândia,
Uberlândia, MG, Brazil

alice.suassuna@hotmail.com

Abstract. The Advancements in biomedical technologies have led to the need for a sector responsible for management of all medical equipment in health establishments, thus coming to clinical engineering. There are three basic types of causes of failures that occur in these equipment: human error, technology failure, and external phenomena. Monitoring maintenance events is essential to understand what leads to these failures and, thus, seek solutions to mitigate them. Thus, the present work aims to analyze the requests for maintenance in the largest trauma hospital in Natal, Rio Grande do Norte, categorizing them in an attempt to understand the maintenance occurrences and carelessness with the equipment. For this, a survey of maintenance calls for biomedical equipment was performed, in the period of 3 months (February to May 2022), at the Monsenhor Walfredo Gurgel Hospital in Natal, Rio Grande do Norte. After data collection, it was found that 51.18% of the calls for maintenance corresponded to human error, and that a large part of the occurrences due to human error were related to problems with dirt and the others to false calls arising from the lack of information about correct operation of this equipment. From the classification, it is understood in a process of listening and observation of these professionals, that errors are caused, above all, by the lack of periodic training of the hospital's medical team. The implementation of a training routine would be a solution to alleviate the occurrences of maintenance in the hospital in question.

Keywords: Medical-hospital equipment · Clinical engineering · Human error · Dirtiness · Training

Lyssandra Paz and Lucas Moura are contributed equally to this work.

1 Introduction

The manual for regularization of medical equipment of Brazilian Health Regulatory Agency (Anvisa) categorize Medical-Hospital Equipment (MHE) as those that serve directly or indirectly for diagnosis, therapy, rehabilitation or monitoring for purposes of the medical, dental, therapeutic or rehabilitation areas [1]. Technological advances in health have also brought the insertion of equipment with refined and complex technologies and, along with these, another preoccupation has also arisen for hospitals: the expenses to preserve the lifespan of these equipment and how to manage them so that they work safely [2].

Clinical engineering is a subarea of biomedical engineering and it is responsible for the management and maintenance of all MHE in Healthcare Establishments [3]. From the implementation to the equipment's obsolescence, the clinical engineer is responsible for ensuring that it is used in the best way, promoting safety and quality in its operation [4]. In the current world scenario, where the Covid-19 pandemic is being experienced, the importance of the management and acquisition of medical equipment and the need and importance of the clinical engineer within the Healthcare Establishments became even more evident [5].

There are three basic types of failure causes that occur in these equipment: human error, which are acts of failure caused by a operator or other person; technology failure, in which a mechanical, electrical, structural or operational failure results in damage to the equipment and; external phenomena, in which items outside of the unit affect the equipment operation [5]. Regarding failures caused by human error, some studies in the literature showed that the main cause of maintenance MHE was due to this type of failure [6–8].

Medical equipment training that are provided to hospital professionals, who are users of these technologies, increases the percentage of functional medical equipment in use and reduces the rate of equipment failure due to operator error and negligence [9]. It is estimated that 20% of all equipment failures can be avoided by training the user [9], this information was reinforced by studies that showed the importance and effectiveness of training hospital staff [8, 10]. Furthermore, a study performed in a city in Iran showed that in 60% of the hospitals only a small number of employees have been trained in the use of MHE, in 20% all the employees who work with the equipment have been trained in the maintenance and use of the equipment and in the remaining 20% of hospitals, the staff has not been trained in the use of the equipment [11], also reinforcing the lack of training within the healthcare establishments.

All the MHE of Monsenhor Walfredo Gurgel Hospital, located in the Natal/RN, is managed by the biomedical engineering staff of the State Department of Public Health of Rio Grande do Norte (SESAP) together with the Equipment Center. The hospital is considered the largest public hospital for trauma care in the state. During a curricular internship for the technical course of biomedical equipment, developed at the hospital, it was observed that many of the maintenance calls and equipment problems came from false calls and operation errors. Therefore, in order to understand and seek ways to alleviate the problems observed in the hospital during the internship period, the present work

aims to analyze the requests for work orders in the Monsenhor Walfredo Gurgel Hospital, categorizing them in an attempt to understand the maintenance occurrences and carelessness with the equipment.

2 Methodology

2.1 Observation

The observational and methodological process of this work was performed at the Monsenhor Walfredo Gurgel hospital. Thus, a quantitative analysis of the hospital's medical equipment maintenance calls was performed. Maintenance calls are made by telephone between the sectors and the hospital's Biomedical Equipment Center. After connecting, technicians move to the equipment to transfer it into the clinical engineering laboratory. Thus, with the appropriate material and environments, the equipment is evaluated. During the process of technical evaluation, the operational tests verify the malfunction or not of the equipment, thus the technician is able to classify the problem and report what happened in physical document.

Through the records of maintenance calls requested by the sector and/or the weekly visits routine to the hospital sectors, it was identified that a portion of the requests attended by the clinical engineering corresponded to problems in the biomedical equipment due to misuse. Among them were mainly: electrocardiographs, laryngoscopes, infusion pumps and defibrillators. It is important to mention that all analyzed equipment has less than five years of service life.

2.2 Data Collection

All maintenance data for electrocardiographs, laryngoscopes, infusion pumps and defibrillators were collected during the period from February 21, 2022 to May 20, 2022. These data were referred to both maintenance calls and misuse identified during weekly predictive maintenance in the sectors. From then on, engineering reported the descriptions in physical document with the objective of recording which equipment was collected, the amount of them, which defects and their possible causes. In addition, there was also the photographic register.

Then the data were exported to a spreadsheet and the analysis and categorization of maintenance calls for the collected period were performed.

3 Results

3.1 General Occurrences of Maintenance on the Biomedical Equipments

In total, the four biomedical equipment analyzed totaled 127 maintenance calls (Table 1). Of these occurrences, 48.8% were true failures, from the technology itself and 51.2% from human error (Fig. 1A). Analyzing by equipment, there were

Table 1. Occurrence of maintenance calls for each equipment during the three months.

Equipment	Total maintenance	True failure	Human error
Defibrillator	14	2	12
Electrocardiograph	8	0	8
Laryngoscope	9	2	7
Infusion pump	96	58	38

about 11% of maintenance calls for defibrillator, 6.3% for electrocardiograph, 7.1% for laryngoscopes and 75.6% for infusion pumps (Fig. 1B).

Regarding maintenance calls due to human error, many occurrences were observed due to dirtiness in the equipment, such as: clotted blood inside the laryngoscopes, dry enteral and parenteral feeding in the connections of the infusion pumps’ drop sensors and dry conductive gel in defibrillator paddles connections (Fig. 2). The graph in Fig. 1C shows the percentage of dirtiness problems for each equipment in relation to other maintenance calls.

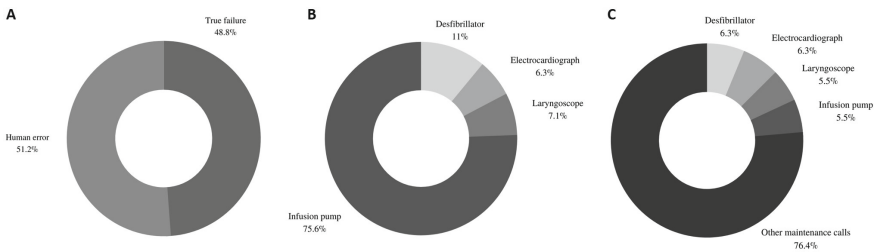


Fig. 1. A) Percentage of occurrences of true maintenance failures and those resulting from human error. B) Percentage of maintenance calls for each equipment. C) Percentage of dirtiness problems in each equipment in relation to other maintenance calls.

For better conclusions, the calls for each of the four observed equipment will be analyzed below. After analyzing the maintenance calls for each equipment, it was possible to categorize the occurrences of failures in the MHE into three situations: true failure, false failure and failure due dirt.

3.2 Laryngoscopy

The records of maintenance calls related to laryngoscopes were due to two points:

- *Two true maintenance calls:* physical breakdown of the device.
- *Seven maintenance calls caused specifically by dirtiness:* Laryngoscopes consist of two parts: a handle and a blade; both of which are autoclave. However,

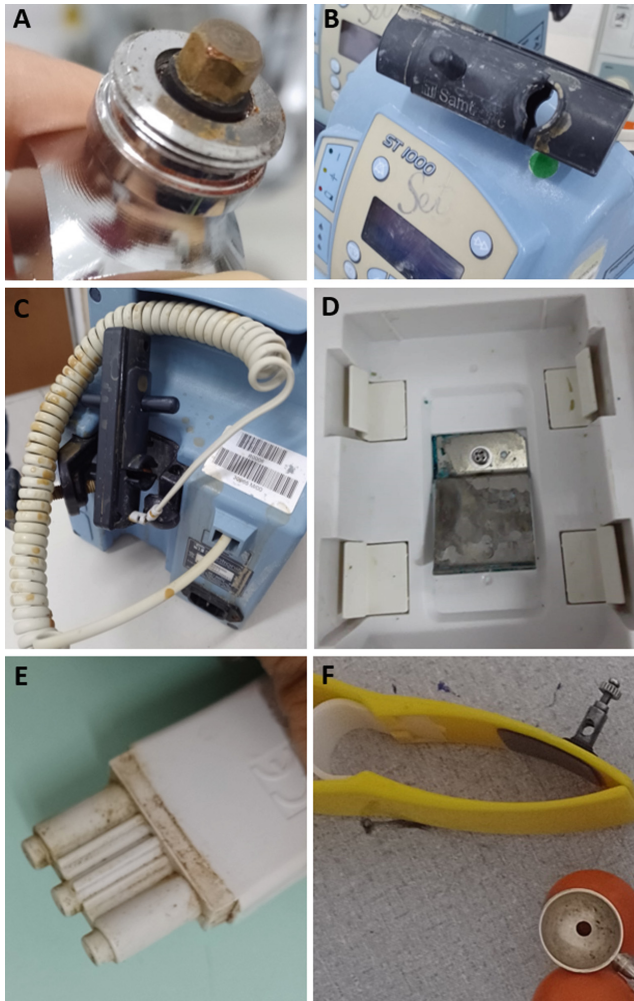


Fig. 2. Images of the dirtiness problems. A) Clotted blood inside the laryngoscopes. B) and C) infusion pumps' drop sensors and. D) Dry conductive gel in defibrillator paddles connections. E) Dirt on the defibrillator ecg cable. F) Ecg electrodes with dried gel.

to perform the autoclaving process, it is necessary to disassemble this parts of the device. As this procedure is not protocoled by the Hospital's Material and Sterilization Center (MSC), then it is not performed. The process that the equipment is submitted consists in a high-level disinfection of the blade, discarding the cable. As disinfection is not performed correctly, in some cases, it is common for dirt to accumulated on the inside of the cable, such as clotted blood (Fig. 2A). This cause poor contact between the handle and the blade, whose connection is necessary for led activation and equipment operation.

Based on the observation of the functioning of the MSC and the need for internal cleaning of the cables, it was possible, initially, to repair five cables considered obsolete and, later, two more cables at the request of the operating room, only performing the necessary thorough cleaning. The graph in Fig. 3A shows the occurrences of laryngoscopy failures.

3.3 Infusion Pump

- *Fifty-eight true maintenance calls*: problems in the door sensor, drip sensor, pressure sensor, battery, blown fuse, software errors and damage to structural parts of the equipment from fall (which could still be related to human error).
- *Thirty-one false maintenance calls*: the team from the equipment's origin sector reported an error in one of the main sensors of the device. Thus, the equipment was collected and subjected to operational tests in its main sensors (drop, air in the line, pressure and door sensor) and tests of usual functionality, performed through the programming of the infusion procedure. After the tests carried out, the usefulness of the electromedical device was proven, then the occurrence was recorded as a false call.
- *Seven maintenance calls caused by dirtiness*: inspections were made in the infusion pumps whose visible dirt indicated carelessness with the equipment (Fig. 2B-C). Misuse, in the analyzed cases, caused the breakage of the drops sensors or air sensors. The graph in Fig. 3B shows the occurrences of infusion pump failures.

3.4 Defibrillator

- *Two true maintenance calls*: both caused by equipment battery problems. In sectoral visits, these equipments are regularly found not connected to the electrical grid. Therefore, although considered as a real defect, these calls are due to misuse;
- *Four false maintenance calls*: during the period of the curricular internship, it was noticed by the biomedical engineering staff that the lack of periodic training linked to the constant change of the sectors' employee, cause human errors related to the negligence in carrying out the daily operational test of this equipment. Many health professionals have technical difficulties when performing the daily operational test of defibrillators, this lack of information is caused, in most cases, by the absence of adequate training. In addition, the equipment becomes inoperative after a period without performing daily operational tests, because of its programming. Both false maintenance calls were related to not performing the test, it was also possible to observe that the requesting sectors were composed of a senior team, or infirmary sectors whose report of need for use is lower. Consequently, these calls are classified as human error, caused by lack of information.
- *Eight maintenance calls caused specifically by dirtiness*: in seven of the eight cases the dirt caused poor contact between the paddles and the equipment (Fig. 2D). In the other case, dirt was present in the connection between parts

of an ecg cable (Fig. 2E). As it was a plug-in cable and it was in direct contact with the patient, dirt was added to this part. The graph in Fig. 3C shows the occurrences of defibrillator failures.

3.5 Electrocardiograph

- *All eight maintenance calls caused specifically by dirtiness*: described as interference in the exam trace. These failures are common due to several factors: electrodes with dried gel (Fig. 2F), inadequate preparation of the patients' skin, the lack of a suitable place to perform the exam and the absence of periodicity of training to nursing technicians.

During the period evaluated, the sector with the most recurrent problems was the electrocardiogram, which is responsible for performing tests for other sectors such as: multiple trauma, clinical care and observation sectors. On April 29, 2022, it was reported that a maintenance call, on a Friday, caused a 24-hour stop in the electrocardiography sector due to interference in the exam trace caused by dirt previously accumulated in the ecg electrodes and, later, on the cable of the electrocardiography device. It is important to note that in this case, even though the equipment was cleaned and the cable changed, it still presented interference due to problems regarding the preparation of the patient's skin and the location of the electrodes. The professionals of this department of the hospital, in particular, did not receive training. One of the causes for this was the difficulty of the professionals with technology, since the implementation of the equipment occurred via the internet, as reported by nurses and secretaries of the sector. From then on, due to not knowing how the electromedical device worked, there was no knowledge of the need to clean the electrodes and use the gel to improve contact, since that the exams are routinely performed in the hospital corridor with the patient under stress and restless.

The graph in Fig. 3D shows the occurrences of electrocardiograph failures. During the attendance to the maintenance calls and sector visits, a simple training was applied to the health staff, showing the functionality and the main reasons for interference in the equipment. Their application made it possible to limit up to two maintenance calls per sector during the evaluated time, with the exception of the electrocardiogram sector, which requested three maintenance calls and one training. In addition, regular maintenance made it possible to formulate a procedure for responding to calls. The sequence of actions to be taken were arranged as follows: cleaning the electrodes, cable and electrode contact areas with the patient and using a little conductive gel to facilitate the performance of the exams.

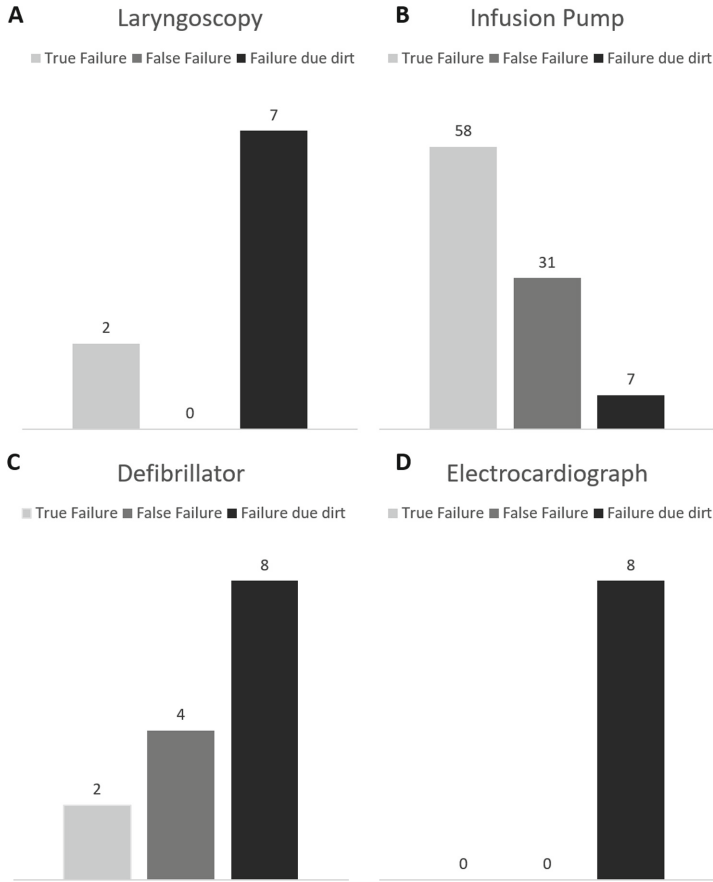


Fig. 3. Occurrences and identification of failures for each analyzed biomedical equipment. A) Laryngoscopy. B) Infusion Pump. C) Defibrillator. E) Electrocardiograph.

4 Discussion

The need to reinforce training methods in hospital medical equipment for health professionals who use them is incontestable [12]. Furthermore, as predicted by Barbosa and Ferraz in [13], and reinforced by Silva et al. in [5], in view of the constant change of professionals who handle the equipment, it is necessary to provide periodic training. In this sense, according to the results presented, it is observed that the data found in the present work corroborate with data from the literature, showing that many of the maintenance problems in medical equipment are caused by human error, often resulting from the lack of training.

In the present work, the maintenance calls for defibrillator presented two failures referring to non-performance of the daily operational test. After the application of simple training and followed by weekly monitoring via sectoral round of these hospital departments, the daily test started to be performed

correctly. Concomitant to the training factor, it is worth discussing the issues of human error, characterized by Lima in [7], listed in this work. As in the data referring to false calls for the infusion pump, thirty-eight occurrences, it is noted that the lack of regular training caused unnecessary maintenance stops, in addition to misuse observed during sector rounds. An example of misuse observed is that the hospital's nursing staff infused drugs with the parenteral setting so that they did not use the air in-line sensor. Furthermore, the infusion pump is considered an equipment very important within hospital, but it is among the main equipment responsible for medical complications and causes of failures [8, 14, 15]. In our study, this fact was also evident, since they were responsible for 75.6% of maintenance occurrence.

Another aspect that was frequently observed in the research was the cases of problems due to dirt, which caused the equipment to not function correctly, and which can also be mitigated with periodic training to the operators. In the case of electrocardiographs, for example, it was noted that the presence of extracorporeal fluids and resected conductive gel made it difficult to acquire the bioelectric signals read during the electrocardiography exam. This problem was also observed by Cummins, Chesemore and White in [16], in a research with defibrillators. Based on this, it is clear that the dirt affected the dynamics of examinations of various medical equipment in the hospital. Therefore, including a process for proper use of the medical equipment, as well as providing a cleaning routine before and after its use and protocol the care to be taken by health professionals would help to reduce these maintenance occurrences.

According to Jamshid et al. in [17], and Sheikhalipour et al. in [18], false maintenance calls also impact on the decrease in performance of the hospital's quality, cost and operating time indicators, as they cause stops that reduce equipment availability time and promote their non-assistance in a medical procedure. As well as was observed in a false call for electrocardiograph maintenance that resulted in a 24-hour stop in the sector that performed electrocardiogram exams.

In addition, it is important to emphasize that dirt indicators do not only impact in the good work of medical equipment. According to Queiroz-Junior et al. in [19], the incorrect cleaning and disinfection of equipment, although not critical items, makes them susceptible to possible contamination. Furthermore, according to Morais et al. in [20], failures in the cleaning and disinfection process of these devices potentiate the development of microorganisms, such as coagulase-negative Staphylococcus.

5 Conclusion

In view of the data presented, it is noted that failures in biomedical equipment caused by human error are still quite present in the hospital (51.18%) and impact the functioning of the institution. Dirtiness considerably influences the medical equipments life cycle, influencing not only the life cycle but also the indicators of quality, time and cost in biomedical engineering and risk of infection, since that cleaning, testing and evaluating the equipment requires the availability of human,

technical and time resources. With this, the importance of periodic availability of biomedical equipment training for the team that uses them is observed. The professional working in the field of clinical engineering must consider not only the demands of equipment but also the limitations of operating individuals. As future suggestions, we see the need to carry out periodic training in the hospital together with the record of calls for predictive maintenance, that is, sector rounds and the report of health professionals who deal with the device in question.

Conflict of Interest. The authors declare that they have no conflict of interest.

Acknowledgments. To the Monsenhor Walfredo Gurgel Hospital and the biomedical engineering sector of the State Department of Public Health of Rio Grande do Norte for allowing the accomplishment of this work.




References

1. BRASIL: Manual para regularização de equipamentos medicos na Anvisa at www.gov.br/anvisa/pt-br/centraisdeconteudo/publicacoes/produtos-para-a-saude/manuais/manual-para-regularizacao-de-equipamentos-medicosna-anvisa.pdf (2021)
2. Rogers, T.: Hospital-based technology assessment. *J. Clin. Eng.* **27**, 276–279 (2002)
3. Hegarty, F., Amooore, J., Scott, R., Blackett, P., McCarthy, J.: The role of clinical engineers in hospitals. *Clin. Eng. (Elsevier)* 93–103 (2014)
4. Araújo, C.: Análise e Simulação de Processos de Manutenção de Equipamentos Médicos no Serviço de Electromedicina. PhD thesis. Instituto Politécnico do Porto(Portugal) (2020)
5. Silva, A., Monteiro, J., Moreira, P., Pedroso, M.: A importância do engenheiro clínico no ambiente hospitalar. *Braz. J. Dev.* **6**, 83579–83585 (2020)
6. Alves, M., et al.: Bombas de infusao: operação, funcionalidade e segurança (2002)
7. Lima, M.: Taxonomia dos modos e causas de falhas aplicada na tecnovigilância de equipamentos médico-hospitalar. *Rev. Bras. Inov. Tecnol. Saúde* 32–41 (2011). ISSN 2236-1103
8. Suassuna, A., Mendes, E., de Menezes, C.D.L., Stransky, B.: Infusion pump training: from course to evaluation. In: XXVI Brazilian Congress on Biomedical Engineering, pp. 783–788. Springer (2019)
9. Oshabaheebwa, S., Namuli, L., Tusabe, M., Nantume, J., EngD, R., Ssekitoleko, T.: Enhancing skills to promote the utilization of medical laboratory equipment in low resource settings. *Health Policy Technol.* **9**, 94–101 (2020)
10. Shukla, K., Muthal, S.: Mishandling of medical devices in hospital ICU: analysis of causes, revenue drains and training needs of ICU Staff. *Indian J. Publ. Health Res. Dev.* **8** (2017)
11. Ghasemi, M., Mazaheri, E., Hadian, M., Karimi, S.: Evaluation of medical equipment management in educational hospitals in Isfahan. *J. Educ. Health Promot.* **11** (2022)
12. Mohess, K., Turner, J.: Development and evaluation of an electronic medical device training passport to identify nurses' training needs. *Nurs. Manag.* **28** (2021)
13. Barbosa, F., Ferraz, N.: Gestão das Tecnologias Biomédicas e seu papel no ensino-aprendizagem do correto manuseio dos equipamentos medico-assistenciais Perspectivas Experimentais e Clínicas, Inovações Biomédicas e Educação em Saúde (PECIBES) **7**, 33–37 (2021). ISSN-2594-9888

14. Holsbach, L., Kliemann, J., Holsbach, N.: Use of an instrument to identify knowledge for safe administration of medications using automatic infusion. *Rev. Bras. Eng. Bioméd.* **29**, 353–362 (2013)
15. ECRI (Emergency Care Research Institute) - Top ten health technology hazards for 2014. www.ecri.org/Resources/Whitepapers-and-reports/2014-Top-10-Hazards-Executive-Brief.pdf (2014)
16. Cummins, R., Chesemore, K., White, R.: Defibrillator failures: causes of problems and recommendations for improvement. *JAMA* **264**, 1019–1025 (1990)
17. Jamshidi, A., Rahimi, S., Ait-kadi, D., Bartolome, A.: Medical devices inspection and maintenance; a literature review. In: IIE Annual Conference. Proceedings: 3895 Institute of Industrial and Systems Engineers (IISE) (2014)
18. Sheikhalipour, Z., Ghahramanian, A., Dadashzadeh, A., Akhuleh, O., Rahmani, F., Fallah, M.: Factors affecting false calls to prehospital emergency medical services and analyzing the recorded false calls in the dispatch center. *Disaster Emerg. Med. J.* (2022)
19. Queiroz Junior, J., Melo, I., Calado, G., Cavalcanti, L., Sobrinho, C.: Identification and resistance profile of bacteria isolated on stethoscopes by health care professionals: systematic review. *Am. J. Infect. Control* **49**, 229–237 (2021)
20. Moraes, C., Ribeiro, N., Costa, D., Furlan, V., Palos, M., Vasconcelos, L.: Contaminação de equipamentos e superfícies de Unidades de Terapia Intensiva de uma maternidade pública por *Staphylococcus coagulase-negativa* (2013)



Indexes for Health Technology Assessment Two Case Studies: Computer Tomography Scan and Linear Accelerator

L. Guzmán-Canizales , J. A. Lozano-Suárez , and M. R. Ortiz-Posadas^(✉) 

Electrical Engineering Department, Universidad Autónoma Metropolitana-Iztapalapa, CP 09340
Mexico City, Mexico
posa@xanum.uam.mx

Abstract. The Computed Tomography Service (CTS) of the National Institute of Pediatrics from Mexico, currently has a 64-slice CT-scan acquired in 2010. The equipment will be soon obsolete since the supplier will no longer provide technical support. In 2020 the CT-scan was evaluated, as well as the productivity of the CTS. Likewise, the Pediatric Radiotherapy Service (SRP) has a linear accelerator old than ten years and is also closed to becoming obsolete due to lack of technical support from the supplier. In 2019, the productivity of the SRP was evaluated as part of an investment project to acquire a new linear accelerator. In both studies, a set of variables and indicators was defined to evaluate different aspects of these two medical equipment. Therefore, the objective of this work was to show that the subset of variables and indicators defined for two devices with different purposes: diagnostic (CT-scan) and therapeutic (linear accelerator), are useful to evaluate any type of medical device. It was defined eight variables and a technical indicator (I_T). The I_T was applied in both medical equipment allowed knowing their technical state and suggesting a period to replace them. In both cases, it is observed that the results are consistent, since they are more than 10 years old, and during the year 2022 they will no longer have technical support from the provider. This scenario makes both the CT-scan and the linear accelerator obsolete equipment. Both equipment should be replaced in the short term.

Keywords: Health Technology Assessment · Computer Tomography Scan · Linear Accelerator

1 Introduction

Health Technology Assessment (HTA) is the systematic evaluation of properties, effects, and/or impacts of health care technology. It should include medical, social, ethical, and economic dimensions, and its main purpose is to inform decision-making in the health area [1]. The indicators are a very useful tool in the HTA. An indicator is an instrument to provide evidence of a particular condition, or measurement of certain specific results. Indicators may provide information on quantitative and qualitative aspects of a program or a project objective. To this effect, several HTA studies use indicators to prioritize the preventive maintenance [2]; prioritize the replacement of medical technology [3]; or estimate patient access to imaging services [4].

The National Institute of Pediatrics from Mexico (INP, its Spanish acronym) is a tertiary public hospital with 243 beds. It has a total of 6165 medical equipment, 3699 are located in clinical and research laboratories, and 2466 in healthcare areas. About 1603 equipment is less than or equal to 10 years old, 1356 is between 11 to 20 years old, and 3206 is more than 20 years old [5]. In this sense, obsolescence is a characteristic related to the medical equipment antiquity. It implies the increasingly difficult to obtain spare parts, accessories, and consumables for its correct operation, with the consequence that the equipment will stop working. Therefore, it will be necessary to acquire a new one to continue providing healthcare services to patients.

The Computed Tomography Service (CTS) of the INP currently has a 64-slice CT-scan acquired in 2010. The equipment will be soon obsolete since the supplier will no longer provide technical support. In 2020 the CT-scan was evaluated considering three aspects: technical and economic performance, and the productivity of the CTA [6]. Likewise, the Pediatric Radiotherapy Service (PRS) has a linear accelerator old than ten years old and is also closed to becoming obsolete due to lack of technical support from the supplier. In 2019, the productivity of the SRP was evaluated as part of an investment project to acquire a new linear accelerator [7]. In both studies, a set of variables and indicators was defined to evaluate different aspects of the medical equipment. To evaluate the technical aspect and the productivity of the medical service where the medical equipment is located, a selection of the variables and indicators defined in each study was made. Therefore, the objective of this work was to show that the subset of variables and indicators defined for two medical equipment with different purposes: diagnostic (CT-scan) and therapeutic (linear accelerator), are useful to evaluate any type of medical device.

2 Methodology

2.1 Technical Evaluation of Medical Equipment

The technical evaluation of medical equipment was performed by applying a technical indicator (I_T) defined for eight variables (x_i) with a weight factor (ρ_i) through the Eq. (1) [6, 7]. Observe in Table 1 that the variable with the highest weight ($\rho_1 = 0.9$) is $x_1 =$ Spare parts available next 5 years; and the lowest weight ($\rho_8 = 0.2$) is $x_8 =$ Maintenance requirement, that describes the level and frequency of maintenance according to the manufacturer's indications, or accumulated experience of technical staff [8]. The variable $x_4 =$ Equipment function, defines the application and environment in which the equipment item will operate, and it considers 10 functions [8].

$$I_T = \sum_{i=1}^n \frac{\rho_i x_i}{4.4} \quad (1)$$

where:

$x_i =$ variable, $i = \{1, \dots, 8\}$ $\rho_i =$ relevance factor for x_i .

$N = 4.4$ is the normalization factor for obtaining the I_T result into $[0, 1]$.

For the interpretation of the quantitative result of I_T a qualitative scale was defined, divided into four intervals that correspond to a deadline for the equipment replacement:
 $[0,0.25) =$ long term (10 years)

Table 1. Variables of the technical indicator (I_T) and their weights [6].

x_i	Variable	ρ_i
x_1	Spare parts available next 5 years	0.9
x_2	Equipment age in operation	0.8
x_3	Days of the equipment out of service	0.7
x_4	Equipment function	0.6
x_5	Equipment failure frequency	0.5
x_6	Physical Risk	0.4
x_7	Consumables available next 5 years	0.3
x_8	Maintenance requirements	0.2

[0.25, 0.5) = medium term (6 years)

[0.5, 0.75) = short term (3 years)

[0.75, 1] = immediately (less than 3 years).

2.2 Epidemiological Analysis of the Medical Service

Epidemiological information was collected from the medical services: number of patients treated, patient characteristics, type of study, and time spent in each study. For the Computed Tomography Service (CTS), the information was obtained from the RIS-PACS (Radiology Information System—Picture Archiving and Communication System) [9], and for the Pediatric Radiotherapy Service (PRS) from the monthly report [10].

2.3 Medical Service Attention Time

It refers to the real time that the medical service attend patients. To calculate this time it was necessary to define two parameters:

Total Operation Time (k_{OT}). It is a constant obtained with the multiplication of the attention daily hours of the medical service (H_D), with the days worked per week (D_W), the weeks worked per year (W_Y), and the number of work shifts (W_S), using Eq. (2).

$$k_{OT} = (H_D)(D_W)(W_Y)(W_S) \quad (2)$$

Equipment Out of Service Time (t_{OS}). There are factors as failures in medical equipment and/or interruptions in the electrical supply, which leave medical equipment out of service. In this sense, the t_{OS} is obtained by adding the time spent on work orders (t_{WO}), preventive maintenance (t_{PM}) and power supply interruptions (t_{PSI}), with Eq. (3).

$$t_{OS} = t_{WO} + t_{PM} + t_{PSI} \quad (3)$$

Therefore, Medical Service Attention Time, (t_{MS}) was calculated with (4)

$$t_{MS} = k_{OT} - t_{OS} \quad (4)$$

2.4 Patient Attention Time

The Patient Attention Time (t_p) is variable and depends on:

- Patient features. First time, regular, emergency or COVID-19, and if the patient needs to be anesthetized.
- Patient's provenance. Patients can come from any of the Institute's 30 medical specialties. Although emergency patients represent almost a third of the total: 1018 patients treated in 2018, 1050 in 2019, and 947 in 2020. On the other hand, there are patients called "referred" from other public hospitals in Mexico City (General Hospital Dr. Manuel Gea González, Women's Hospital, Moctezuma Pediatric Hospital and Federico Gómez Children's Hospital of Mexico, inter alia).
- Anatomical region studied.
- Study type. Simple or contrasted.

These aspects were considered in the estimation of Patient Attention Time in the two medical services considered in this study: Computed Tomography and Pediatric Radiotherapy.

Patient attention time (Computed Tomography) (t_{p-CT}). To calculate this time, three patient types were considered: regular, emergency, and COVID-19, as the attention times in each case are different. Additionally, it was necessary to know these parameters:

The CT study time (t_{S-CT}) of a *regular* patient is calculated with the Eq. (5):

$$t_{S-CT} = \sum_{i,j=1}^n (n_{i,j})(t_{i,j})/60\text{min} \quad (5)$$

where:

n , is the number of studies per year,

t , is the study time,

$i = \{1, 2, \dots, 6\}$ is the study type (Table 4).

$j = \{1, \dots, 4\}$ is the nature of the study (simple, contrasted, with or without anesthesia).

The CT-study time of an *emergency* patient is calculated with the Eq. (6). Note this equation has 10 min factor, which is the time it takes to prepare the patient.

$$t_E = (\text{Patients No.})(10 \text{ min})/60 \text{ min} \quad (6)$$

The CT-study time of a *COVID-19* patient is calculated with the Eq. (7). In this case, sanitizing the room after patient attention takes 80 min.

$$t_C = (\text{COVID19Patient})(80\text{min})/60\text{min} \quad (7)$$

The CT-study time t_{p-CT} for 2018 y 2019 results on:

$$t_{p-CT} = t_{S-CT} + t_e \quad (8)$$

For the year 2020, it was necessary to add to Eq. (8) the attention time of a *COVID-19* patient as shown in (9):

$$t_{p-CT-2020} = t_{S-CT} + t_e + t_C \quad (9)$$

Patient attention time (Pediatric Radiotherapy) (t_{P-PR}). In this case, there are two types of patients: first time and regular. The parameters required for time calculation were:

The total number of patients of each type treated for a specific period (P_A).

First time patient (t_{FT}):

$$t_{FT} = \frac{(P_A)(S_I)(t_{SI})}{60\text{min}} \quad (10)$$

where: S_I = number of initial radiotherapy sessions; t_{SI} = initial radiotherapy sessions time.

Regular time patient (t_{RT}):

$$t_{RT} = \frac{(P_A)(S_R)(t_{SR})}{60\text{min}} \quad (11)$$

Where: S_R = regular radiotherapy sessions per patient; t_{SR} = regular radiotherapy sessions time. Finally:

$$t_{P-PR} = t_{FT} + t_{RT} \quad (12)$$

Equation (12) calculates the time spent in the attention of all oncological patients treated at Pediatric Radiotherapy Service for a certain period.

2.5 Medical Service Productivity

Medical Service Productivity (P_{MS}) was calculated using the proportion between patient attention time (t_P) and medical service attention time (t_{MS}) as in Eq. (13).

$$P_{MS} = \frac{t_P}{t_{MS}} \quad (13)$$

3 Results

3.1 Technical Evaluation of CT-Scan

The technical evaluation of the CT-scan was made with the information of the last three years (2018–2020). The values of variables are shown in Table 2. Note that the variables receive a qualitative value (Q_i) used by the technical staff of the Biomedical Engineering Department (BED). For example, x_4 . Equipment function has a Diagnostic (D) value, this involve that Physic risk (x_6) from equipment is a Misdiagnosis (MD). The CT-scan have a high complex technology therefore, its Maintenance requirements (x_8) are Important (I), which means that it requires highly specialized personnel to carry out preventive/corrective maintenance. Furthermore, note that Equipment failure frequency (x_5), has doubled every year, which shows the deterioration of the CT-scan. Note also that the variables have a quantitative domain (M_i), which is the mapping of the qualitative value (Q_i) to a value in the interval $[0, 1]$ and are the same in the 2018–2019, and change for the year 2020.

The quantitative values (M_i) of the year 2018 (Table 2) were substituted in Eq. (1), to illustrate the application of IT.

$$I_{T2018} = \frac{\sum_{i=1}^n P_i x_i}{4.4} = \frac{(0.9)(1) + (0.8)(0.4) + (0.7)(1) + (0.6)(0.6) + (0.5)(0.4) + (0.4)(0.6) + (0.3)(1) + (0.2)(1)}{4.4} = 0.73$$

According to the qualitative scale, this result indicates that the CT-scan must be replaced in the short term, that is, in three years.

Table 2. Qualitative (Q_i) and quantitative (M_i) values of the variables from technical indicator I_T of 64-slice CT-scan

Variable	2018	2019	M_i	2020	M_i
x_1 Spare parts available next 5 years	No	No	1	No	1
x_2 Equipment age in operation	8	9	0.4	10	0.4
x_3 Days of the equipment out of service	14	11	1	21	1
x_4 Equipment function	D	D	0.6	D	0.6
x_5 Equipment failure frequency	2	4	0.4	8	0.8
x_6 Physical Risk	MD	MD	0.6	MD	0.6
x_7 Consumables available next 5 years	No	No	1	No	1
x_8 Maintenance requirements	I	I	1	I	1

I_T was applied for the three years data and showed that in 2018 and 2019 ($I_T=0.73$), the equipment must be replaced in the short term (three years), that is, for the year 2021. In the year 2022, due to the number of failures $I_T=0.77$ so the equipment should be replaced immediately, within a period of less than 3 years.

3.2 Technical Evaluation of Linear Accelerator

The technical evaluation of the Linear Accelerator was made with the information of 2019 (Table 3). As in the case of the CT-scan, the variables have a qualitative (Q_i) and a quantitative domain (M_i). The equipment has been operating for more than ten years without any failures. However, four days out of service were identified due to preventive maintenance, which were carried out four times a year. Therefore, it presents the maintenance requirement considered as Important (I). The equipment has a Function (x_4) of Treatment (T), and a Physical risk (x_6) of Possible Injury to the Patient or Operator (PIPO).

Table 3. Qualitative (Q_i) and quantitative (M_i) values of the variables from technical indicator I_T of Linear Accelerator

x _i	Variable	Q _i	M _i
x ₁	Spare parts available next 5 years	no	1
x ₂	Equipment age in operation	15	0.8
x ₃	Days of the equipment out of service	4	0.4
x ₄	Equipment function	T	0.8
x ₅	Equipment failure frequency	0	0
x ₆	Physical Risk	PIPO	0.8
x ₇	Consumables available next 5 years	No	1
x ₈	Maintenance requirements	I	1

The application of I_T is illustrated by substituting the quantitative values of 2019 in Eq. (1).

$$I_T = \sum_{i=1}^n \frac{\rho_i x_i}{4.4} = \frac{(0.9)(1) + (0.8)(0.8) + (0.7)(0.4) + (0.6)(0.8) + (0.5)(0) + (0.4)(0.8) + (0.3)(1) + (0.2)(1)}{4.4} = 0.71$$

According to the qualitative scale, the result of the indicator suggests that the linear accelerator should be replaced in the short term, in a period of 3 years.

3.3 Epidemiological Analysis of Computed Tomography Service

Twenty-one types of tomographic studies were identified by anatomical region and three interventional procedures [11]. Based on the experience of radiology technicians, studies by anatomical region can be classified into short and long studies. Angiotomography (cardiac, neck, renal, abdominal) requires a longer preparation time, and are considered in another group. Interventional procedures are classified into punctures (biopsies and drainage), and stereotaxy, the latter also requiring more time. On the other hand, the canceled studies represent a constant time investment of 20 min each one. In addition to the type of studies, the time study (t_s) depends on whether the study is simple (S) or contrasted (C), or if the patient requires anesthesia (A). The times per study are shown in Table 4, and the information by type of study for each year of the 2018–2020 triennium is observed in Table 5. Note that in total, 4239 studies were carried out in 2018, 4115 studies in 2019, and 3284 studies in 2020.

3.4 Epidemiological Analysis of Pediatric Radiotherapy Service

During 2019, the Pediatric Radiotherapy Service (PRS) treated 212 patients. The data relative to the radiation sessions times are shown in Table 6.

Table 4. Type CT-study time (i) in minutes (j)

Study time ($t_{i,j}$)	S ($t_{i,1}$)	S/A ($t_{i,2}$)	C ($t_{i,3}$)	C/A($t_{i,4}$)
1. Short study ($t_{1,j}$)	15	40	35	60
2. Long study ($t_{2,j}$)	35	60	55	80
3. Angiotomography ($t_{3,j}$)	–	–	65	90
4. Puncture ($t_{4,j}$)	–	–	100	125
5. Stereotaxy ($t_{5,j}$)	–	–	–	175
6. Canceled ($t_{6,j}$)	20	–	–	–

Table 5. Patient attention process data in the Pediatric Radiotherapy Service

Parameter description	Value
Treated patients in 2019 (P_A)	212
Initial radiotherapy sesión per patient (S_I)	1
Regular radiotherapy sessions per patient (S_R)	25
Initial radiotherapy sessions time (TS_I)	45 min
Regular radiotherapy sessions time (TS_R)	15 min

3.5 Computed Tomography Service Attention Time

Total Operation Time (k_{CT}). Constant that was calculated by substituting the values of the parameters in Eq. (2):

$$k_{CT} = (51 \text{ weeks})(5 \text{ days})(8 \text{ h})(2 \text{ shift}) = 4080 \text{ h}$$

Equipment Out of Service Time (t_{OS-TC}). It is illustrated by calculating the time for 2018. In this year the CT-scan presented three faults with this number of hours out of service: gantry (168 h), UPS (88 h), electrical supply (72). Substituting these values in (6), the total number of hours out of service for the CT-scan in 2018 was:

$$t_{OS-CT-2018} = (168) + (88) + (72) = 328 \text{ h}$$

Tomography Computed Service Attention Time (t_{TC}). Substituting the data for the year 2018 in Eq. (4):

$$t_{CT-2018} = k - t_{OS-CT-2018} = 4080 - 328 = 3,752 \text{ h}$$

3.6 Patient Attention Time (Computed Tomography)

Study Time (t_{S-CT}). The time for each type of study was calculated. For example, for short studies time of the year 2018, we substituted the corresponding data (Table 5) in

Table 6. CT-studies annually per type

Study type	S	S/A	C	C c/A	Total
<i>2018</i>					
1. Short study	1,953	343	504	125	2,925
2. Long study	580	167	244	76	1,067
3. Angiotomography	–	–	84	140	224
4. Puncture	–	–	10	10	20
5. Stereotaxy	–	–	–	3	3
6. Canceled	30	–	–	–	30
Total	2,563	510	842	354	4,239
<i>2019</i>					
1. Short study	1,959	256	432	100	2,747
2. Long study	661	145	212	74	1,092
3. Angiotomography	–	–	113	128	241
4. Puncture	–	–	7	8	15
5. Stereotaxy	–	–	–	4	4
6. Canceled	16	–	–	–	16
Total	2,636	401	764	314	4,115
<i>2020</i>					
1. Short study	1,500	173	330	94	2,097
2. Long study	569	111	232	72	984
3. Angiotomography	–	–	91	102	193
4. Puncture	–	–	3	3	6
5. Stereotaxy	–	–	–	4	4
6. Canceled	14	–	–	–	14
Total	2,083	284	656	275	3,284

the Eq. (5):

$$t_{S-2018-short} = \frac{(1,953)(15) + (343)(40) + (504)(35) + 125(60)}{60min} = 1,136hrs$$

We do the same in each study type and later the sum was made to obtain the global t_{S-TC} with Eq. (5).

$$t_{S-2018-long} = 830h$$

$$t_{S-2018-angio} = 301h$$

$$t_{S-2018-puncture} = 38h$$

$$t_{S-2018-stereotaxy} = 9h$$

$$t_{S-2018-canceled} = 10h$$

$$t_{S-CT-2018} = (1136 + 830 + 301 + 38 + 9 + 10) = 2324 \text{ h}$$

Emergency patient time (t_E). During 2018, 1018 emergency patients were treated. It was 1050 in 2019, and 1000 in 2020. To illustrate the use of Eq. (6), data from 2018 were substituted.

$$t_{E-2018} = (1018)(10 \text{ min}) / 60 \text{ min} = 170 \text{ h}$$

Patient attention time (t_P). Applying Eq. (8), for 2018 and 2019 it was obtained:

$$t_{P-2018} = 2324 + 170 = 2,494$$

$$t_{P-2019} = 2190 + 175 = 2,365$$

Patient Covid-19 attention time (t_C). 76 Covid-19 patients were treated in 2020, and in each case, an average of 80 min was spent on their attention. Applying Eq. (7) it was obtained:

$$t_C = \frac{76(80 \text{ min})}{60} = 101 \text{ h}$$

Then, the t_P for 2020, was calculated by substituting the information in Eq. (12)

$$t_{P-2020} = 1802 + 167 + 101 = 2,070 \text{ h}$$

3.7 Computed Tomography Service Productivity

Substituting the service attention time (t_{CT}) and the patient attention time (t_{P-CT}) for the year 2018, in Eq. (13) it is obtained that the productivity in that year was:

$$P_{CT-2018} = \frac{t_P}{t_{CT}} = \frac{2494 \text{ h}}{3752 \text{ h}} = 0.66 = 66\%$$

Over the next two years, 2019 and 2020, productivity stood at 62% and 58%, respectively. In 2019 there was a decrease of 4%, and in 2020 it decreased by 4% more. The latter, as mentioned, was due to the fact that the CTS did not attend outpatients for three months and also the service time was reduced due to the COVID-19 pandemic.

3.8 Pediatric Radiotherapy Service Attention Time

The total operation time of the Pediatric Radiotherapy Service (k_{PR}) was calculated by substituting the corresponding values in Eq. (2):

$$k_{PR} = (8h)(5days)(48weeks)(1shift) = 1920h$$

Linear Accelerator Out of Service Time (t_{OS-LA}). Due to the four preventive maintenance interventions carried out, the equipment was out of service four days (32 h) during 2019. Substituting this value in expression (3) obtained: $t_{OS-LA} = 32$ h.

The attention time of the Pediatric Radiotherapy Service (PRS) was calculated with Eq. (4) and the data of the year 2019:

$$t_{P-RP} = 1920h - 32h = 1888h$$

3.9 Patient Attention Time (Pediatric Radiotherapy)

First time patient (t_{FT}). The time for patients starting their radiotherapy treatment was calculated by substituting the data for the year 2019 (Table 6) in Eq. (10):

$$t_{FT} = \frac{(212)(1)(45)}{60} = 159h$$

Regular patient time (t_{RT}). The attention time for patients who continue their radiotherapy treatment was calculated by substituting the data for the year 2019 (Table 6) in Eq. (11):

$$t_{RT} = \frac{(212)(25)(15)}{60} = 1325h$$

Once t_{FT} y t_{RT} were estimated the patient attention time (t_{P-RP}) was obtained by adding these two times, using Eq. (11):

$$t_{P-RP} = 159h + 1325h = 1484h$$

3.10 Pediatric Radiotherapy Service Productivity

The Pediatric Radiotherapy Service productivity (P_{PR}), as for CTS, was calculated using the proportion between the time invested in patient attention (t_p), and the service patient attention time (t_{PR}) through the Eq. (12):

$$P_{PR-2019} = \frac{t_p}{t_{PR}} = \frac{1484h}{1888h} = 0.79 = 79\%$$

This result indicates that the PRS had a productivity of 79% during 2019.

4 Conclusions

The technical indicator (I_T) application in both medical equipment allowed knowing their technical state and suggesting a period to replace them. In the case of the CT-scan, a deterioration was observed due to the increase in the frequency of annual failures, so it must be replaced within a period not exceeding 3 years. The same way, the linear accelerator must also be replaced in the short term (three years). In both cases, it is observed that the results are consistent, since they are more than 10 years old, and during the year 2022 they will no longer have technical support from the provider. This scenario makes both the CT-scan and the linear accelerator obsolete equipment.

The importance of acquiring the two new medical equipment lies in providing safe and effective medical care to the patients attended by the National Institute of Pediatrics, as well as increasing the supply of care and, consequently, increasing the productivity of both Medical Services.

Finally, it was shown that the same set of indicators to evaluate the technical aspect of the medical equipment and the productivity of the medical service where it is located, are useful for the evaluation of medical equipment with different purposes, as were the two study cases presented in this work, since one equipment was for diagnosis (tomograph) and other for therapy (linear accelerator).

Acknowledgment. The authors would like to thank the technical, medical, and paramedical staff of the Computed Tomography Service and the Pediatric Radiotherapy Service of the National Institute of Pediatrics, because without their collaboration the development of this work would not have been possible.

References

1. Pan American Health Organization: Health Technology Assessment. https://www3.paho.org/hq/index.php?option=com_content&view=article&id=9229:2013-tecnologias-sanitarias&Itemid=41687&lang=en
2. Hernández-López, L.A., Pimentel-Aguilar, A.B., Ortiz-Posadas, M.R.: An index to prioritize the preventive maintenance of medical equipment. *Heal. Technol.* **10**(2), 373–375 (2019)
3. Mora-García, T., Piña-Quintero, M.F., Ortiz-Posadas, M.R.: Pattern recognition for supporting the replacement of medical equipment at hospitals. In: Ortiz-Posadas, M. (ed.) *Pattern Recognition Techniques Applied to Biomedical Problems*, pp. 197–215. Springer. Series STEAM-H (Science, Technology, Engineering, Agriculture, Mathematics and Health) (2020)
4. Rosales-López, A., Ortiz-Posadas, M.R.: An indicator to estimate the access to imaging services in the Costa Rican public health system. *J. Digit. Imaging* **27**(1), 41–48 (2014)
5. Piña-Quintero, M.F.: Technical Report from the SERVICE of Electro-Medicine. National Institute of Pediatrics. Mexico City (2017). (in Spanish)
6. Guzmán-Canzales, L., Duarte-Peña, A., Piña-Quintero, M.F. et al.: Functional Evaluation of a 64-Slice Tomograph with Productivity Indicators. In: Mexican Society of Biomedical Engineering. 44th Mexican Conference on Biomedical Engineering, vol. 8(1), pp. 296–299. Guadalajara. Jal (2021). (in Spanish)
7. Lozano-Suárez, J.A., Piña-Quintero, M.F., Ortiz-Posadas, M.R.: Identification and Quantification of Benefits for the Acquisition of a Linear Accelerator. 43th Mexican Conference on Biomedical Engineering, vol. 7(1), pp. 311–318. Virtual Congress (2021). (in Spanish)

8. World Health Organization (WHO): Medical equipment maintenance programme overview. Geneva: WHO (2011). http://apps.who.int/iris/bitstream/handle/10665/44587/9789241501538_eng.pdf?sequence=1. Accessed 3 May 2018
9. National Institute of Pediatrics. Statistical Agenda 2019. Mexico City: Planning Department (2019). (In Spanish)
10. Amador, J.J.: Monthly General Report of the Pediatric Radiotherapy Service 2019. CDMX: National Institute of Pediatrics (2019) (in Spanish)
11. National Institute of Pediatrics: Annual report of RIS/PACS. CDMX: Imaging and Radiology Service (2020). (in Spanish)



A Proposed Model for Calculate the Number of Mammography Machines for the South-West Area of Mexico

Fabiola M. Martinez-Licona^{1,2}(✉)  and Cipactli M. Martinez-Vazquez² 

¹ Electrical Engineering Department, Universidad Autonoma Metropolitana Iztapalapa, Mexico City, Mexico

fmml@xanum.uam.mx

² Universidad Autonoma Metropolitana Biomedical Engineering Academic Program, Iztapalapa, Mexico City, Mexico

Abstract. Breast cancer is a global health problem. Mexican statistics show that 28.2% of new cancer cases in women come from the breast, so efforts must be made to control the burden of the disease. Early detection is an essential part of the social programs aimed at female populations at potential risk, and mammography machines are the technology used to perform screening methods. The possible coverage of a region is mainly affected by the available technological resources. This paper presents a proposal model to determine the number of mammography machines required to meet the State's requirements of Guerrero, Oaxaca and Chiapas, as those in which there are municipalities with the highest social backwardness. The socioeconomic and demographic determinants, as well as the screening mammography demand data, were extracted from official Mexican agencies. The model variables were selected from the categories of target population, epidemiological indicators and infrastructure. Under the author's heuristic assumptions, the analytic hierarchy process produced the weight that led to selecting the final set of variables. The resource allocation principles were used to adapt the Resource Allocation Working Party (RAWP) focus formula from population to equipment to calculate the State Weighted Machines using the mentioned category adjustments. Model results with 2017 and 2020 data showed that, on average, 50% more mammography machines are needed to cover around 46% of the female population 50–64 years old in the studied States. Further study and analysis of the determinants of access to the service and the equipment proposals are necessary.

Keywords: Mammography machines · Breast cancer · Infrastructure resource allocation

1 Introduction

Breast cancer is a global health problem. In 2020, the International Agency for Research on Cancer reported that 11.7% of new cancer cases globally and 28.2% of new cases in women in Mexico belonged to the breast [1]. Early detection represents an essential part of the strategy that includes diagnosis, treatment of the detected disease, and follow-up.

There are two primary components of breast cancer early detection programs: education to promote early diagnosis and screening. Among the possible screening methods is mammography with or without a physical examination of the breasts.

Mammography is a simple radiological study of the breasts with low radiation doses that are carried out using a device specially designed for this purpose, known as a mammograph. There are two modalities of mammography: screening and diagnostic [2]. Screening mammography is applied to women who do not present signs or symptoms; they are used to identify tumors that cannot be perceived or felt and microcalcifications that can give indications of breast cancer. The organized population-based approach to programme implementation allows an operational framework to develop screening processes that effectively manage the actions and outcomes [3]. Mammography applied under this scheme has the potential to reduce the risk of death from breast cancer by about 40% in women from 50 to 69 years old [4].

Despite the potential impact of screening programs, the difficulty in accessing and using health services, the lack of hospital infrastructure, limited access to treatment, and the lack of specialists who operate the necessary equipment limit detection and timely treatment of breast cancer [5]. This situation is more evident concerning coverage with screening mammography. Therefore, national cancer control programs must advance universal health coverage and provide access to health services, especially to the poorest segments of the population. Such is the case of the Southwest area of Mexico; the National Council for the Evaluation of Social Development Policy (CONEVAL) reported that in 2020 the States of Guerrero, Oaxaca and Chiapas had municipalities with the highest social backwardness [5].

The safe and effective operation of mammography machines is an essential part of the success of screening programs, and one crucial action that can guarantee the quality of the procedures and outcomes is to have knowledge of their quantity, location, and physical condition. OECD data shows that in 2019, Mexico had 10.4 mammography equipment per million inhabitants, in contrast to Korea, which reports 63.4, and the United States, 66.9 [7]. The number of units per federal entity is evidence of the degree of service coverage. The Ministry of Health only reports data on the infrastructure of health services, number and location, but a more specific analysis is required with a focus on the needs of the target population to plan both the replacement of obsolete units and the acquisition of equipment that complement the technology park.

This paper presents a proposal to determine the number of mammography machines required to meet the State's requirements of Guerrero, Oaxaca, and Chiapas. The model used principles of resource allocation integrating information from the social, demographic, epidemiological, and equipment contexts.

2 Methods

Identifying the region's prevailing situation is mandatory to determine the equipment demand. An analysis of the selected States was carried out based on socioeconomic and demographic determinants, emphasizing the female population likely to use the screening mammography service. Likewise, the demand for screening mammography studies in the region was estimated based on the target population (cohorts defined by

the WHO [6]). With the information obtained, a model was developed that integrated the components to contextualize the need to the characteristics of each State, which will determine the number of required mammography machines. Each stage is detailed below.

2.1 Determinants of the Region

The statistical information on each State's socioeconomic and demographic determinants, from which we obtained the model variables, was carried out based on [7]. The data were obtained for 2017 and 2020 from the official sites of the following agencies:

- The National Institute of Statistics and Geography (INEGI) [8]
- The National Council for the Evaluation of Social Development Policy (CONEVAL) [9]
- The Mexican Ministry of Health [12].

After selecting the variables derived from the determinants, we decided on those with the most significant relevance concerning screening mammography to detect breast cancer, using Saaty's analytic hierarchy process under heuristic assumptions [10]. The chosen variables are:

- Female population over 18 years old
- Education level
- Type of living place
- Women's age who underwent mammography
- Origin municipality from women who underwent the mammography
- Mammogram outcomes
- Mammogram locations
- Number of mammography machines
- Breast cancer mortality
- Breast cancer mortality municipalities
- Breast cancer morbidity rate

2.2 Screening Mammography Demand

Data were obtained from the number of mammographies reported by the Ministry of Health in each State and the mammography studies carried out with their outcomes. This information complemented the selected set of variables from the previous section and was used to conform the situation of breast cancer screening in Guerrero, Oaxaca and Chiapas. According to WHO suggestions, the data was selected for women over 18 years up to 75, but only the female population from 50 years old was considered for the model since most of the reports agree to select this age to design breast cancer screening organized programs with success [11].

2.3 Model

By applying the analytic hierarchy process, the variables used in the model were defined and tested to determine the number of medical equipment for screening in each State

based on the target population, epidemiological indicators, and the existing infrastructure. Subsequently, the variables that obtained the highest weight from the hierarchical analysis were selected to propose a model based on the classic principles of resource allocation [12]. According to these, resource allocation is based on population-weighted for three factors: age structure, health needs, and costs of delivering services. Then a weighted population WP of an authority is calculated from

$$WP = POP * (1 + a) * (1 + n) * (1 + c) \quad (1)$$

where POP is the unweighted population, a , n , and c are age, needs and cost adjustments, respectively [13]. The result shows the specific weight for each set of characteristics defined by the adjustments and is used as a decision support element. The model was adapted for the case of mammography resource allocation as follows.

State's weighted mammography capacity (SW_{MC}): The objective is to determine the number of mammography machines based on the needs of the target population. So, we proposed changing the emphasis in the original model from the population to the State's mammography capacity, intending to take the result as the basis for the calculation.

Adjustments: The adjustments for age, needs, and costs were modified to reflect the aspects of the target population, infrastructure, and epidemiological information.

So, the formulation for the model is:

$$SW_{MC} = NSW_{MC} * (1 + op) * (1 + i) * (1 + ei) \quad (2)$$

where NSW_{MC} is the unweighted State's current mammography capacity, and op , i , and ei are objective population, infrastructure, and epidemiologic information adjustments.

The number of mammography machines per State was obtained directly by SW_{MC} . Then, we calculated the number of patients that the equipment and the mammography coverage can treat.

$$P_t = FP_{50+}/SW_{MC} \quad (3)$$

$$M_c = 6000/P_t * 100 \quad (4)$$

where P_t is the number of female 50 + patients to be treated by each medical equipment, M_c is the % mammography coverage, and 6000 is the number of mammograms that can be performed in a year considering 20 min per studio, 8 h a day, five days a week and 50 labor weeks in the year [14].

3 Results

3.1 Model Variables

The selection of variables for the model were mammogram locations, female population over 18 years old, women age who underwent mammography, number of mammography machines, mammogram outcomes, and breast cancer morbidity rate. These variables were obtained after applying Saaty's analytic hierarchy process (AHP) in each State

for 2017 and 2020. As an example, Table 1 shows the weights of each variable and the category to which they were assigned for Chiapas in 2020. The weights were obtained by averaging the values assigned heuristically to each variable's impact on the others, verifying their consistency in each case, and analyzing with respect to the possible solutions to the problem posed, which in this case were the categories in which they were classified. The education level variable was exchanged for the breast cancer morbidity rate. Although the results placed it with the lowest weight, it was considered that this data is relevant to incorporate into the model since it provides information directly related to the demand for diagnostic and follow-up services, which require the use of the mammograph.

Table 1. Variable weights from AHP for Chiapas 2020.

Variable	Weight	Category
Mammogram locations	0.158	Infrastructure
Female population 18+	0.142	Target population
Women age who underwent mammography	0.118	Target population
Education level	0.118	Target population
Number of mammography machines	0.095	Infrastructure
Mammogram outcomes	0.090	Epidem. Indicators
Origin municipality from women who underwent the mammography	0.088	Target population
Breast cancer mortality municipalities	0.064	Epidem. Indicators
Type of living place	0.057	Target population
Breast cancer mortality	0.051	Epidem. Indicators
Breast cancer morbidity rate	0.020	Epidem. Indicators

Next, we proceeded to define how to measure each variable and incorporate it into the model.

3.2 Target Population

The two variables associated with this category are the female population 18+ and Women age who underwent mammography. The first variable was adjusted for women undergoing mammography screening, which usually begins after age 50. Then, each State calculated this population based on the reported data. The final values were obtained by calculating the proportion of the population 50+ of the State to the country's ratio (Prop. FP50 + St/Co). The average age of the women who underwent mammography and the relationship between the State average (AvSt) and the country average (AvCo) were calculated. Table 2 presents the values obtained for 2017 and 2020.

Table 2. Target population variables for 2017 and 2020.

Variable	Guerrero	Oaxaca	Chiapas	Mexico
<i>Female population (FP) 50+</i>				
FP 15 + (2017)	1 179 268	1 384 574	1 603 476	40 767 055
(2020)	1 320 619	1 584 001	1 946 645	48 732 991
FP 15–49 (2017)	877 211	1 007 409	1 272 061	30 703 546
(2020)	910 221	1 077 929	1 461 928	33 885 546
FP 50 + (2017)	302 057	377 165	331 415	10 063 509
(2020)	410 398	506 072	484 717	14 847 445
Prop. FP50 + (2017)	0.256	0.272	0.207	0.247
(2020)	0.311	0.319	0.249	0.305
Prop. FP50 + S_t/C_o	1.038	1.104	0.837	
(2020)	1.020	1.049	0.817	
<i>Women age who underwent mammography</i>				
Average (2017)	49.425	51.25	47.5	50.75
(2020)	50.62	51.61	49.58	51.45
Av_{St}/Av_{Co} (2017)	0.974	1.01	0.936	
(2020)	0.948	1.003	0.964	

3.3 Epidemiological Indicators

The variables that belong to this category are Breast cancer morbidity rate and Mammogram outcomes. Incidence of malignant tumor of the breast ($IMTB$) values for women 50+ by State and country were obtained, and then the proportional share for each State ($IMTB_p S_t/C_o$) was calculated. From the data reported on the mammograms performed, the proportion of studies with negative or benign neoplasia results in the target population ($M_{B\&N}$) for each State and the country was calculated and then to obtain the ratio ($M_{B\&C} S_t/C_o$). Table 3 presents the values obtained for 2017 2020.

3.4 Infrastructure

This category includes the number of mammography machines and the mammography locations. The number of machines ($\# Med_Machines$) and the number of hospital institutions ($\# Med_Facilities$) were obtained by State and country. Then, the relationship between equipment and facilities in each case (Med_{Mach}/Med_{Fac}) was calculated, followed by the proportion of this result for each State to the country ($Inf. S_t/C_o$). The number of municipalities in each State and the country ($\# Municipalities$) was obtained for the location variable. The number of municipalities with mammography machines ($\# Munic_Mamm$) was extracted. The ratio of municipalities with mammograms to the total number of municipalities in each case ($Munic_Mamm/Total$) and the proportion of

Table 3. Epidemiological indicator variables for 2017 and 2020.

Variable	Guerrero	Oaxaca	Chiapas	Mexico
<i>Breast cancer morbidity rate</i>				
IMTB 50 + (2017)	40.97	103.58	21.16	3429.17
(2020)	7.56	105.08	43.5	4048.75
IMTB _p S _t /C _o (2017)	0.012	0.030	0.006	
(2020)	0.002	0.026	0.011	
<i>Mammogram outcomes</i>				
M _{B&N} (2017)	0.903	0.946	0.761	0.883
(2020)	0.947	0.746	0.912	0.925
M _{B&C} S _t /C _o (2017)	1.023	1.023	0.862	
(2020)	1.023	1.098	0.986	

this result in each State to the country (*Munic Mamm S_t/C_o*) were calculated. Table 4 presents the values obtained for 2017 and 2020.

3.5 Number of Mammography Machines

The number of mammographers per State was determined by taking the averages of the variables for each category (bold values from Tables 2, 3, 4) and incorporating them into Eq. 2. The unweighted State's current mammography capacity (NSW_{MC}) corresponds to the number of machines for every 60,000 inhabitants aged 50+ in each State based on what was proposed by the Specific Action Program for Breast Cancer 2007–2012 [15]. Then SW_{MC} is the number of mammography machines calculated by the model. The number of patients per unit (P_t) and the coverage percentage of the total number of machines calculated (M_C) were obtained by applying Eqs. 3 and 4. Table 5 presents the values obtained for 2017 and 2020.

Table 6 shows the number and coverage capacity of the reported mammographers (Mamm_{REP} y Cover_{REP}) and the number calculated by the model (Mamm_{CAL} y Cover_{CAL}) for 2017 y 2020.

4 Discussion

One of the resource management problems lies in determining their quantity and location in the region of interest. Demographic determinants often impact these decisions, primarily when focusing on the target population. The potential demand for health programs can be taken as a starting point to identify and address needs in a timely manner. Given the health problem that breast cancer represents, efforts to develop screening programs should focus on the population strata most likely to be at risk. Moreover, as a critical element for the development of screening studies, the mammograph should be considered a resource to manage effectively to meet the programs' objectives.

Table 4. Infrastructure variables for 2017 and 2020.

Variable	Guerrero	Oaxaca	Chiapas	Mexico
<i>Number of mammography machines</i>				
# Med_Machines (2017)	25	14	8	748
(2020)	10	12	26	765
# Med_Facilities (2017)	1 206	1 206	1 793	22 555
(2020)	1 172	1 560	1 787	21 857
Med _{Mach} /Med _{Fac} (2017)	0.021	0.012	0.004	0.033
(2020)	0.009	0.008	0.015	0.035
Inf. S _t /C _o (2017)	0.625	0.350	0.135	
(2020)	0.244	0.220	0.416	
<i>Mammogram locations</i>				
# Municipalities (2017)	81	570	119	2463
(2020)	81	570	214	2469
# Munic_Mamm (2017)	8	11	6	103
(2020)	4	9	10	243
Munic_Mamm/Total (2017)	0.099	0.019	0.05	0.042
(2020)	0.049	0.016	0.047	0.098
Munic_Mamm S _t /C _o (2017)	2.362	0.461	1.206	
(2020)	0.502	0.160	0.475	

In this sense, it was decided to take the female population aged 50+ years as a basis because, in addition to being the range where there is more remarkable agreement on the impact of screening programs, it has been shown that both the population aged 40+ and 65+ years are not cost-effective [16]. Concerning infrastructure, the reported data of the existing equipment by State and the country did not include information on its operating status. This information would allow adjusting the variables related to this category to fit the model. It is important to mention that in the model, the value obtained from considering the number of units per number of people instead of the number of units reported was taken as the basis for the weighting (NSW_{MC}). It was done to propose a scenario closer to an ideal situation. However, this value is not shared by other instances, such as the Pan-American Health Organization PAHO, which in 2016 proposed determining the number of machines for every 100,000 females 50–69 years [17]. The variables related to mortality and morbidity obtained the lowest values in the weighting; this may reflect the heuristic considerations applied in the AHP. The morbidity variable was selected to integrate information directly related to the current demand for equipment, whether for screening or diagnosis; the proposed model requires further treatment for these considerations. The analysis of the variables that determined the number of mammography machines contrasts with studies where a correlation with

Table 5. Number of mammography machines per State 2017 and 2020.

Variable	Guerrero	Oaxaca	Chiapas
Op (2017)	1.006	1.057	0.887
(2020)	1.002	1.026	0.890
Ei (2017)	0.517	0.526	0.434
(2020)	0.513	0.426	0.498
I (2017)	1.493	0.406	0.670
(2020)	0.373	0.190	0.445
NSW _{MC} (2017)	5.034	6.28	5.52
(2020)	6.84	8.43	8.07
SW _{MC} (2017)	38.201	27.74	24.95
(2020)	28.43	28.99	33.07
P _t (2017)	7 948.86	13 470.17	13 256.6
(2020)	14 657.07	17 450.75	14 688.39
Mc (2017)	75.48	44.54	45.26
(2020)	40.93	34.38	40.84

Table 6. Current and calculated mammography capacity 2017 and 2020.

State	Mamm _{REP}	Mamm _{CAL}	Cover _{REP}	Cover _{CAL}
Guerrero (2017)	25	38	49.65	75.48
Guerrero (2020)	10	28	14.61	40.93
Oaxaca (2017)	14	28	22.27	44.54
Oaxaca (2020)	12	29	14.22	34.38
Chiapas (2017)	8	25	14.48	45.26
Chiapas (2020)	26	33	32.18	40.84

the number of radiologists, the female population, or the region surface under study was present [18].

The values in Table 6 show the effect of the variables and the importance of having reliable information to calculate the number of mammography machines. The values reported in three years behaved differently in each state. While in Guerrero, the number of machines decreased by less than half, and in Oaxaca, it decreased to a lesser extent, there was a considerable increase in Chiapas. Since the model uses this information for the calculation, the result is biased by its quality. From the results, it can be inferred that differences in the courses of action were taken in each State concerning the technological recourses provision. However, the number of machines does not guarantee better coverage for screening mammography.

The model based on resource allocation was adapted for a situation where the object of study is the medical equipment and not the population. Although the original model has considerations to account for, it is considered a good reference to start the development of methods to determine the number of resources. The chosen years established two scenarios where there were breast cancer care programs; a specific program for breast cancer (2017) and a general program on women's cancer (2020). The study limitations include the heuristic considerations for the weighting of the model, the quality of the information collected, and the premises established to adapt the model.

5 Conclusions

A model based on resource allocation is proposed to determine the number of mammography machines needed to serve the target population with screening studies in the States of Guerrero, Oaxaca, and Chiapas. The results show a better coverage than obtained based on the reported data (average of 55.093% for 2017 and 38.17% for 2020); however, further study and analysis of the determinants of access to the service and the equipment proposals is necessary. It is planned to continue the research for other regions, propose modifications to the model and integrate the location of resources as part of it.

Conflict of Interest. “The authors declare that they have no conflict of interest.”



References

1. International Agency for Research on Cancer (IARC). <https://bit.ly/3sBfVsb>, <https://gco.iarc.fr/today/data/factsheets/populations/484-mexico-fact-sheets.pdf>
2. National Cancer Institute at <https://www.cancer.gov/types/breast/mammograms-fact-sheet>
3. von Karsa, L., Arrossi, S.: Development and implementation of guidelines for quality assurance in breast cancer screening—the European experience. *Salud Pública de México* **55**, 318–328 (2013)
4. Lauby-Secretan, B. et al.: Breast-cancer screening—viewpoint of the IARC Working Group. *New England J. Med.* **372**(24), 2353–2358 (2015). <https://doi.org/10.1056/NEJMSr1504363>
5. Duggan, C., Dvaladze, A., Rositch, A.F. et al.: The breast health global initiative 2018 global summit on improving breast healthcare through resource-stratified phased implementation: methods and overview. *Cancer* **126**, 2339–2352 (2020). <https://doi.org/10.1002/cncr.32891>
6. National Council for the Evaluation of Social Development Policy (CONEVAL). Municipal poverty measurement. <https://bit.ly/3Mizo9n>
7. Organization for Economic Co-operation and Development (OECD). Mammography machines (indicator). <https://data.oecd.org/healthqt/mammography-machines.htm>
8. World Health Organization: WHO position paper on mammography screening (2014). <https://apps.who.int/iris/bitstream/handle/10665/137339/?sequence=1>
9. Agudelo Botero, M.: Sociodemographic determinants of access to breast cancer screening in Mexico: a review of national surveys. *Salud Colectiva* **9**(1), 79–90 (2013). http://www.scielo.org.ar/pdf/sc/v9n1/en_v9n1a07.pdf
10. National Institute of Statistics and Geography (INEGI). https://www.inegi.org.mx/programas/ccpv/2010/default.html#Datos_abiertos

11. National Council for the Evaluation of Social Development Policy (CONEVAL). <https://www.coneval.org.mx/Paginas/principal.aspx>
12. Ministry of Health. <https://datos.gob.mx/busca/dataset/recursos-en-salud-nivel-central>
13. Saaty, T.: The Analytic Hierarchy Process. McGraw-Hill (1980)
14. National Center for Gender Equity and Reproductive Health: Modelo para la detección, diagnóstico y referencia del cáncer de mama. Secretaría de Salud (2011). https://www.gob.mx/cms/uploads/attachment/file/15174/MODELOCAMA_CNEGSR.pdf
15. Carr-Hill, R., Hardman, G., Martin, S., Peacock, S., Sheldon, T., Smith, P.: A Formula for Distributing NHS Revenues Based in Small Area Use of Hospital Beds. York Centre of Health Economics, University of York (1994)
16. Peacock, S., Smith, P.: The Resource Allocation Consequences of the New NHS Needs Formula. York Centre of Health Economics, University of York (1995)
17. US GAO: US Government Accountability Office. <https://www.gao.gov/assets/gao-06-724.pdf>
18. Ministry of Health: Specific Action Program 2007–2012 Breast Cancer. <https://es.calameo.com/read/0009477201394124b17b0>
19. Mittmann, N., Stout, N.K., Lee, P., Tosteson, A.N., Trentham-Dietz, A., Alagoz, O., Yaffe, M.J: Total cost-effectiveness of mammography screening strategies. Health Rep. **26**(12), 16–25 (1994). <https://www150.statcan.gc.ca/n1/pub/82-003-x/2015012/article/14295-eng.pdf>
20. Pan-American Health Organization: Mammography services quality assurance: Baseline standards for Latin America and the Caribbean (1994) <https://iris.paho.org/handle/10665.2/31402>
21. Autier, P., Ouakrim, D.A.: Determinants of the number of mammography units in 31 countries with significant mammography screening. Br. J. Cancer **99**(7), 1185–1190 (2008). <https://doi.org/10.1038/sj.bjc.6604657>



Productivity Index Applied to Clinical Engineering

D. N. Araújo¹(✉)  and J. W. M. Bassani^{1,2} 

¹ Departamento de Eletrônica E Engenharia Biomédica, Faculdade de Engenharia Elétrica E de Computação, Universidade Estadual de Campinas, Campinas, Brasil
diegonaraujo@outlook.com

² Centro de Engenharia Biomédica, Universidade Estadual de Campinas, Campinas, Brasil

Abstract. In the present work, a productivity index (I_p) was developed based on: the number of concluded service orders (SO), number of worked hours, and complexity of completed SO. This indicator can be used to help measure the productivity of teams and individual workers. I_p was used to evaluate the productivity of a clinical engineering (CE) nucleus of the GETS-CEB-UNICAMP network from 01/01/2018 to 31/12/2019. It was observed that although the CE team presented good productivity, alerts were raised concerning the low productivity of some individuals who require additional attention of the CE manager.

Keywords: Productivity · Indicator · Clinical Engineering

1 Introduction

Electronic devices in healthcare procedures have led to the growth of clinical engineering (CE), which is responsible for applying management techniques and engineering methods to healthcare technology [1].

The clinical engineer has the primary responsibility to manage both the medical equipment (ME) from its acquisition until its deactivation and the technical team responsible for the maintenance of these pieces of equipment. Therefore, his work is primarily to avoid unnecessary costs for the health care units and protect patients and users from potential adverse events resulting from ME malfunction [2].

Every CE team needs to be concerned with maintaining or improving the quality level of its activities. The result of these activities impacts the population's health and the financial result of healthcare organizations.

One of the factors affecting this quality is the productivity of the technical team. Productivity correlates with the efficiency of individuals, i.e. the more productive they are, the faster they complete their activities spending the least amount of resources. Consequently, costs are reduced and performance is increased in the hospital. Therefore, measuring productivity is fundamental for managers to monitor the team and propose actions for improvement [3–5].

The productivity of a process is the ratio of its output to the resources used in production. However, this definition is best applied for evaluating processes of which

output is easily measured, for example, a product. In CE, the output is a service, not a manufactured asset, so measuring productivity requires other means [6].

One way of measuring productivity in processes of which the results are services is to compute the unit production ratio (labor cost ratio by the amount of service performed) [7]. However, this indicator is best used to evaluate individuals performing similar services. In CE, services (maintenance) are rarely similar, so it is not ideal to use this method.

Among the most appropriate indexes for sound management of a CE sector, the majority are for team assessment [8], and only a few represent the productivity of each person. In this case, most have as a methodology the calculation of the number of concluded service orders (nSO) and/or the number of worked hours (nWH) [6, 9–11]. However, other variables could also be considered when measuring productivity, such as the complexity of the completed service orders (cSO).

If two individuals who work the same number of hours are compared, it would be unfair to say that one that has fewer nSO, is less productive than the other, if his solved work orders (SO) were of higher complexity.

The maintenance task complexity is related to the characteristics of the activities necessary to complete it, the characteristics of the professionals who perform the task, and the degree of interdependence of these characteristics [12].

Among the factors that affect the complexity of a task, are the number of solutions, the number of actions required to complete the task and the logical plot—which is the logical sequence of actions to be followed. It is also essential to consider the availability of the necessary tools and equipment, the technical knowledge, psychological pressure, fatigue, and worker's training [12–14].

The objective of this work was to develop a productivity index (I_P) based on the classic nSO and nWH indicators and take into account cSO. This index can be used to help measure the productivity of teams and individual workers.

2 Methodology

2.1 Index Calculation

Equation 1 is used to calculate I_P , where I_{OS} , I_{HT} and I_C are subindexes based on number of concluded service orders (nSO), number of worked hours (nWH) and complexity of the completed service orders (cSO), and a , b and c are weights that, in this work, were assumed equal to 1 (this value can be changed by managers if they want one of the subindexes to have more impact on the result than the others to accomplish for mission dependent aspects of the particular hospital).

$$I_P = \frac{a \cdot I_{OS} + b \cdot I_{HT} + c \cdot I_C}{a + b + c} \quad (1)$$

The calculation of the subindexes is based on the calculation methodology of the I_{CEB} productivity index [15]. Therefore, to calculate them, a number m of months of work of a technician for which nSO, nWH and cSO are available should be obtained. After that, create a vector $T_m(i)$, $i = 1, m$. With this data, the following algorithm applies:

- Order T_m in ascending order;
- Count the number of months with nSO, nWH, and cSO less than or equal to multiples of 5, such that the minimum nSO, nWH, and cSO are $5 \cdot n_{\min}$ and the maximum nSO, nWH, and cSO are $5 \cdot n_{\max}$. The CE team manager chooses the value of $n = n_{\max} - n_{\min}$.
- Convert the obtained count values into a percentage of m and store these values in a vector $P\%(j)$, $j = 1, 2, \dots, n + 1$;
- Calculate the subindex ($I_x = I_{OS}$ or I_{HT} or I_C) using Eq. 2.

$$I_x = 1 - \frac{\sum_{j=1}^{n+1} P\%(j)}{100 \cdot (n + 1)} \tag{2}$$

The values of n_{\max} to calculate I_{OS} , I_{HT} and I_C in this work were 4, 7 and 10, respectively. These values were defined based on the median of nSO, nWH and cSO, in a way that the minimum values of these subindexes to each worker would be at least equal to the median of the whole group. As an example, Fig. 1 shows the nSO values per worker. One-way analysis of variance revealed significant differences between individuals ($p < 0.05$) for this and the other subindexes. The red line indicates the median (of value 20) of the team for nSO. Since $5 \cdot n_{\max} = 20$, then $n_{\max} = 4$. Similarly, 7 and 10 were obtained to calculate I_{HT} and I_C , respectively. Lastly, n_{\min} was considered equal to 1 for the three subindexes.

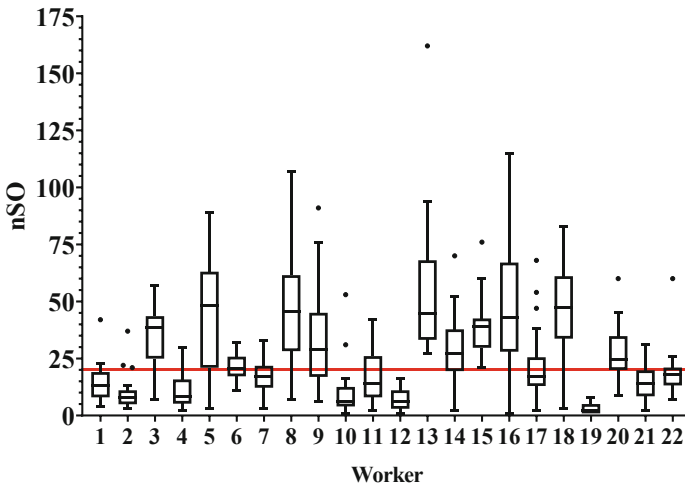


Fig. 1. Number of concluded service orders (nSO) per worker from 01/01/2018 to 31/12/2019. The red line indicates the minimum monthly OS threshold targeted by the manager for subjects, defined according to the median (20) of the group.

After calculating I_p , a score can be assigned to the result. In this work, the following scores were established: A ($1.0 \geq I_p \geq 0.90$); B ($0.90 > I_p \geq 0.70$); C ($0.70 > I_p \geq 0.50$) and D ($0.50 > I_p \geq 0.0$). These scores are based on the classification (Grade

Point Average—GPA) used by American universities and by some Brazilian universities, such as the University of Campinas (UNICAMP), to evaluate the performance of students [16, 17]. However, managers can change the limits of each score according to the characteristics of their team.

2.2 Sensitivity of I_p

To calculate I_p , it is necessary to collect a set of data, so it's necessary to know the minimum number of data to compose this set so that the insertion of new data does not generate a significant change in the result.

This is relevant because every worker has at least one vacation month in the year, and in this month, the data may have low values for one or more subindexes.

It's not recommended that the vacation months of the workers be discarded during data collection because their vacations don't always last thirty days in a row.

In Fig. 2, the sensitivity curve of the subindexes is presented (all present the same curve). It can be seen that the insertion of data considered as bad (≤ 5) in a set with little data can cause significant changes in the result.

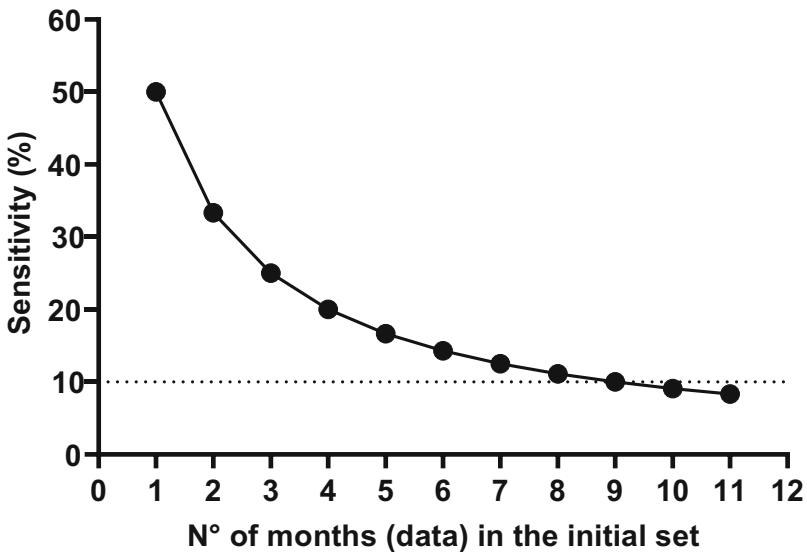


Fig. 2. Subindex sensitivity curve due to the inclusion of a low data value (≤ 5) in a data set initially with a subindex equal to 1. Note that the effect would be a 50% drop in the index for only one month of data collection.

The maximum tolerable variation was assumed to be 10%. Hence, it's only possible to obtain this variation from the inclusion of data in a set that already has nine (Fig. 2), so it is necessary to have at least ten months of data.

This work has been planned to perform the measurements with sets of 12 months of data, so the index calculated in one month corresponds to the data from the previous

12 months. Furthermore, the inclusion of low data-value in a set initially composed of 11 months of data results in a maximum variation of 8.33%.

2.3 Case Study

The data for this work were collected using the software Healthcare Technology Management (GETS), which is used by the CE team at the Center for Biomedical Engineering (CEB) of UNICAMP, where it was developed, and by more than 40 CE Nuclei (NEC) of public hospitals under agreement with the university [18].

Using GETS, it is possible to collect nSO and nWH data, but at the moment, cSO is not available in the software. Since one of the factors that affect the complexity of a task is the number of actions required to perform it, it was assumed that the greater the number of actions required, the greater the time demanded by the task; consequently, the greater the task complexity. This way, complexity scores were assigned according to the median time of activities performed per equipment type. This association between multiple task time and complexity has been confirmed in the daily practice by the CEB's CE team (personal communication from the CEB's manager).

The data collected is from an NEC composed of 22 workers, and the data collection period was 01/01/2018 to 31/12/2019. Since to measure the productivity of individuals, 12-month sets of data were used, from Jan/18 to Dec/19, it is possible to form 13 sets, which were called annual periods (AP). AP 1 begins in Jan/2018 and ends in Dec/2018, AP 2 begins in Feb/2018 and ends in Jan/2019, and so on until AP 13, which begins in Jan/2019 and ends in Dec/2019.

2.4 Statistical Tests

One-way (with D'Agostino-Pearson normality test) and two-way analysis of variance with Bonferroni contrast tests were used. When applicable, Student's t-test was used for comparisons between two means. These calculations were done using Graphpad Prism 8.0.1 software. Furthermore, the randomization test for 1-sample mean and Bootstrap test for 1-sample function were also applied using Minitab 21.1 software. $P < 0.05$ was considered the level of statistical significance.

3 Results

Table 1 shows the average productivity values of workers, from AP 1 to AP 12, and their respective productivities in AP 13. By utilizing this table based on the scores, it is possible to identify the lowest productive individuals in the team (workers 2, 4, 10, 12, 14, 19, 21, and 22). Using the randomization test for the mean by 1 sample, the average productivity of these individuals, from an AP 1 to AP 12, was compared with the last productivity measured against them. Bootstrap for a 1-sample function was also used to determine the confidence interval (95%) for each worker's mean productivity (AP 1 to AP 12). The confidence interval helps to confirm whether the productivity presented by them in AP 13 is significantly different from their mean. It was observed that worker 22 decreased productivity ($p < 0.001$), and workers 4 and 10 improved productivity ($p < 0.05$). The others (workers 2, 12, 14, 19, and 21) had no significant changes in productivity.

Table 1. Mean productivity of the workers (column 1) from AP 1 to AP 12 (column 2) and their productivity in AP 13 (column 3), as well as the concepts (“A”, “B”, “C” or “D”) assigned according to the production values.

Worker	Mean AP 1 to AP 12	AP 13
1	0.72 (B)	0.81 (B)
2	0.51 (C)	0.53 (C)
3	0.87 (B)	0.82 (B)
4	0.45 (D)	0.48 (D)
5	0.88 (B)	0.92 (A)
6	0.79 (B)	0.82 (B)
7	0.76 (B)	0.75 (B)
8	0.94 (A)	0.96 (A)
9	0.88 (B)	0.85 (B)
10	0.20 (D)	0.25 (D)
11	0.68 (C)	0.74 (B)
12	0.28 (D)	0.27 (D)
13	0.96 (A)	0.90 (A)
14	0.60 (C)	0.62 (C)
15	0.86 (B)	0.76 (B)
16	0.89 (B)	0.95 (A)
17	0.78 (B)	0.72 (B)
18	0.96 (A)	0.90 (A)
19	0.22 (D)	0.25 (D)
20	0.79 (B)	0.84 (B)
21	0.60 (C)	0.58 (C)
22	0.72 (B)	0.66 (C)

Figure 3 presents a histogram with the individual productivity information highlighted against the team’s overall productivity. Worker 4 is highlighted, and the team at AP 13.

Note that worker 4, in AP 13, scored $0.4 \leq I_p < 0.5$, thus concept “D”, while the median productivity of the team is in a higher class (concept “B”).

As mentioned in the introduction, there could be cases of individuals with low nSO values, but high cSO values. Therefore, this would not necessarily be an unproductive worker. In Fig. 4, the productivity of worker 1 is presented, considering or not the complexity of his work. If complexity was not considered, the result of the index for him would be lower ($p < 0.0001$) than considering the complexity.

Furthermore, it was also observed that worker 21 performance had opposite behavior from AP 1 to AP 7, that is, he performed high nSO values but low cSO values.

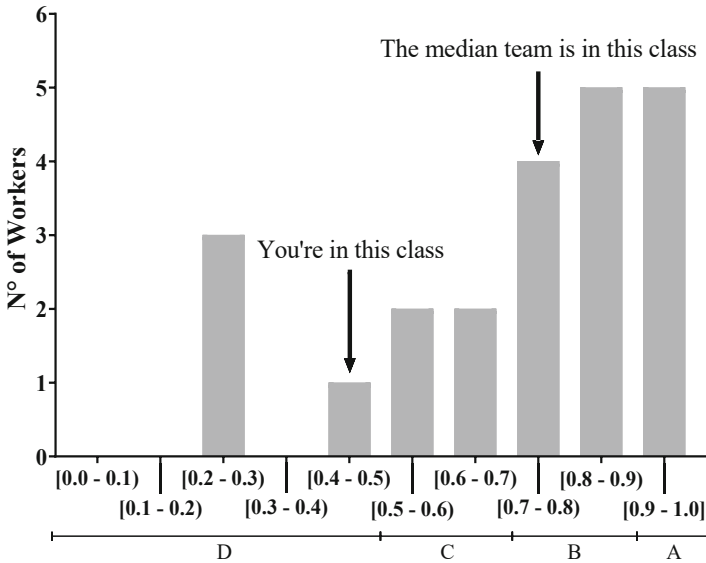


Fig. 3. Productivity histogram during PA 13. The productivity of worker #4 is highlighted. The arrows indicate in which class the worker’s productivity and the median productivity of the team are. The letters at the bottom of the figure indicate to which concept (“A”, “B”, “C” or “D”) the classes belong.

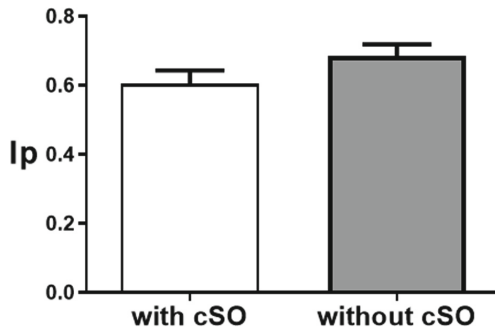


Fig. 4. Effect of complexity on worker 1’s productivity from AP 1 to AP 13.

In Fig. 5 the productivities of workers 1 and 21 are compared in the presence and absence of the cSO effect. The two-factor analysis of variance revealed that the productivity of individuals is not independent of cSO (complexity vs. Individual interaction highly significant, $p < 0.0001$). In other words, the difference in productivity may not be considered independently of the individual vs. complexity interaction.

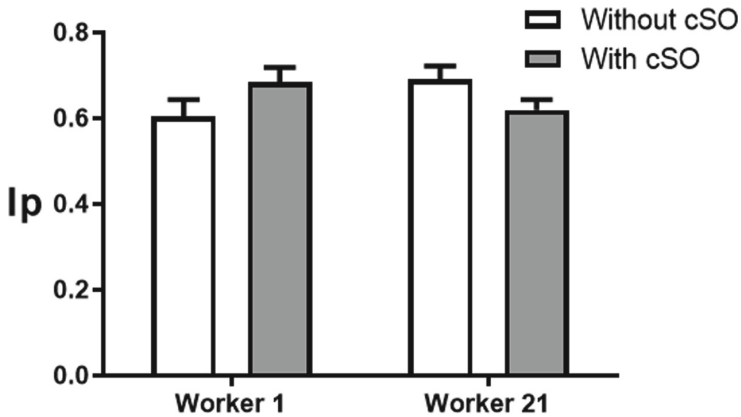


Fig. 5. Comparison of the productivity of workers 1 and 21, considering or not the complexity (cSO), from PA 1 to PA 7.

4 Discussion

The data collected by GETS showed differences between the productivity of the professionals working in the studied NEC and that for the same worker, the nSO, nWH and cSO data may belong to different positions concerning the team medians. Consequently, measuring the productivity of individuals only by the number of work orders completed or the number of hours worked would be a misunderstanding [11, 19].

From 01/01/2018 to 31/12/2019, two-thirds of the workers in the CE team had average productivity in concepts A or B, characterizing good productivity for the team as a whole. However, although the team's productivity was good, some professionals were identified as having low productivity (Table 1). This type of alert (of impartial character) illustrates the need for the CE manager to evaluate the work of these individuals to understand the reasons that made them perform unsatisfactory results and propose actions aimed at their improvement.

It is crucial noting that the use of the index doesn't aim to tax the individuals as productive or unproductive, but to create alerts to the CE manager about the productivity of the workers and from this, to serve as a guide for decision making [20].

AP 13 serves as a "sensor" of what may become the future behavior without the manager's intervention. As for the individuals who presented a significant difference between mean productivity from AP 1 to AP 12 and productivity in AP 13, the manager can assess whether actions taken are causing increased productivity of workers, thus permitting the replication of success cases; and to identify as soon as possible, those with decreasing productivity. So, it is essential to highlight the importance of the critical analysis of the CE manager to ensure that the results are correctly interpreted.

As in Fig. 3, histogram use is feedback to the workers about their performance. It is advised that the CE manager makes this data available periodically. It helps communicate sector expectations, creates a sense of accountability among individuals, and makes the group more integrated [6, 21]. It will be expected that this type of (confidential)

feedback will stimulate self-assessment and even a behavioral self-correction of the team personnel.

At last, considering the effect of complexity in productivity measurement proved to be effective in avoiding biased results since low values of nSO can be compensated with high values of cSO, i.e., individuals' productivity is not independent cSO.

5 Conclusions

A productivity index was developed based on nSO, nWH and cSO. This index made it possible to measure the productivity of a team and individual workers in an NEC of the GETS network.

With the results obtained, it was possible to identify individuals whose productivity was below the expected productivity, considering the good average productivity of the team. At the same time, the indicator demonstrated that considering the complexity of the tasks is a crucial way to improve the accuracy of the evaluations.



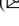


References

1. Goodman, G.: The profession of clinical engineering. *J. Clin. Eng.* **14**(1), 27–37 (1989)
2. Wang, B.: Strategic health technology incorporation. *Synthesis Lect. Biomed. Eng.* **4**(1), 1–71 (2009)
3. Parida, A., Kumar, U.: Maintenance productivity and performance measurement. In: *Handbook of Maintenance Management and Engineering*. Springer (2009)
4. Bond, T.: The Role of Performance Measurement in Continuous Improvement. *International Journal of Operations & Production Management*, MCB UP Ltd (1999)
5. Oliveira, J.C.S.: Análise de indicadores de qualidade e produtividade da manutenção nas indústrias brasileiras. *Revista Gestão da Produção Operações e Sistemas* **9**(3) (2013)
6. Fennigkoh, L.: Cost-effectiveness, and productivity. In: *Clinical Engineering Handbook*. [S.l.]: Elsevier (2004)
7. Lerman, L.V. et al.: Construção de indicadores de produtividade da mão de obra com base no modelo de estratificação. In: *Simpósio de Engenharia de Produção*. [s.n.] (2019)
8. dos Santos, R.M., do Dallora, M.E.L.V.: Avaliação de indicadores de desempenho da área de engenharia clínica: uma proposta para um hospital público universitário. *Medicina (Ribeirão Preto. Online)* **52**(1), 34–46 (2019)
9. Bauld, T.J.: Productivity: standard terminology and definitions. *J. Clin. Eng. LWW* **12**(2), 139–146 (1987)
10. Kawohl, W. et al.: How to Manage the Finances of Your Healthcare Technology Management Teams. *Teaching-aids at Low Cost* (2005)
11. Autio, D.D., Morris, R.L.: Clinical engineering program indicators. In: *Medical Devices and Systems*. [S.l.]: CRC Press LCC (2006)
12. Bonner, S.E.: A model of the effects of audit task complexity. *Account. Organ. Soc.* **19**(3), 213–234 (1994)
13. Park, J.: *The Complexity of Proceduralized Tasks*. Springer (2009)
14. Ge, X., Zhou, Q., Liu, Z.: Assessment of Space Station On-Orbit Maintenance Task Complexity. *Reliability Engineering & System Safety*, Elsevier (2020)
15. Vilela, M.Z., Bassani, J.: Indicador de produção aplicado ao gerenciamento de tecnologia em saúde. In: *IV Latin American Congress on Biomedical Engineering 2007, Bioengineering Solutions for Latin America Health*, pp. 859–862. Springer (2007)

16. Diretoria Acadêmica da UNICAMP: Coeficiente de Rendimento (CR). <https://www.dac.unicamp.br/portal/vida-academica/pos-graduacao/avaliacao-e-frequencia>. Last accessed 03 Mar 2022
17. Loyola University Chicago: The Grading System (2021). https://www.luc.edu/academics/catalog/undergrad/reg_gradinsystem.shtml. Last accessed 03 Mar 2022
18. Eboli, A.C.B. et al.: Gestão de tecnologia em saúde usando o sistema gets-ceb-unicamp. In: Avanços, Desafios e Oportunidades no Complexo Industrial da Saúde em Serviços Tecnológicos. [s.n.], pp. 58–75 (2018)
19. Blossom, A.P., Bradley, J.R.: Mistakes Commonly Made Using Performance Measures to Motivate Employees (1999)
20. Fernandes, D.R.: Uma contribuição sobre a construção de indicadores e sua importância para a gestão empresarial. Revista da FAE 7(1) (2004)
21. Horn, H.: Adding value: how to become a high-performing HTM department. Biomed. Instrum. Technol. 47(6), 478–484 (2013)



Reliability Analysis Techniques Applied to Highly Complex Medical Equipment Maintenance

M. C. C. Rezende¹ , R. P. Santos¹ , F. C. Coelli¹  ,
and R. M. V. R. Almeida² 

¹ Centro Federal de Educação Tecnológica Celso Suckow da Fonseca UnED Itaguaí, Itaguaí, RJ, Brazil

fernandocoelli@gmail.com

² Universidade Federal do Rio de Janeiro/Programa de Engenharia Biomédica – COPPE/UFRJ, Rio de Janeiro, Brazil

Abstract. The objective of this study was to apply reliability concepts in order to define adequate maintenance strategies for a group of highly complex equipment (Computerized Tomography) in the state of Rio de Janeiro. Methods: Equipment were located in 43 health units (private and public) Brazil. Failures claimed by customers and those observed by maintenance operators were identified. These data were collected considering all CT scanners and for each of the four brands present in the database. A FMEA was performed in order to identify failure risks and priorities thus allowing the ranking and prioritizing of the failures detected by the analysis. Each brand of equipment was thus classified according to its risk criticality (high-medium-low); and for each criticality, the most appropriate maintenance strategy (mitigation action) was defined. Additionally, with the observed times between failures, the maintenance indicators MTTF (Mean Time to Failure), MTTR (Mean Time to Repair) and MTBF (Mean Time Between Failure) were calculated. Results: About 200 repair requests from 2017 and 2018 had their information digitized. The most recurrent complained failure was “Failure of System Initialization, followed by “Generator failure” and “table malfunction”. Two of these could be classified as needing “predictive maintenance”, while the third (system initialization failure) was assigned “corrective maintenance). Conclusion: Reliability methods allowed for the definition of optimized maintenance strategies, with a resulting reduction in maintenance costs and an increase in equipment availability to patients.

Keywords: Reliability · Maintenance · CT Scanner · FMAE · Clinical Engineering

1 Introduction

The business model of this century differs from the prior style of competitiveness, mainly because of the current technological changes and increasing globalization [1]. Thus, what used to be considered a competitive advantage, for example, a very high advertising budget no longer has a place in this current scenario [2].

In this context, there is a strong incentive to increase the effectiveness and efficiency of operational activities, enabling not only equipment availability but also greater results for a company [3]. Based on these concepts, companies are increasingly seeking to achieve advantages by using management tools that result in greater productivity and quality for their products and services [4].

For instance, something that is widely observed in the maintenance field is the importance of reducing or eliminating failures [5].

Reliability techniques have been applied in several areas, such as aviation, since the 1940s [6], and have been consolidated as a strategy for performance and productivity gains [7]. These techniques are also great tools to assist in the maintenance management of medical equipment [8]. The application of these concepts allows, for example, for the rationalization of resources and the increase in equipment availability.

Therefore, besides the business sector, maintenance has a relevant role in other sectors, such as the Health Care [9]. Based on the studies of Coelli et al. [10], it was possible to identify the need to deepen the analysis of the reliability of Computed Tomography (CTs) and to seek strategies for the reduction of their failure rates, considering their importance in the diagnosis of a large number of serious diseases [13]. In this context, the Failure Modes and Effects Analysis (FMEA) is an important tool for analysis and definition of maintenance strategies. Its objective is to identify potential failures and how they impact in a process [5, 15]. Born in the American armed forces, it is widely used in the automobile and aeronautics industries. However, the use of this technique in Brazil's Health area is still limited. One of the reasons for that is that despite its potential contribution, data on medical equipment maintenance is hard to obtain in the country.

The objective of this study was to apply reliability concepts such as Mean Time Between Failures (MTBF) and Failure Mode and Effects Analysis (FMEA) to a group of CT scanners maintained by a private company in Rio de Janeiro State, Brazil.

2 Materials and Methods

Data were obtained from the Service Orders (SOs) of the years 2017 and 2018 of a hospital maintenance company located in the State of Rio de Janeiro, Brazil. Equipment were installed in 43 health units, representing 28 private and 15 public and/or SUS associated hospitals and radiology clinics. The equipment consisted of the four most present brands in our market.

The Google Groups tools, Google Forms and Google Sheets were used to automate the analysis of the SOs. The programs Wolfram Mathematica, Tableau Desktop and Microsoft Excel were used for graphical visualization. For parameter estimation calculations and definition of probability distributions the R software was used, and for other calculations Wolfram Mathematica was used.

The type of equipment chosen for analysis was the Computerized Tomography (CT) due to its high number of appearances in the maintenance database. In addition, this is a relevant equipment for the diagnosis of diseases and has very high costs in all utilization stages [10, 11].

The maintenance claims were provided by a hospital maintenance company based in the city of Rio de Janeiro. These maintenance claims were standardized forms filled

out on paper. To collect the data, the information on paper was transposed to an online form using Google Forms. As this form was fed with data from the claims, a Google Sheets spreadsheet was automatically fed, thus creating a digital database.

2.1 Data Collection and Analysis

In this step, an analytical survey of the information pertinent to the reliability calculations was performed. The following items were highlighted:

- The model with the highest number of SOs;
- Failure history in two years;
- Maintenance interventions performed.

The failures reported by customers and those observed by the maintenance operators were also collected. These data were collected both in an aggregated way (considering all CT scanners) and focusing on each of the four brands present in the database.

2.2 Elaboration of the FMEA

The FMEA technique consists of a systematic and progressive analysis of failures and their causes in a process or service. Once the most recurrent failures were identified, the FMEA was prepared, with the objective of qualitatively evaluating the risks provided by such failures. Thus, the failure analysis was performed using the PRN (Primary Risk Number) and RPN (Risk Priority Number) indicators of the FMEA. From these results, we may obtain the severity, occurrence and detection indexes, thus completing the risk classification and allowing for the definition of the maintenance strategy. In this study, only the three most frequent failures were analyzed.

With the definition of the RPN, each equipment brand was classified according to its risk criticality; and for each one, the most adequate maintenance strategy (mitigation action) was defined.

Thus, failures were classified and analyzed by two factors: severity and probability of occurrence. Each factor is defined by an integer value between 2 and 10, and the two factors are multiplied, resulting in the Primary Risk Number (PRN). After this first prioritization, another factor is added to the calculation: detection, also defined by the same range of values above, and which is multiplied by the PRN, resulting in the Risk Priority Number (RPN). Thus, RPN is the product of the three mentioned factors, as shown in Eq. (1) below.

$$\text{RPN} = \text{severity} \times \text{probability of occurrence} \times \text{detection} \quad (1)$$

With the observed times between failures the maintenance indicators MTTF (Mean Time to Failure), MTTR (Mean Time to Repair), MTBF (Mean Time Between Failure), Availability and Failure Rate (λ) and Reliability ($R(t)$) were calculated, and, according to the NBR 5462 Standard [12], Eqs. (2–7) were used to this end [13]. These are most objective and simple implement indicators for reliability studies.

$$\text{MTTF} = (Tt)/(Nf) \quad (2)$$

where $T_t = CT$ total operating time and $N_f =$ number of failures.

$$MTTR = (Tr)/(N_f) \tag{3}$$

where $Tr =$ Repair time

$$MTBF = MTF + MTTR \tag{4}$$

(for repairable items).

$$Availability = MTBF / (MTBF + MTTR) \tag{5}$$

$$\lambda = 1 / MTBF \tag{6}$$

$$R(t) = e^{-\lambda \cdot t} \tag{7}$$

3 Results

We analyzed 112 physical SOs from the year 2017 and 88 from 2018 (scanned). From these data, 200 records were generated referring to the maintenance services. Figure 1 presents the histogram of the client claimed failures, and Fig. 2, of the failures identified by maintenance crews. The most recurrent failure was “System Not Initializing”. The most recurrent item observed was “No failure”. The second was “Generator failure”.

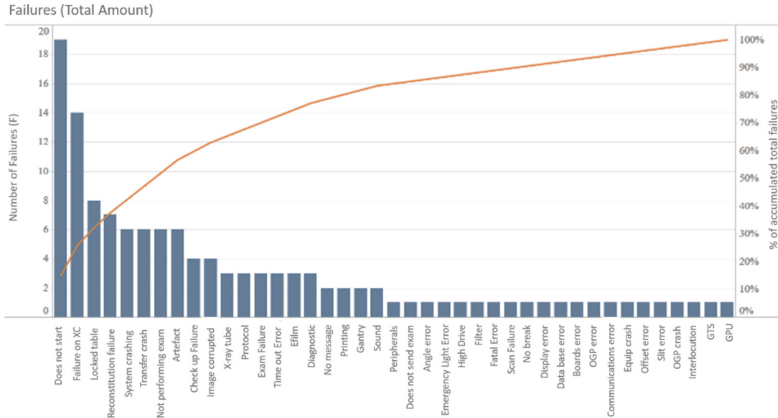


Fig. 1. Histogram for claimed failures in a database for the years 2017 and 2018. CTs, 43 health units in Rio de Janeiro State.

Table 1 presents the number of equipment units for each brand, the number of failures in the analyzed period, and the number of failures per unit of equipment for each brand. Table 2 presents the main failure types, the components responsible for these failures, the risk classification, and the defined maintenance strategy. Table 3 shows the results of the MTTF, MTTR, MTBF, Availability, Failure Rate and Reliability for the studied equipment.

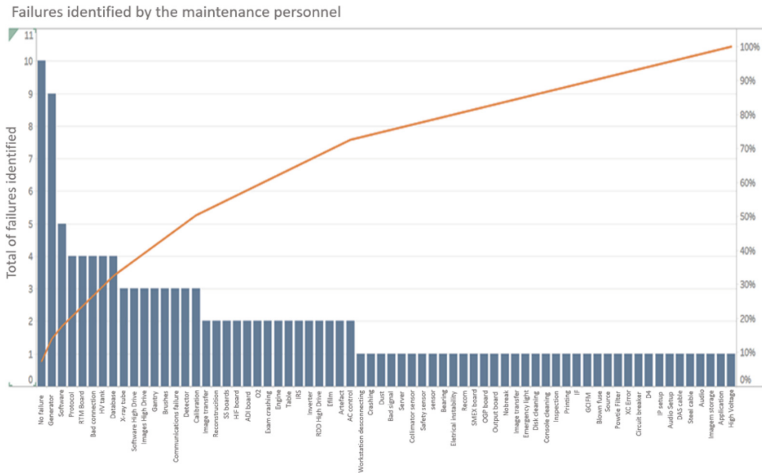


Fig. 2. Failures identified by the maintenance personnel.

Table 1. Number of equipment per brand, number of failures and failures/equipment in a FMEA of a database of CT maintenance SOs for 2017/2018, 43 health units, Rio de Janeiro State.

Brand	Number of equipment	Number of failures	Failures by equipment
1	30	113	3.76
2	12	32	2.66
3	8	35	4.37
4	1	6	6.00

Table 2. Type of failure, component responsible for the failure, Risk Classification (RPN) and defined maintenance strategies.

Component/Function	Failures	Risk classification	Maintenance
System initialization	Software failure	Low	Corrective
System initialization	RTM board failure	Medium	Predictive
XC board	HV generator	Medium	Predictive
Table	Engine failure	Medium	Predictive

4 Discussion

The failures found by the maintenance personnel did not always coincide with those claimed by the clients, denoting a mismatch in the understanding of a same problem. The importance of correcting this mismatch should be emphasized, given that a maintenance team is activated taking into account a received failure report. Also, Fig. 2 shows the

Table 3. Results of the reliability indicators in a database of CT maintenance SOs for 2017/2018, Rio de Janeiro State (in days).

Indicator	Result
MTTF	615.20
MTTR	2.30
MTBF	617.5
Availability	99.6%
Failure rate (λ)	0.00161
Reliability (R(t))	85.04%

occurrence of claims such as “Equipment does not start” and “XC failure”, problems that concern equipment software or X-ray generator, and which are somewhat generic.

Table 1 shows the number of failures by equipment manufacturer. In this case there may be a bias introduced by the small sample size and by the disparity in the number of devices of each brand. For example, while brand 1 had thirty devices, brand 4 had only one. For a more realistic comparison a more homogeneous sample would be necessary with regards to equipment brands. Once the aforementioned bias is controlled, this indicator can be interesting for inter-brand comparison.

Although 200 SOs were studied, only 186 pertained to equipment failures, the remaining 14 referred to calls where the equipment was not defective, services such as training and other miscellaneous client requests.

Table 2 presents the criticality of the failures and the defined type of maintenance according to the most frequent failures. For example, the system startup failure requires corrective maintenance since its occurrence impedes the use of an equipment. On the other hand, this failure does not allow the equipment to function, and therefore its associated risk is low.

Lack of information is frequently mentioned as one of the greatest difficulties in the implementation of the methodology of reliability centered maintenance (RCM) [14]. Therefore, a careful documentation of maintenance intervention events should be suggested to companies and/or health care units. As the present maintenance company did not have a digital database, the database developed in this work was made available for its use. Another important result of this study was sharing the theoretical and practical framework with the maintenance company. It was recommended to the company that, after this study, it should start collecting claims data digitally. As a consequence, the databases would be more organized and would generate reliability parameters for maintenance follow-up, also allowing for future studies with other equipment.

As said, for the criticality and failure strategy definitions, the three most frequent failures were considered in the study. This approach was used in order to simplify the work, although a deeper study would be possible by adding other types of failures.

The most recurrent failure claim was “System Not Initializing”; and the most recurrent observed failure was “No fault” (that is, the device did not present a defect when

tested, although the user complained about an alleged failure). Therefore, this is evidence of training deficiencies in what concerns client failure identification. The better a “pre-diagnosis”, the better the first intervention can be, since the maintenance team could readily decide on what components to use or, for instance who is the best person for dealing with a specific type of failure.

It was also observed that a common failure was related to the (high voltage) CT generator. This is a fundamental part of the equipment, which is susceptible to grid power supply failure. This component is obviously critical given that it operates with high voltages and power. As for power supply problems, units should keep their systems in optimal operating conditions, with periodic grounding and cabling revisions and a constant monitoring of variations in electrical supply levels. Another recommended prevention factor is to avoid using CTs during lighting storms.

Table jamming involves moving components, and can be attributed to wear, use under inadequate weather conditions and misuse, such as allowing paper jamming inside the mechanism.

From the reliability indicators in Table 3, it may be seen that 2.27 days were needed, on average, in order to repair an equipment. This represents a short time period, given that in just over 48 h the equipment was back into operation, despite its possible failure complexity. The time to failure (after the intervention) was 615.2 days. This high value shows that the equipment was well maintained, what can also be seen by the calculated MTBF of 617.5 days. As a consequence, the availability indicator was 99.6%, denoting that an equipment was in operational conditions almost all of the time. In addition, the estimated reliability indicated that 85.04% of the equipment were working in nominal conditions in the 100 days after an intervention.

The risk assessment of the most recurrent failures (XC board failure, table jamming and problems related to the high voltage generator) indicated a need for predictive maintenance strategies, allowing for a reduction in corrective interventions and in the clinics cost per visit. It is important to stress that predictive maintenance strategies detect failure at an early stage, therefore avoiding equipment downtime. Therefore, these interventions are relevant not only financially, but also in terms of equipment downtime, avoiding interruptions in patient care.

It should be noted that the technique applied in this study could be applied to different types of equipment in the Healthcare area. The improvement of maintenance management with these techniques can provide significantly longer equipment availability and resource savings [16–19].

The most commonly identified failures also show the need for clinic personnel training. On the other hand, the estimated reliability indicators point to a fast and adequate response capability of the company in charge of equipment maintenance. As an example, in a hospital in Rio de Janeiro city, 2003, the MTBF identified for a variety of hospital equipment was in the range 6–120 days [19].

5 Conclusion

The application of basic reliability techniques for CT equipment maintenance allowed for the identification of improvement opportunities in the definition of maintenance strategies. The dissemination of these techniques is very important, since they can significantly reduce equipment downtime, with a direct impact on patient care, with reduced waiting times, for example. In this sense, the adoption of this methodology by the public health system of the country could have a great impact in service improvement and resource optimization.

Acknowledgments. Our thanks to CAPES/ME (Proex Program, code 001) and CNPq for supporting this work.

Conflict of Interest

The authors declare that there is no conflict of interest in the present work.

References






1. Ramos, N.K., da Yamaguchi, C.K., Costa, U.M.: Tecnologia da informação e gestão do conhecimento: estratégia de competitividade nas organizações. *Brazil. J. Develop.* **6**(1), 144–161 (2020)
2. Anning-Dorson, T.: Innovation and competitive advantage creation: the role of organisational leadership in service firms from emerging markets. *Int. Mark. Rev.* **35**(4), 580–600 (2018)
3. Silvestri, L., Forcina, A., Introna, V., Santolamazza, A., & Cesarotti, V.: Maintenance transformation through Industry 4.0 technologies: a systematic literature review. *Comput. Indus.* **123**, 103335 (2020)
4. Patil, A., Soni, G., Prakash, A., Karwasra, K.: Maintenance strategy selection: a comprehensive review of current paradigms and solution approaches. *Int. J. Qual. Reliab. Manage.* **39**(3), 675–703 (2021)
5. Lo, H.W., Liou, J.J., Huang, C.N., Chuang, Y.C.: A novel failure mode and effect analysis model for machine tool risk analysis. *Reliab. Eng. Syst. Saf.* **183**, 173–183 (2019)
6. Anderson, R.T., Neri, L.: *Reliability-Centered Maintenance: Management and Engineering Methods*. Elsevier Applied Science, London (1990)
7. Shamayleh, A., Awad, M., Abdulla, A.O.: Criticality-based reliability-centered maintenance for healthcare. *J. Qual. Maint. Eng.* **26**(2), 311–334 (2020)
8. Sezdi, M.: Two different maintenance strategies in the hospital environment: preventive maintenance for older technology devices and predictive maintenance for newer high-tech devices. *J. Healthcare Eng.* **3**, 1–16 (2016)
9. Zamzam, A.H., Wahab, A.K.A., Azizan, M.M., Satapathy, S.C., Lai, K.W., Hasikin, K.: A systematic review of medical equipment reliability assessment in improving the quality of healthcare services. *Front. Public Health* **9**, 753951 (2021)
10. Coelli, F.C. et al.: Reliability analysis of computed tomography. In: *Annals of the XXIV Brazilian Congress on Biomedical Engineering—CBEB 2014*. 2049-51. Uberlândia-MG Brazil (2014)
11. Brasil. Ministério da Saúde: Secretaria de Gestão de Investimentos em Saúde. Projeto REFORSUS Equipamentos Médico-Hospitalares e o Gerenciamento da Manutenção: capacitação a distância/Ministério da Saúde, Secretaria de Gestão de Investimentos em Saúde, Projeto REFORSUS. – Brasília, DF: Ministério da Saúde, Brazil (2002)

12. NBR 5462: Confiabilidade e Manutenibilidade. ABNT:Associação Brasileira de Normas Técnicas.Rio de Janeiro, Brazil (1994)
13. Brenam, J.E., Sahay, C., Lewis, E.E.: Introduction to Reliability Engineering. John Wiley & Sons, New Jersey USA (2022)
14. ABRAMAN, Associação Brasileira de Manutenção: Documento Nacional: a situação da Manutenção no Brasil. Rio de Janeiro, Brazil (2013)
15. European Standards: Failure modes and effects analysis (FMEA and FMECA) - BS EN IEC 60812. Released: 2018–10–15 (2018)
16. Wen, Y., Tang, L., Ho, D.C.W.: A BIM-based space-oriented solution for hospital facilities management. *Facilities* **39**(11) 689–702 (2021)
17. Blanch, P.: An evaluation of ventilator reliability: a multivariate. Failure time analysis of 5 common ventilator brands. *Respir Care* **46**(8), 789–797 (2001)
18. Santos, R.P.: Análise da Ocorrência de Falhas em Equipamentos Cardiológicos em um Hospital de Emergência de Grande Porte no Município do Rio de Janeiro.MSc Dissertation: Universidade Federal do Rio de Janeiro, Rio de Janeiro Brazil (2003)
19. Santos, R.P., Almeida, R.M.V.: Hospital medical equipment maintenance schedules using the mean time between failures. *Cadernos de Saúde Coletiva* **18**(2), 309–314 (2010)

Health Technology, Innovation and Development



Multi-platform Mobile Application for Elderly Care Management

R. S. Navarro¹ , R. K. Chagas¹ , A. Baptista¹ , L. A. M. Pereira² ,
and S. C. Nunez¹ 

¹ Universidade Brasil, Pós Graduação Bioengenharia, São Paulo, Brazil
silvia.nunez@universidadebrasil.edu.br

² Universidade Brasil, Programa de Mestrado em Produção Animal, Descalvado, Brazil

Abstract. The aging of the world population has been occurring in recent decades as a result of the decrease in birth rates and better health care that allow an increase in life expectancy. The lack of contact with the family and unfamiliarity with habits and tastes can reduce the quality of life of the elderly that live under the care of professionals. Technological advances should be used to bridge the gap between families, caregivers, doctors and the elderly. This work aimed to develop an application for mobile devices that facilitates communication between health service providers for elderly people living in long-stay institutions. The CuidaLife App was developed for a software operating system with input modules for registering the elderly, family members, doctors and caregivers. The developed application can be accessed through any smartphone, tablet or computer, as long as it has internet access. Its layout is responsive, it adjusts according to the screen size of the device. The elderly registration modules were designed to allow the exchange of information about the elderly, not only medical, but also including food preferences, habits that are important for well-being. The caregivers module allows the exchange of information between caregiver shifts, with information relevant to the care of the elderly, and the medical module allows access to health information relevant to the monitoring of the elderly. The application worked well and may represent an easy and safe way to improve the quality of life of individuals who depend on third parties for their care.

Keywords: Aging · Computer Programs · Elderly Care · App · Mobile Device · Bioengineering

1 Introduction

The growth in life expectancy changed the world population demography. All over the world, it is common to have the idea that all countries, states and cities are composed of more children, young people and adults than elderly people, however, in face of this transition, it is expected that in the year 2050 there will be more people aged over 60 than under 15, estimated to reach a global elderly population of 2.1 billion compared to 901 million calculated in 2015 [1]. For example, the Brazilian population scenario is undergoing changes, a country that has long been known for having a high rate of young

people, according to statistics, will, by 2025, occupy the 6th position among the oldest countries, due to the increase in number of elderly people [2]. According to Law No. 10,741 of October 1, 2003, an elderly person is one who is 60 years of age or older.

The advance of improving the quality of life in all senses (social, cultural, economic, health care, among others), resulted in a demographic transition marked by a reduction in mortality and birth rates and an increase in the rate of elderly people [3]. Despite this improvement, this data does not mean that everyone enjoyed healthy aging. According to the World Health Organization (WHO), healthy aging is a “process of developing and maintaining the functional capacity that allows well-being in old age”.

In view of the above, a great challenge with the increase in longevity are chronic non-communicable diseases (NCDs), and within this category, dementias stand out, which are disorders characterized by cognitive decline, necessarily involving memory and at least one more domain, such as personality, language, social skills, abstract thinking, among others [4]. NCDs are a challenge in this population as they are causes of functional impairment and quality of life [5]. However, despite an individual being diagnosed with a chronic disease, it is possible to experience aging in the best possible way through processes that build skills and interventions to assist in this phase.

In addition to this challenge, the great transformations of society, such as the insertion of women more and more in the labor market, led to an increase in the number of elderly people within long-stay institutions, due to lack of time, fatigue, comfort, as well as the lower number of children and, consequently, of siblings to assist in this care, among other factors. Transformation that managed to demystify the vision of the old asylum that had the appearance of a “deposit for the elderly”, or a place that welcomes rejected elderly people or even abandoned by the family, a sad place, taxed by loneliness for a welcoming, respected environment, having all the necessary assistance to watch over and care for the life of the elderly, whether they are in full health or weakened [6].

According to ANVISA (National Health Surveillance Agency), long-stay institutions, also called nursing homes, are governmental or non-governmental institutions of a residential nature intended for the collective home of people aged 60 or over, with or without family support, in conditions of freedom, dignity and citizenship [7].

Within the demographic profile that makes up long-stay institutions are people with dementia, who are admitted by decision of third parties, by their own choice or even caused by abandonment because they demand more care, requiring greater availability of time from the caregiver, whether this is a loved one, family member, friend or professional hired at home [8]. The support network with aging decreases and in view of this fact it is very important that institutions seek to preserve family and social ties. In this sense, remote technologies can help communication between family, doctors, institutionalized patients and the nursing team itself [9].

Therefore, it is necessary to improve the innovation of technologies suitable for the elderly, which could assist in the care of this population, to facilitate direct conversation between family and professionals that work in the institution in which the elderly person is located. This study proposes to develop an application for mobile devices or not that facilitates communication between health service providers for elderly people living in long-stay institutions.

2 Methods

Before starting the development of the application, the best way of crossing the information was studied, in order to guarantee the efficiency of the application, object of this work. In this context, it was understood that the application should be divided into three main modules, which allow changes in data entry and access: Administrator, Caregiver, Doctors.

As proposed, the administrator is responsible for providing information about the elderly person, caregivers, doctors, family members, medication, food and examinations of the elderly person to be monitored. It is important to emphasize that, in the registration of caregivers and doctors, they must also receive a username and password to access the system, which will allow their caregivers and doctors to access the information of the elderly person being accompanied by this user.

With the password to access the application, the caregiver, in addition to having access to the elderly's information, such as personal data, family members, preferred food, medication and others, can record food, mediations, discomforts and other events that occur with the elderly. In this way, the application will assemble a history of the occurrences. The idea is that the system allows photos and videos to be archived along with reports of occurrences and events.

One of the main ideas of the system is that doctors have access to patient information, daily occurrences, history of medication given and exams. In this way, it is expected that these data can produce more assertive diagnoses. It is important to note that although the third module was aimed at physicians. It is possible that, in some cases, other people may be registered, for example, the person responsible for a nursing home. It is reaffirmed that the goal is for the application to serve as an electronic medical record with useful information that can help in diagnoses and guarantee the fulfillment of the caregiver's work, avoiding failures and forgetfulness.

So that the application can control an unlimited number of elderly people and their respective caregivers and doctors, a database structure was designed where a given user can control only one elderly person, thus, the database tables are interconnected through the user field, as shown in Fig. 1, in this image, it is also possible to see the fields of the idealized tables.

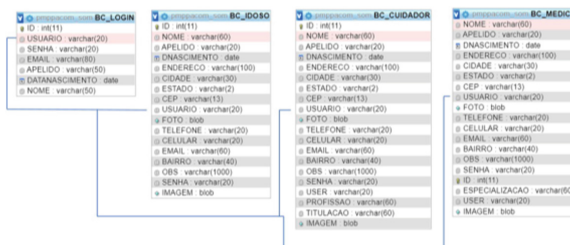


Fig. 1. Structure of the database tables designed to control the elderly, their caregivers, and doctors.

In the same way that the structure of Fig. 1 was assembled, it was also linked to the user, to the other frames: family, medicines, food, medical records and exams.

As proposed, few tables control infinite patients, followed by their caregivers, doctors and family members. The Fig. 2 presents the structure of the aforementioned tables, as well as their fields, types and sizes.



Fig. 2. Structure of the database tables designed to control family members, medication, food, exams and medical records

With this table structure, it is understood that the data can be shared between the different profiles in the system:

- User: responsible for registering the elderly and their information;
- Caregiver: responsible for feeding the actions carried out during the period of care for the elderly;
- Physician: responsible for monitoring the health of the elderly.

After planning the application, the next step was to choose the programming language, initially the idea was to develop an App for mobile phones, however, considering that at times it would be interesting to use the application on desktop or notebook, since some facilities in the use of the keyboard and the arrangement of information on a larger screen, we opted for the use of combined programming languages: PHP, HTML, Java Scripts, CSS and bootstrap, a free framework with a responsive character, which makes responsive programming, that is, it adapts according to the screen size of the equipment, wherever it is running. All the developed programming was stored on an outsourced web server and can be accessed through the link: <www.pmppa.com.br/cuidar>.

3 Results

The development of the software presented below resulted in the application for registration at the INPI number BR12021002074—0_870210078505.

3.1 App Developed

To use the App, just access the link <www.pmppa.com.br/cuidador>, the initial screen is shown in Fig. 3 (A) in the version for computers and notebooks and in Fig. 3 (B) in the version for smartphones.

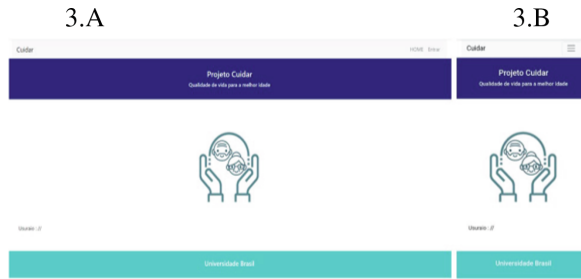


Fig. 3. In 3.A Initial screen of the developed App viewed on desktop computer and for Smartphone in 3.B.

To access the application, the user must click on Enter in the desktop version and, in the case of a smartphone, must first access the menu on the top tab on the left, represented by and dashes, where you will find the option: Enter. Two options will be displayed: login and register user. If it is the first time that the user accesses the system, he must necessarily choose the second option, register a user, however, it should be noted that the same person can register more than one user, as each user controls only one patient.

Once the user is registered, he/she must log in to access the system. Figure 4 shows the screen described in 4A and 4B, the first is the desktop version and the second is the smartphone version.



Fig. 4. In 4.A we present the login screen of the developed App viewed on a desktop computer and in 4.B viewed on a smartphone.

Once the register user option is chosen, the system will open a screen superimposed on the previous screen that will ask the user to fill in the fields: Username, Password, Name of the elderly person, Date of Birth, Surname, Email. The username and password field are responsible for giving the user access to the application. The other fields are information that the application needs to process some screens that will be presented throughout this work. Figure 5 A and B show the screen describing in the first image the desktop version and the smartphone version respectively.

With the registered user, it is already possible to log in to the system, in this case, the application will open a window superimposed on the initial screen, where the user must choose in the category field, if he is a user, who manages the elderly's information, if he is a caregiver, or doctor. Once one of the options is selected, you must enter your login and password, if the data are correct, you will have access to the system according

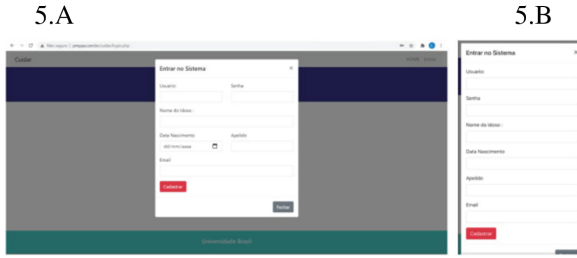


Fig. 5. In 5.A the user registration screen of the developed App viewed on a desktop computer and in 5B the screen viewed on a smartphone.

to your profile (category). Figure 6.A and B present the screen obtained for the desktop version and the smartphone version.

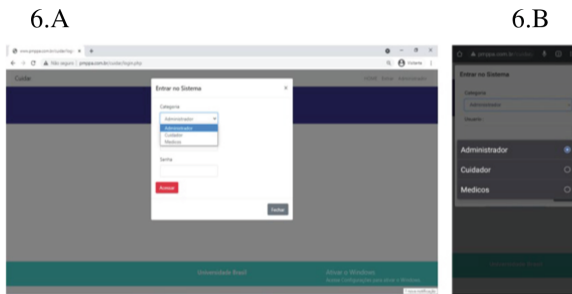


Fig. 6. In 6.A the login screen of the developed App viewed on a desktop computer and in 6.B the smartphone screen.

4 Discussion

The present study developed an App for mobile devices that facilitates communication between family and health service providers of elderly people who need third-party care for basic activities. For the development, the possibility of using a fast and practical platform that facilitates the routine of elderly people who need special care was analyzed, bringing together relevant information between doctors, caregivers and family members, promoting the safe storage of such information.

Although the increase in quality and in life expectancy have made great strides in several sectors, including health care, social and economic activities [10], according to WHO, there is a need to expand this right to everyone who reaches old age, since there is an indispensability of care and maintenance of existing methods for this to occur, as well as the development of new methods that can increasingly improve the way the professionals involved deal with the day to day in homes, institutions and also in households where the elderly may need special care [3].

According to Gaugler et al. [11] approximately two-thirds of residents in long-term care institutions in the United States have some form of dementia. Also according to the authors, the ideal treatment for patients with dementia should adopt a person-centered perspective and focus on maximizing the residents' quality of life.

Person-centered care refers to care that is individualized and adapted to changes in each person's preferences, abilities, and needs. In this context, the software developed in our study seeks to individualize the care of the elderly, from their personal food preferences to communication with family members and other health service personal to provide a personalized routine of behavior, tastes and daily manifestations made by the old man.

It has been increasingly observed the insertion of innovations and information and communication technologies (ICTs) to support health care for patients with dementia, aiming to support the care of these patients at home and improve the quality of life of caregivers [12]. Our software addresses some of the areas of interest pointed out by the researchers. In the case of patients with autonomy of manifestation, there may be the introduction of favorite foods, habits of interest and contact with family members through the program.

For those who have lost their autonomy, the program's caregivers area allows the exchange of information and experiences that can support the service provider in decision-making in the face of demands presented by the elderly, and in the aspect of assisted living, interaction with family members can help the elderly in maintaining contact with habits and customs of their daily life.

The inclusion of the elderly in their preferences is essential to maintain some degree of autonomy and control over daily activities and our software allows information to be exchanged between caregivers regarding the person's own preferences. Receiving care [13].

On Google Play, it was possible to find applications such as The Backup Memory where family members send photos and activities developed with the elderly so that they can try to maintain or establish a connection with family and friends. In the same category, Samsung launched the Memory recaller app. However, no applications were found that had similar characteristics to CuidaLife.

It is necessary that the software developed in this study to be tested by caregivers, family members and the elderly so that its performance can be analyzed, and necessary adjustments can be developed. Technological advances and access to real-time information in a safe and fast way should be explored for the care of elderly people [14] who will increasingly have access to technology because they have lived with it for a good part of their lives, thus, integration from simple software like the one proposed in this study to the development of connected products that can facilitate the care and quality of life of the elderly should be encouraged, including as a public policy in the health field.

5 Conclusions

The present study developed an application for mobile devices as well as for computers that facilitates communication between health service providers for elderly people living in long-stay institutions. The cross-platform mobile application will be able to broadly contribute to communication between professionals, family members and the elderly.

Conflict of Interest. The authors declare that there are no conflicts of interest in carrying out this study.







Declaration of Human Rights. The study was not performed directly or indirectly in humans, not requiring submission to Ethical Committee on Human Experimentation.

References

1. Beard, J.R., Officer, A., De Carvalho, I.A., Sadana, R., Pot, A.M., Michel, J.P., Lloyd-Sherlock, P., Epping-Jordan, J.E., Peeters, G.M.E.E.G., Mahanani, W.R., Thiyagarajan, J.A., Chatterji, S.: The World report on ageing and health: a policy framework for healthy ageing. *Lancet* **387**(10033), 2145–2154 (2016)
2. Miranda, G.M.D., Mendes, A.D.C.G., Silva, A.L.A.D.: O envelhecimento populacional brasileiro: desafios e consequências sociais atuais e futuras. *Revista Brasileira de Geriatria e Gerontologia* **19**(3), 507–519 (2016)
3. World Health Organization: World Report on Ageing and Health. World Health Organization (2015)
4. Buffington, A.L., Lipski, D.M., Westfall, E.: Dementia: an evidence-based review of common presentations and family-based interventions. *J. Am. Osteopath. Assoc.* **113**(10), 768–775 (2013)
5. André, C.: Vascular dementia: a critical review of diagnosis and treatment. *Arquivos de Neuro-Psiquiatria* **56**(3), 498–510 (1998)
6. Noronha, C.V.: Idosos em instituição de longa permanência: Falando de cuidado. *Interface* **14**(33) (2010)
7. Colegiada, D.E.D., De, D.E.S.: Ministério da Saúde - MS Agência Nacional de Vigilância Sanitária (2005)
8. Jesus, I.S., et al.: Cuidado sistematizado a idosos com afecção demencial residentes em instituição de longa permanência. *Rev. Gaúcha Enferm.* **31**(2), 285–292 (2010)
9. Abdi, J., Al-Hindawi, A., Tiffany, N.G., Vizcaychipi, M.: Scoping review on the use of socially assistive robot technology in elderly care. *BMJ Open* **8**, e018815 (2018)
10. D'onofrio, G., et al.: Information and Communication Technologies for the Activities of Daily Living in Older Patients with Dementia: A Systematic Review, pp. 927–935. IOS Press (2017)
11. Gaugler, J.E., Yu, F., Davila, H.W., Shippee, T.: Alzheimer's disease and nursing homes. *Health Aff.* **33**(4), 650–657 (2014)
12. Changizi, M., Kaveh, M.H.: Effectiveness of the mHealth technology in improvement of healthy behaviors in an elderly population—a systematic review. *mHealth* **27**(3), 51 (2017)
13. Veras, R.P., Oliveira, M.: Aging in Brazil: the building of a healthcare model. *Ciencia e Saude Coletiva* **23**(6), 1929–1936 (2018)
14. Zhao, Y.U., Hu, X., Men, D.: Design and Research of Health Aids Based on App in the Elderly. Springer International Publishing (2019)



Comparative Study of Therapeutic Ultrasound and Copaiba Oil Phonophoresis Therapies for Shoulder Tendinitis

J. P. S. Martins^{1,2} , A. B. Fernandes^{1,2} , R. A. Lazo-Osório^{1,2} ,
L. P. Alves^{1,2} , A. B. Villaverde^{1,2} , and C. J. de Lima^{1,2} 

¹ Institute of Biomedical Engineering, Distrito de Eugênio de Melo, Anhembi Morumbi University (UAM), Estrada Dr. Altino Bondensan 500, Distrito de Eugênio de Melo, CEP: 12.247-016, São José Dos Campos, SP, Brazil

dr.joaopedromartins@yahoo.com

² Center of Innovation, Technology and Education, CITE. Estrada Dr. Altino Bondensan 500, Distrito de Eugênio de Melo, CEP: 12.247-016, São José Dos Campos, SP, Brazil

Abstract. Shoulder tendinitis is characterized by inflammation of the rotator cuff tendons, resulting in pain, instability, and limitation of shoulder movements. The injury can be caused by stress, excess movements in daily activities or excessive load on the muscles. The study aimed to evaluate the effectiveness of shoulder tendinitis treatment using therapeutic ultrasound associated with the Copaiba oil incorporated into the coupler gel. The study assessed 30 patients divided into groups: TUS—conventional ultrasound and CP—ultrasound with 10% Copaiba oil gel. Ultrasound parameters: 1 MHz acoustic frequency, 0.5 W/cm² intensity, 100 Hz repetition rate, 20% duty cycle, and 3.5 cm² irradiation area. Ultrasound was applied for 4 min each session, with 12 sessions treatment. The treatment was evaluated by the parameters: quality-of-life, pain intensity, muscle strength (abduction and flexion), and the amplitude of the joint movement of the shoulder (abduction, adduction, flexion, extension, medial and lateral rotations). The treatment evaluation was made by introducing the evolution score index, which compare the values measured post-treatment with the pre-treatment. The ANOVA and Student tests were used for intra and intergroup statistical analysis, respectively, with a significance level of $\alpha < 0.05$. Results show that the group of phonophoresis with Copaiba oil gel presented an improvement in functional capacity, with pain reduction, increase in muscle strength and in joint movement amplitude, when compared with therapeutic ultrasound ($p < 0.05$). Concluding, the anti-inflammatory and analgesic properties of ultrasound can be enhanced by phonophoresis using gel with Copaiba oil.

Keywords: Copaiba gel · Rotator cuff tendinitis · Phonophoresis · Therapeutic ultrasound · Pain relief · Muscle strength and shoulder motion improvements

1 Introduction

Shoulder tendinitis is a condition characterized by inflammation of the rotator cuff tendons, resulting in pain, instability, and considerable limitation of shoulder movements, such as the medial and lateral rotation movements. The injury can be caused by several factors, such as stress, excess movements in daily activities, excessive load on the muscles, or physical inactivity associated with old age [1, 2]. Shoulder pain, range of motion impair, and disability are the most common symptoms in patients with shoulder dysfunction [3]. In view of the increase of the population looking for sports and the excess of competitiveness within all sport competitions there is an increase in the rate of shoulder injuries caused by the practice of sports [4–7]. In this context, it is important to seek the best treatment of athletes' shoulder injuries.

Nam and Lee [8] reported that the conservative treatment of shoulder tendinitis should be always prioritized, i.e., the use of anti-inflammatory drugs, thereby improving quality-of-life without the need for surgical intervention. However, the use of anti-inflammatory drugs can cause adverse effects.

Among the various techniques for the treatment of shoulder tendinitis the therapeutic ultrasound (TUS) is very promising, it promotes a faster recovery process at the injured site [9–11]. Ultrasound generates acoustic waves that cause thermal effects like acceleration of metabolism, changes in nerve conduction velocity, increased blood flow, a temporary increase in the extensibility of collagen structures, and a reduction or control of pain [12]. To maximize the transmission of the mechanical energy of the ultrasound through the skin, a specific coupler gel is applied over the skin.

The addition of a drug to the coupler gel in ultrasound therapy promotes the transport of the active substances of the drug to the location of the lesion, resulting in greater efficacy of the treatment. This technique is non-invasive and without side effects and it is known as phonophoresis [13]. The action of the absorbed drugs depends on the anatomy of the treated area, the hydration degree of the skin, the presence of fat, the patient's metabolism, and how the ultrasound is applied [14].

Several studies have been published in the last few years comparing the effect of the phonophoresis using different drugs on the treatment of diverse musculoskeletal disorders. It is worthy to mention some of them, drug(s)–musculoskeletal disorder: Fish oil–Achilles tendon rupture [15], virgin olive and piroxicam–exercise induced knee pain [16], diclofenac and thicolchioside gel–low back pain [17], piroxicam and dexamethasone sodium phosphate–carpal tunnel syndrome [18], among others.

In the present study, it is investigated the effect of adding an herbal medicine substance to the coupler gel, i.e., Copaiba oil, which has analgesic and anti-inflammatory properties, and it can improve the tendinitis recovery process. Copaiba oil is a natural substance extracted from trees of the species *Copaifera langsdorffii* Desf. (Leguminosae, Caesalpinioideae), and is characterized as a terpenoid [19, 20]. The main compound found in Copaiba oil is β -caryophyllene. This substance presents properties such as local analgesic, anti-inflammatory, and anti-microbial effect [21, 22].

The aim of the present study is to test the hypothesis that a phonophoresis using Copaiba oil enhances the effect of conventional ultrasound on the treatment of shoulder tendinitis.

2 Materials and Methods

A study was conducted experimental, randomized, blinded, controlled, and composed of 30 patients of both sexes suffering of chronic tendinitis of the shoulder for more than 6 months (patients' age: 60.6 ± 6.8 yr). The research project was approved by the University Ethics Committee under the code CAAE: 47345015.0.0000.5494. All patients signed a consent form, and they first underwent a clinical evaluation process by the responsible physiotherapist. Inclusion criteria were medical diagnosis as chronic tendinitis of the shoulder, age between 45 and 70 years, and not using anti-inflammatory or analgesic medication at the time of the study. Exclusion criteria, no chronic tendinitis of the shoulder, age out of the studied range, using anti-inflammatory or analgesic drugs, presenting other pathologies associated with tendinitis, and who were treated with other therapeutic methods recently.

2.1 Treated Groups

The study assessed 30 patients equally divided into two groups: TUS - treated with ultrasound using the conventional water-based gel, and CP-ultrasound with 10% of Copaiba oil added to the coupler gel.

2.2 Ultrasound Equipment

Therapy was conducted using IBRAMED equipment, Sonopulse model (IBRAMED Co, Amparo, São Paulo, Brazil), with 1 MHz acoustic frequency, Spatial Average–Temporal Average (SATA) intensity of 0.5 W/cm^2 , pulsed with 100 Hz repetition rate and 20% duty cycle, and 3.5 cm^2 of Effective Radiation Area (ERA). The equipment was calibrated by the own factory.

2.3 Treatment Description

Copaiba oil (Bioflora, Itajubá, MG, Brazil) added to the coupler gel at a concentration of 10% was used in the present study. The ultrasound was applied by direct coupling with oscillatory rubbing movements for 4 min over an area of $5 \times 5 \text{ cm}$, and 30 min of session, including the prior clinical evaluation. Treatment comprised of 12 sessions, three times a week (28 days).

2.4 Treatment Evaluation

The treatment evaluation was performed by assessing the parameters: quality-of-life using the Health Assessment Questionnaire (HAQ; 15 questions) [10], pain intensity by the visual analog scale (VAS) that classifies the pain on a scale from 0 to 10, being 10 the maximum pain, and muscle strength that was evaluated through a protocol in which the patient performs two specific movements of the shoulder joint (abduction and flexion), using a weight of up to 50 N. Other evaluation parameter was the range of motion, which was measured in degrees with a goniometer. This last parameter was subdivided

into six aspects to evaluate every movement separately: flexion, extension, abduction, adduction, medial rotation, and lateral rotation. Each parameter was measured before and at the 28th day of treatment. The treatment performance was evaluated by using the evolution score index, which is defined as:

$$\text{evolution score} = (\text{score post} - \text{score pre}) - (\text{score post-treatment} - \text{score pre-treatment}) \quad (1)$$

Evolution scores positives for muscle strength and shoulder motion indicate that the patient shows improvement in the corresponding parameter. On the contrary, negative values for pain and HAQ means improvements.

2.5 Statistical Analysis

A one-way ANOVA test followed by Tukey post-hoc test was used for the statistical intragroup analysis of the scores of each parameter before and after treatment. The intergroup analysis was performed by applying a parametric, unpaired, and two-tailed Student t-test to compare the evolution scores of the TUS group with the CP group. The GraphPad Prism 8[®] software (GraphPad Software Inc., La Jolla, CA, USA) was used for intragroup and intergroups statistical analysis, with a significance level of 5% ($p < 0.05$). Results are expressed as Mean \pm SEM.

3 Results and Discussion

Table 1 shows the scores of the 10 parameters that were evaluated in the groups TUS and the phonophoresis CP, as well as the intragroup statistical analysis. The data in Table 1 indicate that both treatments induce an improvement of the patients in all parameters, although at different intensity, being the increase statistically significant for 8 parameters in the CP group, and only 5 parameters of the TUS group.

Evolution scores of the parameters for both groups are depicted in Table 2. The improvement in shoulder tendinitis by both therapies is manifested in the values of the positive evolution scores for muscle intensity and shoulder movement, and negative for pain reduction and the HAQ test. Table 2 also contain the results of the intergroup statistical analysis, which are described as follows:

Evaluation of pain intensity and quality of life. The CP group using the phonophoresis technique induces a statistically significant reduction of pain when compared to the TUS group. On the contrary, in the quality-of-life parameter using the HAQ test the CP group shows a smaller increase than for the TUS group, a result that could be explained by the very subjective characteristic of the HAQ test.

Evaluation of muscle strength. The parameter that evaluates muscle strength was divided into two components, i.e., abduction and flexion movements, to facilitate the understanding and implementation of the assessment. The treatment using phonophoresis presents a significant increase in strength when compared with the ultrasound therapy for both components of the parameter.

Evaluation of range of motion. The assessed shoulder motion parameter comprised six angular movements: flexion, extension, abduction, adduction and, medial and lateral

Table 1. Parameter scores and intragroup statistical analysis for TUS and CP groups: Mean (SEM)

Parameter	Group TUS			Group CP		
	Pre-treatment	Post-treatment	p	Pre-treatment	Post-treatment	p
Pain	6.0 (0.5)	2.4 (0.5)	***	6.8 (0.5)	1.1 (0.3)	***
HAQ	10.3 (1.7)	1,2 (0.3)	***	6.2 (1.3)	2.7 (0.8)	ns
Muscle strength (N)						
Abduction	5.9 (1.8)	10.9 (2.4)	ns	4.6 (1.2)	16.8 (0.9)	***
Flexion	3.5 (0.6)	8.6 (1.1)	ns	7.4 (1.5)	15.5 (1.7)	***
Shoulder motion (°)						
Flexion	135.5 (11.3)	157.5 (8.9)	ns	118.7 (8.5)	178.0 (2.0)	***
Extension	36.4 (1.3)	43.0 (0.8)	***	32.9 (0.8)	45.0 (0.1)	***
Abduction	138.0 (7.1)	164.0 (7.3)	*	162.0 (3.2)	176.5 (3.5)	ns
Adduction	33.5 (1.7)	39.0 (0.7)	ns	28.7 (2.0)	40.0 (0.1)	***
Medial rotation	68.5 (4.7)	83.5 (3.2)	*	62.5 (3.3)	89.0 (0.7)	***
Lateral rotation	75.0 (3.6)	87.0 (2.1)	ns	64.0 (4.6)	88.0 (1.3)	***

A one-way ANOVA test followed by Tukey post-hoc test was used for the statistical intragroup analysis of the scores of each parameter before and after treatment. Statistical analysis with a significance level of 5% ($p < 0.05$).

Parameter units: (N) Newton, (°) degree. TUS: therapeutic ultrasound. CP: Copaiba oil. SEM: standard error of the median. * $p < 0.05$, ** $p < 0.01$, *** $p < 0.001$, ns-not significant.

rotations. It can be observed from the intergroup analysis data shown in Table 2 that the phonophoresis with Copaiba gel induces a statistically significant increase, in relation to therapeutic ultrasound, in the angulation of shoulder movements flexion, extension, adduction, medial and lateral rotations, with statistical uncertainty values of $p < 0.05$ to $p < 0.01$, depending on the parameter studied. On the contrary, although the TUS and CP groups increased angulation in the abduction movement after treatment, the increase was lower for the CP group.

Briefly, the results of this study show that the insertion of 10% Copaiba oil to the gel used in the treatment with therapeutic ultrasound enhances the effect of the ultrasound in the treatment of shoulder tendinitis, in eight of the ten evaluated parameters.

The aim of the present study was to assess the reduction of the painful process in the chronic phase of shoulder tendinitis using two therapies: conventional ultrasound and ultrasound with coupler gel containing the herbal substance Copaiba. In this sense, a reduction in the painful process in the chronic phase was observed in our study for both proposed therapies.

The ultrasound parameters used in the present study optimized the therapeutic effects of the ultrasound on shoulder tendinitis, allowing deeper penetration into the tissue, providing maximum rate tissue regeneration, and avoiding thermal effects in the stratum corneum [23].

Table 2. Intergroup statistical analysis of the evolution scores for TUS and CP groups: mean (SEM)

Parameter	Group TUS	Group CP	p
Pain	-3.6 (0.4)	-5.7 (0.6)	**
HAQ	-9.1 (1.6)	-3.5 (0.8)	**
Muscle strength (N)			
Abduction	5.0 (1.1)	12.2 (1.0)	***
Flexion	5.1 (0.8)	8.1 (1.2)	*
Shoulder motion (°)			
Flexion	22.0 (5.1))	59.2 (8.5)	**
Extension	6.6 (1.3)	12.1 (1.8)	*
Abduction	26.0 (2.2)	14.5 (2.3)	**
Adduction	5.5 (1.4)	11.3 (2.0)	*
Medial rotation	15.0 (3.3)	26.5 (2.8)	**
Lateral rotation	12 (3.1)	24 (3.6)	*

The intergroup analysis was performed by applying a parametric, unpaired, and two-tailed Student t-test to compare the evolution scores of the TUS group with the CP group. The GraphPad Prism 8[®] software (GraphPad Software Inc., La Jolla, CA, USA) was used for intragroup for statistical analysis, with a significance level of 5% ($p < 0.05$). Parameter units: (N) Newton, (°) degree. TUS: therapeutic ultrasound. CP: Copaiba oil. SEM: standard error of the median. * $p < 0.05$, ** $p < 0.01$, *** $p < 0.001$.

The choice of the right medium to be used as an ultrasound coupler is important to obtain the maximum transfer of acoustic power to the tissue. Casarotto et al. [24] reported that gel used with ultrasound presented the highest transmission, an attenuation coefficient and acoustic impedance close to that of the skin, as compared with other materials such as mineral oil, white petrolatum, and degassed water. Based on those findings, we chose to employ the gel as the ultrasound coupler in the present study, alone or combined with Copaiba oil.

Therapeutic ultrasound combined with anti-inflammatory drugs has been widely employed in recent decades. For instance, Jun et al. [25] compared the effect of phonophoresis using Chinese medicinal herbs or sodium diclofenac on the treatment of knee osteoarthritis observing that the two therapies were efficient and no statistically significant difference was found between both drugs.

In a recent work, Altan et al. [17] reported a study on the therapy of acute low back pain using phonophoresis (diclofenac plus thiocolchioside gel) or therapeutic ultrasound. They assessed the parameters Visual numeric scale (VNS), Oswestry Disability Index (ODI), and Shober test. Comparing the two therapies was found that phonophoresis presented a significantly improvement in VNS and ODI parameters.

Our results agree with findings reported in the literature that phonophoresis enhances the effect of the therapeutic ultrasound regarding pain reduction and improvement in functional capacity [15–17, 25].

Several parameters were analyzed in our study for the treatment of shoulder tendinitis. It was found that phonophoresis using the Copaiba oil gel (at 10% concentration) presented statistically significant differences when compared with conventional ultrasound for eight out of the ten studied parameters: pain relief, increased muscle strength (abduction and flexion) and articular movement of the shoulder (flexion, extension, adduction and, medial end lateral rotation). These results indicate that the phonophoresis process enhanced the permeation of drugs when they are included into the gel.

Moreover, Copaiba oil has anti-inflammatory and analgesic activity due to the presence of sesquiterpenes such as β -caryophyllene (main component of the oil). Tung et al. [21], Chavan et al. [22], and Ghelardini et al. [26] highlighted the medicinal activity of β -caryophyllene, due to its anti-inflammatory and analgesic properties.

In this way, the gel with Copaiba oil seems to be effective for the treatment of chronic shoulder tendinitis, improving pain relief and functional capacity; therefore, improving the quality-of-life of the patients.

However, even though these results are promising for shoulder tendinitis treatment, further studies are needed with an augment of the cohort size to corroborate these findings. Likewise, longitudinal studies as the rehabilitation of patients with kinesiotherapy, to strengthen the rotator cuff muscles that were affected by the lesion, and follow up of patients' recovery after therapy are convenient.

Phonophoresis using gel with Copaiba oil seems to be a valuable candidate for a low-cost alternative treatment for shoulder tendinitis.

4 Conclusion

It can be concluded that treatment of shoulder tendinitis with ultrasound using gel containing Copaiba oil (10% concentration) was more efficient than the conventional ultrasound with water-based gel, suggesting that phonophoresis enhances the anti-inflammatory and analgesic activities of ultrasound.

Acknowledgments. JPSM thanks the Coordination for the Improvement of Higher Education Personnel (CAPES) for the PhD scholarship. ABF, RAL-Z, LPA, ABV, and CJL thank the Anima Institute (Brazil) for the grating of their Research Scholarships.

Conflict of Interest. The authors declare that they have no conflict of interest.

References





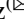

1. Mitchell, C., Adebajo, A., Hay, E., Carr, A.: Shoulder pain: diagnosis and management in primary care. *BMJ*. **331**, 1124–1128 (2005). <https://doi.org/10.1136/bmj.331.7525.1124>
2. Gomoll, A.H., Katz, J.N., Warner, J.J.P., Millett, P.J.: Rotator cuff disorders: recognition and management among patients with shoulder pain. *Arthritis & Rheumatol*. **50**, 3751–3761 (2004). <https://doi.org/10.1002/art.20668>

3. Answer, S., Alghadir, A.H., Al-Eisa, E.S., Iqbal, Z.A.: The relationships between shoulder pain, range of motion, and disability in patients with shoulder dysfunction. *J. Back Musculoskelet. Rehabil.* **31**, 163–167 (2018). <https://doi.org/10.3233/BMR-169762>
4. Oyama, S.: Baseball pitching kinematics, joint loads, and injury prevention. *J. Sport. Health Sci.* **80e91** (2012). <https://doi.org/10.1016/j.jshs.2012.06.004>
5. Weiss, L.J., Wang, D., Hendel, M., Buzzerio, P., Rodeo, S.A.: Management of rotator cuff injuries in the elite athlete. *Curr. Rev. Musculoskelet. Med.* **11**, 102–112 (2018). <https://doi.org/10.1007/s12178-018-9464-5>
6. Joeng, H.S., Na, Y.M., Lee, S.Y., Cho, Y.J.: Injuries among Korean female professional golfers: a prospective study. *J. Sport. Sci. Medicine.* **17**, 492–500 (2018). PMID: 30116123; PMCID: PMC6090400
7. Goodman, A.D., Raducha, J.E., De Froda, S.F., Gil, J.A., Owens, B.D.: Shoulder and elbow injuries in NCAA football players, 2009–2010. through 2013–2014. *Physician Sport.* **47**, 323–328 (2019). <https://doi.org/10.1080/00913847.2018.1554167>
8. Nam, H.S., Lee, S.U.: Conservative management of shoulder pain with common causes. *J Korean Med Assoc.* **57**, 661–666 (2014). <https://doi.org/10.5124/j.2014.57.8.661>
9. Robertson, V.J., Baker, K.G.: A review of therapeutic ultrasound: effectiveness studies. *Phys. Ther.* **81**, 1339–1350 (2001). PMID: 11444997
10. Pribicevic, M., Pollard, H.: A multi-modal treatment approach for the shoulder: a 4 patient case series. *Chiropr Osteopat.* **13**, 20 (2005). <https://doi.org/10.1186/1746-1340-13-20>
11. Naredo, E., Aguado, P., De Miguel, E., Uson, J., Mayordomo, L., Gijon-Baños, J., Martín-Mola, E.: Painful shoulder: comparison of physical examination and ultrasonographic findings. *Ann. Rheum. Dis.* **61**, 132–136 (2002). <https://doi.org/10.1136/ard.61.2.132>
12. Draper, D.O., Castel, J.C., Castel, D.: Rate of temperature increase in human muscle during 1 MHz and 3 MHz continuous ultrasound. *J. Orthop. & Sport. Phys. Ther.* **22**, 142–150 (1995). <https://doi.org/10.2519/jospt.1995.22.4.142>
13. Byll, N.N.: The use of ultrasound as an enhancer for transcutaneous drug delivery: phonophoresis. *Phys. Ther.* **75**, 539–553 (1995). <https://doi.org/10.1093/ptj/75.6.539>
14. Karatay, S., Aygul, R., Melikoglu, M.A., Yildirim, K., Ugur, M., Erdal, A., Akkus, S., Senel, K.: The comparison of phonophoresis, iontophoresis and local steroid injection in carpal tunnel syndrome treatment. *Jt. Bone Spine* **76**, 719–721 (2009). <https://doi.org/10.1016/j.jbspin.2009.02.008>
15. Chan, K.O., Tong, H.H., Ng, G.Y.: Topical fish oil application coupling with therapeutic ultrasound improves tendon healing. *Ultrasound Med. Biol.* **42**, 2983–2989 (2016). <https://doi.org/10.1016/j.ultrasmedbio.2016.08.018>
16. Nakhostin-Roochi, B., Khoshkharesh, F., Bohlooli, S.: Effect of virgin olive oil versus piroxicam phonophoresis on exercise-induced anterior knee pain. *Avicenna J Phytomed.* **6**, 535–541 (2016). PMID: 27761423; PMCID: PMC5052416
17. Altan, L., Kasapoğlu Aksoy, M., Kösegil Öztürk, E.: Efficacy of diclofenac & thiocolchioside gel phonophoresis comparison with ultrasound therapy on acute low back pain; a prospective, double-blind, randomized clinical study. *Ultrasonics* **91**, 201–205 (2019). <https://doi.org/10.1016/j.ultras.2018.08.008>
18. Boonhong, J., Thienkul, W.: Effectiveness of phonophoresis treatment in carpal tunnel syndrome: a randomized double-blind, controlled trial. *PMR* **12**(1), 8–15 (2020). <https://doi.org/10.1002/pmrj.12171>
19. Barbosa, P.C.S., Wiedemann, L.S.M., Medeiros, R.S., Sampaio, P.T.B., Vieira, G., da Veiga-Junior, V.F.: Phytochemical fingerprints of copaiba oils (*Copaifera multijuga* Hayne) determined by multivariate analysis. *Chem. & Biodivers.* **10**, 1350–1360 (2013). <https://doi.org/10.1002/cbdv.201200356>

20. Cascon, V., Gilbert, B.: Characterization of the chemical composition of oleoresins of *Copaifera guianensis* Desf., *Copaifera duckei* Dwyer and *Copaifera multijuga* Hayne. *Phytochem.* **55**, 773–778 (2000). [https://doi.org/10.1016/S0031-9422\(00\)00284-3](https://doi.org/10.1016/S0031-9422(00)00284-3)
21. Tung, Y.T., Chua, M.T., Wang, S.Y., Chang, S.T.: Anti-inflammation activities of essential oil and its constituents from indigenous cinnamon (*Cinnamomum osmophloeum*) twigs. *Bioresour. Technol.* **99**, 3908–3913 (2008). <https://doi.org/10.1016/j.biortech.2007.07.050>
22. Chavan, M.J., Wakte, P.S., Shinde, D.B.: Analgesic and anti-inflammatory activity of caryophyllene oxide from *Annona squamosa* L. bark. *Phytomedicine* **17**, 149–151 (2010). <https://doi.org/10.1016/j.phymed.2.009.05.016>
23. Ansari, N.N., Fathali, M., Naghdi, S., Hasson, S., Jalaie, S., Rastak, M.S.: A randomized, double-blind clinical trial comparing the effects of continuous and pulsed ultrasound in patients with chronic rhinosinusitis. *Physiother.: Theory Pract.* **28**, 85–94 (2012). <https://doi.org/10.3109/09593985.2011.571751>
24. Casarotto, R.A., Adamowski, J.C., Fallopa, F., Bacanelli, F.: Coupling agents in therapeutic ultrasound: acoustic and thermal behavior. *Arch. Phys. Med. Rehabil.* **85**, 162–165 (2004). [https://doi.org/10.1016/S0003-9993\(03\)00293-4](https://doi.org/10.1016/S0003-9993(03)00293-4)
25. Zhao, J., Wang, Q., Wu, J., Shi, X., Qi, Q., Zheng, H., Lang, S., Yang, L., Zhang, D.: Therapeutic effects of low-frequency phonophoresis with a Chinese herbal medicine versus sodium diclofenac for treatment of knee osteoarthritis: a double-blind, randomized, placebo-controlled clinical trial. *J. Tradit. Chin. Med.* **36**, 613–617 (2016). [https://doi.org/10.1016/S0254-6272\(16\)30080-2](https://doi.org/10.1016/S0254-6272(16)30080-2)
26. Ghelardini, C., Galeotti, N., Mannelli, L.D.C., Mazzanti, G., Bartolini, A.: Local anaesthetic activity of beta-caryophyllene. *Il Farmaco* **56**, 387–389 (2001). [https://doi.org/10.1016/S0014-827X\(01\)01092-8](https://doi.org/10.1016/S0014-827X(01)01092-8)



Home Dental Whitening: Preliminary Clinical Study of the Technique and Patients' Perception

A. Baptista , L. H. V. Dantas , R. S. Navarro , A. Pinto , and S. C. Nunez  

Universidade Brasil, Pós-Graduação Bioengenharia, São Paulo, Brazil
silvia.nunez@universidadebrasil.edu.br

Abstract. The demand for treatments aimed at aesthetics in dentistry has been growing more and more and with this comes the need to improve procedures and treatments so that there is greater effectiveness, quality and longevity in them. One of the means of contributing to the evolution is the research and execution of comparative tests, such as this single-blind randomized study that aims to evaluate the home whitening technique performed in dental practice and verify its effectiveness and patient satisfaction. The procedures were performed in 5 patients and all performed in a dental clinic. The technique with a tray and the use of a 6% hydrogen peroxide gel was used. Photographs were taken and analyzes performed with the aid of an appropriate scale. Patients received a questionnaire to assess treatment-related perception. The results showed that, within the parameters analyzed, at-home bleaching proved to be safe and effective. All patients showed improvement in tooth color. In the case of sensitivity, it was reported by 20% of patients, but efficiently controlled with professional intervention. Regarding the perception, the treatment was well evaluated by most patients, however, they reported wanting to perform the treatment with another method and the method mentioned was the whitening performed in the office using the photo-assisted method.

Keywords: Bleaching · Esthetics · Dental chromatic alteration

1 Introduction

In recent years, the search for smile aesthetics has been increasingly valued worldwide. Tooth whitening, in its different modalities, is highly sought after by patients and the target of studies. The field of tooth whitening has evolved and changed with the development of new materials, techniques and equipment [1].

There are many commercial products, with different formulations and concentrations, for performing professional whitening in the office, associated with light sources, or at home or “home bleaching” [2]. The dental element is polychromatic, and the so-called color of the teeth is composed of the elements: hue, chroma and value [3]. The process of tooth whitening or “bleaching” is actually the increase in tooth luminosity [4].

The color scales used evaluate hue and chroma as main points and after tooth whitening, there is a change in the value [1–3].

There are discussions about the effectiveness and side effects, such as sensitivity, and durability between the different whitening methods. The aim of this study is to evaluate the effectiveness of at-home tooth whitening in terms of color change, tooth sensitivity and patient perception.

2 Methods

The preliminary (pilot) clinical uni-blind study, carried out in the Dentistry Clinic of Universidade Brasil (SP), under the responsibility of a duly qualified dental surgeon. The study was performed after approval by the Human Research Ethics Committee CAAE: 89953318.0.0000.5494. The inclusion criteria were older than 18 years, both genders, with the presence of post-eruption stains, non-smokers, cooperating with the procedures, without the presence of hyperplastic or hypoplastic stains, evaluated on hydrated teeth and after drying through trans-illumination, without systemic diseases, that present good conditions of hygiene and oral health. Exclusion criteria were minors, poor hygiene, presence of caries, uncontrolled periodontal disease, gingival recession with or without sensitivity, presence of oral lesions, with a history of allergies related to the products used in the technique.

After the initial analysis, five patients of both sexes were invited to participate in the study. After reading, understanding and agreeing with the free and informed consent form, they were included in the study. Initial photographs of the teeth of all selected patients were taken for analysis of the initial color, the photos were all taken with standardized distance and brightness.

In the case of home bleaching, the patients selected for this group were evaluated for color taking after prophylaxis with pumice stone and rubber cup. The initial photographs were taken and the color was taken with an appropriate scale. Molding was performed with alginate of the upper and lower arches and plaster models were obtained after casting the model in stone-like plaster.

All patients were molded in a conventional way and had their trays made of acetate plates adjusted and tested. Figure 1 shows an example of the plate made for the treatment.



Fig. 1. Custom-made whitening tray for each patient.

Initial photographs were recorded. The Fig. 2 presents an example of an initial photo taken with a color scale.



Fig. 2. Initial color taking, always obtained with the aid of the scale.

After this step, the patients were instructed on the correct use of the bleaching material, as shown in Fig. 3.



Fig. 3. Tray being filled with bleaching material for patient instruction.

Individualized acetate whitening plates were made on the arch models and, after the initial adjustments, they were tested in the patient's mouth to verify adaptation and comfort. Patients then received syringes containing home-use bleaching gel (6% hydrogen peroxide) and were instructed in writing and verbally on the appropriate way of use according to the manufacturer's instructions. Patients were well instructed on the amount of bleaching material to be dispensed in the tray and the recommended usage time.

The time of use was one week and the patients returned for reassessment and color taking. Patients received more bleaching material and were instructed to use it for another seven days. After the end of the entire tooth whitening process, the final photographs were taken to record the result obtained at the end of the treatment.

After one week, patients returned and were evaluated for the presence of tenderness during home treatment. Two of the five patients reported pain in the lower incisor region, however, according to the report, it was not necessary to interrupt the treatment because as soon as the tray was removed, the sensitivity disappeared. Then, photobiomodulation was carried out with a low-power laser (LaserDuo–MMOptics, São Carlos, São Paulo) (Near Infrared Diode Laser 780 nm, 100 mW, 4 J, 40 s, punctual) and application of neutral fluorine phosphate (2%) to minimize post-bleaching sensitivity.

After photobiomodulation therapy, patients received 2% neutral and colorless sodium fluoride applied for 4 min. All were instructed not to ingest any food or drink for one hour after application.

After seven days, the patients returned for final evaluation. New photos were obtained as shown in the example in Fig. 4.



Fig. 4. Final treatment image.

The patient received the Patient Perception Questionnaire for treatment assessment and instructions. The data obtained were tabulated and statistically analyzed.

3 Results and Discussion

Then the initial color taking was performed and according to the results the color distribution was represented in Fig. 5.

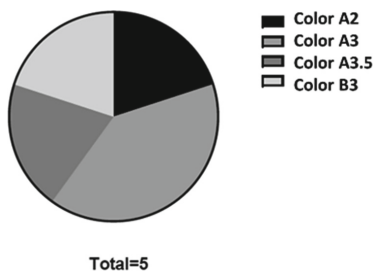


Fig. 5. Graphic representation of the color distribution of the dental elements before treatment

All participants had color change after treatment with increased value in all cases analyzed. The Fig. 6 shows the color change obtained according to the analysis performed with the color scale.

As a final analysis, data related to the patient satisfaction questionnaire were tabulated and the frequency of responses can be seen in Fig. 7.

According to the results of the questionnaire, most patients wanted to undergo tooth whitening for aesthetic improvement. Most patients (60%) admitted to constantly ingesting coloring products in their food.

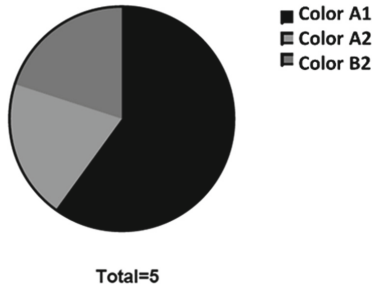


Fig. 6. Graphic representing the color distribution of the dental elements after treatment.

Regarding the perception of treatment, most patients considered the treatment pleasant (60%), for 20% the treatment was not pleasant and for 20% the treatment was unpleasant and uncomfortable. Due to the small sample size, the results should be interpreted with caution.

The perception of unpleasantness and discomfort can be the result of a tray with little adaptation or poorly stored, which can result in changes in shape that can cause discomfort to the patient. Constant checking of the tray during the procedure should be performed so that changes to this device do not interfere with the treatment experience.

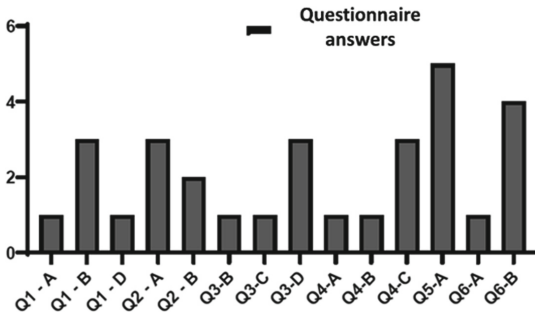


Fig. 7. Distribution of responses obtained with the application of the treatment questionnaire

Regarding the patient’s perception of the result, most participants (60%) did not report having expectations and having considered the treatment to be good. For 20% of the participants the treatment was better than the expectations and 20% considered it worse than the expectations.

In the specific case of this work, as it is a study with voluntary participants, the lack of expectation can be explained by the fact that it is a case of treatment by opportunity. In the case of office patients, however, expectations must be carefully evaluated to avoid post-treatment frustrations. According to Martim et al., even the patient’s personality interferes with the perception and expectation of treatment [18].

Interestingly, although 20% considered the treatment unpleasant, 100% of the patients stated that they would like to undergo the treatment again. As reported in the literature, the appearance of teeth can improve patients’ self-esteem and even if it is not

considered a pleasant treatment, the result would compensate for the effort to obtain it [19].

Regarding the type of treatment that the patients would like to do, 80% answered that they would like to test another method, with the use of light indicated as the desired method. For 20%, the same treatment would be performed in a new intervention.

Many studies presented in the literature seek to study the best way to perform tooth whitening. In general, if performed under the supervision of a dental surgeon, the treatment is safe in any of its forms. Because it is an elective treatment and much more sought after by the patient than indicated by the professional, the patient's expectations must be analyzed so that in addition to the clinical result, satisfaction with the treatment and the professional who performed it is achieved at the end.

4 Conclusions

According to the analysis of the results, we can conclude that tooth whitening performed at home with the help of trays and professional supervision was effective in promoting the removal of dental stains, promoting improvement in the color of the teeth of all volunteers in this study. In the case of sensitivity, it was reported by 20% of patients, but efficiently controlled with professional intervention.

Regarding the perception, the treatment was well evaluated by most patients, but they reported wanting to perform the treatment with another method and the method mentioned was the whitening performed in a photo-assisted office.

5 Statement of Human and Animal Rights

The study was carried out in humans after submission and approval of the project by the Human Research Ethics Committee (number 2.713.367).

Conflict of Interest. The authors declare that there are no conflicts of interest in carrying out this study.




References

1. Ontiveros, J.C., Paravina, R.D.: Color change of vital teeth exposed to bleaching performed with and without supplementary light. *J. Dent.* **37**(11), 840–847 (2009)
2. Horn, D.J., Bulan-Brady, J., Hicks, M.L.: Sphere spectrophotometer versus human evaluation of tooth shade. *J. Endod.* **24**(12), 786–790 (1998)
3. Paravina, R.D.: New shade guide for tooth whitening monitoring: visual assessment. *J. Prosthet. Dent.* **99**(3), 78–84 (2008)
4. Dantas, C.M., Vivian, C.L., Ferreira, L.S., Freitas, P.M., Marques, M.M.: In vitro effect of low intensity laser on the cytotoxicity produced by substances released by bleaching gel. *Braz. Oral Res.* **24**(4), 460–466 (2010)
5. Soares, D.G., Ribeiro, A.P., Lima, A.F., Sacono, N.T., Hebling, J., Costa, C.A.S.: Effect of fluoride-treated enamel on indirect cytotoxicity of a 16% carbamide peroxide bleaching gel to pulp cells. *Braz Dent J.* **24**(2), 121–127 (2013)

6. Martin, J.M., et al.: Effect of fluoride therapies on the surface roughness of human enamel exposed to bleaching agents. *Quintessence Int.* **41**(1), 71–78 (2010)
7. Mandarino, F.: *Clareamento dental*. São Paulo: WebMasters do Laboratório de Pesquisa em Endodontia da FORPUSP (2003)
8. Kina, M., Borghi, A.P.S., Fabre, A.F., Martins, O.C.S., Simonato, L.E., Boer, N.P., Kina, J.: Clareamento dental em dentes vitais: protocolo clínico em consultório. *Arch. Health Investig.* **4**(4) (2015)
9. Clifton, M.C.: Tooth whitening: what we now know. *J. Evid. Based Dent. Pract.* **14**, 70–76 (2014)
10. Maran, B.M., Burey, A., Matos, T.P., Loguercio, A.D., Reis, A. In-office dental bleaching with light versus without light: a systematic review and meta-analysis. *J. Dent.* **70**, 1–13 (2018)
11. Féliz-Matos, L, Hernández, L.M., Abreu, N.: A. Dental bleaching techniques; hydrogen-carbamide peroxides and light sources for activation, an update. Mini review article. *Open Dent. J.* **8**, 264–268 (2015)
12. Peixoto, A.C., et al.: High-concentration carbamide peroxide can reduce the sensitivity caused by in-office tooth bleaching: a single-blinded randomized controlled trial. *J. Appl. Oral Sci.* **26**, e20170573 (2018)
13. Silva, F.B., Chisini, L.A., Demarco, F.F., Horta, B.L., Correa, M.B.: Desire for tooth bleaching and treatment performed in Brazilian adults: findings from a birth cohort. *Braz. Oral Res.* **8**(32), e12 (2018)
14. Tin-Oo, M.M., Saddki, N., Hassan, N.: Factors influencing patient satisfaction with dental appearance and treatments they desire to improve aesthetics. *BMC Oral Health* **11**, 6 (2011)
15. Meireles, S.S., Goettems, M.L., Dantas, R.V.F., Della Bona, A., Santos, I.S., Demarco, F.F.: Changes in oral health related quality of life after dental bleaching in a double-blind randomized clinical trial. *J. Dent.* **42**(2), 114–121 (2014)
16. Meireles, S.S., Santos, I.S., Della Bona, A., Demarco, F.F.: A double-blind randomized clinical trial of two carbamide peroxide tooth bleaching agents: 2-year follow-up. *J. Dent.* **38**(12), 956–63 (2010)
17. Meireles, S.S., Fontes, S.T., Coimbra, L.A.F., Della Bona, A., Demarco, F.F.: Effectiveness of different carbamide peroxide concentrations used for tooth bleaching: an in vitro study. *J. Appl. Oral Sci.* **20**(2), 186–191 (2012)
18. Martin, J., et al.: Personality style in patients looking for tooth bleaching and its correlation with treatment satisfaction. *Braz. Dent. J.* **27**(1), 60–65 (2016)
19. Bersezio, C., Estay, J., Jorquera, G., Peña, M., Araya, C., Angel, P., Fernández, E.: Effectiveness of dental bleaching with 37.5% and 6% hydrogen peroxide and its effect on quality of life. *Oper. Dent.* **44**(2), 146–155 (2019)



Experimental Determination of Vascular Pulsatility During Continuous-Flow LVAD Assistance

Marcelo Mazzetto¹(✉) , Daniel S. Torres², Simão Bacht¹ ,
and Idágene A. Cestari^{1,2} 

¹ Divisão de Bioengenharia, Faculdade de Medicina, Instituto Do Coracao, Hospital das Clinicas HCFMUSP, Universidade de Sao Paulo, Sao Paulo, SP, Brazil
marcelo.mazzetto@incor.usp.br

² Programa de Pos-Graduação Em Engenharia Biomédica da Escola Politecnica de Engenharia, Universidade de Sao Paulo, Av. Prof. Luciano Gualberto, Sao Paulo, SP 380, Brazil

Abstract. Continuous flow ventricular assist devices (CF-VADs) are being used to treat of infant patients with acute heart failure. Because of their operation mode, these devices present an increase in gastrointestinal bleeding and vascular remodeling. To overcome these problems, newer pumps are developing control strategies with pulsatile flow, focusing in minimizing the very high pathological shear stress, which is known to cause platelet activation, hemolysis, and acquired von Willebrand syndrome. In this work, we used an automatic hydraulic simulator to study the interaction of the CF-VAD PedVad Incor prototype as a means to identify important parameters for the development of a control strategy algorithm. The simulator uses a 30 ml pneumatic pump to mimic the native heart, with pressure and flow data recorded digitally. Energy equivalent pressure (EEP) and surplus hemodynamic energy (SHE) were calculated to quantify flow pulsatility. The simulator was set to operate in normal hemodynamic condition and two conditions of heart failures insufficient conditions at 70, 80 and 90 cycles per minute (cpm) with no assistance, partial and full assistance. The results demonstrated that assistance at 50% maximal cardiac output there is an increase in pulsatility. At full assistance there is no flow from the native heart and pulsatility drops to near zero. The application of the simulator for studies that attempt to increase the hemodynamic energy provided by continuous-flow devices is an important tool for the development of novel control strategies for pediatric mechanical circulatory devices.

Keywords: Mechanical circulatory support devices · Cardiovascular hydrodynamics response · Vascular pulsatility control strategy · Continuous flow pump · In vitro testing

1 Introduction

Heart failure (HF) is a clinical condition that can be characterized by functional or mechanical dysfunction of one or both ventricles, leading to an insufficient cardiac output [1]. Patients with advanced heart failure that are refractory to drug therapy and are

waiting for a heart transplant can be candidates for a ventricular assist devices (VADs), to reestablish normal hemodynamic conditions.

VADs can be categorized by the type of flow generated. The first generation VADs had pulsatile flows (P-VADs) usually intended for use as bridge to transplant while newer generations use continuous flow (CF-VADs) and can be used as temporary support or longer periods.

The results obtained with the use of CF-VADs to treat heart failure in adults stimulated the use of adult devices to treat pediatric and infant patients [2]. In vitro testing of devices under development and the investigation of their interaction with the circulation can be speeded with the help of simulators. However, there is a lack of appropriate simulators for testing pediatric ventricular assist devices and their interaction with the circulation.

Hydraulic models with adjustable vascular resistances and compliances in association with pulsatile-flow artificial ventricles allow the construction of simulators sensitive to variations in preload, afterload and heart rate.

VADs may be used to mimic the Frank-Starling response of the natural heart making the simulator applicable to studies of the physiology of mechanical assist circulation. In addition, mock circulation loops (MCLs) can be used to assess the performance of VADs in reestablishing physiological pressures and flows and for the evaluation of the vascular pulsatility under pulsatile (P-VAD) and continuous-flow (CF-VAD) assistance.

Clinical studies associated the use of CF-VADs with gastrointestinal bleeding [3], affecting approximately 40% of patients, compared with 10% of P-VADs patients [3] and with significant pathophysiological implications, for example, severe periarteritis in the kidneys and vascular remodeling [4]. Also, under full assistance, aortic valve leaflets may undergo commissural fusion.

To overcome these problems, some of the newer CF-VADs incorporate a pulsatile mode of operation. But this mode causes high shear stress, which is known to cause platelet activation, hemolysis, and acquired von Willebrand syndrome [5, 6].

The aim of this study is to investigate the interaction of a continuous flow pediatric pump under development in our institution the CF-VAD InCor PedVad prototype. To this end an automated pediatric simulator of the systemic loop of circulation of babies (up to 1-year old) adapted to infants (1 to 5 years old), combining a hydraulic model with an electronic automation system is utilized. A graphical user interface (GUI) is integrated into the simulator providing the settings of simulation options and real time visualization of results. Instantaneous and recorded signals of aortic, left atrial, and left ventricular pressures (AoP, LAP, and LVP, respectively), and left ventricular input and output flows can be displayed in addition to the pressure-volume relationship (PV-loop) [7].

2 Materials and Methods

2.1 Flow Pulsatility Quantification

Energy equivalent pressure (EEP) and surplus hemodynamic energy (SHE) [8, 9] have been used to quantify hemodynamic energies associated with blood flow with focus on energy gradients rather than pressure gradients as the driving force of blood flow, making its use clinically viable.

EEP is used to quantitatively measure differences between steady-state and pulsatile blood flow, and is calculated by Eq. (1):

$$EEP = \frac{\int Q \cdot P \cdot dt}{\int Q \cdot dt} \quad (1)$$

where Q is the instantaneous blood flow, P is the instantaneous pressure, and dt is the change in time. EEP should be higher than mean AoP. With totally continuous flow circulation, EEP becomes equal as mean AoP.

SHE is derived from the difference between EEP and the mean arterial pressure (MAP) and converted to the energy units of erg/cm^3 , calculated by Eq. (2).

$$SHE = 1332 \cdot (EEP - MAP) \quad (2)$$

When EEP equals AoP, the SHE becomes 0 as SHE indicates how much more energy is given to circulation with the same mean AoP. This is the energy loss that may compromise flow in vascular beds with low-flow conditions.

2.2 Mock Circulation Loop

The mock Circulation Loop (MCL) is presented in Fig. 1. The MCL integrates a hydraulic loop and a pneumatically actuated pulsatile infant VAD that mimics the native left ventricle (LV P-VAD, (A)). The loop is designed to generate aortic and left atrial pressures based on components that simulate afterload (systemic vascular resistance, SVR), aortic compliance (AoC), ventricular filling pressure (left ventricle preload, LPL), and arterial inertance.

The CF-VAD (I) input is connected to the atrial compartment (B) and its output is connected to the aortic compartment (C), in parallel to the LV P-VAD (A), simulating a left ventricle heart assistance arrange. In this arrange, the CF-VAD act as a parallel pump, unloading the natural heart, increasing blood flow and systemic pressure.

In the loop, schematically represented in Fig. 2, the pressure in the left atrial compartment (B) gives the left ventricle preload, the aortic compliance is simulated by the mechanical energy stored by the air inside the aortic compartment (C), and the hydraulic resistance is adjusted by a motorized clamp (D), representing the lumped systemic vascular resistance. The tube (3/8", 35 cm) connecting the VAD inflow connector to the aortic compartment gives an equivalent arterial inertance of $0.0192 \text{ mmHg} \cdot \text{s}^2/\text{ml}$ (E).

The pneumatic VAD utilized has a 30 ml blood chamber with two mechanical heart valves (21AJ-501, St. Jude Medical, Saint Paul, MN, USA) to control inflow and outflow. A driving console provides air pulses with duration and frequency defined by the user, and set at 70, 80 and 90 cycles per minute (cpm) and 30% systolic interval for this application.

The loop is filled with a blood analogue fluid (40% glycerin-saline mixture by volume, viscosity 3.5 cps at 21 °C). Three clamp-on ultrasonic flowmeters (SonoTT CT 1/2 × 3/32" and SonoTT CT 3/8 × 3/32", Em-tec GmbH, Finning, Germany) are used to measure instantaneous and mean aortic and left ventricular flows. Aortic, left atrial and left ventricular pressures are measured by Strain Gauge pressure transducers (TruWave

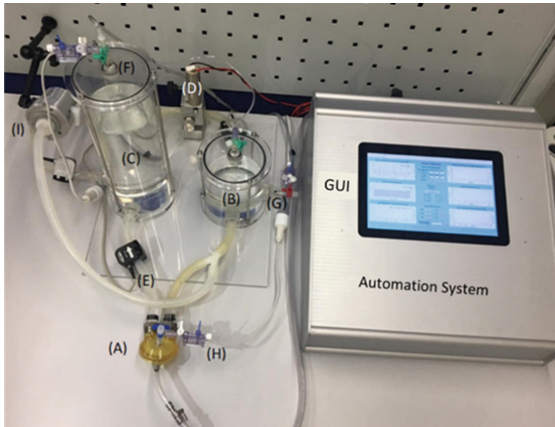


Fig. 1. Mock circulation loop with a CF pump (I), a VAD representing the left ventricle (A); Left atrial compartment (B); Aortic compartment (C); Motorized clamp (D); Aortic pressure measurement and air control ports (F); Left atrial compartment air control port (G); Left atrial pressure measurement port; flowmeter for the LV outflow measurement (E); left ventricle pressure measurement (H).

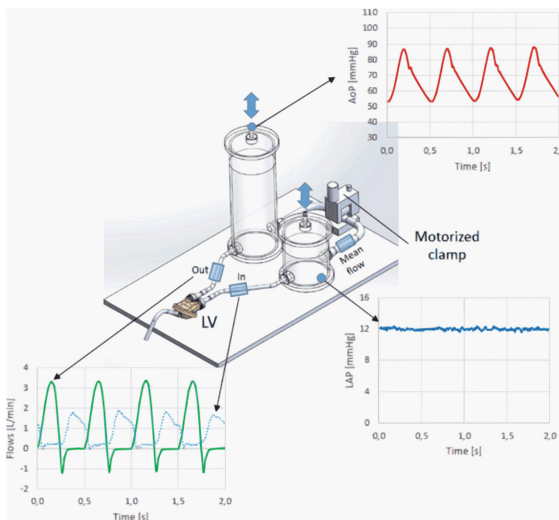


Fig. 2. Schematic of the mock circulation loop with indications for pressure (circle) and flow (rectangles) transducers positions with real time waveforms are displayed. The motorized clamp and the airflow input and output ports (arrows) in the aortic and left atrial compartments.

PX24N, Edward Lifesciences, Irvine, CA, USA) and signals are filtered and amplified. Signals are measured in access ports made on top of the aortic compartment (F), in the outflow of the left atrial compartment (G), and in the VAD blood chamber (H), and are sampled at 1800 Hz using a microcontroller board (Arduino Mega 2560, Ivrea, Italy)

in serial communication (56000 bps, USB) with a miniaturized computer board (Up-Board RE-UP-CHT01-A10 -0464, Aaeon, New Taipei City, Taiwan) that runs the user interface.

A place for VAD connection was defined between the LV and the aortic compartment to simulate LV assistance. Vascular pulsatility was determined during continuous-flow assistance using a centrifugal pump (InCor PedVad Prototype) as CF-VAD.

The mock loop was set to simulate normal circulation condition and heart failure conditions.

3 Results

Table 1 shows hemodynamics data representing the circulation of pediatric patients up to 5 years of age considering normal (condition 1), and decreased myocardial contractility associated to heart failure (conditions 2 and 3) [10, 11].

P-VAD was operated at 70, 80 and 90 cycles per minute (cpm). Results of left ventricle assistance continuous flow VADs in heart failure (condition 2, Table 1) for 90 cpm are shown in Table 2 with no assistance, $\frac{1}{2}$ and full assistance. Systolic, diastolic, pulse and mean AoP, mean aortic flow, EEP and SHE were measured without and with the use of CF-VAD. Three tests were performed after stabilization of the parameters by the automation system in each condition described in Table 1 at 70, 80 and 90 cpm.

Table 1. Physiological ranges for hemodynamic parameter in normal and heart failure simulated conditions.

Parameter, [Units]	Normal (condition 1)	Heart failure (condition 2)	Heart failure (condition 3)
MAP [mmHg]	75–95	50–60	35–45
AoPA [mmHg]	30–45	35–45	25–35
Mean LAP [mmHg]	10–12	15–20	8–12
Mean aortic flow [L/min]	1.30–3.10	0.90–2.40	0.50–1.50
SVR [mmHg.s/mL]	1.40–4.15	1.28–4.89	2.24–8.64
AoC [ml/mmHg]	0.44–0.60	0.31–0.61	0.19–0.40

MAP – Mean aortic pressure; AoPA – Aortic pulse amplitude; LAP – Left atrial pressure; SVR – Systemic vascular resistance; AoC – Aortic compliance.

The waveforms of pressures and flows obtained during simulations of heart under normal and failure conditions are presented in Fig. 3. The aortic pressure pulse decreases under simulated failure conditions 2 and 3, as does the pressure in the P-VAD chamber and, as a consequence, reduction in the flow provided by the P-VAD. We also can observe a pressure increase in the atrial chamber. In a real patient, this pressure overload in the left atrium induces pathophysiological changes, which cause structural and functional remodeling. These changes can alter the electrophysiological characteristics

Table 2. Average hemodynamic data of pressures, flows and energies obtained during simulation of heart failure and during continuous-flow left ventricular assistance for 90 cpm.

Parameter, [Units]	Heart failure (condition 2)	1/2 CF-assistance	Full CF-assistance
AoP _{sys} [mmHg]	101.9 ± 1.6	113.7 ± 0.3	121.7 ± 0.3
AoP _{dia} [mmHg]	68.8 ± 1.1	79.0 ± 0.2	107.7 ± 0.2
MAP [mmHg]	61.1 ± 1.1	77.6 ± 0.9	96.7 ± 0.7
AoPA [mmHg]	33.1 ± 0.6	34.7 ± 1.3	14.0 ± 2.1
Mean LAP [mmHg]	15.7 ± 9.1	0.7 ± 4.2	-7.1 ± 3.5
Mean aortic flow [L/min]	2.1 ± 0.2	2.9 ± 0.3	3.5 ± 0.1
EEP [mmHg]	83.37	97.65	112.29
SHE [erg/cm ³]	816.08	922.27	10.21

AoP_{sys} – Systolic aortic pressure; AoP_{dia} – Diastolic aortic pressure; MAP – Mean aortic pressure; AoPA – Aortic pulse amplitude; LAP – Left atrial pressure; EEP – Energy equivalent pressure; SHE – Surplus hemodynamic energy.

of the LV and increase ectopic atrial activity, culminating in the onset of paroxysmal atrial fibrillation attacks.

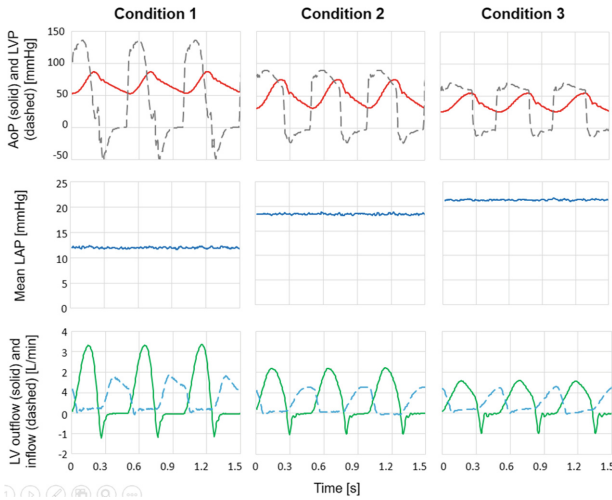


Fig. 3. Waveforms of pressures and flows obtained in three simulated conditions: normal (1) and two levels of heart failure (2 and 3). Aortic pressure (AoP, top, solid); Left ventricular pressure (LVP, top, dashed); Mean left atrial pressure (LAP, middle); left ventricle outflow (bottom, solid) and left ventricle inflow (bottom, dashed). Aortic pressure (AoP, top); Mean left atrial pressure (LAP, middle), and systemic flow (bottom).

EEP and SHE obtained at different frequencies are presented in Figs. 4, 5 and 6. There is an increase of the EEP and SHE during partial assistance in all three heart

frequencies. When the flow of the CF-VAD is increased and full assistance is achieved, SHE is near zero. In this condition, there was only a residual flow from the P-VAD and atrial pressure was drastically reduced.

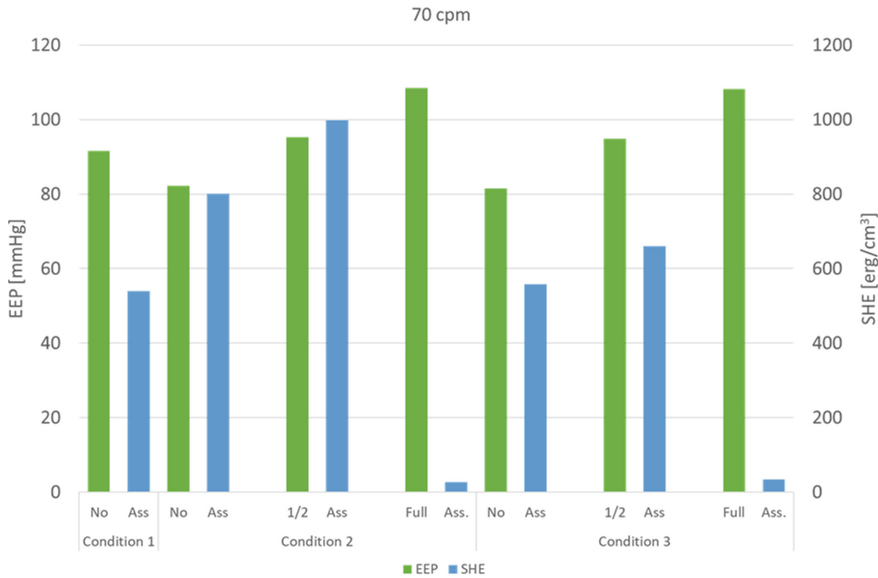


Fig. 4. Energy equivalent pressure (EEP) and surplus hemodynamic energy (SHE) at 70 cpm in conditions 1, 2 and 3 of Table 1.

4 Conclusions

The evaluation of the vascular pulsatility during CF-VAD assistance demonstrate that during partial assistance, there is an increase of surplus hemodynamic energy compared with the heart failure situation. During full assistance, the SHE was drastically reduced and the outflow of the P-VAD, acting as the natural left ventricle, was practically zero. Different control strategies can be investigated using the method described such as the modulations of the speed pump, using square, sine or ramp waves and synchronization with the natural heart activity [12, 13]. This result demonstrates the application of the simulator for studies that attempt to increase the hemodynamic energy provided by continuous-flow devices, being useful to the development of novel pediatric mechanical circulatory devices.

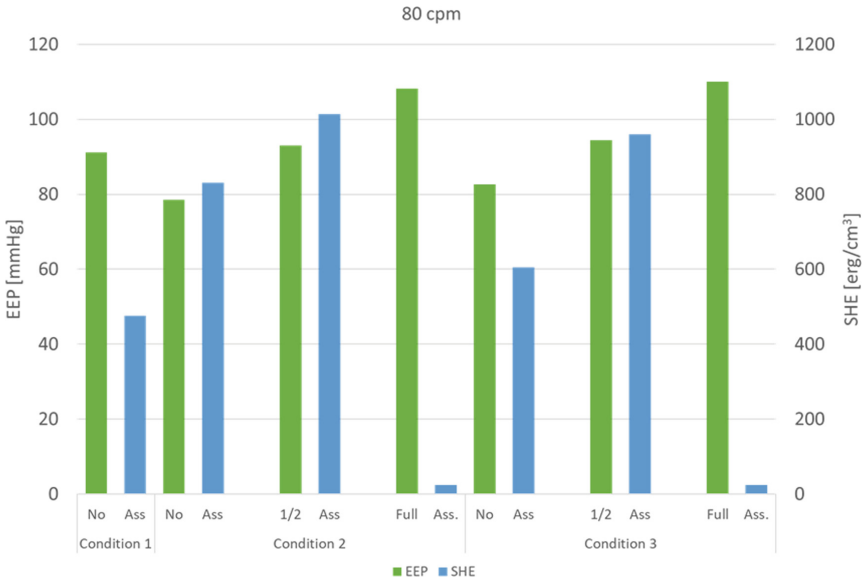


Fig. 5: Energy equivalent pressure (EEP) and surplus hemodynamic energy (SHE) at 80 cpm in conditions 1, 2 and 3 of Table 1.

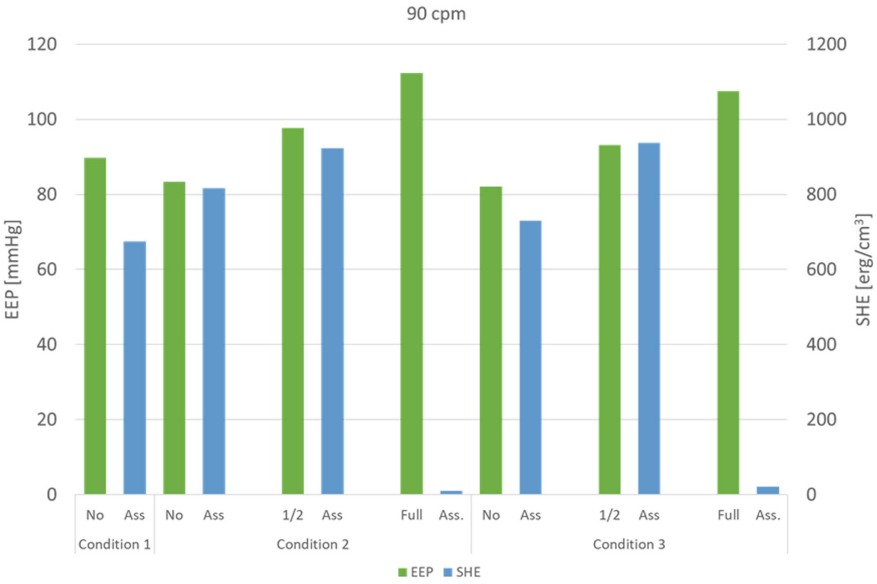


Fig. 6: Energy equivalent pressure (EEP) and surplus hemodynamic energy (SHE) at 90 cpm in conditions 1, 2 and 3 of Table 1.

Acknowledgment. Financial support: São Paulo State Foundation (FAPESP, Grant 2012/50283–6), FINEP (Grant 01.14.0177.00), FINEP (1253/13) and the National Council for Scientific and Technological Development (CNPQ Grant 313846/2021–9).



Conflict of Interest. The authors declare that they have no conflict of interest.

References

1. Kurmani, S., Squire, I.: Acute heart failure: definition, classification and epidemiology. *Curr. Heart Fail. Rep.* **14**(5), 385–392 (2017). <https://doi.org/10.1007/s11897-017-0351-y>
2. Tunuguntla, H., et al.: Destination-therapy ventricular assist device in children: “the future is now.” *Can. J. Cardiol.* **36**(2), 216–222 (2020). <https://doi.org/10.1016/j.cjca.2019.10.033>
3. Crow, S., et al.: Gastrointestinal bleeding rates in recipients of nonpulsatile and pulsatile left ventricular assist devices. *J. Thorac. Cardiovasc. Surg.* **137**(1), 208–215 (2009). <https://doi.org/10.1016/j.jtcvs.2008.07.032>
4. Ootaki, C., et al.: Reduced pulsatility induces periarteritis in kidney: role of the local renin-angiotensin system. *J. Thorac. Cardiovasc. Surg.* **136**(1), 150–158 (2008). <https://doi.org/10.1016/j.jtcvs.2007.12.023>
5. Sharifi, A., Bark, D.: Mechanical forces impacting cleavage of von willebrand factor in laminar and turbulent blood flow. *Fluids*, 1–10 (2021). <https://doi.org/10.3390/fluids6020067>
6. Wang, S., Griffith, B. P., Wu, Z. J.: Device-induced hemostatic disorders in mechanically assisted circulation. *Clin. Appl. Thromb./Hemost.* **27** (2021). <https://doi.org/10.1177/1076029620982374>
7. Torres, D.S., Mazzetto, M., Cestari, I.A.: A novel automated simulator of pediatric systemic circulation: design and applications. *Biomed. Signal Process. Control.* **70**(January) (2021). <https://doi.org/10.1016/j.bspc.2021.102926>
8. Ündar, A., Frazier, O.H., Fraser, C.D.: Defining pulsatile perfusion: quantification in terms of energy equivalent pressure. *Artif. Organs* **23**(8), 712–716 (1999). <https://doi.org/10.1046/j.1525-1594.1999.06409.x>
9. Ündar, A., et al.: Quantification of perfusion modes in terms of surplus hemodynamic energy levels in a simulated pediatric CPB model. *ASAIO J.* **52**(6), 712–717 (2006). <https://doi.org/10.1097/01.mat.0000249013.15237.5e>
10. Goodwin, J.A., et al.: A model for educational simulation of infant cardiovascular physiology. *Anesth. Analg.* **99**(6), 1655–1664 (2004). <https://doi.org/10.1213/01.ane.0000134797.52793.af>
11. Zijlmans, M., et al.: Corrected and improved model for educational simulation of neonatal cardiovascular pathophysiology. *Simul. Healthc.* **4**(1), 49–53 (2009). <https://doi.org/10.1097/SIH.0b013e31818b27a8>
12. Rich, J.D., Burkhoff, D.: HVAD flow waveform morphologies: theoretical foundation and implications for clinical practice. *ASAIO J.* **63**(5), 526–535 (2017). <https://doi.org/10.1097/MAT.0000000000000557>
13. Mapley, M.C. et al.: Analysis of the heart ware HVAD pump characteristics under pulsatile operation. *Biomed. Signal Process. Control.* **68**(March), 102754 (2021). <https://doi.org/10.1016/j.bspc.2021.102754>



Augmented Reality for Gait Rehabilitation: A Scoping Review

Laís Souza Amorim^{1,2}  and Alana Elza Fontes Da Gama^{1,2}  

¹ Voxar Labs, Universidade Federal de Pernambuco, Recife, Brasil
alana.elza@ufpe.br

² Departamento Engenharia Biomédica, Universidade Federal de Pernambuco, Recife, Brasil

Abstract. The purpose of this article is to provide a comprehensive overview of the current applications of Augmented Reality (AR) in gait rehabilitation. To accomplish this, a scoping review was conducted using the Preferred Reporting Items for Systematic Reviews and Meta-Analyses (PRISMA) protocol. A total of 530 articles were initially identified and screened, with 13 ultimately being included in this review. The findings of this review reveal the various ways in which AR has been utilized and tested in gait rehabilitation, which may prove helpful for individuals seeking to develop new technologies, solutions, or tools in this area. By mapping out the current state of the literature, this article provides insights into the potential benefits and limitations of using AR for gait rehabilitation. Overall, the use of AR in gait rehabilitation shows promise as a way to enhance the rehabilitation process and improve patient outcomes. However, more research is needed to fully understand the most effective ways to use AR in this context and to identify any potential drawbacks or limitations. This review serves as a useful starting point for anyone interested in exploring this area further.

Keywords: Augmented reality · Rehabilitation · Gait · Gait training · Smbulation

1 Introduction

Technological tools have been increasingly common in everyday activities, including Augmented Reality, a technology that allows virtual elements to be superimposed on real scenes. Its use has been developed in several spheres [1, 2], including health [3]. For example, in physiotherapy, AR technologies are already being used in rehabilitation for various purposes and in different ways [4, 5], such as for the treatment of stroke patients [6–8] and Parkinson’s patients [9–11, 14]. Some of these applications aim to work with real-time feedback [4–6] to provide more effective visualizations of the movements and have corrections and more assertive orientation by the physical therapists.

In the context of gait rehabilitation, the purpose of applications differ significantly as different types of people need to rehabilitate their gait due to illness, amputation, or injury. And likewise, there is a wide variety of tools and methods used for these studies and applications; devices such as RGB-D sensors [12–14], treadmill [10, 13–15], motion-sensing glasses [8, 9, 11, 16, 17], markers motion capture systems [8, 11,

17–19] and Projective or Spatial AR systems [10, 13, 19] are some of the examples available today.

These applications have and can have many advantages in gait training, either with the immediate treatment or in the analysis of data of calculated and tested spatiotemporal parameters, contributing enormously to the research and planning of future actions of specialists in the area.

The main objective of the present study is to map the current forms of application, proposed and described in the literature, of the Augmented Reality technologies that were developed and tested in gait rehabilitation. This research aims to verify the technologies' patterns, frequency, and feasibility. In this way, we intend to identify the best evidence from the studies and synthesize them to support proposals for changes and contribute to the development of future augmented reality tools in the treatment and rehabilitation of gait.

2 Materials and Methods

This study conducted a scoping review of studies that developed and/or tested AR technologies for gait rehabilitation. The method used to develop this study was the PRISMA protocol [20]. Papers were searched, selected, evaluated, analyzed, and synthesized according to the protocol described below.

Research questions: “How has Augmented Reality been applied in gait rehabilitation in recent years?” and “For what purposes has AR been used in gait training in recent years?”.

Research Strategy and Sources: The search was carried out in the Scopus database between November 3, 2021, and February 23, 2022, classifying articles listed based on the following keywords: “(augmented AND (reality OR projective) AND augmented AND reality) AND rehabilitation AND gait.”

Inclusion and Exclusion Criteria: In order to be included in the scoping review the papers must present, the following inclusion criteria: (1) published between January 2017 and February 2022, (2) language: English and Portuguese, (3) minimum size of 5 pages, (4) that developed and tested AR for and in gait rehabilitation or used a previously existing solution, (5) which tested the proposed technologies on users.

Study Selection and Data Extraction: The research was structured based on the inclusion and exclusion criteria, and the information from the articles was organized and tabulated into categories such as “Used technologies”, “Gait exercise performed” and “Limitations of applied technology”, among other eight categories.

For each of the included studies, parameters were observed, such as technologies used, gait training performed, treatment focus, and limitations of the applied technology, among other measures, being placed in a table format (Table 1), thus performing the study mapping.

3 Results

A total of 530 articles were identified. All of them were pre-selected using the mentioned criteria, and 509 were excluded at the titles and abstract screening phase because they did not, directly or indirectly, mention AR and rehabilitation gait. Of these, 21 were submitted for full reading, and 13 articles were included (Fig. 1).

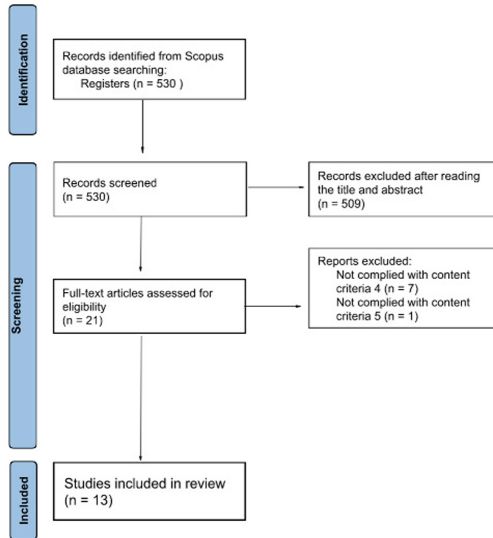


Fig. 1. Article selection process using the PRISMA flowchart [17].

Table 1 presents a mapping of the included studies, containing some descriptions and categories referring to the analyzed studies.

From the selected articles, it was possible to observe that only five studies applied the technologies indirectly and focused on a specific aspect of the gait, such as cadence, angulation, and strength, instead of applying the technologies directly and working on the gait generally.

Regarding technologies, approximately 46.15% of the studies used markers motion capture systems [8, 11, 14, 17–19], and 30.77% used Microsoft HoloLens glasses [8, 11, 16, 17], 23.07% Microsoft Kinect [12–14], 15.38% used the C-Mill treadmill [7, 15], 15.38% used common treadmills [13, 14] and 15.38% used force platforms [12, 18]. Finally, only one study used Epson’s Moverio BT-200 glasses [9], and one used laser shoes [10].

Regarding what was analyzed, all studies focused on analyzing spatiotemporal parameters, such as speed, cadence, step width, and height. A few studies clashed due to the different purposes of the tests and also observed, for example, cognitive states and changes in motor behavior [16], stability and balance [7], peak moments of knee adduction and abduction [18], the center of mass [8] and frequency and duration of gait freezing episodes [9–11].

As for the gait exercises, most of them were performed on a treadmill and steady gait in a straight line, while one study used gait for short periods and with directional changes [16] and another used 180° turns [11]. And only two employed gait with obstacles [8, 13].

Regarding the focus of treatment, there was a huge range of limitations (such as Parkinson's [9–11, 14], stroke [7, 8], cerebral palsy [17], hereditary spastic paraplegia [15], among others) and the purpose of the tests performed, which varied in adapting and identifying gait patterns [9], the study of cognitive interference [16], decrease in the moment of ambulatory knee adduction [18], improvement with gait freezing in Parkinson's patients [9–11] and the effect on cognition and balance from physical exercise games [14].

It was impossible to identify a pattern in the tests carried out with the users, in the profile and in the number of users who tested the tools, and in the frequency of tests. This is because several groups need gait rehabilitation and specific attention to each need.

Regarding tests, only the Timed Up and Go and the 10-m Walk Test were repeated throughout the reading of the 13 articles.

In general, the tests of the analyzed studies showed satisfactory results based on the technology and accuracy tests applied to each one, even with certain limitations of space [16], sensitivity [17] and low dimness of devices [12], and limitations of the technology itself and the way it was used [8, 10, 13, 19].

4 Discussion

The present study analyzed how AR has been used in gait rehabilitation in the last five years and how it can be applied to improve ambulation treatments. In general and excluding the software, it was used and combined in all the studies, seven types of AR technologies talking into motion capture systems [8, 11, 14, 18, 19], glasses [8, 9, 11, 16, 17], RGB-D sensors [12–14], treadmill [7, 13–15], force platforms [12, 18], and laser shoes [10]. That shows us the enormous diversity and possibilities of the technologies available today that can interpret the data of the patients' gaits and rehabilitate them. The same fact is for the tests executed; due to the plurality of the objectives, the tests varied a lot.

Most of the studies, to test the technologies to rehabilitation gait, did not limit to analyzing only the spatiotemporal parameters, essential elements of the gait, and also observed and focused on some other things correlated with the gait, like cognitive states and changes in motor behavior [16], the center of mass [8] and frequency and duration of gait freezing episodes [9–11]. This shows that it is common to analyze the gait, not only observe it in an isolated form, a fact important that must be explored in future research.

About the gait exercises realized, only 4 of the studies performed directional changes [16], 180° turns [11] or gait with obstacles [8, 13]. Based on that, we can assume that it is not frequent to implement AR technologies with challenges and difficulties with obstacles and directional changes, which are common in everyday life and can be investigated and applied in future works.

As previously mentioned, AR in gait rehabilitation has different purposes. Generally, the studies developed cannot cover more than one group of patients due to their more

Table 1. In-depth mapping of included studies

Study	Technology used	What gait exercise was performed?	What is the treatment focus?	Experiments performed (with the user)	Profile and the number of users	Variables	Tests	How often was it tested?	Results/Opinions	Limitations of applied technology
van de Venis et al. [15]	C-Mill	Treadmill march	Gait adaptation for patients with HSP	10 sessions with C-Mill	18 to 70 years diagnosed with HSP able to walk 50m barefoot without support		Obstacle subtask of the E-FAP + 10MWT + miniBEST + Physical activity levels during daily life + ABC + Fall Calendar + WALT + SP	The group that had the intervention received 10h (1h sessions, 2 times a week)	Test not yet completed but has potential	-
Ferraris et al. [12]	Microsoft Kinect v2 + MATLAB + 6 optoelectronic motion cameras + 2 force platforms	Continuous gait in a straight line	-	Walking barefoot along a 10m walkway at comfortable speed	11 stroke patients, mean age 53 years and last stroke event 52 months ago	Gait patterns and SP in a short gait	Timed up and go (TUG)	Apparently only once with each participant	Good agreement, precision and correlation between gait parameters	There are other more accurate and better performing RGB-D sensors

(continued)

Table 1. (continued)

Study	Technology used	What gait exercise was performed?	What is the treatment focus?	Experiments performed (with the user)	Profile and the number of users	Variables	Tests	How often was it tested?	Results/Opinions	Limitations of applied technology
Nema et al. [16]	Microsoft HoloLens + Unity 3D + wireless Xbox One	Short-period marches with directional changes	Study of motor cognitive interference	i) visual discrimination of peripheral targets, ii) spatial navigation from one point to another and iii) visual and navigation tasks simultaneously	21 FP and 24 MP with an average of 24 years	Cognitive states and "confusion" with the presence of virtual objects in the peripheral field + change in motor behavior	Use of reaction time and the NASA TLX questionnaire [18] after each task	Apparently only once with each participant	AR is a research tool suitable for simulating multitasking and dynamic tasks outdoors	Distance used (3 m) is too short to infer behaviors and AS
Guinet et al. [17]	HoloStep (Microsoft HoloLens) + MOCAP System	Continuous gait in a straight line	SP analysis of gait in healthy children and in children with gait disorders caused by cerebral palsy	March at comfortable speed in a straight line along an 8 m path	13 healthy adults aged 18 years and over and 62 children aged 10 to 18 years with cerebral palsy	User position, AS, SL, number and time of steps, cadence, step detection	Using Zeni's algorithm [19] + HoloStep algorithm + 2-min walk test	3 attempts were made	The HoloStep algorithm used in HoloLens was able to identify several parameters and has good accuracy even with people with gait disorders who use walkers or supports	Very high sensitivity of HoloStep, can have a lot of variations if the head position is not stable

(continued)

Table 1. (continued)

Study	Technology used	What gait exercise was performed?	What is the treatment focus?	Experiments performed (with the user)	Profile and the number of users	Variables	Tests	How often was it tested?	Results/Opinions	Limitations of applied technology
Enam et al. [7]	C-Mill + CueFors software	Treadmill march	Training on spatiotemporal and functional mobility outcomes in stroke patients	30 s of calibration and self-selected comfortable walking speed (SSC) capture, then 4 10-min gears at SSC speed, 20% above and 20% below	Healthy: 55 years old, MP and healthy; with intervention: 54 years old, FP and had a stroke 10 years ago No in-tervention: 59 years old, PF and had a stroke 2 years ago	SL, stance time and swing time, plus AS, stability and balance	BBS + DGI + 10MWT + 6MWT + TUG + ProtoKinetics Zeno Walkway + PACES	3 sessions per week for 4 weeks for stroke participants and tested only 1 time with the healthy patient	Significant improvement; increase in AS and significant score on the BBS, the DGI [13] and the PACES	–
Ulrich et al. [18]	Force platform + vicon system	Continuous gait in a straight line	Decreased ambulatory knee adduction moment with osteoarthritis without increasing individual knee flexion moment	Walking at comfortable speed	7 men and 4 women with no history of lower limb surgery, or knee pain or limited mobility, mean age 25 years, 1.80m tall and 69kg	Foot projection angle, SW, SL, peak moments of knee adduction and abduction	Vicon system was used to measure the kinetics of the right knee and the SP	5 attempts to walk at normal speed + 5 min or 10 attempts to walk under the adjusted design gears	AR holds promise for gait retraining with knee osteoarthritis	–

(continued)

Table 1. (continued)

Study	Technology used	What gait exercise was performed?	What is the treatment focus?	Experiments performed (with the user)	Profile and the number of users	Variables	Tests	How often was it tested?	Results/Opinions	Limitations of applied technology
Held et al. [8]	Microsoft HoloLens + Xsens MVN System	Continuous running in a straight line, running with obstacles, running after rotation	Manipulation of the gait pattern of stroke patients	Overcoming obstacles, trampolines, body rotation	1 74-year-old patient who had a right-sided ischemic stroke 7 years ago	Kinematics of the lower limbs and the center of mass	System usability scale and virtual reality symptom questionnaire [20, 21]	1 single session of 10 m walk test and 3 times AR parkour course	The ARISE system is useful for gait and balance rehabilitation	The ARISE system requires technical support for configuration and calibration. And motion sensors are limited by orientation deviation when used for a long time
Janssen et al. (2020) [11]	Microsoft HoloLens + Xsens MVN System + Unity 3D + MATLAB	180° turn	Improve frozen gait after rotation in Parkinson's patients	90 attempts at 180° turns around its axis in a space of 50 cm ²	16 patients diagnosed with Parkinson's, mean age of 69 years, 81% of whom were MP and mean of 10 years living with the disease	Freeze time percentage, frequency and duration of FOG episodes, cadence, peak angular velocity, stride time, stride time coefficient of variation, and step height, and turn time	-	3 sessions, 1 of which training and all held on the same day	AR visual cues had detrimental effects on gait freezing	-

(continued)

Table 1. (continued)

Study	Technology used	What gait exercise was performed?	What is the treatment focus?	Experiments performed (with the user)	Profile and the number of users	Variables	Tests	How often was it tested?	Results/Opinions	Limitations of applied technology
Sekhawat et al. (2018) [13]	Microsoft kinect + unity 3D + treadmill	Continuous running in a straight line, running with obstacles, running after rotation	—	Step on and avoid obstacles	8 hemiplegic individuals, 5 men, mean 44.5 years	Step size, foot length, distance between right foot and left foot	-	8 sessions in two weeks, 15 min for the stepping task and 10 min for the obstacle avoidance task	AR is more effective than biofeedback	Some participants needed to look down at their feet while walking on the treadmill
Barthel et al. [10]	Laser shoes + MoveTest accelerometer	Going forward and backward, walking around curves, going around objects	Decreased frozen gait and change of gait measures in Parkinson's patients	Walk backward and forwards over 10m, walk backward and forwards with countdown, turns, walking to pick up an object and walk around objects	19 individuals diagnosed with Parkinson's with a mean age of 68.68 years	AS, SL, cadence, step time asymmetry, step time variability, double limb support, number of frozen gait episodes	GABS and MDS-UPDRS Part III and FAB, analyzing half-turn while walking, full turn, modified performance oriented gait assessment scale, FOG and test freezing	A total of 10 attempts were made	There was a reduction in the occurrence of gait freezing (2 episodes less) and in the duration of freezing (56.5%)	They used a passive condition, in which it was possible to walk in the same shoes with the laser beams turned off. And some participants had to look down at their feet as they walked

(continued)

Table 1. (continued)

Study	Technology used	What gait exercise was performed?	What is the treatment focus?	Experiments performed (with the user)	Profile and the number of users	Variables	Tests	How often was it tested?	Results/Opinions	Limitations of applied technology
Bemour et al. [19]	Vicon system	Continuous gait in a straight line	Effect of footprint modifications on lower limb flexion and extension angles	Recording of 5 walks at normal speed + 27 walks with parameter modification	10 healthy subjects, 6 men, mean age 25 years	Stride length, SW, foot progression angle, AS	-	-	It was possible to change parameters independently	Unable to assess modification errors and characterize footprint-kinematic relationships (such as linearity and dose-response)
Vallabhajosula et al. [14]	Microsoft Kinect + treadmill + GAITRite system + qualisys System	Treadmill march	Effect of physical exercise games and treadmill on cognition, balance and gait in Parkinson's patients	Each session with 30 min of games and 30 min of treadmill	1 69-year-old diagnosed with Parkinson's 7 years ago	SL, time, AS, peak force in anteroposterior, mediolateral and vertical forces for swing and support legs	Stroop test, short falls efficacy scale (Short FES-I), MiniBEST	3 times in the first week, 1h each session + 2 times a week for the other 7 weeks, 1h per session	There was no effect on cognition, but resulted in improved balance and gait	-
Ahn et al. [9]	Epson's Moverio BT-200	Continuous gait in a straight line	Identification of FOG and improvement of gait pattern in Parkinson's patients	Timed up and go test + 10m walk	10 individuals diagnosed with Parkinson's, 7 men with a mean age of 70.8 years	-	-	2 times each test (TUG and the walk)	Achieves 83.7% accuracy detecting FOG episodes and there was an increase in AS and stride length	-

FOG = Freezing of Gait; SP = Spatiotemporal Parameters, SL = Step Length; SW = Step Width; AS = Average Speed; HSP = Hereditary Spastic Paraplegia; MP = Male People; FP = Female People; E-FAP = Emory Functional Ambulation Profile, 10MWT = 10-m Walk Test, miniBEST = Mini Balance Evaluation Systems Test, ABC = Activities-specific Balance Confidence scale, WALT = Walking Adaptability Ladder Test, BBS = Berg Balance Scale, DGI = Dynamic Gait Index, 6MWT = 6-min walk test, PACES = The Physical Activity Enjoyment Scale, FAB = Frontal Assessment Battery, MDS-UPDRS = Movement Disorder Society–Unified Parkinson's Disease Rating Scale Motor.

differentiated demands. This fact is understandable but dramatically limits the usage of the technologies developed. Besides, verifying patterns in profiles, the number of users, and the frequency of tests in general in all studies is difficult due to the variety of users.

According to the mapping of included studies in Table 1, it was not explicit in the articles that used C-mill the limitations of this technology. Otherwise, besides having handles that guarantee the user's safety, the C-mill provided a significant improvement in gait parameters [7].

About Kinect v2, it was related that the technology improved balance and gait [14], presented good agreement, precision, and correlation between gait parameters [12], and even proved that AR is more effective than biofeedback [13]. In return, one of the studies [12] concluded there are other more accurate and better performing RGB-D sensors than Microsoft Kinect v2. In any other test, some participants needed to look down at their feet while walking on the treadmill while using the Kinect [13], which is a negative point.

Around the glasses HoloLens, the studies concluded that it is a tool suitable for simulating multitasking and dynamic tasks outdoors [16], capable of identifying several parameters, and has good accuracy even with people with gait disorders who use walkers or supports [17]. But, due to the very high sensitivity of HoloStep, it can have a lot of variations if the head position is not stable [17], a fact that can limit the analysis.

The Epson's Moverio BT-200 glasses achieved 83.7% accuracy in detecting FOG episodes and increased AS and stride length [9]; negative aspects of the use of technology were not explained.

With the laser shoes, there was a reduction in gait freezing (2 episodes less) and the duration of freezing (56.5%) [10]. A disadvantage of this application was that some participants had to look down at their feet as they walked [10].

5 Conclusion

Given the results obtained and the patterns analyzed, it is concluded that Augmented Reality is a promising tool in Gait Rehabilitation. Due to the great variety of applications, it is possible, due to the great diversity of applications, to intervene in various needs within the rehabilitation. To test or develop a gait rehabilitation tool using AR, it's necessary to analyze the benefits and limitations of available technologies already mentioned to assess and decide which ones satisfy certain objectives.

It was also possible to observe the extreme importance of spatiotemporal parameters, not only in the evaluation but also in the rehabilitation of ambulation, so that they can be used as a reference and, through the collection of these parameters, health professionals can identify the greatest needs of patients.

A portable system capable of rehabilitating the gait using, for example, a cellphone, was not registered yet. Also, none of the studies had the objective or mentioned the application of tools for telerehabilitation, for the possibility of using the technology at home to complement the rehabilitation already carried out in the clinics, and also concerned with access issues, saving time, and optimizing the treatment.

Thus, a complete and simpler system must be developed aimed at assisted rehabilitation at home. It would also be interesting if it covered more than one type of patient who need gait rehabilitation.

References

1. Kirner, C., Siscoutto, R.: Realidade Virtual e Aumentada. In: Symposium on Virtual and Augmented Reality (2007)
2. Costa, R.M., Ribeiro, M.W.: Aplicações de Realidade Virtual e Aumentada. In: XI Simpósio de Realidade Virtual e Aumentada (2009).
3. Nunes, F., Costa, R.M., Oliveira, A.C. et al.: Aplicações médicas usando Realidade Virtual e Realidade Aumentada. In: Symposium of Virtual Reality (2007)
4. Sousa, M., Vieira, J., Medeiros, D., Arsenio, A., Jorge, J.: SleeveAR. In: Proceedings of the 21st International Conference on Intelligent User Interfaces, pp. 175–185. <https://doi.org/10.1145/2856767.2856773> (2016)
5. Barioni, R.R., Chaves, T.M., Figueiredo, L., Teichrieb, V., Neto, E.V., da Gama, A.E.F.: ARkanoidAR: an augmented reality system to guide biomechanical movements at sagittal plane. In: 19th Symposium on Virtual and Augmented Reality (SVR), pp. 207–214. <https://doi.org/10.1109/SVR.2017.34> (2017)
6. Alamri, A., Cha, J., el Saddik, A.: AR-REHAB: an augmented reality framework for poststroke-patient rehabilitation. *IEEE Trans. Instrum. Meas.* **59**(10), 2554–2563 (2010). <https://doi.org/10.1109/TIM.2010.2057750>
7. Enam, N., Veerubhotla, A., Ehrenberg, N., et al.: Augmented-reality guided treadmill training as a modality to improve functional mobility post-stroke: a proof-of-concept case series. *Top. Stroke Rehabil.* **28**(8), 624–630 (2021). <https://doi.org/10.1080/10749357.2020.1864987>
8. Held, J.P.O., Yu, K., Pyles, C., et al.: Augmented reality-based rehabilitation of gait impairments: case report. *JMIR Mhealth Uhealth* **8**(5), e17804 (2020). <https://doi.org/10.2196/17804>
9. Ahn, D., Chung, H., Lee, H-W., et al.: Smart gait-aid glasses for Parkinson’s disease patients. *IEEE Trans. Biomed. Eng.* **64**(10), 2394–2402 (2017). <https://doi.org/10.1109/TBME.2017.2655344>
10. Barthel, C., Nonnekes, J., van Helvert, M., et al.: The laser shoes. *Neurol.* **90**(2), e164–e171 (2018). <https://doi.org/10.1212/WNL.0000000000004795>
11. Janssen, S., de Ruyter van Steveninck, J., Salim, H.S. et al.: The effects of augmented reality visual cues on turning in place in Parkinson’s disease patients with freezing of gait. *Front. Neurol.* **11**. <https://doi.org/10.3389/fneur.2020.00185> (2020)
12. Ferraris, C., Cimolin, V., Vismara, L. et al.: Monitoring of gait parameters in post-stroke individuals: a feasibility study using RGB-D sensors. *Sensors.* **21**(17), 5945. <https://doi.org/10.3390/s21175945> (2021)
13. Sekhavat, Y.A., Namani, M.S.: Projection-based AR: effective visual feedback in gait rehabilitation. *IEEE Trans. Hum.-Mach. Syst.* **48**(6), 626–636 (2018). <https://doi.org/10.1109/THMS.2018.2860579>
14. Vallabhajosula, S., McMillion, A.K., Freund, J.E.: The effects of exergaming and treadmill training on gait, balance, and cognition in a person with Parkinson’s disease: a case study. *Physiother. Theory Pract.* **33**(12), 920–931 (2017). <https://doi.org/10.1080/09593985.2017.1359867>
15. van de Venis, L., van de Warrenburg, B.P.C., Weerdesteijn, V., van Lith, B.J.H., Geurts, A.C.H., Nonnekes, J.: Improving gait adaptability in patients with hereditary spastic paraplegia (Move-HSP): study protocol for a randomized controlled trial. *Trials.* **22**(1), 32. <https://doi.org/10.1186/s13063-020-04932-9> (2021)
16. Nenna, F., Zorzi, M., Gamberini, L.: Augmented reality as a research tool: investigating cognitive-motor dual-task during outdoor navigation. *Int. J. Hum.-Comput. Stud.* **152**, 102644. <https://doi.org/10.1016/j.ijhcs.2021.102644> (2021)

17. Guinet, A.-L., Bouyer, G., Otmane, S., Desailly, E.: Validity of hololens augmented reality head mounted display for measuring gait parameters in healthy adults and children with cerebral palsy. *Sensors* **21**(8), 2697 (2021). <https://doi.org/10.3390/s21082697>
18. Ulrich, B., Cosendey, K., Jolles, B.M., Favre, J.: Decreasing the ambulatory knee adduction moment without increasing the knee flexion moment individually through modifications in footprint parameters: a feasibility study for a dual kinetic change in healthy subjects. *J. Biomech.* **111**, 110004. <https://doi.org/10.1016/j.jbiomech.2020.110004>. (2020)
19. Bennour, S., Ulrich, B., Legrand, T., Jolles, B.M., Favre, J.: A gait retraining system using augmented-reality to modify footprint parameters: effects on lower-limb sagittal-plane kinematics. *J. Biomech.* **66**, 26–35 (2018). <https://doi.org/10.1016/j.jbiomech.2017.10.030>
20. Page, M.J., McKenzie, J.E., Bossuyt, P.M., Boutron, I., Hoffmann, T.C., Mulrow, C.D., et al.: The PRISMA 2020 statement: an updated guideline for reporting systematic reviews. *BMJ* **372**, n71 (2021). <https://doi.org/10.1136/bmj.n71>
21. Hart, S.G., Staveland, L.E.: Development of NASA-TLX (Task Load Index): results of empirical and theoretical research, pp. 139–183. [https://doi.org/10.1016/S0166-4115\(08\)62386-9](https://doi.org/10.1016/S0166-4115(08)62386-9) (1988)
22. Zeni, J.A., Richards, J.G., Higginson, J.S.: Two simple methods for determining gait events during treadmill and overground walking using kinematic data. *Gait Posture* **27**(4), 710–714 (2008). <https://doi.org/10.1016/j.gaitpost.2007.07.007>
23. Ames, S.L., Wolffsohn, J.S., McBrien, N.A.: The development of a symptom questionnaire for assessing virtual reality viewing using a head-mounted display. *Optom. Vis. Sci.* **82**(3), 168–176 (2005). <https://doi.org/10.1097/01.OPX.0000156307.95086.6>
24. Bangor, A., Kortum, P.T., Miller, J.T.: An empirical evaluation of the system usability scale. *Int. J. Hum.-Comput. Interact.* **24**(6), 574–594 (2008). <https://doi.org/10.1080/10447310802205776>



IoT System for Elbow Angle Assessment Applied to Orthosis Device

Beatriz Cunha^(✉), Jean Schmith, and Rodrigo Marques de Figueiredo

Polytechnic School, Unisinos University, São Leopoldo Av. Unisinos, 950, São Leopoldo, Brazil
cunhabeatrizc@gmail.com

Abstract. Joints, mobile structures of the musculoskeletal system, contribute to the autonomy and mobility of human beings, however they are requested by several events that may compromise their integrity impacting physiological activities. In these cases, medical assistance may be necessary and can be accompanied by the use of dynamic orthoses, which can promote immobilization and dynamic control of the structure. IoT fundamental can be applied to these devices and benefits the rehabilitation as it allows continuous and remote monitoring, but these type of devices are scarce in the market. The presented work developed a prototype of an orthosis with continuous monitoring elbow angle assessment during flexion and extension. The work encompassed structural, electro-electronic and software development. From the methodology proposed, it was possible to obtain good results since the data was properly acquired and displayed as well as the orthosis structure met the requirements in agreement to the validation method using the widespread software Kinovea. In this way, it was possible to develop an orthosis prototype for the elbow joint angle assessment using IoT fundamentals as a proof of concept.

Keywords: Joint · Elbow · Orthoses · Monitoring · Internet of things

1 Introduction

The use of orthoses, external support devices applied to the body, provide therapeutic effects to injured joints and limbs, since it promotes the immobilization and dynamic control of musculoskeletal structures resulting in tissue recovery [1]. Concomitantly with the usage of orthoses, the medical prescription may include physical rehabilitation exercises supervised by physical therapists, which contribute to the recovery of joint functional integrity. Furthermore, the patient's and professional's commitment to the exercises protocol and medical prescription is a determining factor for the total rehabilitation of the injured area, being commonly necessary the presence and regular attendance of both subjects [2]. However, given the change in social habits, attendance at medical appointments can be impaired or even made unfeasible.

The rehabilitation program of an injured joint can encompass several dynamic exercise protocols in order to decrease inflammatory responses in the musculoskeletal tissue and still restore the full motor functionality of the limb [3,4]. The effects of prolonged and not guided immobilization can promote the reduction of the use of muscular structures, compromising the patient's well-being regarded to the total time of return to its daily activities [5]. According to Fournier et al. [6] the muscle is a biological structure with adaptable responses to a scenario of reduced use. These responses can relate to the decrease of muscle electrical activation, a percentage reduction of slow contraction fibers and a decrease in the physiological cross-sectional area of muscle fibers, which can represent a picture of muscle hypotrophy and decreased force generation [7].

Studies conducted by Macdougall et al. [8] and Macdougall et al. [9] corroborate the findings of Fournier et al. [6]. After five weeks of immobilization of the upper limb with the elbow joint at 120°, a reduction of 34% and $35 \pm 18.8\%$ in muscle strength of the elbow extensors was observed in isokinetic and concentric contractions, respectively. When evaluating the impact of four weeks immobilization of the elbow in 90° regarded to force magnitude and muscle electrical activation, Yue et al. [10] found a loss of 35% of maximal strength of the elbow flexor muscles in the first week, in addition to a reduction of at least 10% in the duration of electrical activity of the biceps brachii.

As shown, it can be noticed negative impacts promoted by prolonged immobilization of upper limbs and yet can be caused by the inability of presence follow up of the rehabilitation protocol in physical therapy sessions. In this sense, the advancement of technology contributes in a positive way, since fundamentals of engineering and Internet of Things (IoT) allow the interaction between doctor and patient in a remote and assisted way. However, telemedicine devices that guarantee remote joint kinematics assessment are scarce.

The development of tools for this scenario is essential for maintaining the health and well-being of patients with injuries to the musculoskeletal system. Furthermore, it can positively impact the socioeconomic scenario by reducing the total expenses of medical centers and reducing the average time for patients for re-enter their regular activities, in addition to contributing to technological advances in the areas of engineering and medicine.

In view of the discussed premises, the presented work proposes the development of a prototyped system of orthosis with adjustable angulation of the elbow joint. The system proposed can continually monitor the angular position of the elbow during flexion and extension movements. Further, it pursues the development of a friendly interface for graphical displacement of data, thus enabling the analysis and extraction of control parameters and clinical interest regarding the monitoring of the prescribed medical protocol.

2 Theoretical Foundation

2.1 Kinematic, Biomechanical and Anatomical Aspects of the Elbow Joint

The human body is composed of several tissues and systems that together contribute to the total functionality of the individual. Mobility, protection, stability, blood cells production and minerals metabolic reserve is provided by the musculoskeletal system, which consists of bones, tendons, ligaments, muscles and joints [11].

Joints play a fundamental role in terms of mobility and maintenance of physiological activities as they allow the individual to eat, for instance. These structures correspond to the meeting point between two or more bones and provide an area of movement from the active action of muscles and bone handle [12]. Also, in addition for enabling movement, joints preserve other biological structures, since they transfer and shed forces generated by gravity and muscle action [13].

Regarding the upper portion of the human body, it is possible to find a set of structures that comprehends the elbow joint. Located in the middle part of the upper limb, this joint not only connects the arm to the forearm, but also allows protection, feed and other physiological activities. The elbow joint it is contemplated by two joints: humeroulnar and humeroradial; characterizing the agreement between the humerus and ulna and humerus and radius, respectively [14]. The elbow joint, classified as synovial hinged joint, most allows flexion and extension movements [14].

According to Chapleau et al. [15], during the passive extension movement it is possible to verify the value of 5° beyond neutral extension (0°) for the maximum range of motion. For flexion, the maximum perceived amplitude is 145° . Miyazaki et al. [16] and Morrey [17] describe a functional arc for the elbow of 100° contemplated by the limiting angles of extension and flexion of 30° and 130° , respectively. Hamill, Knutzen and Derrick [12] proposed a range of active and passive flexion of 145° and 160° , respectively. For the hyperextension movement, it was determined angulation of 5° to 10° after the extension limit. Yet, it is noticed that the amplitude of the elbow joint varies from 20° to 140° during the performance of daily activities.

2.2 State of Art of Orthoses

In a scenario of upper limb rehabilitation, several protocols can be used based on the clinical status of the patient. In this context, orthoses can be used as a complementary therapeutic tool for treatment aiming the immobilization and stabilization, preventing and correcting deformities, protecting and helping healing processes [2, 18]. Depending of the functionality, material or design, orthoses can be categorized in several classifications. Regarding the kinematic behavior in can be noticed two large groups: static and dynamics. In what refers to the last feature, mechanisms of articulation and motorization can be found [2]. Regardless of their category, these devices are considered therapeutic resources, there-

fore must be individually prescribed after medical evaluation, since the orthosis model must be patient-oriented [19].

Dynamic orthoses allow controlled mobility of the joint, as well as restoring joint range of motion and promoting restoration of muscle strength [20]. A study carried out by Elui, Oliveira and Santos [21] showed a correction of 85.5% and 53% in patients affected by mobile claw after use of dynamic orthosis in thermoplastic and leather material, respectively.

Prolonged immobilization of the elbow joint may trigger a picture of damage to the integrity of musculoskeletal structures [6,8,9]. To avoid this condition, dynamic orthoses can be prescribed. Regarding the elbow joint, it is possible to find available articulated dynamic orthoses which allow the angular adjustment of the joint according to physician-guided protocol. These devices can promote this adjustments given, for instance, every 10° of increment for the range between 90° and 120° . This pace can be constant or vary in certain range of amplitude, this feature, however, is pertinent to the device manufacturer and its use must be in accordance with the protocol and medical evaluation.

The insertion of technologies, in the sense of remote and continuous analysis of the movement, for the purpose of adding value to the device and benefiting the patient is hardly found in orthoses. The analysis in remote and real-time significantly impact in the doctor's decisions, since he may adapt the protocol according to the performance of the patient. IoT fundamentals are studied and applied in rehabilitation devices and biomechanical analysis to not only provide feedback on user performance, but also promote visual and remote feedback. Studies applying IoT fundamentals in musculoskeletal devices can be found in [22–24].

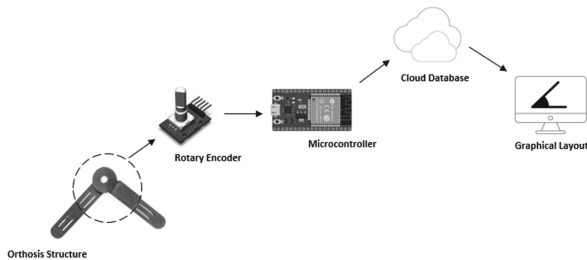


Fig. 1. Proposed project architecture

3 Materials and Methods

The proposed methodology, presented in Fig. 1, made possible the development of the prototyped orthosis. The methodology sought to encompass processes that would integrate the structural development of the orthosis, prototyped electronic

system for acquiring data and communication between a cloud database and graphical interface.

Searching for the most accurate fit anthropometric, measurements were performed on the right upper limb segment of one subject (24 years old, female), as a proof of concept. According to studies conducted by Netter [25], three anatomical points were used as reference for the measurement: insertion of the deltoid muscle, lateral epicondyle and styloid process of the ulna; with those three references, the length of the arm and forearm as well as the width of these two structures were analyzed. These anthropometric measurements were used as reference for the design of the device's structure and directly impacts on its performance.

The kinematics required by the presented work was possible by the mechanical principals stipulated and carried out by the development of the structure. As required, the orthosis must execute flexion and extension angular movements in the range of 90° and 180° with no obstructions. In order to promote the intermediary angular adjustments a pin was used through a slit, so the subject could limit the movement according to what was needed. For the intermediary adjustments using the pin the following angular positions were used: 102° , 115° , 128° , 141° , 154° and 167° . The positions were chosen according to elbow orthosis with angular adjustments already available on the market.

The device structure was modeled in SolidWorks software and in its entirety is composed of four parts that guarantee mechanical operation. While three pieces acts together in order to perform flexion and extension among to the elbow, the last one protects the microcontroller. In order to properly fix the orthosis, elastic bands were used on the upper arm and forearm.

The device was manufactured by a 3D printer machine using the Fusion and Deposition Method (FDM). This method guarantee functional advantages to the device over conventional methods, such as efficiency, accessibility and sustainability [26]. It was used Polyethylene Glycol Terephthalate (PETG) as filament. This thermoplastic combines properties of ductility and strength from Acrylonitrile Butadiene Styrene (ABS) with the printability of Polylactic Acid (PLA). It presents good tenacity, flexibility and ease of processing [27].

For the electronics system it was used a Rotary Encoder KY-040 and a microcontroller ESP32. The combination of these devices made it possible to determine the angular position of the elbow joint and process it for further data analysis.

The first mentioned device, Rotary Encoder KY-040, interprets a rotational movement and transforms it into digital pulses used to measure angular displacements. Since this device is used for determining of angular positions, it is possible to find its application in different knowledge areas. De Castro and Assis [28] applied the rotary encoder to obtain the angular position of joints during gate in an electromechanical exoskeleton.

After acquiring the angular position of the elbow joint it is necessary a device that processes, interprets and controls this variable. The microcontroller ESP32 was used for this purpose, since it has built-in WiFi and DualCore functionality.

The WiFi module was fundamental to transfer the data acquired to the database and the DualCore functionality increases the performance of the system as a whole, since it allows the simultaneously tasks for reading Encoder signal and transferring the processed data to database. Similar to this work, Takao et al. [29] used the ESP32 when determining the superficial tension band of the deltoid ligament. Nassour et al. [30] used the same device when analyzing and controlling the acquired signals by a glove sensor which identifies and replicates movements performed by the hand.

The data acquired is transmitted by the microcontroller through the WiFi to a cloud database which will be responsible for storing the angular amplitude performed by the patient while wearing the orthosis. Also, this database has communication with the graphical interface available for its analysis populating it. In this work, Google Sheets was used as a cloud database since it is a web application.

To ensure interpretation and visualization remotely of the angular variable of the patient's behavior, a graphical environment had to be modeled. It is understood, therefore, that in this scenario it is necessary a tool capable of assisting the critical analysis and decision-making. In this work was used Google Data Studio, a dashboard tool for information management, since it has an ideal communication between the database used for data storage.

For data validation, it was realized a global compliance analysis and verified ergonomics aspects in dynamic and static scenario, as well as a critical performance analysis through image analysis software Kinovea (version 0.9.5). This last mentioned analysis meets studies from Elrahim and Hassan [31] and according to Richardson et al. [32] this software is capable of performing two-dimensional analysis up to 1° degree of deviation. The subject was instructed to position himself perpendicularly to the camera being found at the same level as the elbow joint so image distortion effects were avoided. After that, the subject performed random flexion and extension movements and two images were taken from each angular position analyzed for further comparison between the output from ESP32 at that same moment.

4 Results and Discussion

The presented work prototyped an external aid device for the continuous and remote monitoring of the elbow joint angle through an IoT system, thus provide practical and reliable analysis of the patient's clinical status. Still, it sought the prototyping of a structure that allows the gradual adjustment of the angular joint amplitude, promoting dynamic mobility in addition enabling remote medical assistance. The results obtained are described in the following subsections.

4.1 Modeling and Structural Development

The structure of the orthosis was prototyped from SolidWorks modeling and manufactured in PETG using FDM technique. The temperature of the printer

bed and extrusion was 90°C and 250°C , respectively, following the manufacturer's instructions.

When analyzing it globally it can be affirmed that the structure demonstrates satisfactory results since the mechanical operation was not compromised, in the same way all the pieces had their structure met to the design modeled. Regarding the dimensions after printing it was possible to achieve satisfactory results as well. However, decrements of approximately 1 mm in the dimensions of both pieces that fix the device to the arm and in the piece that protects the microcontroller. This fact may be related to the phenomenon of contraction of the material used due to the temperature of the printing table and room, as Mano [33] describes. To this end, new printing tests are necessary in order to approximate the actual dimensions to the projected ones. Also, the design of the adjustment pin was not encompassed by the scope of the work, so a screw with the net dimensions was used to intermediary adjust the orthosis.

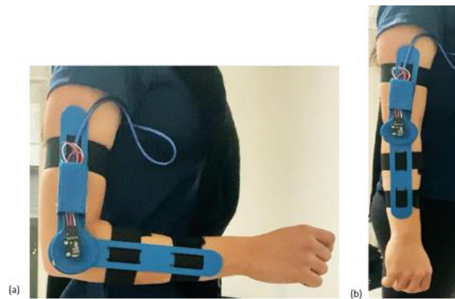


Fig. 2. Orthosis fit in (a) 90° and (b) 180°

When analyzing the fit of the prototype to the subject's arm in a static situation, it is possible to verify satisfactory results since the orthosis is securely fixed through elastic bands without causing discomfort to the arm. In addition, the area of the encoder axis attached to the pieces A, B and C is adjusted under the region of the lateral epicondyle when the elbow is in 90° and when 180° , as Fig. 2(a) and (b) demonstrate, respectively.

With regard to the dynamic adjustment of the orthosis to the right upper limb it was verified satisfactory results since the device kept fixed during flexion and extension movement. This is further corroborated by the correct angular measurement.

4.2 Electronic Circuit Prototypation

The Rotary Encoder KY-040 establishes connection with the ESP32 board and it is attached at the center of the axis of rotation in the orthosis structure. By verifying and comparing the angles provided by the Serial output of ESP32 and the position characterized in the electronic system, it is possible to claim that

good results were obtained, since all the angles and their respective positions were identified and are in accordance with the spatial arrangement of the chamfer found in the encoder shaft. After the experiments, the presented resolution of the Encoder agreed for the elbow joint angle measurement.

4.3 Database Configuration

Due to the DualCore characteristic of the ESP32 one task was responsible for accessing and transmit the angle acquired to the database. The transmission event of acquired data to the database contemplates interactions between the tasks encompassed by the microcontroller function, WiFi connections and interactions between servers. The transmission average time from the ESP32 to the database was 6.2 s when analyzing 20 samples. However, a cumulative behavior of this delay can be noticed when analyzing the Serial output time and database time. This behavior can be attributed to the inherent conditions of connection and data transmission, however it did not have impact on the quality of the transmitted data since no loss was noticed. The quality of the transmitted data can be notice as shown in Fig. 3, where several flexion and extension movements were made for testing purposes. It can be noticed agreement between the pace established for the angle joint measurements. Yet, in what refers to data integrity, all relevant information about elbow movement could be captured, once the projected microsystem and coding were designed to function by interruption.

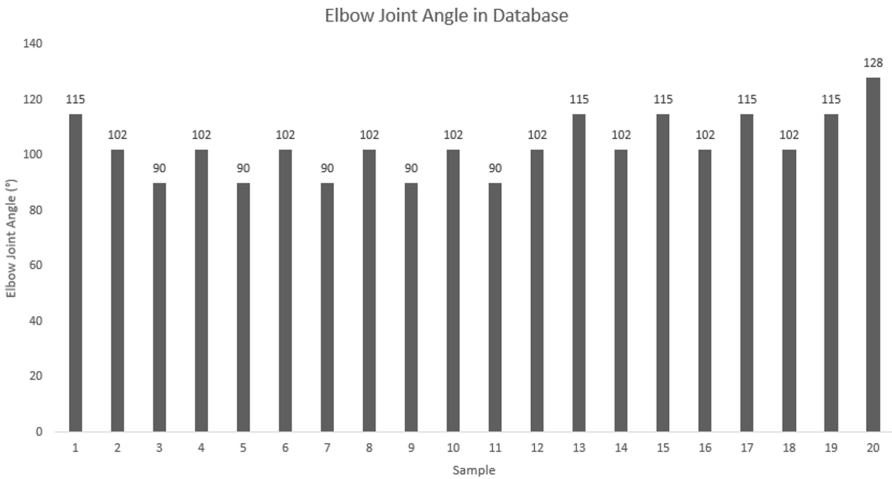


Fig. 3. Elbow angle joint analysis in database

4.4 Graphical Interface Configuration

For the graphical visualization of the elbow angular movements an interface was developed using Google Data Studio. This interface accesses the database every

6 s and provides an up-to-date view of the angular behavior, thus maintaining compliance with the data collected and arranged in the database.

Through the interface it is possible to analyze the number of times that the subject had his articulation arranged during the use as well as a behavioral view of the movements performed over time. For a better experience, it can be selected the period of time for the analysis.

4.5 Performance Validation

It is extremely important that the orthosis is able to identify correctly the angle of the elbow, transmitting to the database in order to display it graphically. According to the methodology described, the performance validation was performed using images processing techniques by Kinovea. When analyzing 2 samples for each angle of interest (16 samples in total) it was possible to verify divergences in all angles evaluated, as presented in Table 1. Despite showing divergences, the results are satisfactory and can be attributed to the fixation of the device on the user's arm, the device structure itself, subject movement and the analysis method, since the points used as guidance were made through the software and can be affected by the analyst. Still, this difference does not present relevance in clinical analysis. The greater difference can be noticed at the angle of 180° followed by the angle of 115°, however more investigation needs to be conducted in order to find the reason for this behavior.

Table 1. Angle performance comparison between Serial output and image analysis

Serial angle (°)	Image angle (°)	Difference (°)
90	89.4	0.6
115	114.1	0.9
128	127.8	0.2
167	167.7	0.7
154	154	0
128	128.9	0.9
141	141.4	0.4
115	113.9	1.8
90	90.3	0.3
102	101.2	0.8
102	101.3	0.7
141	140.8	0.2
154	153.5	0.5
167	166.4	0.6
180	178.1	1.9
180	177.5	2.5

5 Conclusion

Prolonged immobilization of musculoskeletal structures can represent adverse clinical conditions to the patient, such as muscle atrophy and stiffness. In this sense, the use of articulated orthoses guarantees benefits to the user since it promotes their autonomy and speed up the reintegration into society.

Orthoses that perform continuous and remote monitoring of the elbow articulation are hardly found on the market, so the presented work developed a prototype of an articulated orthosis with continuous monitoring of this joint. Also, it developed a graphical software interface to data visualization enabling critical and agile analysis by the doctor and patient. From the methodological processes developed, it was possible to develop a structural and electronic prototype that, through application of IoT fundamentals, provides satisfactory remote displacement of data.

Although using prototyping methods of manufacture, the PETG provided good characteristics to the device, such as lightness. The electronic circuit showed good results since all proposed angles could be identified. The graphical view demonstrates a good user experience and meets the requirements. The validation through image analysis presented a good error agreement with the need of clinical analysis.

Despite the good results, it is suggested as future works structural changes in order to provide better ergonomics and resistance to the device, in addition to making the design more attractive to the user. Yet, with regard to performance, it is suggested studies applied the communication and data transmission in order to reduce the time for acquiring and displacement in the graphical interface. Finally, it is suggested as next step apply the study in a bigger population in order to obtain more relevant statistics results as the proposed device is a proof of concept.

References







1. Vasconcelos, G., Matiello, A.: *Órtese e Prótese*, pp. 12–13. Grupo A, Porto Alegre (2019)
2. McKee, P., Morgan, L.: *Orthotics in Rehabilitation: Splinting the Hand and Body*. FA Davis (1998)
3. Butterfield, T.A., Best, T.M., Merrick, M.A.: The dual roles of neutrophils and macrophages in inflammation: a critical balance between tissue damage and repair. *J. Athl. Train.* **41**(4), 457 (2006)
4. Schaible, H.-G., et al.: The role of proinflammatory cytokines in the generation and maintenance of joint pain. *Ann. N. Y. Acad. Sci.* **1193**(1), 60–69 (2010)
5. Appell, H.-J.: Muscular atrophy following immobilisation. *Sports Med.* **10**(1), 42–58 (1990)
6. Fournier, M., et al.: Is limb immobilization a model of muscle disuse? *Exp. Neurol.* **80**(1), 147–156 (1983)
7. Lieber, R.L., et al.: Differential response of the dog quadriceps muscle to external skeletal fixation of the knee. *Muscle & Nerve: Off. J. Am. Assoc. Electrodiagn. Med.* **11**(3), 193–201 (1988)

8. MacDougall, J.D., et al.: Effects of strength training and immobilization on human muscle fibres. *Eur. J. Appl. Physiol. Occup. Physiol.* **43**(1), 25–34 (1980)
9. MacDougall, J.D., et al.: Biochemical adaptation of human skeletal muscle to heavy resistance training and immobilization. *J. Appl. Physiol.* **43**(4), 700–703 (1977)
10. Yue, G.H., et al.: Task-dependent effect of limb immobilization on the fatigability of the elbow flexor muscles in humans. *Exp. Physiol. Transl. Integr.* **82**(3), 567–592 (1997)
11. Koeppen, B.M., Stanton, B.A.: *Berne and Levy Physiology e-book*. Elsevier Health Sciences (2017)
12. Hamill, J., et al.: *Bases biomecánicas do movimento humano*. [Revisão Técnica] (1999)
13. Hall, S.J.: *Biomecânica Básica*. Grupo Gen-Guanabara Koogan (2000)
14. Neumann, D.A.: *Cinesiologia do aparelho musculoesquelético: fundamentos para reabilitação*. Elsevier Health Sciences (2010)
15. Chapleau, J., et al.: Validity of goniometric elbow measurements: comparative study with a radiographic method. *Clin. Orthop. Relat. Res.* [®] **469**(11), 3134–3140 (2011)
16. Miyazaki, A.N., et al.: Avaliação dos resultados do tratamento cirúrgico da triade terrivel do cotovelo. *Rev. Bras. Ortop.* **49**, 271–278 (2014)
17. Morrey, B.F., Askew, L.J., Chao, E.Y.: A biomechanical study of normal functional elbow motion. *J. Bone Joint Surg. Am.* **63**(6), 872–877 (1981)
18. King, S., Thomas, J.J., Rice, M.S.: The immediate and short-term effects of a wrist extension orthosis on upper-extremity kinematics and range of shoulder motion. *Am. J. Occup. Therapy* **57**(5), 517–524 (2003)
19. Rodrigues, A.C.T., Marques, T., Marciano, L.H.S.C.: Instrumentos de avaliação funcional da mão: uma análise crítica de cinco testes. *Rev. Inst. Adolfo Lutz* **72**(1) (2013)
20. Gonçalves, B.A., Francisco, N.P.F.: Órteses: orientações e cuidados. In: *Anais 14º Encontro Latino Americano de Iniciação Científica e 10º Encontro Latino Americano de Pós-Graduação-Universidade do Vale do Paraíba* (2011)
21. Elui, V.M.C., de Oliveira, M.H.P., dos Santos, C.B.: Órteses: um importante recurso no tratamento da mão em garra móvel de Hansenianos. *Hansenologia Internationalis: hanseníase e outras doenças infecciosas* **26**(2), 105–111 (2001)
22. Zhang, W., Tomizuka, M., Byl, N.: A wireless human motion monitoring system for smart rehabilitation. *J. Dyn. Syst. Meas. Control* **138**(11) (2016)
23. Aoike, K., et al.: Gait analysis of normal subjects by using force sensor and six inertial sensor with wireless module. In: *2016 IEEE International Conference on Systems, Man, and Cybernetics (SMC)*, pp. 001257–001260. IEEE (2016)
24. Chiaradia, D., et al.: Design and embedded control of a soft elbow exosuit. In: *2018 IEEE International Conference on Soft Robotics (RoboSoft)*, pp. 565–571. IEEE (2018)
25. Netter, F.H.: *Netter Atlas de Anatomia Humana*. Elsevier Brasil (2018)
26. Woodson, T., Alcantara, J.T., do Nascimento, M.S.: Is 3D printing an inclusive innovation?: An examination of 3D printing in Brazil. *Technovation* **80**, 54–62 (2019)
27. Santana, L., et al.: A comparative study between PETG and PLA for 3D printing through thermal, chemical and mechanical characterization. *Matéria (Rio de Janeiro)* **23** (2018)
28. de Castro Assis, W.O.: Contribuição para o desenvolvimento de exoesqueletos-projeto do circuito eletrônico para um exoesqueleto em tamanho real (2016)

29. Takao, M., et al.: Strain pattern of each ligamentous band of the superficial deltoid ligament: a cadaver study. *BMC Musculoskelet. Disord.* **21**(1), 1–7 (2020)
30. Nassour, J., et al.: A robust data-driven soft sensory glove for human hand motions identification and replication. *IEEE Sens. J.* **20**(21), 12972–12979 (2020)
31. Abd Elrahim, R.M., Hassan, K.A.: Realiability of computerized software in measuring elbow joint range of motion. *Turk. J. Physiother. Rehabil.* **32**(3) (2021)
32. Richardson, J.L.: Effect of step rate on foot strike pattern and running economy in novice runners (2013)
33. Mano, E.B.: Polimeros como materiais de engenharia. Editora Blucher (1991)



Analysis of the Exposure of PLA Surfaces to Ozone Gas, Ozonated Water, and Ultraviolet Radiation, Preliminary Evaluation

M. C. O. Carvalho¹(✉) , F. T. C. S. Balbina¹ , L. L. Azevedo^{1,3} ,
G. V. Schmitz² , A. B. Fernandes^{1,3} , and C. J. Lima^{1,3} 

¹ Biomedical Engineering Center, Anhembi Morumbi University, São José Dos Campos, SP, Brazil

mayconcarvalhoms@gmail.com

² Undergraduate Course in Biomedicine, Anhembi Morumbi University, São José Dos Campos, SP, Brazil

³ Center for Innovation in Technology and Education (CITE), São José Dos Campos, SP, Brazil

Abstract. 3D printing, also known as additive manufacturing (AM), has been used in automobiles, aerospace, mechanical systems, medicines, and biological systems, among other environments. The present study aimed to evaluate possible alterations induced after exposure to ozone (O₃), both in the gaseous form and dissolved in water, and ultraviolet (UV) radiation, in materials that are used in three-dimensional (3D) printing, since they have a great potential for use in health. The material analyzed as polylactic acid (PLA), is the filament most commonly used. To evaluate the degradation of this material, objects were printed on a 3D printer, and the samples were divided into 3 groups Ozone Gas (O₃), Ozonated Water, and UV light, and monitored in two cycles of 90 min of exposure. Optical microscopy was used to evaluate the alterations of the surfaces exposed to the different treatments. The tested materials showed resistance to exposure to O₃ in the gas and liquid phases, but UV exposure showed that PLA was degraded. The data obtained suggest that this material can be used to manufacture parts to be used and exposed to O₃ gas, as well as ozonated water. In this sense, the use of PLA is promising in health equipment and instruments, such as components for ozone therapy, and/or disinfection equipment that uses ozone or ozonated water.

Keywords: Ozone · PLA · Surface modification · UV radiation

1 Introduction

3D printing, also known as additive manufacturing (AM), has been used in automotive, aerospace, mechanical systems, medicines, and biological systems, among other environments [1, 2]. The main advantage of 3D printing is the ability to build complex shapes economically using a wide variety of materials. By using this technology, consumers and industries can quickly prototype early-stage product designs [3].

Medical applications for 3D printing have expanded greatly in recent years and it is expected to revolutionize health, as the application of 3D printing in medicine can provide many benefits, including customization and customisation of medical products, medicines, and equipment; increasing the effectiveness of known procedures and increase the reproduction of innovative techniques [4].

Among the main processes of 3D printing is the casting modeling (FDM) or manufacture of molten filaments (FFF), which belongs to the process of extrusion of materials, and is becoming the most popular due to its extrusion systems presenting lower cost and flexible, including thermoplastic materials [5]. However, the phenomena of chemical, photodynamic, and thermal degradation of 3D printed thermo-plastics are an inevitable problem for long-term reliability.

Components created through 3D printing technology come into contact with different environments in common practice, especially in the case of engineering, where there is a high probability that they will be exposed to considerably adverse effects, one of which is contact with agents causing chemical degradation, these can then have a fundamental impact on the properties and durability of these components [6].

Ozone stands out for its high oxidation potential, being the second strongest oxidizing agent, second only to fluoride [7]. The water solubility of O_3 is higher than in oxygen, so when dissolved in water, ozone decomposes much faster than in oxygen or air [8].

Both O_3 and UV radiation quickly damage unprotected polymers, which can considerably reduce their service life. In particular, highly unsaturated polymers (i.e., rubbers) are known to undergo a major degradation by O_3 , due to their double bonds, while saturated polymers also react, but much more slowly [9].

UV treatment can mainly affect the properties of the surface region with minimal influence on volume properties depending on the choice of UV lamp and optical geometry [10].

The objective of this study was to perform the analysis of the surfaces of parts constituted of PLA after exposure to ozone gas, ozonated water, and UV separately, and thus, later, to verify whether or not there was a degradation of the material.

2 Materials and Methods

2.1 Fused Deposition Modeling

The test samples were manufactured using Fused Deposition Modeling (FDM) technology, using thermoplastic Poly Lactic Acid (PLA). PLA samples were designed using the Inventor[®] Professional 2020 CAD Software and printed using the 3D printer (MakerBot Replicator+), in association with your printing software (MakerBot Print, version 4.10.1.2056). The experiment was carried out in sample pieces of connectors to flow liquids and gases so that each part produced is composed of half of the connector already mentioned, in this sense the final sample was assembled by the junction of the two pieces printed by the system, Fig. 1.

The print fill density has been adjusted to 100% to inhibit leaks. To join the two pieces and ensure a better seal, Polytetrafluoroethylene (PTFE) tape was used.

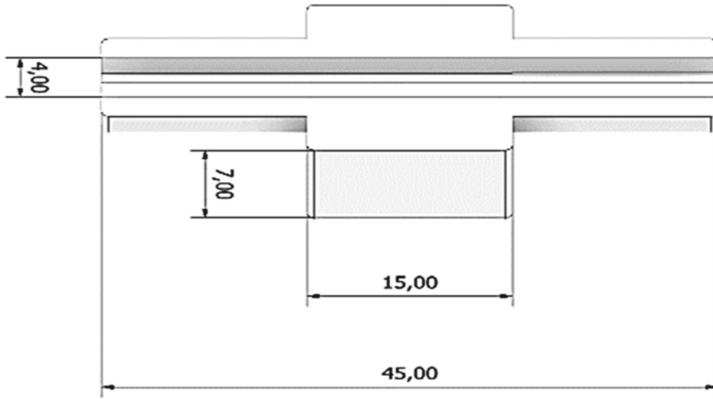


Fig. 1. The three-dimensional design of the connector is composed of two symmetrical parts, to obtain the sample with flat internal surfaces, and to perform exposures to O₃, UV, and ozonized water.

The samples were divided into 3 groups O₃ (gas), Ozonated Water, and UV, and monitored in two cycles of 90 min of exposure, with an interval of 90 min between them. Each test was performed considering two exposure surfaces.

2.2 Exposure to Ozone Gas

To perform the ozonation of the printed parts, an ozone generator (Ozone & Life, O&L 1.5RM), at its inlet was connected to an oxygen cylinder in conjunction with a pressure-reducing valve, and flow regulator, specifically adjusted in 1/4 L/min. At the outlet of the ozone generator, the PLA part was connected to a flexible silicone duct as shown in Fig. 2. Ozonation occurred within a chapel with exhaustion in two cycles of 90 min of exposure to a concentration of 48 mg.

2.3 Exposure to Ozonated Water

A hydraulic apparatus containing a reservoir for storing distilled water was developed. This reservoir has an outlet where a pump of the centrifugal type was coupled, and to this was connected a three-way valve (Venturi). The entry of hollow zone gas through the third access route of this valve, thus produces the mixture with pumped water, after passing through the Venturi the ozonized water will drain the two surfaces that make up the PLA connector, which returns by draining the reservoir, thus closing the hydraulic circuit. The excess ozone gas during this process is collected through a flexible tube, from the reservoir cover, the surplus O₃ was processed and discarded to the external medium through the exhaust system as shown in Fig. 3. A sensor that instantly obtains the dissolved ozone value was used to perform the analysis of ozone concentration in water using the tri-electrode measurement method (DOZ30, Clean[®]).

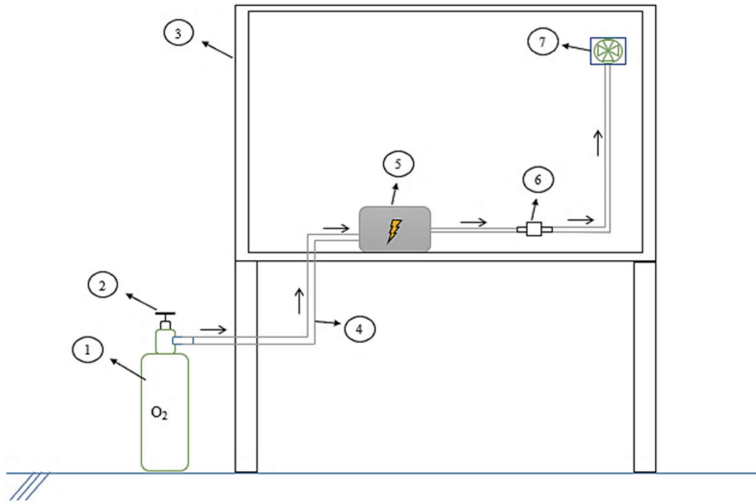


Fig. 2. Mounting equipment for the exposure of electrical parts to ozone gas. (1) Oxygen cylinder, (2) Pressure reducing valve and flow control, (3) Chapel with exhaust, (4) Silicone hose, (5) generator O₃, (6) PLA printed connector, (7) Overall disposal exhaust fan

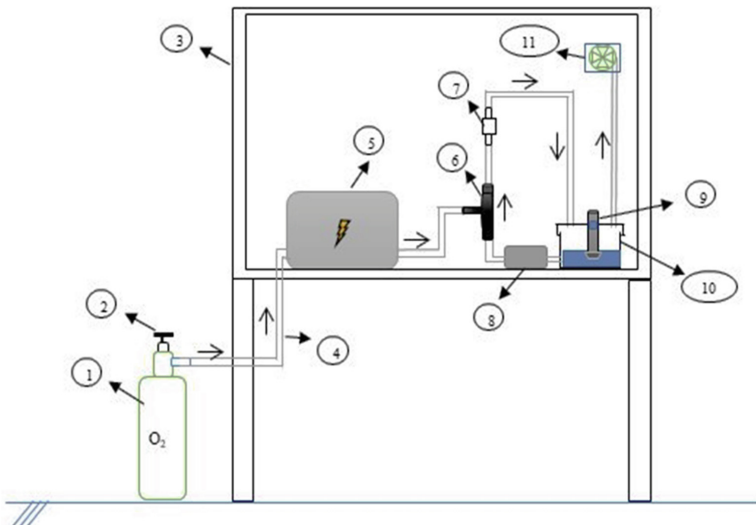


Fig. 3. Assembly was performed for the experimentation of exposure of parts containing flat surfaces of PLA, to ozonized water in a fluid dynamic situation. (1) Oxygen cylinder, (2) Pressure reducing valve and flow regulator, (3) Exhaust chapel, (4) Silicone hose, (5) O₃ generator, (6) Venturi valve, (7) sample connector printed in PLA, (8) Water pump, (9) Ozone sensor (10) Water tank, (11) Exhaust fan for the ozone not used.

2.4 Exposure to Ultraviolet (UV)

This stage was carried out in the Optical Diagnosis laboratory at the Center for Innovation, Technology, and Education (CITÉ) Technological Park of São José dos Campos/SP. To perform the exposure of the PLA part to the UV, a chamber constructed with medium-density fiber panels was used, in this, there are mercury gas lamps of the “germicidal” type, which emit light radiation in the spectral bands UV-A + UV-B, (26 W, Zoo Med, CA, USA, 2 units; 26 W, Exo Terra, MA, USA, 2 units; and 15 W, Sylvania, Bavaria, Germany, 1 unit) (Fig. 4). Two cycles for each time 90 min of exposure were performed.

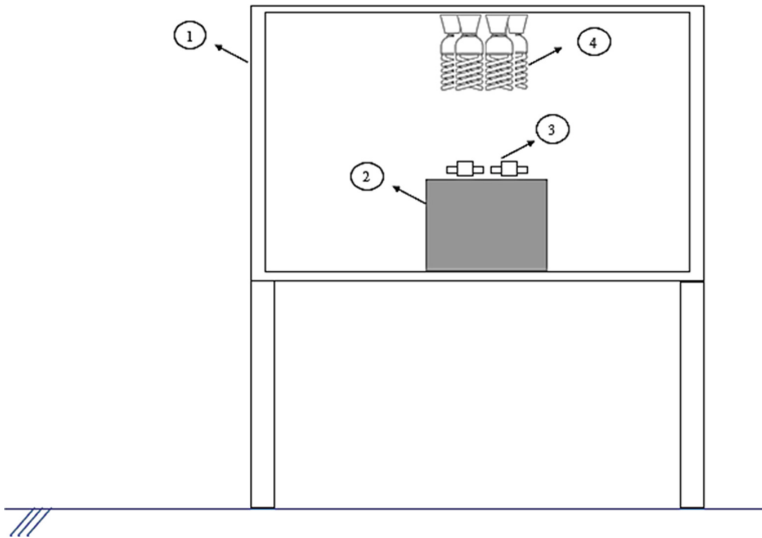


Fig. 4. Schematic representation of assembly for the exposure of sample parts constituted of PLA before UV radiation. (1) Reflective chamber for exposure, (2) Base with 40 cm height (3) PLA samples with separate symmetrical parts to allow the incidence of radiation, (4) UV lamps - A + UV - B.

2.5 Analysis of Parts Using an Optical Microscope

The images of microscopic optics were obtained in the Biomedical Instrumentation laboratory at the Center for Innovation, Technology, and Education (CITÉ) of the Technological Park of São José dos Campos/SP, through the optical microscope (Opton TNB-01T). The microscope is equipped with a set of lenses that offer magnifications of $\times 10$, $\times 40$, $\times 100$, and $\times 1000$ and a digital camera coupled to a computer for capturing images.

Optical microscopy was used as a non-destructive technique to investigate the surface of the parts. A more detailed analysis was performed in $\times 40$ magnification with the change of focus depth/microscope position, to also visualize surface reliefs.

3 Results

Through the data collected from the ozone sensor, the curve of dissolved ozone concentration in the reservoir water was obtained, where it was verified that the maximum concentration reached 7.73 mg.L^{-1} . The data comprise the average of the two ozonation tests using distilled water for each 90 min cycle. The second curve indicated by the dashed line represents the average curve of the measurement points according to the polynomial equation representing the correlation coefficient (R2). This mathematical function, shown in Fig. 5, allows the calculation of ozone concentration in water as a function of ozonation time.

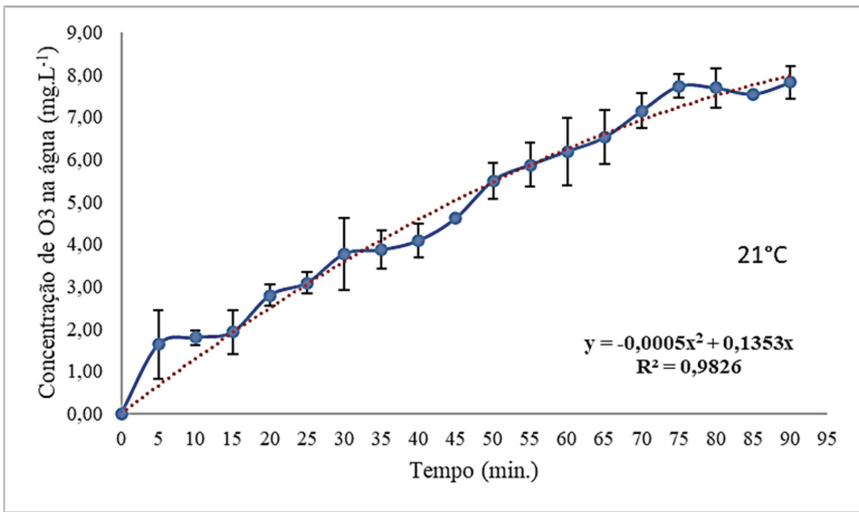


Fig. 5. Determination of the ozone concentration (mg.L^{-1}) dissolved in the water according to time.

When evaluating through the optical microscope it was possible to visualize that even after the second 90-min exposure cycle to the ozone gas in high concentration there was no degradation of the PLA part (Fig. 6).

After exposure of PLA pieces to ozonated water, it was observed that there was no degradation even after exposure to the second cycle of 90 min (Fig. 7).

When performing the analysis through the optical microscope it was possible to observe that after the second cycle of exposure of 90 min to the UV there was the degradation of the PLA part, with a reduction of the material, even eliminating parts and increasing the depth of the grooves as it is possible to observe through the indications in Fig. 8.

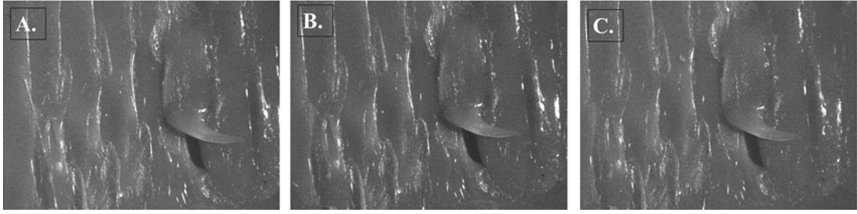


Fig. 6. Images were obtained from surfaces exposed to the flow of ozone gas, using the optical microscope with an x40 lens. (A) Before exposure to ozone gas. (B) After the first 90 min cycle of ozone gas actuation. (C) After the second cycle of 90 min of exposure to O_3 .

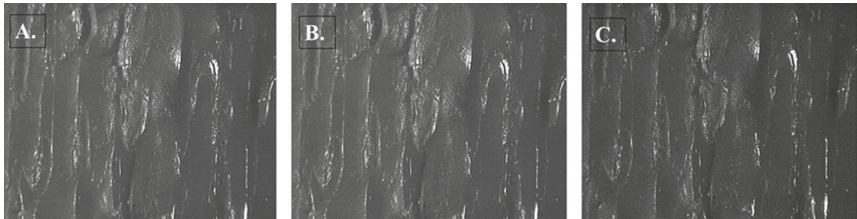


Fig. 7. Images were obtained from samples exposed to the ozonized water in fluid dynamic conditions, using an optical microscope with an x40 lens. (A) Before exposure to ozone water. (B) After the first 90 min cycle. (C) After the second cycle of 90 min.

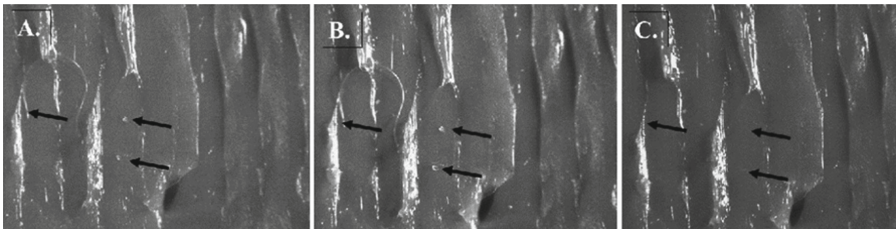


Fig. 8. Images were obtained through the microscope with an x40 lens, before exposure to UV light. (A) Before UV exposure. (B) After the first 90 min cycle of UV exposure. (C) After the second cycle of 90 min of UV exposure. The Arrows indicate where the material was degraded.

4 Discussion

3D Printing is an area of manufacturing engineering that is characterized by stages of building parts by automatic deposition layer by layer from a virtual model controlled by computer programs [3]. Recently due to the critical lack of personal protective equipment that occurred during the COVID-19 pandemic, the researchers [11], after analyzing the possibility of using 3D printing for the development of masks, found that despite the porosity, PLA can be considered appropriate material for this use.

Metal/mechanical machining and forming technology demand machines, devices, tools, and molds in the course of relatively high time and cost. The advantage of using part printing systems, with the use of 3D printers, is to obtain low production cost parts

with different geometries and details without the organizational need for machining and assembly [12].

The manufactured parts are macroscopic objects, and the current study was focused on their ability to resist exposure to high ozone concentration both in their gaseous phase and dissolved in water and UV radiation, due to the use of these agents in health. Knowing that these agents cause the degradation of organic materials and polymers in general, this study aimed to evaluate the degree of damage due to the actions of the agents already mentioned. The results of optical microscopy showed that ozonized water and ozone gas did not degrade the surfaces of PLA parts.

According to Madrid Declaration on Ozone Therapy [13], the estimated time of ozonation of the water (double-distilled) is from 5 to 10 min for the volume used, since the time of exposition of wounds to O₃ gas is used periods of 5, 10, and 20 min [13]. In the present study, cycles with longer periods were carried out, aiming at greater exposure of the parts to oxidizing agents.

Ozonation is a promising technology, but it presents certain challenges because the materials used to produce this gas and its use systems must present characteristics of resistance to the degradation of this agent [14, 15]. Stainless steel, glass, and Teflon have good resistance to ozone when in moderate concentrations. Copper alloys are susceptible to oxidation, and polyvinyl chloride (PVC) and polyethylene (PE) are generally resistant at low concentrations [14]. In the case of natural rubber, rapid disintegration may occur [14, 15], while silicone has short-term resistance, but oxidizes in prolonged exposure [15].

The preliminary results of this study showed that PLA is a compatible material for the development of parts that act in systems in which the environment has ozone in the gas phase or diluted in water. Thus, due to the ease of obtaining different geometries of parts via 3D printing technology, it has become a viable alternative to the traditional machining and forming machine for the development of parts to be used in health, such as components for ozone therapy or disinfection equipment that use ozone or ozonized water as the main agent.

As can be seen in Fig. 8 there was a degradation of the surface of the PLA piece after the second cycle of UV exposure, corroborating the study conducted by [16]. This work performed by the author already mentioned, it was analyzed the photochemical action that UV-B radiation could cause in the mechanical properties of 3D printed parts made of PLA. After mechanical tests, the authors verified that the resistance decreased slightly for PLA samples submitted to a 24-h exposure, as well as post-exposure to UV-B radiation, which simulates the effect of the SUN's UV action, and the tested parts darkened, instating an increase in reflectivity.

It has been reported that UV radiation, O₃, and other oxygen-related species can oxidize the polymer surface and shorten its shelf life. According to [17] the intensity of UV radiation and the longer exposure time led to gradual photo-oxidation of the PLA surface, which results in visible surface deformation. The longer effect of O₃ concentration, atomic oxygen, and UV radiation causes the disintegration of the ester bonds that make up the material, with PLA samples becoming hydrophilic [10].

In a study carried out by [18], where the possibility of using 3D printing materials for applications in active particle generators, O₃ and UV radiation from electrical discharges

was investigated, they concluded that from a macroscopic point of view, PLA and ABS could be used, at least on the experimental use scale, despite surface damage due to UV exposure.

5 Conclusion

In the present study, the possibility of using 3D printing materials for health applications related to exposure to ozone gas and ozonized water was evaluated. As test samples, PLA parts were used, which were integrated into the ozonation system with the potential to replace stainless steel connectors, for example, becoming a viable alternative with lower production cost and customizable, so that they can be used in health. The analysis of the surface by optical microscopy, after exposure of the groups to O₃ and ozonized water, leads to the conclusion that the use of PLA in parts that will be exposed to ozone gas and ozonized water is promising. The pieces printed in PLA showed mechanical stability and potentially high sealing, also corroborating the ecological aspects, the PLA is biodegradable and free of petroleum derivatives. Another advantage is the possibility of customizing and creating parts through 3D printing as needed in protocols involving ozone.

Acknowledgment. This study was financed in part by the Coordination for the Improvement of Higher Education Personnel - Brazil (CAPES) - Finance Code 001.

Conflict of Interest. The authors declare that they have no conflict of interest.







References

1. Liu, L., Sun, W., Xu, Q., et al.: Carbohydr. Polym. **207**, 297–316 (2019). <https://doi.org/10.1016/j.carbpol.2018.11.077>
2. Grimmelsmann, N., Kreuziger, M., Korger, M., et al.: Adhesion of 3D printed material on textile substrates. Rapid Prototyp. J (2018). <https://doi.org/10.1108/rpj-05-2016-0086>
3. Manoj, A., Ramesh, C.: Biodegradable filament for 3D printing process: a review. J. Eng. Sci. **18**, 11–19 (2022). <https://doi.org/10.30919/es8d616>
4. Ventola, C.L.: Medical applications for 3D printing: current and projected uses. PPTTEK **39**(10), 704 (2014)
5. Tran, T.N., Bayer, I.S., Heredia-Guerrero, J.A., et al.: Cocoa shell waste biofilaments for 3D printing applications. Macromol. Mater. Eng. **302**(11), 1700219 (2017). <https://doi.org/10.1002/mame.201700219>
6. Kaspar, V., Rozlivka, J.: Chemical degradation of 3D printed products. Manuf. Technol. **20**(1), 45–48 (2020). <https://doi.org/10.21062/mft.2020.010>
7. Silva, S.B., Mello Luvielmo, M., Geyer, M.C., et al.: Potentialities of the use of ozone in food processing. Sem-ina: Ciênc. Agrár. **32**(2), 659–682 (2011). <https://doi.org/10.5433/1679-0359.2011v32n2p659>
8. Brodowska, A.J., Nowak, A., Śmigielski, K.: Ozone in the food industry: principles of ozone treatment, mechanisms of action, and applications: an overview. Crit. Rev. Food Sci. Nutr. **58**(13), 2176–2201 (2018). <https://doi.org/10.1080/10408398.2017.1308313>

9. Lee, R., Coote, M.L.: Mechanistic insights into ozone-initiated oxidative degradation of saturated hydrocarbons and polymers. *Phys. Chem. Chem. Phys.* **18**(35), 24663–24671 (2016). <https://doi.org/10.1039/c6cp05064f>
10. Koo, G.H., Jang, J.: Surface modification of poly (lactic acid) by UV/Ozone irradiation. *Fibers Polym.* **9**(6), 674–678 (2008). <https://doi.org/10.1007/s12221-008-0106-1>
11. Vaňková, E., Kašparová, P., Khun, J., et al.: Polylactic acid as a suitable material for 3D printing of protective masks in times of COVID-19 pandemic. *PeerJ* **8**, e10259 (2020). <https://doi.org/10.7717/peerj.10259>
12. Gokhare, V.G., Raut, D.N., Shinde, D.K.: A review paper on 3D-printing aspects and various processes used in 3D-printing. *Int. J. Eng. Technol.* **6**(06), 953–958 (2017)
13. Schwartz, A., et al.: Madrid Declaration on Ozone Therapy. In: ISCO3. Faculdade do Centro Oeste Paulista. Madrid (2010). <https://www.oz.org.br/biblioteca/Madrid-declaration-on-ozone-therapy-/210>
14. Fellows, P.J. (2018). *Food Processing Technology: Principles and Practice*. Artmed Publisher
15. Pirani, S. M. G. (2011). *Application of ozone in food industries*
16. Amza, C.G., Zapciu, A., Baciú, F., et al.: Aging of 3D printed polymers under sterilizing UV-C radiation. *Polym. J.* **13**(24), 4467 (2021). <https://doi.org/10.3390/polym13244467>
17. Eren, H.A., Avinc, O., Uysal, P., et al.: The effects of ozone treatment on polylactic acid (PLA) fibers. *Text. Res. J.* **81**(11), 1091–1099 (2011). <https://doi.org/10.1177/0040517510397576>
18. Mikeš, J., Pekárek, S., Babčenko, O., et al.: 3D printing materials for generators of active particles based on electrical discharges. *Plasma Process. Polym.* **17**(1), 1900150 (2020). <https://doi.org/10.1002/ppap.201900150>



Therapeutic Approaches in the Sequence of Pierre Robin: A Systematic Review of the Literature

J. E. P. Nunes¹ , R. S. Navarro¹ , M. S. A. Mota¹ , B. P. Santos² ,
G. P. Nunes³ , and N. A. Parizotto¹ 

¹ Brazil University, Scientific and Technological Institute, São Paulo, Brazil
jpavini@hotmail.com

² Medicine School, University of the State of Mato Grosso, Cáceres, Brazil

³ Medical School, Várzea Grande University Center, Várzea Grande, Brazil

Abstract. Pierre Robin sequence (PRS) is characterized by micrognathia, glossoptosis and respiratory obstruction with or without cleft palate. These facial abnormalities trigger breathing problems and eating difficulties of varying degrees of complexity. Despite the various therapeutic possibilities currently available, there is the problem of not having a treatment protocol for PRS. The aim of this study is to analyze, through a systematic review of primary clinical studies, the best treatment strategy for SPR. When analyzing surgery risks and postoperative results of surgical interventions to treat patients with SPRS, it is possible to observe that such procedures are safe, in addition to being largely resolutive and effective in the long term, compared to conservative approaches.

Keywords: Pierre robin sequence · Glossoptosis · Micrognathia · Cleft palate

1 Introduction

Pierre Robin sequence (PRS) is a triad of congenital facial abnormalities characterized by: micrognathia, glossoptosis and respiratory obstruction, with or without cleft palate, originally described in 1923 by French stomatologist Pierre Robin [1, 2].

PRS, sometimes referred to as a syndrome, is a sequence in which a primary anomaly leads to multiple secondary anomalies. The initial abnormality is believed to be poor growth of the mandible that occurs between the 7th and 11th week of gestation, significantly reducing the oropharyngeal space. Secondary outcomes are glossoptosis and cleft palate, caused by the anatomical readaptation of the tongue in the reduced space [3, 4]. In this sense, the organ moves superiorly and posteriorly, causing a mechanical impairment in the fusion of the palatal platforms, preventing the correct closure of the palate [4].

PRS is a rare disease that affects 1:8500 to 1:14000 live births [5]. This congenital condition may present alone or in association with syndromes and other malformations, with Stickler Syndrome, Velocardiofacial Syndrome and Treacher Collins Syndrome

being the most prevalent [5, 6]. PRS presents in the neonatal period. Anatomical abnormalities manifest with marked clinical features such as respiratory distress, which can range from mild difficulty breathing to choking attacks, in addition to feeding difficulties that may occur with reduced food intake, prolonged oral feeding (more than 30 min), fatigue, gagging, vomiting, regurgitation and insufficient weight gain which, in combination with other factors, can lead to severe protein-calorie malnutrition [5–7].

Early and effective management is decisive in the prognosis and quality of life of patients with PRS. However, the proper conduct of treatment will depend on the severity of the airway obstruction. To perform the risk stratification of symptoms and to outline the best therapeutic approach, classification scales are used [6].

Among the current treatment options, the first line is based on the so-called conservative approaches, which are the prone or lateral postural maneuvers. When positioning fails to help the patient improve, non-surgical invasive alternatives are the next options, such as nasopharyngeal intubation and positive pressure [7]. Approaches such as glossoptosis, palatoplasty and distraction osteogenesis of the jaw are invasive surgical treatments. At the extreme of therapeutic approaches is the tracheostomy, used in patients with a high degree of impairment [7].

Despite the various therapeutic possibilities, there is the problem of not having a treatment protocol for PRS. Therefore, the objective of this study is to analyze, through a systematic review of primary clinical studies, the best treatment strategy for Pierre Robin. In this sense, it is considered from conservative management to current treatments, which present improvements in breathing and eating difficulties and provide an increase in the quality of life for the patient, as well as a decrease in severe and fatal cases of PRS.

2 Méthod

2.1 Research Strategy

The question that guided this Systematic Literature Review was “What is the best treatment strategy for Pierre Robin Sequence?”. The study was conducted according to the recommendations of the “Cochrane Manual of Systematic Reviews of Interventions” [8].

High sensitivity searches were performed in the following electronic databases: PUBMED, VHL, EMBASE (via ELSEVIER) and COCHRANE, using the following terms: “Pierre Robin Sequence”, “Glossoptosis”, “Micrognathia” and “Cleft Palate” listed in the Health Sciences Descriptors (DeCS) and Medical Subject Headings (MeSH). The combination of descriptors was done using the Boolean operators OR and AND and the high sensitivity strings were built following the particularities of each search engine. No language and time filter was applied, as the study does not aim to limit the search for the best scientific evidence, and articles published until April 2022 were included.

2.2 Article Selection Criteria

The research results were analyzed individually by two blind researchers, following the inclusion criteria: primary observational cross-sectional studies, cohort, clinical trial and

case series dealing with treatment strategy in SPR. Exclusion criteria were: duplicate studies, studies with unavailable full text, publications in which the diagnosis of Pierre Robin was uncertain and articles that did not specifically address Pierre Robin. For the analysis of methodological reliability, only studies with a score >6 on the PEDro scale were included. The choice of articles took place in three stages: the first selection was based on the title; then, the abstract was read; finally, the articles that remained were selected based on the analysis of the full text. During the screening and selection process of the studies, the RAYYAN software was used in order to guarantee the reliability of the blinding of this step. In cases of disagreement between researchers, texts for which the final decision was consensual were excluded.

2.3 Data Analysis

The selected articles were analyzed according to the following aspects: study design, sample characteristics, type of procedure and intervention characteristics, main results and conclusions.

3 Results

Initially, the high-sensitivity search strategies identified a total of 17,423 articles in the four electronic databases, from which animal, in vitro, simulation and secondary studies were automatically excluded through the filters on the search engines. Thus, 299 articles remained in the selection and then, with the help of the RAYYAN tool, 21 duplicates were eliminated. Still with the help of software developed specifically for screening abstracts and titles of systematic reviews, the blinding step was activated and two reviewers made the selection by title and abstract. At this stage, 201 studies were excluded, leaving a total of 77 articles. There were disagreements between the evaluators and, after resolving these conflicts, a total of 57 studies were elected to read the full text. After applying the inclusion and exclusion criteria, as well as the methodological reliability analysis score (PEDro Scale), 8 articles were accepted for this review (Fig. 1). Table 1 presents a summary of the main information analyzed in each study.

4 Discussion

This study reaffirms the need to develop an internationally recognized clinical protocol in order to guide the various health services for the treatment of patients with Pierre Robin sequence. Most of the articles qualitatively analyzed in this systematic review highlighted the need for new studies of high value in scientific evidence involving all the therapeutic approach strategies used in PRS. One of the characteristics of this condition is the heterogeneity of clinical manifestations, which is hardly addressed in clinical studies due to strict methodological criteria.

The choice of the best therapeutic approach is directly related to the degree of respiratory function impairment and feeding difficulties. The literature, in general, mentions the use of prone and lateral positioning maneuvers as the first line of treatment. However, probably because it is a very conservative procedure, no clinical studies were found

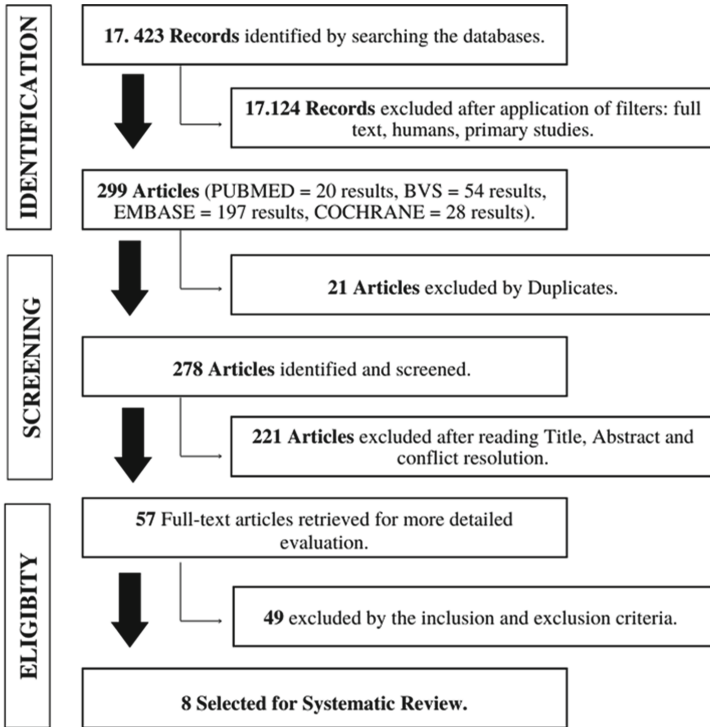


Fig. 1. Systematic review flowchart recommended by PRISMA

in this regard. In a study developed at the Hospital for Rehabilitation of Craniofacial Anomalies of Bauru (HRAC-USP) by Marques et al. [9], thirty children with PRS, were treated with prolonged nasopharyngeal intubation (NTI) in order to test the best type of diet. One group of infants received a highcalorie diet (milk formula supplemented with 5 to 7% polymers of glucose and 3 to 5% medium-chain triglycerides), and another group of infants received formula alone. The choice of diet for each infant was randomized. In both groups, the children started the diets before 1 month of age and were maintained until 6 months of age. The study showed, through the analysis of weight and length, that children with a high-calorie diet showed an improvement in their nutritional status and, consequently, in their respiratory conditions, allowing for an earlier suspension of NTI.

NTI is an invasive and temporary treatment, as there may be improvement in the condition or the need for more invasive measures. Devices like the epiglottic plate show promise. And it was analyzed in two studies as an alternative to NTI.

Bacher et al. [10] carried out a study showing that the preepiglottic stick plate (PEBP) with velar extension can offer a safe and effective alternative capable of avoiding more invasive interventions until the cleft palate can be surgically closed. The prospective and observational study included 15 babies up to 3 months of age undergoing orthodontic

Table 1. List of articles selected for qualitative analysis

Author	Sample	Procedure	Conclusion
Marques et al. [9]	9 babies 0–6 months old	Nasopharyngeal intubation (NPI) and hypercaloric diet	The hypercaloric diet led to an improvement in the nutritional status and, probably, in the respiratory conditions of patients with isolated RS, allowing an earlier suspension of NPI
Bacher et al. (2009)	15 babies up to 3 months old	Oral device Pre-epiglottic stick plate (PEBP) Oral device Pre-epiglottic stick plate (PEBP)	PEBP with velar extension can be a safe and effective alternative to avoid more invasive interventions until the cleft can be surgically closed
Poetas et al. [11]	49 babies > 1 year old	Oral device Pre-epiglottic stick plate (PEBP) Oral device Pre-epiglottic stick plate (PEBP)	This study confirms the effectiveness of PEBP treatment in improving upper airway obstruction and feeding problems, which are the main clinical complications of infants with PRS. Collaborate collaborative work is needed to compare this with other treatment approaches
Morovic [15]	31 babies	Osteogenic distraction of the mandible	Mandibular distraction is a successful method for young patients with PRS to relieve airway obstruction, improve feeding, and prevent early tracheotomy or decannulation in previously tracheotomized patients

(continued)

treatment without randomization. Using a maxillary plaster used as a mold, the PEBP was custom built, covering both the palate, including the cleft, and the alveolar ridges.

Table 1. (continued)

Author	Sample	Procedure	Conclusion
Lozano-Cifuentes et al. [12]	31 babies - 3–90 days old	Osteogenic distraction of the mandible	Patients with PRS treated with mandibular distraction for airway clearance with a maxillomandibular overjet of 7 mm or greater had less treatment failure with $p < 0.01$
Jiayu et al. [16]	100 babies between 15 days—14 months of age	Osteogenic distraction of the mandible	Patients' physiques improved after distraction osteogenesis surgery, mainly reflected by weight gain and growth curves in length. Body shape also progressed, indicating that the nutritional status of patients after surgery also improved
Carpes [15]	53 babies between 10—23 months of age	Palatoplasty. Rating by polysomnography	The prevalence of obstructive sleep apnea found was 61.9% before palatoplasty, and 33.3% postoperatively. Palatoplasty indicated a positive result in relation to sleep-disordered breathing
Cardim et al. [14]	12 babies	Operative technique. Orthoglossopelvis-plasty	Orthoglossopelvis-plasty allowed the unlocking of airway obstruction generated by poor lingual positioning, improved feeding function and mandibular development, with low surgical morbidity and few complications

The oral appliance included a velar extension of about 2 to 3 cm in length, moving the dorsum of the tongue forward, thus widening the hypopharyngeal space. Positioning in terms of angle and length was controlled and adjusted by nasal endoscopy. Patients underwent sleep studies at admission, at discharge and after three months of discharge, and body weight was monitored weekly. The study suggests that this protrusion is sufficient to reduce the frequency of apneas not only in the acute phase, but also up to 3 months after the initial admission.

A cohort study conducted in Germany by Poetas et al. [11] reaffirms the effectiveness of PEBP in improving upper airway obstruction and weight gain in PRS infants. The median length of stay for orthodontic treatment was 3 weeks, the effectiveness of the plaque in relieving upper airway obstruction was confirmed by additional sleep studies, and 69% of babies were discharged without a feeding tube after starting PEBP treatment. Both INF with a high-calorie diet and the pre-epiglottic stick plate are temporary alternatives pending a definitive therapeutic option, such as a surgical technique. The surgical procedure of mandibular distraction is widely studied in the literature, as well as in several case reports in which the technique proved to be beneficial in the resolution of respiratory obstruction and feeding difficulties. The objective of jaw distraction osteogenesis (MDO) is to induce tissue neoformation between two segments of a bone and trigger bone neoformation from the surgical separation of two structures.

Morovic [12] submitted 31 patients with PRS to mandibular distraction, which resulted in relief of airway obstruction in all cases. Two cases underwent tracheotomy at birth, which was removed during the process and two other patients had pulmonary hypertension and clinical signs also reversed after distraction. Her weight charts improved significantly after the surgery. Post-distraction feeding was greatly facilitated, with reduced time (average of 20 min) due to more effective swallowing. In the long-term followup, they did not present respiratory obstruction, and in all cases early distraction was the only and definitive treatment. The nutritional evolution of 100% of the patients was positive.

In Buenos Aires, Argentina, Lozano-Cifuentes et al. [13] performed a prospective randomized comparative study in patients diagnosed with PRS undergoing osteogenesis by mandibular distraction. Through the maxillomandibular discrepancy, the study found that there was an association between greater or lesser success in the outcome of the procedure. Patients with PRS treated with mandibular distraction for airway clearance with a maxillomandibular overjet of 7 mm or more had fewer treatment failures with $p < 0.01$.

Recently, a study carried out in Malaysia by Jiayu et al. [14] showed that bilateral distraction osteogenic surgery of the mandible also has a positive effect on the nutritional status of children with PRS. In this study, all patients were fed whole milk and t tests for independent samples were used to analyze pre- and postoperative indicators. The WFA percentile increased from 14.16 ± 2.17 to $15.01 \pm 1.85\%$ ($P = 0.0048$), the WFA z score increased from -2.40 ± 0.18 to -1.90 ± 0.14 after surgery ($P = 0.0010$), the LFA percentile increased from 20.04 ± 3.48 to $33.67 \pm 4.29\%$ ($P = 0.0098$), the LFA z score increased from -2.09 ± 0.19 to -1.42 ± 0.23 ($P = 0.0009$), the BMI z score increased from -1.95 ± 0.22 to -1.39 ± 0.16 ($P = 0.0408$), ALB increased from 37.06 ± 0.51 to 42.85 ± 0.30 g/L ($P < 0.001$), which indicates that the physique of patients improved after distraction osteogenesis surgery, reflected mainly by weight lifting and

growth curves in length; body shape also improved, indicating that the nutritional status of patients after surgery also improved.

The osteogenic distraction of the mandible was used in most studies as a permanent and resolute procedure, however, in some cases a new procedure is necessary to correct any problems.

Carpes [15] evaluated the effects of palatoplasty on obstructive sleep apnea using polysomnography (PSG) in 53 patients diagnosed with PRS. The prevalence of obstructive sleep apnea found was 61.9% before palatoplasty, and 33.3% postoperatively. Palatoplasty indicated a positive result in relation to sleep-disordered breathing, reducing both the rates of respiratory events and their severity.

A Brazilian study carried out at the Benefício Portuguesa Hospital of São Paulo, Núcleo de Cirurgia Plástica Avançada developed a new operative technique for lingual repositioning of PRS patients with glossoptosis. Cadim et al. [16] followed 12 patients, previously submitted to conservative treatment with postural maneuvers of lateral/ventral decubitus, use of nasopharyngeal cannula and speech therapy without success. The surgical indication for muscular and functional reorganization of the tongue with the “Orthoglossopelveplasty” technique was given by physical and speech-language examinations. The results were analyzed in relation to the evolution of the treated patients, in terms of morbidity and mortality data, and the need for tracheostomy and/or gastrostomy.

Four patients were operated on with this technique and 8 associated with osteogenic distraction of the mandible. The evolution of the patients was as follows: 3 cases evolved with no need for tracheostomy and gastrostomy; 2 cases, with the need for postoperative tracheostomy (due to laryngomalacia and tracheal stenosis); in 1 case it evolved with the need for postoperative gastrostomy (due to Edwards syndrome); 2 cases, with the need for postoperative tracheostomy and gastrostomy (due to laryngomalacia); in 4 cases that had previous tracheostomy and gastrostomy evolved with: tracheostomy and gastrostomy removal, tracheostomy removal programming, gastrostomy removal and death (died during cardiac surgery) respectively. The study states that the performance of orthoglossopelveplasty is effective, functional and anatomical, with less surgical extension and complications. It is important to highlight that there are positive and negative aspects of both conservative and surgical approaches. Surgical interventions are shown to be safe, resolute and effective, compared to conservative actions. In the studies of high methodological qualities selected in the present systematic review, there is a lack of information to establish specific protocols, due to the great variability of symptoms and clinical manifestations, which makes it difficult to establish restrictive methodologies.

5 Conclusion

When analyzing surgery risks and postoperative results of surgical interventions to treat patients with PRS, it is possible to observe that such procedures are safe, in addition to being largely resolute and effective in the long term, compared to conservative approaches.

Due to the diversity of approaches in the treatment of PRS, observed in most of the articles analyzed in this systematic review, as well as the heterogeneity of clinical manifestations of this condition, the relevance and urgency of establishing a clinical

protocol for elaboration, analysis and international recognition is evident., which seeks to allocate, in the various health sectors, a gold standard treatment for patients with PRS.

The cost-benefit of the numerous therapeutic procedures for SPR must be considered. In addition, it is suggested the integration and partnership of international and national health reference centers in the elaboration of the protocol, in order to analyze, through sleep studies and weight and growth charts, which treatment approaches are suitable for each patient. More effectively and efficiently in its patient population.

Conflict of Interests. The authors declare that there are no conflicts of interest in carrying out this study.










References

1. Robin, P.: A queda da base da língua considerada como um novo causa de desconforto na respiração nasofaríngea. *Bull Acad Natl. Med (Paris)*. **89**(34–41), 2 (1923)
2. Robin, P.: Glossoptose por atresia e hipotrofia da mandíbula. *Am J Dis Criança*. **48**, 541–547 (1934)
3. Tan, T.Y., Kilpatrick, N., Farlie, P.G.: Developmental and genetic perspectives on Pierre Robin sequence. *Am. J. Med. Genet., C: Semin. Med. Genet.* **163**, 295–305 (2013)
4. Scott, A.R., Tibesar, R.J., Sidman, J.D.: Pierre Robin sequence: evaluation, management, indications for surgery, and pitfalls. *Otolaryngol. Clin. North Am.* **45**, 695–710 (2012)
5. Evans, K.N., Sie, K.C., Hopper, R.A., Glass, R.P., Hing, A.V., Cunningham, M.L.: Robin sequence: from diagnosis to development of an effective management plan. *Pediatr.* **127**(5), 936–48 (2011). PMID: 21464188. <https://doi.org/10.1542/peds.2010-2615>
6. Marques, I.L.: Sequência de Pierre Robin: diagnóstico e abordagens terapêuticas. *Anais (2013)*. ISSN: 2318–3314
7. Marques, I.L., Sousa, T.V., Carneiro, A.F., Barbieir, M.A., Bettiol, H., Gutierrez, M.R.: Experiência clínica com lactentes com sequência de Robin: um estudo prospectivo. *Fissura Palatina Craniofac J.* **38**, 171–178 (2001)
8. Higgins, J.P.T., Thomas, J., Chandler, J., Cumpston, M., Li, T., Page, M.J., Welch, V.A. (eds.): *Cochrane Handbook for Systematic Reviews of Interventions* versão 6.3 (atualizado em fevereiro de 2022). Cochrane (2022). Disponível em www.training.cochrane.org/handbook
9. Marques, I.L., Peres, S.P., Bettiol, H., Barbieri, M.A., Andrea, M., De Souza, L.: Revista fenda palatina-craniofacial. **41**(1), 53–58 (2004). adicionado ao CENTRAL: 31 de outubro de 2004 | 2004 Edição 4 <https://doi.org/10.1597/02-043>
10. Bacher, M., Sautermeister, J., Urschitz, M.S., Buchenau, W., Arand, J., Poets, C.F.: An oral appliance with velar extension for treatment of obstructive sleep apnea in infants with Pierre Robin sequence. *Cleft Palate Craniofac. J.* **48**(3), 331–336 (2011). <https://doi.org/10.1597/09-091>
11. Poetas, C.F., Maas, C., Buchenau, W., Arand, J., Vierzig, A., Braumann, B., Muller-Hagedorn, S.: Revista Orphanet de doenças raras. **12**(1), 1–6 (2017). | adicionado ao CENTRAL: 30 de abril de 2017 | Edição 4 <https://doi.org/10.1186/s13023-017-0602-8>
12. Lozano-Cifuentes, A., Siguén, M.I., Ayrad, Y.M., Díaz, P.A., Apa, S.N.: Secuencia de Pierre Robin: implicación de la fisura palatina en la distracción mandibular. *Cir. plást. iberolatinoam.* [Internet]. [citado 2022 Mayo 26]; **44**(3), 281–286 (2018). <https://doi.org/10.4321/s0376-78922018000300008>

13. Carpes, A.F.: Avaliação polissonográfica e endoscópica em crianças com seqüência de Robin isolada submetidas a palatoplastia [tese]. Faculdade de Medicina, Universidade de São Paulo, São Paulo (2015)
14. Cadim, V.L.N., Peixoto, J.H., Silva, A.S.: “Ortoglossopelveplastia” e o algoritmo de sua utilização na seqüência de Pierre-Robin. *Rev. Bras. Cir. Plást.* **34**(2), 228–236 (2019)
15. Morovic, I.C.G.: Manejo real en síndrome de Pierre Robin. *Rev. chil. pediatra* (2004). <https://doi.org/10.4067/S0370-41062004000100005>
16. Jiayu, L., Jing, S., Yiyang, C., e Fan, L.: Estudo sobre o Efeito da Bilateral Distração da Mandíbula Osteogênese sobre o estado nutricional dos bebês Com Sequência Pierre-Robin. *Fronte. Pediatra* **9**, 771333 (2021). <https://doi.org/10.3389/fped.2021.771333>



Cardiopulmonary Exercise Testing Data Processing and Storage Tools

G. B. Penteado¹ , V. R. Uemoto^{1,2} , F. C. Araujo³ , R. D. D. Buchler⁴ ,
C. A. C. Hossri⁴ , R. S. Meneghelo¹ , R. V. Freitas² , R. A. Hortegal² ,
and H. T. Moriya^{1,2} 

¹ Biomedical Engineering Laboratory, University of São Paulo, São Paulo, Brazil
vinicius.uemoto@dantepazzanese.org.br

² Personalized Cardiovascular Medicine Section, Dante Pazzanese Cardiology Institute, São Paulo, Brazil

³ FCA Sports, Belo Horizonte, Brazil

⁴ RehabilitationSection, Dante Pazzanese Cardiology Institute, São Paulo, Brazil

Abstract. Conducting a clinical study is a complex and challenging task, so using technology to facilitate the process is necessary for the medical and scientific community. Data digitization is needed to store and process it. Digitization speeds up data visualization techniques so scientists can analyze it most effectively depending on their goals. In this project, we developed two digital tools related to the cardiopulmonary exercise test (CPET) data, one for digitizing PDF reports and the other for generating databases. The latter was a web-based database visualization dashboard. Users can select parameters of interest and check for differences among subgroups. Basic statistical tests are performed for each variable under analysis, and its results are presented in numerical and graphical formats. The initial statistical tests and the derived recommendation will guide the research team in deeper statistical analysis and robust analysis supporting more decisive conclusions. We ended up with the first version for both tools and validated it using patients' CPET data from the Dante Pazzanese Institute of Cardiology. We conducted a pilot study to verify if the tools served their purpose and observed that both programs worked as planned. The tools can be further tailored to be clinically or research-oriented. On the analysis of CPET's results, the conclusions for our example study were in line with what is presented in the bibliography for cardiorespiratory physiology.

Keywords: First keyword · Second keyword · Third keyword

1 First Section

1.1 A Subsection Sample

Data digitization and database generation are crucial steps in the clinical research process. Here we present two tools developed and used to analyze the patients' data in the Personalized Cardiovascular Medicine Section (PCMS) of the Dante Pazzanese Institute of Cardiology (DPIC). The PCMS main research line concerns studying and understanding heart failure with preserved ejection fraction's effects on patients and how to

detect and classify subjects with this disease [1]. All patients in this project underwent cardiopulmonary exercise tests (CPET) as part of the PCMS screening routine.

Since the CPET equipment does not allow users to access the raw data recorded during the exam, we developed specific tools to help extract and organize the data. The first tool is based on the optical character recognition (OCR) script to obtain and store the relevant data from the auto-generated PDF reports. The second is a web-based dashboard that runs basic statistical tests on the database and allows users to visualize the results besides charting the desired variables. These tools were necessary to extract the patient's data from the PDF reports and perform post-processing and preliminary statistical tests to automate data collection and analysis.

2 The Cardiopulmonary Exercise Test Data Processing

Cardiopulmonary Exercise Test

The CPET consists of an exercise test in which subjects complete a progressive and maximal effort on a treadmill or a bicycle ergometer. Several physiological variables are monitored during the trial, including a 12-lead electrocardiogram (ECG), breath-by-breath gas analysis (O_2 and CO_2), oximetry, blood pressure, etc. Through comparisons with normative knowledge databases, trained physicians can diagnose cardiovascular, respiratory, or metabolic diseases in their patients. In the following list, we can see the primary variables measured during a CPET [2].

- O_2 , CO_2 , and ventilated volumes
- O_2 and CO_2 partial pressures
- Heart rate, blood pressure
- Workload
- Aerobic and anaerobic thresholds
- Respiratory exchange ratio (RER)
- VE/VCO_2 slope
- Oxygen uptake efficiency slope (OUES)

In this study, all subjects were submitted to a CPET in a laboratory equipped with a gas exchange analysis system (Ultima Cardi O_2 breath-by-breath gas analyzer, MGC Diagnostics, USA), a 12-lead ECG (Cardio Perfect Systems, Welch Allyn, USA), a treadmill (TMX428CP, TrackMaster, USA), a sphygmomanometer and a finger oximeter. All patients had the measurement devices adequately attached to them while running on the treadmill. The CPET workload was increased until the patient's exhaustion. Local institutional and national review boards approved the data collection protocols used at PCMS (CAAE 39592920.3.000.5462).

2.1 Difficulties in Data Storage and Digitalization

All the data obtained during the test must be stored in a database throughout the process. However, neither the software nor the hardware allows the user to access the raw data. The only data available after the test is an auto-generated PDF report by the CPET software (Breeze 8.6, MGC Diagnostics, USA). The report has some interpolated data and the measured values for significant physiological moments of the test. These include resting, ventilatory thresholds, and maximal VO_2 consumption and work [3]. Therefore, to create a database, it was necessary to extract as much relevant information as possible from the report, store it and make it available in a user-friendly interface, including fundamental statistical analysis.

3 Data Process, Storage, and Analysis Tools

3.1 Script for Obtaining and Storing the Data

To digitize the data from the reports, we developed a Python-based script that converts the PDF report into a string using OCR. Then, the desired data was extracted from the files and merged into a CSV file used as the dashboard tool's database.

The script required two inputs from the user: 1) load the exported PDF file of each patient's CPET, and 2) set the undetected ventilatory thresholds or overlap them manually if needed. The workflow of the script is illustrated in Fig. 1.

3.2 Web-Based Dashboard for Data Visualization and Statistical Analysis

A dashboard was built to provide preliminary statistical and visualization analysis for scientists using the database. Different physiological parameters and patient subgroups can be quickly selected and compared, including a few statistical tests and auto-generation instructive charts. The charts can be exported as PNG files for use in research publications. The statistical analyses were chosen and validated according to the current recommended practices for biostatistics [4].

There are two dropdown menus at the top left box of the dashboard's main page (Fig. 2). The one on top is dedicated to CPET-derived parameters. At the same time, the one below it is committed to clinically significant moments of the test (resting, aerobic threshold (AT), respiratory compensation point (RCP), maximum VO_2 consumption, or maximum workload). Relative values are also available through the checkbox above the first dropdown menu. They are computed as the ratio of the absolute values and the predicted (normative) data.

After picking the parameters of the desired analysis, the statistical analysis is computed. First, a normality test is done to verify which hypothesis test will be used. A simple t-student/ANOVA is selected if a normal distribution is confirmed. Otherwise, a Kruskal-Wallis test is done. The bottom left box (Fig. 3) has a table on top with a comparison between groups. The table is followed by the p-value, the minimum sample size [4] for each group, and the normality test result of the parameters selected.

A subpage (Fig. 4) of the dashboard allows users to see the individual records of the database. Users can access it at the top main menu. When the page is loaded, filters are



Fig. 1. Digitalization and Storage script workflow.

available to sort subjects that have a specific value or are in a determined range. The feature is useful when searching for outliers or editing records with known reporting errors.

3.3 Tools Validation

To validate the developed tools, we conducted a comparative study between male and female PMCS patients.

We used the script to create the database from the PDF files from the gas analyzer and its respective software to generate reports for 102 PCMS patients. Using this database in the dashboard, we compared all the available variables at the most critical instants of time (AT, RCP, VO_2 max, and maximum workload). The respective p-values and minimum population sizes from these comparisons that showed differences among the different groups could be seen in Table 1 [4].

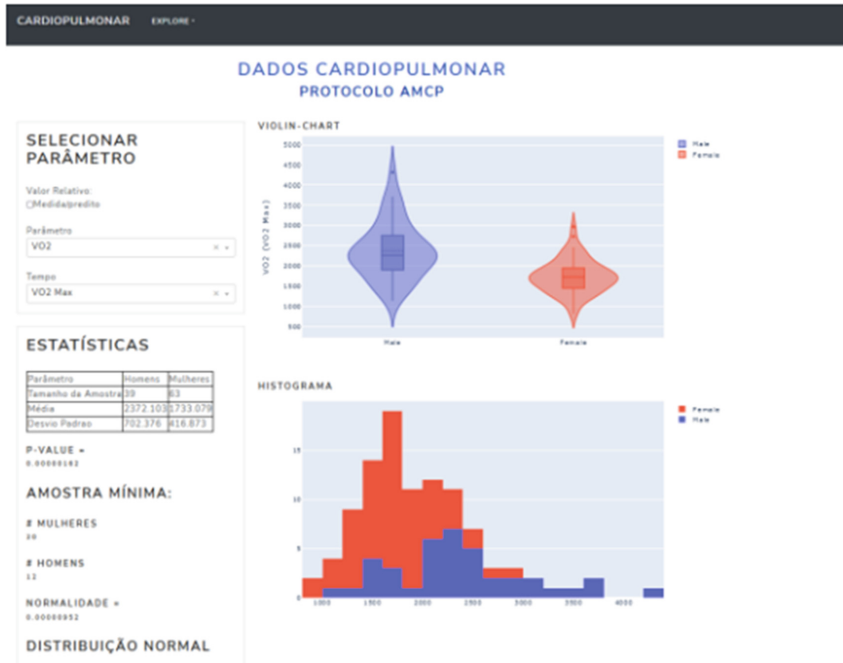


Fig. 2. Dashboard's main page with all graphs (right), parameters selection (top left box), and all statistical results for the chosen parameter (bottom left box).

As shown in Table 1, most of the differences that can be seen between men and women that were submitted to the CPET are mostly presented when comparing absolute gas volume values throughout the entire exam and for some relative values at significant CPET moments.

Hormonal and anatomical variations could explain the differences between genders, promoting unequal gas volume consumption or exhalation during the test [5, 6].

4 Conclusions

After the validation study, we observed that the developed tools and workflow could be used to digitalize, store, and analyze data from simple reports of the CPET tests. Currently, the software and hardware do not allow users to access and export the data freely, and the PDF files are the only way to export some data from each exam.

It is important to reiterate that the developed tools were made exclusively for exams using a specific combination of gas-analyzer hardware and software. It can be easily adapted to any other equipment-program variety. Currently, the dashboard tool provides a comparison between genders, but it can be easily extended to new groups or classifications.



Fig. 3. Results from the statistical analysis. The table on top is formatted to show the subgroups in columns, while the rows display the sample size, mean value, and standard deviation. At the bottom, we have the p-value of the groups’ comparison, the minimum sample size for each group, and the normality test result of the parameters selected.

We plan to integrate both tools in the subsequent iterations, so they do not need to be run separately. We are also planning to implement them in the rehabilitation.

section of the DPIC after making some adaptations. It would follow the section’s research line to improve and optimize projects using CPET’s data.

ID	VO2 (REST)	VO2 (LA)	VO2 (RCP)	VO2 (VO2 MAX)
[Redacted]	163	946		1284
[Redacted]	451	1189	1310	2184
[Redacted]	157	886		1589
[Redacted]	386	1691	2904	3392
[Redacted]	148	1238	1685	1925
[Redacted]	544	1946	2331	2729
[Redacted]	193	887	1222	1498
[Redacted]	286	1142	1594	1698
[Redacted]	285	1874	1797	2149
[Redacted]	211	1835	1377	1632
[Redacted]	178	596		869
[Redacted]	290	1368	1798	1957
[Redacted]	443	1855	1533	1793
[Redacted]	498	1822	1389	1496
[Redacted]	284	911	1242	1388

Fig. 4. Part of the subpage showing individual records of the chosen VO_2 variable. Black rectangles purposely covered the patient institutional ID. Filters fields are available on the second row.

Table 1. Significant differences detected between gender

Parameter (Time)	Minimum Population Size		p-Value (%)
	Women	Men	
	Example		
	Women	Men	
VCO ₂ (VO ₂ MAX)	19	12	<0,01
VO ₂ (VO ₂ MAX)	20	12	<0,01
VO ₂ (AT)	25	15	<0,01
VE (VO ₂ MAX)	27	17	0,01
VO ₂ (WORK MAX)	36	19	0,01
VCO ₂ (AT)	29	18	0,01
VO ₂ (RCP)	27	17	0,01
VCO ₂ (WORK MAX)	33	20	0,01
VCO ₂ (RCP)	27	17	0,03
Relative VE (AT)	35	22	0,04

(continued)

Table 1. (continued)

Parameter (Time)	Minimum Population Size		p-Value (%)
	Women	Men	
	Example		
	Women	Men	
Relative VO ₂ (AT)	44	27	0,04
VE (AT)	36	22	0,06
Relative VCO ₂ (AT)	45	28	0,07
VE (WORK MAX)	42	26	0,18
Relative VE (RCP)	38	29	0,21
Relative VO ₂ (RCP)	51	39	0,31
VE (RCP)	42	26	0,48
Relative VCO ₂ (RCP)	59	45	1,26
Relative VO ₂ (VO ₂ MAX)	95	59	1,30
PETO ₂ (AT)	133	82	1,64
Relative VO ₂ (WORK MAX)	144	89	2,33
METS (VO ₂ MAX)	65	40	2,61
PETO ₂ (RCP)	89	55	3,01

References

1. Uemoto, R.V., et al.: The impact of isometric handgrip testing in left atrial reservoir function. *Eur. Hear. J.-Cardiovasc. Imaging* 23. Supplement_1 (2022): jeab289- 104
2. Herdy, A.H., Ritt, L.E.F., Stein, R., Araujo, C.G.S., De Milani, M., Meneghelo, R.S., Ferraz, A.S., Hossri, C.A.C., Almeida, A.E.M., De Fernandes-silva, M.M., Serra, S.M.: *Teste Cardiopulmonar De Exercício: Fundamentos, Aplicabilidade E Interpretação. Arquivos Brasileiros De Cardiologia*
3. MEDICAL GRAPHICS CORPORATION.: *Breeze Manual: Printed Documentation*, p. 467. Saint Paul, Minessota, USA
4. Motulsky, H.: *Intuitive Biostatistics: Anonmathematical Guide to Statistical Thinking*. 4th edn, p. 568. Oxford University Press, New York, 2018
5. Wasserman, K., Hansen, J.E., Sue, D, Whipp, B.J., Casaburi, R.: *Principles of exercise testing and interpretation*. Lippincott Williams and Wilkins, Philadelphia (2012)
6. Hossri, C.A.C.: *Efeitos da reabilitação cardiopulmonar sobre o tempo de tolerância ao exercício e a cinética do consumo de oxigênio em cardiopatas isquêmicos. Dissertação (Doutorado em Pneumologia) - Faculdade de Medicina, Universidade de São Paulo, São Paulo (2014)*



Application for Mobile Devices to Measure Daily Protein Intake in the Elderly: PROT + First Results

F. C. D. Silva¹(✉) , A. P. S. Martins² , F. C. D. F.C.D.Silva³ , L. E. Simonato⁴ ,
and D. S. F. Magalhães¹ 

¹ Scientific and Technological Institute, Universidade Brasil, São Paulo, Brazil
fabio_carniello@hotmail.com

² UBS Santa Clara, Atibaia, Brazil

³ Centro Universitário Padre Albino, Catanduva, Brazil

⁴ Dental School, Universidade Brasil, Fernandópolis, Brazil

Abstract. Among the various domains of a Comprehensive Geriatric Assessment, nutritional assessment stands out for its important relationships with major geriatric syndromes, such as frailty syndrome and sarcopenia. In this context, the development of an application to assess the daily protein intake facilitates the identification of low protein intake and the nutritional risk of this user. In this work, we developed and evaluated the usability of a protein intake control application to be used by the elderly. The application was developed targeting the population of users over 60 years old, regardless of schooling, in the presence or absence of dementia. System Usability Scale (SUS) was used for usability evaluation with the users ($n = 18$). The PROT + offers an easy use mobile application for elderly, helping the users and their families to access an evaluation based on household measures to control their protein intake daily. There were significant differences for usability between the 60–69 and 70–79 age groups.

Keywords: mHealth · Protein · Elderly · Sarcopenia · App

1 Introduction

The use of various electronic devices is already part of the daily life of the general population and, increasingly, has reached the elderly [1]. These technologies are useful in several areas, and one that has gained increasing prominence is the application of these tools in the health scenario [2]. The scientific community has been constantly dedicated to developing safe technological tools which enable the generation of high quality information and that result in greater patient safety, as well as improve outcomes in the approach of its users [3].

In addition to the caloric and micronutrient component of the diet, the daily intake of protein by the elderly is one of the focuses of nutritional assessment and its parameters considered ideal were recently reformulated [4].

This work is justified by the need to control the diet of elderly people and to facilitate the monitoring of protein intake by relatives and doctors. Its objective was to develop an application for mobile devices which enables to perform a 24-h food recall by the elderly patient, in an automated way, with the possibility of being helped by their family members, when necessary. Furthermore, we evaluate its usability with the elderly group.

2 Materials and Methods

A development study based on software engineering, which proposes the development of an application, in an iterative process flow, based on the need to make the process of evaluating nutritional adequacy in the elderly, exclusively for the ingestion of proteins, more agile and easy to apply by the user, motivating the perception of risks of malnutrition by the elderly person or by family members.

A. 24-hour food record

Data entry was structured through text, with the automatic filling feature to make the process more intuitive. The “multiple passes” method was adapted to structure the sequence of the questionnaire. After selecting the food, the standardized measure to quantify was a household measure, easier for the elder user. This way of quantifying was chosen to bring the application closer to the patient’s reality and reduce the burden on the user, minimizing the exhaustion that the need to weigh food could cause. The database chosen was the nutritional composition table proposed by Fernanda Schmitz Goulart Delgado and Vitória de Resende Salles.

B. App development and minimum system requirements

Unity development pack was used for programming in C Sharp (C#). For the app usage 2Gb of RAM and 80 Mb of memory is required, and Android 5 or newer.

C. Usability test

System Usability Scale (SUS) [5] was used for usability evaluation. 18 individuals aged over 60 years and who obtained a score greater than 8 in the 10-CS Cognitive Screening Questionnaire participated in the research. This project was approved in Ethics Committee of UB under #5,357,578.

3 Results and Discussion

With the application finished, named PROT+, we show below some screens that exemplify its operation. Figure 1A shows the opening screen, offering the options to start a new test or access previously performed tests. Figure 1B shows the screen where we differentiate the patient’s health condition, before carrying out the assessment.

Figure 2A shows the insertion of a 50g bread for breakfast and B the graph obtained for a day, showing the percentage of protein intake for the day.

For usability assessment, after withdrawing 2 subjects who scored less than 8 on the 10-CS questionnaire, the median for 60–69yo, 70–79yo and 80 + yo were 95 (IQR 8.75), 85 (IQR 33.75) and 87.5 (IQR 10) as shown in Fig. 3.



Fig. 1: Opening screens of the PROT + App. (A) shows the opening screen, offering the options to start a new test or access previously performed tests. (B) shows the screen where we differentiate the patient's health condition, before carrying out the assessment.



Fig. 2: In use screens of the PROT + App. (A) shows the insertion of a 50g bread for breakfast. (B) the graph obtained for a day, showing the percentage of protein intake for the day.

4 Conclusions

The PROT + offers an easy use mobile application for elderly, helping the users and their families to access an evaluation based on household measures to control their protein intake daily. There were significant differences for usability between the 60–69 and 70–79 age groups.

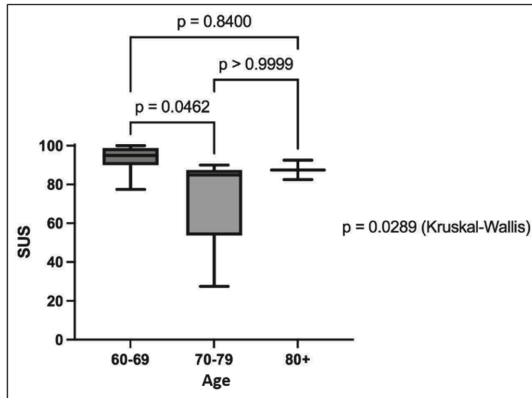


Fig. 3: Usability evaluation of the app. Kruskal-Wallis with Dunn's post-hoc were used for group comparison.

References

1. Elavsky, S., Knapova, L., Klocek, A., Smahel, D.: Mobile health interventions for physical activity, sedentary behavior, and sleep in adults aged 50 years and older: a systematic literature review. *J. Aging Phys. Act.* **27**(4), 565–593 (2019). <https://doi.org/10.1123/japa.2017-0410>
2. Chauvin, J., Lomazzi, M.: The digital technology revolution and its impact on the public's health. *Eur. J. Public Health* **27**(6), 947 (2017). <https://doi.org/10.1093/eurpub/ckx134>
3. Brenner, S.K., et al.: Effects of health information technology on patient outcomes: a systematic review. *J. Am. Med. Inform. Assoc.* **23**(5), 1016–1036 (2016). <https://doi.org/10.1093/jamia/ocv138>
4. Bauer, J., et al.: Evidence-Based recommendations for optimal dietary protein intake in older people: a position paper from the PROT-AGE study group. *J. Am. Med. Dir. Assoc.* **14**(8), 542–559, 1 ago (2013)
5. Brooke, J.: System usability scale (SUS): a quick-and-dirty method of system evaluation user information. *Read., UK: Digit. Equip. Co Ltd.* **43**, 1–7 (1986)



Qualitative Analysis of Different Formulations of Losartan Potassium Using Raman Spectroscopy

T. R. O. Heinzelmann¹ (✉) , C. J. Lima^{1,2} , H. C. Carvalho^{2,3} ,
A. B. Fernanades^{1,2} , and L. Silveira^{1,2} 

¹ Biomedical Engineering Center, Anhembi Morumbi University, São José Dos Campos, SP, Brazil

tatiheinzelmann@gmail.com

² Center for Innovation in Technology and Education (CITE), São José Dos Campos, SP, Brazil

³ Federal Technological University of Paraná (UTFPR), Campo Mourão, PR, Brazil

Abstract. Raman spectroscopy has demonstrated great potential as an alternative technique for drug analysis due to its molecular specificity, speed and simplicity of analysis. In this study, the potential of Raman spectroscopy for qualitative analysis of losartan potassium in 50 mg tablets in different commercially available pharmaceutical formulations (reference, similar and generic) was evaluated. The spectra were obtained from a dispersive Raman spectrometer (830 nm and 300 mW excitation) coupled to a fiber optic probe (Raman probe). Spectra with integration time of 30 s were collected in triplicate. The average spectra of the triplicates from each sample were examined. Comparing the Raman spectra obtained by the literature, it was observed that all have peaks in height and width similar to losartan. Some peaks presented “blue shift”, suggesting hydrolysis of the losartan. Small differences in peak intensities were observed at locations where the spectrum of the losartan molecule does not show peaks, suggesting that they are related to the different excipients used in the production of the drug in the different formulations. It was concluded that the six commercial presentations contain the active ingredient losartan potassium, with very similar Raman spectra.

Keywords: Raman spectroscopy · Losartan potassium · Pharmaceutical formulation

1 Introduction

Raman spectroscopy is a vibrational technique based on the inelastic scattering of light with matter, discovered in 1928 by C.V. Raman and K.S. Krishnan, where the laser radiation is directed onto a sample and interacts with the molecules, resulting in information about the vibrational energy of chemical bonds [1, 2]. Over the past three decades, the range of applications has increased following the technological advances of lasers, spectrographs and detectors [3].

The Raman technique has become a popular tool in the pharmaceutical field due to its versatility in several applications, such as identification and quantification of active pharmaceutical ingredients (API) and excipients and determination of the homogeneity of formulations to control the overall pharmaceutical analysis process [4, 5]. Raman has the benefit of presenting information on the molecular composition of the studied material, being non-invasive, having a rapid evaluation and not destroying the sample [1].

Losartan potassium (losartan) is an anti-hypertensive drug, selective and competitive antagonist of the angiotensin II receptor (type AT1), that interferes with the renin-angiotensin system, a significant natural blood pressure regulator. It is a drug widely marketed worldwide, mainly indicated for hypertension, especially for people who have cough related to angiotensin conversion enzyme (ACE) inhibitors. It is also indicated for cardiac insufficiency and in cases of progression of diabetic neuropathy. Figure 1 and Fig. 2 illustrate its chemical and space structures [6–8].

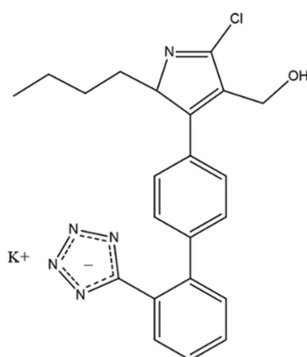


Fig. 1. Chemical structure of the losartan molecule.

In Brazil, losartan is marketed without obligatory medical prescription and the drug is available in reference, generic and similar forms, all approved and registered by the Brazilian Health Regulatory Agency (ANVISA) [9].

The reference drug is the innovative drug whose efficacy, safety and quality have been scientifically demonstrated by clinical studies, registered with the responsible federal agency, and marketed for the first time in the country. A generic drug is a drug that has the same active ingredient in the same dosage and pharmaceutical form; it contains the exact same active ingredient as the reference drug and produces the same therapeutic effect, that can be inter-changeable due to its equivalent effectiveness and safety. A similar drug contains the same active ingredient as its reference drug and can only be replaced by the same after undergoing laboratory tests that prove its equivalence [10].

Ensuring the quality of medicines is an important and complex task and involves some criteria such as purity, efficacy, formula uniformity, bioavailability, and stability [11]. The API is one of the main components of the pharmaceutical formulation and its quality has a direct impact on the final quality of the drug [12].

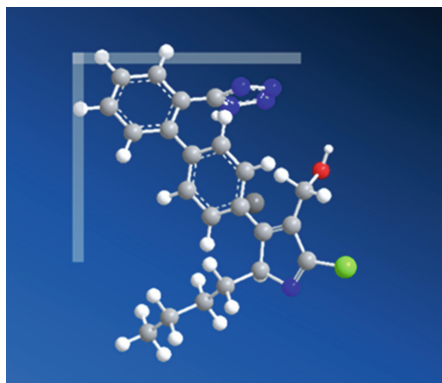


Fig. 2. Spatial representation of the losartan molecule.

When changes occur in the crystalline formations of solid API (polymorphism), the drug absorption process can be altered and, consequently, its effectiveness may change [12]. These changes are caused by the capacity of the solid material to have two or more crystalline forms, determined by its chemical structure and can occur in the API during the drug production and/or storage process [13, 14].

Although crystalline forms have structural differences, it is a challenge to be able to distinguish them precisely [13]. The detection of polymorphism can be done by different techniques, such as infrared spectroscopy, nuclear magnetic resonance, x-ray diffraction, among others, but currently, Raman spectroscopy has been widely used due to its good spectral resolution [12, 14]. A study identified the existence of two polymorphic forms of losartan, a low temperature stable form and a high temperature stable form. Raman spectroscopy has been shown to be effective in identifying crystalline forms, identifying subtle molecular changes in each one [15].

This work proposes the use of Raman spectroscopy in the qualitative analysis of drugs, with the direct determination of the presence of losartan in commercial formulations acquired in drugstores.

2 Materials and Methods

2.1 Samples

For this study, six commercial samples of losartan potassium 50 mg were purchased from local drugstores, in the form of coated tablets from different producers. The drugs were identified as one reference, one similar and four generics. Before the beginning of the analyses, three tablets from each box were taken, the surface of each tablet was scraped with a scalpel to remove the coating film, providing a better reading of the active ingredient and excipients by the Raman spectrometer.

2.2 Raman Spectroscopy

The experiment was performed at the Optical Diagnosis Laboratory at the Center for Innovation in Technology and Education (CITE), São José dos Campos Technological

Park, São José dos Campos, SP, Brazil. The drugs were submitted to a dispersive Raman spectrometer (model Dimension P1, Lambda Solutions Inc., MA, USA), which uses diode laser excitation (830 nm, 300 mW), imaging a spectrograph with diffraction grating (1200 lines/mm) and CCD camera (100 × 1340 pixels), generating high resolution Raman spectra in the range of 400 to 1800 cm^{-1} . The spectra are collected by a fiber-optic Raman probe coupled to the spectrograph as shown in Fig. 3.

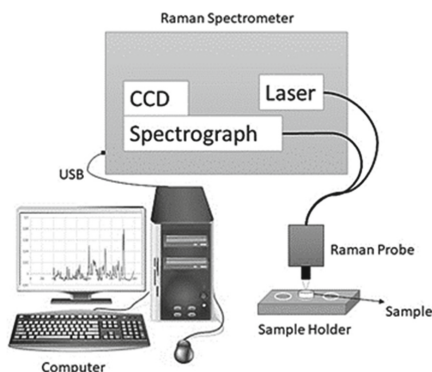


Fig. 3. Diagram of the dispersive Raman spectrometer used to collect the losartan spectra.

The tablets were placed in the focal position of the Raman probe to collect the Raman signal. The signal scattered by the sample was collected by the probe, dispersed by the spectrograph/CCD and stored in the computer for further spectra processing. All samples were analyzed on the same day under the same experimental conditions.

For each losartan tablet, triplicate Raman spectra were gathered with an exposure time of 30 s. After collection, Raman spectra were pre-processed to remove spikes from cosmic rays, background fluorescence (background signal), and then normalized by the area under the curve. The mean spectrum was calculated for each sample.

2.3 Sample Spectral Analysis

The mean spectra of the six formulations were plotted using Excel® 2019 software for comparison. The Raman bands of the formulations were compared to verify their spectral similarities with the standard spectrum of losartan found in the literature, thus qualitatively evaluating the presence of the API in these commercial drugs. The spectra of four main excipients used in the production of the drugs were also verified and compared with their respective pure Raman spectra found in the literature. The excipients analyzed were: microcrystalline cellulose (polysaccharide, used mainly as a binding agent), lactose (natural disaccharide, used as a filler or diluent), silicon dioxide (anti-caking agent) and magnesium stearate (lubricating agent).

3 Results

The mean spectra of the losartan samples are represented in Fig. 4. The main Raman peaks for losartan obtained in the literature are presented in Table 1.

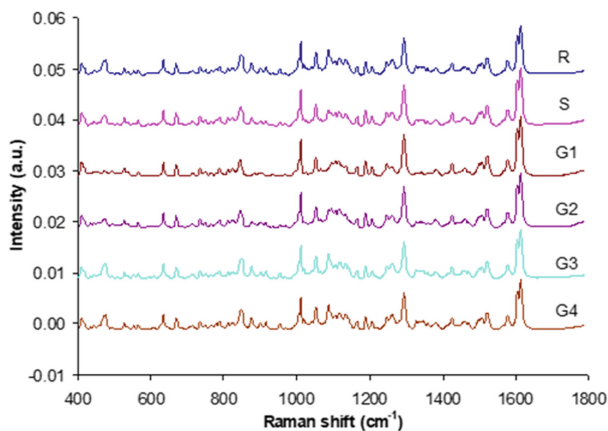


Fig. 4. Mean Raman spectra of losartan potassium 50 mg samples in different formulations. (R) Reference drug, (S) Similar drug, (G1, G2, G3, G4) Generic drugs.

Table 1. Raman bands for losartan [16]

Losartan potassium	
Raman bands (cm^{-1})	325, 414, 530, 540, 637, 673, 813, 905, 994, 1012, 1052, 1165, 1188, 1260, 1292, 1425, 1461, 1506, 1522, 1578, 1606, 1610, 2873, 2912, 3061

The differences in the Raman spectra of the reference drug compared to similar and generic drugs are shown in Fig. 5.

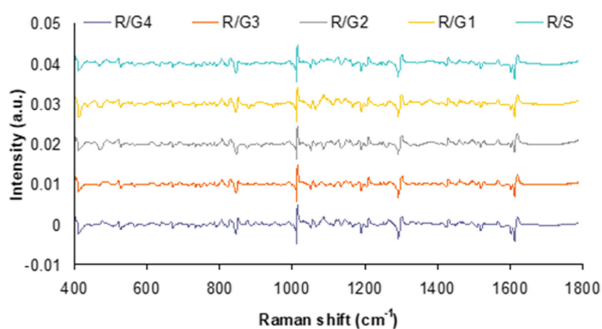


Fig. 5. Differences in the Raman spectra of the reference drug compared to other drugs. (R) Reference drug, (S) Similar drug, (G1, G2, G3, G4) Generic drugs.

The Raman bands of four main excipients found in the analyzed drugs (microcrystalline cellulose, lactose, starch and magnesium stearate), obtained in the literature, are presented in Table 2.

Table 2. Raman bands of excipients [17]

Name	Raman bands (cm ⁻¹)
Microcrystalline cellulose	343(w), 378(s), 435(m), 457(m), 517(m), 894(w), 1093(vs), 1120(s), 1152(m), 1335(m), 1378(m), 1473(w)
Lactose	256(w), 353(vs), 374(s), 395(m), 474(m), 551(w), 629(w), 847(m), 873(m), 912(w), 950(w), 1015(w), 1037(w), 1049(w), 1083(m), 1117(w), 1139(w), 1258(w), 1323(w), 1344(w), 1377(w)
Starch	302(w), 359(w), 409(w), 439(w), 477(vs), 576(w), 867(w), 940(m), 1050(w), 1081(m), 1126(m), 1261(w), 1338(w), 1379(w), 1458(w)
Magnesium stearate	888(w), 945(w), 1061(s), 1102(w), 1128(s), 1294(vs), 1437(s), 1458(m)

(w) weak, (m) medium, (s) strong, (vs) very strong peak intensity.

4 Discussion

Raman spectroscopy has been subject of great interest in the pharmaceutical industry, mainly due to the fact that it can test products in a non-destructive, fast and real-time way, thus being a good method for quality control [1].

Regulatory agencies around the world have strongly encouraged to integrate real-time analytical processes into manufacturing processes. In 2002, the American Food and Drug Administration (FDA) agency launched an initiative to encourage innovation in manufacturing technology and quality system. In 2003, the European Medicines Agency (EMA) released guidance documents on analytical technology processes and real-time testing and the International Conference on Harmonization (ICH) reinforced the FDA and EMA recommendations, which have been implemented since 2009 in the USA, European Union and Japan [6].

This study aimed to qualitatively evaluate the different commercial formulations, according to the conditions determined by the current legislation so that the drugs can be considered similar and generic. Before starting the analysis by Raman spectroscopy, all the tablets tested had the coating film scraped so that there was no interference in the reading of the active ingredient [18].

The Raman bands of losartan were demonstrated in Table 1, according to Mizera, 2015 [16]. Their peaks were compared with the analyzed drugs, and it was possible to identify the peaks of losartan in the six tested commercial formulations. As shown in Fig. 4, all spectra were very similar, with only small differences in peak intensities at positions where the spectrum of the losartan molecule does not present peaks, suggesting that they are related to the different excipients used in drug manufacturing and also in their different concentrations.

The differences in the Raman spectra of the reference drug, compared to similar and generic drugs seen in Fig. 5 showed a small frequency shift (“blue shift”) in the main peaks, which may suggest hydrolysis of the losartan.

The Raman spectra of the six commercial drugs analyzed were compared with the spectra of four main excipients found in these drugs (Table 2), according to Veij, 2008 [17], that analyzed 43 excipients divided into seven categories, all widely used in drug manufacturing, thus providing a reference to aid the interpretation of Raman spectra during analysis. It was observed that the main peaks of the excipients coincide with the positions where the differences between the spectra of the analyzed drugs occurred, corroborating the idea that these spectral differences are due to the fact that the drugs may have different excipients in their compositions and these, even when the same, may present different concentrations and are in accordance with current legislation [10], as long as they guarantee the bioequivalence and bioavailability of the drugs.

Since the study is a qualitative analysis, it was not demonstrated the bioequivalence and bioavailability required by the current legislation; for that, other tests would be necessary.

Many studies focus on the API of the drugs and do not give much attention to the excipients present in these formulations, which makes it especially difficult to interpret Raman spectra during drug's qualitative and quantitative analyses.

A review by Frosch, 2019 [19] showed that the interest in the use of this technology for drug monitoring has grown over the years. According to Web of Science statistics, the number of published articles using the words "Raman" and "drugs" tripled between 2010 and 2018.

Due to the growing number of drugs sold in Brazil, since the approval of Law 9787 in 1999, which establishes the generic drug, there are still doubts about the quality of generic and similar drugs in relation to the reference drugs. A bibliographic survey of articles published from 2015 to 2020 shows that although these drugs need to undergo quality tests before being marketed when analyzing the content of the active ingredient of similar drugs, unsatisfactory results were found, in disagreement with the standards of quality established by the Brazilian Pharmacopoeia, which a drug came to present a percentage lower than 70% [20].

In addition to being a tool for quality control and real-time monitoring during the drug manufacturing process, the Raman technique has also shown promise in identifying counterfeit drugs, as demonstrated by Sanada, 2021 [21], who evaluated counterfeit erectile dysfunction drugs using a compact Raman spectrometer.

Raman spectroscopy has been used to evaluate the quality of drugs for some years and has remained a tool of great interest in the pharmaceutical area due to its constant technological evolution that allows an increasing sensitivity to identify the biomolecular composition of the material studied, better showing its molecular alterations, according to a study, which quantitatively analyzed the solid dosage forms of losartan potassium [22].

5 Conclusion

This study showed that dispersive Raman spectroscopy was able to identify the presence of the API losartan in all six commercial formulations tested, with peaks in height and width similar to losartan. Peak shifts ("blue shift") in positions of the losartan in the difference spectrum suggests hydrolysis of the active ingredient. Only small differences were observed in some peak positions where the losartan spectrum does not show

peaks, suggesting that they are related to different excipients or excipients with different concentrations in the different drug formulations.

Acknowledgment. T.R.O. Heinzelmann acknowledges Coordination for the Improvement of Higher Education Personnel (CAPES) for the master fellowship—Finance Code 001. L. Silveira Jr. Acknowledges National Council for Scientific and Technological Development (CNPq) for the productivity fellowship—Process No. 314167/2021-8. C. J. Lima, A. B. Fernandes and L. Silveira Jr. Acknowledge Anima Institute (AI) for the research fellowship.

Conflict of Interest. The authors declare that they have no conflict of interest.







References

1. Alula, M.T., Mengesha, Z.T., Mwenesongole, E.: Advances in surface-enhanced Raman spectroscopy of pharmaceuticals: a review. *Vib. Spectrosc.* **98**, 50–63 (2018). <https://doi.org/10.1016/j.vibspec.2018.06.013>
2. Bório, V.G., Fernandes, A.U., Silveira, L., Jr.: Characterization of an ultraviolet irradiation chamber to monitor molecular photodegradation by Raman spectroscopy. *Instrum. Sci. Technol.* **44**(2), 189–198 (2016). <https://doi.org/10.1080/10739149.2015.1081936>
3. Esmonde-White, K.A., Cuellar, M., Uerpmann, C., et al.: Raman spectroscopy as a process analytical technology for pharmaceutical manufacturing and bioprocessing. *Anal. Bioanal. Chem.* **409**(3), 637–649 (2017). <https://doi.org/10.1007/s00216-016-9824-1>
4. Cailletaud, J., De Bleye, C., Dumont, E., et al.: Critical review of surface-enhanced Raman spectroscopy applications in the pharmaceutical field. *J. Pharm. Biomed.* **147**, 458–472 (2018). <https://doi.org/10.1016/j.jpba.2017.06.056>
5. Bajwa, J., Nawaz, H., Majeed, M.I., et al.: Quantitative analysis of solid dosage forms of cefixime using Raman spectroscopy. *Spectrochim. Acta A Mol. Biomol. Spectrosc.* **238**, 118446 (2020). <https://doi.org/10.1016/j.saa.2020.118446>
6. Jeeva, A.S., Chandran, M., Krishnakumar, K.: A review of analytical methods for estimation of amlodipin, hydrochlorothiazide and losartan potassium in pharmaceutical formulations. *Int. Res. J. Pharm. Med. Sci.* **1**, 75–77 (2018)
7. Bakr, N.A., Saad, S., Elshabrawy, Y., et al.: First-derivative synchronous spectrofluorimetric for estimation of losartan potassium and atorvastatin in their pure forms and in tablets. *Luminescence* **35**(4), 561–571 (2020). <https://doi.org/10.1002/bio.3755>
8. Etcheverry, S.B., Ferrer, E.G., Naso, L., et al.: Losartan and its interaction with copper (II): Biological effects. *Bioorg. Med. Chem.* **15**, 6418–6424 (2007). <https://doi.org/10.1016/j.bmc.2007.06.056>
9. BRASIL. ANVISA at http://antigo.anvisa.gov.br/documents/10181/2921766/RDC_98_2016_COMP.pdf/dcb09ea1-e222-4192-98c5-54a13426dc4aat
10. BRASIL. Lei 9787 at http://www.planalto.gov.br/ccivil_03/leis/9787.htm
11. Martínez, J.C., Guzmán-Sepúlveda, J.R., Bolanõz Evia, G.R., et al.: Enhanced quality control in pharmaceutical applications by combining Raman spectroscopy and machine learning techniques. *Int. J. Thermophys.* **39**, 79 (2018). <https://doi.org/10.1007/s10765-018-2391-2>
12. Guzmán, E.L., Rentería, S.A.A., Pescador, M.G.N., et al.: Pharmaceutical polymorphisms and its influence on the dissolution profile of two pioglitazone brands. *Afr. J. Pharm. Pharmacol.* **13**(16):273–279 (2019). <https://doi.org/10.5897/AJPP2019.5079>
13. Higashi, K., Ueda, K., Moribe, K.: Recent progress of structural study of polymorphic pharmaceutical drugs. *Adv. Drug Deliv. Rev.* **117**, 71–85 (2016). <https://doi.org/10.1016/j.addr.2016.12.001>

14. Da Silveira, A.A., Pereira, A.E.T., De Oliveira, I.S., et al.: Drug polymorphism in the drug quality control: a review. *Electron. J. Collect. Health* **29**, 791 (2019)
15. Raghavan, K., Dwivedi, A., Campbell, G.C., Jr., et al.: A spectroscopy Investigation of Losartan Polymorphs. *Pharm. Res.* **10**(6), 900–904 (1993)
16. Mizera, M., Lewadowska, K., Talaczynska, A., et al.: Computational study of influence of diffuse basis functions on geometry optimization and spectroscopy properties of losartan potassium. *Spectrochim. Acta A Mol. Biomol. Spectrosc.* **137**, 1029–1038 (2015). <https://doi.org/10.1016/j.saa.2014.09.036>
17. De Veij, M., Vandenabeele, P., et al.: Reference database of Raman spectra of pharmaceutical excipients. *J. Raman Spectrosc.* **40**, 297–307 (2009). <https://doi.org/10.1002/jrs.2125>
18. Roggo, Y., Degardin, K., Margot, P.: Identification of pharmaceutical tablets by Raman spectroscopy and chemometrics. *Talanta* **81**, 988–995 (2010). <https://doi.org/10.1016/j.talanta.2010.01.046>
19. Frosch, T., Knebl, A., Frosch, T.: Recent advances in nano-photonics techniques for pharmaceutical drug monitoring with emphasis on Raman spectroscopy. *Nanophotonics* **9**(1), 19–37 (2019)
20. Santos, T.S., Souza, O.G.B., Melo Neto, B., et al.: Quality assessment of similar, generic and reference drugs sold in Brazil: a literature review. *Res., Soc. Dev.* **9**(7), 1–12 (2020). <https://doi.org/10.33448/rsd-v9i7.4355>
21. Sanada, T., Yoshida, N., Kimura, K., et al.: Discrimination of falsified erectile dysfunction medicines by use of an ultra-compact Raman scattering spectrometer. *Pharmacy* **9**(1), 3 (2021). <https://doi.org/10.3390/pharmacy9010003>
22. Shafaq, S., Majeed, MI, Nawaz H et al. (2022) Quantitative analysis of solid dosage forms of Losartan potassium by Raman spectroscopy. *Spectrochim. Acta A Mol. Biomol. Spectrosc.* **272**. <https://doi.org/10.1016/j.saa.2022.120996>



Application Development for Canine Hearing Monitoring

R. S. Navarro¹ , D. C. L. Martins¹ , A. Baptista¹ , L. A. M. Pereira² ,
and S. C. Nunez¹  

¹ Universidade Brasil, Pós-Graduação Bioengenharia, São Paulo, Brazil
silvia.nunez@universidadebrasil.edu.br

² Universidade Brasil, Programa de Mestrado Em Produção Animal, Descalvado, Brazil

Abstract. Otitis is an inflammatory disease of the external auditory canal, being common in dogs. The treatment is complex, involves multiple antimicrobials and depends on the owner's involvement. Diagnosis in the initial stages are difficult to assess. With the increase in access to mobile App, this technology can help diagnose and monitor the evolution of canine hearing loss. The objective of the study was to develop an App for canine hearing monitoring aiming to introduce an innovative product in this sector. After evaluating available products, a software was designed in Java Script language for use on computers and cell phones with Android system, the device should reproduce sounds with a specific range to evaluate bass and treble sounds that can be affected differently in the hearing loss process. The developed application allows user and animal registration, on the test screen, it emits frequencies ranging from 20 Hz to 40,000 Hz with an intensity of about 45 dB in all bands, which represents an uncomfortable sound intensity, but not an irritating one, with 5 s of duration the frequencies correspond to the canine hearing range. The App's screens are intuitive and easy to manipulate and allow the storage of results with specific dates, which can permit the tutor or the veterinarian to follow the evolution of the animal's hearing degree. The App presented functionality and after registration at the National Institute of Industrial Property is available on the web page and it will be tested in clinical practice.

Keywords: Canine Otitis · Deafness · Mobile Application

1 Introduction

Otitis is an inflammation of the external auditory canal, which affects several species, being more common in dogs due to its anatomical features; long and pendulous ears, excess hair, narrow ear canals, and because it is a humid and hot region, become the favorite place for fungi, bacteria and mites. Some breeds develop this disease more easily such as Golden Retriever, Basset Hond, Cocker Spaniel, Labrador, German Shepherd, Beagle [1].

The most frequent symptoms and signs are intensive itching, excess wax, odor, edema, shaking the head several times from side to side, crying when scratching, ear

discharge, lack of appetite generated by the pain. [1, 2]. This disease does not have a single cause, several factors can cause infections [1].

Hearing loss in animals doesn't just occur in elderly pets. Hearing impairment can be permanent, temporary or occur gradually and the diagnosis of hearing loss in its first stages is very difficult. Audiometry tests in dogs' use a stimulus elicited into the animal's canal, and a brainstem auditory evoked response waveform is analyzed to determine a pass or fail hearing screening result [3].

The softest sound an animal can hear at a specific frequency is called the threshold of hearing. The animal can hear sounds that are above its threshold without impairment until a certain combination of intensity and duration is reached. Above this threshold, the animal's hearing threshold may be temporarily or permanently worsened. When this happens, the sounds must be louder to be detected. If the threshold returns to near-normal levels after some time, this condition is called a temporary threshold shift or TTS. If the threshold does not return to near-normal levels, the effect is called a permanent threshold shift or PTS. PTS can occur because of repeated occurrences of TTS, or it can occur as a result of a single exposure to very loud sound [4]. Thus, it is important that the sound emitted remains within the animal's hearing threshold with adequate intensity and duration for the safety of the test [5].

During the treatment of canine otitis, the effectiveness of the procedure can be measured by the hearing threshold. Eger and Lindsay (1997) [4] carried out a study where the auditory function was measured in normal dogs and in dogs with otitis through auditory brainstem evoked response tests. Data were obtained from 86 normal ears and 105 ears with otitis, categorized into four degrees of severity. Data were analyzed to illustrate the differences between auditory function in normal and abnormal ears and to estimate the degree of impairment associated with different degrees of pathology.

While severe hearing loss appeared to be present in dogs with more severe otitis, only two individuals were identified as being totally deaf in the affected ears and no dogs were identified in which the cleaning and examination processes had caused damage to hearing function. Cleaning the ear canal produced measurable improvements in hearing in several dogs, indicating the profound effect of physical obstruction of the external ear canal by debris. The authors concluded that most dogs with chronic otitis external are not completely deaf and that the hearing impairment that occurs has characteristics of conductive hearing loss.

The home treatment of external otitis is time consuming for the tutors and if the animal does not present typical signs of otitis (i.e., bad smell, pain, scratching the ear) the tutors may not perceive the diseases and abandon the treatment [6].

Audiometry test in veterinary practice is expensive and difficult to find. Nowadays the test a medical procedure performed under anesthesia [7].

Some home methods are recommended for canine hearing testing, and these include making sounds without causing vibration on the floor and observing the animal's reactions that can be as small as ears lifting, looking in the direction of the noise, standing up or wagging the tail. However, these tests are performed only within the audible range of the sound frequency spectrum for humans and do not demonstrate the frequencies that are affected by the disease [3].

Faced with the lack of an alternative method for evaluating the canine auditory response, we propose an innovative project in the sector, where, through specialized software that emits frequencies between 20 Hz and 40,000 Hz, with the intention of being used by veterinarians and animal tutors to follow-up treatment of canine otitis in order of to prevent hearing loss due to a common infection.

With the increased access to applications for mobile devices, the use of this technology as an aid in the diagnosis and monitoring of the evolution of canine otitis can be useful for both caregivers and professionals. Based on the search that we carried out evaluating products available in the application market, we verified that there is a gap in analysis segmented by sound frequency. Apps for dog training are available with behavior control purposes emitting different sound frequencies. We did not find any device that had the proposed of audiometric analysis.

Therefore, the development of an application in this area can present an innovation in the animal health care sector. The objective of this study was to develop an App for auditory monitoring of dogs emitting sound frequency starting at 20 Hz and intensifying until close to ultrasounds of the order of 40,000 Hz, with an intensity of about 45 dB in all bands and approximate duration of 5 s, so no temporary threshold shift would occur affecting the test results.

2 Methods

2.1 Development of App

Surveys were carried out by active search of software specialized in sounds for dogs, software related to hearing in general and software that could emit sound frequencies from 100 Hz to 100,000 Hz. The search was carried out in applications for IOS and Android, in addition to searches for computer software open to the public. The keywords used in the search were “Canine audiometry”, Sounds for dogs, Sound frequency generators, hearing. Several software’s were found with the purpose of training and dressage, the available software’s generate sounds with a frequency of 100 Hz to 50000 Hz. Applications were found with the purpose of generating sounds to provide behavioral changes in the animal.

3 App AudioPet

Before starting to program the application, we studied the best way to create an efficient, easy-to-use application that can monitor the animal’s hearing loss as it ages. In this context, it was understood that the application should be divided into three modules:

- Access to the application and user registration.
- Hearing test and test result.
- History of tests performed.

As proposed, initially the application user needs to register and then log in for access. The main advantage of controlling access to the application is that the access to history of animal tests is possible. In order to ensure wide use of the application, the idea is

that the registration is carried out with little information, just to guarantee the possibility access the recorded data.

Bearing in mind that the user field is the key to access the system, the application will check if the registered user already exists in the database, if so, it will warn you for a new choice, avoiding errors in the history of the exams performed.

In the hearing and result test module, an application was designed that, after requesting the animal's data, to record the history, shows the choice of frequencies from 20 to 40,000Hz on the screen, each of these will have a button to turn the sound on and off, followed by a field for recording whether the animal heard the emitted sound.

At the end of the exam, the application will calculate the percentage of the animal's hearing responses and will issue some considerations according to the responses obtained. In the last module foreseen, the tests performed will be stored, in this way, it is possible to monitor the animal's hearing loss.

It should be noted that there are no test limits. The structure of the idealized database tables is shown in Fig. 1. In one database are stored the application user data and in the other the information about the animal and the tests performed. The interconnection between the tables is done through the user field, present in both tables.

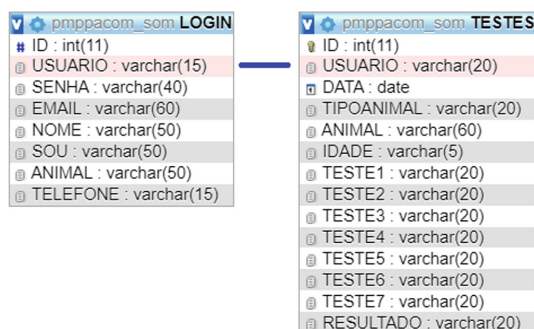


Fig. 1. Structure of the idealized database tables

4 Results and Discussion

The developed application can be accessed from any smartphone, tablet, or computer, as long as it has internet access. Its layout is responsive, that is, it adjusts according to the screen size of the device.

To use the application, the user just needs to access the link <www.pmpa.com.br/som>, the initial screen is shown in Fig. 2 in 1 in the version for computers and notebooks and in 2 the version for smartphones.

To access the application, the user must click on Enter in the desktop version and, in the case of a smartphone, he must first access the menu located on the upper left-hand tab, represented by three small dashes, where he will find the option: Enter. Two options will be displayed: login and register user. If it is the first time that the user accesses the

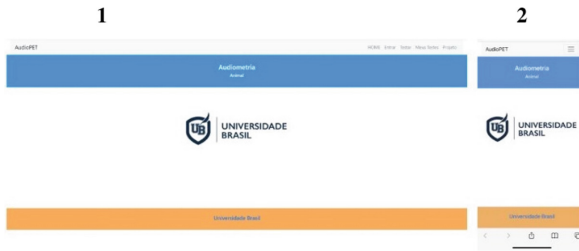


Fig. 2. In initial screen of the developed application viewed on a desktop computer and at 2 the screen of the developed application viewed in a smartphone

system, he must necessarily choose the second option. Once registered, the user must log in to access the application’s functions. Figure 3 1 and 2 show the screen described for desktop and smartphone respectively.



Fig. 3. In 1 the access screen of the software viewed on a desktop computer and at 2 the access screen for smartphone

Once the option “register user” is chosen, the system will open a screen superimposed on the previous screen that will ask the user to fill in the fields: user, password, name, I am (veterinary doctor, zoo technician, student, pet tutor, entrepreneur, and others), telephone and email.

The username and password fields are responsible for giving the user access to the application. Figure 4 1 and 2 presents the screen described the first image for desktop and the second is the smartphone version.

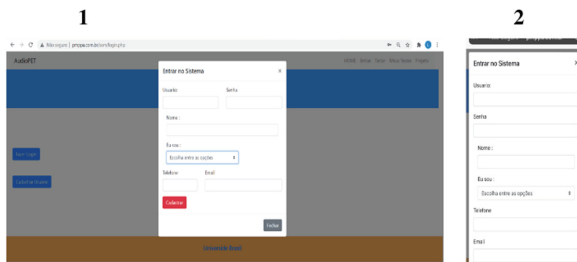


Fig. 4. In 1 the desktop screen of the software is presented and in 2 the smartphone version

With the registered user, it will be possible to log in to the application, in this case, a window superimposed on the previous screen will open, where the user must enter their username and password, if the data are correct, access to the application is released. Figure 5 in 1 and 2 shows the screen described the first image in the desktop version and the second in the smartphone version.

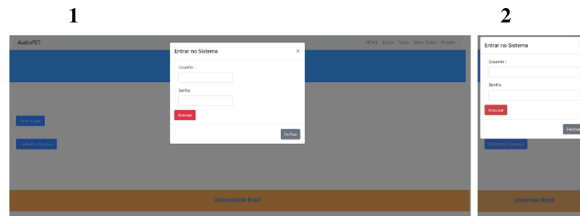


Fig. 5. In 1 the user login screen viewed on desktop computer and in 2 the same screen on a smartphone

Once the application is accessed, the user can choose from the menu the options: test, my tests and project. In the first option, the user is led to fill in the data of the animal to be tested, where it is requested: date, type of animal (canine and feline), name of the animal and age. After completing the form, the user must click on start test.

On the test screen, the user will find eight test options, in each of the options the frequency to be tested is displayed, a button to start the test, a button to turn off and a field to inform if the animal heard the sound tested or did not hear. The eight frequencies tested are: 20 Hz, 1000 Hz, 5000 Hz, 10000 Hz, 20000 Hz, 30000 Hz and 40000 Hz. Figure 6 in 1 and 2 presents the screens for desktop and smartphone respectively.

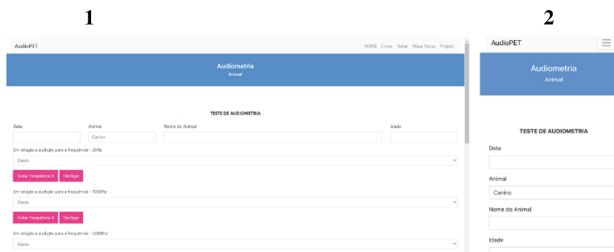


Fig. 6. In 1 audiometry test screen viewed on desktop computer and the same screen visualized on the smartphone

At the end of the test, the application will issue the result in percentage, accompanied by a comment according to the measured hearing. Figure 7 1 and 2 presents the screen describing the desktop version and the smartphone version.

In the option “my tests”, the user of the application finds the history of the tests carried out, if he understands that any test should be disregarded, the user simply clicks on the trash can icon to delete the record. It should be noted that for better visualization, if there are more than 8 records, they will be divided into pages that can be accessed

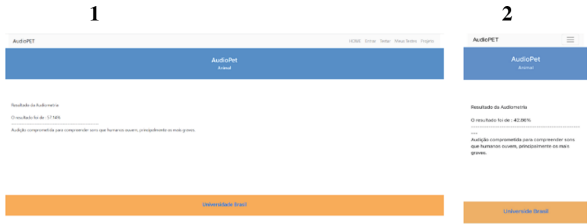


Fig. 7. Audiometry test result screen viewed on desktop computer and in 2 the smartphone version

by page advance and retreat icons. Figure 8 1 and 2 shows the screen described the first image in the desktop version and the second in the smartphone version.

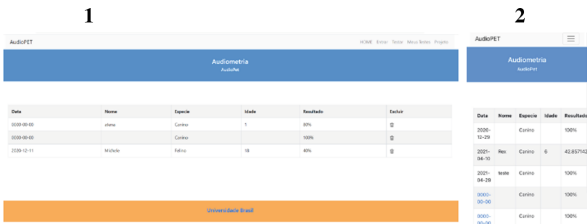


Fig. 8. In 1 the screen of history of audiometry tests performed by the user viewed on desktop computer and in 2 smartphone version

Finally, in the project menu item, the application user will find an explanation of the developed project, according to Fig. 9 for desktop and smartphone in 1 and 2.

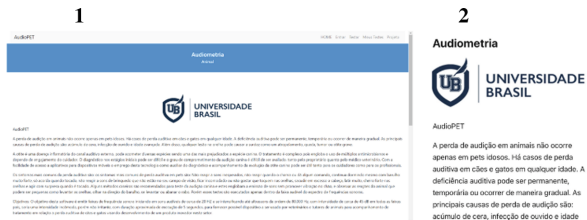


Fig. 9. Screen of the menu project item viewed on a desktop (1) and smartphone (2)

In the software for veterinary medical purposes or for assessing, the degree of canine hearing was found in the searches and the available frequencies emitted by some dog training Apps do not include the canine auditory spectrum (100 Hz to 100,000 Hz). Some applications aiming human hearing testing are available, but they cover a small frequency range, usually from 100 Hz to 15000 Hz. This fact motivated the authors to develop the App for auditory monitoring of dogs, emitting sound frequencies starting at 20 Hz and intensifying until close to ultrasounds of the order of 40,000 Hz, with an intensity of about 45 dB in all bands and approximate duration of 5 s.

As pointed out by Sidiras et al. (2021) [8], even regarding human hearing loss control, efforts should be made to develop a strategy and implementation of user-operated audiometry tests since the control can be pivotal to prevent permanent deafness.

It will be important as future steps that the App developed in this study start tests with tutors, veterinarians and zootechnicians, therefore we provide easy access to the software so it could be tested and further improved, if necessary, after evaluation by veterinarians. The clinical use of a technology as an aid in the diagnosis and monitoring of the evolution of canine otitis treatment can be useful to implement a more accurate and efficient treatments.

5 Conclusions

The present study developed an App that is easy to use and could be a useful tool for monitoring the hearing health of domestic animals.

Conflict of Interest. The authors declare that there are no conflicts of interest in carrying out this study.




Statement of Animal Rights. The study was not performed directly or indirectly on animals, not requiring submission to the Ethics Committee for the Use of Animals.

References

1. Silva, C.F., Alves, B.H., Almeida Júnior, S.T., et al.: Otite externa e média em cães: revisão de literatura. *BJDV* **7**(11), 103426–104248 (2021)
2. Linzmeier, G.L., Endo, R.M., Lot, R.F.E.: Otite externa. *Rev. Cient. Eletr. Med. Vet.* **12**, 1–6 (2009)
3. Sims, M.H.: Evoked response audiometry in dogs. *Progress in Vet. Neurol.* **1**(3), 275–283 (2010)
4. Eger, C.E., Lindsay, P.: Effects of otitis on hearing in dogs characterized by brainstem auditory evoked response testing. *J. Small Anim. Pract.* **38**(9), 380–386 (1997)
5. Rabinowitz, P.M.: The Public Health Significance of Noise-Induced Hearing Loss. In: Le Prell, C.G., Henderson, D., Fay, R.R., Popper, A.N. (eds.) *Noise-Induced Hearing Loss*. SHAR, vol. 40, pp. 13–25. Springer, New York (2012). https://doi.org/10.1007/978-1-4419-9523-0_2
6. Bajwa, J.: Canine otitis externa - Treatment and complications. *Can. Vet. J.* **60**(1), 97–99 (2019)
7. Schacks, S., Rohn, K., Hauschild, G.: Frequency-specific electric response audiometry (ERA) and its clinical application in the diagnosis of hearing defects in the dog. *Vet. Q.* **28**(1), 14–22 (2006)
8. Sidiras, C., Sanchez-Lopez, R., Pedersen, E.R., Sørensen, C.B., Nielsen, J., Schmidt, J.H.: User-operated audiometry project (UAud) – introducing an automated user-operated system for audiometric testing into everyday clinic practice. *Front. Digit. Health* **3**, 724748 (2021)



Design of Technical Support for Stand-Up

Y. J. Fonseca^(✉) , R. A. Espinosa , and M. E. Lambertinez 

Universidad ECCI, Kra 100 # 139-68, 110311 Bogotá, Colombia
yeisonj.fonsecar@eccí.edu.co

Abstract. This article contains the design of a technical aid for stand-up support in patients with lower limb immobilization syndrome or with reduced mobility. The methodology applied in this article consisted initially in the definition of the design that complied with the necessary requirements for a correct stand up, the height and weight of the user were taken into account, then the pieces of the structure were designed, these pieces were designed independently in order to facilitate the final assembly of the technical aid, then the electronic circuit was designed using the proteus software, finally the final design and assembly was performed using the Autodesk Inventor Professional version 2021 software. We achieved the simulation and articulation of each of the parts that compose the structure of the technical aid to know how it works. The final result of the design will allow the ascent and descent of the patient in a controlled, safe and supervised way by the personnel in charge of the user.

Keywords: — Technical assistance · Stand-up · Design · Linear actuated

1 Introduction

Elderly adults suffer a deterioration of their motor skills due to bone decalcification and muscle deterioration, in addition to other diseases that develop primarily with age, according to the WHO (World Health Organization), more than one billion people worldwide are elderly adults with disabilities who need technical assistance[1].

These physical conditions confine elderly adults to places and spaces with little movement, increasing deterioration due to lack of exercise leading to restrictions that affect the performance of daily activities, such as getting up from a chair, walking, or moving heavy objects, which reduces the quality of life of an elderly adult.

WHO defines technical aids as devices, instruments or programs that provide their users with greater independence [2], to move beyond the advantages offered by assistive technology, there is a difference between need, demand and supply, that needs technical assistance does not mean that it is easy to find in the market. Currently only 10% of people with these needs have access to them [1].

In 1999 Liljedahl Gunnar, presented the design of a system of technical aids for standing up, this consisted of a mobile lifting crane that held the patient in a wave-type sling. In 2009, Hunzikier Kurt developed a prototype with hydraulic action and

parallelogram mechanism used in physical rehabilitation therapies, which consists of changing the patient's position from sitting to standing.

In the same year Perk Heinrich, presented a standing design that was adapted to a wheelchair with a parallelogram mechanism. Consisting of an actuator from the base to the backrest joint, causing a necessary force that displaces the chair, placing the person in a standing position. [3].

For the management of immobility syndrome, occupational therapy is currently used. Occupational therapy is used, which proposes an intervention that does not change the psychological characteristics, but improves the performance of activities of daily living, by activating them through various methods that compensate for appropriate equipment and assistance.

It is important to emphasize that, in order to carry out a good management of these treatments in the elderly, prevention and therapeutic aspects must be taken into account, rehabilitation and palliative care without neglecting social and family aspects. [3].

Today, the sololift crane allows patients, guardians and health care personnel in institutions to transfer to a wheelchair, beds or chairs in a safe, fast and risk-free manner for patients with reduced mobility [4].

According to the registry of localization and characterization of persons with disabilities (RLCPD), the following is indicated, established that in Colombia 22% of people in 2018 suffered from lower limb disabilities, also recognized the need for the use of a technical aid such as a lift, standing frame (crane, stander, etc.), cane, walker or crutch) and 81% reported that they were already using one of these aids [2], However, these people require a greater effort from the user to reach a full standing position, in the case of cranes, they require higher structural conditions because of their dimensions [5].

This study proposes the development of a technical aid that allows patients to stand upright in order to facilitate their mobility, this assistive technology is currently in the design phase and has not been tested on patients, consists of a linear actuator that raises and lowers the upper arms, which contain the supports that hold the patient, is easy to handle and is indicated for patients with immobilization syndrome. Designed in 6061 aluminum, capable of supporting 150 kg of weight, is easy to maintain and clean.

2 Materials and Methods

This section describes the design process of the standing aid, which is made up of 4 stages, as shown in Fig. 1.

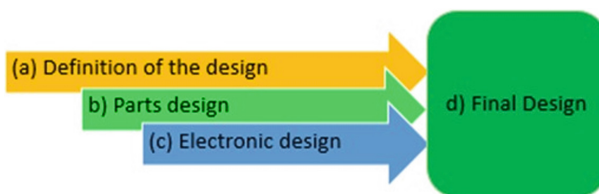


Fig. 1. Stages of the design process. Own source.

2.1 Design Definition

To determine the final design of the technical aid, the following features were taken into account: patient safety, used technology and ergonomics, anthropometric characteristics of the patient were also taken into account, weight and height, in this phase, the complete structure of the final technical aid was drafted, in which it was sectioned by parts (described in stage b) to facilitate its elaboration and final assembly in software.

2.2 Design of Parts

The design of the technical aid for stand-up upright, consists of 8 pieces, which were created independently to be later assembled and assembled, as shown in Fig. 2, these parts were designed using Autodesk Inventor software, anthropometric measurements of a patient weighing 90 kg were also taken into account, parts are designed in 6061 aluminum, which has good resistance to weight and is easy to weld.

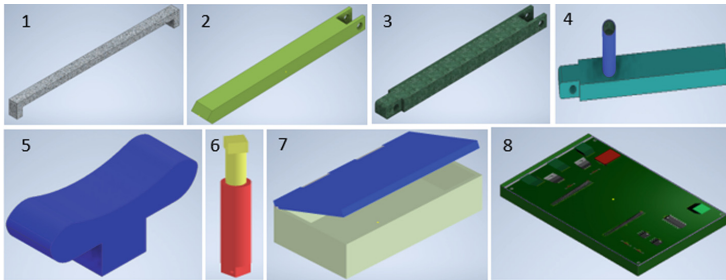


Fig. 2. Individual design of each part

The following are the 8 pieces that were designed to achieve the final assembly:

1. Chassis base: Supports the structure of the technical aid.
2. Arm 2 and 3: serves as a support for arm 3.
3. Arm 4: this is where the pushbuttons used to control the vertical movement of the technical aid are located.
4. Axillary support: offers comfort and supports the weight of the patient.
5. Linear actuator: its function is to raise and lower the structure that allows the patient to stand upright.
6. Electronic card storage box: serves to protect the electronic card.
7. Electronic board: contains the electronic components used for the operation of the technical aid.

2.3 Electronic Design

In this stage, the study of the electronic design phases was carried out, as shown in Fig. 3, The electrical circuit was then designed in Proteus software (Fig. 4).

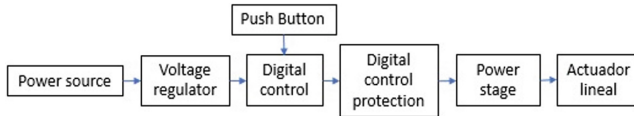


Fig. 3. Electronic schematic design phases.

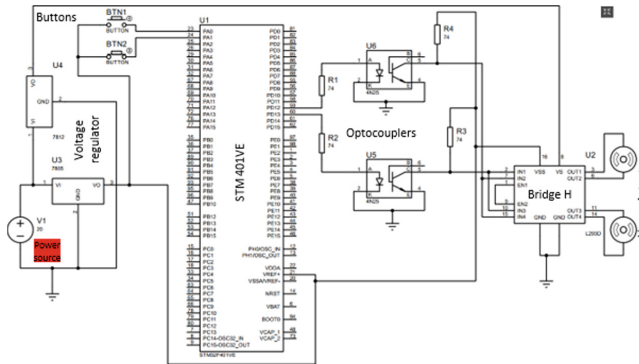


Fig. 4. Electronic design of the technical aid. Own source.

2.4 Final Assembly

The stand-up aid consists of a linear actuator that ascends and descends supporting the structure that holds the patient. This aid is easy to use and is indicated for patients with immobilization syndrome, its parts are designed in 6061 aluminum, which is capable of supporting up to 150 kg of weight, being in this way easy to maintain and clean.

The assembly was performed using Autodesk Inventor software, in which the parts described in the first stage were taken and the respective couplings between the parts were made, resulting in the final assembly shown in Fig. 5.

The following is a description of each of the parts listed in Fig. 5.

1. Structure.
2. Axillary supports.
3. Push button for lowering and raising the technical aid.
4. Linear actuator.
5. Housing and electrical circuit.

3 Results

A heavy-duty electric linear actuator with good thrust and pull characteristics was used, withstanding a maximum load of 1500 N, works with a travel speed of 14 mm/s, a duty cycle of 25% and operating frequency of 20%, is powered by 12 VDC and a maximum load current of 3 A.

Figure 6, we can observe that the technical aid has a vertical displacement, has a linear actuator that has a length of 20 cm and an angle of 30° with respect to arm 2 in

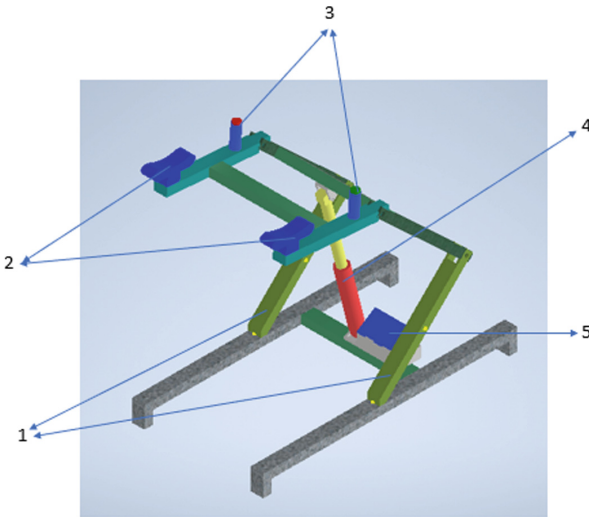


Fig. 5. Identification of parts in the final assembly. Own source.

its initial position and the final position of the linear actuator reaches a length of 95 cm and an angle of 60° with respect to arm 2.

The technical aid has a red pushbutton for activating the lowering of the linear actuator and a green push button for activating the raising of the linear actuator the patient can be verticalized.

To start the assistive device, make sure that the actuator is in its initial position (lowered) and position the patient in front of the assistive device, making sure that the patient is attached to the axillary supports and safety harness, after this press the ascent button until the patient is fully verticalized.

This technical aid will allow the user greater mobility and independence to carry out daily activities, It also seeks to satisfy the medical and social needs of the user and, above all, to offer safety and security, affordability and quality for good performance, as well as practical maintenance.

4 Conclusions

The technical aid proposed in this article presents robust properties that will allow it to be used in people weighing up to 150 kg, with electronic operation that facilitates controlled ascent and descent, minimizing the effort made by the patient, thanks to its axillary supports it offers greater safety and comfort, compared to the article (Design of a standing equipment) published in the UC engineering magazine on April 1, 2013 [6], where a mechanical operation based on levers and pedals is described.

There are currently many technologies that offer similar features, However, these require complex pre-installation conditions, as well as ample space for its proper operation, their acquisition implies a high cost since they require a specialized and frequent maintenance service.

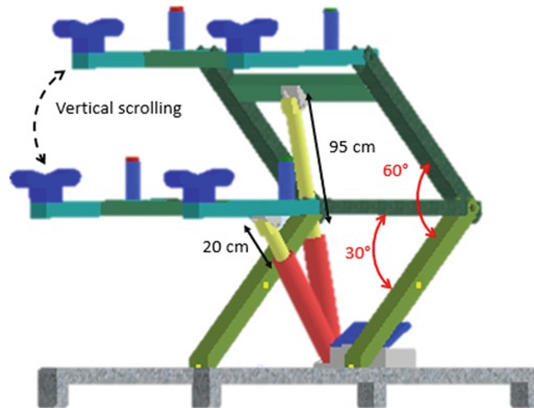


Fig. 6. Simulation of technical assistance operation. Own source.

Although this prototype offers many benefits for its users, has not yet been tested in patients because it is still in the design phase.

The development of this technical aid is intended to achieve greater patient autonomy, as standing up will require less effort, improving their quality of life and making it easier for their caregivers to work.

The design and simulation of the structure and electronic card of the technical aid for stand-up was achieved, taking into account the need to verticalize the patient with reduced immobilization syndrome in a simple and safe manner.

The design of this technical aid will support up to 150 kg, this will enable a wider range of users of this support product to be reached. However, prior evaluation is required for the use of the equipment in case the user exceeds the established characteristics for safe operation.

Acknowledgment. We thank ECCI University for allowing us to be part of the EMB-IEEE Biomedical Applications Seminar.

Conflict of Interest. The authors declare that they have no conflict of interest.







References

1. O. M. d. I. Health: World Health Organization. Pan American Health Organization (2022). [Online]. <https://www.paho.org/es/temas/discapacidad>. [Last accessed: 08 August 2022]
2. C. S. Jaramillo Losada, J.: Evaluation of technical aids. Editorial University Santiago de Cali, pp. 351–384 (2020)
3. Ronald Saavedra, E.G.T.S.A.: Design of a stand up equipment. Engineering UC Magazine **20**(1), 25–33 (2013)
4. Ochoa Sergio, C. M.: Proyecto Melissa. Universidad distrital francisco José de Caldas, Bogotá, November 2015

5. Vasquez, L.F.B.: Control system for the mobility and extension of a wheelchair. Technical University of Ambato, Ambato - Ecuador (2017)
6. Ronald Saavedra, E. G. T. S. A.: Design of a stand up system. Eng. UC Mag. **20**(1), 25–33 (2013)



Use of Ozonized Oil in Chronic Wounds of Lower Limbs: Preliminary Results

T. K. Serra^{1,2}(✉) , L. Dos Santos¹ , L. Assis¹ , J. C. Tarocco¹ ,
P. C. O. Z. Pimente¹ , and C. Tim¹ 

¹ Brazilian University, Scientific and Technological Institute, Biomedical Engineering, Carolina Fonseca, 235, São Paulo, Brazil

thallitacescr@gmail.com, carla.tim@universidadebrasil.edu.br

² State University of Maranhão: Nursing, São Luís, Brazil

Abstract. A randomized, double-blind clinical trial approved by the Research Ethics Committee (no. 4,246,236) was conducted in which elected patients had chronic wounds in the lower extremities. Participants aged 55 to 70 years, of both genders, with wounds on the lower limbs for more than 12 weeks of vascular, diabetic or traumatic etiology. 08 patients were randomly assigned in two groups: Group 1 – patients with chronic wounds received treatment with ozonated sunflower oil, concentration of 600 m²/kg; (milliequivalent/kg) and Group 2 – patients with chronic wounds who underwent treatment with traditional sunflower oil. All patients, when necessary, before starting treatment received debridement necrotic tissues was performed. To perform the bandage, the wound was first cleaned with 0.9% saline solution and then ozonized or traditional sunflower oil were administered throughout the wound bed, and then covered with sterile dry gauze, padding in bandage, and fixed with adhesive. All patients received the same procedure three times a week for 12 weeks. The results showed that the wounds of group 1, ozonized sunflower oil, improve in the aspects of the wounds with the presence of granulation tissue and absence of signs of infection and occurred reduction or complete repair of wounds. In the conventional curative group, with non-ozonized traditional sunflower oil, one wound completely repaired, however the other lesions continued with seroso type exudation, with the presence of edema at the wound site, presence of sign and signs of infection. In view of the above, it was observed that the use of ozonized sunflower oil promoted bactericidal and restorative effects.

Keywords: Treatment · Wound · Ozonized oil · Repair · Tissue damage · Sunflower oil

1 Introduction

The structural and physiological rupture of the integumentary system is called a wound [1, 2]. Immediately after the injury of the tissue integumentary, begins a complex repair process, which includes the interaction of a series of biological events and phenomena capable of stimulating the process of tissue repair, namely inflammation: proliferation,

proliferation [3]. Nonetheless, in the course of this process, changes may occur that culminate in repair deficiency and, consequently, in the delay or even in the absence of tissue repair, thus, as wounds become chronic [1]. The bandage is the standard treatment of these wounds, its main objective is to provide a physical barrier of temporary protection; absorb wound drainage; and provide the moisture needed to optimize re-epithelialization [4]. Ozone therapy has been an adjunct wound treatment, contributing to tissue repair in an economically viable, noninvasive way and without side effects [5].

The ozone molecule has antimicrobial effect without causing resistance [6]. In addition, the literature shows that ozone therapy improving the inflammatory response by stimulating the synthesis and release of cytokines and growth factors such as epidermal growth factor (EGF), platelets derived growth factor derivative (PDGF), growth transformer factor (TGF) and vascular endothelial growth factor (VEGF), growth transformer factor (TGF) and vascular endothelial growth factor (VEGF) [7–9]. Ozone can be used in different forms, such as gaseous or dissolved in water or oil (ozonized solutions) [9]. The advantage of ozonized oil is that expenses can reach a decrease proportional to 25% if equated with antibiotic expenses [8, 10].

In addition, ozonized oil has anti-inflammatory and analgesic effects, increasing the release of growth factors capable of contributing to tissue repair [12]. Although ozonized solutions are auxiliary in tissue repair, there is no standardized protocol for the treatment of skin wounds or even comparative studies to evaluate the advantages and disadvantages of ozonized oil. Therefore, this study aimed to evaluate and compare the effects of ozonized sunflower oil with traditional sunflower oil in the treatment of chronic wounds.

2 Material and Methods

A randomized, double-blind clinical trial approved by the Research Ethics Committee (no. 4,246,236) was conducted in which elected patients had chronic wounds in the lower extremities. Eight participants were selected by the means of active search in all health units of the municipality and dissemination of the project to the community by pamphlet and social network. After surveying the candidates participating in the research, they were evaluated to verify whether they were eligible using the following criteria: Inclusion: Patients aged 30 to 70 years, both genders, with wounds on the lower limbs more than 12 weeks of vascular, diabetic or traumatic etiology. Exclusion: Bedridden patients, neoplasms, leprosy, patients with neurological problems, pregnant patients, patients with HIV (Human Immunodeficiency Virus).

Patients were randomly assigned in two groups: Group 1 – Patients with chronic wounds received treatment with ozonized sunflower oil, concentration of 600 m^2/kg ; (milliequivalent/kg); Group 2 – Patients with chronic wounds who underwent treatment with traditional sunflower oil.

2.1 Intervention

All patients, when necessary, received adequate debridement of necrotic tissues. To perform the dressing, the first wound was cleaned with 0.9% saline solution and then

ozonized sunflower oil or traditional sunflower oil was administered throughout the wound bed, and then covered with sterile dry gauze, padding in bandage and fixed with adhesive. All patients received the same procedure three times a week for 12 weeks.

2.2 Clinical Assessment

The patient's anamnesis was performed by applying the patient data collection instrument, which included information on the main complaint, history of family disease, main comorbidities, lifestyle, blood glucose measurement and blood pressure measurement. Next, the clinical evaluation of the lesions in which the following clinical aspects were evaluated was performed: wound site, tissue characteristics, exudated amount, edge characteristics, injured skin, based on the protocol used by Campos et al. [13]. These data were obtained before starting the intervention in all participants involved in the research and in cases where the wounds did not repair after 12 weeks of treatment. Clinical evaluation was performed again. As the wound areas were photographed at the beginning and end of treatment using a digital camera.

2.3 Microorganism Analysis

The analysis of microorganisms was performed by collecting the swab from the lesion(s) in the first treatment session. The patient who still presented lesions after 12 weeks was collected in a new swab analysis. The material was collected by an adequate and qualified professional for this procedure, respecting the asepsis techniques and biosafety standards.

3 Results

The study was conducted in 08 patients of both genders, being 5 women and 3 men aged 55 to 70 years, 50% of term venous wounds, 37.5% diabetic and 12.5% traumatic and in relation to wound time, all were more than 12, in the evaluation of weeks of comorbidity weeks the patients evaluated fear diabetes, hypertension and venous insufficiency, only 1 patient did not present comorbidity.

During the treatment, 3 wounds had total repair, two belonging to the group receiving ozonized sunflower oil closed and one receiving conventional dressing. As initial morphological alterations in both groups showed that at the beginning of treatment they presented alterations, characterized by irregular edges, total loss of skin thickness with extensive destruction, muscle damage or support structures, intense edema, presence of exudate, macerated and presence of sides. After treatment, Fig. 1 shows complete repair or reduction of wounds, improvement in wound aspects with the presence of granulation tissue and absence of signs of infection.

Figure 2 represents the wounds belonging to group 2, conventional dressing group with non-ozonized sunflower oil. After the 12-week period, one wound completely noticed, however the too many lesions continued with serosotype exudation, with the presence of edema at the wound site, presence of crumbles and signs of infection.

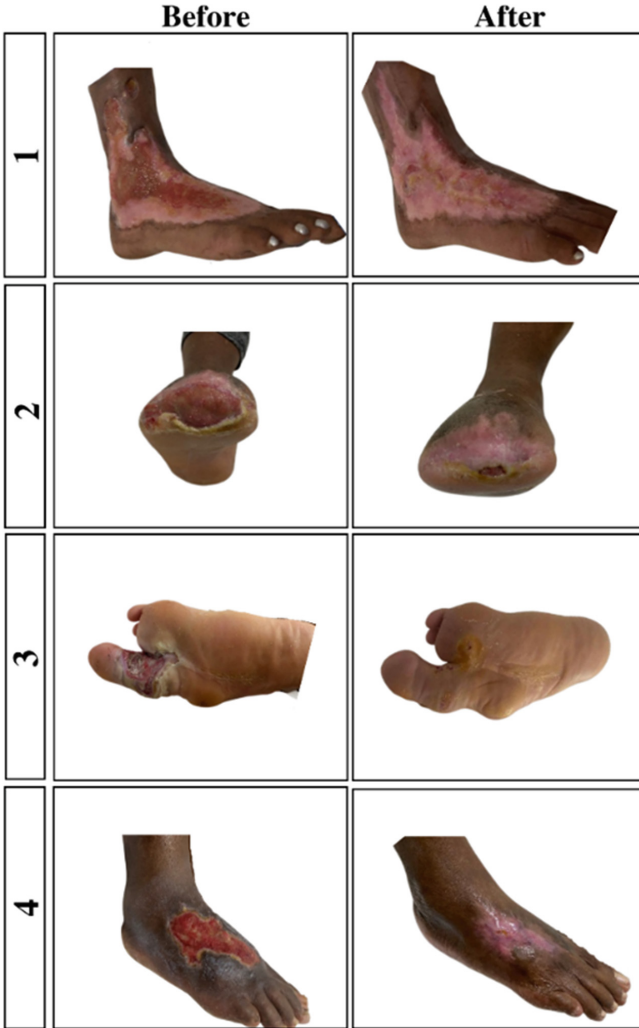


Fig. 1. Wounds treated with ozonized sunflower oil – Group 1

Due to the skin lesions presenting clinical signs of infection samples were collected to identify microorganisms. The results show that in the 8 wounds treated in this study, 13 species of bacteria were identified (Table 1).

The patients of group 1, ozonized sunflower oil, showed greater presence of microorganisms in the lesions, the patients had more than 1 species of bacteria, than the wounds belonging to group 2, traditional sunflower oil.

The most detected species of bacteria in the groups were *Pseudomonas aeruginosa* 38.4%, *Klebsiella pneumoniae* 23.7% and *Klebsiella oxytoca*, *Morganella*, *Enterococcus faecalis*, *Proteus mirabilis* and *Providencia stuartii*, 7.6% with one.

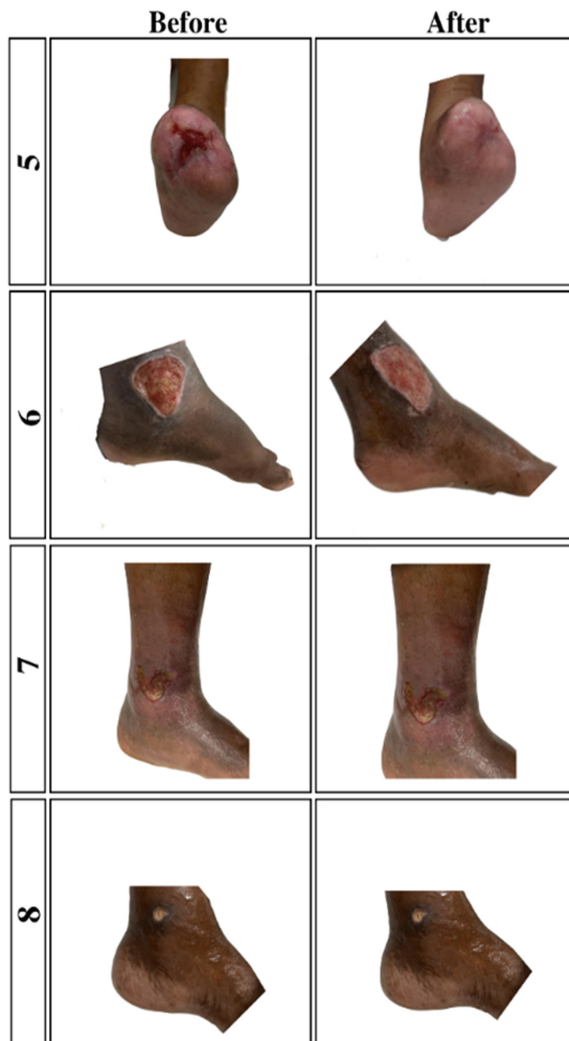


Fig. 2. Wounds treated with traditional sunflower oil – Group 2

After the 12-week period, the wounds that did not fully notice were reevaluated and it was observed that two patients belonging to group 1, ozonized sunflower oil, still had an injured area, as wounds were not infected. However, as wounds belonging to group 2, conventional dressing with traditional sunflower oil, still presented the presence of the same bacteria initially identified (Table 2).

Table 1. Microorganisms present in wounds before treatment

Patient	Bacterium	Level
<i>Group 1</i>		
1	<i>Morganella Morganii</i>	Abundant
	<i>Klebsiella pneumoniae</i>	Abundant
	<i>Enterococcus faecalis</i>	Abundant
2	<i>Mirabilis</i>	Abundant
	<i>Klebsiella pneumoniae</i>	Lightweight
	<i>Pseudomonas aeruginosa</i>	Lightweight
3	<i>Pseudomonas aeruginosa</i>	Lightweight
	<i>Klebsiella pneumoniae</i>	Lightweight
4	<i>Oxytouch klebsiella</i>	Lightweight
	<i>Pseudomonas aeruginosa</i>	Lightweight
<i>Group 2</i>		
5	<i>Pseudomonas aeruginosa</i>	Lightweight
6	<i>Stuartii Provides</i>	Lightweight
7	Negative	–
8	<i>Pseudomonas aeruginosa</i>	Lightweight

Table 2. Microorganisms present in wounds after treatment

Patient	Bacterium	Level
<i>Group 1</i>		
1	Negative	–
2	Negative	–
3	No injury	–
4	No injury	–
<i>Group 2</i>		
5	No injury	–
6	<i>Stuartii Provides</i>	Lightweight
7	Negative	–
8	<i>Pseudomonas aeruginosa</i>	Lightweight

4 Discussion

The present study observed that the use of ozonized sunflower oil promoted bactericidal effect and stimulated the process of skin repair of chronic wounds. These findings are in accordance with the study by Zanardi et al. [14] that observed, *in vitro*, the bactericidal effect of ozonized sesame oil in Gram-positive and Gram-negative bacteria (*Staphylococcus aureus*, *Enterococcus faecalis*, *Pseudomonas aeruginosa*, *Escherichia coli* and *Candida albicans*), which are often detected in wounds in humans. Furthermore, the authors declare that the application of ozonized oil is very promising in a variety of skin and mucosal infections, due to its bactericidal effect, and also warn that, before the application of ozonized oil, the damaged surface of the skin should be cleaned with the removal of necrotic tissue and excess liquid exudate.

Similarly, in an *in vivo* study, it was observed that the use of camellia oil ozonized in excisional wounds on the back of rats accelerated the process of skin repair [15].

Positive results were observed in clinical studies, Campanati et al. [16] compared the use of ozonized oil with hyaluronic gel in the treatment of 30 patients with second-degree skin burn. Each skin burn was subdivided into two symmetrical parts, one part was treated with occlusive dressing of ozonized oil and the lateral part of the lesion was treated with topical application of hyaluronic acid in gel, once a day, for 12 weeks. The authors found that all treated lesions improved regardless of the treatment used, and that ozonated oil was as effective as hyaluronic acid in improving erythema, tension, itching and burning sensation reported by patients.

In view of the above, the use of ozonized sunflower oil may be an alternative treatment for chronic and/or infected skin lesions.

5 Conclusions

The present study demonstrates the potential reparative effect of ozonized sunflower oil in the treatment of chronic wounds and promoted the bactericidal effect on treated wounds.

Acknowledgment. We would like to acknowledge the contributions of the funding agency CAPES for the financial support of the present research.

Conflict of Interest. The authors declare that they have no conflict of interest.












References

1. Reinke, J., Sorg, H.: Wound repair and regeneration. *Eur. Surg. Res.* **49**, 35–43 (2012). <https://doi.org/10.1159/000339613>
2. Hameedaldeen, A., Liu, J., Batres, A., et al.: FOXO1, TGF- β regulation and wound healing. *Int. J. Mol. Sci.* **15**, 16257–16269 (2014). <https://doi.org/10.3390/ijms150916257>
3. Guo, S., Dipietro, L.: Factors affecting wound healing. *J. Dent. Res.*, 219–229 (2010). <https://doi.org/10.1177/0022034509359125>

4. Demidova-Rice, T., Hamblin, M., Herman, I.: Acute and impaired wound healing: pathophysiology and current methods for drug delivery, part 1: normal and chronic wounds: biology, causes, and approaches to care. *Adv. Skin Wound Care* **25**, 304–314 (2012). <https://doi.org/10.1097/01.ASW.0000416006.55218.d0>
5. Majd, S., Khorasgani, M., Moshtaghian, S., et al.: Application of nano chitosan/PVA fiber as a curative potential for diabetic rats induced by streptozotocin. *Int. J. Biol. Macromol.* **92**, 1162–1168 (2016). <https://doi.org/10.1016/j.ijbiomac.2016.06.035>
6. Lin, H., Venault, A., Chang, Y.: Zwitterionized chitosan base membranas macias para cicatrização de feridas diabéticas. *Sci* **591**, 117319 (2019). <https://doi.org/10.1016/j.memsci.2019.117319>
7. Akturk, A., Van Netten, J., Scheer, R., et al.: Ulcer-free survival dias e úlceras curativas em pacientes com úlceras diabéticas: Um estudo prospectivo de coorte. *Int. Ferida J.* **16**, 1365–1372 (2019). <https://doi.org/10.1111/iwj.13199>
8. Atkin, L.: Chronic wounds: the challenges of proper management. *Frei. J. Comunitário de Enfermagem* **24**:S26–S32 (2019). <https://doi.org/10.12968/bjcn.2019.24.Sup9.S26.31479336>
9. Valacchi, G., Fortino, V., Bocci, V.: The double action of ozone on the skin. *Br. J. Dermatol.* **153**, 1096–1100 (2005)
10. Fitzpatrick, E., Holland, O., Vanderlelie, J.: Ozone therapy for the treatment of chronic wounds: a systematic review. *Int. Wound J.* **15**, 633–644 (2018)
11. Melo, M., Alves, L., Carvalho, H., et al.: Ozone therapy in CO₂ laser-induced burns on rat skin. *XXIV Congr. Bras. Eng. Biomédica* **24**, 2671–2674 (2014)
12. Guinesi, A., Andolfatto, C., Filho, I., et al.: Ozonized oils: a qualitative and quantitative analysis. *Braz. Dent. J.* **22**, 1 (2011)
13. Campos, A., Borges-Branco, A., Groth, A.: Cicatrização de feridas. *Arq. Bras. Cir. Dig.* **20**, 51–58 (2007). <https://doi.org/10.1590/S0102-67202007000100010>
14. Zanardi, I., Burgassi, S., Paccagnini, E., et al.: What is the best strategy for enhancing the effects of topically applied ozonated oils in cutaneous infections? *Biomed. Res. Int.* **27**, 702949 (2013). <https://doi.org/10.1155/2013/702949>
15. Xiao, W., Tang, H., Wu, M., et al.: Ozone oil promotes wound healing by increasing the migration of fibroblasts via PI3K/Akt/mTOR signaling pathway. *Biosci. Rep.* **37**, 1–11 (2017). <https://doi.org/10.1042/BSR20170658>
16. Campanati, A., De Blasio, S., Giuliano, A., et al.: Topical ozonated oil versus hyaluronic gel for the treatment of partial- to full-thickness second-degree burns: a prospective, comparative, single-blind, non-randomised, controlled clinical trial. *Burns* **23**, 579036 (2013). <https://doi.org/10.1016/j.burns.2013.03.002>



COVIData: A Web Platform for Tracking, Classification and Monitoring Cases Suspects of COVID-19

Beatriz L. Gandolfi¹ , Clarissa S. R. Merino¹ , Vitor I. da Silva² ,
Diego S. Costa² , Gabriel de M. Fiali² , André S. Carneiro¹ ,
Luiz R. C. da Silva² , Camila C. Rocha² , Giovanna B. Lins³,
Saul C. Leite² , and Fernanda N. Almeida¹  

- ¹ Center for Engineering, Modeling and Applied Social Sciences, Federal University of ABC, São Bernardo do Campo, Brazil
fernanda.almeida@ufabc.edu.br
- ² Center for Mathematics, Computing and Cognition, Federal University of ABC, Santo André, Brazil
- ³ Center for Natural and Human Sciences, Federal University of ABC, Santo André, Brazil

Abstract. The high speed spread of SARS-CoV-2 through out the entire globe has ignited the warning about the importance and need to collect data from patients possibly infected, on a massive scale, in order to understand spreading dynamics of this particular disease. Having stated that, this article aims to present the entire development of the web platform COVIData, created by students and researchers of the Federal University of ABC (UFABC) while in partnership with Inter-municipal Consortium of ABC, resulting in a tool directed to people' self-screening their symptoms and being able to have an immediate identification of whether they are or not possibly infected. The tool consists of a detailed questionnaire based on scientific data on the most common symptoms of the disease. The questionnaire has been validated by healthcare professionals to verify the correlation of symptoms described by individuals using COVIData with SARS-CoV-2 infection. Furthermore, as a result, data analysis may be made and enhanced viewing the possibility to discuss, develop and implement public policies that help facing the disease.

Keywords: COVID-19 · Self-screening · Health monitoring · Public health · Decision support system · Database

1 Introduction

Since the coronavirus outbreak in China, late 2019, to the present time (August 2022), more than 593 million people have been reported as infected with SARS-CoV-2 around the globe [13]. The sudden spread of the disease has struck up

a global alert about the need to understand its different manifestation forms, as well as the many spreading ways it has and is transmitted through society, bearing in mind not only to detect the entire behavior spectrum of the new virus, but also the need for public health and public management to make decisions and face the challenges and consequences it shall up-bring by facing this pandemic.

Having lasted over 02 years and being something population has to deal with on a daily basis, meanwhile going back to their “normal lives”, COVID-19 is still a topic on demand and many studies are still carried on in this regard in order to make sure we will not face its pandemic status once again.

Once the panorama of increasing cases accelerating over time, the concern with under-reportation of cases was born, especially in places with lack of information access, such as not so much developed countries or even rural or low income areas. These factors revealed the huge challenge of lack of communication spread which lead to lack of knowledge, from these citizens, on the pandemic itself and also on prevention methods, vaccination and follow up in cases of infection.

Contemplating the previously stated facts, on regards of finding ways to identify possible infected and contaminating patients without conducting clinical examinations has become an urgent and extremely important matter so that one may to try to curb the geographical spread of the virus and to advise these patients to perform proper social isolation and take compatible hygiene measures. Moreover, once the self-assessment, to be further explained, is performed and gives as a result a possible positive to COVID-19 infection, the individual receives indications of what to do and what not to do next, avoiding the spread of COVID-19.

One way to identify these possible cases of COVID-19 is to offer tools that allow screening the symptoms experienced by the population, as an attempt to avoid the fast-paced spread of this disease, especially given that tests and masks are not mandatory for most situations and not all are vaccinated still.

In addition to being possible to classify people as suspects based on protocols of the World Health Organization and the Health Ministry of Brazil, tools such as the one presented may also offer the possibility to collect quality information in real-time about the characteristics of the population such as age, gender and body mass index (BMI), their pre-existing diseases, geographical location and how the disease manifests itself in different ways according to these factors.

Once we are able to track and have these quality data in hand, it is possible to generate solid insights into the disease behavior in a predetermined region to boost government measures to tackle the disease and its uncontrolled spread in the population, which can lead to the collapse of the health system resulting in deaths due to lack of adequate care.

Last, with the advances of social media usage and podcast, we were able to share useful and valuable information, even fighting back the so called “Fake News” (false or misleading information) and spread topics that were relevant for the population including: vaccination, health safety measures, mental health

helping tools as well as UFABC updates on returning to in person classes and also community updates and news.

Many initiatives addressing the mechanisms previously mentioned have been launched all over the world, such as the CDC screening system in partnership with Apple Inc. [5] and the application ‘Corona Virus - SUS’ [16] concomitant with the Brazilian framework are solid examples. Nonetheless, both tools are exclusively dedicated to doing a self-assessment of symptoms and do not expand its functionalities to analyze the community transmission of the virus in the regions where the screenings are carried out and the symptoms particularities.

Thus, the COVIData web platform is a tool for self-screening the population, easy to use and access, estimating a possible infection and suggesting next steps to be taken, also helping the debate, development and implementation of public policies that help to face the pandemic we are experiencing.

The platform itself aims to reach the public with the report of symptoms of COVID-19, in real time, through a detailed questionnaire, based on scientific knowledge and on the most common symptoms of the disease. This questionnaire was validated by world health professionals. The platform allowing the tracking of the geographic location of identified as symptomatic individuals and helping the early identification of cases, leading to help in blocking the spread of the disease.

In addition, through social media and podcast, the platform seeks constant communication with the scientific community and society, aiming at broad knowledge and dissemination of true information about the pandemic and the like. The COVIData emerged amid concerned within the notification and monitoring of suspected cases of COVID-19 in the ABC Paulista area (metropolitan region of São Paulo).

Efforts were established addressing the creation of a simple and intuitive web application that could be accessed in any location from any personal device, being those computers or mobiles. The web platform is concerned and aiming to identify potentially infected citizens using a self-assessment of patients’ symptoms and pre-existing health conditions, also tracking geographically people who have already perform the screening. By these means, it is possible to create a database with all the information provided by users to understand how the disease spreads and manifests itself in the ABC population.

2 Methods and Approach

2.1 Development of the Screening Method

At first sight, we focus on creating a web platform which counts with a complete screening flowchart that understood symptoms that are being recently identified in clinical research around the world, updated and evidence-based. The questionnaire - result of the flowchart - was applied through an electronic web form, hosted on the UFABC web server. The user, before being directed to the platform’s questionnaire, must accept to participate in the survey (the acceptance form was also made available electronically). The Terms of Use of the tracing

tool was registered in the Ethics Committee's with the protocol number CAEE: 33797120.4.0000.5594.

During the period in which the web platform was implemented and given the lack of knowledge about the dissemination aspects of the SARS-CoV-2 virus, analyzing and understanding the behavior of this virus in clinical cases of infected patients was followed by several studies [3, 18]. Through these studies and the follow-up of cases, we were able to notice as studies on clinical cases are treated segmentally around the world, clinical manifestations may vary according to the group of patients analyzed.

In spite of the fact that the most well-known symptoms of the coronavirus infection being dry cough and shortness of breath associated with fever, studies indicate that other symptoms such as diarrhea, headaches, and myalgia [1, 8, 20] are quite common in COVID-19 patients, and may as well go unnoticed or mistaken as symptoms for different diseases other than COVID-19, for example, flu.

Another study presented by the University of Mons has shown that a relevant part of the individuals afflicted by loss of smell and taste [9, 10]. Others works published alongside Europe and China also have shown mental confusion and migraine [11, 15, 19], and dermatological manifestations [12, 17] as possible symptoms of COVID-19.

In addition to symptoms that manifest with the disease, variables like how characteristics gender, age and comorbidities, for example, diabetes, cardiovascular diseases, immunosuppressive diseases are related to the number of infected and coronavirus results are also discussed [4, 21].

Using the information contained in these studies, as well as the COVID-19 management protocol of the Health Ministry of Brazil [14], a flowchart was developed (Fig. 1), consisting in questions about the most widespread symptoms about the coronavirus. This symptoms are similar as a respiratory syndrome and were also related with symptoms that were identified by researchers as previously cited. We were also include in the COVIData the pre-existing illnesses and personal characteristics (Fig. 1).

The workflows were built based on a scoring scheme. These score has been added to each question marked as 'yes' by the user. The final sum of the screening questions score served to classify the user as 'not suspicious', 'mild suspicious', 'average suspicious', 'high suspicious'. In those cases, in which the suspicion of COVID-19 infection is confirmed, the website informs user important recommendations on social isolation, hygiene and guidelines for medical advice seeking and provides the address with telephone of the health centers and hospitals closest to the user for assistance. As the screening tool uses the user's geographic location, it was possible to indicate the nearest hospitals and health centers to the user.

An utterly important fact that COVIData is not intended to act as a diagnosis web platform. The result of the questionnaire indicates a suggestion about the possibility of SARS-CoV-2 virus infection.

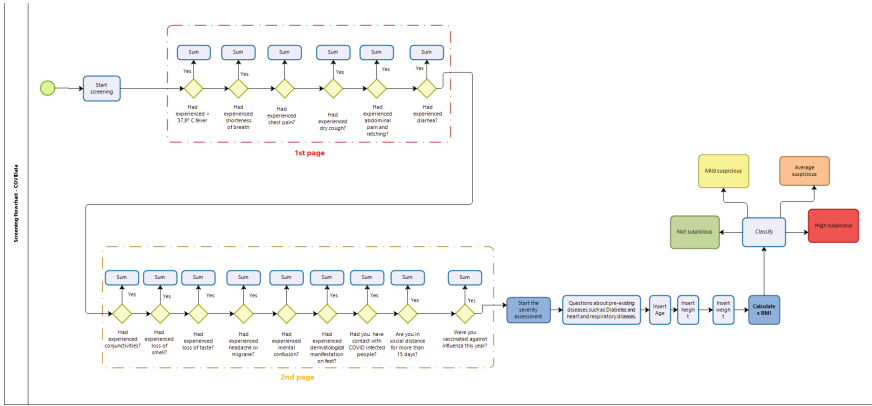


Fig. 1. COVIData simplified screening workflow.

2.2 Partnership and Additional Features

The implementation of the platform made it possible to generate several public health and population management insights, so the initiative started at the Federal University of ABC could also count on a partnership with the Inter-municipal Consortium of ABC, which is currently responsible for planning and articulating regional actions in seven cities of the metropolitan region of São Paulo, Brazil. Relying on this partnership, it was possible to direct the geographical analysis of the geo-location data captured through the IP and GPS of the devices used to access the platform combined to clinical data obtained to positively impact the area close to the UFABC and provide information to supplement the updating of the number of COVID-19 in these cities.

What is more, in addition to the screening functionality, once the user is classified as suspect, the tool provides a registration tab that is customized according to the ABC Inter-Municipal Consortium membership cities’ data of interest. From this registration, it is possible to drive services in collaboration with this municipalities and their Health Departments. Were developed, 3 functional fronts: registration for tele-monitoring carried out by the health departments, registration to address the patient for clinical testing in partnership with the Federal University of ABC, and a personalized study on the prevalence of the disease in one of the consortium’s member city.

On the first registration front that directs patients for tele-monitoring, those who had been classified as ‘suspects by SARS-CoV-2 infection’ have the possibility to register. When the user requests registration, the following data is requested: address, phone number, ethnic group, occupation and other information that may be important for the development of public policies. In this case, city halls and health departments are responsible by the tele-monitoring structure. The data collected in these tele-consultation will return to the COVIData platform, to create more robust information about population experiencing coronavirus symptoms.

2.3 Information Spreading

Since the beginning of the pandemic, there has been an increase in the spread of so-called fake news, which not only led to the alienation of the population, but also to a poor management of the pandemic and aggravation of the unfavorable situation in which we find ourselves numerous times with the collapse of the health system.

People who didn't understand well what the virus was, if there really was a virus, how to prevent it, what treatments or measures to take when infected population, not always with great accuracy or veracity.

Thus, it was decided to create a communication and social media group on the platform, in order to search for new relevant information about COVID-19 and the like (variants, vaccination, tests, etc.) and transmit it in a simple and cohesive way to as many people as possible.

Thus, this group was responsible for creating the social networks of COVIData UFABC (Instagram and Facebook), in addition to communicating with the platform's followers through their message portals and institutional email.

After the creation of social media, the issue regarding the inclusion of their users was raised. Thus, we started to insert tools such as enabling the option of reading text and comments on Facebook and Instagram, avoiding the use of special characters, in addition to creating a Podcast with monthly updates of the project in which the topics covered in the publications are taken spoken to the population.

Finally, with the unexpected extension of the pandemic for more than a year, issues of Mental Health and Well-Being were raised, leading to the prioritization of publications and interaction with the public aimed at this point.

3 The COVIData Implementation

The Web platform COVIData was developed using mostly *JavaScript* often abbreviated JS. This language is a high-level programming language primarily designed to run in browsers and manipulate web page behaviors. The JS is one of the most important technologies aimed at the front-end and, joining the trio HTML, CSS and PHP, they form a group of languages that cover practically all the requirements of the development of a complete, dynamic and with good performance page. With its scripts it is possible to include, in a static page, dynamic elements such as maps, forms, numerical operations, animations, interactive infographics and much more.

The JS frameworks we used for development were different for the frontend and backend. For the frontend, React JS was used. The Front-end is closely related to the graphical interface of the project. That is, it is where the application is developed with which the user will interact directly, whether in software, websites, applications, etc. Therefore, it is essential that the developer has a concern for the user experience.

React (also known as React.js or ReactJS) is a free and open-source front-end JavaScript library for building user interfaces based on UI components.

It is maintained by Meta (formerly Facebook) and a community of individual developers and companies. React can be used as a basis in the development of single-page, mobile, or server-rendered applications with frameworks like Next.js. However, React is only concerned with state management and rendering that state to the DOM, so creating React applications usually requires the use of additional libraries for routing, as well as certain client-side functionality.

For backend, we used NodeJS with Express. The backend is the structure that enables the system to operate, while the front-end is responsible for the visual part, such as presentation, design, languages, colors, among others. Even though they have different roles, these applications are closely linked so that electronic environments operate in sync.

Node.js can be defined as a server-side Javascript execution environment. This means that with Node.js it is possible to create Javascript applications to run as a standalone application on a machine, not depending on a browser for execution, as we are used to. Despite being recent, Node.js is already used by large companies in the technology market, such as Netflix, Uber and LinkedIn.

The main reason for its adoption is its high scalability. In addition, its architecture, flexibility and low cost make it a good choice for implementing Microservices and Serverless architecture components. Even the main providers of Cloud products and services already support the development of scalable solutions using Node.js.

For the database we use MongoDB (<https://www.mongodb.com/>). This source-available cross-platform is an open source, high performance and flexible database, being considered the main NoSQL database. NoSQL databases have some advantages over other types, especially when we need scalability, flexibility, good performance and ease of queries.

MongoDB is document-oriented, that is, data is stored as documents, unlike relational model databases, where we work with records in rows and columns. Documents can be described as data in key-value format, in this case, using JSON (JavaScript Object Notation) format (<https://www.json.org/>).

4 Results

The COVIData tool (<https://covidata.ufabc.edu.br/>) was made available on April 2020. In the first two weeks of use (from launching to May 2020), 7012 screenings were carried out throughout Brazil. The database was then processed and filtered to select the ones carried out in the Grande ABC region and to remove duplicated or inconsistent data. Altogether, after this treatment, 2672 screenings were considered as interest data. From these, 1106 users were classified as suspected of COVID infection according to their responses. The distribution of the levels of suspicion was: 59% without suspicion, 6% mild suspicion, 4% medium suspicion, 31% severe suspicion.

Using the geolocation information linked to these screenings, it was possible to track which cities owned the highest number of suspected cases. Using the Leaflet [2] package was generated an interactive graph with the estimated density of screenings classified as suspected of being infected by COVID-19 (Fig. 2).

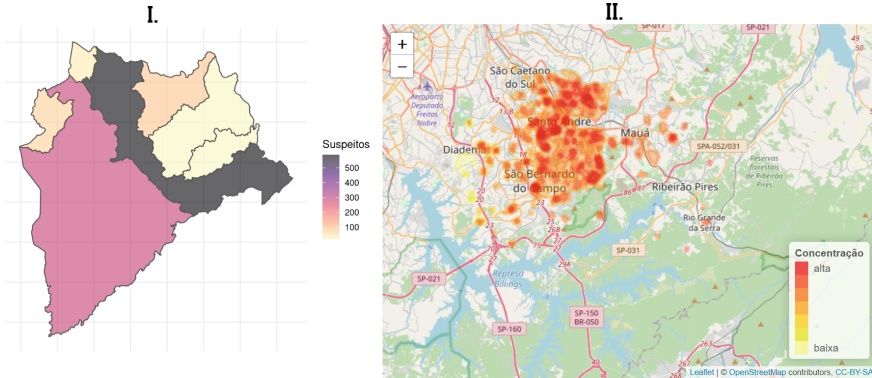


Fig. 2. I. Suspected cases identified for the ABC region and II. Interactive graph of the estimated density of screens classified as suspicious

At this very first moment right after the availability of the platform, the aim of the tool was to provide simple, quick and easy information to both the consortium and the population - who has access to reports directly on the platform's website. The graphics presented by COVIData show statistics about of the number of cases and their distribution over age groups and gender, as well as the frequency with which symptoms were reported for the different classifications of suspicion (Fig. 3) and generated. From the age groups graphic, it is visible the suspicion is concentrated among individuals between 20 and 60 years old. Although studies have [1] shown that elderly patients have more symptoms and have a higher risk of death, the sample demonstrates that the elderly are not the main focus of COVID-19 in the region.

Regarding gender, the suspicion of infection was more prevalent among women, representing 59% of the total. Again, the sample did not corroborate with published research that showed the prevalence among men and women is the same despite the fact that the disease has higher mortality among men [6].

Through the graphs which show symptoms, it was also possible to observe that for individuals classified as serious suspects, the frequency in which the different symptoms are reported was more balanced, while for users without suspicion and with mild suspicion the symptoms “headache” and “coughs” are reported much more frequently than other symptoms. Despite the balance in the frequency of symptoms reported by those classified as serious suspects, it was possible to identify that symptoms such as respiratory distress, chest pain, and loss of taste and smell become more relevant in patients with the highest levels of suspicion.

Finally, after much study and analysis of topics related to social media, the creation of arts, videos and podcast was carried out, with weekly publications on days and times of greater access, in addition to the use of tools such as stories to reach a greater number of people, even with the possible fatigue that the COVID-19 issue has caused after so long a pandemic [7].

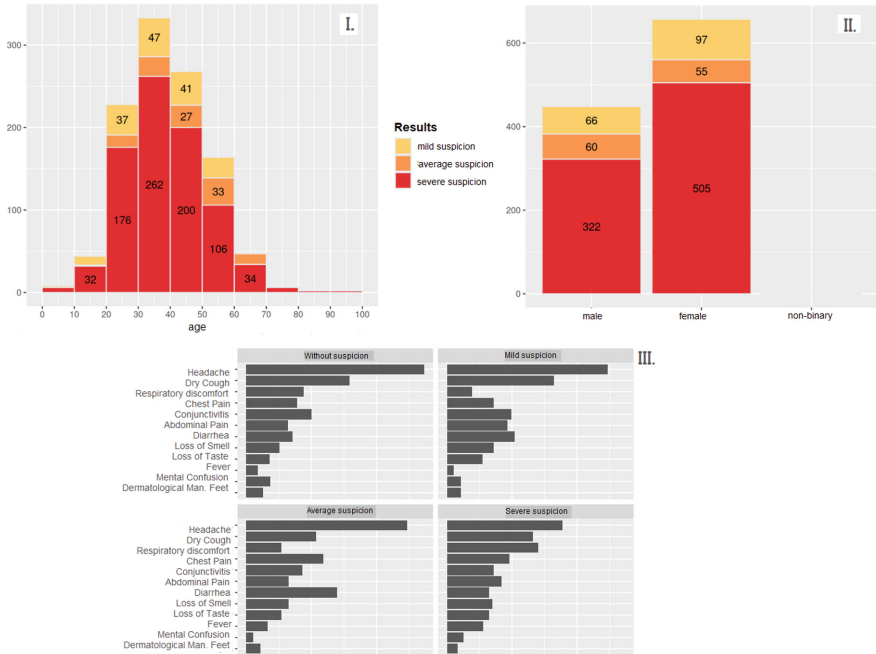


Fig. 3. I. Prevalence of cases by age, II. Prevalence of cases by gender, III. Frequency of symptoms according to risk classification

5 Conclusion

By these means, we may state that both a accurate diagnosis and follow-up and immediate responses have been of immeasurable need while we attempt to fight back and direct our efforts on the non-spread of Coronavirus disease.

It's also important to enhance the fact that, when we bear in mind facing pandemics like the one we've been facing for the last months (COVID-19) having tools which may be of immediate response is a must as the disease spreads more and more as the time passes.

Withal, the purposed tool targets not only a pre-diagnosis of COVID-19 but also helps people out on how to prevent themselves, what to do next concerning their infection suspicious level and also build up many analysis within the multiple data collected; ending up in benefits conjointly of use to many health organizations and governmental attitudes to be taken.

Conflict of Interest. The authors declare that they have no conflict of interest.

Acknowledgments. The authors would like to thank the Federal University of ABC to the support.


References

1. Clinical findings in a group of patients infected with the 2019 novel coronavirus (SARS-Cov-2) outside of Wuhan, China: retrospective case series. *BMJ* **368** (2020). <https://doi.org/10.1136/bmj.m792>. eprint: <https://www.bmj.com/content/368/bmj.m792.full.pdf>. www.bmj.com/content/368/bmj.m792
2. Cheng, J., Karambelkar, B., Xie, Y.: leaflet: Create Interactive Web Maps with the JavaScript “Leaflet” Library. R package version 2.1.1 (2022). <http://www.CRAN.R-project.org/package=leaflet>
3. Cheng, X., et al.: Symptom clustering patterns and population characteristics of COVID-19 based on text clustering method. *Front. Public Health* (2022). <https://doi.org/10.3389/fpubh.2022.795734>
4. Fang, L., Karakiulakis, G., Roth, M.: Are patients with hypertension and diabetes mellitus at increased risk for COVID-19 infection? *Lancet. Respir. Med.* **8**(4), e21 (2020)
5. Apple Inc.: Centers of Disease Control, and Prevention CDC. Coronavirus (COVID-19) (2020). www.apple.com/covid19/
6. Jin, J.-M., et al.: Gender differences in patients with COVID-19: focus on severity and mortality. *Front. Publ. Health* **8**, 152 (2020). ISSN: 2296–2565. www.frontiersin.org/article/10.3389/fpubh.2020.00152
7. Chávez-Martínez, O., Avila-Malpica, R., Gímez-Rivera, L., Franco-Rico, J.: Los servicios de información ante la pandemia por COVID-19/information services facing the COVID-19 pandemic. *Rev. Méd. Inst. Mex. Seguro Soc.* **60**(1), 1–3 (2022). ISSN: 2448-5667. <https://www.revistamedica.imss.gob.mx/editorial/index.php/revistamedica/article/view/4480>
8. van Kessel, S.A.M., et al.: Post-acute and long-COVID-19 symptoms in patients with mild diseases: a systematic review. *Family Pract.* **39**(1), 159–167 (2021). ISSN: 1460-2229. <https://doi.org/10.1093/fampra/cmab076>. eprint: <https://www.academic.oup.com/fampra/article-pdf/39/1/159/42243810/cmab076.pdf>
9. Lechien, J.R., et al.: Objective olfactory testing in patients presenting with sudden onset olfactory dysfunction as the first manifestation of confirmed COVID-19. *Infection*. Medrxiv (2020)
10. Lechien, J.R., et al.: Olfactory and gustatory dysfunctions as a clinical presentation of mild-to-moderate forms of the coronavirus disease (COVID-19): a multicenter European study. In: *European Archives of Oto-Rhino-Laryngology*, pp. 1–11 (2020)
11. Li, Y., et al.: Acute cerebrovascular disease following COVID-19: a single center, retrospective, observational study (2020)
12. Mazzotta, F., Troccoli, T.: Acute acro-ischemia in the child at the time of COVID-19. In: *Dermatologia Pediatrica, Bari* (2020)
13. World Health Organization. WHO - Coronavirus Disease (COVID-19) Dashboard (2022). <https://www.covid19.who.int/>
14. Protocolo de Manejo Clínico da Covid-19 na Atenção Especializada (2020). https://www.bvsm.sau.de.gov.br/bvs/publicacoes/manejo_clinico_covid-19_atencao_especializada.pdf
15. Rocha-Filho, P.A.S., et al.: Headache, anosmia, ageusia and other neurological symptoms in COVID-19: a cross-sectional study. *J. Headache Pain* (2022). <https://doi.org/10.1186/s10194-021-01367-8>
16. Ministério de Saúde Brasil. Coronavirus - SUS (2020). <https://www.play.google.com/store/apps/details?id=br.gov.datasus.guardioes&hl=ptBR>

17. Gholizadeh Mesgarha, M., Pour Mohammad, A., Shaka, Z., Goodarzi, A., Seirafian-pour, F., Pourriyahi, H.: A systematic review on mucocutaneous presentations after COVID-19 vaccination and expert recommendations about vaccination of important immune-mediated dermatologic disorders. *Dermatol. Ther.* (2022). <https://doi.org/10.1111/dth.15461>
18. Silva, B.R.O., et al.: Clinical-epidemiology aspect of inpatients with moderate or severe COVID-19 in a Brazilian macroregion: disease and countermeasures. *Front. Cell Infect. Microbiol.* (2022)
19. Vetter, P., et al.: Clinical Features of Covid-19 (2020)
20. Xu, X.-W., et al.: Clinical findings in a group of patients infected with the 2019 novel coronavirus (SARS-Cov-2) outside of Wuhan, China: retrospective case series. *BMJ* **368** (2020). <https://doi.org/10.1136/bmj.m606>. eprint: <https://www.bmj.com/content/368/bmj.m606.full.pdf>. <https://www.bmj.com/content/368/bmj.m606>
21. Zhou, F., et al.: Clinical course and risk factors for mortality of adult inpatients with COVID-19 in Wuhan, China: a retrospective cohort study. *The Lancet* (2020)



Mechanical Ventilator and Oxygen Concentrator System: Tinki's Proof of Concept

Pierol Quispe^{1,2}(✉) , Daniela Gómez-Alzate¹ , and Sandra Pérez-Buitrago¹ 

¹ Pontificia Universidad Católica del Peru, San Miguel, 15088 Lima, Peru

² Universidad Peruana Cayetano Heredia, San Martin de Porres, 15102 Lima, Peru
pierol.quispe@pucp.edu.pe

Abstract. The last two years have not only revealed profound deficiencies of the Peruvian health system, but have also led to its collapse on more than one occasion. Within this, medical oxygen production suffered serious problems which led to the shortage of this gas, widely used in mechanical ventilation of patients with respiratory diseases like COVID-19. Given this context, new alternative solutions must aim to eliminate reliance on conventional oxygen sources, therefore, oxygen concentrators were considered to be used as source of mechanical ventilators. In agreement with other studies, this work aims to evaluate the feasibility of a system that couples a MASI mechanical ventilator with COVOX oxygen concentrator, called the Tinki system, in terms of the fraction of inspired oxygen (FiO_2). For flows greater than 7 L/min, FiO_2 levels above 80% were obtained. The continuous change of valves and the use of Pressure control mode for ventilation, ensure around 92% in comparison to other set-ups, behaviour that can be maintained over 6 h. Although the results are encouraging, further research is required.

Keywords: Mechanical ventilation · Oxygen concentrator · Delivered FiO_2

1 Introduction

The COVID-19 pandemic highlighted the extensive limitations of the Latin American health systems, especially the Peruvian case. Before its arrival, some of the main problems that Peru faced within the health sector were the lack of technological resources and supplies, budget cuts, disorganization of human resources, lack and disconformity of personnel, and debilitated primary care services [1]. At the end of 2019, the Ministry of Health (MINSA) reported that Peru only had 13.6 doctors per 10,000 inhabitants, and 0.4 ICU beds and 5 mechanical ventilators per 100,000 inhabitants [2]. The COVID-19 outbreak greatly amplified these problems and led to a rapid collapse of the health system. By December 2020, the National Registry of IPRESS (institutions providing health

services) inspected 247 second-level hospitals belonging to public health institutions and determined that 97% of them had inadequate installed capacity (precarious infrastructure or insufficient/inoperative medical equipment). The fact that this figure almost double that of 2019, demonstrates the magnitude of the pandemic's impact. Unfortunately, all of this led to the death of 87,069 (8.84% mortality) during the first wave (March–October 2020) and 113,264 (9.11% mortality), during the second one (November 2020–October 2021) [3].

A determining factor that substantially aggravated the situation was the shortage of medicinal oxygen, used for both mechanical ventilation and oxygen therapy. The problem progressively scaled until the demand for this gas rose to 250 TPD during 2020. In response to this, the number of oxygen plants augmented to more than 400, capable of supplying up to 300 TPD [4]. However, not all plants functioned properly. In July 2021, the Ombudsman's Office presented the results of the supervision carried out on the management and availability of medical oxygen in 66 hospitals along the country, where it was detected that 17 oxygen plants located in 11 regions were inoperative. It was also reported that most operating plants would have been delivering only 70% of their capacity daily. Although at this time Peru is not in the midst of a new wave, the National Registry of Medicinal Oxygen (Renoxi) indicates that the oxygen reserves of 11 regions present medium risk, which indicates an availability of oxygen for 15 days, and the rest maintain a low risk, which means its availability for 15–70 days [?]. Another problem is the Peruvian geography since there are several rural areas whose accessibility is complicated and therefore, the distribution of oxygen to these places. In several cases it complicates access to rural areas, which directly impacts the distribution of oxygen tanks. This worsens when local plants stop operating (as has happened), which offloads supply responsibility to plants in other locations or regions, thus producing an over-demand that requires their production beyond their provided capacity. In this way, the supply systems ends up collapsing.

Consequently, oxygen supply for the mechanical ventilation of patients that suffers from respiratory diseases is in danger, therefore, future solutions must aim to eliminate reliance on conventional oxygen sources (such as cylinders or wall oxygen outlets in health centers). Oxygen concentrators (OC) are biomedical devices that produce oxygen from the ambient air, so they are considered an inexhaustible source of oxygen once connected to the electrical network. Due to this great advantage, different researchers have studied the possibility of unifying OCs with mechanical ventilators in a single system, in order to assess its viability. Cardinale, M. et al. enabled such a system using an Elisée 350 ventilator with two Newlife Intensity 10 OCs (with a max. flow of 10 L/min, each), with the aim of testing whether it could obtain $FiO_2 > 0.8$, which could treat ARDS. To do this, they configured the ventilator's minute volume between 4 and 15 L/min and modified the flow of the concentrators between 4 and 20 L/min. The results revealed that for minute volumes between 4 and 10 L/min, flows greater than 16 L/min reached the target FiO_2 , reaching up to 0.95 [6]. In fact, it was determined that by increasing the OC's flow, the respiratory rate (hence minute

volume), FiO_2 increases. Moreover, Bordes et al. documented the use of a Pulmonetics LTV 1000 ventilator with a SeQual Integra CO (up to 10 L/min), which obtained encouraged results too. With minute volumes between 4 and 6 L/min and flows over 8 L/min, $FiO_2 > 0.80$ were found, with a maximum of 0.9, that is, only 0.04 below the maximum originally delivered by the concentrator. The study confirms that the changes in PEEP and tidal volume have no significant difference, but the decrease in I:E does increase FiO_2 [7]. Furthermore, Rybak et al. carried out the proof of concept of a system that coupled an Impact 754 mechanical ventilator with a CO SeQual Saros 3000 (up to 6 L/min), with the aim of evaluating its operation in austere environments with low (365 masl) and high (1981 masl) altitude. For this, the CO was set at 3 and 6 L/min, while the ventilator was set to volume control and the respiratory rate varied between 4 and 20 breaths/min. In the case of low altitude, the system was able to deliver an FiO_2 of 0.9 for respiratory rates less than 10 breaths/minute, and surprisingly, for high altitude this was only reduced to 4 breaths/minute [8].

On the other hand, during 2020, the Pontifical Catholic University of Peru (PUCP) in alliance with private companies, took on the task of developing and manufacturing medical devices in response to the overwhelming demand. The first was MASI, an emergency mechanical ventilator. This device bases its operation on the automated compression of an Ambu resuscitator and allows imparting 3 ventilatory modes: volume control, pressure control and pressure support; relied on flow and pressure sensing. MASI was used in intensive care units throughout Peru, especially during the second wave of the pandemic [9]. The second was COVOX, an OC that also meets the high demand of its commercial counterparts, but also contributes to oxygen shortages for patients requiring oxygen therapy. This equipment is capable of delivering up to 15 L/min and guaranteeing oxygen concentrations greater than 90% [10]. Although its use has not yet reached clinical instances, this device recently completed its technical validation and is seeking approval from Peruvian regulatory entities.

The present work aims to discover if a system that couples MASI with COVOX, called the Tinki system, could deliver high values of fraction of inspired oxygen (FiO_2) to the patient's ventilatory circuit as occurs in ventilation with conventional sources. As it was reviewed, the scientific literature has demonstrated the in-vitro success of these systems, therefore, it is expected that Tinki can match or exceed the performance reported in these studies and thus provide a self-sustaining alternative to oxygen therapy with mechanical ventilation.

2 Methodology

The Tinki system (Fig. 1) consists of a COVOX oxygen concentrator, whose oxygen outlet is connected to the oxygen inlet of the MASI mechanical ventilator using a 10 mm pneumatic hose; while the ventilator's oxygen output is connected by a corrugated tube to a conventional ventilatory pneumatic circuit (inspiration/expiration valve, PEEP valve, and the ventilator's flow and oxygen sensor). A Fluke VT-650 gas flow analyzer was then coupled with a Fluke

AccuLung II (compliance: 25 mL/mbar, resistance: 20 mbar/L/s) test lung. It is worth mentioning that the union of both devices was carried out only by means of mechanical connections, so no digital or electronic communication was established between the devices' logic units.

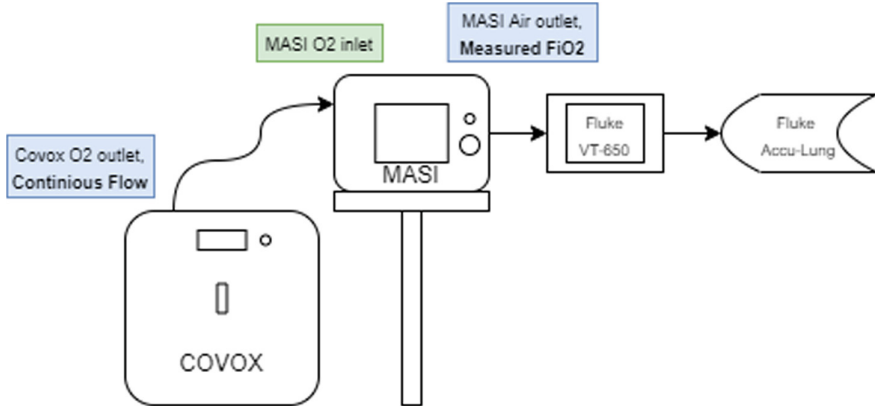


Fig. 1. Representation of the Tinkin system tested in this work

For system testing, MASI was configured with ventilatory parameters commonly applied to patients in a clinical setting. To perform pressure control (PC) and volume control (VC) modes, a tidal volume of 400 mL and a peak inspiratory pressure of 20 cm H₂O, were respectively set. In both cases, it was specified:

- Respiratory Rate: 20 rpm
- Trigger Flow: 4 L/min
- Inspiration Time: 1.0
- Inspiratory to Expiratory time: 1/2
- PEEP: 7.0 cm H₂O.

In the set-up, the only element that was exchangeable for the assays, was the security valve of MASI's Ambu resuscitator, which prevents the Ambu from collapsing due to over-pressure. When this reaches its limit it opens to relief the pressure by allowing air to enter. The mix of the external air with the one inside the Ambu will definitely impact FiO_2 , and the limit-pressure could decrease depending on the valve's status. This is why this item is also matter of interest during the assays, as it could affect the performance of the Tinkin system.

It should be noted that prior to carrying out the tests, the flow analyzer was calibrated using a 98.5% medicinal oxygen tank.

2.1 Oxygen Versus Flow Calibration

To carry out the calibration between the oxygen delivered by the ventilator and the outlet flow of the concentrator, the flows of the latter were varied between

3 and 15 L/min and measurements were taken after 3 min from the start of its operation, using the flow analyzer. This was done in both PC and VC modes and the repetitions were averaged. Also, 2 sets of tests were done, one before and one after changing the security valves of the Ambu bag.

2.2 FiO_2 Stability Test in Time

After performing the previous calibrations, stability tests were carried out over time. For this, a flow of 8 L/min and PC mode were set; the rest of the parameters were the same as in the previous test. The system's performance with respect to delivered FiO_2 was measured for 6 continuous hours. Two tests were carried out, one before and one after changing the safety valves.

3 Results

3.1 Oxygen Versus Flow Calibration

All the graphs show a linear growth from 3 to 7 L/min, a plateau phase up to 12 L/min and a slight decrease for higher flows. It is worth paying attention to the Plateau phase of the graph, since in it all the FiO_2 values are positioned above 80%, while the most significant differences are observed with respect to the change of valves. After valves replacement, PC's plateau phase maintained an average value of 91.9%, while before the change it did so at 88.8%, thus giving a difference of 3.1%. Similarly, the VC's remained at 91.1% with the new valves, but prior to the change its FiO_2 was at 87%, which makes a difference of 4.1%. Also, it can be stated that PC mode maintains greater FiO_2 compared to VC mode. Surprisingly, a FiO_2 very closer to 90% was obtained with 6 L/min in PC with new valves (PC-NV), meaning that high FiO_2 levels could be obtained using less flow and so, less energy consumption.

3.2 FiO_2 Stability Test in Time

Figure 3 shows that the performance of the system is visibly better when working with the new (replaced) valves. With this condition, FiO_2 rises to 93%, which is 2.1% above the maximum obtained without the replacement. In addition, the maximum and minimum difference between the two tests is 4.9% and 1%, respectively. Despite the difference in values, both graphs show a similar morphology until minutes before the fifth hour. Initially they present a growth, followed by an evident fall and then a plateau. The last one prevails over time for the changed valves, while for the other, the FiO_2 increases again, thus creating a valley.

Ventilator FiO_2 vs Concentrator Flow: Before and after valve replacement

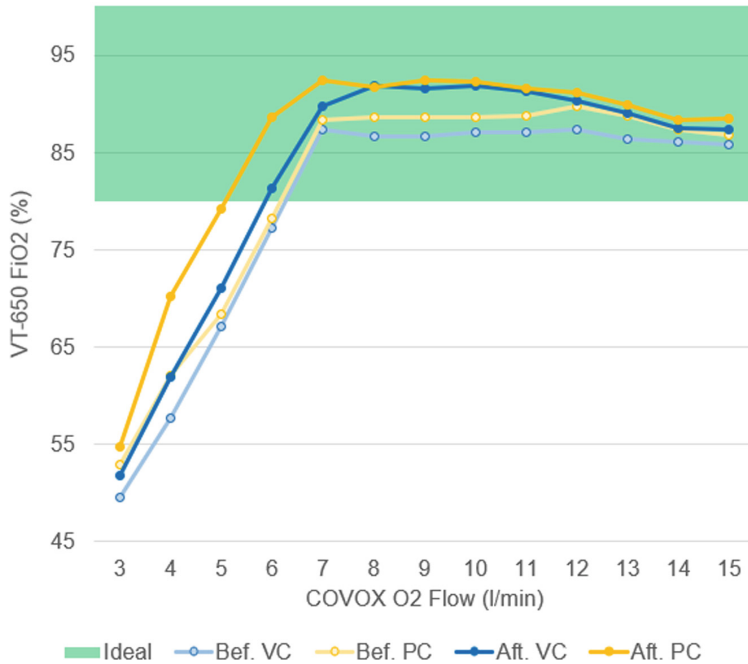


Fig. 2. Effect of oxygen flow from the concentrator on the FiO_2 delivered by the ventilator. “Bef.” and “Aft.” make reference to before and after replacing the Ambu’s security valve, respectively

4 Discussion

It is important to outline that Tinki system indeed delivers high values of FiO_2 . This became evident at the plateau phase of the Fig. 2, where FiO_2 arises over 80% and eventually it reaches 92% for PC-NV. This is a clear indicator that Tinki system could potentially be used to treat ARDS, relying in the fact that medical literature reports and/or recommend the use of FiO_2 greater than 70%, and even better, 80% in these patients [6,11]. Surprisingly, a FiO_2 very closer to 90% was obtained with 6 L/min, meaning that high FiO_2 levels could be obtained using less flow and so, less energy consumption.

Furthermore, the status of the security valves and the mode of ventilation impacts directly on the provided FiO_2 . Actually, valve replacement assures a consistent increase of FiO_2 , with a gain greater than 3% in both modes, and PC mode resulted 0.8% greater than VC for this case. These percentages become really significant when dealing with critically ill patients who rigorously require FiO_2 values greater than 90%, like in the case of severe COVID-19, where ideally a FiO_2 of 100% is needed [12]. Nevertheless, obtain as much as 100% is impos-

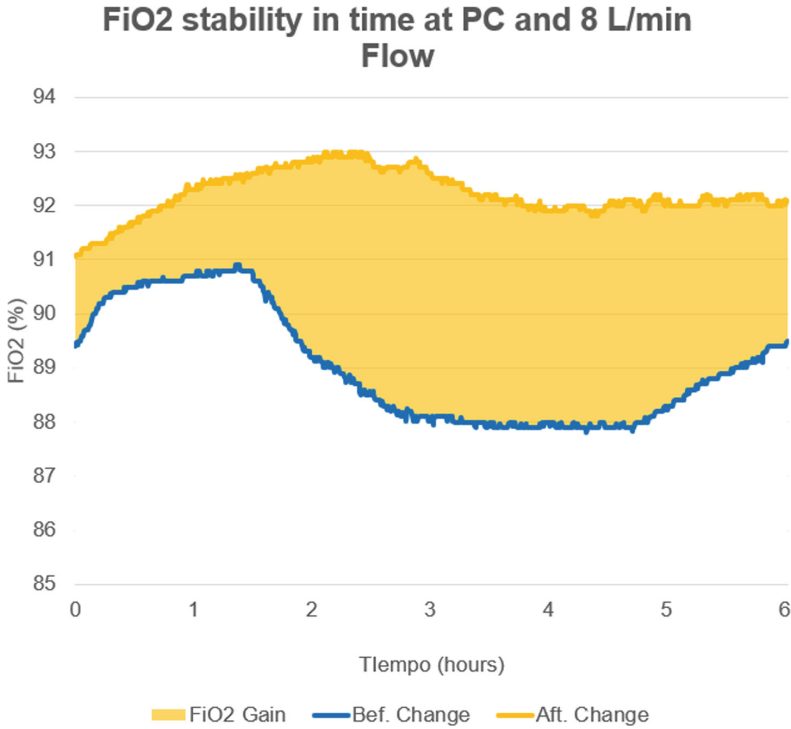


Fig. 3. *FiO₂* stability test results over 6 h before and after the change of valves

sible for Tinki given that COVOX works on zeolite sieves, a nitrogen-selective adsorption agent that filtrate oxygen and rise its concentration to a theoretical maximum of 95.7%, being this a limitation of the system [13].

It is true that a 3-min test is not enough to ensure that the system can really respond to a clinical case, in which mechanical ventilation is provided for prolonged periods; that is why stability tests over time were carried out. This consisted of measuring the *FiO₂* delivered by the Tinki system for 6 h, configured as previously indicated for PC ventilation and a fixed flow of 8 L/min, a configuration that in the previous test (of 3 min) demonstrated high *FiO₂* values. The results obtained after changing the valves show that the Tinki system can not only to deliver a *FiO₂* greater than 90%, but is also capable of sustaining it on average at 92.2% with a standard deviation of 0.4%, which is appropriate for ARDS treatment as stated early. In contrast, before the valve change, the average was 89% with a standard deviation of 1.1%.

During the experimentation it was determined that the time of use of the valves to consider them as new, and thus obtain the results that were categorized as “recently replaced”, is one day. This suggests that to apply the Tinki model in clinical practice, it would be necessary to replace the valves on a daily basis. This process consists of opening the MASI top cover (prepared for easy access),

extracting the Ambu resuscitator and unscrewing the safety valve area, then the valves are manually removed and replaced with new ones. This process requires no tools and can be done in less than 3 min by any health-care professional.

To execute ventilation, MASI receives as input a value of FiO_2 that it will require from the oxygen source; if this is not met, an alarm will be triggered. To facilitate this, the device performs a calculation to request a certain flow from the source (the one manipulated by the user) which during its design was modeled as a conventional medical oxygen tank with FiO_2 of 100%. Given that COVOX provides FiO_2 between 90 and 96%, the flows calculated by MASI did not match the ones necessary for COVOX to reach the FiO_2 required initially. To solve this, the calibration carried out in the present work can serve as a starting point for a group of calibration tests that assess different sets of ventilatory parameters (variations of peak pressure or minute volume) to characterize the usability of Tinki as a system. With this data, future work can automatize this process through a closed-loop control. In relation to this, there are research works that have studied similar scopes applying feed-back control to enhance the system's performance by including the patient as the plant. To do this, physiological parameters such as SpO_2 were measured to be used as the variables responsible for determining the patient's status and changing the FiO_2 delivered as a function of flow [14, 15].

In the other hand, it is necessary that these tests are carried out in different geographical areas, in which the altitude varies the initial concentration of oxygen. This factor considerably affects the FiO_2 of COVOX as a source and therefore will compromise the system. The presented tests in this work were made in the district of San Miguel in Lima, at an altitude of just 45 masl, however, there are regions in the country such as the city of Arequipa (2,335 masl) or Cuzco (3,399 meters masl), where environmental conditions change drastically.

This is only an initial preliminary study on the performance of the Tinki system, it is appropriate to test different configurations of MASI to better characterize its operation.

5 Conclusions

In conclusion, this work reveals that it is feasible to implement the Tinki system, which uses an oxygen concentrator (COVOX) as gas source for a mechanical ventilator (MASI) to obtain a FiO_2 greater than 90%. The experimentation showed that continuous flows greater than 7 L/min ensure FiO_2 over 80% regardless of the ventilation mode or the state of the valves, with which, according to the bibliography, it is possible to treat respiratory symptoms such as ARDS. Likewise, the results showed that the fact of replacing the safety valves of the Ambu resuscitator (which is part of the MASI) had a positive impact on the FiO_2 levels obtained, and regarding to the same reason PC configuration outperforms the VC. Both points were reaffirmed with the PC-NV stability test, which after 6 h, FiO_2 values reached and remained around 92%. From this study, the possibility of characterizing the operation of the system will be opened in order to

automate it through a control algorithm that varies the flow based on a desired FiO_2 . On the other hand, although the results are encouraging, it will be necessary to explore new configurations and evaluate their performance in various contexts that represent the Peruvian reality.

Conflict of Interest. The authors declare that they have no conflict of interest.

Acknowledgments. The development of this work was supported by PROCENCIA 026-2021. We extend a special thanks to Eng. Mauricio Córdova for collaborating during the formulation and execution of the system tests. The author thanks to Salvador Quispe, Editha Sánchez, Naibeth Quispe, Mayfe Quispe and Domitila Cadenillas for the continuous encouragement.


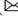



References

1. Herrera-Añazco, P., Uyen-Cateriano, A., Mezones-Holguin, E., et al.: Some lessons that Peru did not learn before the second wave of Covid-19. *Int. J. Health Plann. Manag.* **36**, 995–998 (2021). <https://doi.org/10.1002/hpm.3135>
2. Diagnosis of infrastructure and equipment gaps in the health sector (2022). Peruvian Ministry of Health. www.minsa.gob.pe/Recursos/OTRANS/08Proyectos/2022/diagnostico-brechas-infraestructura-sector-salud-2022.pdf. Accessed 5 May 2022
3. Current Situation of COVID-19: Peru 2020–2022 (2022). Peruvian Ministry of Health. www.dge.gob.pe/portal/docs/tools/coronavirus/coronavirus140122.pdf. Accessed 14 May 2022
4. Herrera-Añazco, P., Uyen-Cateriano, A., Mezones-Holguin, E., et al.: Some lessons that Peru did not learn before the second wave of Covid-19. *Int. J. Health Plann. Manag.* **36**, 995–998 (2021). <https://doi.org/10.1002/hpm.3135>
5. Reportes Gerenciales de oxígeno (2022). Peruvian Ministry of Health. www.minsa.gob.pe/reunis/data/renoxi_reporte_gerencial.asp. Accessed 16 May 2022
6. Cardinale, M., Cungi, P.-J., Bordes, J., et al.: Maintaining a high inspired oxygen fraction with the Elisée 350 turbine transport ventilator connected to two portable oxygen concentrators in an austere environment. *J. Trauma Acute Care Surg.* (2020). <https://doi.org/10.1097/ta.0000000000002792>
7. Bordes, J., d'Aranda, E., Savoie, P., et al.: FiO_2 delivered by a turbine portable ventilator with an oxygen concentrator in an austere environment. *J. Emerg. Med.* **47**, 306–312 (2014). <https://doi.org/10.1016/j.jemermed.2014.04.033>
8. Rybak, M., Huffman, L.C., Nahouraii, R., et al.: Ultraportable oxygen concentrator use in U.S. army special operations forward area surgery: a proof of concept in multiple environments. *Military Medicine* (2017). <https://doi.org/10.7205/milmed-d-16-00100>
9. Chang, J., Acosta, A., Benavides-Aspiazu, J., et al.: Masi: a mechanical ventilator based on a manual resuscitator with telemedicine capabilities for patients with ARDS during the COVID-19 crisis. *HardwareX* (2021). <https://doi.org/10.1016/j.ohx.2021.e00187>
10. Rubio, J., Rojas, C., Sanchez, M., et al.: Covox: providing oxygen during the COVID-19 health emergency. *HardwareX* (2023). <https://doi.org/10.1016/j.ohx.2022.e00383>

11. Allardet-Servent, J., Forel, J.-M., Roch, A., et al.: FiO_2 and acute respiratory distress syndrome definition during lung protective ventilation. *Crit. Care Med.* (2009). <https://doi.org/10.1097/ccm.0b013e31819261db>
12. Barahona, C., Avedaño, C.: Capítulo 5: Ventilación mecánica invasiva en COVID-19. In: *Manejo del paciente con coronavirus - COVID-19 en la población adulta*. Bogotá (2021)
13. Ackley, M.W.: Medical oxygen concentrators: a review of progress in air separation technology. *Adsorption* **25**, 1437–1474 (2019). <https://doi.org/10.1007/s10450-019-00155-w>
14. Johannigman, J.A., Branson, R., Lecroy, D., Beck, G.: Autonomous control of inspired oxygen concentration during mechanical ventilation of the critically injured trauma patient. *J. Trauma: Injury, Infect. Crit. Care* **66**, 386–392 (2009). <https://doi.org/10.1097/ta.0b013e318197a4bb>
15. Gangidine, M.M., Blakeman, T.C., Branson, R.D., Johannigman, J.A.: System design verification for closed loop control of oxygenation with concentrator integration. *Mil. Med.* **181**, 177–183 (2016). <https://doi.org/10.7205/milmed-d-15-00150>



Optimized Performance Pulse Oximeter Based on the MAX30102 Commercial Sensor

Ricardo Cebada-Fuentes¹  , José Valladares-Pérez¹ ,
José Antonio García-García² , and Celia Sánchez-Pérez¹ 

¹ Instituto de Ciencias Aplicadas y Tecnología, Universidad Nacional Autónoma de México, Ciudad de México 04510, Mexico

ricardo.cebada@icat.unam.mx

² Hospital General de México “Dr. Eduardo Liceaga”, Dirección de Educación y Capacitación en Salud, Ciudad de México 06720, Mexico

Abstract. Pulse oximeters are devices that use the photoplethysmography technique to estimate oxygen saturation in blood and heart rate. The MAX30102 is a sensor for reflective photoplethysmography with signal-conditioning and digitalization stages embedded in a single chip that facilitate its implementation in wearable devices. However, there are limitations and external factors that affect its performance in a significant way. This paper suggests a pulse oximeter based on the MAX30102 whose performance has been optimized through the design of algorithms adapted to the signals of this particular sensor. The performance of two heart rate measurement algorithms is compared, one based on a pulse counter and the other on the Fast Fourier Transform (FFT). The proposal covers from the algorithms design to the manufacture of a functional prototype tested with volunteers. Results indicate an accuracy of $\pm 1.39\%$ for the measurement of oxygen saturation and ± 2.04 bpm for heart rate. The Bland-Altman analysis of the pilot test results indicate that prototype measurements are comparable to those of a high-end oximeter taken as reference.

Keywords: MAX30102 · Photoplethysmography · Pulse oximetry · FFT · Bland-Altman

1 Introduction

Photoplethysmography is a non-invasive technique that allows the estimation of the amount of oxygenated hemoglobin (HbO_2) in blood respect to total hemoglobin. It consists in applying light at different wavelengths, typically red ($\lambda = 660$ nm) and infrared ($\lambda = 880$ nm), in an area of the body irrigated with arterial blood to analyze the attenuated light by absorption due to the different tissues through which it passes [2]. The detection of this dimmed light produces a variable amplitude signal called photoplethysmogram signal or PPG, which

has a continuous intensity (DC) and a pulsatile intensity (AC) components [1]. Pulse oximeters use this technique to determine oxygen saturation (SpO_2) and heart rate (HR) quickly and continuously.

During Covid-19 pandemic, the use of pulse oximeters became an obligatory practice among physicians for the monitoring of patients, both in hospitals and remotely [3]. The Pan-American Health Organization (PAHO) has established the technical and functional specifications that clinical pulse oximeters must follow. As technical requirements, it is pointed out that SpO_2 and HR measurements must be carried out with a minimum accuracy of $\pm 3\%$ and ± 3 bpm, respectively, as well as with a one-unit resolution [9]. Among the most important features required are the display of the photoplethysmography waveform, visual and audible alarms for out-of-range measurements, charging indicator, battery status, signal quality indicator and internal data storage [9].

The MAX30102 is a reflection-type photoplethysmography sensor widely used in the development of wearable devices. One of its advantages is that it integrates within the same chip, a conditioning and digitalization stage for the PPG signal that reduces the number of electronic components necessary to implement this sensor in a practical application. Similarly, its intrinsic operating parameters such as sampling rate (SR), LED current (I_{LED}), pulse width and analog to digital converter resolution (ADC) are fully programmable to the user by modifying memory registers via the I^2C protocol [10]. Obtaining a good quality PPG signal with this sensor depends to a great extent on finding an optimal combination of these parameters.

There are several works in which the development of pulse oximeters based on the MAX30102 is suggested, however, very few of them address the search for an optimal configuration of its intrinsic parameters and the design of SpO_2 and HR calculation algorithms appropriate to the particularities of this sensor in which its limitations are taken into account [5,6]. Similarly, few papers address the development of a complete pulse oximeter from the algorithms design to the manufacture of a fully functional prototype that meets the PAHO requirements and that has been subjected to tests with users [13].

In this paper, an optimized performance finger pulse oximeter based on the MAX30102 is presented. This performance optimization is achieved by two ways. The first one, is to obtain the optimal values for the intrinsic parameters LED current (I_{LED}) and sampling rate (SR), with which a high quality PPG signal is obtained. The second way is the development of SpO_2 and HR calculation algorithms adequate for the MAX30102 signals considering both the sensor and microcontroller limitations. Under this approach, the performance of two HR calculation algorithms is compared, one based on the analysis of the PPG signal intensity, and the other, based on a frequency analysis. Finally, a pilot test of the prototype functioning is carried out in a group of 15 healthy people comparing it with a high-end commercial oximeter.

2 Design and Implementation

2.1 General Description of the Developed Pulse Oximeter

The design of the proposed pulse oximeter was performed taking various commercial oximeters as models and considering key elements such as ergonomics and finger restrain mechanisms. The outer case of the prototype was manufactured using 3D printing with polylactic acid polymers (PLA) and thermoplastic polyurethane (TPU) and is held together by a screw-spring mechanism that exerts an adjustable pressure on the finger. Finding the right magnitude for this pressure is one of the key factors that determine the quality of the PPG signal, since excessive pressure will completely deform it.

Some of the main operating features of this prototype are the display of the photoplethysmography waveform, bluetooth connectivity for data storage, visual and audible alarms for SpO_2 and/or HR out-of-range measurements, charge monitor and battery status, signal intensity indicator and battery charge via a USB-C connection. These features fully comply with the functionality requirements established by PAHO [9].

For the development of the pulse oximeter an ESP32 Expressif Systems microcontroller was used as the central processing unit. Figure 1 shows the functional prototype in operation.

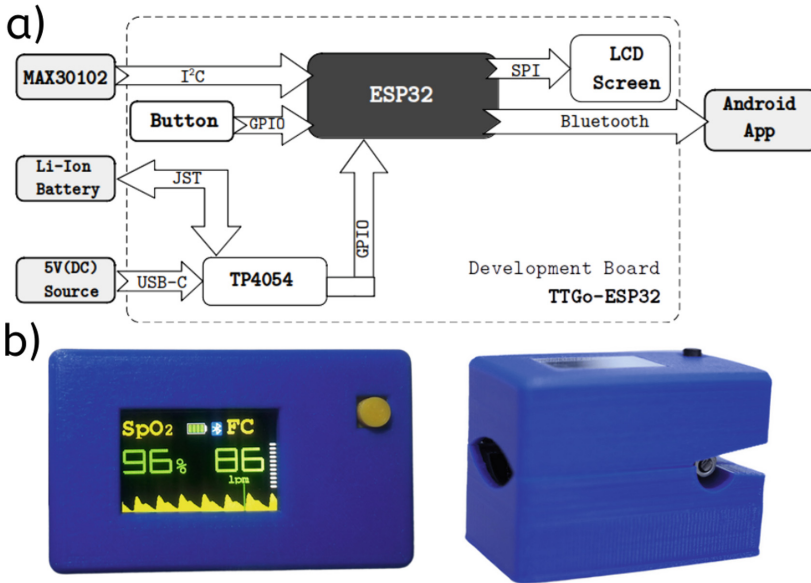


Fig. 1. a) Block diagram of the interconnection of the prototype components. b) Functional prototype operating.

2.2 Acquisition and Conditioning of the PPG Signal

The acquisition of PPG signals is done digitally through the I^2C protocol. Since the sensor has an embedded conditioning stage, there is no need for additional electronic components as post processing is done digitally. Because the proposed algorithms for calculating HR are design to work with the pulsatile components, an IIR type digital low-pass filter was implemented with a cut-off frequency $f_c = 0.05$ Hz.

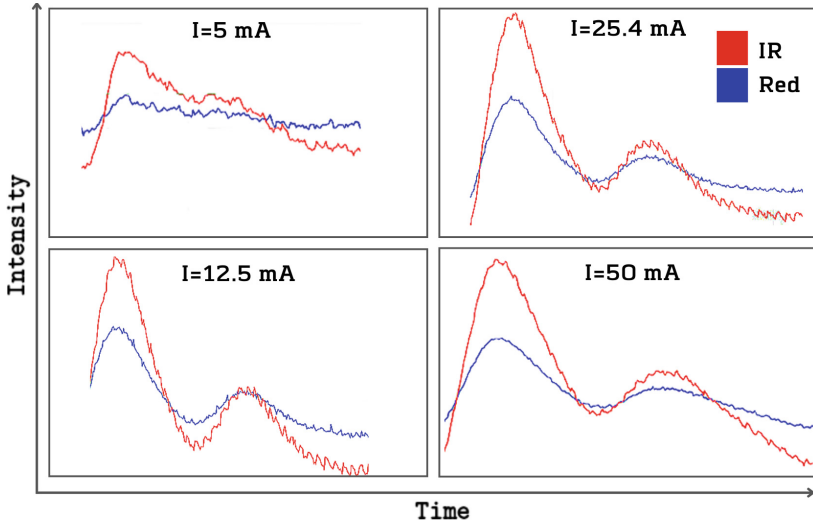


Fig. 2. Quality of PPG signal for different I_{LED} values.

One of the parameters that determine the PPG signal quality is the brightness intensity of the light emitting sources, which is directly linked to the current intensity supplied to them. In the MAX30102, this current can be varied between 0 and 50 mA at intervals of 0.2 mA and it was determined that the best signal quality is obtained for values greater than 40 mA. Lower current values can cause deformities in the PPG signal or produce higher noise levels (Fig. 2) that would affect the performance of the measurement algorithms.

2.3 SpO_2 Calculation

The calculation of oxygen saturation is based on the fact that oxygenated (HbO_2) and deoxygenated (Hb) hemoglobin have different absorption properties for visible and infrared wavelengths. This difference allows to estimate the proportion of HbO_2 to total hemoglobin in arterial blood from the value of the ratio of ratios (R) of the AC and DC components [4] (Eq. 1).

$$R = \frac{(AC_{rms}/DC)_R}{(AC_{rms}/DC)_{IR}} \quad (1)$$

The relationship between R and SpO_2 is determined experimentally through ABG (*Arterial Blood Gas*) tests in volunteers with which a linear approximation of Lambert-Beer law is obtained (Eq. 2). The values of the coefficients α and β depend on the type of sensor and are usually provided by the manufacturer in the sensor's datasheet. In the case of the MAX30102 the values of these coefficients are $\alpha = -17$ y $\beta = 104$ [7].

$$\%SpO_2 = \alpha R + \beta \quad (2)$$

2.4 Heart Rate Calculation

The heart rate (HR) indicates the number of heart beats within a minute and is calculated from the frequency of the PPG signal. There are several methods to determine this frequency but in general they can be classified into two categories: methods that analyze the intensity of the signal and methods that perform decomposition into frequencies. Both methods were studied in this paper with a particular approach in the MAX30102 to determine its advantages and limitations in a practical implementation.

The methods of intensity analysis consist mainly of detection and peak counting algorithms that require few computational resources but are susceptible to failures in the presence of noise. It has been noted that two of the factors affecting the performance of the MAX30102 are movement in the measurement area and low blood perfusion [11]. The movement deforms the PPG signal by inducing fake peaks and sudden amplitude changes, while low perfusion causes significant attenuation on the pulse's amplitude and an increase in the base noise level. That is why the suggested algorithm seeks to detect these alterations on the PPG signal and discriminate them in the final calculation of the HR so as not to affect the measurement.

The proposed algorithm comprises a peak detection stage inspired by an algorithm proposed by Arguello, to which a number of additional conditions have been added to improve the detection for the specific case of the MAX30102 signals [14]. This algorithm works under the assumption that a PPG signal is a strictly increasing function. That is, if the function is denoted by f , then all the points that make it up fulfill the following condition in time (t):

$$f(t_{i+1}) > f(t_i) \quad \text{if} \quad t_{i+1} > t_i \quad (3)$$

A peak is detected when a sign change occurs on the slope of the signal. To differentiate a systolic peak from a diastolic one the algorithm counts the number of times that the condition of Eq. 3 (*num_upsteps*) is met and evaluates whether this number of occurrences reaches a threshold value, in which case it is concluded that a peak has been detected. Because PPG signals have amplitude variations, this threshold is recalculated dynamically according to the total number of samples that make up the rising flank of a systolic peak and which depends on the sampling rate (SR) of the sensor.

One of the additional conditions proposed compares the amplitude of a signal sample ($samp(i)$) with a threshold value (PPG_{MV}) that is equal to 1.5 times the

mean value of the PPG signal calculated for a 50-second window that is updated in real time. This allows to improve the detection of pulses in the presence of slight movements and low intensity noise. Similarly, it was added a condition for resetting the threshold value when there is a substantial increase in the amplitude of the signal due to sudden movement. The flow chart of the suggested algorithm is shown in Fig. 3.

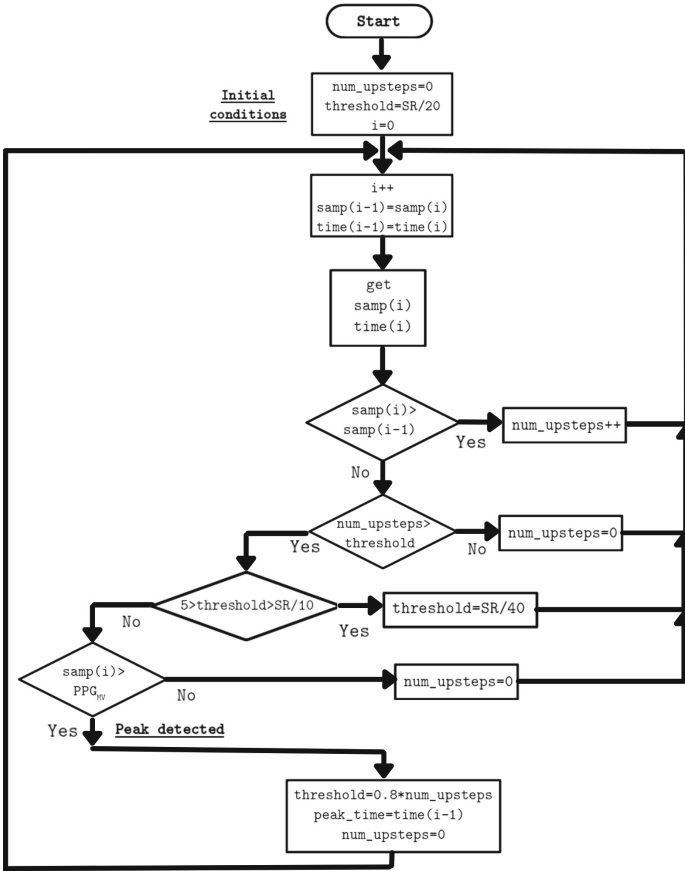


Fig. 3. Flowchart of the proposed algorithm for the detection of peaks in the PPG signal for later use in the calculation of HR.

Unlike the methods used in the intensity based analysis, the frequency methods perform a spectral decomposition of the signal in its fundamental components by using algorithms such as the Discrete Fourier Transform (DFT). In practice, DFT is solved by optimized algorithms such as the Fast Fourier Transform (FFT) which greatly reduces the number of operations required [15]. Some research where the FFT has been used to calculate HR point out that the results

are very similar to those obtained with pulse counting algorithms [16]. For this research, the applied FFT algorithm was a 512-point radix-2 Cooley-Tukey algorithm.

An important advantage of this method is that it has a higher noise immunity compared to pulse counters, however, to calculate HR with the desired resolution of 1 bpm it is necessary for the FFT to calculate the PPG signal frequency with a minimum resolution of 0.016 Hz. This means that the number of data (N) required for a given sampling rate (SR) and frequency bin (N_{bin}), has to be very large, as indicated in Eq. 4 [17]. In a practical implementation this represents a disadvantage due to SRAM memory limitations of the used microcontroller.

$$f_{FFT} = N_{bin} \frac{SR}{N} \quad (4)$$

In the case of MAX30102, in order to maximize the FFT resolution, the maximum possible sample rate of the sensor ($SR = 50$ mps) should be used. Preliminary tests with the ESP32 showed that the largest number of floating point variables that can be stored for the implemented FFT is 512, which implies that the maximum resolution in the frequency calculation is 0.097 Hz, equivalent to 5.8 bpm in heart rate units.

2.5 Comparison of HR Calculation Algorithms

To evaluate the operation of the proposed algorithms, a series of computer tests were carried out with simulated PPG signals for different HR and SNR (*Signal to Noise Ratio*) values and it was concluded that the FFT had a better performance in presence of noise and movement than the intensity algorithm as expected (Fig. 4), however, because of the limited SRAM memory in the microcontroller, the 5.8 bpm resolution in the calculation of the HR does not meet the PAHO requirement of one-unit resolution. For this reason, it was decided to use the intensity based algorithm in the in the final prototype.

3 Results

A series of validation tests were performed to determine the accuracy of the prototype. SpO_2 and HR measurements were compared with those of a high-end commercial oximeter model Masimo[®] MightySat. Table 1 shows a summary of the absolute ($\overline{\varepsilon_a}$) and relative ($\overline{\varepsilon_r\%}$) average errors obtained after testing the final prototype on a healthy volunteer. The results indicate accuracies of 1.39% and 2.04 bpm for SpO_2 and HR, respectively, which clearly meets the PAHO requirements.

To evaluate the performance of the prototype in a real environment, it was considered necessary to carry out a pilot study in a small sample of healthy people.

To carry out this study, verbal informed consent was obtained from the participants, which is authorized in Mexico for minimal risk and non-invasive research

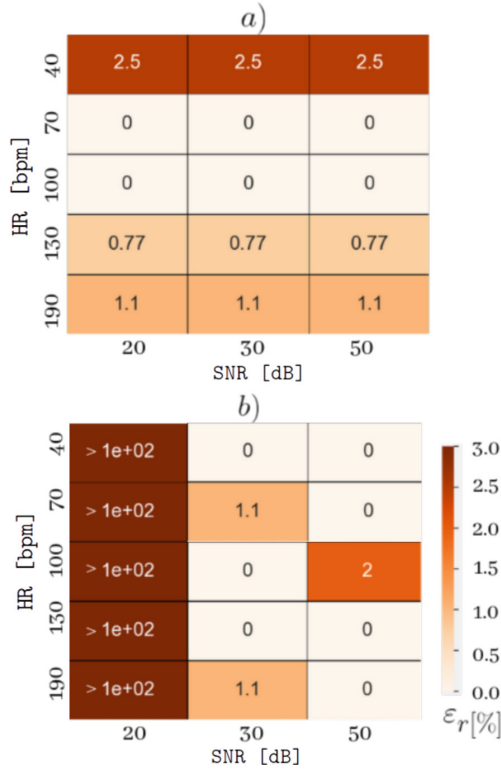


Fig. 4. Heatmap of the relative error ε_r in the calculation of HR performed with simulated PPG signals with different combinations of HR and SNR values using a) 512 point FFT and b) intensity based algorithm.

such as pulse oximetry, as indicated in articles 17 and 23 of Chap. 1 of the Mexican General Health Law [12].

The performance of the prototype was compared with that of the same high-end oximeter used in the validation tests. A total of 15 people participated in the test. 60% were female and the rest were male. The average age was 41 years (± 16) and the third part of the sample said they had suffered from COVID-19 in the last year.

Experimental methodology: 3 measurements were taken for each test subject. Both oximeters were placed simultaneously on the right hand: the prototype on the index finger and the reference on the middle finger. The first measurement was recorded one minute after placing the oximeters, the second, passed 3 min, and the third after 5 min.

Based on the results obtained, a concordance analysis was done using the Bland-Altman method, in which concordance limits are established to study the level of agreement between two instruments or measurement methods. After applying the Student’s T-test to the sample, it was observed that the difference

Table 1. Absolute ($\overline{\varepsilon_a}$) and relative ($\overline{\varepsilon_r\%}$) errors in the measurement of SpO_2 and HR with the working prototype.

Variable	$\overline{\varepsilon_a}$	$\overline{\varepsilon_r\%}$
SpO_2	1.39 %	1.49
HR	2.04 bpm	2.31

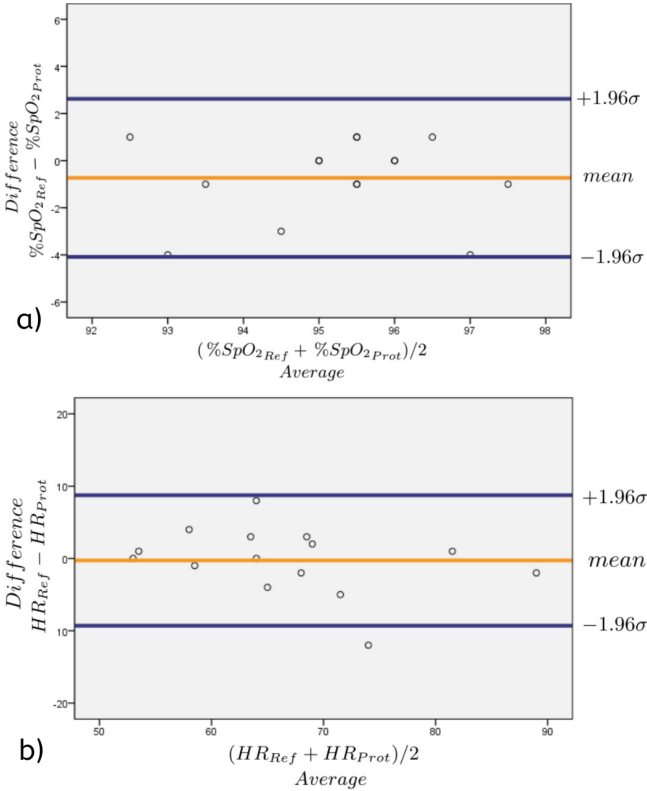


Fig. 5. Bland-Altman plots for a) SpO_2 measurements and b) HR measurements.

between the SpO_2 and HR measurements of both oximeters had a p value of $p > 0.05$, which indicates that they are not statistically significant. As for the Bland-Altman analysis, the dispersion graphs were made by plotting the differences between the reference measurements (*Ref*) and those of the prototype (*Prot*) against their corresponding average values. The confidence intervals which group 95% of the data were plotted at ± 1.96 standard deviation (σ) from the average value of the differences as shown in Fig. 5 [8].

It is clear that the Bland-Altman analysis show different results from those reported in Table 1. This difference can be attributed to several factors, but

mainly it is due to the different methodology follow in the pilot test. Whereas in validation tests measurements from the prototype and the reference oximeter were recorded just once, those of the pilot test were recorded three times separated by 2 min, and since the values of SpO_2 and HR are not static, the results displayed by the prototype can be different because the response time of each oximeter is not the same. In any case, this does not imply a greater error.

4 Conclusions

An optimized performance pulse oximeter based on the MAX30102 was obtained. The developed prototype meets the technical and functional requirements established by the Pan American Health Organization for clinical pulse oximeters. Results show that the proposed algorithms calculate SpO_2 and HR with one-unit resolution and accuracies of 1.39% and 2.04 bpm, respectively.

Two algorithms to calculate HR were proposed. The FFT showed a better performance than the intensity based algorithm for PPG signals with low SNR values and fake peaks induced by movement. However, to guarantee its correct operation, a microcontroller with greater SRAM memory capacity must be used. Finally, the Bland-Altman analysis of the pilot test results indicate that the measurements of the prototype are comparable to those of a high-end commercial oximeter. However, it is advisable to carry out a validation with a larger number of people.

Conflict of Interest. The authors declare that they have no conflict of interest.

Acknowledgments. The authors acknowledge financial support from UNAM-PAPIIT grant iv100320 and SECTEI grant SECTEI/080/2020. Ricardo Cebada-Fuentes and José Valladares-Pérez thank CONACYT for the Ph.D. studies grant (CVU:1005230) and (CVU:929080).









References

1. Chan, E.D., Chan, M.M., Chan, M.M.: Pulse oximetry: understanding its basic principles facilitates appreciation of its limitations. *Respir. Med. (Elsevier)* **107**, 789–799 (2013)
2. Allen, J.: Photoplethysmography and its application in clinical physiological measurement. *Physiol. Meas.* **28**, R1 (2007)
3. Badgujar, K.C., Badgujar, A.B., Dhangar, D.V., Badgujar, V.C.: Importance and use of pulse oximeter in COVID-19 pandemic: general factors affecting the sensitivity of pulse oximeter. *Indian Chem. Eng.* **62**, 374–384 (2020)
4. Webster, J.G.: *Design of Pulse Oximeters*. CRC Press (1997)
5. Shruthi, P., Resmi, R.: Heart rate monitoring using pulse oximetry and development of fitness application. In: 2nd International Conference on Intelligent Computing, Instrumentation and Control Technologies (ICICICT), vol. 1, pp. 1568–1570. IEEE (2019)
6. Andika, I.P.A., Rahmawati, T., Mak'ruf, M.R.: Pulse oximeter portable. *J. Electron. Electromed. Eng. Med. Inf.* **1**, 28–32 (2019)

7. Integrated Maxim: Recommended Configurations and Operating Profiles for MAX30101/MAX30102 EV Kits. www.maximintegrated.com/en/design/technical-documents/userguides-and-manuals/6/6409.html (2018)
8. Kaur, P., Stoltzfus, J.C.: Bland-Altman plot: a brief overview. *Int. J. Acad. Med.* **3**, 110 (2017)
9. Pan American Health Organization: Technical and Regulatory Aspects of the Use of Pulse Oximeters in Monitoring COVID-19 Patients
10. Integrated Maxim. MAX30102 Datasheet. www.maximintegrated.com/en/products/interface/sensor-interface/MAX30102.html
11. Fine, J., Branan, K.L., Rodriguez, A.J., Boonya-Ananta, T., Ramella-Roman, J.C., McShane, M.J.: Sources of inaccuracy in photoplethysmography for continuous cardiovascular monitoring. *Biosensors* **11**, 126 (2021)
12. Ley General de Salud and CAPITULO ÚNICO. Ley General de Salud
13. Skrvan, A., Hudec, R., Matuska, S.: Design of a cheap pulse Oximeter for home care systems. *ELEKTRO (ELEKTRO)*, pp. 1–6. IEEE (2022)
14. Prada, A., Javier, E., Maldonado, S., Daniel, R.: A novel and low-complexity peak detection algorithm for heart rate estimation from low-amplitude photoplethysmographic (PPG) signals. *J. Med. Eng. Technol.* **42**, 569–577 (2018)
15. Rao, K.R., Kim, D.N., Hwang, J.J.: *Fast Fourier Transform: Algorithms and Applications*. Springer (2010)
16. Sani, N.H.M., Mansor, W., Lee, K.Y., Zainudin, N.A., Mahrim, S.A.: Determination of heart rate from photoplethysmogram using Fast Fourier transform. In: *International Conference on BioSignal Analysis, Processing and Systems (ICBAPS)*, pp. 168–170. IEEE (2015)
17. Zonst, A.E.: *Understanding the Fast Fourier Transform: Applications*. Citrus Press (1995)



Antimicrobial Photodynamic Therapy with Methylene Blue and Urea in *Escherichia Coli* and *Staphylococcus Aureus*

P. I. B. P. Silva , M. A. K. Saleh , A. Baptista , D. Honorato , S. Campos ,
S. C. Nunez , and R. S. Navarro  

Universidade Brasil, Pós Graduação Bioengenharia, São Paulo, SP, Brazil
ricardo.navarro@universidadebrasil.edu.br

Abstract. Antimicrobial Photodynamic Therapy (aPDT) is the technique in which a photosensitizing agent (PS) in the presence of oxygen is activated by light of a specific wavelength, resonant to the PS, generating reactive oxygen species through the photodynamic process, promoting the microbial death from oxidative damage. The aim of this study was to evaluate the efficacy of aPDT with methylene blue (MB) and MB with urea (UMB) in bacteria as a proof of concept of the urea-disaggregating action on phenothiazine PS. Sterile dental diamond burs were contaminated with gram negative *Escherichia coli* (*E. coli*) and gram positive *Staphylococcus aureus* (*S. aureus*) bacteria (10⁸ CFU/mL) and divided into three groups (n = 9): GMB (MB + red laser- RL), GUMB (urea +MB + RL), GC (control-without treatment). The contaminated diamond burs were immersed in tubes with aqueous solution of MB (60 µM) (GMB) or MB diluted in urea (60 µM) (GUMB). After 1 min, irradiation was performed with RL (660 nm, 100 mW, 18 J, 3 min), in contact below and above the tube. The results presented in colony forming units (CFU/ml) showed that the MB and UMB groups showed significantly greater microbial reduction than GC (p < 0.05), for all microorganisms. The microbial reduction of the group with urea (GUMB) was not superior to the group without urea (GMB). It can be concluded that aPDT with MB and UMB promoted effective antimicrobial actions, the disaggregation factor that urea has in phenothiazine PS, in this in vitro experiment, was not determinant in microorganisms in suspension.

Keywords: Antimicrobial · Methylene blue · Photodynamic therapy · Urea

1 Introduction

Antimicrobial Photodynamic Therapy (aPDT) is used for oncological treatment and antimicrobial therapy, proving to be an effective method through oxidative processes. aPDT is a photosensitizing agent (PS), it is activated by light of specific wavelength resonant to the PS, triggering the production of singlet oxygen, superoxides and free radicals (reactive oxygen species), which are cytotoxic to target cells [3, 4]. This treatment modality is also called antimicrobial photodynamic chemotherapy, photoactivated disinfection or light activated disinfection.

Reactive oxygen production is characterized by photochemical oxygen consumption and occurs by inducing two types of reactions. In the type I reaction there is a transfer of electrons or hydrogen, leading to the production of different types of free radicals, superoxides, hydroxyl radicals and hydrogen peroxide, while in the type II reaction there is energy transfer to oxygen by the change in electron spin, leading to the production of singlet or superoxide oxygen, which are highly reactive species [6]. Both lead to cell death by the oxidation of biological molecules such as proteins, nucleic acids and lipids [7]. The action of aPDT extends to bacteria, fungi, yeasts, viruses and protozoa, depending on the SF and light source used, being therefore very useful in combating localized infections [8].

The therapy has different action on gram-positive and gram-negative bacteria, due to structural differences in cell walls. The former are more susceptible to elimination by aPDT. Gram-negative bacteria have a complex outer membrane, with two lipid layers that act as a barrier between the cell and the environment, which makes it difficult to kill them [5].

The success of aPDT depends on the interaction of the light source (laser or LED) with natural or synthetic PS, in the presence of oxygen. The PS must present favorable photo physical, chemical and biological properties. The ability to penetrate bacterial cells is a high absorption coefficient in the region of the light excitation spectrum, ability to transfer energy to species, in addition to having local action and presenting a short time interval between the period of administration and tissue absorption.

Phenothiazine PS are composed of a tricyclic aromatic ring, such as methylene blue (MB) and toluidine blue (TB), they are performed for photodynamic therapy studies [1,8] and are activated by light in the spectrum from 620 to 700 nm (red wavelength [4, 8]. MB and TB have similar chemical and physicochemical characteristics, with hydrophilic nature, low molecular weight and positive charge that facilitates the passage through the bacterial wall [4], inducing damage to the nucleic acids, proteins and lipids [12] The TB has the additional advantage of an affinity for the lipopolysaccharide (LPS) of Gram-negative bacteria and is, in general, more effective than MB.

The addition of urea to aqueous formulations of PS could improve the efficiency of phenothiazine photosensitizers [13] due to its characteristics that lead to PS breakdown as MB tends to aggregate, negatively interfering with the generation of singlet oxygen [14, 15].

Urea weakens hydrophobic bonds, changes the dielectric constant, and increases the surface tension of water, which generally causes a decrease in substrate-substrate interactions, such as those found in ion pairs. Urea stabilizes the solution monomers (and consequently reduces dimer concentration) of MB, allowing aPDT to be more efficient in *Candida albicans* [13].

This study proposes to evaluate in vitro the effectiveness of the decontamination process with MB and TB with urea in dental diamond burs using aPDT with red laser in gram negative bacteria *E. coli* and gram positive bacteria *S. aureus*, being a proof of concept to determine a more refined methodology in new experiments both in vitro and in vivo. The hypothesis of this study is that the addition of urea to methylene blue increases the efficacy of phenothiazine PS.

2 Methods

2.1 Bacterial Samples and Cultivation

Bacterial samples of *E. coli* (ATCC 25922) and *S. aureus* (ATCC 25923) provided by the microbiology laboratory at Universidade Brasil (São Paulo) to conduct the research. For the cultivation of microorganisms, 100 μL of the bacteria solution were incubated in 10 mL of sterile BHI broth, in a test tube and kept in a bacteriological oven (37 °C, 8 h). Tubes with bacteria were standardized with turbidity 7 on the Mc Farland scale, which corresponds to the approximate number of bacteria in the order of 21×10^8 .

2.2 Procedures

Conical diamond burs (DB) (Fava, São Paulo, Brazil) for dental use were sterilized and individually immersed in test tubes containing broths with 10^8 CFU/mL of *E. coli* and *S. aureus* in suspension. After a period in a bacteriological oven (37°C, 16 h) the contaminated DB were divided into three groups (n = 9): GMB (treatment group with MB + red laser – RL), GUMB (MB with urea additive + RL), GC (control group without treatment) (Table 1).

Table 1. Experimental groups

Methylene blue (MB) treatment group	Methylene blue (MB) + Red laser	n = 9
Treatment group with urea-added methylene blue (UMB)	Methylene blue (MB) + urea + Red laser	n = 9
Control Group – no treatment (C)	PS (–) Red laser (–)	n = 9

The contaminated DB were individually immersed in 1.5 ml tubes containing 60 μM aqueous MB solution diluted in MiliQ water (GMB) or 60 μM MB diluted in urea aqueous solution (GUMB) for 1 min (pre-irradiation – TPI). Soon after, irradiation was performed with a red laser (Laser DUO®, MM Optics; Brazil) with a wavelength of 660 nm, power of 100 mW. Irradiation was performed perpendicularly in contact with the tube for 3 min (18 J), 1.5 min above (9 J) and 1.5 min (9 J) below the tube (Fig. 1). Before irradiation, the energy of the Laser equipment was measured.

Afterwards, the diamond burs were removed from the tubes containing the FS and placed in a new tube containing sterile PBS. After centrifugation, the PBS supernatant and the diamond tip were discarded, leaving only the pellet at the end of the tube, in which 100 μL of sterile PBS was added. From this content, 100 μL was taken and placed in the microplate for serial dilution. After serial dilution, 10 μL of each dilution were taken to inoculate plates containing BHI culture medium to determine the number of colony forming units (CFU) for each diamond bur. The plates were placed in a bacteriological oven (37 °C, 16 h). This procedure was performed in triplicate and the results obtained were expressed in CFU.

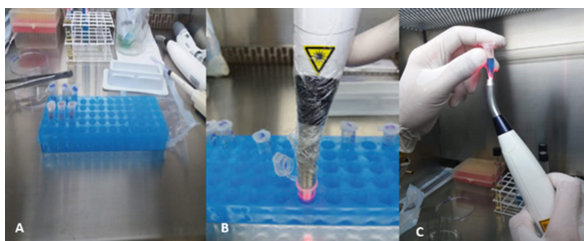


Fig. 1. Illustrative images of the experiment: **A** – Pre-irradiation time; **B** – Irradiation with red laser above the tube containing PS; **C** – laser irradiation under the tube.

3 Results

The samples of microbiological material were collected and submitted to laboratory processing to perform the colony forming units (CFU) count at different dilutions. The experiment was carried out in triplicate and from the original CFU data of each group, calculations of the averages of the different groups were performed.

The statistical analysis of the data (CFU/ml) showed, by the Shapiro-Wilk test, the non-normal distribution of the data in the curve. From this, the Kruskal-Wallis test was performed, in this, as it is a non-parametric test, the original average values (CFU/ml) were transformed into average ranks, and later, the Dunn's Test was used to compare the groups ($p < 0.05$).

As seen in the box-plot chart (Fig. 2). The inferential statistical analysis of the data showed that the MB and UMB groups showed significantly greater microbial reduction ($p < 0.05$) for the *E. coli* compared to the C group. The same can be observed for the *S. aureus*, showing significant greater microbial reduction ($p < 0.05$) in the MB and UMB groups compared to the C group. Such findings, with the limitations of the in vitro study, show the antimicrobial effectiveness of Photodynamic Therapy with MB and UMB in the parameters evaluated in the present study.

No statistically significant differences ($p > 0.05$) were observed between *E. coli* and *S. aureus* bacteria for GC, GMB and GUMB. Such findings show that the study as a proof of concept, did not confirm the disaggregating effectiveness of urea associated with MB in aPDT in vitro.

The action of urea in association with methylene blue on aPDT did not promote effects on different gram-positive and gram-negative bacterial species, and the action should be considered due to differences in the structural and compositional characteristics of these bacteria.

It is interesting to note that there were no statistically significant differences ($p > 0.05$) between the aPDT groups treated with MB or UMB, despite a trend of superiority of UMB for *E. coli* in relation to UMB for *S. aureus*, even being microorganisms with different structural characteristics, being a positive gram and a negative gram.

Finally, the values were converted into results of the microbial survival fraction (CFU/ml) showing the clear difference of remaining microorganisms between the MB and UMB groups and the C group for *E. coli* and *S. aureus* bacteria, becoming evident

the antimicrobial effectiveness of aPDT, and similarity of both techniques with MB and UMB, as confirmed by the statistical analysis (Figs. 3 and 4).

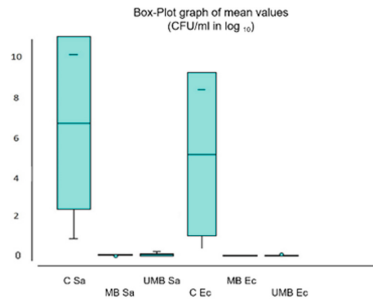


Fig. 2. Box-Plot graph of mean values (\pm SD) (CFU/ml in log) of groups C *E. coli* (C Ec), MB *E. coli* (MB Ec), UMB *E. coli* (UMB Ec), C *S. aureus* (C Sa), MB *S. aureus* (MB Sa), UMB *S. aureus* (UMB Sa)

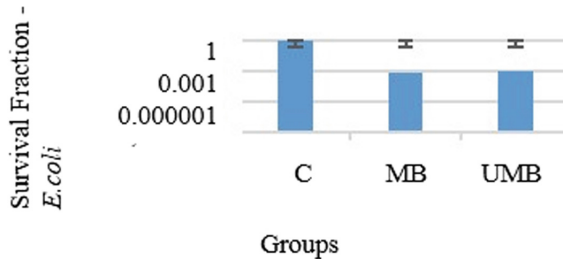


Fig. 3. Graph of the results of the Microbial Survival Fraction (CFU/ml) of groups C, MB and UMB for Gram negative bacteria *E. coli*

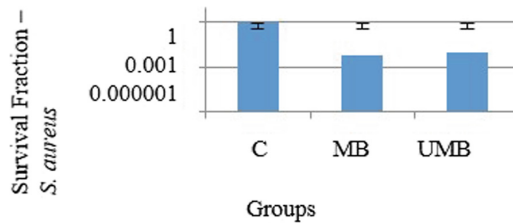


Fig. 4. Graph of the results of the Microbial Survival Fraction (CFU/ml) of groups C, MB and UMB for Gram positive *S. aureus*

4 Discussion

Antimicrobial photodynamic therapy (aPDT) has effective antimicrobial action and applications in different areas of health, and is a therapy based on the association of a PS, a source of light with a specific wavelength and oxygen, generating the production of species through the photodynamic process. Reactive oxygen specimens (ROS)

promoting microbial death by oxidative damage. MB is the main PS used in studies and clinical practice. They are currently looking for new PS or association with chemical compounds, aiming to increase antimicrobial effectiveness [5, 6, 9–11].

This study is intended to be a proof of concept in the use of aPDT with phenothiazine PS added with urea, to determine parameters and define a protocol for use to be followed in other in vitro and in vivo experiments, as MB tends to aggregate, negatively interfering with the generation of singlet oxygen [6, 11]. The MB and UMB groups showed greater reduction of microorganisms compared to the control group, for Gram negative (*E. coli*) and positive (*S. aureus*) bacteria in suspension condition. However, the urea group (UMB) did not perform better than the MB group, and urea was not, therefore, in this in vitro experiment, a determining factor in bacterial reduction, with microorganisms in suspension and not in biofilm.

MB has been widely used in aPDT. However, the mechanisms of action (Type I or Type II) are defined by their aggregation state. In this sense, the identification of aggregation, mechanisms of action and effectiveness against microorganisms, as well as the establishment of means and formulations that can favor the most effective mechanisms, is essential to improve the effectiveness of aPDT [7, 12, 13].

Despite the different available and effective treatments with antibiotics, alternative treatments are increasingly being sought, and their prescription is controlled by health regulatory agencies around the world [14]. Due to the indiscriminate use of antibiotic therapy, leading to microbial resistance, being the cause of morbidity and mortality due to the so-called “super-resistant” bacteria found mainly in the hospital environment, the systemic side effects of the drugs, the cost to the health system, initial action therapy, drug interaction in patients who use medications for underlying diseases is encouraged and the target of study of alternative therapies [5, 6, 11, 13, 14].

In alternative or adjuvant antimicrobial therapies, efficacy, speed, cost, low toxicity and safety in clinical application are sought. Within this context, aPDT comes across as a therapeutic resource in different clinical conditions in the health area [1, 6, 14].

Sodium dodecyl sulfate was the only one that improved the effectiveness of AM on aPDT in a culture of *C. Albicans* in which several vehicles were tested, in biofilm, including 1 mol/L urea [11]. This study shows that the possible breakdown of MB by urea, in this case, was not so efficient, in line with our work. But MB with urea had a shorter exposure time to totally eliminate *C. albicans* compared to MB without urea in another experiment [6]. The use of MB in gel form was tested to improve the generation of reactive oxygen species, comparing carbopol gel (CBP) and hydroxyethylcellulose (HEC) gel with 10% urea addition, 10% ethanol or water. The best results were obtained in CBP with 10% ethanol and 10% HEC in water [15]. In contrast, our study showed that urea did not obtain much lower results when added to MB.

MB was evaluated in deionized water and 0.9% saline solution for bacterial reduction in *E. coli*, with the best bacterial reduction being the MB associated with deionized water [16] in agreement with our experiment that used the mixture of MB with deionized water in the MB group. What should be considered is that the application of aPDT in vivo, as it contains secretions and several other substances that are not found in in vitro situations, may cause the urea disaggregating power to promote greater antimicrobial action, in addition to providing a decrease in the exposure time. As it is an in vitro study, in the

present study urea, despite exerting PF disaggregation, did not result in a better bacterial decrease than the group that used only MB.

5 Conclusions

The present study showed that aPDT with MB or MB with urea promoted superior microbial reduction compared to the control group, for Gram negative (*E. coli*) and Gram positive (*S. aureus*) bacteria in suspension. The microbial reduction of aPDT in the group with urea (UMB) was not higher than in the group without urea (MB). The disaggregation factor that urea has in phenothiazine PS, in this experiment, was not decisive to reduce the amount of microorganisms in suspension.

Conflict of Interest. The authors declare that there are no conflicts of interest in carrying out this study.

Statement of Animal Rights. The study was carried out after submission and approval by the Ethics Committee for the Use of Animals from Brazil University, protocol approval number IC18-19/016), following the precepts of ethics and animal welfare recommended by CONCEA.

References

1. Trindade, A.C., Figueiredo, J.A.P., Steier, L., Weber, J.B.B.: Photodynamic therapy in endodontics: a literature review. *Photomed. Laser Surg.* **33**(3), 175–182 (2015)
2. Singh, S., Nagpal, R., Manuja, R., Manuja, N., Tyagi, S.P.: Photodynamic therapy: an adjunct to conventional root canal disinfection strategies. *Aust. Endod. J.* **41**, 54–71 (2015)
3. Melo, M.A., et al.: Photodynamic antimicrobial chemotherapy and ultraconservative caries removal for management of deep caries lesion. *Photo diagnosis Photodyn Ther* **12**(4), 581–586 (2015)
4. Bumb, S.S., Bhaskar, D.J., Agali, C.R., Punia, H., Gupta, V., Singh, V., Kadtane, S., Chandra, S. Assessment of photodynamic therapy (PDT) in disinfection of deeper dentinal tubules in a root canal system: an in vitro study. *J Clin Diagn Res* **8**(11), ZC67-ZC71 (2014)
5. Garcia, V., et al.: Effect of the concentration of phenothiazine photosensitizers in antimicrobial photodynamic therapy on bone loss and the immune inflammatory response of induced periodontitis in rats. *J Periodontol Res* **49**, 584–594 (2014)
6. Nuñez, S.C., et al.: Urea enhances the photodynamic efficiency of methylene blue. *J. Photochem. Photobiol., B* **150**, 31–37 (2015)
7. Nunez, S.C., Garcez, A.S., Ribeiro, M.S.: PDT Terapia Fotodinâmica Antimicrobiana na Odontologia **2**, 153–154 (2019)
8. Centers for Disease Control and Prevention. Guidelines for Infection Control in Dental Health-Care Settings MMWR 2003, 52 (No. RR-17) (2003)
9. Garcez, A.S., et al.: Effects of photodynamic therapy on Gram-positive and Gram-negative bacterial biofilms by bioluminescence imaging and scanning electron microscopic analysis. *Photomed. Laser Surg.* **31**, 519–525 (2013)
10. Soares, R.B., Myakawa, W., Navarro, R.S., Baptista, A., Ribeiro, M.S., Nunez, S.C.: Photodynamic therapy to destroy pneumonia associated microorganisms using external irradiation source. In *Light-Based Diagnosis and Treatment of Infectious Diseases*, Proceedings of SPIE **10479**, 1047917 (2018)

11. Da Collina, G.A., et al.: Controlling Methylene Blue aggregation: a more efficient alternative to treat *Candida albicans* infections using Photodynamic Therapy. *Photochem. Photobiol. Sci.* **17**(10), 1355–1364 (2018)
12. Demidova, T.N., Hamblin, M.R.: Photodynamic therapy targeted to pathogens. *Int. J. Immunopathol. Pharmacol.* **17**, 245–254 (2004)
13. Hamblin, M.R., Hasan, T.: Photodynamic therapy: a new antimicrobial approach to infectious disease? *Photochem. Photobiol. Sci.* **3**, 436–450 (2004)
14. Barroso, R.A.: Eficácia da Terapia Fotodinâmica mediada pelo fotossensibilizador *Hypericum perforatum* e Laser em baixa intensidade sobre Biofilmes monotípicos de *Propionebacterium acnes*. Dissertação de Mestrado Programa de Pós-Graduação em Engenharia Biomédica, Universidade Brasil. São Paulo, p. 35 (2018)
15. Costa, L.A.G., Pereira, H.K.M., Fontes, A., Falcão, J.S.A., Santos, B.S.: Géis poliméricos contendo azul de metileno como novas formulações para terapia fotodinâmica. *Encontro Brasileiro para Inovação Terapêutica*, 377–380 (2017)
16. Núñez, S.C., et al.: Effects of ionic strength on the antimicrobial photodynamic efficiency of methylene blue. *Photochem. Photobiol. Sci.* **13**(3), 595 (2014)



360 Immersion System: A Work at Height Safety Training Experience with Physiological Monitoring

Guilherme Agnolin¹ (✉) , Maira Miekto Botome¹ , Bruno Pires Bastos^{1,2} ,
Lazaro Ismael Hardy Llins¹ , Bruno Garcia da Rocha¹ ,
and Marcela Purificação¹ 

¹ SESI Innovation Center for Health Technologies (CIS Tech), Florianopolis, Brazil
guilherme-agnolin@sesisc.org.br

² Post-Graduation Program in Production Engineering (PPGEP), Universidade Federal de Santa Catarina (UFSC), Florianopolis, Brazil

Abstract. The application of technology in the area of occupational health and safety (OSH) presents many opportunities for improving applied research to boost innovation in activities involving work at height. Workplace training and qualifications are tools to contribute to the safety of employees. The implementation of immersive Virtual Reality (VR) has the purpose to cause different stimuli in the human body. The methodology explains the collection of physiological data from workers in training at two different stages, providing them with distinctive audio-visual experiences. First, the physiological parameters are collected, using the electrocardiograph, without the use of the VR goggles. In a second moment, the parameters are, once again collected, but with the use of the VR goggles by the individual. Hence, this work aims to develop a platform for registering occupational safety training for activities at height and to monitor the physiological indicators of these workers. Occupational data and dashboards are generated for managers to base decisions more assertively and monitor the occurrence of these training. Thus, the organization improves its ability to train workers more interactively and dynamically through the application of the 360 Immersion System, enhancing the absorption of the contents of OSH training and allowing the replication of the training in a faster and easier way, promoting safer behaviors in the work environment.

Keywords: Training · Health monitoring · ECG · Height workers · API

1 Introduction

Work at height can be understood as an activity performed above ground level in which there is a risk for the worker in such a condition to fall [1, 2]. The obligation to attend OSH training and use personal protective equipment to carry out work activities at a certain level of height is a requirement that depends on the legislation of each country. In the Brazilian context, work at height is characterized by any activity performed above two

meters from the lower level, as recommended by Regulatory Norm 35 (NR 35-Work at Height). This norm makes it mandatory for employers to provide training to individuals working at heights, in addition to other essential requirements and recommendations for this type of work.

As it is a risky activity, training with a high level of effectiveness becomes essential for the worker's safety. However, the training carried out for the execution of work at heights is not always practical and duly effective. Thereby, the use of more interactive and dynamic learning formats can promote a greater engagement of the individual with relevant information and, consequently, a better comprehension.

Virtual Reality (VR) is capable of strongly assist the organizational process of implementing new experiences for training workers. This tool uses special goggles and allows the user to be placed in an exclusive real-life environment, filmed with 360 degrees technology. It is also possible to add digital elements to the simulation (augmented reality) and, as an application of computer technology, create a realistic effect in an interactive and three-dimensional world [3]. These characteristics of VR provide the individual a feeling of being part of the environment, not only as an observer but as an active participant in the virtual simulation [4].

It is worth highlighting the role of the 360 degrees immersion tool or immersive VR linked with strategies for applying virtual reality in labor skills learning processes. This VR technique, used in occupational safety training, provides immersive learning to the user, free from the risks inherent in the work activity while simulating real actions and situations that users may encounter in their professional daily life [5]. Therefore, it is possible to make the learning process more stimulating and interactive for the learner, favoring the engagement and assimilation of content and activities more effectively and, consequently, contributing to the adoption of safer behavior within their work environment.

In the health area data are essential to the decision-making process, since, through them, professionals can establish an action plan to monitor and control the spread of diseases; assess the health status of patients; effectively manage drug inventories; among other relevant situations. Thus, developing data visualization through interactive dashboards can be a way to contribute to assertiveness in health area decision-making processes [6].

The preventive assessment of individuals' health and the analysis of physiological parameters can be relevant ways to assist in carrying out clinical diagnoses. In addition, such analysis allows individuals to monitor their current health status, following its evolution over time or identifying changes when exposed to different contexts. As an example of such parameters, there are bioelectrical signals generated by nerve and muscle cells from different sources, such as bioimpedance signals, bioacoustics signals, biomagnetism, and biomechanical signals, among other classifications. The potential use is the biological signal itself, which can be measured using surface electrodes that act as sensors. The electric field generated by the action of many cells, distributed in the proximity of the electrodes, constitutes the bio-electric signal, which is characterized as the type of signal of interest for the development of the present research [7].

Biomedical instrumentation is an area that works with the development of systems (hardware and software) to assist health professionals in diagnosing and monitoring

patients, investigating pathologies, or assisting them during medical treatment. This knowledge sphere uses concepts of physiology, electronics (analog and/or digital), programming, and digital signal processing, among others [8] to deliver, in a more effective way, the results that best help health professionals in the execution of their activities.

At the same time, health data is generated and collected at increasing speeds and volumes, making essential their fast and assertive visualization. Currently, it is extremely important to transform raw data into relevant information that can support the decision-making process of individuals, companies, or the government [6]. To corroborate and improve this process, technology has revealed great potential in its applications, such as the Internet of Things (IoT) applied to the development of technological solutions in the health area.

It is possible to explore the use of non-invasive devices in other less widespread applications as a means of promoting health care for the population [9]. For example, mobile applications that connect to other electronic devices to obtain data about the user's health were developed, sending accurate information that can assist in the detection and treatment of possible physiological changes [10].

The use of IoT is intended to improve the user experience and the results of such applications. It is important to highlight that the existence of this method is due to the integration of electronic devices embedded with a communication network, where information transfer takes place [11]. This technological tool aims to minimize the direct participation of the human factor in processes [12, 13], where relevant results found IoT a useful strategy for data collection quality and conservation.

One of the most relevant advantages of technology implementation in healthcare is the minimization of the need for maintenance support, synchronized with healthcare opportunities [11]. These characteristics can be extended to any environment, system, or situation, expanding and diversifying even more health technology applications and uses.

In this context, the present research is aimed to develop a platform for registering occupational safety training focus in work at height activities while monitoring physiological parameters. It is intended to use immersive virtual reality, integrated with the measurements of the users' physiological parameters, so the organizations can train workers more interactively and dynamically, enhancing the absorption of the contents, promoting safer behaviors in the work environment.

2 Methodology

The present work aims to develop a method for monitoring the physiological parameters of frequency heart rate (HRV) in a short period, using an electrocardiogram signal. This paper describes the building of the IoT system to train individuals that work at heights through the development of a device to collect the signals by employing an Electrocardiograph. Therefore, the proposed solution is divided into three stages: Input, Processing, and Output (result) of data, as shown in Fig. 1 of the Operational Diagram.

The first stage begins with data acquisition. The Quest 2 virtual reality goggles (A) allow the simulation of realistic scenarios of work at height through a video with 360 degrees technology. This video provides an immersion effect to the individual and it

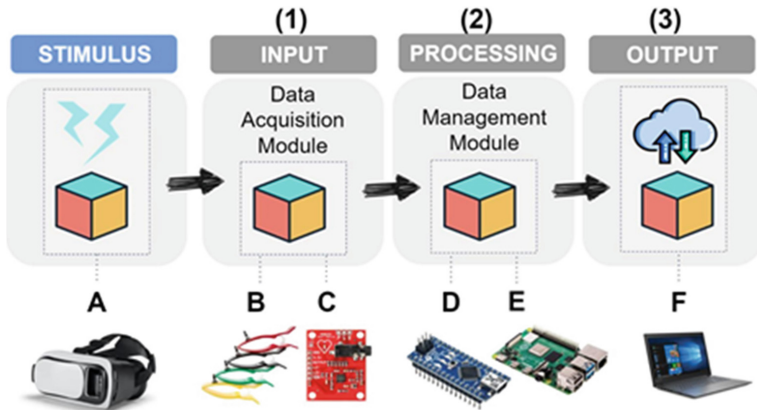


Fig. 1. Operational diagram.

might cause physiological variations in HRV, ranging from ultra-low to high frequency, and the Beats Per Minute (BPM) levels.

The use of heart rate as a marker of changes in individuals, submitted to the virtual reality experience at heights, was based on triggered physiological patterns in situations of stress reported in similar studies. The first answer to stress is the stimulation of the sympathetic activity of the autonomic nervous system (ANS), which innervates various tissues and influences the cardiovascular system [14].

Therefore, it is possible to check the quick fight or flight reaction, stimulate releasing of the sympathetic system, and trigger uplift processes heart rate (BPM) [14]. Still, in the Input stage, the voltage measured on the electrodes (B) is treated by the AD8232 module (C), which amplifies, extracts and filters small signals that are subject to noisy conditions. The processed data helps to obtain the ECG signal, as shown in Fig. 2. This signal has an amplitude of the peak between approximately 1 mV and 5 mV, a frequency range between 0.05–100 Hz for clinical records, and a range between 0.5–50 Hz for monitoring records [7].

It is important to note that, in many cases, the “data acquisition” is not able to deliver a complete signal without noise, however, we can carry out filtering through the software with the Neurokit2 library. This library demonstrates better results in signal quality and indicators. To eliminate the undesirable effects of the signal it is required more RAM from the controller, increasing the computational effort of the system.

In the second stage, the Arduino Nano controller (D) collects the data and sends it to the serial protocol in the processing center. This communication strategy solves two problems: data transmission and the power supply 3.3 – V for the AD8232 module. Raspberry Pi 3B + (E) receives and starts the analysis of the information transferred by the microcontroller. The Neurokit2 library determines the definition of physiological indicators and filters the data to facilitate the R peak values. The following equation calculates the BPM values.

$$BPM = \frac{PR \times 60}{PC} \quad (1)$$

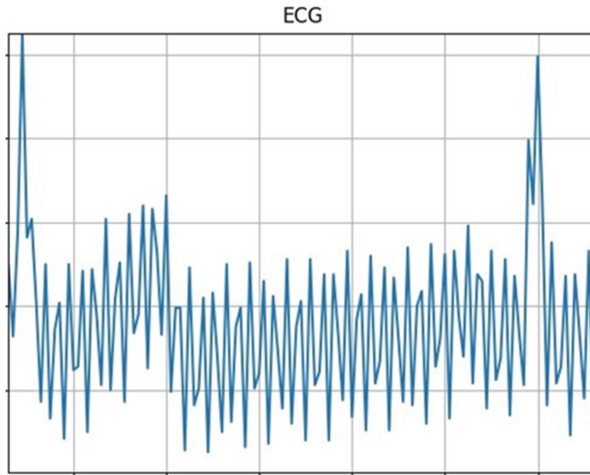


Fig. 2. ECG signal collected with noise.

The last stage (F), imports and protects the obtained results through the Programming Interface of Application (API). The Microsoft Azure platform stores the information in the Web application. The services in this environment allow the registration of the physiological parameters of the workers from the training that took place in VR through the simulation goggles. The built application can manage and replicate the training and may represent smaller costs for other companies to put into practice.

3 Results

The development of new management strategies within the Health and Safety at Work field is an emerging necessity in society, mainly in the industry of construction. Technology and immersive virtual reality devices have been considered promising alternatives in the learning process. They can also contribute to the safety culture of organizations. When users get immersed in a virtual environment, they have practical experiences due to the simulation of the work environment. They are even exposed to dangerous situations in the virtual environment and suffer simulated accidents as part of their learning process.

After creating all the architecture for the solution, it was possible to structure and develop the planning for its practical application through a predetermined protocol. Furthermore, during the ideal implementation of the prototype, users must be accompanied by an instructor to assist them during the use of the solution. It is also advisable that the individuals who carry out work activities addressed in the training simulation via VR goggles are the target audience of the application, which may vary depending on the occupation area of the company that adopts the solution.

A protocol designed in this study intends to instruct individuals to use the prototype correctly and safely to obtain greater accuracy in the collected data and their results. The protocol presents two macro stages: one to collect the heart rate (BPM) with the

VR goggles off, and the second to collect it while the users wear the VR goggles. It is relevant to highlight that each data collection lasts between, approximately, one minute and fifteen seconds and one minute and thirty seconds.

Macro stage one: data collection with the VR goggles off.

1 – Clarification about the purpose of the data collection: the instructor, who monitors the worker that uses the solution, must choose an environment that presents thermal, acoustic, and physical comfort and with an internet connection to enable the training. The instructor must explain the purpose of the data collection and the importance of following all recommendations during the training.

2 – The user's proper positioning in the environment: after the first procedure, the worker must sit on a comfortable chair that upholds their arms and back; their knees should be at a ninety-degree angle and their feet flat on the ground.

3 – Proper positioning of the electrodes on the user: the electrodes (tweezer-like) must be on the user's wrists (both right and left) and their left ankle. Besides, the electrodes present colors and letters to ensure their proper positioning. The user must not perform sudden movements during the procedure to avoid mistakes throughout the data collection. It is also important to mention that all the necessary guidelines to carry out the ideal collection of the parameters are displayed when starting the training platform.

4 – The start of the data recording through the web platform: the instructor must verify whether the previous steps comply with the recommendations for using the solution. After that, the instructor must start the software, and the data collection from the user-assisted begins. It is essential to mention that both training and users who participate in it must be previously registered on the solution's web platform to optimize the time during the data collection.

Macro stage two: data collection with the use of the VR goggles.

The second recording stage occurs after the first collection. There is a little time gap between the macro steps to place the VR goggles correctly on the assisted user. During this macro stage, steps one, two, and four from the macro stage one must be done one more time in the same way. However, step number three presents new activities that the users must accomplish. In this second collection, there are two additional steps: the fifth step, the Self-Assessment by the worker, and the sixth step, the dashboard generation with the collected data.

3 – Proper positioning of both VR glasses and electrodes: after the correct positioning of the electrodes (according to step 3 in Macro Step 1) the instructor must place and adjust the VR goggles correctly on the user's head and eyes, so s/he feel comfortable wearing them. After that, a video with the immersive simulation of the work activity appears to the user in the environment inside the VR goggles, which only the user can visualize. The user needs to press the button "start" using one of the VR controllers, and the activity starts. Concerning the proposed solution, the user will watch a recording of the work activity at heights made with a 360 degrees camera during the training simulation.

4 – The start of the data recording through the web platform: the instructor must verify whether the previous steps comply with the recommendations for using the solution.

After that, the instructor must start the software, and the data collection from the user-assisted begins.

5 – Self-Assessment by the worker: at the end of the second collection of the parameters, the user must perform a well-being self-assessment which consists of three questions about the experience during the simulation. Concerning the proposed solution, the self-assessment corresponds to questions that suffered some adaptations from the acrophobia questionnaire (fear of heights), originally elaborated by Cohen [15].

6 – Dashboard creation and presentation: after gathering the data from the worker's collections, a dashboard with some information concerning the user's experience, such as the training, the self-assessment questionnaire, and the recorded heart rate (BPM), will be generated.

After performing both well-being and acrophobia self-assessment, the system presents a screen with information about the assisted user and their two collections, as shown in Fig. 3. In this screen, the users can see their previously registered identification data such as name, age, department/area, actual occupation, identification number, the attended training, pre-existing health conditions, and physical activity practice. The last two items are answered by the workers during their registration on the platform to identify their health conditions and certain diseases that may influence the results of the collections. This last action has the purpose of minimizing errors in final readings.

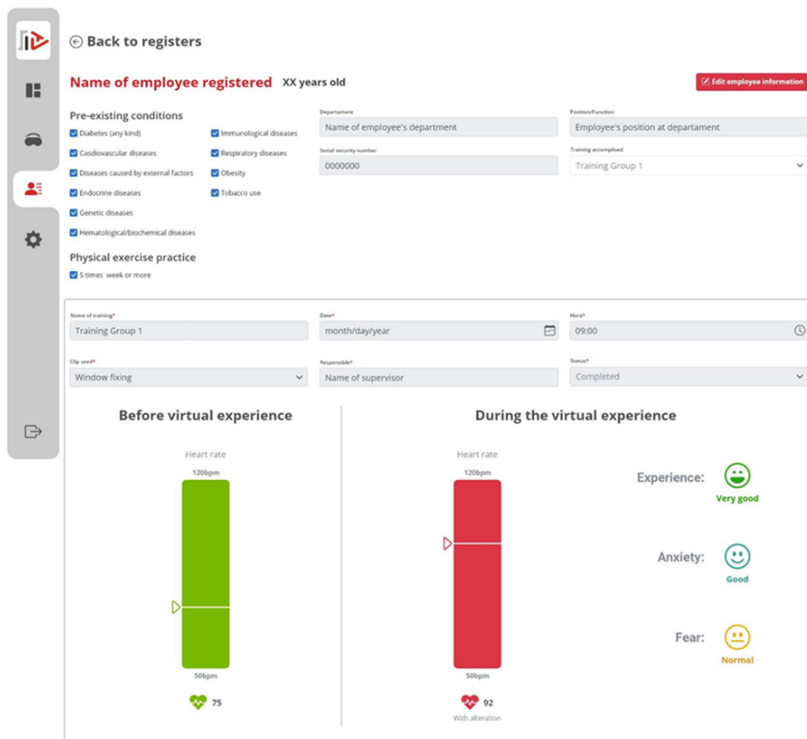


Fig. 3. User's parameter collection screen.

Below the user's information, it is possible to visualize a board with additional data about the training, such as the date and time of the testing, the 360 degrees video used during the simulation, the training status, and the instructor who applied the test. Furthermore, two charts, which show the results of the heartbeats before and during the virtual experience, are generated to indicate the heart rate and its possible changes. The use of the heart rate and its variation, collected in real-time, may enhance clinical practice by developing some devices that carry out the collection and analysis of electrocardiographic signals of the RR intervals [16].

Based on the user's responses to the well-being/acrophobia self-assessment, information such as their self-perception of the experience with the VR training, anxiety, and fear of height appears beside the charts. All this information is considered variables inside the 360 degrees simulation of the work activities at height.

Moreover, it is possible to generate another dashboard for the manager with all data from the training and the collection registered on the platform. This second dashboard presents information such as the number of participants, how many pieces of training occurred, data about the user's aptitude and their inaptitude to perform the work at height, and the percentage of trained workers. It is also possible to identify the categorization of suitable and unsuitable workers after the simulation, how the experience with VR proceeded, the anxiety levels, and fear during the video execution through the goggles. The self-assessment answered by the user can serve as a basis for assessing whether the user's perception is consistent with the BPMs collected from it.

Due to the immersive training inside a simulated environment, the user will be able to face risky situations without compromising their physical integrity. The developed solution carries out the user's heart rate collection (BPM) without the VR goggles and a second collection while s/he got immersed in the virtual training. Therefore, the system can conduct a correlation between the physiological parameters collected in both situations. In addition, along with the acrophobia self-assessment, the platform generates an indicator that shows the stress levels, attention, anxiety, and fear of height with and without the virtual experience.

In this context, an innovative product arises based on immersive technologies connected to an active learning methodology and physiological parameters collection. It generates some data that can assist the health and safety at work management in some organizations. This study prioritized the heartbeat (BPM) as a result. Moreover, the solution may be adapted and applied to other industry segments and projects since it becomes possible to work with other physiological indicators, even in different applications in the Health and Safety field.

4 Conclusions

In this work, we implemented an IoT system for monitoring the physiological parameters of frequency heart rate (HRV), using immersive virtual reality to obtain indicators of physiological characteristics of workers during work at height training.

The solution presented is modular, making it possible to modify the type of training and register other kinds of themes within the software, making it easier to replicate the solution. A plan to apply the pilot in the civil construction industries of Santa Catarina State is a possible next step to the current project.

The possible results of the project can contribute to the reduction of the company's costs with training, making them more interactive and dynamic and bringing the apprentice closer to their work reality and the variables that it presents. The user can also experience risk situations in an immersive environment, making his response in the event of an accident more adequate.

The dangerous nature of the work in industrial plants induced managers to look for innovative solutions, focusing on the prevalence of training outside the work environment, avoiding inefficiency, high costs, or exposure of workers to risks.

Furthermore, the virtual reality simulation allows users to explore the scenario at their own pace, controlling their progress. This participatory form of learning provides greater realism to the education process, given that the simulation allows users to make associations with real situations. Accordingly, users' attention can be increased and influenced, as well as the behaviors and decisions taken, aiming to promote a safe culture in the work environment.

Acknowledgments. The research was supported by the Research and Innovation Support Foundation – FAPESC – by the hiring of scholarship holders who contributed to the development of the project. In addition, the project had the financial support of the SESI Innovation Technical Call (Industry Social Service) of the year 2019.

References

1. Rey-Becerra, E., Barrero L. H., Ellegast, R., Kluge, A.: The effectiveness of virtual safety training in work at heights: a literature review. *Appl. Ergon.* **94** (2021)
2. HSE UK. Working at Height. A Brief Guide (2014)
3. Grajewski, D., Górski, F., Zawadzki, P., Hamrol, A.: Application of virtual reality techniques in design of ergonomic manufacturing workplaces. *Procedia Comput. Sci.* **25**, 289–301 (2013)
4. Zheng, J.M., Chan, K.W., Gibson, I.: Virtual reality. *IEEE Potentials* **17**, 20–23 (1998)
5. Bhoir, S., Esmaili, B.: State-of-the-art review of virtual reality environment applications in construction safety. *AEI*: 457– 468 (2015)
6. Novaes, L., Bonelli, J., Sousa, M.: Visualização de dados aplicada à saúde. Departamento de Artes e Design (2020)
7. Rathke, J.E.: Sistema de processamento de sinais biomédicos: módulos didáticos de aquisição de ECG, EMG, EOG e conversão analógico-digital de biosinais. Dissertação (mestrado) - Universidade Federal de Santa Catarina, Centro Tecnológico. Programa de Pós-Graduação em Engenharia Elétrica (2008)
8. Pesquisa em Engenharia Biomédica, <http://www.ieb.ufsc.br>, last accessed 2022/04/01
9. Katzis, K., Berbakov, L., Gardašević, G., Šveljo, O.: Breaking barriers in emerging biomedical applications. *Entropy* **24**(2), 226 (2022)
10. Xu, B., Xu, L.D., Cai, H., Xie, C., Hu, J., Bu, F.: Ubiquitous Data Accessing method in IoT-based information system for emergency medical services. *IEEE Trans. Ind. Inform.* **10**, 1578–1586 (2014)
11. Alekya, R., Boddeti, N.D., Salomi Monica, K., Dr. Prabha, R., Dr. Venkatesh, V.: IoT based smart healthcare monitoring systems: a literature review. *Eur. J. Mol. Clin. Med.* **7**(11), 2761–2769 (2021)
12. Morais, R., Valente, A., Serôdio, C.: A Wireless Sensor Network for Smart Irrigation and Environmental Monitoring: A Position Article (2005)

13. Agrawal, S., Das Manik, L.: Internet of Things—a paradigm shift of future Internet applications in 2011. In: Nirma University International Conference on Engineering, pp. 1–7 (2011)
14. Mendes, H. A.: Efeitos do estresse mental agudo sobre a resposta autonômica cardiovascular em bombeiros militares. Universidade Federal de Santa Catarina Master's thesis, Florianópolis (2019)
15. Cohen, D.C.: Comparison of self-report and overt-behavioral procedures for assessing acrophobia. *Behav. Ther.* **8**, 17–23 (1977)
16. Marães, V.: Frequência cardíaca e sua variabilidade: análises e aplicações. *Revista Andaluza de Medicina del Deporte* **3**(1), 33–42 (2010)

Metrology and Quality of Healthcare Technologies



Mass Estimation in Body Photography for Obesity Assessment Using Deep Learning and Linear Regression

Alexandre G. Silva¹✉, Lucas N. Ziza², Rangel Arthur²,
and Franklin C. Flores³

¹ Department of Informatics and Statistics, Federal University of Santa Catarina, Florianópolis, SC, Brazil

alexandre.goncalves.silva@ufsc.br

² School of Technology, University of Campinas, Limeira, SP, Brazil

³ Department of Informatics, State University of Maringá, Maringá, PR, Brazil

Abstract. This work presents a computer vision method for estimating the mass (weight) of people, based on the automatic interpretation of anthropometric attributes in low resolution, non-standardized almost full body photographs. Human body keypoints are obtained by deep learning, relationships between measurements are defined as features, and a regression architecture is trained for 405 images. When applying the model to another 100 unknown images, the correlation between actual and estimated mass measurements is 0.7216, with correct classification of obesity for 71% of cases.

Keywords: Anthropometry · Mass estimation · Obesity classification · Computer vision

1 Introduction

Body fat measurement is an important way of evaluating diets and training, as well as serving as a parameter for health risk factor analysis. Obesity, according to 2016 data from the World Health Organization (WHO), is one of the main factors of preventable death worldwide, with increasing prevalence rates.¹ In Brazilian capital cities, among adults, 19% are obese and 35% are overweight; in Florianópolis, for example, 49.8% of the population is overweight [7]. On another spectrum, eating disorders (such as anorexia), dysfunctions with eating disorders, conditions of extreme poverty, among other situations, promote significant weight loss, and require proper monitoring. In this sense, a practical and fast means, such as a common mobile device with a camera (cell phone), for body fat assessment, can represent an outstanding tool in medical clinics and hospitals. No commercial technique for assessing body fat is exact and all approaches are estimates. The *Dual-Energy X-ray Absorptiometry* (DEXA or DXA) method is

¹ <http://www.who.int/en/news-room/fact-sheets/detail/obesity-and-overweight>.

the most accurate² and widely accepted method for measuring body composition in clinical settings [3]. In practice, indirect, cost-free and approximate methods are used.

The Body Mass Index (BMI), given by Eq. 1, is the most practiced in the evaluation of fat and adopted by the WHO as an international predictor of obesity. In Fig. 1, a chart with values of mass (in kilograms) and stature (in meters) shows the classification, by colors, of the individual’s situation.³ Normality is highlighted in the region in yellow. For the other colors, there are non-ideal conditions. The BMI formula requires only a weighing scale and a tape measure, but it has problems such as not considering gender differences.

$$BMI = \frac{mass}{stature^2} \tag{1}$$

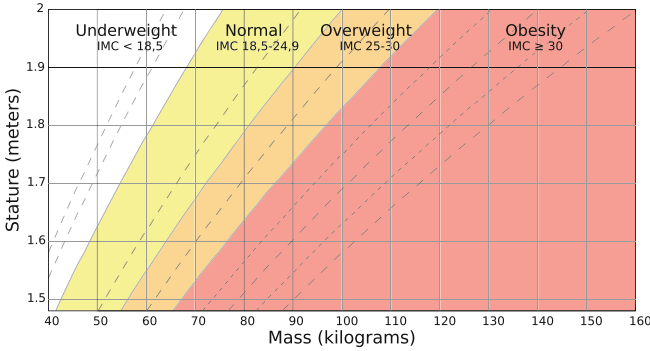


Fig. 1. Body Mass Index (BMI) chart (Adapted from https://commons.wikimedia.org/wiki/File:Body_mass_index_chart.svg).

Recently, a new model called Relative Fat Mass (RFM), in addition to discarding the use of a weighing scale, and requiring only a measuring tape to determine stature and waist circumference, proved to be a more reliable alternative for body assessment. The RFM expression is given by Eq. 2, being the calculation more accurate than other 300 formulas [8] (including BMI), and has become the closest to DEXA densitometry [12]. The indicated constants are

² The best methods for determining the body composition of a living human are called “four component models” (4CM) which divide the body into water, protein, mineral and fat using radioactive isotopes to determine total body water and potassium, but are impractical even in most clinical scenarios (source: <http://fellrnr.com/wiki/DEXA>).

³ We chose to use “mass”, because “weight”, strictly speaking, is the force acting on the object due to gravity. “Stature” was also used in preference to person’s “height”. In the context of this work, “weight” and “height” can eventually be exchanged for “mass” and “stature”, respectively.

derived using linear regression. This formula is composed of the inverse of the Waist(circumference)-to-Stature Ratio (WSR) [6]. Despite the applicability of this equation, its validity for specific populations still needs to be evaluated⁴ [4].

$$RFM = 64 - \left(20 \frac{stature}{waist} \right) + (12 \text{ sex}) \quad (2)$$

$$sex = \begin{cases} 0 & \text{for male} \\ 1 & \text{for female} \end{cases}$$

In the context of this work, [2] implement a system based on whole-body images for weight estimation. They assess the correlation between extracted anthropometric measurements and BMI values. A dataset with 5900 images of 2950 people is produced, with proper labeling as to gender, height and mass. Five anthropometric characteristics for frontal 2D images of the body are proposed and measured automatically by computational methods (deep learning): head width, waist width, hip width, thigh width and abdominal area. The predictive accuracy was 81% for the obese category and 64% for the overweight (there were few samples of underweight people, resulting in poor performance in these cases).

In turn, [13] develop a volume feature extractor (more than a dozen circumferences or perimeters are estimated), from the generation of frontal and lateral full-body silhouettes, followed by regression, based on methods of learning, trained in a dataset of 3D scans for mapping and reconstruction of body shape models.

With recent advances in deep learning methods, based on convolutional neural networks, many object recognition applications have become possible by computer vision. In this work, there is a special interest in methods for the analysis of human postures [2, 5, 11], so that they can be adapted to extract anthropometric parameters, based only on a single photographic image, efficiently, automatically and without physical contact with the individual. We propose a system for estimating mass from almost full body (the extremities of the upper and lower limbs, such as areas around the hands and feet, are not necessary) and frontal RGB images, obtained by cameras with basic settings, fully automatically, using indirect methods – for example, mass can be approximated based on measurements of the arm, abdomen and calf [9].

The datasets, computational tools and features for model training are presented in Sect. 2. The results are illustrated in Sect. 3. Conclusions and future works are in Sect. 4.

2 Methodology

In this work, anthropometric markers (*keypoints*) are determined by *deep learning* and the mass estimation is calculated by traditional regression technique.

⁴ <https://lanutri.injc.ufrj.br/2020/07/01/medidas-antropometricas-alternativas-na-obesidade/>.

2.1 Image Dataset

The photos are of people standing, positioned in front of the camera, acquired from public internet pages, in significant quantity and at random. Images with lateral or profile positioning, or images that did not contemplate the head area, upper limbs up to the elbows, and lower limbs up to the knees, were discarded (this region is called almost full body).

The training dataset consists of 405 photos from <https://www.height-weight-chart.com/>, being selected 255 images of women and 150 of men, following the stature and mass distribution of Fig. 2, with female averages of 1.65 ± 0.09 m and 76.49 ± 26.14 kg, and for males of 1.84 ± 0.09 m and 92.17 ± 28.05 kg. In this dataset and according to BMI, there are 35 underweight individuals, 144 with normal weight, 98 overweight and 128 obese.

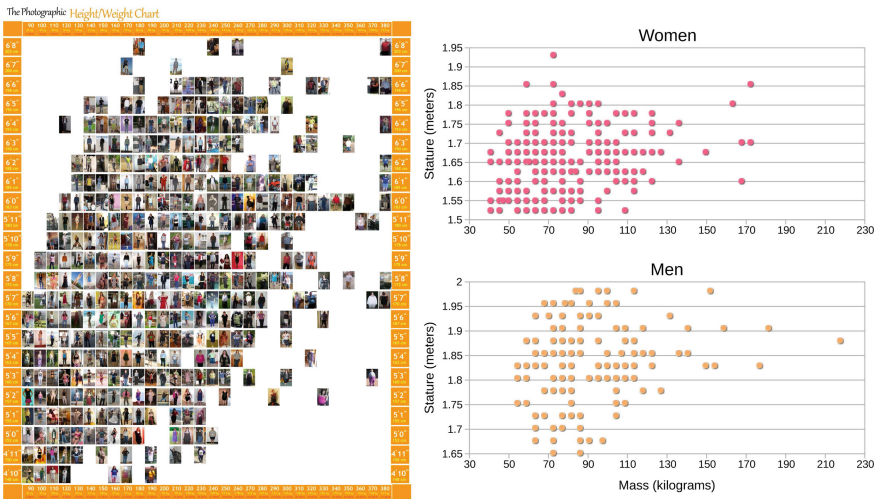


Fig. 2. Distribution of photographs (left), according to mass on the horizontal axis and stature on the vertical axis (taken from [height-weight-chart.com](https://www.height-weight-chart.com)). Distribution of selected images, separated into female and male (right).

The test dataset consists of 100 photos selected from <https://www.reddit.com/r/progresspics/>, 73 of which are female with an average stature of 1.67 ± 0.07 m and average mass of 90.00 ± 26.10 kg, and 27 males with averages of 1.83 ± 0.07 m and 117.72 ± 41.08 kg. In this dataset and according to BMI, there is 1 underweight individual, 15 with normal weight, 33 overweight and 51 with obesity.

2.2 Posture Estimation

For posture estimation, the architecture *MoveNet* [10] is used, considering a single image per person and model training in the “Lightning” version for critical latency.⁵ The acquisition of 17 keypoints of the human body is based on *MobileNetV2* with the addition of a *Feature Pyramid Network* (FPN). The model training was done with two datasets, COCO⁶ and another one internal to *Google* called *Active*, in order to make it appropriate for the physical activity and health applications.

2.3 Regression

The regression is performed using ordinary least squares linear regression, which fits a linear model with coefficients $w = (w_1, \dots, w_p)$ to minimize the residual sum of squares between the observed targets in the dataset, and the targets predicted by the approximation $y = w_1 x_1 + b_1 + \dots w_p x_p + b_p$, where, in machine learning, w is often referred to as the weight of a relationship and b is referred to as the *bias*.

2.4 Features

The *MoveNet* architecture automatically generates 17 keypoints from a person’s photo. Figure 3(a) shows an example of the processing output. Figure 3(b) describes the position and meaning of each keypoint. Additionally, in this work, the midpoint m_1 between 5 and 6, and the midpoint m_2 , between 11 and 12, are determined by Eq. 3.

$$\begin{aligned} m_1 &= \left(\frac{x_5 + x_6}{2}, \frac{y_5 + y_6}{2} \right) \\ m_2 &= \left(\frac{x_{11} + x_{12}}{2}, \frac{y_{11} + y_{12}}{2} \right) \end{aligned} \quad (3)$$

With the new points m_1 and m_2 , it is possible to describe two more line segments, highlighted in green in Fig. 3(b), whose lengths (squared) are calculated in Eq. 4.

$$\begin{aligned} d_{5,6} &= (x_5 - x_6)^2 + (y_5 - y_6)^2 \\ d_{0,m_1} &= (x_0 - x_{m_1})^2 + (y_0 - y_{m_1})^2 \\ d_{m_1,m_2} &= (x_{m_1} - x_{m_2})^2 + (y_{m_1} - y_{m_2})^2 \end{aligned} \quad (4)$$

The average length (squared) from hip to knee, considering both legs, can also be easily determined by Eq. 5.

$$\begin{aligned} d_{11,13} &= (x_{11} - x_{13})^2 + (y_{11} - y_{13})^2 \\ d_{12,14} &= (x_{12} - x_{14})^2 + (y_{12} - y_{14})^2 \\ d_{leg} &= \frac{d_{11,13} + d_{12,14}}{2} \end{aligned} \quad (5)$$

⁵ <https://tfhub.dev/s?q=movenet>.

⁶ <https://cocodataset.org/>.

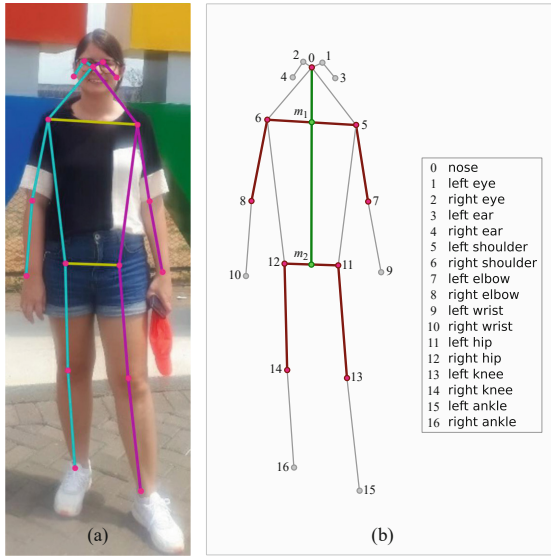


Fig. 3. *MoveNet* keypoints. (a) Result for a sample (magenta segments on the left and cyan segments on the right of the body). (b) Enumeration of keypoints with addition of points and segments in green.

The average length (squared) from shoulder to elbow, in turn, is calculated by Eq. 6.

$$\begin{aligned}
 d_{5,7} &= (x_5 - x_7)^2 + (y_5 - y_7)^2 \\
 d_{6,8} &= (x_6 - x_8)^2 + (y_6 - y_8)^2 \\
 d_{arm} &= \frac{d_{5,7} + d_{6,8}}{2}
 \end{aligned}
 \tag{6}$$

The lengths are squared only to avoid the radix calculation, whereas the interest is only in the proportions. The value of H from Eq. 7 refers to the height from marker 0 to the knee and will be a divisor for the other lengths (squared), so that each feature is, in fact, an invariant index to the scale (dimensions) of the image.

$$H = d_{0,m_1} + d_{m_1,m_2} + d_{leg}
 \tag{7}$$

The features for training the model are, therefore, determined from anthropometric proportions, so that there is no need for standardization of image resolution or rigorous positioning of individuals. Equation 8 describes the five features used by the regression architecture, the first two, sex and stature, being informed by the individual, and the following three, automatically calculated based on the

photo processing.

$$A = \left(sex, stature, \frac{d_{5,6}}{H}, \frac{d_{m_1,m_2}}{H}, \frac{d_{arm}}{H} \right) \tag{8}$$

$$sex = \begin{cases} 0 & \text{for male} \\ 1 & \text{for female} \end{cases}$$

3 Results

The training of the linear regression model is done from the five features of Eq. 8, calculated for the 405 samples of the first dataset of images, and the real mass of each individual (informed on the web pages, in which the images were acquired). Once trained, predictions are made for the 100 different samples that make up the second dataset. Figure 4 illustrates the comparison between the real mass (in kilograms) reported and the mass estimated by the model (in kilograms) for each sample.

Figure 5 shows the linear regression (in orange) involving the real measurements and those calculated by the model. Correlation analysis produced a Pearson coefficient of $r = 0.7216$. Figure 6, in turn, shows a Bland-Altman plot, indicating that 95% of the time, the automatic measurement differs from the real measurement by at most ± 44.9886 kg and on average this difference is 7.4553 kg.

When testing the method as a health indicator, and considering that there is no information on waist circumference (the analysis of the RFM is not possible), a comparison of the BMI classification was carried out, both for the real calculation and for the the calculation based on the mass estimate obtained by the developed model. In this way, the confusion matrix of Fig. 7 is obtained. It is observed that the method is a good indicator to identify overweight and, mainly, obesity, but it is not yet able to identify weight normality (the test set has only 1 underweight individual).

Thus, it was decided to restrict the estimated BMI calculation to a binary classification, in order to answer whether the individual is obese or not. This particular classifier worked for 71% of the cases, as per the confusion matrix in Fig. 8.

4 Conclusion

Given the complexity of the problem, the lack of minimum resolution or any other type of standardization for image acquisition (there is a significant distinction between the average mass of the training dataset and the test dataset), the correlation between mass measurements above 0.7216 is considered satisfactory. The method, as a BMI classifier, is only useful in verifying occurrences of obesity with 71%. Therefore, the developed system can be applied, at the limit, as a screening method or informal automated monitoring. A medical specialist is

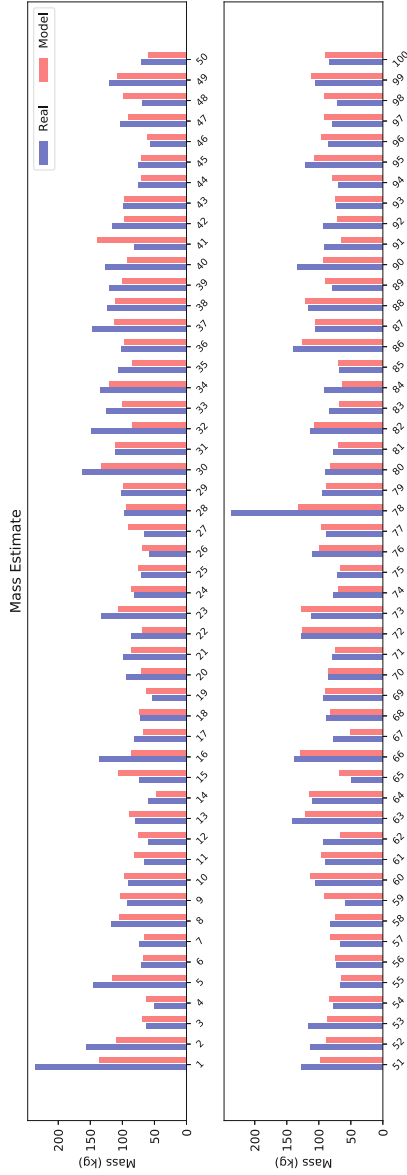


Fig. 4. Comparisons between reported mass and mass prediction for 100 test dataset images.

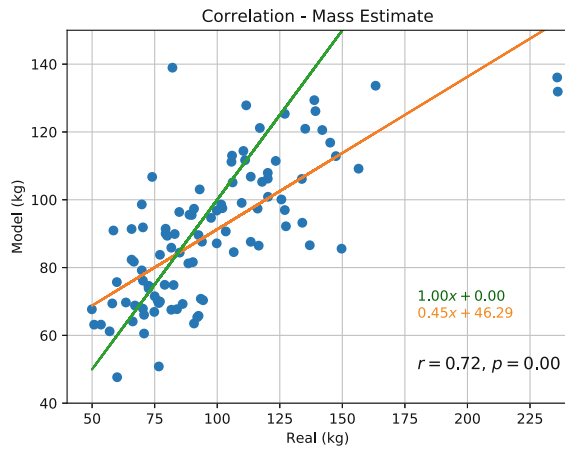


Fig. 5. Correlation between real and model-calculated mass measurements.

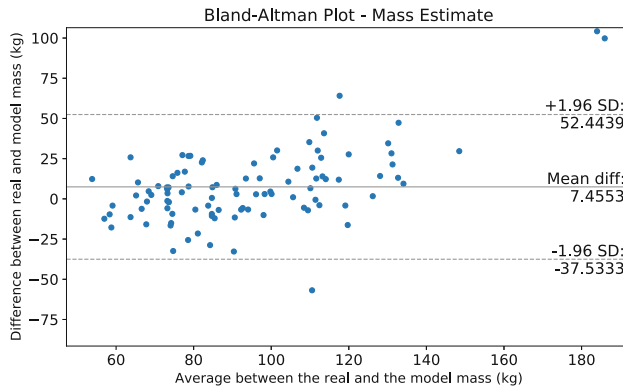


Fig. 6. Bland-Altman plot for analysis of differences between real mass measurements and those calculated by the model.

required to confirm the results. To improve the quality of mass inference, an essential future work would be the semantic segmentation of the human body, especially for estimating the area of the abdomen, which can be related to the waist circumference, an important parameter for health risk analysis [1].

The DEXA densitometry test, although accurate, is expensive, and has been almost universally approximated by the simple and low-cost BMI classifications and, more closely, by the RFM. Based on this result, estimates of stature and waist circumference become the main anthropometric features for assessing body fat, which could be observed by future computer vision systems.

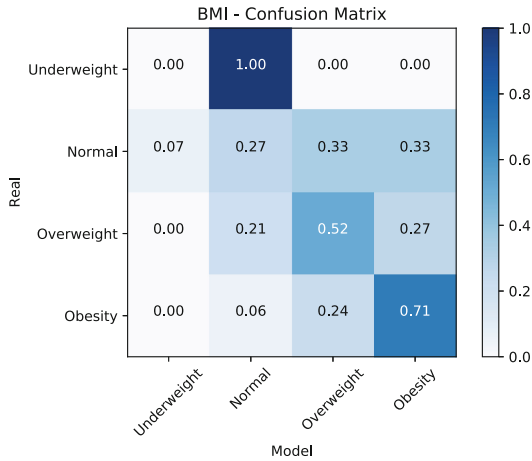


Fig. 7. Normalized confusion matrix between real and model-calculated BMI values.

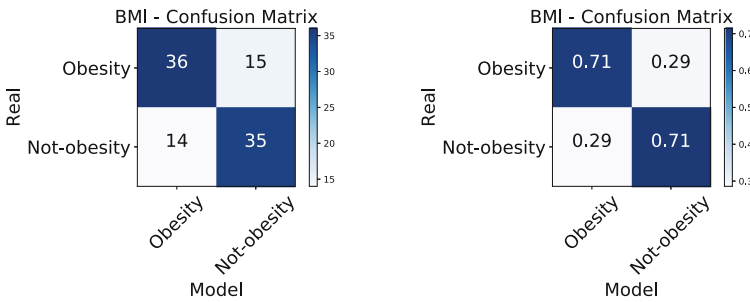


Fig. 8. Amount (left) and normalized (right) confusion matrix between real and model-calculated BMI values for obesity verification.

Conflict of Interest. The authors declare that they have no conflict of interest.

Acknowledgments. The authors thank UFSC, Unicamp and UEM for supporting this research.

References

1. Fontes, A., de Oliveira, L., Vanderlei, F., Garner, D., Valenti, V.: Waist-stature ratio and its relationship with autonomic recovery from aerobic exercise in healthy men. *Sci. Rep.* **8**(16093), 1–10 (2018). October
2. Jiang, M., Guo, G.: Body weight analysis from human body images. *IEEE Trans. Inf. Forensics Secur.* **14**(10), 2676–2688 (2019). Oct
3. Kakinami, L., Henderson, M., Chiolero, A., Cole, T.J., Paradis, G.: Identifying the best body mass index metric to assess adiposity change in children. *Arch. Dis. Child.* **99**(11), 1020–1024 (2014)

4. LANUTRI: Medidas antropométricas alternativas na obesidade. Equipe Técnica do Laboratório de Avaliação Nutricional (LANUTRI) do Instituto de Nutrição Josué de Castro (INJC) da UFRJ (julho 2020), pp. 1–8
5. Liu, Y., Sowmya, A., Khamis, H.: Single camera multi-view anthropometric measurement of human height and mid-upper arm circumference using linear regression. *PLOS ONE* **13**(4), 1–22 (2018)
6. Milagres, L., Martinho, K., Milagres, D., Franco, F., Ribeiro, A., Novaes, J.: Relação cintura/estatura e índice de conicidade estão associados a fatores de risco cardiometabólico em idosos. *Ciência & Saúde Coletiva* **24**, 1451–1461 (2019)
7. Monteiro, C.A., Claro, R.M., de Fátima Marinho de Souza, M., Coelho, M.R.S., Mendes, A.C.R., de Oliveira, P.P.V., Santos, M.A.S., Stopa, S.R., da Silva, S.U., Barufaldi, L.A., de Paula Lobo, A., Maia, E.G., da Silva, L.E.S.: Vigitel Brasil 2017: vigilância de fatores de risco e proteção para doenças crônicas por inquérito telefônico. Technical report, Ministério da Saúde, Brasília (2018)
8. Rativa, D., Fernandes, B.J.T., Roque, A.: Height and weight estimation from anthropometric measurements using machine learning regressions. *IEEE J. Transl. Eng. Health Med.* **6**, 1–9 (2018)
9. Silva, A.G., Arthur, R., Flores, F.C., Moreira, A.P.C.A.: Avaliação de gordura corporal de pacientes por visão computacional: uma revisão bibliográfica. *J. Health Informatics* **12**, 31–36 (2020)
10. Votel, R., Li, N.: Next-generation pose detection with MoveNet and tensorflow.js. *TensorFlow Blog* (May 2021)
11. Wei, S., Ramakrishna, V., Kanade, T., Sheikh, Y.: Convolutional pose machines. In: 2016 IEEE Conference on Computer Vision and Pattern Recognition (CVPR), pp. 4724–4732 (2016)
12. Woolcott, O., Bergman, R.: Relative fat mass (RFM) as a new estimator of whole-body fat percentage—a cross-sectional study in American adult individuals. *Sci. Rep.* **8**(10980), 1–11 (2018)
13. Yan, S., Kämäräinen, J.K.: Learning Anthropometry from Rendered Humans (2021)



Development of a Neonatal Lung Simulator with Variable Compliance

S. G. Mello^{1,2}(✉) , A. E. Lino-Alvarado¹ , G. D. Valério¹ ,
C. A. Estevam² , M. S. Dias² , K. N. Barros² ,
A. F. G. Ferreira Junior^{1,2} , and H. T. Moriya²

¹ Laboratório de Engenharia Biomédica, Universidade de São Paulo, São Paulo, Brazil

² Instituto de Pesquisas Tecnológicas do Estado de São Paulo, São Paulo, Brazil
saragm@usp.br

Abstract. A set of test scenarios is required to conduct a bench evaluation of lung ventilators during volume and pressure control ventilation. In general, test lung simulators that mimic fixed values of lung resistance and compliance are employed along with specific ventilatory settings in these test scenarios. Different values of resistance and compliance are necessary to emulate patients ranging from an adult to a neonate. However, it is difficult to find on the market lung simulators mimicking neonatal values of static compliance and low tidal volume, in specific values of 0.5 mL/hPa and 5 ml volume. This compliance value is required to assess lung ventilators under a control test setup of volume and pressure neonatal ventilation prescribed by the NBR ISO IEC standard 80601-2-12:2014. To cope with this particular limitation, a low-cost device was developed and characterized at the Institute of Technological Research (IPT). The developed device was able to reach values of compliance of 0.5 mL/hPa for volumes of 4, 5, and 6 mL, with a 10% acceptable tolerance, as required by the ISO standard. Thus it enables to the assessment of lung ventilators under the test scenarios required by the ISO standard.

Keywords: Neonatal · Lung simulator · Compliance · Neonatal ventilation · Evaluation of mechanical ventilation

1 Introduction

At hospitals, in neonatal intensive care units, it is found lung ventilators that provide support to neonates suffering from respiratory failure. Due to the fact that lung ventilators are essential components in a patient's recovery, these medical equipment need to be tested to assess their operation. In Brazil, the standard NBR ISO IEC 80601-2-12:2014 describes the required performance tests for lung ventilators. One of these tests evaluates volume and pressure control ventilation by using test scenarios, in which it is set values of resistance and static compliance with an acceptable tolerance of 10%. These parameters are set in a lung simulator, generally composed of bellows and springs.

Static lung compliance is viscoelastic lung propriety that measures its elasticity. It is given by the ratio between the change in volume and the change in pleural pressure at the end of inspiration, and it can be calculated by Eq. 1.

$$C = \frac{\Delta V}{\Delta P} \quad (1)$$

In individuals, the lung compliance is affected by the flexibility of the fibers of the lung tissue, by the surface tension elastic force of the fluids lining the walls of the alveoli, by the surfactant secreted by the alveolar epithelial cells lining the alveoli, and by the lung volume [1].

Clinically, these parameters guide medical diagnosis by allowing clinicians to determine the patient's lung condition. For instance, stiffness of the lung as seen in patients with Acute Respiratory Distress Syndrome (ARDS) is characterized by low compliance, whereas a lung with low elastic recoil, as seen in emphysema, has a high compliance [2]. Hence, it is necessary to consider this parameter during the development of a lung ventilator because it will have to provide the same ventilatory support in spite of the plethora of possible patient values of compliance and resistance.

The commercial lung simulator (Adult/Infant TTL, Michigan Instruments, EUA), which is widely employed to assess lung ventilators [3–5], has a compliance lower limit of 1 mL/cm H₂O in the infant setting. However, the NBR ISO IEC 80601-2-12:2014 requires the lung ventilator to be tested with the compliance ranging from 0.5 to 50 mL/cm H₂O for volumes ranging from 5 to 500 mL, as seen in its tables 201.103 and 201.104 [6]. In addition, the last three tests require a static compliance of 0.5 mL/cm H₂O for volumes of 5 mL, and it is important to note that in the ISO IEC 80601-2-12:2020, that will substitute the ISO standard of 2014, also has these tests as mandatory. These measurements are relevant due to conditions such as the Newborn Respiratory Distress Syndrome, since the low quantity of surfactant in the alveoli of newborns increases the tendency of their lung to collapse. This condition is fatal and requires a continuous positive pressure with the use of a lung ventilator [1]. As a result, the following project has had the objective of developing a device that enables the simulation of the lowest value of compliance required by the ISO standard.

2 Methodology

2.1 Construction

The test device was developed at the Institute for Technological Research (IPT), in São Paulo, Brazil. First, a flexible silicon bellow neonatal test lung (Test Lung 50 ml, Neotech Medical, India), with a volume of 50 mL and compliance of 1 mL/cm H₂O, was fitted in between two acrylic circular plates with the dimensions specified in Fig. 1, the front, top, left side and isometric views of the neonatal lung simulator.

Then, to reach the target value of compliance a set of 3 springs made with 0.5 mm steel wires and 8 coils was attached to the holes in the border of the

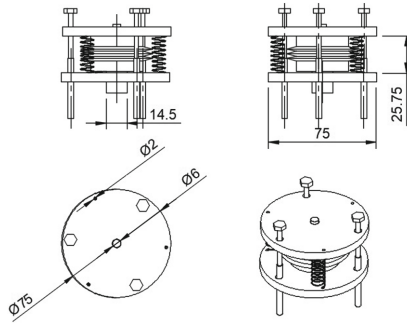


Fig. 1. Dimensions of the device and isometric views of the neonatal lung simulator

acrylic plates. In addition, three screws M4 were used to maintain the alignment and for displacement. The exploded view of the neonatal test lung system can be visualized in the Fig. 2.

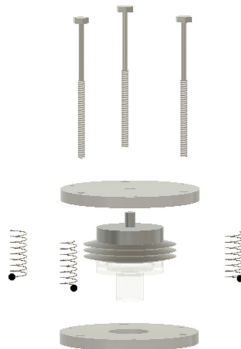


Fig. 2. Neonatal lung simulator with variable compliance

2.2 Measurement Setup

For the characterization of the system's compliance, it was used a ventilator analyzer (PF300 FlowAnalyser, IMT Analytics, Switzerland) calibrated in terms of low volume and pressure. Flow and volume signals were sampled and recorded at a frequency of 200 Hz.

The setup employed to measure the system's compliance is presented in Fig. 3. The intended volumes were delivered with a glass syringe through a circuit connected to the analyzer to finally insufflate the system.

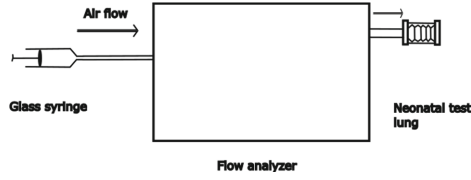


Fig. 3. Measurement setup

2.3 Characterization

Each target volume (4, 5, and 6 mL) was delivered three times with the glass syringe. As a result, we recorded values of flow, pressure, and volume to calculate the static compliance using Eq. 1. The computation of the static compliance was done one second after the system reach a plateau of pressure. In Fig. 4, pressure and pressure curves were shown.

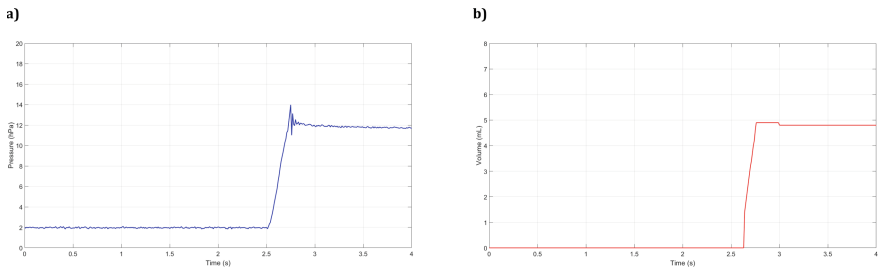


Fig. 4. Recorded values of tests. **a** Pressure curve. **b** Volume curve

3 Results

In Table 1 the average of static compliance and standard deviation for each measured volume can be visualized. It were obtained compliance values of (0.507 ± 0.020) , (0.491 ± 0.040) , and (0.529 ± 0.013) mL/hPa for volumes of 4, 5, and 6 mL, respectively.

4 Discussion

There are different models of neonatal lung ventilators available on the market. Over the years different studies showed that these equipment had differences in performance [7,8]; so, it is important that these lung ventilators are evaluate in controlled scenarios regarding their performance in ventilation modes.

Table 1. Measured values of compliance for volumes of 4, 5 and 6 mL

Volume (mL)	Compliance (mL/hPa)	Average compliance (mL/hPa)	Standard deviation (mL/h)
4.0	0.510	0.507	0.020
	0.529		
	0.481		
5.0	0.548	0.491	0.040
	0.464		
	0.461		
6.0	0.546	0.529	0.013
	0.516		
	0.461		

Due to the fact that dynamic compliance of the lungs are depended on the rate of respiration that varies according to ventilator settings and it is adjusted to fit the patient's condition; which is to say that the amount of gas reaching the internal lungs fluctuates in the function of the respiratory rate [9], the dynamic compliance could not give information about the static characteristics of the lung. This is why the measurement of the static compliance is clinically used as a tool of diagnostic [10]. Having pointed it out, it seems critical that lung ventilators can correctly inform the clinicians of the neonate's lung value.

The developed device could help with this regard because it emulates the compliance values lower than the test lungs developed in other studies [11], with the objective of meeting the normative requirements for evaluation of pulmonary ventilation equipment for newborns.

The development of this device was motivated by the necessity of meeting the requirements of the tables 201.103 and 201.104 of the standard NBR ISO IEC 80601-2-12:2014 and ISO IEC 80601-2-12:2020, since the adjustable compliance of the lung simulator available in the laboratory has a lower limit of 1 mL/cm H₂O and total volume of 100 mL. There are neonatal lung simulators commercially available with lower values of compliance, but their prices range around R\$2000.00, whereas the developed device costs R\$500.00. It is important to note that the device meets the 10% acceptable tolerance required by the ISO standard for the three measured volumes, and that it can be adjusted for different values of compliance between 0 and 1 mL/cm H₂O. This can be useful for testing a lung ventilator in physiological conditions beyond those required by the ISO standard.

5 Conclusion

In summary, this study developed and characterized a neonatal lung simulator with a compliance of 0.5 mL/cm H₂O for a tidal volume of 5 ml. This device fits

the requirement for testing lung ventilators in a control test scenario of pressure and volume ventilation prescribed in the standards NBR ISO IEC 80601-2-12:2014 and ISO IEC 80601-2-12:2020.

Conflict of Interest. The author(s) declare to have no potential conflicts of interest with respect to the research, authorship, and/or publication of this article.

Acknowledgements. This study was financed in part by the endowment fund from Escola Politécnica of University of São Paulo “Amigos da Poli” and the São Paulo State Government (42960P - Comitê de Crise do COVID-19).

References

1. Desai, J., Moustarah, F.: Pulmonary compliance. StatPearls [Internet] (2021)
2. Faustino, E.: Mecânica pulmonar de pacientes em suporte ventilatório na unidade de terapia intensiva. Conceitos e monitorização. *Rev. Bras. Ter. Intensiva*. **19**, 161–169 (2007)
3. Alvarado, A., Oliveira Rosa, D., Mello, S., Dias, M., Barbosa, M., Nascimento Barros, K., Lemos, B., Lima Vitorasso, R., Bartholomeu, V., Americano, P., et al.: Quality assessment of emergency corrective maintenance of critical care ventilators within the context of COVID-19 in Sao Paulo, Brazil. *Glob. Clin. Eng. J.* **4**, 27–36 (2021)
4. Richard, J., Carlucci, A., Breton, L., Langlais, N., Jaber, S., Maggiore, S., Fougere, S., Harf, A., Brochard, L.: Bench testing of pressure support ventilation with three different generations of ventilators. *Intensive Care Med.* **28**, 1049–1057 (2002)
5. Conti, G., Piastra, M.: Mechanical ventilation for children. *Curr. Opin. Crit. Care* **22**, 60–66 (2016)
6. Normas Técnicas (ABNT), A. ABNT NBR ISO 80601-2-12: 2014. Equipamento eletromédico. Parte 2-12: Requisitos particulares para a segurança básica e o desempenho essencial de ventiladores para cuidados críticos. ABNT (2014)
7. Juvet, P., Hubert, P., Jarreau, P.: Assessment of neonatal ventilator performances. *Intensive Care Med.* **21**, 753–758 (1995)
8. Juvet, P., Hubert, P., Isabey, D.: Assessment of high-frequency neonatal ventilator performances. *Intensive Care Med.* **23**, 208–213 (1997)
9. Bates, J.: Lung Mechanics: An Inverse Modeling Approach. Cambridge University Press (2009)
10. Olinsky, A., Bryan, A., Bryan, M.: A simple method of measuring total respiratory system compliance in newborn infants. *S. Afr. Med. J.* **50**, 128–130 (1976)
11. Abdullah, Z., Basiuras, A., Duman, A., Garcia, L. V.: Pediatric and Neonatal lung simulator. Escola Politécnica Superior D’Enginyeria de Vilanova I La Geltrú 1–215 (2014)



Typical Values in Digital Mammography Within the Framework of Diagnostic Reference Levels

J. V. Real^{1,2}(✉)  and A. L. M. C. Malthez¹ 

¹ Graduate Program in Biomedical Engineering, Federal University of Technology - Paraná, Curitiba, Brazil

real.jessicavilla@gmail.com

² Clinical Hospital Complex of the Federal University of Paraná/Diagnostic Imaging Unit, Curitiba, Brazil

Abstract. In the context of diagnostic reference levels (DRLs), typical values of mean glandular dose were established from a survey of mammographic examinations performed in a university hospital in Curitiba, Paraná, Brazil. This study represents an initial approach to the implementation of DRLs at the specific medical institution, as a means to improve the activities related to the radiological protection of patients managed by the Diagnostic Imaging Unit.

Keywords: Typical values · Diagnostic reference levels · Digital mammography

1 Introduction

According to recent estimates provided by the International Agency for Research on Cancer (IARC), breast cancer is the most frequently diagnosed cancer and leading cause of cancer death among women worldwide [1]. Brazilian National Cancer Institute (INCA) also recently estimates that breast cancer incidence is dominant within Brazilian female population (excluding nonmelanoma skin cancer) [2], as well as reports an increasing trend of breast cancer mortality rate [3].

As a major type of cancer commonly observed in women, breast cancer early detection is of primary concern. Mammography is generally the basic breast examination used for early detection of cancer in women presenting no clinical symptoms (screening mammography) and in women manifesting certain clinical symptoms (diagnostic mammography) [4]. Due to the high radiosensitivity of the breast tissue, strategies must be implemented to ensure that mammographic images provide the essential diagnostic information with the lowest possible radiation dose. A potential approach to this optimization of radiological protection is through the establishment of diagnostic reference levels (DRLs).

The concept of DRLs was introduced [5] and refined [6, 7] by the International Commission on Radiological Protection (ICRP), which recommends the use of DRLs as tools to assist the optimization of protection in the medical exposure of patients to ionizing radiation. As a term for a form of investigation level used in the optimization

process of radiological protection, a DRL is a supplement to professional evaluation and does not determine a dividing line between appropriate and inadequate medical practice. DRLs can be regarded as useful resources for identifying situations where optimization of protection may be required.

Specifically, a DRL *quantity* is a commonly and easily measured or determined radiation metric that assesses the amount of ionizing radiation used to perform a certain medical imaging task. Now, a DRL *value* is usually set at the 75th percentile of the distribution of the medians of distributions of the suitable DRL quantity, with these latter ones being collected from surveys or registries at several distinct medical facilities within a country (in this case, defining a national DRL value) and within a local area with a few health facilities (in such case, determining a local DRL value). Also in the context of DRLs, *typical values* can be implemented for a single medical facility with various imaging rooms or units, or in the case of a single equipment associated with a particular imaging technique. Therefore, a DRL value is a suggestive criterion that can be applied for decision making regarding optimization of radiological protection by indicating, for instance, examinations, equipment units or health facilities presenting DRL quantities exceeding locally or nationally established DRL values.

In the case of mammography, the mean glandular dose (MGD) is the recommended DRL quantity to be employed, even though it is a measure of organ dose rather than the amount of ionizing radiation used in breast imaging [7]. The International Atomic Energy Agency (IAEA) provides acceptable and achievable limits for MGD, which correspond to superior (maximum) and desirable values for the performance of a mammography equipment, respectively [8]. Brazilian regulations [9] similarly follow these IAEA recommendations, but unfortunately national DRLs for mammography are currently not established in Brazil by an official regulatory agency.

Regarding the radiological protection of patients undergoing digital mammography examinations, the aim of this study was to determine typical values (also here referred to as institutional doses) according to the methodology proposed and recommended by the ICRP publication 135, i.e., in the framework of DRLs. Moreover, the typical values obtained in this survey were compared to a similar study performed at institutional level, as well as to internationally established DRLs.

2 Materials and Methods

2.1 Patient Data Collection and Equipment

The collection of data accomplished in this study was approved by the Ethics Committee on Human Research of the Clinical Hospital Complex of the Federal University of Paraná (CHC-UFPR), with Certificate of Presentation for Ethical Appraisal (CAAE) No. 53273721.6.0000.0096 and Committee Opinion No. 5.157.771.

Anonymized patient data were collected retrospectively between February and April 2022 from 72 examinations performed on a single digital mammography system (Hologic Selenia Dimensions) installed at the CHC-UFPR and operational since 2018. This equipment is submitted to a periodic quality control (QC) program by the Medical Physics Department of the CHC-UFPR, which consists of evaluating compression force, automatic exposure control, detector performance, system resolution, x-ray equipment

characteristics, dosimetry, collimation system, image quality and image display quality, in accordance with the current Brazilian regulation [9].

Each mammographic examination included 4 views (2 for each breast) corresponding to the craniocaudal (CC) and mediolateral oblique (MLO) projections, therefore resulting in 288 views (mammograms). Also, the data collected from these mammograms were irrespective of clinical indication, i.e., with no distinction between screening and diagnostic examinations. The survey included only female patients without breast implant and all mammograms were acquired in the conventional mode (2D view) without magnification and using automatic exposure control (AEC).

The relevant parameters for this study were manually gathered from the control console of the mammography system, namely, patient age, projection, compression force, compressed breast thickness (CBT) and mean glandular dose (MGD).

2.2 Patient Dosimetry

The MGD is the quantity recommended by the ICRP for the establishment of DRLs (and typical values) in mammography. The aforementioned mammography system displays MGD values (denoted as organ dose) from estimates using Boone's method, which utilizes Wu's equation,

$$\text{MGD} = K \times D_{GN}, \quad (1)$$

where K is the incident air kerma (IAK) and D_{GN} is the normalized glandular dose per unit IAK, which is parametrized for different anode/filter combinations and glandularities [10].

It is assumed in this study that the organ dose displayed by the mammography unit provides a value as accurate as the MGD which would be estimated from measurements of different technical parameters associated with the x-ray tube performance.

2.3 Data Analysis

In the framework of DRLs, it must be emphasized that only typical values (not local values) could be established in this survey due to the presence of a single digital mammography system at the CHC-UFPR. Furthermore, the relatively low number of examinations evaluated was due to the lack of an automated data collection software, only enabling a manual process of data gathering.

Within the DRLs methodology, typical values in mammography should be strictly established from the median (50th percentile) of the distribution of MGD values. However, mean, 75th and 95th percentiles values are also calculated and presented here in order to perform a proper comparison with another studies.

According to the ICRP, a minimum sample size of 50 patients is recommended for the analysis and would be representative of the specific area of the survey. This condition is met here (72 patients). Also, in order to obtain typical values for a standard thickness characteristic of the local population, a restrict but equivalent analysis should be performed for the most frequent CBT range, which is in fact realized here.

3 Results

The mean, standard deviation (SD) and range values of patient age were 56.26, 10.54 and 26–84 years, respectively. The mean, SD and range values of CBT and compression force for all, CC and MLO projections are presented in Table 1.

The mean, median, range, 75th and 95th percentile values of MGD for all, CC and MLO projections are presented in Table 2. These same statistical parameters are exhibited in Table 3 for the most frequent CBT range of 50–59 mm, which can be identified from the distributions of Fig. 1.

Table 4 presents average values of the MGD for the thickness of equivalent breast along with the Brazilian regulation.

Table 1. Compressed breast thickness (CBT) and compression force for all views. CC, cranio-caudal; MLO, mediolateral oblique; SD, standard deviation; N, number of views.

Projection		CBT (mm)	Compression Force (N)
All (N = 288)	Mean ± SD	52.0 ± 12.1	125.1 ± 20.7
	Range	18.0 – 89.0	11.9 – 173.6
CC (N = 144)	Mean ± SD	49.4 – 10.6	123.4 – 21.3
	Range	18.0 – 76.0	11.9 – 168.6
MLO (N = 144)	Mean ± SD	54.6 – 13.0	126.9 – 20.0
	Range	19.0 – 89.0	338.0 – 173.6

Table 2. Mean, median, range (indicate in parenthesis), 75th and 95th percentile values of the mean glandular dose (MGD) for all views. SD, standard deviation; CC, cranio caudal; MLO, mediolateral oblique.

Projection	MGD (mGy)			
	Mean ± SD	Median	75th percentile	95th percentile
All (N = 288)	1.9 ± 0.6 (0.6 – 4.5)	1.81	2.34	3.28
CC (N = 144)	1.8 ± 0.5 (0.6 – 3.5)	1.69	2.05	2.92
MLO (N = 144)	2.1 ± 0.7 (0.6 – 4.5)	2.01	2.56	3.49

4 Discussion

The compression of the breast is a standard practice in mammography (by limiting, for instance, image motion artifacts and scattering effects) and the CBT influences the amount of dose absorbed in the breast tissue. As a means to account for the breast size

Table 3. Mean, median, range (indicate in parenthesis), 75th and 95th percentile values of the mean glandular dose (MGD) for the compressed breast thickness (CBT) range of 50–59 mm. SD, standard deviation; CC, crania caudal; MLO, mediolateral oblique.

Projection	MGD (mGy)			
	Mean ± SD	Median	75th percentile	95th percentile
All (N = 109)	2.0 ± 0.4 (1.3 – 3.7)	1.95	2.22	2.80
CC (N = 50)	1.9 ± 0.4 (1.3 – 3.0)	1.87	2.16	2.77
MLO (N = 59)	2.0 ± 0.4 (1.4 – 3.7)	2.01	2.28	2.79

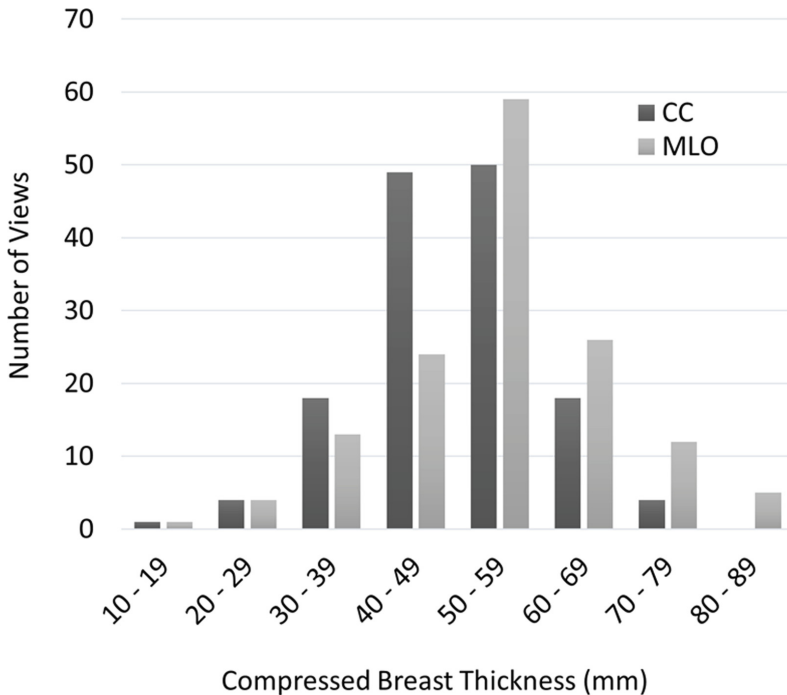


Fig. 1. Compressed breast thickness (CBT) distributions for craniocaudal (CC) and mediolateral oblique (MLO) projections.

variation between individuals, and consequently CBT variation, ICRP 135 recommends that data should be collected for at least 50 patients. Although phantoms may represent convenient instruments for a performance assessment of mammography systems, they do

Table 4. Average values of the mean glandular dose (MGD) for thickness of equivalent breast and achievable and acceptable levels of MGD to equivalent breast according to Brazilian regulations. SD, standard deviation; CC, cranio caudal; MLO, mediolateral oblique.

Thickness of equivalent breast (mm)	MGD (mGy)			
	CC Mean \pm SD	MLO Mean \pm SD	Achievable level to equivalent breast	Acceptable level to equivalent breast
≤ 21	0.9 \pm 0.3	0.8 \pm 0.3	0.6	1.0
22–32	1.1 \pm 0.2	1.2 \pm 0.2	1.0	1.5
33–45	1.4 \pm 0.2	1.4 \pm 0.2	1.6	2.0
46–53	1.8 \pm 0.4	1.8 \pm 0.4	2.0	2.5
54–60	2.0 \pm 0.4	2.1 \pm 0.4	2.4	3.0
61–75	2.6 \pm 0.5	2.9 \pm 0.6	3.6	4.5

not evaluate the full range of breast sizes for which examinations are performed. Therefore, their use should not replace patient dose surveys when considering the establishment of DRLs for optimization of radiological protection in mammography.

As can be noticed from Table 1, the mean value of CBT for all views is higher in the case of MLO projection, which can be expected due to the pectoral muscle present in the field of view during the examination related to this projection. In this case, AEC must compensate for muscle attenuation of the x-ray beam (i.e., more amount of radiation is required for appropriate image quality). Previous studies [11–14] have been reporting higher values for MLO, comparing the MGD values between MLO and CC projections. In our case, no significant differences were found between the two projections considering similar thickness of compressed breast (Table 4).

As presented in Table 4, the average values of the MGD are compatible with achievable levels and lower than acceptable levels given by the Brazilian regulation body.

Table 5 presents the mean, median, 75th and 95th percentiles derived from the distribution of MGD values collected in this survey, as well as shows the same information collated from similar studies in digital mammography. All the selected studies satisfy the condition of minimum sample size of at least 50 patients to account for the variation in CBT between individuals.

Using the same mammography system (Hologic Selenia Dimensions) as employed in this survey, Lekatou et al. [14] also performed a study at institutional level and reported lower MGD values than those presented here. The relatively small differences of mean CBT ranges between these two studies would suggest that there is margin for improvement at the institution of our study. The MGD values derived here were also higher than those found in international studies realized in Greece, Japan, Italy and Norway [15–17], as can be observed from Table 5. The differences could be explained by factors like age and breast density of the evaluated patients. However, care must be taken by implying this discrepancy to be characteristic of local populations, and a more elaborate analysis should be employed.

In order to obtain typical values for a standard thickness with an even more robust representation of the local population, the same analysis used here should be performed for the most frequent CBT range in a survey comprising a relatively large number of patients.

Table 5. Average values of the mean glandular dose (MGD) for thickness of equivalent breast and achievable and acceptable levels of MGD to equivalent breast according to Brazilian regulations. SD, standard deviation; CC, cranio caudal; MLO, mediolateral oblique.

Author (s) year	Country	Type	CBT range (mm) (mean)	MGD (mGy)			
				Mean	Median	75th percentile	95th percentile
This Study (2022)	Brazil	Institutional (Typical values)	All: 18–89 (52.1)	All: 1.96	All: 1.81	All: 2.34	All: 3.28
			CC: 18–76 (49.4)	CC: 1.79	CC: 1.69	CC: 2.05	CC: 2.92
			MLO: 19–89 (54.7)	MLO: 2.14	MLO: 2.01	MLO: 2.56	MLO: 3.49
			50–59	All: 2.02 CC: 1.95 MLO: 2.07	All: 1.95 CC: 1.87 MLO: 2.01	All: 2.22 CC: 2.16 MLO: 2.28	All: 2.80 CC: 2.77 MLO: 2.79
Lekatou et al. (2019) [14]	Greece	Institutional (Typical values)	All: 26–99 (56.3)	All: 1.25	All: 1.2	All: 1.51	All: 1.86
			CC: 26–91 (53.9)	CC: 1.18	CC: 1.13	CC: 1.4	CC: 1.77
			MLO: 27–99 (58.6)	MLO: 1.32	MLO: 1.3	MLO: 1.59	MLO: 1.89
			55–65	All: 1.33 CC: 1.3 MLO: 1.36	All: 1.29 CC: 1.24 MLO: 1.32	All: 1.44 CC: 1.41 MLO: 1.48	All: 1.77 CC: 1.76 MLO: 1.78
Asada et al. (2016) [15]	Japan	National	(42.0)	All: 1.57	All: 1.63	All: 1.84	–

(continued)

Table 5. (continued)

Author (s) year	Country	Type	CBT range (mm) (mean)	MGD (mGy)			
				Mean	Median	75th percentile	95th percentile
Gennaro et al. (2020) [16]	Italy	National	(53.5)	1.24	1.19	–	2.01
Østerås et al. (2018) [17]	Norway	Unspecified	14–101 (53.4)	All: 1.74	All: 1.63	All: 2.1	–

5 Conclusions

The dose survey presented here is intended to aid the optimization of radiological protection of patients at institutional level, within the activities already conducted by the Diagnostic Imaging Unit at the CHC-UFPR. Typical values for digital mammography were calculated and these values were found to be greater than similar published studies. In a simple analysis, this fact would suggest that there is room for improvement in the routine of mammography examinations. A more detailed assessment should be used to confirm the possibility of optimization.

The accuracy of the displayed (organ dose) MGD values by the mammography system is assumed here. Further investigation is intended to be performed in order to address possible differences (under- or overestimation) between these values and those calculated from an alternative dosimetry method. Possible discrepancies must be accounted for in the establishment of DRLs and typical values.

The introduction of an automated acquisition software for data collection and the implementation of an equivalent analysis to digital breast tomosynthesis are interesting perspectives to further extend and improve this work.

The survey performed here can contribute to future work involving the establishment of local DRLs for digital mammography, which can provide a useful tool in the process of optimization of radiological protection of patients.





Conflict of Interest . The authors declare that they have no conflict of interest.

References

1. Sung, H., et al.: Global cancer statistics 2020: GLOBOCAN estimates of incidence and mortality worldwide for 36 cancers in 185 countries. *CA Cancer J. Clin.* **71**, 209–249 (2021)
2. Instituto Nacional de Câncer José Alencar Gomes da Silva: Estimativa 2020 – incidência de câncer no Brasil. Instituto Nacional de Câncer José Alencar Gomes da Silva, Rio de Janeiro (2019)
3. Instituto Nacional de Câncer José Alencar Gomes da Silva: A situação do câncer de mama no Brasil - síntese de dados dos sistemas de informação. Instituto Nacional de Câncer José Alencar Gomes da Silva, Rio de Janeiro (2019)
4. International Agency for Research on Cancer: IARC Handbooks of Cancer Prevention, Breast Cancer Screening, vol. 15. IARC Press, Lyon (2016)
5. International Commission on Radiological Protection: Radiological Protection and Safety in Medicine, ICRP Publication 73, Ann. ICRP 26(2). Elsevier Science Ltd, Oxford (1996),
6. International Commission on Radiological Protection: The 2007 Recommendations of the International Commission on Radiological Protection, ICRP Publication 103, Ann. ICRP 37(2–4). Elsevier Science Ltd, Oxford (2007)
7. International Commission on Radiological Protection: Diagnostic Reference Levels in Medical Imaging, ICRP Publication 135, Ann. ICRP 46 (1). Sage Publishing (2017)
8. International Atomic Energy Agency: Quality Assurance Programme for Digital Mammography, IAEA Human Health Series No. 17. IAEA, Vienna (2011)
9. ANVISA at <https://www.in.gov.br/en/web/dou/-/instrucao-normativa-in-n-92-de-de-maio-de-2021-322985226>, last accessed 2022/09/25
10. Suleiman, M.E., Brennan, P.C., McEntee, M.F.: Mean glandular dose in digital mammography: a dose calculation method comparison. *J. Med. Imaging* **4**(1), 013502 (2017)
11. Young, K.C., Oduko, J.M.: Radiation doses received in the United Kingdom breast screening programme in 2010 to 2012. *Br. J. Radiol.* **89**, 20150831 (2016)
12. Joseph, D.Z., Nzotta, C.C., Skam, J.D., Umar, M.S., Musa, D.Y.: Diagnostic reference levels for mammography examinations in North Eastern Nigeria. *Afr. J. Med. Health Sci.* **17**(1), 54–59 (2018)
13. Parmaksız, A., Ataç, G.K., Bulur, E., İnal, T., Alhan, A.: Average glandular doses and national diagnostic reference levels in mammography examinations in Turkey. *Radiat. Prot. Dosimetry* **190**(1), 100–107 (2020)
14. Lekatou, A., Metaxas, V., Messaris, G., Antzele, P., Tzavellas, G., Panayiotakis, G.: Institutional breast doses in digital mammography. *Radiat. Prot. Dosimetry* **185**(2), 239–251 (2019)
15. Asada, Y., Suzuki, S., Minami, K., Shirakawa, S., Kobayashi, M.: Survey of patient exposure from general radiography and mammography in Japan in 2014. *J. Radiol. Prot.* **36**(2), N8–N18 (2016)
16. Gennaro, G., Bigolaro, S., Hill, M.L., Stramare, R., Caumo, F.: Accuracy of mammography dosimetry in the era of the European Directive 2013/59/Euratom transposition. *Eur. J. Radiology* **127**, 108986 (2020)
17. Østerås, B.H., Skaane, P., Gullien, R., Martinsen, A.C.T.: Average glandular dose in paired digital mammography and digital breast tomosynthesis acquisitions in a population based screening program: effects of measuring breast density, air kerma and beam quality. *Phys. Med. Biology* **63**, 035006 (2018)



Metrological Conformity Assessment of Pulmonary Ventilators During the Covid-19 Pandemic in Brazil

Benedito Vital Ribeiro Junior^(✉) , Henrique Alves de Amorim ,
Matheus Cardoso Moraes , and Thiago Martini Pereira 

Universidade Federal de São Paulo, Instituto de Ciência E Tecnologia, São José Dos Campos,
Brazil

benedito.vital@unifesp.br

Abstract. In the health area, service rendering regarding maintenance, calibration, verification, and assays is highly demanded to incorporate new technologies and innovations in procedures and clinical treatment. Physiological life support measures aided by equipment play a fundamental role in the daily life of intensive care units (ICU) during the COVID-19 pandemic. Mechanical ventilation, also known as ventilatory support, is essential for maintaining life; it is a method for treating patients with acute or chronic respiratory problems. Its main objective is to maintain gas exchange. However, it can worsen the patient's clinical condition without adequate calibration. This leads to death. Thus, conducting a metrological assessment of medical and hospital equipment is crucial. The goal of the present study is to perform a metrological study following Technical Standards and Technical Manuals, ABNT NBR IEC 60601–2-12 - 2004 and ABNT NBR ISO 80601–2-12 – 2014, to demonstrate the safety and performance of lung ventilators by evaluating the main ventilatory parameters.

Keywords: Metrology · Covid-19 · Pulmonary ventilators · Clinical engineering

1 Introduction

COVID-19, transmitted by the Severe Acute Respiratory Syndrome Coronavirus 2 (SARS-CoV-2) virus, began its person-to-person transmission cycle in China around December 2019. Four months after the first report of contagion, the COVID-19 has already reached a global scale [1]. On March 11, 2020, COVID-19 was classified as a pandemic by the World Health Organization [1]. COVID-19 is estimated to have infected about 511 million people, and more than 6.2 million have died [2, 3]. The disease presents different forms of manifestation, from an upper and lower respiratory tract infection to severe pulmonary involvement leading to acute respiratory failure and death. Contact with aerosol particles expelled by infected people is the main form of spread [4]. There is no evidence that early treatments can prevent the disease [5]. Pandemic control occurs by the application of vaccines [6]. Since 2020, different pharmaceutical companies have intensively acted in the technological development of vaccines to combat the coronavirus [6].

Mechanical ventilation, also known as ventilatory support, is a method for treating patients with acute or chronic respiratory failure. Its main objective is to maintain gas exchange, that is, to correct hypoxemia and respiratory acidosis associated with hypercapnia. Ventilatory support is responsible for relieving the work of the respiratory muscles (in acute situations of high metabolic demand), reversing or preventing respiratory muscle fatigue, reducing oxygen consumption and respiratory discomfort, besides allowing the application of specific therapies [9].

Positive end-expiratory pressure (PEEP), and inspiratory pressure of peak (P_{insp}) are critical parameters for the patient's treatment with mechanical ventilation. PEEP, for example, deals with the positive pressure that will remain in the airways at the end of the respiratory cycle (end of expiration) that is greater than the atmospheric pressure in mechanically ventilated patients [18]. Physiologically, PEEP is caused by the closure of the epiglottis and air damming in the respiratory system. Such pressure prevents atelectasis from occurring, and this mechanism is lost when the patient is submitted to ventilatory support [19]. In recent years, professionals in the field and scientists have placed great emphasis on the use of higher PEEP to prevent atelectrauma [11].

The pandemic has drastically affected the logistics and maintenance of healthcare support equipment. Medical centers have faced challenges, such as lack of qualified professionals, lack of ICU beds, and low numbers of ICU beds in public and private hospitals. Since COVID-19 is fundamentally a respiratory disease, the use of mechanical ventilators in patients with extensive pulmonary involvement is essential.

In addition to providing such equipment, it is vital that the ventilators comply with the calibration procedures indicated by the technical standards and manufacturers, mainly in a metrological way.

To ensure safe results and reliable measurements, besides establishing more specific technical criteria, a set of technical standards were prepared by ABNT NBR IEC 60601-2-12 of 2004 and ABNT NBR ISO 80601-2-12 of 2014, Electromedical Equipment, item 2–12: specific requirements for the basic safety and essential performance of critical care ventilators.

One of the major challenges of calibration is the standardization of the manufacturers' permissible tolerance ranges of the measurement parameters; in addition, the uncertainty of measurement in the technical data is not included in their specifications or their tolerances. Each manufacturer defines its test accuracy in its technical manuals [14]. The measured values with dubious results compromised the validation of the process regarding its precision, and, consequently, jeopardized the patient's safety.

In September 2021, twelve low-quality lung ventilators, purchased in March 2021 with exemption from bidding in Brazil, were halted after presenting failures that may have caused the deaths of hospitalized patients with Covid-19. The equipment stopped cycling, compromising the main ventilatory parameters, such as pressure and FiO₂ [22].

There are studies in the literature on the Performance of Mechanical ventilators [23–27]; however, they use different methods for assessing conformity with the International Standard ASTM F1100–90 of 1990. Specifically, they considered the measurement of the parameters; such as, tidal Volume, PEEP, and P_{insp}. However, the literature has not presented a comparison of equipment's performance between metrological conditions,

the Technical Manuals, the ABNT NBR IEC 60601-2-12 – 2004 and ABNT NBR ISO 80601-2-12 – 2014.

Faced with the high demand for ICU equipment during the pandemic and to minimize harmful events associated with mechanical ventilation equipment, the present work aims to develop a comparative metrological study on the performance of pulmonary ventilators following the manufacturers' manuals and the ABNT NBR Standards. IEC 60601-2-12 – 2004 and ABNT NBR ISO 80601-2-12 – 2014 investigate the most important parameters for safe and reliable ventilation: tidal Volume, PEEP and P_{insp}.

2 Objective

Comparing the metrological performance of mechanical ventilation equipment following the manufacturers' manuals and the ABNT NBR IEC 60601-2-12 – 2004 and ABNT NBR ISO 80601-2-12 – 2014 Standards.

3 Methodology

The study was carried out in the ICU sectors of several Hospital Units in the states of São Paulo, Rio de Janeiro, and the Federal District from November 2019 to December 2020. Thirty-six lung ventilators from three different brands were selected, between national and imported equipment. Equipment brands were omitted from the article. All the equipment evaluated has been recorded at the National Health Surveillance Agency (ANVISA).

The metrological analysis consists in determining the error (E) and measurement uncertainty (U) of lung ventilators placed for cycling and using connections, sensors, ventilation circuits, and gas network connected to a calibrated lung ventilator analyzer with traceability by the Brazilian Calibration Network (RBC). Four (4) measurements were performed per point on each ventilator for the parameters: Tidal Volume, Positive End Expiratory Pressure (PEEP), and Peak Inspiratory Pressure (P_{insp}). The calibrated points were: 700 mL for Volume, 15 cm H₂O for PEEP, and 30 cm H₂O for P_{insp}. This number of measuring (4) was considering equipment accessing limitations, yet respecting ISO GUM 2008 and Nit-Dicla-21 – INMETRO ($n > 1$).

The equipment was calibrated against the reference standards according to internal procedures in a controlled environment at a temperature of 22 °C and relative humidity of around 50% RH.

Specific forms were used and transcribed into a spreadsheet with a calculation memorial validated for each measurement parameter for data collection. The methodology used to estimate the measurement uncertainty is the same as described by ISO GUM 2008 [16] and NIT DICLA 021 [17].

The uncertainty of the measurement result is composed of the calculations of several components grouped in two categories: Type A: those that were determined using statistical analysis in a series of observations: repeatability of the standard readings, arithmetic mean, standard deviation, and deviation average standard. Type B: those determined by any other means: the resolution of the reference standard equipment, measurement uncertainty of the reference standard, and resolution of the equipment under test [16].

The Probability Distribution of the uncertainty components is calculated by a random variable probabilistic function, assuming a value within a range of values. The following distributions were used for the calculation memorial: Rectangular, Triangular, Normal, and t-Student [17].

The practical degrees of freedom estimate the standard uncertainty $u(y)$, associated with the output estimate y from the Welch-Satterthwaite equation [16].

The uncertainties reported in the results were combined and expanded by coverage factors k , duly corresponding to the degrees of freedom and a coverage probability of approximately 95% [17]. All the uncertainty calculations were performed following ISO GUM and EA4/02 standards and INMETRO's normative and guidance documents.

The ventilators were separated into three major brands and evaluated by parameters separately. ISO GUM - ISO 14253-2:2011 establishes that, in the absence of another specification (imposed by normative document, regulation, etc.), the following calibration acceptance criterion is used: "The sum of the module of the result of the measurement with the associated uncertainty module shall be less than or equal to the Maximum Permissible Error (MPE) for the equipment". Thus, the MPE acceptance criterion is given by expression [21]:

$$| \text{Error} | + | \text{Uncertainty} | \leq | \text{MPE} |,$$

in which:

Error: Difference between the measured value of a quantity and a reference value.

Uncertainty: It is the expanded uncertainty associated with the corrected result.

MPE: Maximum permissible error.

4 Analysis of Data and Results

In the parameters tidal Volume, measured point: 700 mL of the scale, PEEP (Positive End Expiratory Pressure), measured point: 15 cm H₂O, and P_Ins (Peak Inspiratory Pressure), measured point: 30 cm H₂O, we obtained the following results in comparison with the Standards (Fig. 1):

Volume/PEEP/P_Ins: **conform**

In the Current Volume parameter, 97% obtained results within the standards established by the NBR ISO 80601-2-12 and NBR IEC 60601-2-12 Standards, and only 3% did not meet the criteria or tolerance of the standards.

For the PEEP parameter, 45% were within the standards established by the NBR ISO 80601-2-12 and NBR IEC 60601-2-12 Standards, and 55% were not.

In the analysis of the P_Ins parameter, we found that 56% of the pieces of equipment are within the standards established by the NBR ISO 80601-2-12 and NBR IEC 60601-2-12 Standards, and 44% are not.

In the analysis of the same parameters, we obtained the following results in comparison with the manufacturers' manuals (Fig. 2):

Volume/PEEP/P_Ins: **conform**

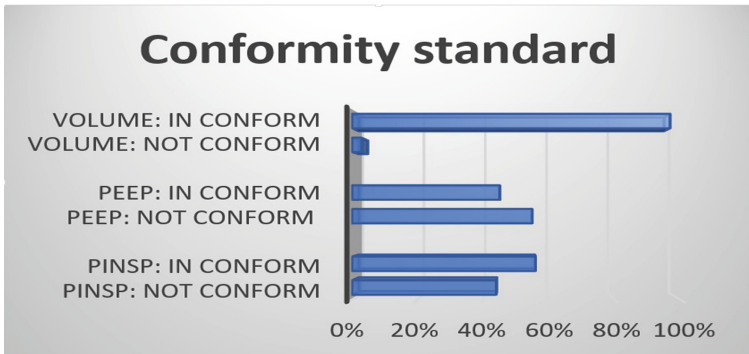


Fig. 1. Conformity standard (*source personal archive*).

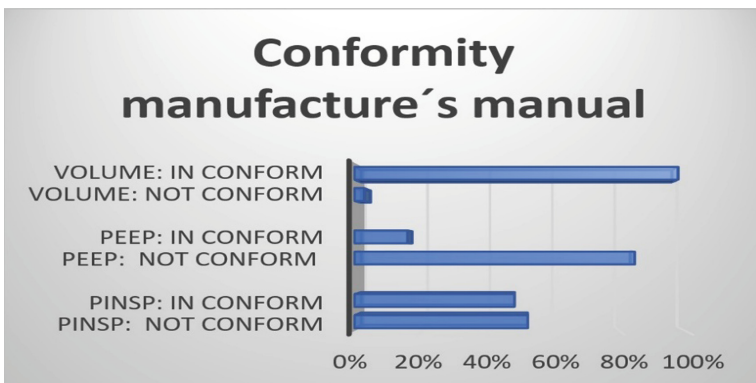


Fig. 2. Conformity manufacture's manual (*source personal archive*).

In the Current Volume parameter, we found the same results of compliance with the standards; that is, 97% obtained results within the standards established by the manufacturers' manuals, and only 3% did not meet the criteria or tolerance of the manuals.

From the analysis of these same parameters, we obtained the following results compared to the manufacturers' manuals.

In evaluating the PEEP parameter, only 16% were within the standards established by the manufacturers' manuals, and 84% were outside the metrological standards established by these manuals.

As for the PInsp parameter, from a sample of thirty-six pieces of equipment evaluated, 48% were within the tolerance standards of the manuals, and 52% did not reach the results established by these documents.

5 Discussion and Conclusion

Our study demonstrated the safety and performance of lung ventilators by metrological reliability. The metrological characteristics, measurement error, and uncertainty found in the equipment evaluated were determined for analysis purposes. These characteristics

point to significant concern and care that we have to have with life support equipment, especially with pulmonary ventilators (PV).

Among the three parameters investigated, the one involving pressure, Positive End Expiratory Pressure (PEEP) and Peak Inspiratory Pressure (P_{Insp}), did not presented satisfactory results. This is due to the restricted tolerance range established by the NBR ISO 80601-2-12, NBR IEC 60601-2-12 Standards, and the manufacturers' technical manuals.

Observing the tests of the Tidal Volume parameter in general, we observed satisfactory results, approximately 97% of the MV within acceptable safety limits.

One of the significant problems that we found in the study is related to the standardization of the permissible tolerance ranges of the measurement parameters; in addition to not including in their specifications their high accuracy of measurement uncertainty in the technical data, each manufacturer defines its precision of test in their technical manuals [14]. Regarding the Standards, they only thoroughly provide for pressure and volume specifications, treating the other parameters superficially, thus leaving parameters such as Respiratory Rate, Inspiratory Fraction of O₂ (FiO₂), and Inspiratory Flow outside our study.

Another critical point to note would be improving the current technology for parameter records, which we call analyzers or reference standards. These measuring instruments deserve to have high precision in their measurements, representing a higher resolution than the test equipment.

It would be of great importance to improve methods and results, also that manuals and standards add measurement uncertainty to their evaluation methods; results would therefore be more satisfactory.

Other factors that we observed and that led to unsatisfactory results were the equipment evaluation with a large number of accumulated working hours. Devices have been used on a large scale in the ICU sectors due to the high demand during the pandemic. Most of the time, equipment is overloaded and made available to the patient without replacing its respective preventive maintenance kits, as recommended by the manufacturers, somehow compromising the results and, consequently, the proper performance of the equipment. According to authors such as Blanch (2001), after a VP accumulates 40,000 h of work, its reliability and performance decrease drastically [20].

In mid-September 2021, in Americana, in the interior of the state of São Paulo, twelve low-quality pulmonary ventilators, purchased with exemption from a March 2021 bidding process, were cast aside after presenting failures that may have caused the deaths of hospitalized patients with Covid-19. The equipment stopped cycling, compromising the main ventilatory parameters, such as pressure and FiO₂ [22].

There has notably been greater involvement and consensus among manufacturers of medical-hospital equipment, analyzers and simulators, the Technical Standards Committee from Anvisa, and also from the most significant metrological authority in the country, Inmetro. There is greater concern about minimizing problems and risks leading to legal suits regarding patients' safety and health.







References

1. World Health Organization. Novel Coronavirus (2019-nCoV) (accessed June 13, 2021) <https://www.who.int/emergencies/diseases/novel-coronavirus-2019/situation-reports>
2. WHO Director-General's opening remarks at the media briefing on COVID-19—11 March 2020. 2020[cited 6 Apr 2020]. Available: <https://www.who.int/dg/speeches/detail/who-director-general-s-openingremarks-at-the-media-briefing-on-covid-19-11-march-2020>
3. World Health Organization. Coronavirus disease 2019 (COVID-19) Situation Report (accessed June 13, 21) Available: <https://www.who.int/emergencies/diseases/novel-coronavirus-2019>
4. Iyengar, K., Bahl, S., Vaishya, R., Vaish, A.: Challenges and solutions in meeting up the urgent requirement of ventilators for COVID-10 patients; Epub 2020 May 5
5. Liu, Q., Xu, K., Wang, X., Wang, W.: From SARS to COVID-19: What lessons have we learned? *J. Infect. Public Health* **13**, 1611–1618 (2020). <http://www.elsevier.com/jiph>
6. Abbasi, J.: COVID-19 and mRNA vaccines—first large test for a new approach. *JAMA* **324**(12), 1125–1127 (2020). <https://doi.org/10.1001/jama.2020.16866>
7. Nardini, S., Sanguinetti, C.M., De Benedetto, F., et al.: SARS-CoV-2 pandemic in Italy: ethical and organizational considerations. *Multidiscip Respir Med.* **15**(1), 672 (2020). Published 2020 May 25. <https://doi.org/10.4081/mrm.2020.672>
8. Allocating ventilators in a pandemic (accessed March 24, 2020), <https://healthmangement.org/c/icu/news/allocating-ventilators-in-a-pandemic;2020>
9. Early severe acute respiratory distress syndrome: What's going on? Part II: controlled vs. Spontaneous ventilation? *Anaesthesiol. Intensiv. Ther.* **48**(5), 339–351 (2016). ISSN 1642-5758. <https://doi.org/10.5603/AIT.2016.0057>, www.ait.viamedica.pl
10. Hess, D.R.: *J. Aerosol Med.* **20**(1), S85–S99 (2007). <https://doi.org/10.1089/jam.2007.0574>
11. Respiratory Support in COVID-19 Patients, with a Focus on Resource-Limited Settings. *Am J. Trop. Med Hyg.*, **102**(6), 1191–1197 (2020)
12. ABNT Standard 15943:2011, Guidelines for a program for the management of healthcare infrastructure and healthcare equipment, 2011-05-28
13. Resolution RDC No. 509, May 27, 2021. Provides for the management of health technologies in health facilities
14. Standard ABNT NBR ISO 80601-2-12:2014; Medical electrical equipment Part 1–12: Particular requirements for basic safety and essential performance of critical care ventilators
15. Evaluation of PEEP and prone positioning in early COVID-19 ARDS, *EclinicalMedicine* **28** (2020) 100579; www.journals.elsevier.com/eclinicalmedicine
16. Gum, I.S.O.: – Assessment of measurement data – guide to the expression of measurement uncertainty. *JCGM* **100**, 2008 (2008)
17. NIT-DICLA-021, Expression of Measurement Uncertainty, Rev. No. 10, Jul/20
18. Andres, M.C.L., Jorge, M.I.: Ventilator management. NCBI bookshelf. A service of the National Library of Medicine, National Institutes of Health. University of Pennsylvania (2020)
19. Recommendations from the Brazilian Intensive Medicine Association for the approach of COVID-19 in intensive medicine: AMIB – April Update (2020)
20. Blanch, P.: An evaluation of ventilator reliability: a multivariate, failure time analysis of 5 common ventilators brands. *Respir. Care* **46**(8), 789–797 (2001)
21. Mendes, A.: Pedro Paulo Novellino do ROSARIO. Metrology and Measurement Uncertainty – Concepts and Applications. LTC - Publication (2019)
22. CNN Brasil (2021) <https://www.cnnbrasil.com.br/nacional/mortes-apos-uso-de-respiradores-sao-investigadas-no-interior-de-sao-paulo/>
23. López Uribe, Ichinose M. Roberto, Neto A. Giannella. Performance of Mechanical Ventilators in Intensive Care Units: Metrological Considerations. Master's Thesis - COPPE UFRJ, Oct/2011

24. Coelho, R.B., Giannella Neto, A.: Sistema de Avaliação de Ventiladores Pulmonares, vol. 11, p. 17–40. Revista Brasileira de Engenharia – Caderno de Engenharia Biomédica, Rio de Janeiro (1995)
25. Daniel Marinho, S.: Sistema para Ensaio de Desempenho de Ventiladores Pulmonares. UFSC, Florianópolis (2007)
26. Romero, J.C.: Confiabilidade Metrológica de Ventiladores Pulmonares. Pontifícia Universidade Católica do Rio de Janeiro, Dissertação de Mestrado em Metrologia para Qualidade e Inovação (2006)
27. Uechi, C.A.S.: Confiabilidade Metrológica de Ventiladores Pulmonares para Cuidados Críticos. UnB – Universidade de Brasília – FGA – Faculdade Gama, Brasília-DF (2012)



Influence of Phototype, Sweating and Moisturizing Lotions on Human Skin Emissivity: A Possible Cause of Screening Errors of Feverish People in Sanitary Barriers

Andrielle Ninke¹ , João Thomaz Lemos² , Pablo Rodrigues Muniz² ,
Reginaldo Barbosa Nunes² , Hércules Lázaro Morais Campos³ ,
and Josemar Simão⁴ 

¹ Federal Institute of Espírito Santo (IFES)/Campus Vitória, Undergraduate Electrical Engineering Course, Vitória, Brazil
andrieleninke@gmail.com

² Federal Institute of Espírito Santo (IFES)/Campus Vitória, Graduate Program in Sustainable Technologies, Vitória, Brazil

³ University of Amazonas (UFAM)/Institute of Health and Biotechnology Federal, Coari, Brazil

⁴ Federal Institute of Espírito Santo (IFES)/Campus Vitória, Electrotechnical Course, Vitória, Brazil

Abstract. Due to the Coronavirus Disease 2019 (Covid-19) pandemic scenario, the implementation of sanitary barriers to screening feverish individuals in places of large circulation of people was adopted, aiming to contain the disease spread. Since contamination by the virus occurs through contact and one of the most common symptoms is fever, measuring the temperature of passers-by through non-contact infrared thermography has been a technique used in sanitary barriers. One of the main factors that significantly change the temperature value indicated by thermal imagers is the emissivity of the inspected surface. Skin emissivity, a dimensionless quantity, is found in the literature with a recurrent value of 0.98. The objective of this study is to investigate whether this value is also valid for skin with sweating or using moisturizing lotions, as well as, for different phototypes. Thus, tests and evaluation of emissivity with volunteers in laboratory can answer these questions. The partial results include 37 volunteers of five skin tones of the Fitzpatrick scale, which has six phototypes. Volunteer's thermographic images were obtained in different situations: dry skin, using moisturizing lotion, and sweaty skin. From the analysis of these images by software and using the tape method, it was possible to estimate the skin emissivity value for each situation. With the emissivity data in hand, a statistical analysis was carried out to assess whether the influence of the conditions studied is significant for the emissivity value and consequently for the temperature measured by the instruments based on the principle of infrared thermography.

Keywords: Error analysis · Thermography · Emissivity

1 Introduction

The advent of the Coronavirus Disease 2019 (Covid-19) pandemic, a severe acute respiratory syndrome, brought a great demand for mechanisms to contain the advancement of the disease since it has a high transmission rate. One of the most common symptoms among Covid-19 patients is fever, a biological response to infections [1, 2]. Fever is also a common symptom in other pandemics recorded in our recent history, such as H1N1, Ebola and, more recently, it is a symptom presented in cases of Monkeypox [1, 3]. Therefore, for a first screening, identifying and segregating febrile individuals in places of great movement of people as well as in geographic borders is a way to prevent the spread of the disease [2, 4]. In a sanitary barrier, the temperature measurement needs to be fast and safe, and non-contact, in order to interfere minimally with the flow of passers-by and reduce the transmission risk. In this scenario, mercury thermometers become unfeasible, since it does not present a quick result, requires contact between operator and patient, and sterilization before each use.

Instruments based on infrared thermography have been used to determine temperature without contact with rapid diagnosis [1, 4–6]. These instruments capture the emission of infrared radiation from all bodies with a temperature above absolute zero (0 K or $-273.15\text{ }^{\circ}\text{C}$), based on Plank's Law [7, 8]. So, it is possible to estimate the temperature of the analyzed body, knowing other parameters, among them, the emissivity.

Emissivity represents the efficiency of absorption and emission of radiation of a body, for a given temperature, in relation to a blackbody at the same temperature, which is a perfect emitter and whose emissivity is equal to one. In nature, there are no bodies with this ideal characteristic, that is, a portion of the radiation is reflected or transmitted, giving real bodies an emissivity lower than one [9].

For human skin, there is no consensus regarding the value of its emissivity, ranging from 0.97 to 0.99. The value of 0.98 is usually adopted [9]. This work goals to analyze whether the presence of sweating, the use of moisturizing lotions, and the skin phototype modify this parameter since in sanitary barriers such situation has a great probability to happen, since several characteristics of the inspected surface can affect the emissivity [10], which is the factor with the greatest impact on the measurement error by infrared thermography [11].

For this, at this stage of the research thermographic images of 37 volunteers, of five different skin tones, in dry skin conditions, with moisturizing lotion, and sweating were analyzed. The obtained results were treated metrologically aiming to estimate the emissivity of the human body.

2 Methodology

A technique widely used to assess the emissivity of objects and bodies is the tape method. The method consists of using a reference of known emissivity, in this case 3M Scotch 33 electrical tape with an emissivity equal to 0.96 [12], and applying it to the surface where the emissivity should be determined, then proceeding with an evaluation of thermographic images of the region. This method was chosen to estimate the emissivity of the skin of the volunteers in this research. The thermographic images

were obtained from a FLIR E60 thermal imager and analyze it with help of the image processing software of the thermal imager. For this test, the region chosen was the forehead, commonly adopted as Region of Interest (ROI) in sanitary barrier based on human thermography [13–15]. This region is commonly used in trade barriers because it generally allows direct view from the thermal imager, as it is uncovered, and does not require intervention in the normal flow of passers-by [16, 17]. So that a portion of the electrical tape was applied to the right region of the forehead of the volunteers, leaving the left side free for comparison purposes. Through the thermographic image, the emissivity of the electrical tape is informed in the software and then the emissivity to be determined is manually adjusted until the temperature of the left region of the forehead (without the electrical tape) presents the initial temperature of the electrical tape [9].

Considering that the face temperature is not necessarily symmetric [14, 15], from the thermographic image of the volunteers without the electrical tape, obtained at the end of the test, the right and left sides of the forehead were compared and the temperature difference between them was considered for using the tape method. Thus, the adjustment of the emissivity on the forehead's left side took into account the initial temperature of the electrical tape plus or minus the temperature difference.

Figure 1 presents the thermographic image of a volunteer after analysis based on the tape method, it is possible to see the reference electrical tape on the right side of the volunteer's forehead.

So far, 37 healthy volunteers participated in the experiment. All of them read and signed the consent form agreeing with the conditions of participation in the research. The Research Ethics Committee of the Federal Institute of Espírito Santo, linked to the National Research Ethics Commission of the Ministry of Health of Brazil, approved this research under the Certificate of Presentation and Ethical Appreciation (CAAE) 52572521.2.0000.5072, opinion number 5.103.274, on November 12, 2021.

The experiments were carried out in the Laboratory of Energy, at Federal Institute of Espírito Santo. Ambient temperature and relative humidity were measured. These data were input in the thermovisor's software, Flirt Tools[®], to properly calculate the volunteer's temperature. The experiment was divided into three stages. The first was with dry skin, without sweat or moisturizing lotion. In the second the volunteers were invited to apply a moisturizing lotion on the forehead, taking care not to apply it on the reference tape. Finally, after removing the moisturizing lotion, the volunteers performed an eight-minute trot with the objective of presenting sweating on the face. Before capturing the thermal images of the first stage, the volunteers rested for about 15 min in the laboratory after applying the electrical tape to their face, so that the skin and tape could acclimate. The images were obtained sequentially respecting the preparation time of each part of the procedure.

All images were analyzed by the FLIR Tools[®] software and the emissivity values determined for each step were recorded. The results obtained, in addition to being divided into the three stages of the experiment, were also organized according to the skin phototype of each volunteer. For that, three of the researchers proceeded to classify the skin color of the volunteers from their real images, also obtained by the thermal imager,

based on the Fitzpatrick color scale [18], presented in Fig. 2. The color chosen by the majority defined the skin phototype assigned to the volunteer.

So far, there have been no volunteers whose skin tone was VI (dark brown) in the Fitzpatrick scale, as it is a rare skin tone in the locality where the experiment is being performed. Furthermore, volunteers whose skin phototype are I (very fair) and V (brown) made up a statistically small sample. Thus, analyzes were performed for colors I (very fair), II (fair), III (medium), IV (olive), and V (brown) of the Fitzpatrick scale.

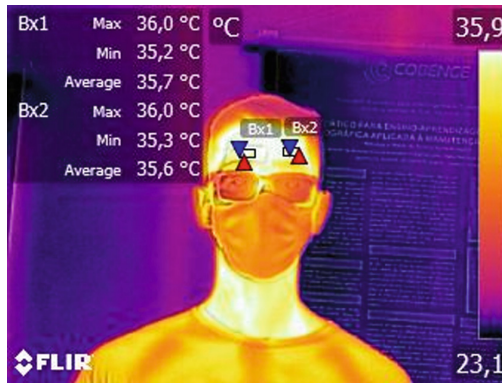


Fig. 1. Thermographic image of a volunteer’s face with the electrical tape on the right side of the forehead.



Fig. 2. Fitzpatrick Skin Color Scale [9]

3 Results

Table 1 presents the number of samples (n) and the degree of freedom (v) for each situation and skin phototype. Although the number of volunteers of certain skin color is fixed, in some stages of the experiment some results, considered outliers, were excluded [19].

The average emissivity value and its respective standard deviation, depending on the skin phototype and the stage of the experiment, are organized in Table 2.

Although the recommended confidence level for metrological analyzes is approximately 95% [20], this work adopts the level of 90%, since the partial results did not yet reach a sample quantity considered reasonable by the literature [21]. To obtain a

confidence level of 90.0% in the measurement uncertainty, the expanded uncertainty of each result was determined [22], through Eq. (1):

$$U = t.u \quad (1)$$

U : Expanded measurement uncertainty

t : Student's t coefficient for 90.0% confidence level and ν degrees of freedom

u : Standard uncertainty

Table 1. Number of samples and degree of freedom for each situation and skin phototype

Skin condition	Skin phototype				
	I	II	III	IV	V
Dry skin	$n = 4;$ $\nu = 3$	$n = 12;$ $\nu = 11$	$n = 9;$ $\nu = 8$	$n = 4;$ $\nu = 3$	$n = 5;$ $\nu = 4$
Skin with moisturizing lotion	$n = 3;$ $\nu = 2$	$n = 9;$ $\nu = 8$	$n = 10;$ $\nu = 9$	$n = 4;$ $\nu = 3$	$n = 4;$ $\nu = 3$
Sweaty skin	$n = 4;$ $\nu = 3$	$n = 11;$ $\nu = 10$	$n = 11;$ $\nu = 10$	$n = 3;$ $\nu = 2$	$n = 4;$ $\nu = 3$

Table 2. Skin emissivity and its standard uncertainty

Skin condition	Skin phototype				
	I	II	III	IV	V
Dry skin	0.98 ± 0.03	0.98 ± 0.02	0.96 ± 0.03	0.98 ± 0.03	0.97 ± 0.02
Skin with moisturizing lotion	0.83 ± 0.04	0.88 ± 0.03	0.84 ± 0.03	0.86 ± 0.03	0.90 ± 0.04
Sweaty skin	0.81 ± 0.04	0.78 ± 0.05	0.80 ± 0.04	0.76 ± 0.04	0.76 ± 0.07

Table 3 presents the emissivity value for each skin condition and phototype, and its expanded uncertainty.

In the first instance, the influence of skin phototype on emissivity was analyzed. The normalized error is a metrological tool that allows inferring how close two results are. The closer the error is to zero, the greater the metrological compatibility between them. Normalized errors greater than unity imply that the two results are not metrologically compatible with each other, within the same confidence level adopted for the uncertainty calculation [23]. The normalized error is determined through Eq. (2).

$$E_n = \frac{|x_i - x_j|}{\sqrt{U_i^2 + U_j^2}} \quad (2)$$

E_n : Normalized error

x_i, x_j : Two results to be compared

U_i, U_j : Standard uncertainty of the respective results

Table 3. Skin emissivity and its expanded uncertainty

Skin condition	Skin phototype				
	I	II	III	IV	V
Dry skin	0.98 ± 0.07	0.98 ± 0.04	0.96 ± 0.06	0.98 ± 0.06	0.97 ± 0.04
Skin with moisturizing lotion	0.83 ± 0.10	0.88 ± 0.05	0.84 ± 0.06	0.86 ± 0.06	0.90 ± 0.09
Sweaty skin	0.81 ± 0.10	0.78 ± 0.09	0.80 ± 0.08	0.76 ± 0.13	0.76 ± 0.17

A comparison was made between the emissivity obtained for each stage of the experiment between the skin phototypes. Table 4 presents the normalized error for emissivity comparing skin phototypes for dry skin condition, with moisturizing lotion and with sweating.

The comparison through normalized error between the emissivity results obtained for the same skin condition (dry, with sweating, or with moisturizing lotion), and different phototypes, indicates that the skin phototype has no significant influence on the emissivity value, because the normalized error is less than one for all possible comparisons between the analyzed skin tones.

Table 4. Normalized error for emissivity comparing skin phototypes

Skin tones compared	Dry skin	Skin with moisturizing lotion	Sweating skin
I e II	0.01	0.35	0.21
I e III	0.20	0.04	0.10
I e IV	0.00	0.22	0.28
I e V	0.06	0.43	0.27
II e III	0.27	0.47	0.13
II e IV	0.01	0.18	0.11
II e V	0.10	0.17	0.13
III e IV	0.22	0.27	0.21
III e V	0.19	0.53	0.21
IV e V	0.08	0.35	0.03

Based on this conclusion, the emissivity results obtained for skin phototypes I, II, III, VI and V were grouped and classified only by the respective skin condition.

The same analyses, mean emissivity and its standard and expanded uncertainty, were performed considering only the classification according to the skin condition. Tables 5 and 6 present the number of samples and degrees of freedom and emissivity values for each skin condition, respectively.

To assess whether the skin condition influences its emissivity value, the normalized error was calculated, comparing the conditions with each other. Table 7 presents the normalized error for each condition.

Table 5. Number of samples and degree of freedom for each skin condition

Skin condition	<i>n</i>	<i>v</i>
Dry skin	34	33
Skin with moisturizing lotion	31	30
Sweaty skin	33	32

Evaluating the results presented in Table 7, it is noted that, with more than 90% confidence, dry skin presents emissivity metrologically incompatible with skin with moisturizing lotion. The same can be said for the comparison between dry skin and sweaty skin, as well as for skin with moisturizing lotion and sweaty skin.

Checking the emissivity values presented in Table 6; 0.97 for dry skin, 0.86 for skin with moisturizing lotion, and 0.79 for skin with sweating; it appears that such situations lead to erroneous measurements of skin temperature, and consequently, errors in the screening of febrile people. In a simulation performed in the Flir Tools[®] software processing the images of the volunteers and adopting the recommended emissivity of 0.98, for dry skin the volunteers would have an apparent forehead temperature of 35.2 °C, 33.5 °C for skin with moisturizing lotion, and 33.7 °C for skin with sweating. This shows that passers-by who applied moisturizing lotion or with sweaty skin on sanitary barriers would have systematic temperature measurement errors. Such errors would lead to measurement results lower than the conventional true values, very possibly implying non-detection of feverish people.

Table 6. Skin emissivity and its standard and expanded uncertainty

	Dry skin	Skin with moisturizing lotion	Sweaty skin
Base value and standard uncertainty	0.97 ± 0.03	0.86 ± 0.04	0.79 ± 0.05
Base value and expanded uncertainty	0.97 ± 0.04	0.86 ± 0.07	0.79 ± 0.08

Table 7. Normalized error for emissivity of dry skin, with moisturizing lotion and with sweating

Skin condition compared	Normalized Error
Dry skin and with moisturizing lotion	2.23
Dry and sweaty skin	3.22
Skin with moisturizing lotion and sweating	1.14

4 Compliance with Ethical Requirements

The Research Ethics Committee of the Federal Institute of Espírito Santo, linked to the National Research Ethics Commission of the Ministry of Health of Brazil, approved this research under the Certificate of Presentation and Ethical Appreciation (CAAE) 52572521.2.0000.5072, opinion number 5.103.274, on November 12, 2021.

5 Conclusions

It was possible to conclude through the analysis of the normalized error that the skin phototype does not influence its emissivity value. This is a positive factor for sanitary barriers since it would not be necessary to implement any procedure to consider this factor in the temperature measurement.

Grouping all the results, previously classified by phototype, and analyzing only the influence of the skin condition, the mean skin emissivity values for the dry skin condition, with moisturizing lotion and with sweating were, respectively: 0.97, 0.86, and 0.79. The metrological analysis leads to the conclusion that the skin conditions should be considered in the temperature measurement by infrared thermography since they significantly modify the skin emissivity value. For application in a sanitary barrier, this variation in the emissivity value for the conditions studied should be taken into account, otherwise feverish people with sweaty skin or with moisturizing lotion will hardly be screened. However, this verification would make it impossible to screen feverish people quickly, with little interference and without contact. This research is continuing to, in addition to obtaining more data with more volunteers for greater metrological robustness, develop a system based on Artificial Intelligence to recognize the situation of the skin of passersby, applying the necessary corrections for temperature measurement, enabling the sanitary barrier of low interference in the flow of people with greater reliability.

Acknowledgment. The authors thank the volunteers and the Energy Laboratory of Ifes Campus Vitória for collaborating in the field research with volunteers. This work was also supported by the Federal Institute of Espírito Santo and the National Council for Scientific and Technological Development (CNPq).

This work was supported by FAPES (Espírito Santo Research and Innovation Support Foundation), grant numbers 03/2020 (Induced Demand Assessment–COVID-19 Project), and 04/2021 (Research Support); IFES (Federal Institute of Espírito Santo), grant numbers 10/2021 (Institutional Support Program for Stricto Sensu Graduate Studies – PROPÓS), 02/2022 (Institutional Scientific Initiation Scholarship Program – Pibic), 07/2022 and 08/2022 (Institutional Program

for Scientific Diffusion – PRODIF); and CNPq (National Council for Scientific and Technological Development), grant number 02/2020 (Productivity Scholarship in Technological Development and Innovative Extension - DT).

Conflict of Interest The authors declare that they have no conflict of interest.

References

1. Silvino, V.O., Gomes, R.B.B., Ribeiro, S.L.G., Moreira, D.D.L., Dos Santos, M.A.P.: Identifying febrile humans using infrared thermography screening: possible applications during covid-19 outbreak. *Rev. Context. Saúde* **20**(38), 5–9 (2020)
2. Zhou, Y., et al.: Clinical evaluation of fever-screening thermography: impact of consensus guidelines and facial measurement location. *J. Biomed. Opt.* **25**(09), 1–21 (2020)
3. Wilson, M.E., Hughes, J.M., McCollum, A.M., Damon, I.K.: Human monkeypox. *Clin. Infect. Dis.* **58**(2), 260–267 (2014)
4. Chen, G., et al.: Validity of the use of wrist and forehead temperatures in screening the general population for covid-19: a prospective real-world study. *Iran. J. Public Health* **49**, 57–66 (2020)
5. Ghassemi, P., Pfefer, T.J., Casamento, J.P., Simpson, R., Wang, Q.: Best practices for standardized performance testing of infrared thermographs intended for fever screening. *PLoS One* **13**(9), e0203302 (2018)
6. Priego Quesada, J.I., Kunzler, M.R., Carpes, F.P.: Methodological aspects of infrared thermography in human assessment. In: Priego Quesada, J.I. (ed.) *Application of Infrared Thermography in Sports Science*, pp. 49–79. Springer International Publishing, Cham
7. Brioschi, M.L., Lucas, R.W.C.: *Termografia Aplicada à Fisioterapia*. 1a. Florianópolis (2016)
8. Muniz, P.R., Mendes, M.A.: *Termografia infravermelha aplicada à manutenção elétrica: dos fundamentos ao diagnóstico*. Edifes, Vitória, ES (2019)
9. Charlton, M., et al.: The effect of constitutive pigmentation on the measured emissivity of human skin. *PLoS One* **15**(11), 1–9 (2020)
10. Vollmer, M., Möllmann, K.P.: *Infrared Thermal Imaging: Fundamentals, Research and Applications*. Wiley, Weinheim (2010)
11. Muniz, P.R., De Araújo Kalid, R., Cani, S.P.N., Da Silva Magalhães, R.: Handy method to estimate uncertainty of temperature measurement by infrared thermography. *Opt. Eng.* **53**(7), 074101 (2014)
12. FLIR: *User's Manual FLIR EXX Series*, p. 100 (2005)
13. Derruau, S., Bogard, F., Exartier-Menard, G., Mauprivez, C., Polidori, G.: Medical infrared thermography in odontogenic facial cellulitis as a clinical decision support tool. A technical note. *Diagnostics* **11**(11), 2045 (2021)
14. Haddad, D.S., Brioschi, M.L., Baladi, M.G., Arita, E.S.: A new evaluation of heat distribution on facial skin surface by infrared thermography. *Dentomaxillofacial Radiol.* **45**(4), 20150264 (2016)
15. Da Silva, J.R., et al.: Recognition of human face regions under adverse conditions—face masks and glasses—in thermographic sanitary barriers through learning transfer from an object detector. *Machines* **10**(1), 43 (2022)
16. Flir Systems: *Skin temperature screening software flir screen-est* (2020)
17. Teledyne FLIR LLC: *Thermal Imaging for Detecting Elevated Body Temperature* (2020)
18. Goldsmith, L.A., Katz, S.I., Gilchrest, B.A.: *Fitzpatrick's Dermatology in General Medicine*, 8th edn. The McGraw-Hill Companies, New York, NY (2012)

19. Chemie, S.K.: Die neue Norm ISO/IEC 17043 Conformity Assessment—General Requirements for Proficiency Testing, vol. 2010 (2010)
20. BIPM, et al.: Guia Para a Expressão da Incerteza de Medição Associação. ABNT, INMETRO, Rio de Janeiro (2003)
21. Martins, M.A.F.M.: Contribuições para a avaliação da incerteza de medição no regime estacionário. Universidade Federal da Bahia (2010)
22. Junior, A.A.G., De Sousa, A.R.: Fundamentos de metrologia científica e industrial, vol. 1 (2008)
23. ISO/IEC 17025:2005 General requirements for the competence of testing and calibration laboratories



Assessing the Quality of Behavioral Data Obtained by Human Observers Using Cohen's Kappa and Accessory Metrics: Development of the Algorithms and an Open-Source Library

João Antônio Marcolan^(✉) , Jefferson Luiz Brum Marques ,
and José Marino-Neto 

Institute of Biomedical Engineering -IEB -UFSC, Department of Electrical
Engineering (EEL), Federal University of Santa Catarina, 88040-900 Florianópolis,
SC, Brazil

jamarcolan@gmail.com

Abstract. Behavioral recordings made by human observers (HOs) are central to animal pre-clinical behavioral models (ABM) of neurobiological diseases, where behaviors (e.g., swimming or immobility) are transcribed from video recordings of experiments by HOs. These models face criticism due to their vulnerability to reproducibility issues; evaluation of HO's reliability during training can help to control this source of error. Here, we propose and test algorithms for estimation of Cohen's Kappa (K) index and accessory measures (maximum K, prevalence, bias) associated with bootstrapping (BS) of behavioral ratings produced during a real experiment using the rat's Forced Swimming Test (FST), to evaluate intra-Hos reliability for the recorded categories. Present results indicate that the use of replicas after BS faithfully mirrors most of the concordance attributes of the original transcripts while allowing a statistical evaluation of intra-HO's reliability, and their differences concerning the maximum agreement (Kmax), and the probabilities of under- or over-estimation of K (bias and prevalence). The use of these tools can inform and optimize the performance of HOs in the use of ABM, without requiring time-intensive re-testing, favoring the reproducibility of the data obtained by these procedures.

Keywords: Intra-observer reliability tests · Behavioral models ·
Bootstrap · Confidence intervals · Cohen's K

1 Introduction

Behavioral recordings by human raters are central to preclinical animal behavioral models of neuro-biological diseases, such as anxiety and depression, as well as to the study of drugs potentially useful to treat these conditions ([19]). In these models, behavioral categories (like swimming or eating) are recorded (transcribed from video recordings) by human observers (HOs). These models

are facing considerable criticism regarding their vulnerability to reproducibility issues (e.g., [17]), arising from multiple methodological causes (e.g., [16]). These causes may include failure to assess and control for intra- or inter-observer reliability (e.g., using analyses such as Cohen’s Kappa(K) analyses and its associated indexes; [2, 6]). As suggested by a recent systematic review on the use and report of reliability assessment on the Forced Swimming Test literature (FST, a relevant model in behavioral pharmacology for the study of antidepressant drugs), these tests are rarely employed [10]. Despite their relevance for quality of data collection and long-standing literature, there is a lack of accessible, open-source tools to estimate intra- and inter-rater reliability, available to neurobehavioral researchers.

Here, we propose and test algorithms for the calculation of K and associated measures (Maximum K achievable, or Kmax, Prevalence (or P), and Bias (or B; [15]) of behavioral ratings produced during a real experiment using the rat’s FST Test, aimed to estimate and evaluate inter-and intra-HO reliability for all and each of the recorded behavioral categories. Estimation and assessment of these indexes are laborious, time-consuming, and demand repeated ratings of multiple samples by multiple researchers. To improve the suitability of these tests without sacrificing their meaning and precision, we also propose and test an approach to infer the population’s K, Kmax and Cohen’s “d” using bootstrapping of pairs of real observations. This method is preferred to estimate confidence intervals (CI) of reliability indexes like K because its results tolerate non-Gaussian distributions of data [8, 20]. The algorithms presented here were coded in a freely available open-source stand-alone application and library, (<https://github.com/EthoWatcher/Reliability>).

2 Materials and Methods

The tests and algorithms described below were coded using C++ 11, the resulting images were developed in Python 3.6.13, run in Windows 10, and are available on a Github repository (<https://github.com/EthoWatcher/Reliability>). These tests were carried out using transcriptions of a video taken from a real rat FST experiment (one adult male rat, recorded for 4 min), performed by a single HO in 2 sessions 15 days apart (as part of a study approved by the Ethics Committee of the Federal University of Santa Catarina; CEUA-UFSC, PP00764). HO was trained to use the transcription tool ([11, 12], <https://github.com/EthoWatcher/ethowatcher>) and a catalog of 6 categories usual for FST studies [4, 9]. Each transcription resulted in a sequence of 7200 annotations (one for every frame in the video, Fig 1). For the bootstrapping (BS) tests, these 2 samples were paired and resampled 1667 times by a BS algorithm developed and coded after [13, 18]. Original or resampled (post-BS procedures) pairs of transcriptions were used to build intra-HO catalog agreement matrices (CAM; Table 1A) and catalog maximum agreement matrices (CAMmax; Table 1B), that were developed according to an adaptation of the AMmax of Sim and Wright (2005). Categorical agreement matrices (CTAM, Table 1C) and categorical maximum agreement matrices

(CTAMax) for each behavioral category in the catalog were also built. K and related indexes (Kmax, B, P and Cohen’s “d”, see below) were estimated from CAM, CTAM, CAMmax and CTAMax, to determine the intra-HO’s reliability in using the entire catalog, as well as HO’s performance for each category.

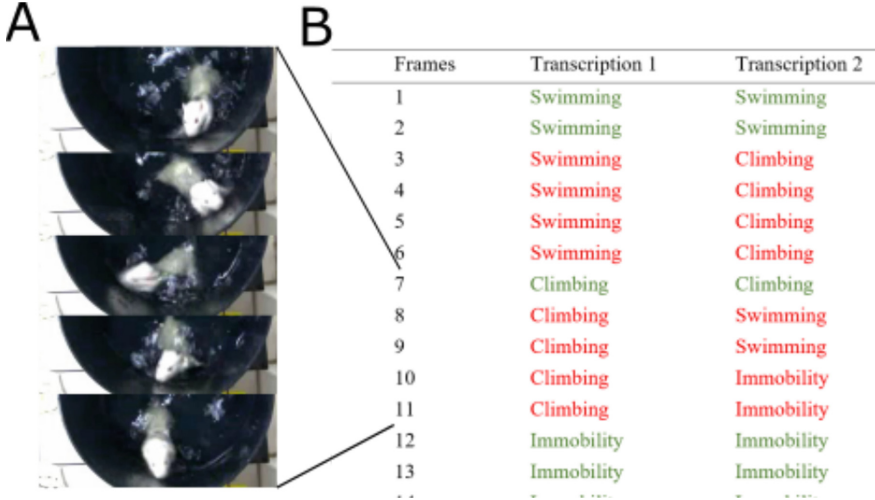


Fig. 1. A. Video frames of an experimental FST in rats. B. Resulting transcription of corresponding frame pairs side-by-side; behaviors in green are agreements, and in red indicates disagreements between transcriptions 1 and 2 of the same video sample taken by the same HO 15 days apart.

The first step was to transform CAM (Table 1A, $N \times N$, for N behaviors) into a CTAM (Table 1C) for each behavior. The algorithm arranges the CAM so that the selected behavior is positioned in its 1st row and its 1st column of CTAM. Using the notation indicated in Table 1A, the CAM cell *a* indicates the frequency of intra-HO agreements on “Swimming” (S) occurrence in the 2 transcriptions; the agreement on Not-S occurrence in both transcriptions is the average between cells *e* and *i*; 3) In the CTAM, disagreements (cells *b* and *c*, Table 1C) are the average of cells *b* and *c*, and of the cells *d* and *g* respectively of the Table 1A. From the CTAM, reliability indexes for the HO for each behavior can be then estimated (see below).

In addition to the CTAM and the CAM, a CTAMmax and a CAMmax were obtained by changing the main diagonal cells so that they contain the highest possible values of agreement frequencies while keeping the marginal values (Kmax; [15]). K max can be compared with K to estimate if there is (or not) room for performance improvement [15]. The higher the difference between the K and the corresponding Kmax, the higher the chance of improving the HO’s performance (e.g., by increasing training or refining the catalog).

The second step is to find the CAMmax and CTAMax for each behavior in the catalog. CTAMmax was determined by a modification of the methodology described by Sim and Wright (2005), to allow finding the CAMmax. This modification establishes the agreement diagonal as the minimum value between the marginals of the respective lines and columns [15]. Then a backtracking algorithm [14] is used to find the values of the other cells and to calculate the marginals. The backtracking algorithm selects a value for the cell and tests if it is valid. Validity occurs when a) the value of the sum of the column or row cells must result exactly in the marginal values (if the number is in the last cell of the row and/or column) or when b) the value is any number that, when added to the other values selected of the row or column, is lower than or equal to the values of the marginal of the corresponding column or row (if there are remaining cells to be determined). When the selected number is valid by these criteria, the algorithm repeats these procedures for the next cell, and so on.

After determining the CAM, CAMmax, CTAM, and CTAMmax we calculate the K, for each matrix, using formula (1).

$$K = \frac{Po - Pc}{Pc - 1} \tag{1}$$

where Po = proportion of observed agreements, Pc = proportion of agreements expected by chance. Using Table 1A, the Po can be calculated using formula (2) and Pc using formula (3).

$$Po = \frac{a + e + i}{n} \tag{2}$$

where $a, e,$ and i are cells located in the main diagonal and n = number of paired rating

$$Pc = \sum_{n=1}^{q-c} \frac{PiPj}{n} \tag{3}$$

where $q-c$ = number of behavioral categories, Pj indicates the marginals of transcription 2 and Pi is the marginals of transcription 1.

K ranges from -1 (total disagreement) to 1 (complete agreement), while $K = 0$ indicates random agreement. The benchmark for Cohen’s K interpretation proposed by Landis and Koch (1977), determined that $K < 0$ corresponds to a poor agreement, while K ranging $0.01-0.2$ = slight agreement; $0.21-0.4$ = fair agreement; $0.41-0.6$ = moderate agreement; $0.61-0.80$ = substantial agreement; $0.81-1$ = almost perfect agreement [7]. The Prevalence index (P) indicates the homogeneity of the frequencies of the categories on which the transcriptions agree, and using the notation in Table 1C, can be calculated by the formula (4).

$$Prevalence = \frac{abs(a - d)}{n} \tag{4}$$

where $abs(a - d)$ = absolute value of the difference between the frequencies of these cells and n = number of paired ratings. The higher the P-value, the more the measured K can be undervalued in the performance of the observer. As an

Table 1. An example of an intra-observer (A) catalog agreement matrix (CAM), (B) catalog maximum agreement matrix (CAMax); and (C) categorical agreement matrix (CTAM). Numbers refer to the frequency of agreements for each category. Note that the superscript right letters in the upper right-hand corners of the cells indicate the notation used in respective agreement formulas

A (CAM)		Trascription 2			Total
		Swimming	Climbing	Immobility	
Transcription 1	Swimming	2 ^a	4 ^b	0 ^c	6
	Climbing	2 ^d	1 ^e	2 ^f	5
	Immobility	0 ^g	0 ^h	3 ⁱ	3
Total		4	5	5	14 ⁿ

B (CAMmax)		Trascription 2			Total
		Swimming	Climbing	Immobility	
Transcription 1	Swimming	4 ^a	0 ^b	2 ^c	6
	Climbing	0 ^d	5 ^e	0 ^f	5
	Immobility	0 ^g	0 ^h	3 ⁱ	3
Total		4	5	5	14 ⁿ

C (CTAM)		Trascription 2	
		Swimming	Not Swimming
Transcription 1	Swimming	2 ^a	2 ^b
	Not Swimming	1 ^c	2 ^d

example, a “slight” K value associated with a high P suggests that the observer can be better than the K indicates. P values near zero suggest that the estimated K is accurately indicating the observer’s (bad or good) performance. So, the more the P approaches zero, the more reliable is the K values in estimating agreement.

Bias (B) indicates the homogeneity of frequencies at which transcriptions disagree. Using the notation in Table 1C. B can be calculated by the formula (5).

$$Bias = \frac{abs(b - c)}{n} \tag{5}$$

where $abs(a - c)$ = absolute value of the difference between the frequencies of these cells and the n = number of paired ratings. In contrast to P, the higher the B, the more the observed K value overestimates the real agreement between the transcriptions. B values near zero suggest that the estimated K is accurately indicating the observer’s (bad or good) performance [15].

B and P are calculated for CAM and CAMmax, using an approach modified here from that was proposed [15] to allow for calculations for N x N matrices, for $N > 2$ (N = number of categories in the catalog). This was achieved by (1) selected the cells located on the central diagonal, for the calculation of the prevalence, or cells located outside the central diagonal, to calculate the bias; (2) constructed for each selected cell a vector with origin at (0, 0), directed along the X-axis, and with intensity determined by its value, Fig. 2A; (3) applied to each of the vectors a linear transformation that rotated them so that the angular difference between the vectors was uniform, Fig. 2B; (4) summing the positioned vectors, and with the module of this vector divided by the n =number of paired ratings, prevalence or bias was calculated. We repeat this operation for every possible combination of vectors and extract the largest value.

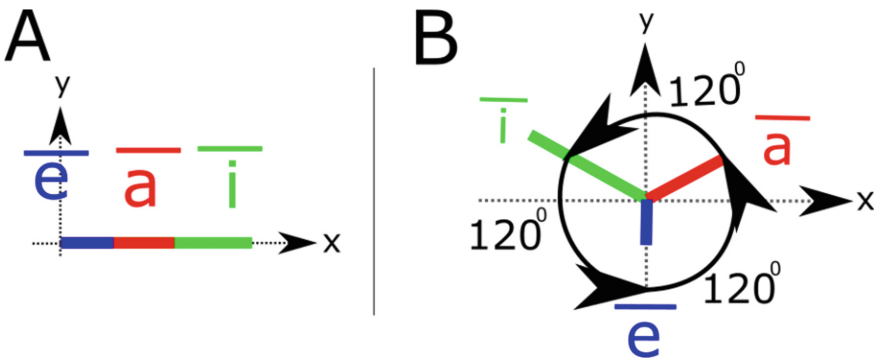


Fig. 2. Example of calculation of P of CAM from Table 1A. A) the first step of the algorithm that positions the cells values on the cartesian plane; B) the second step of the algorithm that rotates the vector in a way that all have evenly angles, The length of blue bars represents the ‘e’ cell value, red bars represent the ‘a’ cell value and green bars represent ‘i’ cell value from CAM matrix of Table 1A. The black solid lines represent the angle among vectors.

After calculating the K, P, and B of the CAM, CAMmax, CTAM and CTAMmax constructed for the original pair of transcriptions from the FST video, a set of new agreement matrices were built from those 1667 pairs of transcriptions obtained after the BS procedures. To build these new transcriptions and their corresponding agreement matrices, a list of random numbers with replacement (ranging from 1 to 7200, the total number of frames in each transcription) was generated and associated with each frame of the paired original transcription (according to [13, 18]). With each bootstrap replica was calculated the K, P, and B from the CAM, CAMmax, CTAM and CTAMmax, in a way that was possible to generate a frequency distribution for each agreement descriptor.

The frequency distributions of K and Kmax were used to calculate the distance (Cohen's d) between these descriptors using the formula (6) [5].

$$K = \frac{M_{max} - M_o}{Pooled\ sample\ SD} \frac{N - 3}{N - 2.25} \sqrt{\frac{N - 2}{N}} \quad (6)$$

where M_{max} = average of Kmax from the bootstrap replicas, M_o = average of K from the bootstrap replicas, N = number of bootstrap replicas. The standard deviation (SD) pooled for all the BS replicas was estimated by formula (7).

$$Pooled\ sample\ SD = \sqrt{\frac{SD_{max}^2 + SD_o^2}{2}} \quad (7)$$

where SD_{max} = standard deviation of Kmax for the BS replicas and SD_o standard deviation of K from the BS replicas. Cohen's d between the K and Kmax allows an estimate of the distance between the means of the distributions in SD (e.g. d = 2 indicates that there is a distance of 2 SD between K and Kmax distributions). The higher the d value, the higher the possibility of improvement in the HO's performance (e.g., through more training). Furthermore, a 95% CI was calculated using the percentile interval technique ([18]) for the frequency distribution of each agreement descriptor, which is useful to estimate the range of possible values for each descriptor. The 95% CI of K and Kmax can be used to test for significant distances between them: if they don't overlap, it is possible to affirm that they are significantly different, assuming a 5% error of type I in this conclusion [1, 3]. Thus, by observing the d value between K and Kmax 95% CIs it is possible to assess which categories can be refined, or better trained.

3 Results and Discussion

The frequency distribution of K and Kmax values generated from 1667 bootstrapped replicas from each category of the catalog and for the overall catalog is compared to the same values estimated for the original pair of transcriptions as shown in Fig. 3. K values (Fig. 3A–E) indicate that the HO's reliability in the FST video was 0.77 (a K value indicative of "substantial" intra-observer agreement, according to [7]). That contrasts with the almost perfect agreement (by the same benchmark) shown when recording some behaviors (e.g., swimming or immobility) or just a fair performance when rating headshaking.

BS procedures preserved the mean K values essentially similar to those observed for the original pair of transcriptions (as indicated by the K deltas); their narrow frequency distributions and C.I. values are confined to the same benchmark “diagnoses” found for original transcriptions. Interestingly, BS procedures overestimated the K values for the poorest performances (those showing the widest distributions: diving and headshaking). Kmax values and distributions (Figs. 3 and 4) can further refine the reliability analysis: significant differences between BS replicas average K and the average Kmax suggest that performance in the overall catalog can be improved (by training or better defining the categories) from 0.77 (substantial) to 0.99 (nearly perfect, the same is valid for swimming or immobility).

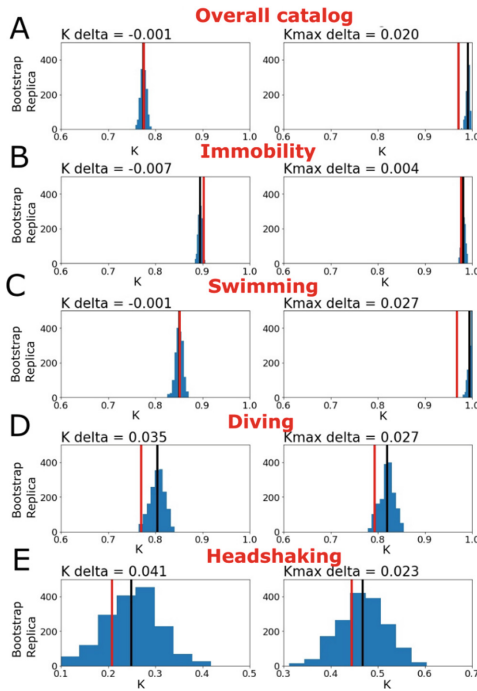


Fig. 3. Frequency distribution ($n = 1667$ bootstrap replicas) of K and Kmax for the overall catalog and of each behavioral category. Red lines represent K (left column of figures) or Kmax (right column of graphs) observed for the original pair of transcriptions, while black lines represent the average of the bootstrapped replicas. $K\delta$ and $Kmax\delta$ are the differences between the K and Kmax values of the original pair of transcriptions and the mean value obtained for the bootstrapped replicas

The substantial K obtained for diving is too close to its maximum achievable (Fig. 4D), suggesting that there is no room for further improvement in the performance of the observer regarding this behavior. This analysis also indicates that

while headshaking reliability can increase, the maximum K achievable remains at the “moderate” levels.

Analysis of B and P values of bootstrapped replicas (Fig. 4A–E) can further refine the interpretation of the K and Kmax. Because it is possible to evalu-

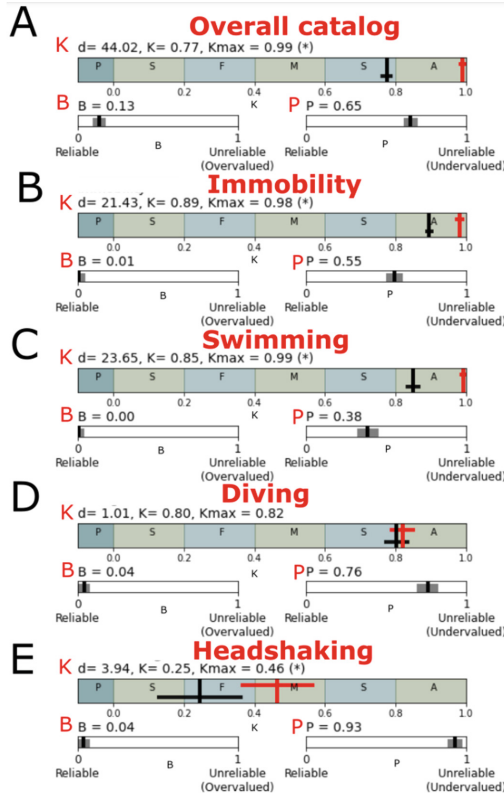


Fig. 4. A summary of the K, P, B and the K-Kmax distance for the overall catalog (A) and single behavioral categories (B–E) for the 1667 replicas obtained by the BS algorithms. The average K values (black vertical bars) and their respective confidence intervals (black horizontal bars) are represented with the respective Kmax averages (red vertical lines) and their confidence intervals (red horizontal lines). $d =$ Cohen’s d between Kmax and K in Standard deviations. (*) indicates that K and K max are significantly different ($p < 0.05$; according to [1,3]). The gray rectangles in this graph indicate the K level according to the benchmark of [7] for K so that P indicates $K < 0$ (poor agreement), S for K of 0.01–0.2 (slight agreement); F for K of 0.21–0.4 (fair agreement); M for K of 0.41–0.6 (moderate agreement); S for K of 0.61–0.80 (substantial agreement); A for K of 0.81–1 (almost perfect agreement). In the B graph, the average bias (or B) of the BS replicas values (black vertical bars) and their respective confidence intervals (black horizontal bars) are represented. In the P graph, the average prevalence (or P) of the BS replicas values (black vertical bars) and their respective confidence intervals (black horizontal bars) are represented

ate if the K calculated is unreliable and with the direction they are skewed. B indicates that none of K calculated from the catalog and for each category are skewed towards overvaluation. Implying that all K values estimated are at least conservative. Complementing, the P values indicate if the K calculated are reliable or skewed towards undervaluation. Using this as criteria the most unreliable K value was for Headshaking, implying that the K calculated for this category is better than shown in Fig. 4E. P informs that every category is skewed toward undervaluation, meaning that the K values calculated are conservatives.

4 Conclusions

Present results indicate that the use of replicas after BS faithfully mirrors most of the concordance attributes of the original transcripts while allowing a statistical evaluation of intra-HO's reliability, their differences in relation to the maximum agreement (Kmax), and the probabilities of under- or overestimation of K (bias and prevalence). The use of these tools can inform and optimize the performance of HOs in the use of ABM, without requiring time-intensive re-testing, favoring the reproducibility of the data obtained by these procedures.

References

1. Austin, P.C., Hux, J.E.: A brief note on overlapping confidence intervals. *J. Vasc. Surg.* **36**(1), 194–195 (2002). PMID: 12096281. <https://doi.org/10.1067/mva.2002.125015>
2. Chaturvedi, S.R.B.H., Shweta, R.C.: Evaluation of inter-rater agreement and inter-rater reliability for observational data: an overview of concepts and methods (2015)
3. Cumming, G.: Inference by eye: reading the overlap of independent confidence intervals. *Stat. Med.* **28**(2), 205–220 (2009)
4. Domingues, K., Lima, F.B., Linder, A.E., Melleu, F.F., Poli, A., Spezia, I., Lino de Oliveira, C.: Sexually dimorphic responses of rats to fluoxetine in the forced swimming test are unrelated to the function of the serotonin transporter in the brain. *Synapse* **74**(1), e22130 (2020)
5. Durlak, J.A.: How to select, calculate, and interpret effect sizes. *J. Pediatr. Psychol.* **34**(9), 917–928 (2009)
6. Gisev, N., Bell, J.S., Chen, T.F.: Interrater agreement and interrater reliability: key concepts, approaches, and applications. *Res. Social Adm. Pharm.* **9**(3), 330–3 (2013)
7. Landis, J.R., Koch, G.G.: The measurement of observer agreement for categorical data. *Biometrics* 159–174 (1977)
8. Lee, J., Fung, K.P.: Confidence interval of the kappa coefficient by bootstrap resampling [letter]. *Psychiatry Res.* **49**(97), 98 (1993)
9. Marchesini, G.: MorphoKinematicFST, um banco de dados unificado de dados categóricos, cinemáticos e morfológicos de ratos submetidos ao Teste do Nado Forçado (FST), validado por procedimentos metrológicos. M.Sc. Dissertation, Federal University of Santa Catarina, Technological Center, Postgraduate Program in Electrical Engineering, Florianópolis. <https://repositorio.ufsc.br/handle/123456789/215435> (2019)

10. Marchesini, G., Lino-de-Oliveira, C., Marino-Neto, J.: The use of reliability metrics for observational studies in rats submitted to the forced swim test (FST): a systematic review. *Acta Neuropsychiatr.* **31**(S2), 1–54 (2019). <https://doi.org/10.1017/neu.2019.38>
11. Marcolan, J.: Ferramenta de código aberto para análise de comportamento e aquisição de vídeo em “tempo real” usando técnicas de visão computacional e processamento paralelo. M.Sc. Dissertation, Federal University of Santa Catarina, Technological Center, Postgraduate Program in Electrical Engineering, Florianópolis. <https://repositorio.ufsc.br/handle/123456789/189477> (2017)
12. Marcolan, J., Marino-Neto, J.: ETHOWATCHER OS - Brazilian National Intellectual Property Institute license on protocol number BR512019002103-7 (2019)
13. McKenzie, D.P., Mackinnon, A.J., Péladeau, N., Onghena, P., Bruce, P.C., Clarke, D.M., McGorry, P.D.: Comparing correlated kappas by resampling: is one level of agreement significantly different from another? *J. Psychiatr. Res.* **30**(6), 483–492 (1996)
14. Rossi, F., Van Beek, P., Walsh, T. (Eds.): *Handbook of Constraint Programming*. Elsevier (2006)
15. Sim, J., Wright, C.C.: The kappa statistic in reliability studies: use, interpretation, and sample size requirements. *Phys. Ther.* **85**(3), 257–268 (2005)
16. Smalheiser, N.R., Graetz, E.E., Yu, Z., Wang, J.: Effect size, sample size and power of forced swim test assays in mice: guidelines for investigators to optimize reproducibility. *PLoS ONE* **16**(2), e0243668 (2021)
17. Spruijt, B.M., Peters, S.M., de Heer, R.C., Pothuizen, H.H., van der Harst, J.E.: Reproducibility and relevance of future behavioral sciences should benefit from a cross fertilization of past recommendations and today’s technology: “Back to the future.” *J. Neurosci. Methods* **234**, 2–12 (2014)
18. Tibshirani, R.J., Efron, B.: *An Introduction to the Bootstrap*. Monographs on Statistics and Applied Probability, vol. 57, pp. 1–436 (1993)
19. Willner, P., Belzung, C.: Treatment-resistant depression: are animal models of depression fit for purpose? *Psychopharmacology* **232**(19), 3473–3495 (2015)
20. Wright, D.B., London, K., Field, A.P.: Using bootstrap estimation and the plug-in principle for clinical psychology data. *J. Exp. Psychopathol.* **2**(2), 252–270 (2011)



Assessment of Lung Ventilators' Pressure Alarms System in a Controlled Scenario

S. G. Mello^{1,2} , A. E. Lino-Alvarado¹ , R. L. Vitorasso¹ , D. A. O. Rosa¹ ,
M. H. G. Lopes¹ , A. F. G. Ferreira Junior^{1,2} , and H. T. Moriya¹ 

¹ Biomedical Engineering Laboratory, University of Sao Paulo, São Paulo, Brazil
saragm@usp.br

² Laboratory of Final Uses and Energy Management, Energy Center, Institute for Technological Research, São Paulo, Brazil

Abstract. Lung ventilator's alarm system ought to ensure patient care by warning clinicians about the patient's condition. This study aims to present and discuss a technical evaluation of the lung ventilators alarms (higher-pressure, PEEP and obstruction) prescribed in ISO IEC 80601-2-12 performed during the Covid 19 pandemic in equipment that was distributed to meet the demand of critical patients. In subitem 201.12.4.105, the lung ventilator's alarm system had to detect when the higher-pressure alarm was reached by the airway-pressure measurement at the ventilator breathing system, and then triggered a high priority alarm. PEEP alarm condition is described in subitem 201.12.4.106 and the obstruction alarm in subitem 201.12.4.107. Ten different lung ventilators were analyzed based on table 201.101 from ISO 80601-2-12. Only one of ten lung ventilators correctly alarmed obstruction and reduced the pressure level to PEEP. Three of them did not present a PEEP alarm and one lung ventilator equipment allowed to disable the high airway pressure alarm. This study demonstrates the current limitations of the lung ventilators' alarms in a controlled scenario. The studied lung ventilators presented incongruity with the ISO 80601-2-12, especially the obstruction alarm.

Keywords: Mechanical ventilation · Lung ventilator · Pressure alarm · Alarm management · Support

1 Introduction

Lung ventilator's alarm system has an important role in alerting medical staff about changes in the patient's physical-pathological condition or technical failures of the equipment in ICUs. Clinicians are able to adjust alarm limits for specific parameters to fit the monitoring patient's requirements to provide safe ventilation. In the case of an adverse event, the alarm system generates an audible and visual signal to alert the clinicians. These alarms are classified according to their priority: lower, medium, and high. The high priority alarm indicates a dangerous event and requires rapid intervention. The medium priority alarm implies an event that could lead to hazardous conditions and need an evaluation of the ventilatory parameters. The low-priority message works as a reminder of the current status of the system and patient to the professional.

Not attending to the alarms may result in aggravating patient condition or death [1, 2]. However, in the hospitals, clinicians have been overwhelmed by many displaying alarms that mostly do not require intervention, as a result, clinicians have become less sensitive [3]. This problem has been described in the literature as alarm fatigue that was acknowledged as a safety problem by the ECRI Institute and The Joint Commission [4, 5].

A well-calibrated and functioning alarm system has a primary objective of ensuring rapid patient care, but also preventing false positive alarm scenarios. These false positive alarms could lead to excessive exposure of the patient to noise and erroneous team notifications [6].

The recommendations for alarm systems are prescribed in ISO IEC 80601-2-12 "Requirements for basic safety and essential performance of critical care ventilators" [7], ISO IEC 10651-3: "Emergency and transport ventilators" [8], and ISO IEC 10651-6: "Home-care ventilatory support devices" [9]. In Brazil, available lung ventilators in the market should complain the Brazilian adaptations of these standards to get approval from the Brazilian Health Regulatory Agency.

In response to the sanitary crisis in Brazil due to the Covid-19, several models of lung ventilators have been distributed across the country to cope with the pandemic. This study aims to present and discuss a technical evaluation of the lung ventilators alarms (higher-pressure, PEEP, and obstruction) in accordance with ABNT NBR ISO IEC 80601-2-12:2014. Alarm priority was evaluated following item 6.1.2 of ABNT NBR IEC 80601-1-8:2010 A1 2014.

2 Methods

This study was conducted in the Institute for Technological Research (IPT), Brazil. In total, we evaluated [10] different models of lung ventilators (Table 1) that are available in the Brazilian market. Due to confidentiality reasons, we did not detail equipment models. For this study, a set of tests was chosen from ABNT NBR ISO IEC 80601-2-12:2014, which is a Brazilian adoption of ISO 80601-2-12:2011 published by the National Agency of Sanitary Vigilance. The set includes requirements indicated in table 201.101 from the standard (airway pressure, obstruction, and PEEP). Additionally, another group of tests prescribed in the standard was employed to cover hazardous points in equipment failure. All selected tests were indicated in Table 2. The standard ABNT NBR IEC 80601-1-8:2010 A1 2014, item 6.1.2, was used to determine the alarm priority.

We tested the lung ventilators using a lung simulator (Dual Adult TTL, Michigan Instruments, USA). Lung ventilator pressure values were evaluated using a ventilator analyzer (AVM100, NÉOS, Brazil) calibrated by the Metrologic Reference Laboratory - LRM, certificate number L 6134/20. The measurement setup is shown in Fig. 1.

Each test was conducted as detailed in ABNT NBR ISO IEC 80601-2-12:2014. The results were reported and presented as compliant or not compliant.

After the lung ventilator had passed the self-test, the device was fully charged. Then, the subitem 201.12.4.105 was evaluated as described in the standard. The lung ventilator's alarm system had to detect when the higher-pressure alarm limit was reached by the airway-pressure measurement at the ventilator breathing system, and then triggered

Table 1. Country from all studied lung ventilators.

ID	Country
A	USA
B	Brazil
C	Brazil
D	Brazil
E	China
F	USA
G	Brazil
H	China
I	China
J	China

**Fig. 1.** Measurement setup.**Table 2.** Evaluated items from the 80601-2-12 studied in this work.

Subitem	Requirement	Priority
201.12.4.105	High airway pressure alarm condition and protection device	High
201.12.4.106	PEEP alarm conditions	High
201.12.4.107	Obstruction alarm conditions	High

a high priority alarm. Additionally, the lung ventilator had to reduce the airway-pressure level to PEEP value or below PEEP.

PEEP alarm condition (subitem 201.12.4.106) was assessed to verify whether the lung ventilator's alarm system indicated when the airway-pressure at the end of the expiration phase was below PEEP (low PEEP) or above PEEP (high PEEP). The priority had to be at least medium.

Other assessed alarm condition is the obstruction alarm (subitem 201.12.4.107), lung ventilator's monitor alarm system had to detect when an obstruction occurs in any part of the breathing tube, the exhalation valve or the breathing system filter. This fault should trigger a high priority alarm, and the lung ventilator had to reduce the airway-pressure level to a PEEP or atmospheric within one respiratory cycle.

3 Results

Tables 3 and 4 depict the pressure alarm results.

Table 3. Alarm results from all lung ventilators.

Ventilators	PEEP alarm condition (high and low PEEP) (201.12.4.106)	High airway pressure alarm condition and protection device (201.12.4.105)
A	C	C
B	C	C
C	C	C ^a
D	C	C
E	C	C
F	C	C
G	NC	C
H	NC	C
I	NC	NC
J	C	C

^a The lung ventilator permitted the alarm deactivation. Where, C: compliant and NC: not compliant.

Three lung ventilators (G, H and I) did not present PEEP alarm. All lung ventilators alarmed high pressure and presented the necessary protective means. However, lung ventilator "I" did not alarm high pressure as high priority, and lung ventilator C permitted alarm inactivation.

Lung ventilator did not alarm obstruction. However, it was considered compliant because it alerts the fault and reduces the pressure according to the standard requirement.

Finally, the obstruction alarm results were listed in Table 4. Only lung ventilator C correctly alarmed obstruction and reduced the pressure to PEEP. Although the ventilator E did not indicate obstruction during the alarm condition, it was considered compliant because it alerted and reduced the pressure to PEEP according to the standard requirement.

4 Discussion

The motivation for the conduction of this study was related to the fact that many lung ventilators (presented in the results and to be discussed) failed to fulfill all prerogatives described by the standard. Not only, because morbidity and mortality are related to lung

Table 4. Obstruction alarm results Subsect. 201.12.4.107.

Ventilators	Alarms			Pressure		Obstruction alarm results
	Obstruction	Other alarm	No alarm	Reduces pressure	Do not reduce pressure	
B		●			●	NC
C	●			●		C
D		●			●	NC
E		●		●		C*
F			●		●	NC
G			●		●	NC
H			●		●	NC
I			●*		●*	NC

ventilator alarm management [1, 2] but the assessment of mechanical ventilator alarming is clinically relevant.

In ABNT NBR ISO IEC 80601-2-12:2014, Subsect. 201.12.4.106, it is prescribed that the lung ventilator must alarm high PEEP within 3 cycles. Lung ventilators G, H and I failed to alarm high and low PEEP, lung ventilator G presented a divergence between the ventilators' manual and Subsect. 201.12.4.106. In the manual, the alarm window was 9 cycles. Hence, there are two main problems to be reported in this work about PEEP alarms: the non-conformity to the standards (G, H and I), and the disparity between manual and the ABNT NBR ISO IEC 80601-2-12:2014 (G). In addition, it is mandatory to present a high PEEP alarm and is optional to present a low PEEP alarm.

The mandatory characteristic of the high PEEP alarm is related to a protection mechanism. Besides the high PEEP alarm, the IEC ISO 80601-2-12:2014 prescribes (Subsect. 201.12.4.105) an alarm related to high airway pressure and a protective device. Recently, it has been discussed the 30 cmH₂O and suggested 32 cmH₂O plateau pressure as the upper safety limit for mechanical ventilation.¹⁰ Regardless of the 30 or 32 cmH₂O recommendation, there must be a protective mechanism in pressure in order to avoid barotrauma.

From our data, all ventilators presented the desirable protective response. However, one ventilator (I) did not alert a high priority alarm when it was required, a high priority alarm in this case was the standard recommendation. The alarm priority is associated with the risk related to that individual alarm [11]. Another ventilator (C) in this study permitted the inactivation of the high-pressure alarm. This feature is not desirable and can be troublesome because one can deactivate the alarm and forgets to report.

Finally, the obstruction alarm had the highest number of divergences from the standard. Two (A and J) out of ten lung ventilators were not evaluated. Only one lung ventilator (C) correctly alarmed obstruction and reduced the pressure to PEEP, which means that only one completely fulfilled the Subsect. 201.12.4.107 requirements. The lung ventilator (E) alarmed a different parameter with high priority level and reduced

the pressure to PEEP, which can protect the patient but can mislead the action of hospital staff to overcome the fault.

One limitation of this study was the non-application of more tests of the collateral standard in the studied ventilators. More specifically, the collateral standard IEC 80601-1-8 "Electromedical equipment Part 1-8: General requirements for basic safety and essential performance - Collateral standard: General requirements, tests and guidelines for alarm systems in electromedical equipment and systems electromedical devices" was created to ensure that there is a clear visual and auditory identification for the alarm operator and to inform its possible harms for the patient [12].

Another consideration is the fact that only one sample, as presented in Table 1, was evaluated per model. The focus of this project was to assess mechanical ventilators during the COVID-19 pandemic in Brazil. However, even with a few items of the ABNT NBR ISO IEC 80601-2-12:2014 applied in this study and one sample per batch, it was important to verify that the lung ventilators demonstrated inadequacy. It is recommended to conduct a study with a larger sample number for better discussion of the results.

5 Conclusion

In conclusion, this study demonstrates the current limitations of the lung ventilation alarm system in a controlled scenario. Despite the fact that assessed lung ventilators were already available on the market, they presented incongruity with the ABNT NBR ISO IEC 80601-2-12:2014, especially the obstruction alarm.

Acknowledgment. This study was financed in part by the endowment fund from Escola Politécnica of University of São Paulo "Amigos da Poli", São Paulo State Government (42960P - Comitê de Crise do COVID-19), the Coordenacao de Aperfeicoamento de Pessoal de Nivel Superior - Brazil (CAPES) - Finance Code 001 and the Conselho Nacional de Pesquisa e Desenvolvimento Científico e Tecnológico - Brazil (CNPq) (381120/2020-1 to RLV and 308280/2019-9 to HTM).

Conflict of Interest. The author(s) declare to have no potential conflicts of interest with respect to the research, authorship, and/or publication of this article.




References

1. Pham, J.C., Williams, T.L., Sparnon, E.M., Cillie, T.K., Scharen, H.F.: Marella WM ventitor-related adverse events: a taxonomy and findings from 3 incident reporting systems. *Respir. Care. Care* **61**(5), 621–631 (2016)
2. Walsh, B.K.: Waugh JB alarm strategies and surveillance for mechanical ventilation. *Respir. Care. Care* **65**(6), 820–831 (2020)
3. Scott, J.B., De Vaux, L., Dills, C., et al.: Mechanical ventilation alarms and alarm fatigue. *Respir. Care.* **64**(10), 1308–13 (2019)
4. Joint Commission Medical Device Alarm Safety in Hospitals: Sentin. event alert No. **50**, 1–3 (2013)
5. Horkan, A.M.: Alarm fatigue and patient safety. *Nephrol. Nurs. J.* **41**(1), 83–86 (2014)

6. Cvach, M.M., Stokes, J.E., Manzoor, S.H., et al.: Ventilator alarms in intensive care units: frequency, duration, priority, and relationship to ventilator parameters. *Anesth. & Analg.* **130**(1), e9-e13 (2020). <https://doi.org/10.1213/ane.0000000000003801>
7. Associação Brasileira de Normas Técnicas. NBR ISO 80601-2-12:2014 Requisitos particulares para a segurança básica e o desempenho essencial de ventiladores para cuidados críticos (2014)
8. ISO 10651-3:1997.: Lung ventilators for medical use—part 3: particular requirements for emergency and transport ventilators (1997)
9. ISO 10651-6: 2004.: Lung ventilators for medical use-particular requirements for basic safety and essential performance-part 6: home-care ventilatory support devices (2004)
10. Gattinoni, L., Marini, J., Collino, F., et al.: The future of mechanical ventilation: lessons from the present and the past. *Crit. Care* (2017)
11. Phillips, J.: Clinical alarms: complexity and common sense. *Crit. Care Nurs. Clin. N. Am.* **18**(2), 145–56, ix. (2006)
12. Bolton, M.L., Zheng, X., Li, M., et al.: An experimental validation of masking in IEC 60601-1-8: 2006-compliant alarm sounds. *Hum. Factors.* **62**(6), 954–72. [https://doi.org/10.1177/0018720819862911\(2020\)](https://doi.org/10.1177/0018720819862911(2020))



Maternal Near Miss in the State of Rio Grande Do Norte (Brazil) Between 2003 to 2019: A Preliminary Analysis of Identification and Monitoring

T. S. Rêgo , S. P. Silva , D. V. Vieira , R. A. O. Freitas-Júnior ,
and A. C. Rodrigues ^(✉) 

Graduate Program in Neuroengineering. Edmond and Lily Safra International Institute of Neuroscience, Santos Dumont Institute. Av. Alberto Santos Dumont, Macaíba, RN 1560, Zona Rural. 59280-000, Brazil
abner.neto@isd.org.br

Abstract. The decline in maternal mortality rate is one of the global goals established by the United Nations. The analysis of maternal near miss makes it possible to identify the morbidities to which women are exposed and, consequently, to recognize the weaknesses of the health system in a region. A temporal trend ecological study was carried out, aiming to identify and monitor cases of maternal near miss between 2003 and 2019 in Rio Grande do Norte, Brazil. With the data made available by the Hospital Information System (SIH) of the Unified Health System (SUS) and with the help of the PySUS library, in Python programming language, it was possible to identify the years of higher incidences of maternal near miss and the main risks that pregnant or postpartum women suffer in the state.

Keywords: Maternal near miss · Maternal morbidity · SUS · SIH · Women's health

1 Introduction

Combating maternal mortality has been an emerging global mobilization. Efforts have been initiated for the prevention and detection of obstetric complications, aiming to reduce estimates such as those of the 1980s, in which approximately 500,000 women died annually from preventable causes related to pregnancy [1].

As the understanding of these rates deepened, social and economic aspects were also interpreted as determinants for maternal mortality cases, reflecting human development in a country [1–3]. Then, factors such as educational level, income, place of birth, social support, and accessibility to health care can be strongly related to maternal mortality rates in a region [1, 2, 4, 5].

In 2015, a global initiative called the Sustainable Development Goals (SDGs) was instated by United Nations (UN). In this are expanded efforts to eliminate preventable maternal mortality, with the goal of reducing the global maternal mortality ratio to below

70 maternal deaths per 100,000 live births by the year 2030 [1]. In Brazil, the maternal death ratio recorded in 2015 was estimated at 62 deaths per 100,000 live births [6]. Therefore, the goal set for Brazil was the reduction to less than 30 maternal deaths per 100,000 live births [1].

The efforts for the extinction of preventable maternal death are far beyond the quality perspective of a country's health system. Pregnancy is a natural condition of the organism, and, therefore, it is a woman's social right to have access to quality obstetric services [2]. Neglect in access, care, and exposure to life-threatening risks are factors that reflect not only a deficient health system but also a situation of social injustice and violation of fundamental human rights [2].

Maternal near miss (MNM) is a concept used for a woman who almost died but survived a complication that occurred during pregnancy, delivery, or puerperium [7–9]. Although the SDGs set the reduction of maternal mortality as a goal, understanding the risks women face at all stages of pregnancy, and the sequelae that exposure to these risks can bring to their health, are vital to identifying the factors that can lead them to death [7].

In parallel to the analysis of maternal mortality, MNM is also directly related to the country's development index, quality of health care, ease of access to basic care networks, among others [2, 4, 10].

For the consolidation of the concept of MNM, it was necessary a consensual delimitation about events that would characterize a life risk to the pregnant woman [9]. According to studies conducted by experts, under the seal of the World Health Organization (WHO), the characterization of maternal near miss would be based on 25 clinical, laboratory, and management criteria [8, 9]. In addition, the classification criteria established by the Mantel [11] and Waterstone [12] studies are also widely used.

In Brazil, the Unified Health System (SUS) has an Informatics Department (DATA-SUS) that aims to provide information and computer support for the hospital and administrative [13] planning, operation, and control processes. The Hospital Information System (SIH) database has great potential to identify cases of a maternal near miss, since it is an extensive source of information on hospital morbidity in the country [9]. The data made available by the Mortality Information System (SIM) enable the identification of the main causes of maternal mortality [9].

Previous studies have used the SIH and SIM databases together with the MNM criteria by means of the codes of procedures used in obstetric care and the codes of diagnoses by means of the International Classification of Diseases – 10th revision (ICD-10) [10].

Based on the information about maternal near miss and on the global goals established for Brazil, the state of Rio Grande do Norte was chosen for a preliminary analysis of identification and monitoring about maternal health in the years made available in the SIH and SIM databases (2003 to 2019).

2 Materials and Methods

2.1 Computational Tools

For the development of this analysis, the Python programming language was used. The manipulation of the data made available by DATASUS was carried out by the PySUS [14] library, which has auxiliary codes to simplify data handling. The GeoPandas [15] library was also used, which allows the handling of geospatial data in Python. Graphs were generated using the Matplotlib library [16].

2.2 Data Acquisition and Analysis

Sex and Age Criteria. According to article 2, § 3º, of Ordinance number 1,119 of the Ministry of Health [17], the fertile age of women between 10 and 49 years old is now considered for the purposes of identifying female deaths in the Mortality Information System (SIM) in Brazil. Based on this fact, for the identification of maternal near miss cases, the cases of females within the age range of 10 to 49 years were filtered, consistent with previous work in the literature [3].

Prenatal and Maternal Near Miss Criteria. For the selection of pregnant or postpartum women in the sample, the numbers of prenatal registrations are analyzed, so that only women with such a registration are selected.

The identification of maternal near miss cases was due to the filtering of the information made available by DATASUS. The three classification criteria that currently exist were used in parallel: Waterstone [12], Mantel [11] and WHO [8], with the aid of the ICD-10 codes that represented each occurrence of maternal morbidity or mortality.

The differentiation between the criteria is due to the degree of specificity of occurrences in hospitalization. In [8], for example, 25 clinical, laboratory and management criteria are addressed. In [11], several markers included in dysfunctions are considered: cardiac, immunological, respiratory, renal, hepatic, metabolic, and coagulation. In [12], in turn, health markers are considered: severe preeclampsia, eclampsia, HELLP syndrome (hemolysis, high levels of liver enzymes, and low plaque counts), severe bleeding, sepsis, uterine rupture, acute abdomen, and disease caused by the human immunodeficiency virus.

2.3 Maternal Near Miss Rate

With the sample filtered, the maternal near miss rate (MNMR) was calculated for each available registration year. This rate, demonstrated in [4], is represented by the following equation:

$$\text{MNMR} = \left(\frac{\alpha \text{MNM}}{\beta} \right) \times 1000 \quad (1)$$

where αMNM is the number of maternal near miss cases and β represents the number of women hospitalized for obstetric procedures.

For the numbers of hospitalized women, the hospital admission authorization data available in the SIH were used.

2.4 Statistical Analysis

In order to investigate the acquired sample, identify the difference in mapped MNM cases, and the correlation between the three classification criteria, IBM SPSS® software was used for statistical analyses. In this study, Fisher’s exact test and Pearson’s correlation were performed. A statistical significance level of 5% was set.

3 Results

3.1 SIH Analysis

The resulting sample from the survey between the years 2003 to 2019, after applying all criteria, was 1701 cases of women who suffered maternal near miss according to Waterstone [12], 367 cases according to the WHO [8] criteria, and 7 cases according to the Mantel [11] criteria. The most common maternal morbidities recorded according to Waterstone include pre-eclampsia (n = 1330), severe bleeding (n = 263), and eclampsia (n = 89). According to WHO, cases of hypovolemic shock (n = 263) and eclampsia (n = 95) were mostly identified. Mantel, in turn, identified cases of sepsis (n = 5), severe hemorrhage (n = 1), and acute renal failure (n = 1).

For the purpose of identifying the sample acquired, the data were divided according to the age considered advanced for maternity (35 years) [18]. Thus, the data were arranged in Table 1 between women aged ≤34 years and those aged ≥35 years. No statistically significant associations were found between the age intervals in each of the criteria, ($\chi^2_{waterstone} (17) = 17.05, p = .451$), ($\chi^2_{who} (15) = 19.75, p = .173$), ($\chi^2_{mantel} (4) = 5.50, p = .429$) by Fisher’s exact test (Table 1). In addition, the sample was divided according to the existence of risk in pregnancy (Table 1). No statistically significant relationships were found between the groups without risk and with risk on Mantel’s criterion, ($\chi^2_{mantel} (4) = 5.50, p = .429$) by Fisher’s exact test. However, significant differences were found between pregnancy type and Waterstone ($\chi^2_{waterstone} (17) = 222.5, p < .001$) and WHO ($\chi^2_{who} (15) = 83.38, p < .001$) criteria by the same analysis (Table 1).

Table 1. SIH Sample description

Age	Waterstone		OMS		Mantel	
	n (%)	p-value	n (%)	p-value	n (%)	p-value
≤ 34 years old	1539 (90.48)	.451	326 (88.83)	.173	6 (85.71)	.429
≥ 35 years old	162 (9.52)		41 (11.17)		1 (14.29)	
Total	1701 (100)		367 (100)		7 (100)	
Type of pregnancy	n (%)	p-value	n (%)	p-value	n (%)	p-value
No risk pregnancy	87 (5.11)	0.000*	40 (10.90)	0.000*	1 (14.29)	.429
Risk pregnancy	1614 (94.89)		327 (89.10)		6 (85.71)	
Total	1701 (100)		367 (100)		7 (100)	

Figure 1 shows the variation in maternal near miss rates for each year of analysis in the state of Rio Grande do Norte, under the evaluation of each MNM identification criterion.

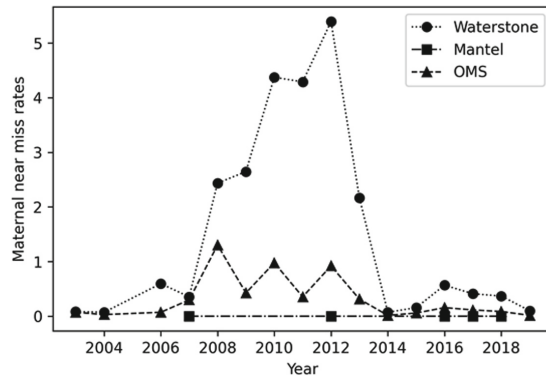


Fig. 1. MNMR in Rio Grande do Norte, Brazil.

The correlation calculation between the maternal near miss criteria was also performed. Where a strong, positive, and significant correlation was found between the Waterstone [12] criteria and the WHO [8] criteria ($r(16) = 0.765, p = 0.001$).

3.2 SIM Analysis

Monitoring of maternal mortality with causes included in the maternal near miss criteria was performed. The resulting samples between the years 2003 to 2019 were: 1439 cases of deaths in Waterstone [12] criteria, 2327 in WHO [8] criteria and 2221 in Mantel [11] criteria. Figure 2 depicts the cases by year and by criteria.

By Waterstone [12], the most common cause recorded was sepsis ($n = 1411$). By WHO [8] and Mantel [11], the occurrences of sepsis ($n = 1411$) and related to respiratory dysfunction ($n = 470$), mainly cases of embolism ($n = 432$).

4 Discussion

This study aimed to provide a complete picture of maternal near miss in the state of Rio Grande do Norte, in the Northeast region of Brazil. With the analysis of the SIH database in the years 2003 to 2019, and the use, in parallel, of the three MNM classification criteria, we obtained 1701, 367, and 7 cases eligible for classification according to Waterstone [12], WHO [8], and Mantel [11], respectively. The age of pregnant or postpartum women did not significantly influence the numbers of near miss in any criteria (Table 1), unlike other analyses found in the literature [4]. However, the type of pregnancy was shown to have a significant influence on these cases for Waterstone and WHO, with women with at-risk pregnancies being the most likely to experience maternal near miss (Table 1).

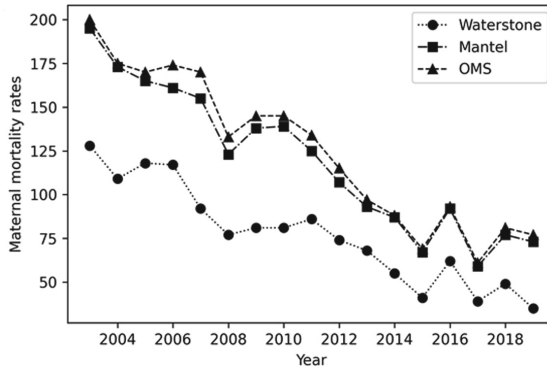


Fig. 2. Maternal deaths according to the near miss criteria in Rio Grande do Norte, Brazil.

There was an increasing trend in the rate of MNM between the years 2008 to 2012 (Fig. 1). A similar result was found by [10] when analyzing the northeastern region of Brazil. According to [10], regions with less development have an increase in maternal near miss rates over the years. Several factors may be influential in these numbers, such as inadequate maternal health care and the accessibility of the pregnant or puerperal woman to specialized hospitals [10]. In addition, [19] finds that one reason for the growth in rates is the improvement in the quality of morbidity registration and information about care.

In parallel to the analysis of the SIH, maternal mortality cases with causes that fit the MNM criteria in the SIM were also filtered (Fig. 2). Applying the filters of sex, age, prenatal, and near miss criteria, the temporal trends of maternal mortality according to Waterstone [12], WHO [8], and Mantel [11] were demonstrated. The three criteria showed decreasing rates over the years, with an increase in cases between the years 2009 and 2012. A similar result was found in [19] with data on maternal mortality in Brazil. Moreover, the most common occurrences that led women to death were related to sepsis, while the most common cases that led to MNM are related to preeclampsia, eclampsia, severe hemorrhage, and hypovolemic shock. Such results contribute to the understanding of the aspects of improvement in maternal health care needed in the SUS.

This study also sought to provide a comparative analysis of the three current MNM criteria. The Waterstone [12] and WHO [8] criteria showed a strong and positive correlation ($r = 0.765$) with each other in characterizing cases, and a good performance in classification. However, difficulties were encountered in identifying cases with the Mantel [11] criteria. In the application of this criterion, the resulting samples of maternal near miss per year were low, being almost zeroed out when calculating the rate of MNM. Because of this, it was not possible to calculate the correlation with the other variables.

Finally, it is worth emphasizing the importance of a public online health data tool. The SIH and SIM databases have an important potential for morbidity and mortality analysis in the country, enabling an extensive range of epidemiological analysis in Brazil. However, until now, this means is used for payment purposes by the Health Units, resulting in the poor filling of spreadsheets and low reliability of the available data [9,

10]. Studies like this one have been increasing in the literature to ratify the importance of filling out the spreadsheet for Brazilian public health analysis.

The analysis performed in this research is preliminary, with the purpose of being expanded to all Brazilian states. Understanding the factors that expose women unnecessarily to life risks or lead to death from preventable causes is of utmost importance for the future provision of quality care, for equity in women's health care, and ultimately for the achievement of the global goal set by the UN.

5 Conclusion

The results of the present study demonstrated the temporal trend of maternal near miss rates in the state of Rio Grande do Norte, Brazil. Periods of growth and decrease of these rates were identified, which may be influenced by socioeconomic factors of the population in each year of registration. Through this analysis, it was also possible to identify the main morbidities that lead women to be at risk during pregnancy, delivery, or the puerperium, when assisted by the SUS. Complementarily, the study offered an overview of maternal mortality and its main causes. Furthermore, the study emphasizes the importance of the availability of complete data in DATASUS, since maternal near miss is a promising alternative for the identification of aggravating factors in maternal health and consequent reduction of mortality. Through this approach, the achievement of the global goal set by the UN will be feasible.

Acknowledgements. The authors would like to acknowledge the support and funding from the Bill & Melinda Gates Foundation, Coordenação de Aperfeiçoamento de Pessoal de Nível Superior – Brasil (CAPES) – Finance Code 001, Conselho Nacional de Desenvolvimento Científico e Tecnológico (CNPq) and Ministério da Educação (MEC).

Conflict of Interest. The authors declare that they have no conflict of interest.




References

1. Souza, J.P.: A mortalidade materna e os novos objetivos de desenvolvimento sustentável (2016–2030). *Rev. bras. Ginecol. Obstet.* **37**(12), 549–551 (2015)
2. Freitas-Júnior, R.A.O.: Mortalidade materna evitável enquanto injustiça social. *Revista Brasileira de Saúde Materno Infantil* **20**(2), 607–614 (2020)
3. Herdt, H.M.C.W., Magajewski, F.R.L., Linzmeyer, A., Tomazzoni, R.R., Domingues, N.P., Domingues, M.P.: Temporal trend of near miss and its regional variations in Brazil from 2010 to 2018. *Rev. Bras. Ginecol. Obstet.* **43**(2), 97–106 (2021)
4. Rosendo, T.S., Roncalli, A.G., Azevedo, G.D.: Prevalence of maternal morbidity and its association with socioeconomic factors: a population-based survey of a city in northeastern Brazil. *Rev. Bras. Ginecol. Obstet.* **39**(11), 587–595 (2013)
5. Graaf, J.P., Steegers, E.A.P., Bonsel, G.J.: Inequalities in perinatal and maternal health. *Curr. Opin. Obstet. Gynecol.* **25**(2), 98–108 (2013)
6. IPEA Instituto: Pesquisa Econômica Aplicada. ODS-Metas Nacionais dos Objetivos de Desenvolvimento Sustentável (2018)

7. Souza, J.P., Cecatti, J.G., Parpinelli, M.A., Serruya, S.J., Amaral, E.: Appropriate criteria for identification of near-miss maternal morbidity in tertiary care facilities: a cross sectional study. *BMC Pregnancy Childbirth* **7**(20), 1–8 (2007)
8. Say, L., Souza, J.P., Pattinson, R.C.: Maternal near miss—towards a standard tool for monitoring quality of maternal health care. *Best Pract. Res. Clin. Obstet. Gynaecol.* **23**(3), 287–296 (2009)
9. Nakamura-Pereira, M., Mendes-Silva, W., Dias, M.A.B., Reichenheim, M.E., Lobato, G.: Sistema de Informações Hospitalares do Sistema Único de Saúde (SIH-SUS): uma avaliação do seu desempenho para a identificação do near miss materno. *Cad. Saude Publica* **29**(7), 1333–1345 (2013)
10. Carvalho, B.A.S., et al.: Tendência temporal do Near Miss materno no Brasil entre 2000 e 2012. *Revista Brasileira de Saúde Materno Infantil* **19**(1), 115–124 (2019)
11. Mantel, G.D., Buchmann, E., Rees, H., Pattinson, R.C.: Severe acute maternal morbidity: a pilot study of a definition for a nearmiss. *BJOG: Int. J. Obstet. Gynaecol.* **105**(9), 985–990 (1998)
12. Waterstone, M., Bewley, S., Wolfe, C.: Incidence and predictors of severe obstetric morbidity: case-control study. *Obstet. Gynecol. Surv.* **57**, 139–140 (2002)
13. Araújo, C.R.L., Dias, L.C., Dias, E.P., Gonzalez, F.L., Santos, H.L., Silva, M.E.M., Serpa, N.S.C.: Departamento de Informatica do SUS—DATASUS A Experiência de Disseminação de Informações em Saúde. In: *A experiência brasileira em sistemas de informação em saúde*, pp. 109–128. Editora do Ministério da Saúde, Brasília (2009)
14. PySUS, <https://pysus.readthedocs.io/en/latest/>, last accessed 2022/01/27
15. GeoPandas, <https://geopandas.org/en/stable/>, last accessed 2022/01/27
16. Matplotlib Homepage, <https://matplotlib.org/>, last accessed 2022/01/27
17. Ministério da Saúde, <https://bvsmms.saude.gov.br/bvs/saudelegis/gm/2008/prt111905062008>, last accessed 2022/01/31
18. Frederiksen, L.E., et al.: Risk of adverse pregnancy outcomes at advanced maternal age. *Obstet. Gynecol.* **131**(3), 457–463 (2018)
19. Rodrigues, N.C., et al.: Temporal and spatial evolution of maternal and neonatal mortality rates in Brazil, 1997–2012. *J. Pediatr. (Rio J)* **92**(6), 567–573 (2016)



Radiation Dose Optimization for Contrast-Free Adult Skull CT Protocol

F. N. Torres¹ , J. V. Real^{1,2} , and A. M. Malthez¹ 

¹ Curitiba, Brazil

flavianasctorres@gmail.com

² Clinic Hospital Complex of Federal University of Parana, Curitiba, Brazil

Abstract. Among all radiological techniques, computed tomography delivers the highest radiation dose to the patient. Aiming for the radiological protection of those, this project set out to optimize the Contrast-free adult skull protocol of the Clinic Hospital Complex of the Federal University of Parana. Four different suggested protocols were submitted to quality control tests to analyze whether it was possible to reduce the dose without a significant loss in the image quality and decide, among those, which one could be implemented at the hospital. Two out of the four suggestions obtained satisfactory results.

Keywords: Radiation dose · Computed tomography · Imaging diagnosis · Dose optimization

1 Introduction

Developed by Godfrey Hounsfield in the sixties, Computed Tomography (CT) has the same basic principles as conventional radiography, a method through which images are acquired by exposing a medium to x-rays. The CT scan contains an x-ray tube located inside a gantry, which rotates 360° around the patient's table and obtains 'sliced' high-quality images of the irradiated structure [1].

Due to its high-definition images, CT has become an indispensable tool in radio-diagnostics. Therefore, international radiation protection institutions, such as the International Commission on Radiation Protection (ICRP), the American Association of Physicists in Medicine (AAPM) and International Atomic Energy Agency (IAEA), established recommendations for both imaging quality assurance and dose optimization, which consists of procedures specifically created to maintain a high diagnostic and treatment quality for the patients [2–4]. The Brazilian body responsible for regulatory in image diagnosis, ANVISA (*Agência Nacional de Vigilância Sanitária*), established in the current resolution the quality assurance tests in at RDC 611, and IN 93 regarding CT's quality assurance [5, 6]. Therefore, there is not a Brazilian technical document that described the methodology to run the tests. In this case, international documents and protocols can be adopted, as the IAEA N19 recommendations [4].

Although there is no limit value for medical exposure, the radiological protection of patients during diagnostic procedures should be improved, keeping the radiation dose as

low as it can be to obtain an image good enough for diagnosis and treatments. Thus, the need arises to search for ways to optimize the patient's radiation dose, especially in CT exams - which has one of the highest rates of exposure in medical imaging -, not only to improve image quality but also to prevent patient exposure as much as possible [7].

Therefore, the main goal of this article was to optimize the Contrast-free adult skull protocol, retaining (or improving) the image quality for clinical diagnosis, whilst also reducing the patient's absorbed dose in CT examinations at the Clinic Hospital Complex of the Federal University of Parana (CHC-UFPR). A secondary goal was to evaluate the influence of the combination of different CT parameter values, such as the product of tube current and beam time (mAs), pitch and equipment's rotation time, and their influence on the volumetric CT dose index (CTDI_{vol}), which is used as a reference index dose in CT examination. And lastly, to examine imaging quality parameters such as noise, CT number uniformity, accuracy, spatial resolution and figure of merit (FOM), for each suggested protocol to define the best one among the options.

2 Materials and Methods

This study was developed at CHC-UFPR Diagnostic Imaging Unit using a Philips MX 16-Slice CT scan (Koninklijke Philips N.V., Eindhoven, Netherlands) (see Fig. 1).

The evaluation of the suggested protocols was based on a comparison between five different exposures made in the head phantom simulator (see Fig. 2), changing operational parameters for each one.

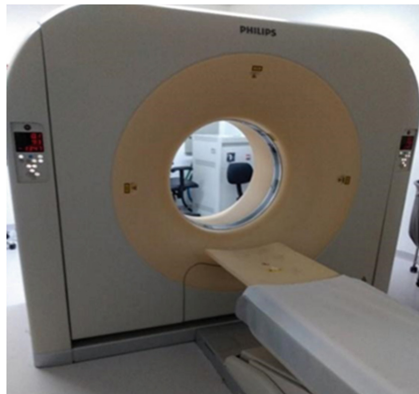


Fig. 1. MX 16-Slice scanner by Philips at the CHC-UFPR. Its x-ray tube contains a maximum capacity of 140 kV with an operating current of 355 mA for that voltage, and maximum output power of 50 kW.

The quality assurance tests were made by analyzing sliced images of two out of the three layers the simulator possesses. Firstly the "Water layer" for the evaluation of noise level, FOM, CT number uniformity, and accuracy. Secondly and lastly, the images of the multi-pin layer of the phantom were considered for evaluating special resolution.



Fig. 2. Head-16 Simulator used in daily MX 16 scanner's quality tests at the CHC-UFPR.

To avoid unnecessary exposures, patient dose values for each protocol parameter set were simulated on the impactscore.org website, where it is possible to calculate, according to the manufacturer and scan model, all the patient dosimetry together with exposure factors.

Although it demonstrates how to change the parameters to minimize the CTDIvol, this simulation could not be used to compare the values obtained in the CT's adult skull test acquisitions directly, because it only shows a theoretical value available on their database. Since the website's database did not have the same equipment as the one used in this study, the Philips Brilliance 16 model was used in the simulation, as it contains a similar configuration to the CHC-UFPR equipment, only as a base to choose which parameters would be changed on the real protocol suggestions. Table 1 presents the CTDIvol values simulated by ImpactScan in each suggestion.

Table 1. Brilliance-16 CTDIvol simulated values obtained using ImpactScan.org.

Protocol	Simulated CTDIvol (mGy)	Real CTDIvol (mGy)
Routine	46.8	46.25
1	43.7	–
2	43.6	–
3	40.4	–
4	43.6	–

It is worth mentioning that the simulation parameter values are not the same as those acquired in the real tests, because Philips CT scans have pre-established values of mAs, pitch and rotation time that cannot be changed manually, only selected from a list. Therefore, the values presented on Table 2 are not the same used on the ImpactScan simulation because they vary from one scan to another.

Aside from routine acquisition protocol, the other four suggested exposures with the Head-16 simulator were done by using different operation parameter values (see Table 2) to evaluate dose optimization and image quality conditions.

These parameters: operation current by effective time product, as well as pitch and tube's rotation time were changed, whilst maintaining the same high voltage tube for each one of them.

Table 2. Operational parameter values for each suggested protocol acquired with the MX 16-Slice scanner.

Protocol	High voltage tube (kV)	Product of operating current by time (mAs)	Pitch	Rotation time (s)
Routine	120	300	0.6713	0.75
1	120	280	0.6713	0.60
2	120	280	0.6042	0.60
3	120	260	0.5035	0.60
4	120	280	0.5035	0.75

The image analysis was made using the ImageJ software (see Fig. 3), which allows calculating the mean and standard deviation of regions of interest (ROIs) delimited in each measurement performed.

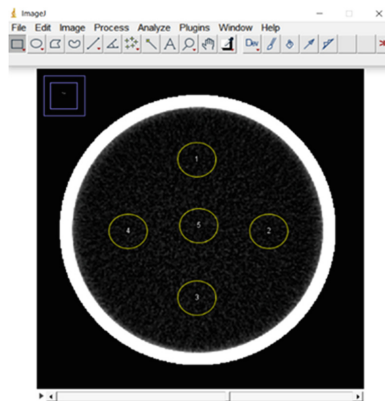


Fig. 3. ImageJ software with a CT image containing 5 circular ROIs, acquired from the head simulator's water layer.

2.1 Spatial Resolution

Following the manufacturer's instructions, the evaluation of the spatial resolution was performed by using the image 'cut' referring to the multi-pin layer of the Head-16

simulator (see Fig. 2). In this layer, there is an arrangement of 7 rows, each with a set of 5 pins of different thicknesses, spaced differently where row number 1 has the smallest space between the pins and row 7 the largest. The criterion was that all pins should be visible in the CT image.

To maintain a standard in image visualization and reliability in the visual analysis it was decided to use the ImageJ software for evaluating the image structures to minimize possible human eye mistakes. Profiles of each row of pins were plotted by arranging a linear ROI on top of the rows (see Fig. 4) so that the gray value of each could be measured.

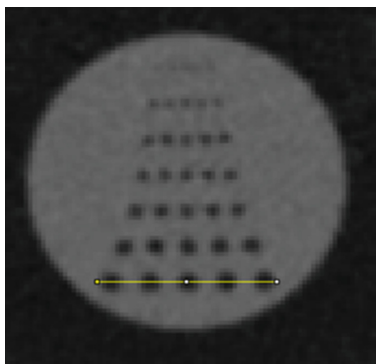


Fig. 4. CT Image showing the rows of pins with a linear ROI positioned on the 7th row, acquired from the multi-pin layer used for the evaluation of spatial resolution.

The plots had a wave pattern where the valleys represented the pins and the crests the spacing between them. In the plot, 5 valleys should be visualized (see Fig. 5).

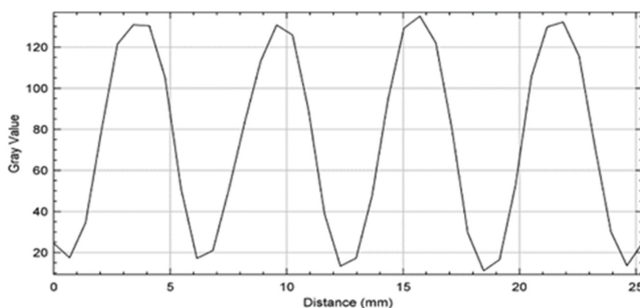


Fig. 5. Wave pattern on Gray Value versus Distance graph, plotted using the ImageJ software.

2.2 The Figure of Merit (FOM)

The FOM can be used as an image quality metric, since the higher it is, the lower the dose delivered to the patient will be. It was possible to compare the optimization between

the acquisition methods relating image quality parameters (such as spatial resolution or noise) with image acquisition parameters (such as slice thickness or dose). The equation is given by:

$$FOM = \frac{CNR^2}{CTDI_{VOL}} \quad (1)$$

where CNR is the contrast-to-noise ratio squared divided by the value of CTDI_{VOL} of each protocol suggested and used in the routine of CHC-UFPR.

CTDI_{VOL}'s value was obtained from the dose description of each protocol and the CNR was defined by subtracting the mean numerical signal of the background region of the image and the mean signal referring to the image object, divided by the standard deviation of the background signal as the following equation:

$$CNR = \frac{S_F - S_O}{\sigma} \quad (2)$$

with S_F being the mean signal of the background region of the image, S_O being the mean signal referring to the image object and σ the standard deviation of the background signal.

2.3 Noise Level (N)

Noise level (N) was estimated by dividing the value of the standard deviation (σ) of the central ROI on the water layer of the simulator by the difference between water and air's CT numbers (approximately 1000), multiplied by 100%, as the equation:

$$N = \frac{\sigma_{ROI}}{1000} \times 100\% \quad (3)$$

According to IN 93, the CT image's noise tolerance must be less than, or equal to 15% added to the reference value used in the QC test.

2.4 CT Number's Accuracy and Uniformity

To perform the CT number's uniformity and accuracy tests 5 ROIs were positioned in the water layer image to analyze the mean signal in these regions. One ROI is in the central zone and the other four are in peripheral regions of the slice, corresponding to 3, 6, 9 and 12 o'clock positions (Fig. 3).

Accuracy (ΔCT) was calculated by the difference between the value of the CT number measured in the central ROI and the nominal CT value, this being zero for water and 1000 for air as shown in the equation:

$$\Delta CT = CT_C - CT_{NOM} \quad (4)$$

where CT_C is the CT number in the central region and CT_{NOM} being the nominal CT number for water.

Uniformity (U) was calculated by subtracting the peripheral CT number (CTP) and the central CT number (CTC), both corresponding to the signal measured in the image's placed ROI as the equation follows:

$$U = CT_P - CT_C \quad (5)$$

The values of CT numbers tolerance limits for accuracy and uniformity, following IN 93 were (0 ± 5) HU (for water), and ≤ 5 HU, respectively.

3 Results and Discussion

3.1 Spatial Resolution

The plot of the profiles of the first row of pins for all the protocols studied is shown in Fig. 6. In it, it is possible to observe the five valleys, although poorly defined, for all the protocols studied, except for the routine protocol. The protocols with better visualization of the valleys in the profiles were protocols 1 (red), 2 (light green), and 3 (dark blue).

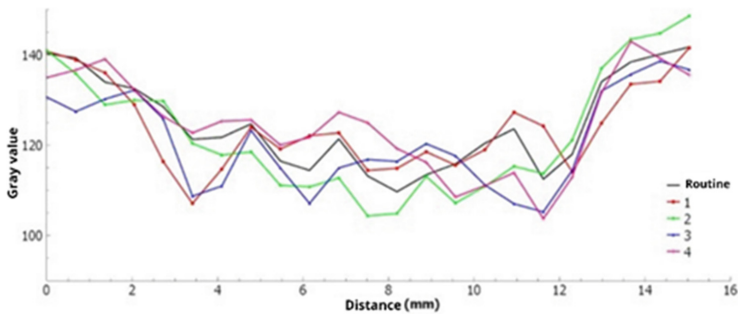


Fig. 6. Comparison between the plotted profiles using the 1st row for each protocol.

In row number 7 (see Fig. 7) it was possible to identify each of the pins in all the suggested protocols, including the routine protocol, as recommended in the instruction manual of the phantom.

It is worth mentioning that row 1 has the smallest pins with the smallest spacing between them, while row 7 has the biggest pins with the biggest spacings. In this way, better visualization of the wave pattern is expected in the plot of the profiles of row number 7.

3.2 The Figure of Merit (FOM)

As the aim was to obtain the highest possible FOM, it was analyzed that all acquisitions, except for number 4, had a higher FOM than the reference protocol, as shown in Table 3, as well as the CTDIVOL values obtained in each acquisition.

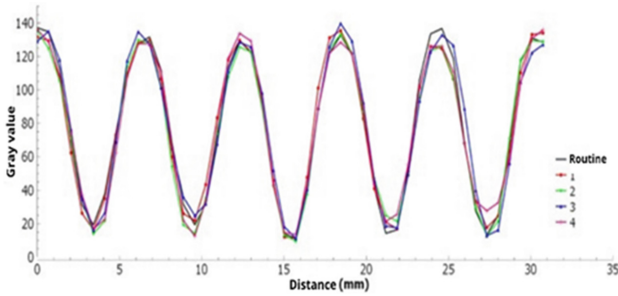


Fig. 7. Comparison between the plotted profiles using the 7th row for each protocol.

Table 3. CTDIvol and FOM comparison between all suggested protocols.

Protocol	NCR	CTDIvol (mGy)	FOM
Routine	27.80	46.25	16.71
1	28.80	43.21	19.18
2	31.01	43.11	22.31
3	26.53	40.09	17.55
4	26.33	43.29	16.01

3.3 Noise Level (N) and CT Number’s Accuracy and Uniformity

For the noise level test, following IN 93, the variation value regarding the reference level should not exceed 15%. Therefore, using the routine protocol as a baseline, the noise level would have to be less than or equal to 4.513, or less than 0.45%.

All acquisitions obtained noise levels within the recommendations. As the parameters in each suggested protocol were designed to reduce the CTDIvol, a small increase in the noise level was already expected concerning the protocol used in the routine, because the lower the dose value, the higher the level of noise. Noise in the image. It was observed that protocol 3 exceeds the tolerance value and that lower levels were obtained with suggested protocols 1 and 4.

Regarding the uniformity of the CT number, also following IN 93, the value of deviation from the reference value should be less than or equal to ± 5 HU. It is worth mentioning that the deviations in the uniformity value of all acquisitions were minimal and did not reach 0.4 HU.

In the evaluation of the CT number’s accuracy, all values found were within the recommendations for evaluation in the water of (0 ± 5) HU, according to IN 93. All results are shown in Table 4.

It was noted that acquisition 3, in the accuracy assessment, was the closest to the tolerance value of 5 HU and that protocols 1 and 4 had the smallest accuracy variation compared to the routine.

Table 4. Noise, uniformity and accuracy test results for each acquired protocol.

Protocol	σ ROI	Noise level (%)	Uniformity (HU)	Accuracy (HU)
Routine	3.925	0.39	-0.174	3.925
1	4.151	0.42	-0.057	4.151
2	4.354	0.44	-0.322	4.354
3	4.537	0.45	-0.385	4.537
4	4.179	0.42	-0.331	4.179

Thus, among the evaluated protocols, numbers 3 and 4 were outside the acceptance criteria, while protocols 1 and 2 were compliant in all proposed quality tests, as shown in Table 5.

Table 5. Performed tests' List containing the acceptance criteria for each parameter and results for each protocol acquired.

Parameters	Acceptance criteria	Routine (reference protocol)	1	2	3	4
Spatial resolution	To visualize five peaks in the plot (manufacturer's recommendation)	✓ ¹	✓	✓	✓	✓
FOM	Higher than, or equal to the reference number	✓	✓	✓	✓	×
Noise	≤15% above the reference value	✓	✓	✓	×	✓
Accuracy	0 ± 5 (water)	✓	✓	✓	✓	✓
Uniformity	≤5 HU	✓	✓	✓	✓	✓

Table 6 shows the comparison of the quality parameters between the routine protocol and the suggestions for protocols 1 and 2. Observing the values in the table, it is noted that protocol 1 presented noise, uniformity, and accuracy values closer to the values obtained with the routine protocol when compared to protocol 2.

However, the acquisition with protocol 2 also brings a reduction in the value of CTDIVOL and a greater increase in FOM, that is, better image quality is obtained with an optimization of the dose. Therefore, considering the acceptance criteria for image quality in CT scans, within all protocols, only numbers 1 and 2 showed satisfactory results.

In addition, with these two protocols, a reduction in CTDIVOL of approximately 6.5% was obtained, and an increase of an average of 28.2% in FOM concerning the protocol already used in the routine.

¹ "✓" for compliant and "×" for non-compliant.

Table 6. Results comparison between routine's reference values and the acquired protocols 1 and 2.

Parameters	Reference value	Protocol 1	Protocol 2
CTDI _{vol} (mGy)	46.25	43.21	43.11
FOM	16.71	19.18	22.31
Noise (%)	0.39	0.42	0.44
Uniformity (HU)	-0.174	-0.057	-0.322
Accuracy (HU)	3.925	4.151	4.354

4 Conclusions

In this study, the CT Contrast-free adult skull protocol was optimized by changing some acquisition parameters such as rotation time, pitch, and tube current product by beam time, to reduce the CTDI_{vol} value, maintaining the image quality.

In all protocols proposed, a significant reduction in the value of CTDI_{vol} was observed due to the change in the value of the current product of operation by time, from 300 to 280 mAs.

Thus, it is suggested that UDIM carry out an analysis of the images acquired with protocols 1 and 2 together with radiologists to compare the quality of the images because, in addition to the quantitative evaluation of the parameters, a qualitative evaluation is also necessary to enable the establishment of a new protocol that best fits the physician's criteria for the hospital's medical report.

References

1. Seeram, E.: Studyguide for Computed Tomography: Physical Principles, Clinical Applications, and Quality Control, 4th edn. Saunders, United States (2015)
2. Tauhata, L., Salati, I., Di Prinzio, R., Di Prinzio, A.: Radioproteção e Dosimetria: Fundamentos, 10th edn. IRD/CNEN, Rio de Janeiro (2014)
3. Samei, E., Bakalyar, D., Boedeker, K. L., et al.: Performance Evaluation of Computed Tomography Systems. In: AAPM Task Group 233 Report, pp 1–71. American Association of Physicists in Medicine, United States (2019)
4. International Atomic Energy Agency.: Quality Assurance Programme for Computed Tomography: Diagnostic and Therapy applications. In: IAEA Human Health Series, Austria (2012)
5. Agência Nacional de Vigilância Sanitária.: Radiodiagnóstico Médico: Desempenho De Equipamentos e Segurança. 1st ed. Editora Anvisa, Brasília (2005)
6. Agência Nacional de Vigilância Sanitária.: RDC 611: Instrução Normativa No 93. Ministério da Saúde, Brasília (2022)
7. Rehani, M. M.: ICRP and IAEA Actions on Radiation Protection in Computed Tomography. In: Annals of the ICRP, vol. 41, pp. 154–160. IAEA, Austria (2012)

Author Index

A

Agnolin, Guilherme 357
Almeida, Fernanda N. 317
Almeida, R. M. V. R. 184
Alves, L. P. 203
Amorim, Laís Souza 228
Araújo, D. N. 174
Araujo, F. C. 273
Arthur, Rangel 369
Assis, L. 309
Azevedo, L. L. 253

B

Bacht, Simão 219
Báez, Edgar D. 67
Balbina, F. T. C. S. 253
Baptista, A. 195, 212, 294, 349
Barreneche-Ospina, Juan 43
Barreto, Tiago 139
Barros, Frieda Saicla 118
Barros, K. N. 380
Bassani, J. W. M. 174
Brandão, Mariana Ribeiro 23, 78, 128
Buchler, R. D. D. 273

C

Campos, Hércules Lázaro Morais 403
Campos, S. 349
Cardona-Alzate, Daniela 43
Carvalho, André S. 317
Carvalho, H. C. 285
Carvalho, M. C. O. 253
Cebada-Fuentes, Ricardo 338
Cestari, Idágene A. 219
Chagas, R. K. 195
Coelli, F. C. 184
Costa, Diego S. 317
Cunha, Beatriz 241

D

Da Gama, Alana Elza Fontes 228

da Silva, Ana Maria Marques 55
da Silva, Luiz R. C. 317
da Silva, Vitor I. 317
Dantas, L. H. V. 212
de Amorim, Henrique Alves 395
de Fátima Camillo Ribeiro, Débora 14
de Figueiredo, Rodrigo Marques 241
de la Cruz, C. 31
de Lima, C. J. 203
de M. Fiali, Gabriel 317
Dias, M. S. 380
Dos Santos, L. 309

E

Espinosa, R. A. 302
Estevam, C. A. 380

F

F.C.D.Silva, F. C. D. 281
Fernandes, A. B. 285
Fernandes, A. B. 203, 253
Ferreira Junior, A. F. G. 380
Flores, Franklin C. 369
Fonseca, Y. J. 302
Francisco, Maicon 88
Freitas, R. V. 273
Freitas-Júnior, R. A. O. 431

G

Gandolfi, Beatriz L. 317
Garcia da Rocha, Bruno 357
García-García, José Antonio 338
García-Ramos, Javier 43
Gómez-Alzate, Daniela 328
Guzmán-Canizales, L. 150

H

Heinzelmann, T. R. O. 285
Hembecker, Paula Karina 14
Hernandez-Contreras, Indira 98

Honorato, D. 349
 Hortegal, R. A. 273
 Hossri, C. A. C. 273

I

Ismael Hardy Llins, Lazaro 357

J

Junior, A. F. G. Ferreira 424
 Júnior, Alexandre Holzbach 128
 Junior, Benedito Vital Ribeiro 395

K

Koch, N. C. B. L. 107

L

Lambertinez, M. E. 302
 Lazo-Osório, R. A. 203
 Leite, Saul C. 317
 Lemos, João Thomaz 403
 Lima, C. J. 253, 285
 Lima, Marcelo 139
 Lino-Alvarado, A. E. 380, 424
 Lins, Giovanna B. 317
 Lopes, M. H. G. 424
 Lozano-Suárez, J. A. 150

M

Maciel, Jonas 23
 Magalhães, D. S. F. 281
 Malthez, A. L. M. C. 386
 Malthez, A. M. 439
 Mamani, C. 31
 Manuel-Galeano, Juan 43
 Marcolan, João Antônio 413
 Marino-Neto, José 413
 Marques, Jefferson Luiz Brum 88, 413
 Martinez-Licon, Fabiola M. 98, 163
 Martinez-Vazquez, Cipactli M. 163
 Martins, A. P. S. 281
 Martins, D. C. L. 294
 Martins, J. P. S. 203
 Martins, Juliano 23
 Mazzetto, Marcelo 219
 Mello, S. G. 380, 424
 Meneghelo, R. S. 273
 Merino, Clarissa S. R. 317
 Mieko Botome, Maira 357
 Moraes, Matheus Cardoso 395

Moriya, H. T. 273, 380, 424
 Mota, M. S. A. 263
 Moura, Lucas 139
 Muniz, Pablo Rodrigues 403

N

Nakato, Adriane Muller 14
 Navarro, R. S. 195, 212, 263, 294, 349
 Ninke, Andriele 403
 Nohama, Percy 14
 Nunes, G. P. 263
 Nunes, J. E. P. 263
 Nunes, Reginaldo Barbosa 403
 Nunez, S. C. 195, 212, 294, 349

O

Ojeda, Renato Garcia 23, 78, 128
 Oliva, Hellen Hillary 14
 Oliveira, T. R. 107
 Ortiz-Posadas, M. R. 3, 150

P

Parizotto, N. A. 263
 Paz, Lyssandra 139
 Penteadó, G. B. 273
 Pereira, L. A. M. 195, 294
 Pereira, Thiago Martini 395
 Pérez-Buitrago, Sandra 328
 Pimente, P. C. O. Z. 309
 Pimentel-Aguilar, A. B. 3
 Pinto, A. 212
 Pires Bastos, Bruno 357
 Pisarello, Maria I. 67
 Porto, Maria Eduarda Rossari 14
 Purificação, Marcela 357

Q

Quispe, Pierol 328

R

Real, J. V. 386, 439
 Rêgo, T. S. 431
 Rezende, M. C. C. 184
 Rocha, Camila C. 317
 Rodrigues, A. C. 431
 Rodríguez-Vera, R. 3
 Romani, A. P. 107
 Rosa, D. A. O. 424
 Rosa, Perseu Filho 118

S

Saldarriaga-Saldarriaga, Óscar 43
Saleh, M. A. K. 349
Sánchez-Pérez, Celia 338
Santos, B. P. 263
Santos, R. P. 184
Schmith, Jean 241
Schmitz, G. V. 253
Serra, T. K. 309
Silva, Alexandre G. 369
Silva, F. C. D. 281
Silva, P. I. B. P. 349
Silva, S. P. 431
Silveira, L. 285
Simão, Josemar 403
Simonato, L. E. 281
Suassuna, Alice 139

T

Tanaka, H. 107
Tarocco, J. C. 309

Tim, C. 309
Toledo, E. 31
Torres, Daniel S. 219
Torres, F. N. 439
Trinca, William Correia 55

U

Uemoto, V. R. 273
Uribe-Herrera, Lucía 43

V

Valério, G. D. 380
Valladares-Pérez, José 338
Vallejos, Sofia J. 67
Vieira, D. V. 431
Villaverde, A. B. 203
Vitorasso, R. L. 424

Z

Zapata-Álvarez, Mabel 43
Ziza, Lucas N. 369